

## **Abstract**

Holocene coastal deposits of NW Germany consist of many lithological facies, e.g., tidal flat, brackish, and lagoonal sediments as well as peat layers in response to climate-driven sea-level changes. In the scope of an interdisciplinary project, initiated by the ICBM, nine drill cores from the marshlands of Lower Saxony were analysed at high-resolution (1,435 samples) for their inorganic-geochemical composition (e.g. bulk parameters, major and trace elements) by using, e.g., XRF, ICP-OES, and ICP-MS. One core originates from the marshlands close to the river Weser (Loxstedt), while the remaining drill sites are situated within (Arngast) or close to (Schweiburg, Wangerland) the present Jade Bay. The major aim of the project is to provide information about type and provenance of deposited material, depositional dynamics, palaeosalinity and early diagenetic processes of mineral formation. The synopsis of these results should reveal a detailed reconstruction of the palaeoenvironmental development of the study area.

The individual lithological facies can be differentiated by varying proportions of the major components quartz, clay, carbonate, and organic matter. The tidal flat facies occur as sand, mixed, and mud flat sediments. While the sand flat sediments contain elevated amounts of quartz and heavy minerals as seen in enrichments of Si, Ti, Y, and Zr, the mixed and mud flats are characterized by a higher abundance of clay and carbonate indicated for instance by increasing contents of Al and TIC. The brackish and lagoonal sediments were formed under comparatively calm depositional conditions indicated by increasing amounts of clay. Despite of slightly higher TOC contents and lower amounts of heavy minerals the brackish sediments show a geochemical composition similar to the mud flat facies. On the other hand, the carbonate-free lagoonal sediments reveal an almost shale-like element pattern.

The lagoonal facies forms the transition to fen reed peat and is, therefore, characterized by enhanced amounts of TOC owing to the occurrence of reed rhizomes. The peat layers of the investigated cores can be subdivided in basal peats and intercalated peats. The basal peats overlay Pleistocene sands and consist in the lower parts of fen woodland and partly bog peat whereas the uppermost parts are formed mainly by reed peat. The intercalated peats are situated between clastic sediments and comprise predominantly reed peat which grew under a continuous seawater influence. In comparison to a reference peat core from the heathland (Aurich Moor) especially the

intercalated reed peats show elevated contents of lithogenic elements (e.g. Al, Si, Ti) due to the influence of the rising North Sea.

As the inorganic-geochemical characteristics of the individual facies correlate with depositional factors like wave-energy and resulting lithofacies changes, this study allows a detailed reconstruction of the palaeoenvironmental development. Thus, the results obtained from the four locations enable a classification in open, sheltered, and estuarine intertidal systems. The Wangerland site reflects a sheltered intertidal system which is, however, partly influenced by tidal channel activities. The same is true for the Schweiburg core but the formation of a natural levee led to enhanced freshening in the upper part of the core. On the other hand, the Arngast location reflects an open tidal system which is unfortunately influenced by processes of redeposition in the upper part. The Loxstedt site could be classified as an estuarine intertidal system due to the proximity to the river Weser. Nevertheless, the river influence was not constant during the Holocene. Diatom studies reveal that the river Weser reached its present location next to the drill site 2,650 years BP which is also evidenced by enhanced Mn contents in tidal flat sediments.

The Holocene coastal peats are predominantly characterized by elevated amounts of pyrite as a result of microbial reduction of seawater sulphate. However, the Fe source seems to be the freshwater environment. The pyrite enrichments can be explained by two different scenarios. On one hand, pyrite formation coincides with peat growing, which is decisive for the reed peats. Hence, a brackish water zone has to be assumed for the peat-forming environment which is influenced by iron-rich freshwater and sulphate-rich seawater. On the other hand, unusually high amounts of pyrite (maximum 49.8%) found within several limnic basal peats at botanical transition zones point to a process occurring after peat formation. These basal peats often contain thin clastic layers due to tidal channel activities which led to an uplift of the peat at the aforementioned transition zones. As a result of the uplift an input of clastic material seems possible. When the peat settles down clastic layers remain whose interfaces to the peat may have acted as aquifers for waters of higher salinity. Therefore, an enhanced formation of pyrite was possible due to the combination of sulphate-rich groundwater and iron-rich peatland waters.

The peat layers are also characterized by enrichments in redox-sensitive trace metals (As, Mo, Re, U) and Cd. By contrast, the trace metals Co, Cr, Cu, Mn, Ni, Pb, Tl, and

Zn reflect the geogenic background. Seawater is suggested to be the main source for As, Cd, Mo, Re, and U whereas the remaining elements were contributed by freshwater. While pyrite shows its highest accumulation in basal peats, the redox-sensitive trace metals As, Mo, Re, and U are highly enriched in the intercalated reed peats. As the intercalated reed peats were formed under the direct influence of brackish water, the saline groundwater entering the basal peats is most likely affected by diagenetic processes which led to a partial depletion in redox-sensitive trace metals.

The comparison of Holocene and recent tidal flat sediments reveals a significant enrichment of Zr in the recent sediments reflecting higher amounts of heavy minerals. This seems to indicate an increase in depositional energy from the Holocene to the recent situation. The Holocene tidal flat sediments contain elevated amounts of mud when compared with recent deposits which show a significant lack of this fine-fraction. This phenomenon is possibly related to modern dike-building. The mainland dike seems to act as an energy barrier for the deposition of the fine-fraction. Thus, the examination of SPM from this area demonstrates that the clay-fraction of the sediments is predominantly suspended in the water column and may be exported from the backbarrier area into the open North Sea.

### **Kurzfassung**

Holozäne Ablagerungen des nordwestdeutschen Küstenraums setzen sich aus einer Vielzahl lithologischer Einheiten zusammen. So bildeten sich im Küstenraum überwiegend Wattsedimente, brackische und lagunäre Ablagerungen sowie Torfe als Reaktion auf den klimatisch bedingten Meeresspiegelanstieg. Im Rahmen eines interdisziplinären Forschungsprojektes des ICBM wurden neun Bohrkern aus den Marschen Niedersachsens in hoher Auflösung (1.435 Proben) auf ihre anorganisch-geochemische Zusammensetzung (u.a. Pauschalparameter, Haupt- und Spurenelemente) mittels RFA, ICP-OES und ICP-MS untersucht. Ein Bohrkern stammt aus der Marsch nahe der Weser (Loxstedt), während die verbleibenden Bohrlokationen innerhalb (Arngast) bzw. nahe (Schweiburg, Wangerland) dem heutigen Jadebusen gelegen sind. Hauptziel des Projektes ist es, Erkenntnisse über Art und Herkunft des sedimentierten Materials, Ablagerungsenergetik, Paläosalinität und frühdiagenetische Prozesse der

Mineralneubildung zu gewinnen. Die Synthese dieser Ergebnisse soll zu einer detaillierten Rekonstruktion der Paläoumweltbedingungen im Untersuchungsgebiet führen.

Die einzelnen lithologischen Fazies lassen sich anhand variierender Gehalte der Hauptkomponenten Quarz, Ton, Karbonat und organisches Material unterscheiden. Die Wattsedimente lassen sich darüber hinaus in Sandwatt-, Mischwatt- und Schlickwattsedimente unterteilen. Die Sandwattsedimente enthalten erhöhte Gehalte an Quarz und Schwermineralen, die sich durch Anreicherungen von Si, Ti, Y und Zr nachweisen lassen. Im Gegensatz dazu zeichnen sich die Misch- und Schlickwattablagerungen durch höhere Anteile an Ton und Karbonat aus, die u.a. durch Al und TIC repräsentiert werden. Die brackischen und lagunären Sedimente bildeten sich unter vergleichsweise ruhigen Ablagerungsbedingungen, was zu einer weiteren Erhöhung des Tonanteils führte.

Abgesehen von erhöhten TOC-Gehalten bzw. einem niedrigeren Anteil an Schwermineralen zeigen die brackischen Sedimente eine ähnliche Geochemie wie die Schlickwattfazies. Andererseits zeichnen sich die karbonatfreien lagunären Ablagerungen durch eine dem mittleren Tonschiefer ähnliche Zusammensetzung aus. Da die lagunäre Fazies den Übergang zu Niedermoor-Schilftorfen darstellt, unterscheidet sie sich zudem durch erhöhte TOC-Gehalte aufgrund von Schilfrhizomen von den übrigen klastischen Sedimenten.

Die Torfe der untersuchten Kerne lassen sich in Basaltorfe und sogenannte „schwimmende Torfe“ unterteilen. Die Basaltorfe bildeten sich auf dem pleistozänen Untergrund und bestehen an ihrer Basis meist aus Bruchwaldtorf, der teilweise in Hochmoortorf übergeht. In den oberen Bereichen der Basaltorfe finden sich überwiegend Schilftorfe als Resultat des ansteigenden Meeresspiegels. Die „schwimmenden Torfe“ sind zwischen klastischen Sedimenten eingeschaltet und bestehen zum größten Teil aus Schilftorf, der sich unter einem kontinuierlichen Meerwassereinfluß bildete. Im Vergleich zu einem Torfkern von der Geest (Auricher Moor) zeigen insbesondere die „schwimmenden Torfe“ erhöhte Gehalte an lithogenen Elementen (z. B. Al, Si, Ti) aufgrund des Einflusses der naherrückenden Nordsee.

Da die anorganisch-geochemischen Eigenschaften der einzelnen Fazies mit den Ablagerungsbedingungen (z.B. Wellenenergie) und den daraus resultierenden lithofaziellen Wechseln korrelieren, erlaubt die vorliegende Arbeit eine detaillierte

Rekonstruktion der Paläoumweltbedingungen. Auf Basis der erhaltenen Ergebnisse spiegeln die vier Bohrlokationen die Bedingungen eines offenen, geschützten und ästuarinen intertidalen Systems wider. So lassen sich die Bohrkerne aus dem Wangerland einer geschützten Buchtensituation zuordnen, die jedoch teilweise durch Rinnensysteme beeinflusst ist. Entsprechendes gilt für die Lokation Schweiburg, wobei die Ausbildung eines Uferwalls zu einer deutlichen Aussüßung im oberen Bereich des Kerns führte. Der Arngast-Kern hingegen spiegelt ein offenes intertidales System wider. Allerdings ist der obere Bereich des Kerns durch rezente Umlagerungsprozesse beeinflusst. Die Loxstedt-Kerne entstammen einem ästuarin beeinflussten System, was sich aus der Nähe zur Weser erklärt. Jedoch war der Einfluß der Weser nicht konstant über das gesamte Holozän. So zeigen Diatomeen-Analysen, daß die Weser ihre heutige Position erst nach 2.650 Jahren vor heute erreichte. Dieses Ergebnis läßt sich ebenfalls durch variierende Mn-Gehalte in den Wattsedimenten nachweisen.

Die untersuchten Torfe des Küstenholozäns enthalten oftmals hohe Anreicherungen von Pyrit aufgrund mikrobieller Reduktion von Meerwassersulfat, wobei die Fe-Quelle jedoch das Süßwasser darstellt. Diese Pyrit-Anreicherungen lassen sich durch zwei unterschiedliche Szenarien erklären. Speziell in den Schilftorfen fand die Pyrit-Bildung parallel zum Torfwachstum statt. So ist eine Brackwasserzone anzunehmen, die aus sulfatreichem Meerwasser und eisenreichem Süßwasser gebildet wird. Andererseits zeigen einige limnische Basaltorfe ungewöhnlich hohe Pyrit-Anreicherungen (max. 49.8%) an botanischen Übergängen, die auf einen Prozeß nach der Torfbildung hindeuten. Diese Basaltorfe enthalten dünne Lagen aus klastischem Material aufgrund von Rinnenaktivitäten, die zu einem teilweisen Aufschwimmen der Torfe an obigen Übergängen führten. Durch das Aufschwimmen des Torfs wurde das Eindringen von partikulärem Material möglich, so daß nach erfolgter Torfsetzung feine klastische Lagen zurückblieben. Die Grenzflächen zwischen Torf und Klastika bzw. die klastischen Lagen selbst können im weiteren Verlauf als Leiter für Wasser erhöhter Salinität fungieren. So besteht die Möglichkeit, daß durch die Kombination von sulfatreichem Grundwasser und eisenreichen Torfwässern eine erhöhte Bildung von Pyrit erfolgte.

Die Torfe zeichnen sich darüberhinaus durch Anreicherungen von redox-sensiblen Spurenelementen (As, Mo, Re, U) und Cd aus. Im Gegensatz zu diesen Elementen, spiegeln Co, Cr, Cu, Mn, Ni, Pb, Tl und Zn den geogenen Hintergrund wider. Die

Hauptquelle für As, Cd, Mo, Re und U stellt das Meerwasser dar, während die verbleibenden Elemente durch Süßwasser eingetragen werden. Im Gegensatz zur Verteilung von Pyrit finden sich die höchsten Spurenelementanreicherungen in den „schwimmenden Torfen“, die unter direktem Einfluß von Brackwasser gebildet worden sind. Andererseits läßt sich vermuten, daß das saline Grundwasser, das in die Basaltorfe gelangte, diagenetischen Prozessen unterworfen war, die zu einer Verarmung an redox-sensiblen Spurenelementen führten.

Der Vergleich von holozänen und rezenten Wattsedimenten zeigt erhebliche Anreicherungen von Zr in den rezenten Sedimenten, die auf ein erhöhtes Vorkommen von Schwermineralen hinweisen. Dieser Unterschied scheint auf einen Anstieg der Ablagerungsenergetik vom Holozän zur rezenten Situation hinzudeuten. So enthalten die holozänen Wattsedimente einen höheren Schlickanteil, während in den rezenten Ablagerungen eine signifikante Verarmung der Feinfraktion festzustellen ist. Dieses Phänomen ist vermutlich auf den modernen Deichbau zurückzuführen. So scheinen die Deiche als Energiebarriere zu wirken, die die Sedimentation von feinem Material verhindert. Die Untersuchung von Schwebstoffen aus diesem Gebiet zeigt, daß die Feinfraktion der Sedimente zu einem Großteil in der Wassersäule suspendiert ist, von wo aus sie in die offene Nordsee transportiert werden kann.

## Chapter 1

### 1.1. Introduction

The coastal lowlands of NW Germany consist of barrier islands, back tidal areas, sheltered and open tidal flats, bay flats, and estuaries. Their development began about 7,500 years BP caused by the Holocene sea-level rise. At that time the first approach of brackish water reached the area of the present East Frisian Islands (Streif, 1990). During the maximum of the Weichselian Glacial 18,000 years BP the sea level was about 110-130 m below the present level (Cameron *et al.*, 1987; Long *et al.*, 1988) whereas 7,500 years BP the sea level was about 25 m lower than today. Within the following 5,500 years a so-called Holocene sedimentary wedge was formed in the coastlands of NW Germany, which partly reaches a maximum thickness of 35 m (Hoselmann and Streif, 1997).

Holocene coastal deposits consist of many lithofacies, e.g., tidal flat, brackish, and lagoonal sediments as well as sedentary peat layers. The peat layers can be differentiated into basal and intercalated peats. The basal peats overlay Pleistocene sands while the latter are situated between clastic sediments (Streif, 1990). The occurrence of the individual lithofacies reflects the response of the depositional area to sea level fluctuations and palaeoenvironmental changes, respectively. These changes are supposed to be manifested in the geochemical composition of the Holocene coastal deposits. However, geochemical investigations are rare (e.g. Ludwig *et al.*, 1973; Behre *et al.*, 1985) when compared with sedimentological or palaeobotanical studies (e.g. Streif, 1971; Barckhausen *et al.*, 1977; Linke, 1979, 1982; Preuss, 1979; Barckhausen and Müller, 1984).

Therefore, an interdisciplinary project was initiated by the Institute of Chemistry and Biology of the Marine Environment (ICBM) and Terramare Research Centre, Wilhelmshaven, as part of the DFG priority program "Changes in the geo-biosphere during the last 15,000 years - continental sediments as evidence of changing environmental conditions". This project involves inorganic-geochemical analyses (e.g. major and trace elements), which were performed by the author, as well as organic-geochemical (e.g. biomarker, amino acids) and microfacies (e.g. diatoms, thin sections) investigations. The results obtained from inorganic-geochemical analyses were, except for Chapter 2.4 and 3.2, combined with microfacies and organic-geochemical

investigations carried out by the following working groups: i) Marine Chemistry (G. Liebezeit, D. Vetter; Terramare), ii) Microfacies (G. Gerdes, F. Watermann; ICBM Marine Station), and iii) Organic Geochemistry (D. Gramberg, J. Rullkötter, B. Scholz-Böttcher; ICBM). Thus, all measurements concerning bulk parameters, major and trace elements were carried out by the author. Additionally, the author was directly involved in SEM investigations and fermentation experiments, which are presented in Chapter 3.1. Exceptions are bulk parameters measurements of the Loxstedt core GE432 performed by D. Gramberg as well as data of recent tidal flat sediments, suspended particulate matter, and North Sea water carried out by A. Hild, J. Hinrichs, and G. P. Klinkhammer. Therefore, the work performed by the author can be clearly separated in the individual chapters from the investigations of the co-authors.

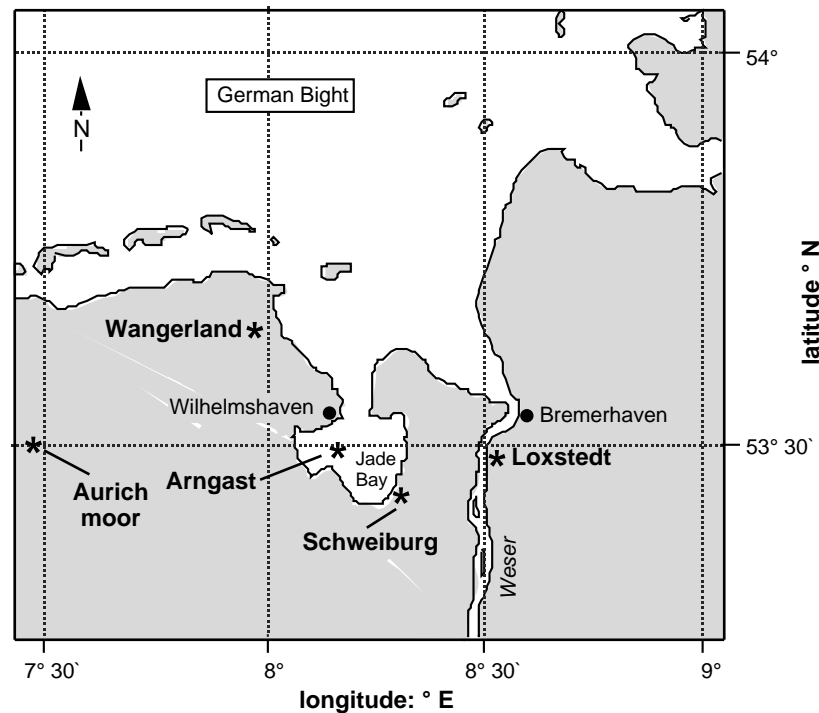


Figure 1.1: Map of the study area showing the drilling locations.

The aim of the project is to provide information about type and provenance of deposited material, depositional dynamics, palaeosalinity and early diagenetic effects. Over all the synthesis of the individual results should reveal a detailed reconstruction of the palaeoenvironmental development of the study area (Figure 1.1).

The work presented here bases on nine cores from the marshlands of Lower Saxony that were drilled with the technical support of the Geological Survey of the Federal



State of Lower Saxony, Hannover. The cores originated from four locations that represent a sheltered bay, an open tidal flat area, and a river influenced intertidal system. In addition, one core was drilled with a drilling system of the Niedersächsisches Institut für historische Küstenforschung, Wilhelmshaven, in the Aurich Moor (Figure 1.1).

## **1.2. Summary**

As mentioned above this work forms part of an interdisciplinary project. Hence, the inorganic-geochemical data collected for the present study were combined in most chapters with organic-geochemical and microfacies results. The ultimate goal of this work was to reconstruct the palaeoenvironmental development of the study area, thus all chapters deal with this superordinate aim. The results can be summarized as follows:

The investigated Holocene deposits consist predominantly of tidal flat, brackish, and lagoonal sediments as well as peat layers. Hence, Chapter 2 deals with a general characterization of these individual lithofacies. In Chapter 2.1 preliminary results are presented which base on the examination of two parallel cores from the Loxstedt site close to the river Weser. Both cores were combined to one composite profile on the basis of inorganic-geochemical data. A factor analysis carried out by using the inorganic-geochemical data set reveals that Holocene deposits consist of a mixture of four major components, i.e., organic matter, clay, carbonate, and quartz (heavy minerals). As the abundance of these characteristic components shows large variations within the core profile, lithofacies changes can be clearly identified. These changes are also evidenced by diatom inventories. In contrast, organic-geochemical analyses focus on molecular peat composition and provide information about the origin of organic matter within the clastic sediments. During the work it turned out that the combination of inorganic-geochemical data and diatom inventories provides a useful tool to reconstruct palaeoenvironmental conditions. Therefore, in Chapters 2.2 and 2.3 the combination of both methods are presented.

Chapter 2.2 focus again on the Loxstedt site while in Chapter 2.3 one core (W5) from a core transect (five cores), drilled in the marshlands of the Wangerland, is chosen for a detailed discussion. The Loxstedt core reflects a very dynamic system in response to sea-level fluctuations and influence of the river Weser. The basis of the Loxstedt core

forms a basal peat which contains a freshwater mud layer. This section was formed independent of the sea-level rise as evidenced for instance by P enrichments which point towards the occurrence of vivianite, an indicator mineral for limnic conditions. Limnic conditions were also evidenced by the absence of marine diatoms in most parts of the basal peat. The examination of rare earth elements reveals similarities to mean Jungwurm loess indicating that eolian material contributed significant amounts to the detrital fraction of the basal peat. The clastic sediments of the core reflect strongly varying hydrodynamics and depositional energy, respectively. Thus, Si/Al- and Zr/Al-ratios, which serve as indicators for quartz and heavy minerals, provide evidence for the occurrence of two sand flat layers in the upper and lower part of the core. The central part of the core is dominated by mixed flat and brackish sediments as well as by several reed peat layers which are situated between lagoonal sediments. The occurrence of reed peat beds and lagoonal sediments reflect a slowly rising or stagnating sea level and low salinity, respectively.

Chapter 2.2 provides the first insight into early diagenetic processes of mineral formation. Despite of the aforementioned occurrence of vivianite, the intercalated peat layers are characterized by elevated amounts of pyrite owing to microbial reduction of seawater sulphate. The investigation of stable sulphur isotopes in peat samples reveals that pyrite formation occurred under open and closed system conditions depending on sulphate availability and proximity to the coastline, respectively. Therefore,  $^{34}\text{S}$  values can be used to differentiate between direct (e.g. tidal flushing) or indirect (e.g. diffusion) seawater influence.

By contrast, the Wangerland area is characterized by comparatively calm depositional conditions owing to its sheltered bay situation. For instance Si/Al- and Zr/Al-ratios of core W5 (Chapter 2.3) show that this core contains no sand flat but mud and mixed flat sediments. This core documents two transgressive and one regressive phase as reflected by the occurrence of a basal reed peat and an intercalated reed peat which were overlaid by clastic sediments mainly of marine origin. Enrichments of lithogenic elements (e.g. Al, Rb, Si, Zr) within the lower part of the basal peat of this core reflect the occurrence of several thin clastic layers of 1 to 3 mm thickness as a result of tidal channel activities.

Chapter 2.4 provides an overview of the inorganic-geochemical composition of the main Holocene coastal sediments (i.e., tidal flat, brackish, and lagoonal sediments) as

well as peat layers. Tidal flat sediments contain elevated amounts of quartz and heavy minerals as seen in enrichments of Si, Ti, Y, and Zr, while the brackish and lagoonal sediments were formed under comparatively calm depositional conditions. However, the occurrence of biogenic carbonate in the brackish sediments, as seen in enrichments of Ca and Sr, reflect a distinctly higher salinity for this facies in comparison to the almost carbonate-free and shale-like composed lagoonal sediments. In contrast, the lagoonal facies contains higher amounts of total organic carbon (TOC) and total sulphur (TS) which is predominantly the result of reed growing under a considerably lower mean salinity (<10‰). Therefore, a higher availability of organic matter favoured the formation of pyrite in the lagoonal sediments. The peat layers (fen and bog peat) of the drill cores can be subdivided into basal and intercalated peats. In comparison to a reference peat core from the heathland (Aurich Moor), the coastal peats contain elevated amounts of lithogenic elements (e.g. Al, Mg, Si, Ti). The intercalated peats received their lithogenic material predominantly from tidal flushing. Despite of eolian input, some basal peats are influenced by tidal channel activities which led to the aforementioned occurrence of thin clastic layers. Chapter 2.4 also provides a comparison of the four drilling locations in order to elucidate palaeoenvironmental differences. Three locations are situated within (Arngast) or close to (Schweiburg, Wangerland) the present Jade Bay while the Loxstedt site originates from the right bank of the river Weser. On the basis of the geochemical characteristics of the individual lithofacies estimates about the exposition to the coastline are possible. High enrichments of As and Mo seen in the basal and intercalated peat of the Arngast core reflect an open intertidal system and a continuous seawater influence during peat formation. Both trace metals occur in seawater as oxoanions and are characterized by a high seawater concentration in seawater in comparison to the geogenic background. On the other hand, lower contents of redox-sensitive trace metals seen in the intercalated peat of the Schweiburg core reflect a complete silting up process which culminated in the formation of bog peat. This silting up process is most likely encouraged by the development of a natural levee within the ancient Jade Bay. The basal peats of the Wangerland cores show elevated As and Mo contents as well. However, these enrichments are favoured by the occurrence of clastic layers within the basal peats which enable an indirect input of seawater. The Loxstedt core reflects an estuarine intertidal system as seen in enrichments of Mn and TOC in the clastic sediments.

However, the influence of the river Weser changed during the Holocene which could be evidenced by varying contents of Mn in the tidal flat sediments. In addition, diatom studies have shown, that the river Weser reached its present location about 2,650 years BP (see Chapter 2.2).

A further aim of this study is the investigation of early diagenetic processes of mineral formation, i.e., pyrite formation as indicated in Chapter 2.2. Thus, Chapter 3 deals with the formation of pyrite in Holocene coastal peats and its effects on trace metal distribution. Chapter 3.1 focus on the peat layers (basal and intercalated peats) of the Wangerland core W5 which contains some unusually high amounts of pyrite. The TS content of the peat layers of core W5 averages 7.8% owing to microbial reduction of seawater sulphate under almost open system conditions. Although the average TS content is comparable to the Loxstedt site (e.g. Chapter 2.1), a maximum value of 28.2% seen within the lower part of the basal peat at the transition of fen and bog peat is rather striking. These pyrite enrichments coincide with the occurrence of the aforementioned clastic layers (Chapter 2.3). The uppermost part of the basal peat is formed by reed peat which also contains elevated amounts of pyrite while the contents of the intercalated reed peat are distinctly lower. In contrast to sulphate the main Fe carrier phase is thought to be freshwater, which suggests the occurrence of a brackish water zone for the Holocene peat-forming environment. As diatom studies reveal a lower salinity during the formation of the basal reed peat in comparison to the intercalated reed peat, the higher amounts of pyrite within the basal reed peat can be explained by a higher Fe availability. On the other hand, the pyrite enrichments in the lower part of the basal peat cannot be explained by a direct influence of brackish water because this part consists of fen woodland and bog peat reflecting limnic and S-limited conditions, respectively. The pyrite enrichments coincide with the clastic layers within the basal peat and point towards a process occurring after peat formation. Tidal channel activities led to an uplift of the basal peat at transition zones (e.g. fen and bog peat) and allowed the deposition of clastic material. For that reason clastic layers of marine origin as evidenced by the occurrence of pelagic diatoms remained. The resulting clastic material/peat interface acted as an aquifer for waters of higher salinity, which led, in combination with Fe-rich peatland waters, to an enhanced formation of pyrite.

In addition to pyrite most of the peat layers are also enriched in redox-sensitive trace metals. Chapter 3.2 deals with the trace metal distribution in the peats of the

Wangerland cores with respect to element sources and fixation. The trace metals Mo and Re show highest enrichments in the peat layers followed by As, Cd, and U. In contrast Co, Cr, Cu, Mn, Ni, Pb, Tl, V, and Zn reflect more or less the geogenic background. The trace metal inventory of the peats can be explained by the occurrence of the above mentioned brackish water zone. Thus, seawater is the decisive source for As, Cd, Mo, Re, and U whereas the remaining elements are contributed by freshwater. Leaching experiments have shown that As, Co, Mo, Re, and Tl are predominantly fixed as sulphides and/or incorporated into pyrite while U is bound to organic matter. The remaining trace metals show no distinct trends, only Cr reveals a strong relation to the lithogenic detritus. In contrast to the pyrite distribution the redox-sensitive trace metals As, Mo, Re, and U are highly enriched in the intercalated reed peats, which were formed under a direct influence of seawater and brackish water, respectively. The saline groundwater which enters the basal peats after their formation is most likely depleted in redox-sensitive trace metals due to diagenetic processes.

In Chapter 4 the geochemistry of the Holocene tidal flat sediments is compared with recent sediments from the Jade Bay (location Arngast) and from the Spiekeroog backbarrier area carried out by A. Hild (ICBM). The use of Ti and especially Zr, which occur in sediments as part of heavy minerals (e.g. zircon, ilmenite, rutile) reveal a rise in depositional energy between the Holocene and the recent situation. On the basis of this change the recent tidal flat sediments are characterized by a significant lack of fine-grained material and higher amounts of heavy minerals, respectively. According to sedimentological investigations by Flemming and Nyandwi (1994) this phenomenon may possibly be traced back to the onset of human influence on the coastal morphology, e.g., by dike-building. The examination of suspended particulate matter (SPM) performed by A. Hild and J. Hinrichs (ICBM) demonstrates that in the present situation the fine-grained material is predominantly suspended in the water column of the tidal flat area and therefore may be exported into the open North Sea. This finding is also evidenced by the examination of  $^{206}\text{Pb}/^{207}\text{Pb}$  ratios. Thus,  $^{206}\text{Pb}/^{207}\text{Pb}$  ratios of SPM tend towards the anthropogenic signal of app. 1.4 with increasing distance from the coast while the recent tidal flat sediments show values similar to the geogenic background (1.2), which is represented by the Holocene samples, indicating the small amount of SPM deposited in the recent situation.

## Chapter 2

### 2.1. Geochemical and microfacies characterization of a Holocene depositional sequence in northwest Germany

O. Dellwig, D. Gramberg, D. Vetter, F. Watermann, J. Barckhausen, H.-J. Brumsack, G. Gerdes, G. Liebezeit, J. Rullkötter, B. M. Scholz-Böttcher and H. Streif

**Abstract** - Holocene depositional sequences in the coastal zone of the North Sea reflect climate-driven sea level changes that led to lateral interfingering of marine, brackish, lagoonal and limnic sediments and peat layers. This succession is reflected in an 18 m sediment core drilled in the marsh lands of the river Weser. The core spanning the entire Holocene was analysed at high stratigraphic resolution for major and minor elements, bulk and molecular constituents and microfacies characteristics. Abundant triterpenoids in sediments of the basal organic unit indicate nutrient-rich limnic paleoconditions not yet influenced by the rising sea level. Lithological description of several sedimentary units overlying the basal sequence initially suggested a mainly lagoonal setting with occasional influence by tidal channel activities; geochemical and microfacies analyses confirmed repeated marine ingressions. Marine conditions are indicated by pyrite enrichment, the presence of sterathiols formed by the reaction of sterols with reduced sulfur species, and the occurrence of marine pelagic diatoms. Towards the top of the sedimentary sequence, estuarine conditions become more and more pronounced as the river Weser established its modern course whereas it had been quite variable previously. Estuarine conditions are reflected by sterol and amino acid distributions and by limnic diatom species that are mixed with marine pelagic forms. Although the majority of the clastic units consist of silty to clayey sediments, some intercalated quartz sand layers reflect the increase of hydrodynamic energy characteristic of lower tidal flats and channels. Lumps of reworked peat within fine clastic deposits also reflect high energy events. Even a dark layer within the upper clastic unit, formerly considered a fossil soil horizon, is not the direct result of regression-induced soil development, but originates mainly from eroded fossil organic material from the basal unit. This interpretation was established by biomarker analysis and radiocarbon dating.

## Introduction

The sediments in the coastal area of northwest Germany have been strongly influenced by long- and short-term sea level fluctuations as a response to climatic changes during the past 18,000 years. This results in postglacial Holocene depositional sequences that are characterized by an alternating lateral interfingering of marine, brackish, lagoonal, and limnic deposits as well as peat layers (Preuß, 1979; Streif, 1990). At the last glacial maximum, the sea level was 110 to 130 m lower than today. The coastline was located north of the Doggerbank, and northwest Germany was a permafrost area.

Based on lithological criteria, radiocarbon dating, pollen analysis, archaeological findings, it was possible to reconstruct the sea-level rise in the German Bight and adjacent coastal areas for the time since 8,600 years BP (e.g. Behre, 1993; Behre and Streif, 1980; Streif, 1990, Streif 1993 and references cited herein; Figure 2.1.1).

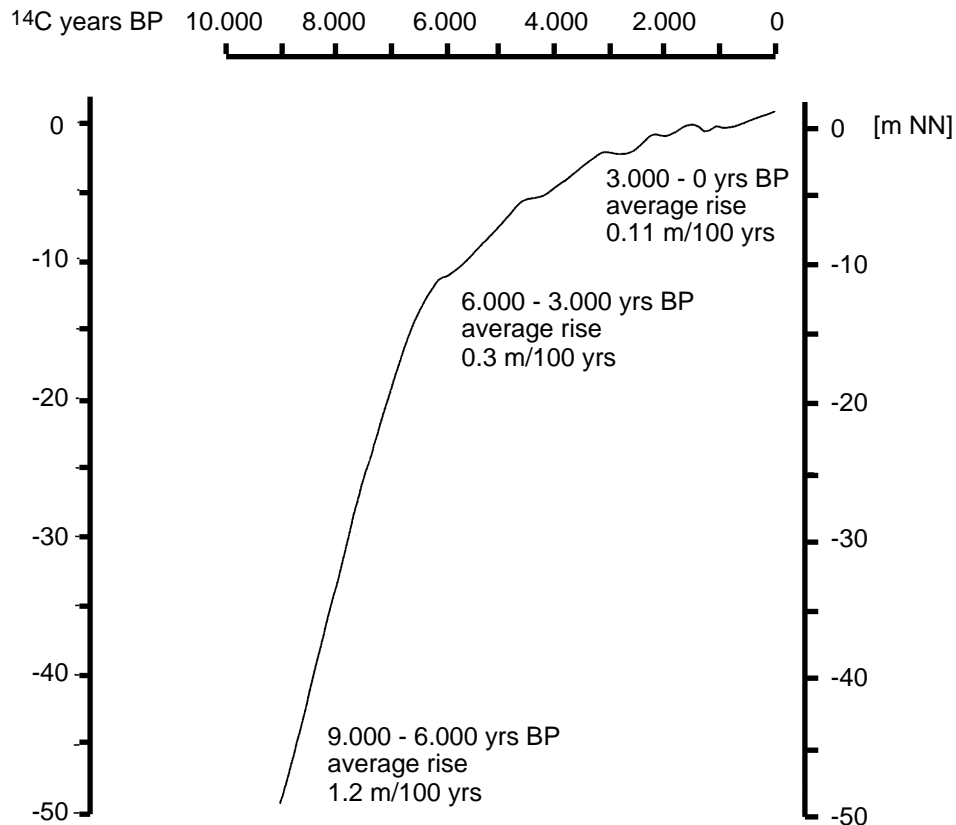


Figure 2.1.1: Reconstructed sea-level rise for the North Sea area (after Behre, 1993) related to the German zero datum (NN).

The general sea-level rise affected the Loxstedt area, in the following manner. Under the influence of a rapidly rising sea level, the basal peat became transgressively overlain by tidal flat and brackish sediments. In the course of the following period of a gently rising sea level a sequence of clayey-silty deposits with intercalated peat layers was formed, indicating repeated phases of transgressive and regressive coastal development. Such sequences consisting of tidal flat and brackish sediments with intercalated layers of limnic-semiterrestrial peat are characteristic for the time span between 6,500 and 2,000 years BP. However, the phases of peat formation are not strictly synchronous. According to the local environmental conditions their formation differs in time and in spatial extension.

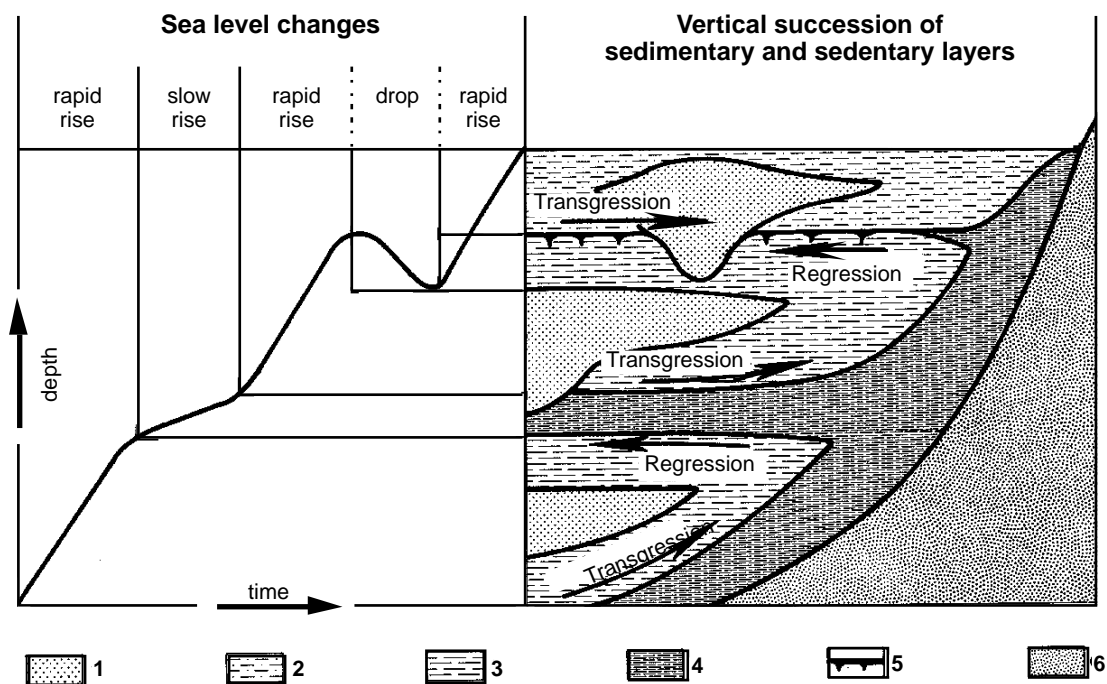


Figure 2.1.2: Schematic relationship between sea level changes and the vertical succession of sedimentary and sedimentary layers (after Streif, 1990): 1 = channel deposits, 2 = tidal flat deposits, 3 = brackish and lagoonal deposits, 4 = peat, 5 = fossil soil horizon, 6 = Pleistocene sands.

Behre and Streif (1980) and Behre (1993) demonstrated that phases of temporal lowering of the sea level are related with soil formation on the top of clastic sediments, with the decomposition of peat, or with rapid changes from fen peat to raised bog peat



vegetation. During the last 2,000 years the sea level has risen slowly with little variations in rate. The increasing influence of dike building that started 900 years BP terminated the former relation of sea level changes and deposited facies. The relation between transgression, stagnation and regression phases and deposited facies is shown schematically in Figure 2.1.2. Most of the investigations on the Holocene depositional sequences in northern Germany were focused on their lithological (e.g. Preuß, 1979) and biofacies data (mainly palynological, e.g. Overbeck, 1975). Little information is available regarding the geochemistry of these sequences (e.g. Ludwig *et al.*, 1973).

The present investigation is part of the PAGES (terrestrial) priority program "Bio-geochemical changes over the last 15,000 years - continental sediments as an expression of changing environmental conditions" initiated by the Deutsche Forschungsgemeinschaft (DFG). The aim of this contribution is the characterization of a typical Holocene sedimentary succession based on combined inorganic, molecular organic and microfacies parameters. For this reason an 18 m sediment core covering the entire Holocene was drilled in the marsh lands of the river Weser where riverine and estuarine changes interplay (Preuß, 1979). Here, preliminary results are presented and discussed.

### **Regional setting and lithology**

Two parallel sediment cores were drilled one meter apart in the marsh area of the river Weser close to Loxstedt in summer 1994 (Figure 2.1.3). Drilling was carried out by the Geological Survey of the Federal State of Lower Saxony, Hannover, Germany (NLfB) using the technique described by Streif (1971). Radiocarbon dating was performed by M. A. Geyh (NLfB) as described in Geyh (1971). The radiocarbon data are given as conventional (non-calibrated)  $^{14}\text{C}$  years before present (BP). The initial lithologic descriptions refer to Archive No. 2517 Loxstedt, GE 430 and GE 432. Based on i) lithological description, ii) bulk parameters and iii) major element distribution, both parallel cores were combined to give a single representative sequence. Figure 2.1.4

shows the composite lithological profile of the two cores. This combined lithology is used in the depth profiles of the geochemical and microfacies data representation.

#### *Organic basal unit*

The unit spans the depth interval from 17.86 to 17.00 m below land surface. It is characterized by two distinct peat layers with intercalated limnic mud. The base of the unit has a  $^{14}\text{C}$  age of approximately 10,000 years BP. Its upper layer has been dated 7,540 years BP. These data suggest a growth of the unit over a time span of about 2,500 years. On the other hand, the total thickness of the unit of only 65 cm may reflect erosion and compaction processes. The occurrence of the basal peat is not related to the contemporary sea level, but is highly influenced by local hydrological conditions (Preuß, 1979).

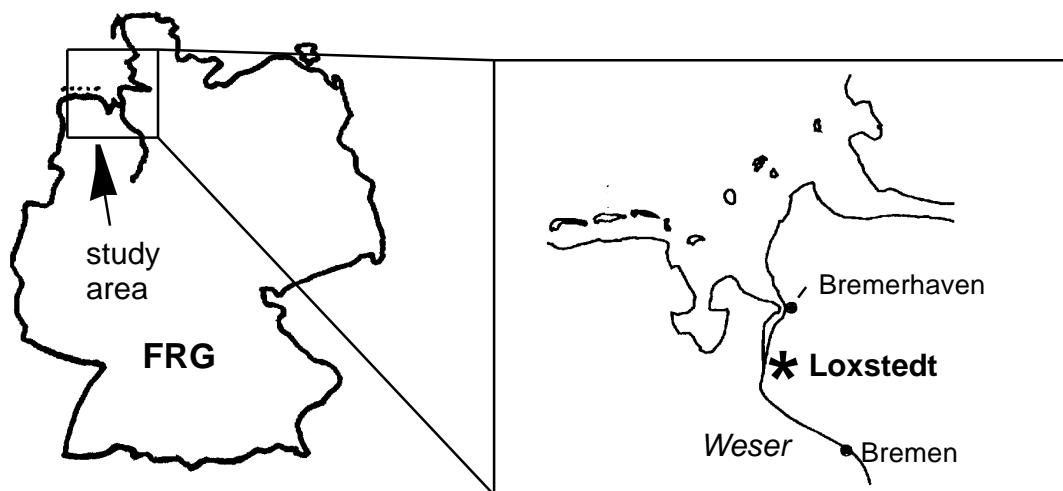


Figure 2.1.3: Drilling location in the Weser marsh lands, Northwest Germany.

#### *Lower clastic unit*

This approximately 5 m thick unit extends from 17.00 to 12.03 m and was deposited over a period of only 1,500 years due to an accelerated sea-level rise (cf. Figure 2.1.2). The sediments of the lower part of this unit (15.36 - 17.00 m) are influenced by tidal

and channel activities. The upper part of the unit (12.03 - 15.36 m) consists of brackish deposits.

#### *Organic-clastic interfingering unit*

This sequence extends from 12.03 to 7.30 m. The lowest layer of the unit has been dated at  $6,160 \pm 110$  years BP, the uppermost at  $2,630 \pm 200$  years BP. Six *Phragmites* peat horizons and intercalated lagoonal sediment layers are documented which reflect regressive and transgressive phases of the coastal development. While the lagoonal sediments are rooted by *Phragmites* rhizomes, the peat is interspersed with clay.

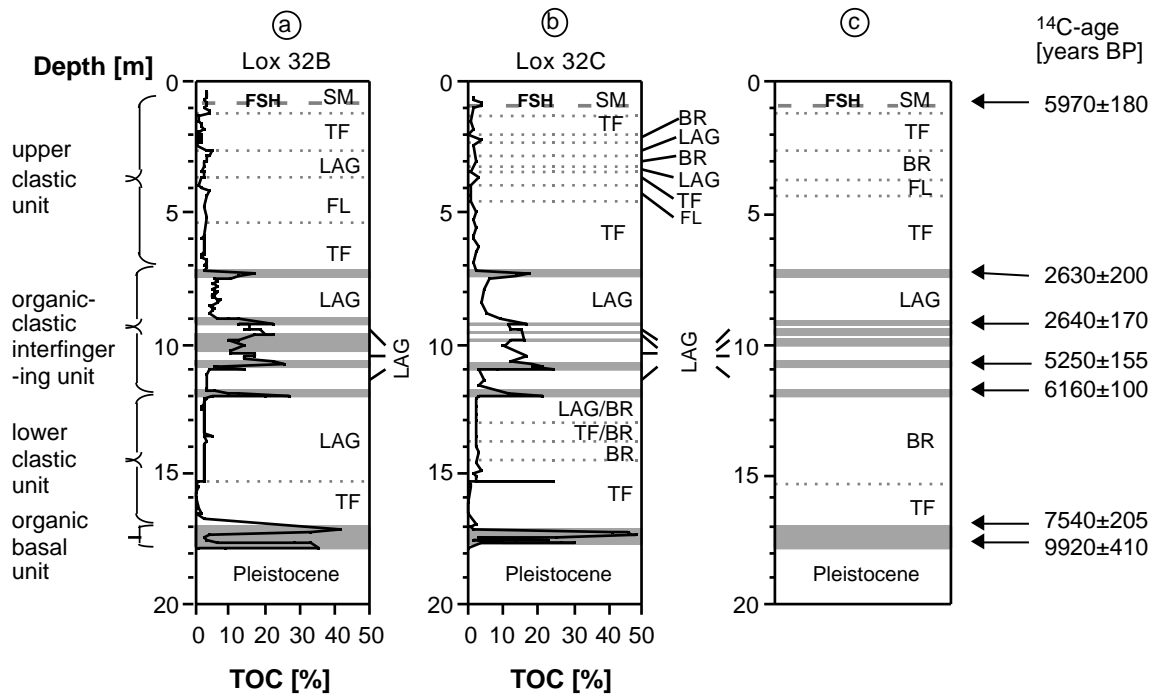


Figure 2.1.4: (a) and (b) Depth profiles of TOC values of the Loxstedt core 32B and 32C. (c) Composite lithology of both cores (based on lithological descriptions and geochemical and microfacies analysis) with  $^{14}\text{C}$  age data. (BR = brackish, FSH = fossil soil horizon, FL = fluvial levee, LAG = lagoonal, SM = salt marsh, TF = tidal flat).

#### *Upper clastic unit*

This unit extends from 7.30 to 0.52 m. Only a rough approximation of the age of this unit is possible. According to Preuß (1979), the upper clastic unit was deposited over a

period of approximately 800 years. The lowest deposits of the unit reveal tidal and channel activities, thus reflecting transgressive conditions. The overlying sediments document an increasing influence of fluvial, levee-type and brackish conditions. Towards the top of the core, tidal flat and saltmarsh sediments occur; the latter contain a thin dark layer initially described as “fossil soil horizon” (FSH). Radiocarbon dating of this layer close to the top revealed an age of 5,650 years BP in contradiction to the position within the stratigraphic record.

### **Material and methods**

*Geochemical analyses* - The cores were sampled in 1 to 10 cm intervals depending on the lithology and the samples were deep frozen immediately. Samples were centrifuged at 6,000 rpm to recover porewater, except for those samples used for extractable lipid analysis. All sediment samples were freeze-dried for two to four days and then ground and homogenised in an agate ball mill.

Total carbon (TC) and total sulfur (TS) contents were determined using an S/C analyser (Leco SC-444). The contents of inorganic carbon (IC) were measured coulometrically by a UIC Coulometer. Total organic carbon (TOC) was calculated from the difference of TC and IC. Total nitrogen was determined using an elemental analyser model Vario El N (Carlo Erba).

A total number of 300 samples were analysed for major and minor elements by X-ray fluorescence spectroscopy (Philips PW 2400) on fused borate glass beads. For preparation of the glass beads, 0.6 g of dry sediment, 3.6 g lithium tetraborate and 1 g ammonium nitrate were heated to 500°C. After this procedure the material was fused at 1100°C in platinum crucibles. Samples with TOC contents >10% were heated to 500°C to remove TOC prior to adding Li tetraborate.

Protein hydrolysis was accomplished with 6N HCl at 110°C for 24 hours under nitrogen. After hydrolysis the amino acids were analysed by HPLC as their OPT-derivates after precolumn derivatisation (Behrends, 1994).

For lipid analysis samples of 5-10 g were ultrasonically extracted with dichloromethane /methanol (99:1) by using an ultrathorax F18. After asphaltene precipitation with *n*-hexane, the *n*-hexane soluble portion was separated by an MPLC-system according to Radke *et al.* (1980) into a nonaromatic hydrocarbon fraction and an aromatic hydrocarbon fraction using *n*-hexane. The heterocompound fraction (NSO) was recovered from the precolumn of the MPLC system with dichloromethane/methanol (9:1). The latter fraction was separated into six subfractions for molecular characterization of the polar lipids (Gramberg *et al.*, 1995). The polar lipids were derivatised with MSTFA (N-methyl-N-trimethylsilyltrifluoroacetamide). GC analysis was carried out on a Hewlett Packard 5890 series II instrument equipped with a temperature programmable injector (Gerstel KAS 3) and a flame ionization detector (FID) or a Finnigan SSQ 710 B mass spectrometer, respectively. A DB 5 (JandW) fused silica capillary column (30 m x 0.25 mm, 0.25 µm film thickness) was used with helium as carrier gas. The temperature of the GC oven was programmed from 60°C (1 min isothermal) to 305°C (50 min isothermal) at 3°C/min. The injector temperature was programmed from 60°C (5 s hold time) to 300°C (60 s hold time) at 8°C/s. The GC-MS system was operated at 70 eV with a scan range of  $m/z$  50-700 and a scan time of 1 scan/s.

*Microfacies analysis* - Littoral and pelagic diatoms were analysed in selected samples. In this report, only the pelagic species will be considered. The samples were homogenised and divided into two parts after drying. One subsample was treated with 15% hydrogen peroxide for one hour, then suspended in water and passed through sieves of 500 µm and 63 µm mesh size. The fractions were dried (12 h at 60°C). The diatom contents were analysed in subsample triplicates of 50 mg. Diatom counts of the fraction >63 µm were made at 64 x magnification.

The second part of the sample was treated following the method of Schrader (1973): 0.5 g dried sediment was weighed, boiled for 20 min with 50 ml of a mixture of acetic acid (99%) and hydrogen peroxide (30%) in a ratio of 1:1. The sample was centrifuged eleven times, and the pellets were diluted with deionised water. After shaking for 1 min

in a solution of 0.5% sodium pyrophosphate, the sample was centrifuged four times. The pellets were fixed in two drops of formaldehyde and diluted with 50 ml of deionized water. Diatom counts were made in triplicate of 1 ml of the sample using counting chambers (Utermöhl, 1958). Counting was done with an inverted microscope at 400x magnification. The quantitative determination of species composition was based on maximum counts of 100-400 frustules of each species (Lund *et al.*, 1958). Frustule fragments  $>1/2$  were counted as a whole frustule (Schrader and Gersonde, 1978).

Taxonomy of the pelagic diatoms was facilitated by mounting the diatoms in Naphrax resin. The species were identified using a light microscope at 1000x magnification. In several cases an electron microscope also was used for taxonomic identification. Species identification was based on Drebes (1974), Hustedt (1930, 1957), Krammer (1986), Pankow (1990), and Round *et al.* (1990). The pelagic diatom species were classified according to the salinity groups summarized in Table 2.1.1 (Simonsen, 1962).

Table 2.1.1: Salinity groups and subcategories after Simonsen (1962).

Group	Subcategories	Salinity groups	Salinity range [‰]
I	oligoeuryhaline	polyhalobe	35-30
II	meioeuryhaline	polyhalobe	35-20
II	pleioeuryhaline	olighalobe	0-20
IV	meso/meioeuryhaline	oligohalobe	0-10

## Results and discussion

### *Bulk parameters*

Within the lithological succession, the changes between lagoonal and marine clastic sediments and sedentary organic layers correspond well to the results of measurements of bulk parameters (Figures 2.1.4 and 2.1.5).

*Total organic carbon (TOC)* - The highest TOC enrichment, up to 47.5%, characterizes the two peat layers of the organic basal unit (Figure 2.1.4). The intercalated silty and sandy muds are distinguished by their low TOC contents. The sediments of the

overlying lower clastic unit show TOC values in the range of 0.26 to 4.79% (average 2.09%). A conspicuous enrichment in the tidal flat sediments in this unit is directly related to a peat lump (23.2% TOC). In comparison to the basal peats, the *Phragmites* peat beds of the organic-clastic interfingering unit show slightly lower enrichment of TOC as a result of dilution with clastic material. The lagoonal sediments of the interfingering unit are rooted by *Phragmites* rhizomes. Therefore, higher TOC contents occur in comparison to the other clastic sediments.

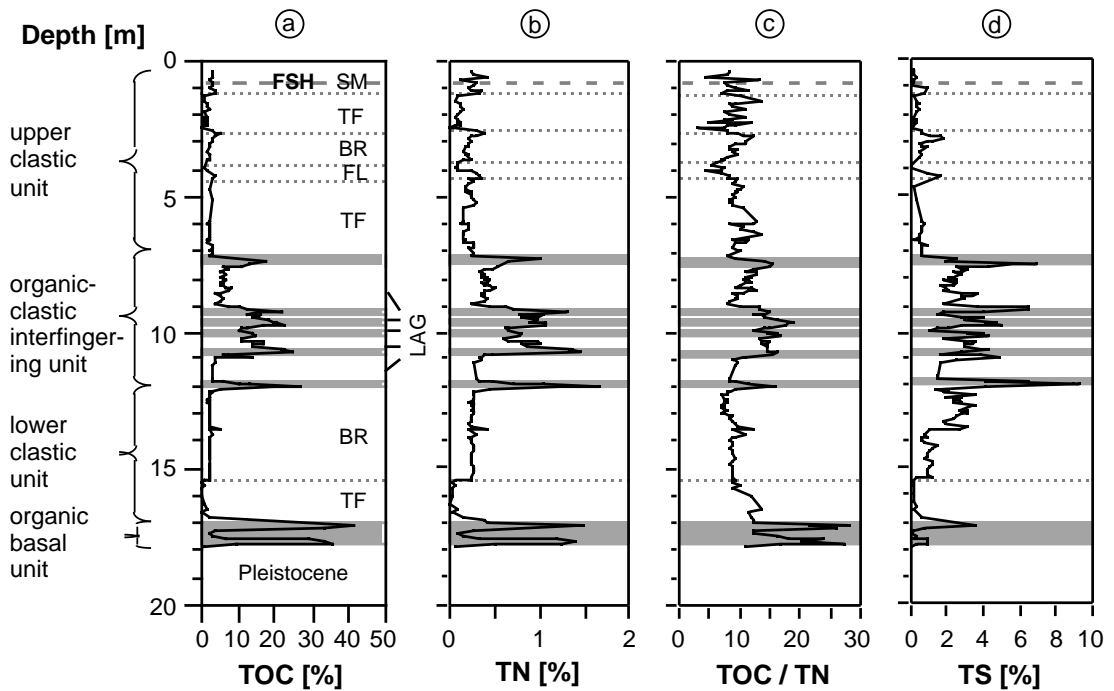


Figure 2.1.5: (a) Depth profile of TOC values. (b) Depth profile of TN values. (c) Depth profile of TOC/TN ratios. (d) Depth profile of TS values. (BR=brackish, FSH=fossil soil horizon, FL=fluvial levee, LAG=lagoonal, SM=salt marsh, TF=tidal flat).

The deposits of the upper clastic unit show a TOC pattern similar to that of the lower clastic unit. The uppermost tidal flat sediments are characterized by the lowest TOC values, although slightly higher in comparison to the tidal flat sediments of the lower clastic unit, possibly due to an increasing influence of the river Weser. The salt marsh sediments at the top of the core contain a thin dark layer (FSH) with a comparatively high TOC content (3.7 %).

*Total nitrogen (TN)* - The total nitrogen (TN) content (Figure 2.1.5b) increases in the organic layers. Nitrogen is predominantly fixed in the organic matter, which was verified by measurements of inorganic nitrogen ( $N_{ex}$ ).  $N_{ex}$  is low with mean values below 1%  $N_{ex}$  in total nitrogen.

*TOC/TN ratios* - The TOC/TN ratios are a useful tool for the characterization of the dominating sources of organic matter. Non-vascular organisms (e.g. marine algae) exhibit TOC/TN ratios of about seven (Meyers and Ishiwatari, 1993) due to their low cellulose content. Because of the enhanced cellulose content vascular higher land plants possess TOC/TN ratios of  $>20$  (Meyers and Ishiwatari, 1993). Ratios  $>20$  were determined only in the peats of the organic basal unit (Figure 2.1.5c). Here, the peat-forming vegetation was more strongly influenced by bushes and wood. In contrast, the cellulose-poor reed peat beds of the interfingering unit show TOC/TN ratios of about 15. In the lower and upper clastic units the marine signal appears to be blurred out by terrestrial influence. However, other parameters will indicate well the marine influence in the basal part of the lower clastic unit (e.g. diatoms, see discussion below). The low absolute TN contents of these sediments, which are close to the detection limit of the instrument used, may render the TOC/TN ratios less reliable for interpretation.

*Total sulfur (TS)* - The organic basal unit is characterized by varying contents of TS (Figure 2.1.5d). The TS enrichment in the upper peat layer of this unit apparently is related to flooding, gradual transgression or vertical diffusion of sea water and subsequent microbial sulfate reduction. The low TS signals of the basal peat and of the overlying muds indicate the limnic origin of these deposits.

The TS contents increase in the brackish sediments of the lower clastic unit and reach maximum values in the *Phragmites* peat layers of the organic clastic interfingering unit. Especially these peat beds offer ideal conditions for sulfate-reducing bacteria if enough sulfate is present. Thus, both sulfate from brackish water and sufficient organic matter as a carbon source for the bacteria must have been available. This implies that the formally limnic organic-clastic interfingering unit, where the sulfate content should be fairly low, must have been frequently under the influence of brackish water. The sulfur



in the sediments is predominantly fixed as pyrite (Dellwig *et al.*, 1996) and to a minor extent also in the organic matter (e.g. in sterathliols of the extractable fraction).

### *Major and minor elements*

To assess the main depositional characteristics of the investigated sequence a principal component analysis (Jöreskog *et al.*, 1976) of the elemental data was carried out. The elements Si, Al, Ca, Mn, Rb, Sr, TS, IC, and TOC were chosen for factor analysis. Figure 2.1.6 shows the three factors plotted versus depth for the entire core. The calculation of the factor for individual samples is based on the following formula:  $F_x = \sum f_{xi} \cdot (c_i / c_{max})$ . For every factor ( $F_x$ ), the sum of the product of the factor loading ( $f_{xi}$ ) and the concentration ( $c_i$ ) (normalised to the maximum concentration ( $c_{max}$ ) for every above mentioned element (i) was calculated and plotted versus depth.

The three factors obtained show that the investigated Holocene sediment sequence may be regarded as a mixture of the four end members quartz, organic matter, clay minerals, and carbonate. The relative proportions of these components are different in the individual lithological units.

Factor 1 describes the negative relationship between quartz and organic matter content. The varimax-rotated factor loadings, which vary between +1 and -1, are -0.93 for Si and +0.89 for TOC, respectively. The higher the numerical value of the factor loading, the higher the element is correlated with the factor. Another element which is positively correlated with factor 1 is S (+0.72) owing to the above-mentioned pyrite formation in TOC-rich peat beds. Several minor elements, which may be fixed as sulfides (As, Co, Mo, and Ni) or bound to organic matter (V and U), were enriched in the peat beds as well. Their distribution, except for the lowest basal peat, is similar to the TS-profile (Dellwig *et al.*, 1996). The peat layers are discernable in the profile of factor 1 (Figure 2.1.6a) with high positive values similar to the TOC content of Figure 2.1.5a. The lagoonal sediments of the interfingering unit show higher amounts of organic matter as well. The sandy tidal flat sediments of the upper and lower clastic units are characterized by negative values due to high quartz contents. Here, high energy conditions prevented the sedimentation of fine-grained material like clay

minerals or carbonates. In contrast to the sandy deposits of the lower tidal flat layer, the upper clastic unit does not differ significantly from the brackish sediments and can be regarded as a mixed flat layer.

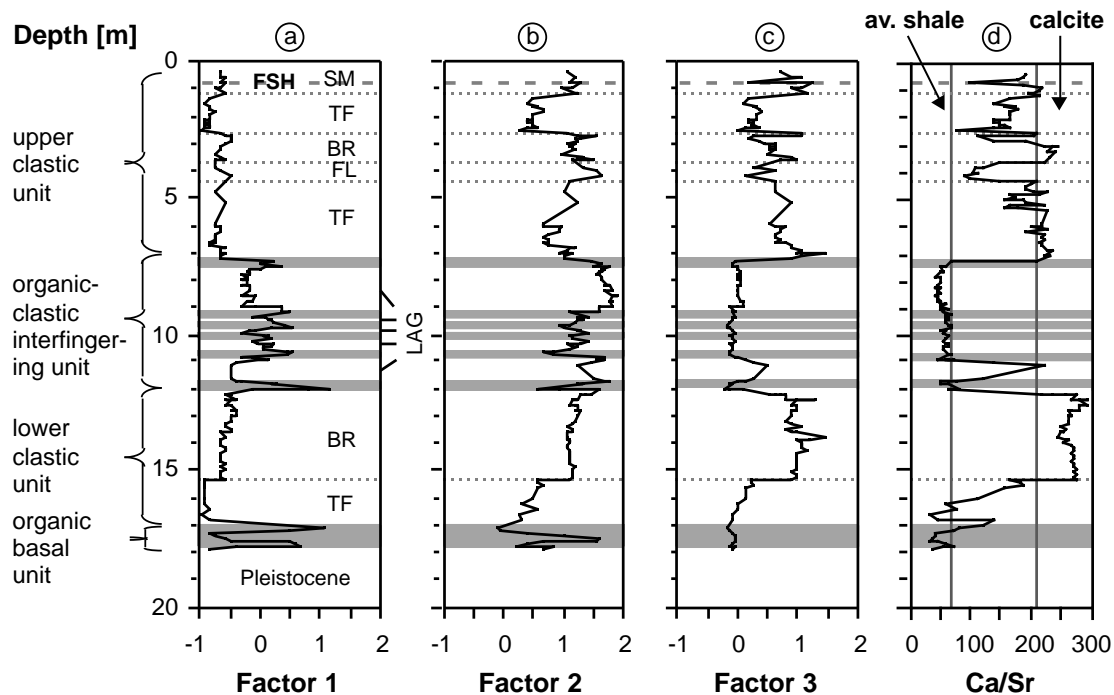


Figure 2.1.6: Depth profiles of factor analysis results and Ca/Sr-ratios. (BR=brackish, FSH=fossil soil horizon, FL=fluvial levee, LAG=lagoonal, SM=salt marsh, TF=tidal flat).

Factor 2 represents the clay mineral components. The elements Al and Rb are assigned to this factor with loadings of +0.99 for Al and +0.95 for Rb, respectively. Thus, Al is predominantly fixed in phyllosilicates and Rb, which does not form mineral phases by its own, is a typical minor element enriched in clay minerals (Wedepohl, 1969). The plot of factor 2 (Figure 2.1.6 b) delineates the clay mineral content, which increases in the lagoonal and brackish sediments. The mixed flat unit has slightly lower and more variable fine-grained components. The sandy tidal flat sediments are dominated by quartz and therefore show the lowest clay contents. The peak in the organic basal unit is due to a silty mud.

Factor 3 describes the carbonate contents. High positive factor loadings were found for IC (+0.84) and Ca (+0.89) because of the presence of calcite ( $\text{CaCO}_3$ ). The minor

elements Sr (+0.88) and Mn (+0.85) are highly correlated with factor 3 as well. Sr is incorporated in calcite (Pingitore and Eastman, 1985). Mn is reduced to  $Mn^{2+}$  under suboxic conditions and can be fixed as carbonate, e.g., in rhodochrosite (Berner, 1981). An increasing carbonate content is visible in the tidal flat layer of the lower clastic unit, which reaches comparatively high contents in the overlaying brackish sediments (Figure 2.1.6c). The organic-clastic interfingering unit shows predominantly low carbonate contents. The mixed flat layer of the upper clastic unit again exhibits quite high carbonate contents.

The Ca/Sr-ratios presented in Figure 2.1.6d are a useful tool for differentiating between the sources of the deposited material, because biogenic carbonate and detrital material have different Ca/Sr ratios. The Ca/Sr-ratio of biogenic calcite varies between 210 and 380 (Pingitore and Eastman, 1985) while average shale, which represents the detrital component of sediments with a high abundance of clay minerals, has a ratio of about 70 (Wedepohl, 1971). The brackish sediments and those of the mixed flat layer have an average Ca/Sr-ratio of about 240, which indicates a marine influence. The Ca/Sr-ratios of most of the lagoonal sediments are close to the average shale with an average ratio of about 60. An increase in Ca/Sr-ratios is seen for the lowest lagoonal section (10.80-11.89 m). Here, a stronger marine influence, similar to the brackish sediments, can be assumed in comparison to the overlying lagoonal sediments. Exceptional are the Ca/Sr-ratios of the two sandy tidal flat layers in the lower and upper clastic units. The lower sand flat layer shows an average Ca/Sr-ratio of 113 (range 32-186), which increases towards the brackish sediments. However, the upper sandy tidal flat has a higher average ratio of 162 (range 136-214), as a result of increasing estuarine conditions in the upper clastic unit.

#### *Amino acids*

The vertical variation of total hydrolysable amino acids (THAA) generally follows the TOC profile (Figure 2.1.7a). Highest concentrations were found in the peat layers, the lowest in the upper clastic unit with extreme values of 0.5 and 474  $\mu\text{mol/g}$  dry weight. The relative proportion of amino acid nitrogen in the total nitrogen pool is highly

variable and ranges from 0.2 to 74% AA-N (Figure 2.1.7b). Even within one facies type this variability is obvious as, e.g., in the brackish sediments of the lower clastic unit.

The comparison of THAA in similar facies types (*viz.* the brackish units in Figure 2.1.7b) suggests that diagenetic changes, which would be indicated by decreasing concentrations with depth, are not obvious. Compared to the upper clastic unit, the tidal flat sediments in the lower clastic unit have higher THAA concentrations which also represent a higher relative proportion in the total nitrogen pool (Figure 2.1.7b). This suggests different sources of organic material in lithologically uniform units. These differences might be due to the change from marine conditions in the lower clastic unit to more estuarine conditions in the upper clastic unit.

To minimise dilution effects by the widely varying amounts of inorganic material, THAA data were normalised to TOC. Figure 2.1.7c shows the downcore variation of THAA. The normalised data show variable concentrations in the peat layers within a range from 40 to 520 mg THAA/g TOC, intermediate values in brackish water sediments and partially also in mixed flat sediments. The upper samples including sandy tidal flat and salt marsh sediments have the lowest THAA concentrations.

Cowie (1990) used TOC-normalised amino acid yields to differentiate between unaltered vascular plants (4-13 mg THAA/g TOC for wood; 70-170 mg THAA/g TOC for leaves, grasses and needles) and phytoplankton, bacteria and fungi (< 500 mg THAA/g TOC). While this approach proved useful for sediment trap material in coastal environments (Cowie *et al.*, 1992), it does not take into account early diagenetic degradation or dilution by amino acid-poor material. Thus, while the peat layers have values <100 mg THAA/g TOC confirming a terrestrial origin, the brackish and marine sediments rarely exceed 200 mg THAA/g TOC (Figure 2.1.7c). The molecular composition of THAA is similar throughout the core and independent of facies variations. The amino acid spectrum is dominated by alanine with about 29 mol% followed by aspartic acid, glycine plus threonine and tyrosine at about 10 mol% each. Relative standard deviations were highest for alanine, leucine and methionine. These were, however, too small to be used for diagnostic purposes. This molecular composition differs from data in the literature for marine sediments. Here, glycine plus

threonine, serine and the acidic amino acids generally dominate (e.g. Cowie, 1990). On the other hand, the Loxstedt core shows a pronounced similarity to sea surface sediments where terrestrial material dominates the organic components (e.g. in the sediments of the Bering Sea; B. Behrends, pers. commun., 1997).

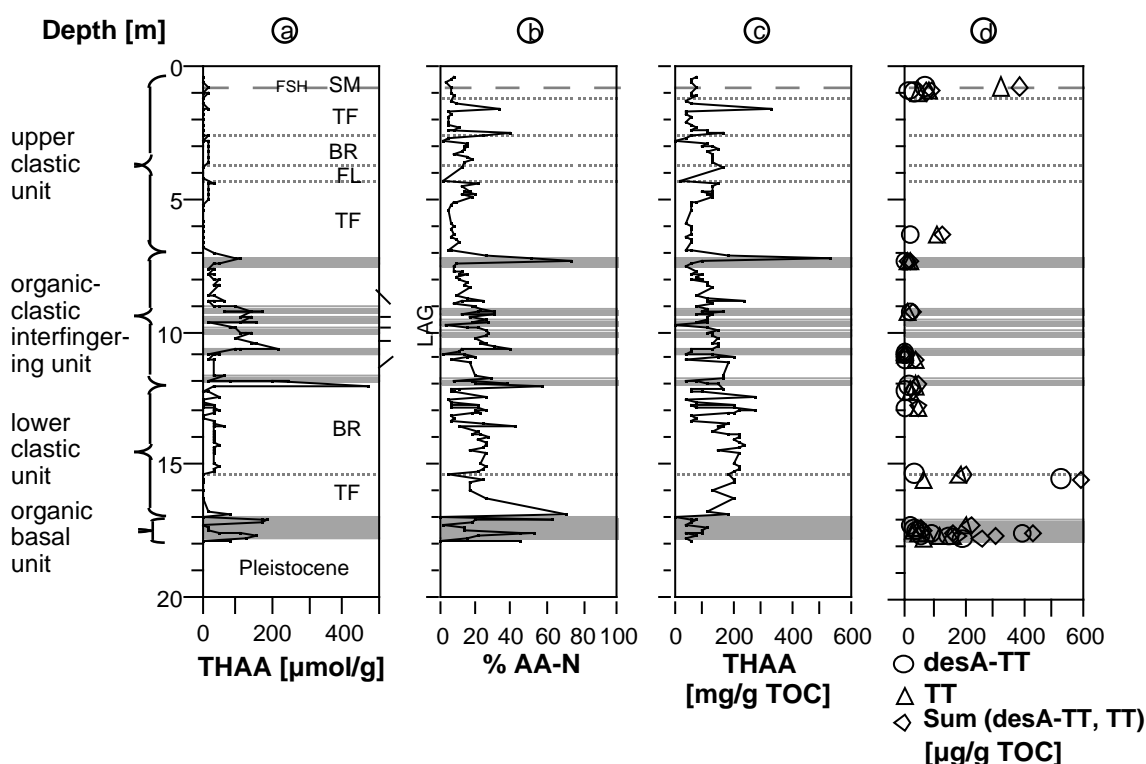


Figure 2.1.7: a) Depth profile of absolute yields of total amino acids ( $\mu\text{mol/g}$  dry weight). b) Depth profile of relative contributions of amino acid nitrogen to the total nitrogen pool (%AA-N). c) Depth profile of total organic carbon-normalized amino acid yields (THAA,  $\text{mg/g TOC}$ ). d) Depth profile of *des-A*-triterpenoid summed of triterpenoid alcohol and ketone and total triterpenoid concentrations. (BR=brackish, FSH=fossil soil horizon, FL=fluvial levee, LAG=lagoonal, SM=salt marsh, TF=tidal flat).

### Steroid and triterpenoid distributions

A set of 24 samples mainly from TOC-rich but also from some TOC-poor sediment layers was selected for detailed lipid studies. In this report, only compound group abundances will be discussed. Molecular distribution patterns will be presented

elsewhere. The investigation was restricted to free lipids in the nonaromatic hydrocarbon and the aromatic hydrocarbon fraction as well as three NSO compound subfractions.

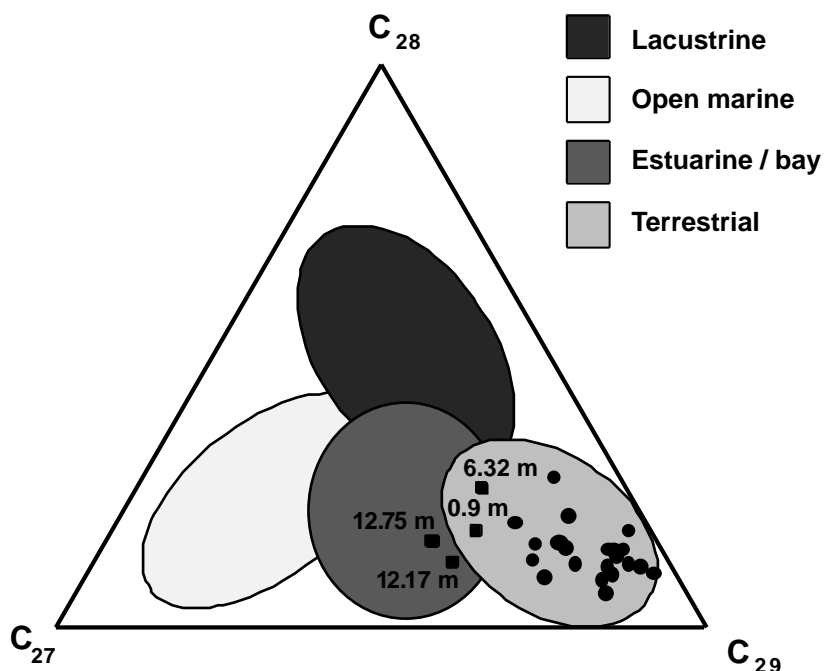


Figure 2.1.8: Triangular plot of the sterol carbon number distribution after Huang and Meinschein (1979). Samples marked with ■ indicate a more estuarine influence (see text).

All samples investigated contain  $C_{27}$ ,  $C_{28}$ , and  $C_{29}$  sterols which represent one of the dominating compound classes of the extractable polar lipids. The most abundant sterols are cholest-5-en- $3\beta$ -ol, 5 (H)-cholestan- $3\beta$ -ol, 24-methyl-5 (H)-cholest-22-en- $3\beta$ -ol, 24-methylcholest-5,22-dien- $3\beta$ -ol, 24-methylcholest-5-en- $3\beta$ -ol, 24-methyl-5 (H)-cholestan- $3\beta$ -ol, 24-ethyl-5 (H)-cholest-22-en- $3\beta$ -ol, 24-ethylcholest-5,22-dien- $3\beta$ -ol, 24-ethylcholest-5-en- $3\beta$ -ol and 24-ethyl-5 (H)-cholestan- $3\beta$ -ol. For each carbon number species, the  $^5$  monounsaturated and the saturated derivatives are the prevailing compounds. The distribution of all samples is dominated by the  $C_{29}$  sterols in accordance with the origin of the organic matter from mainly terrestrial higher plant debris. This is reflected in a triangular plot after Huang and Meinschein (1979) based on the sterol carbon number distribution (Figure 2.1.8). Only four samples, two from the

upper clastic unit (including the salt marsh and the tidal flat layers) and two from the lower clastic unit (the brackish layers), show a more estuarine influenced organic matter composition. This difference is consistent with the depositional conditions and indicates a diminished terrestrial supply in the estuarine paleoenvironments.

A specific group of biomarkers representative of higher land plants are the 3-oxygenated triterpenoids (e.g. Pant and Rastogi, 1979). Figure 2.1.7d shows the depth profile of the extractable triterpenoid contents of 24 samples given as the sum of triterpenoid alcohols and ketones, the sum of *des*-A-triterpenoids and the total amount of triterpenoids. The organic basal unit shows a clear enrichment of triterpenoids, particularly in the TOC-rich peat layers, e.g. at 17.18 and 17.61 m. The latter is described as *Carex* peat layer in the detailed lithologic description. Compared to the TOC-rich layers, a slight decrease was found in the TOC-poor layers, e.g. in the sandy mud at 17.4 m, but even here the total amounts of triterpenoids are much higher than in other TOC-poor layers of the Holocene sequence. High triterpenoid contents reflect a strong supply of plant debris (from bushes, shrubs and trees). This is consistent with the plant community typical of a fen bog with a strong nutrient supply. In contrast to this, vegetation communities dominated by grass are known to be poor sources of triterpenoids (Pant and Rastogi, 1979). The unexpectedly high amount of triterpenoids in the *Carex* peat is consistent with earlier investigations where high contents of total triterpenoids were described (Dehmer, 1988).

The high portion of *des*-A-triterpenoids point to an increased bacterial degradation of the organic matter (OM) (Ries-Kautt and Albrecht, 1989; Trendel *et al.*, 1989). Usually, the amounts of *des*-A-triterpenoids increase with increasing diagenetic reworking of the organic matter. In the *Carex* peat sample the contents of triterpenoid alcohols and ketones and of *des*-A-triterpenoids are in a similar range, which indicates favourable conditions for organic matter preservation due to the depositional regime.

Another distinct enrichment of triterpenoids was detected in two samples of the lower clastic unit, both from the upper part of the tidal flat layer. Here, in an unexpectedly TOC-rich sample high amounts of triterpenoid alcohols and ketones are present, while the content of *des*-A-triterpenoids is relatively low. Hence, the main part

of the organic matter is of higher plant origin, possibly an eroded peat lump due to channel activity, but it seems to be little microbially degraded. An adjacent sample with a very low TOC value (0.76%) shows the highest triterpenoid portion relative to TOC of all samples investigated. As in the former sample it is indicative of a strong contribution of higher plant material (peat debris?), here in a finely dispersed form resulting from high-energy erosion processes, e.g., in tidal channels. The dominance of *des*-A-triterpenoids gives evidence that the OM is microbially degraded.

The brackish sediments of the lower clastic unit are poor in triterpenoids. The relatively close vicinity of these samples to the lowest *Phragmites* peat layer of the organic-clastic interfingering unit and their content of rootlets make a *Phragmites* origin plausible. The peat layers of the organic-clastic interfingering unit show similar triterpenoid contents. In most cases functionalised and *des*-A-triterpenoids are present in similar proportions. In the literature *Phragmites* peats are described as poor in triterpenoids (Dehmer, 1988). Investigations of *Phragmites* plants led to similar results (Behrens, 1996). In comparison to the fen peat forming vegetation of the organic basal unit the *Phragmites* community can be clearly distinguished by its low triterpenoid content.

In the upper clastic unit four samples were investigated, a TOC-poor sample of the tidal flat and three samples of salt marsh sediments. The tidal flat layer of the upper clastic unit shows a relatively high triterpenoid content. Other results of our investigations point to a lower depositional energy compared to the tidal flat layer of the lower clastic unit. Hence, the remaining amount of triterpenoids indicates a possibly more fluvial and eolian deposition of organic matter from surrounding higher plants.

A distinct enrichment of triterpenoids is evident in a dark layer in the uppermost part of the core, the so-called fossil soil horizon (FSH). A grass-dominated and therefore triterpenoid-poor vegetation is expected for such a horizon. The evidently high content of triterpenoids (Figure 2.1.7d) and above all the  $^{14}\text{C}$ -age of the FSH sample (Figure 2.1.4) led to the conclusion that this layer originates from reworked OM of bushes and trees (mainly peats) of the basal unit mixed with younger material of the salt marsh. A possible reason could be a flooding/storm event that spread eroded organic matter over



the salt marsh/juvenile horizon. Similar layers with high amounts of reworked and redeposited organic matter are known from fossil algal mats on the East Frisian islands (Streif, 1990).

As expected, organosulfur compounds are poorly represented in the extractable fractions of these sediments and their characterization was not the goal of this study. However, the distinct presence of 2- and 3-sterathiols in the aromatic fraction of some samples is remarkable. These were tentatively identified by their mass spectra and comparison with published data (Adam *et al.*, 1991). While C<sub>27</sub> and C<sub>28</sub> sterathiols are present as well, the C<sub>29</sub> sterathiols are the most prominent ones. This is in accordance with the dominance of their C<sub>29</sub> sterol precursors in the mostly terrigenous plant material (Figure 2.1.7d). Sterathiols were only detected in samples of the organic-clastic interfingering unit (peats and rootlet-containing clay layers) and the so-called FSH. Although the formation of sterathiols is due to the early diagenetic incorporation of reduced sulfur species into sterenes (Adam *et al.*, 1991), the bacterial formation of these species is bound to the presence of sulfate and organic material. Hence, as mentioned before (TS bulk parameter), the presence of sterathiols can be taken as an indicator for frequent marine influenced depositional conditions in the organic-clastic interfingering unit.

#### *Pelagic diatoms*

All sampled intervals of the core contain pelagic diatoms. Fourteen species of seven genera were identified, including polyhaline and oligohaline taxa. Both ecologic groups occur together, although at different depths. The ratio of cell numbers per weight of sediment between both polyhaline and oligohaline species is expressed in Figure 2.1.9a.

The organic basal unit is characterized by a ratio <1 between oligohaline and polyhaline pelagic diatoms, indicating limnic or fluvial influence. In the lower clastic unit, the values change to ratios >1 (Figure 2.1.9a), underlining the effect of the sea-level rise accompanied by import of polyhaline marine pelagic diatoms (e.g. *Coscinodiscus* spp. and *Actinoptychus senarius*) into the area of deposition. Even in sediment and peat layers of the organic-clastic interfingering unit, polyhaline diatoms

occur, reflecting marine influence. Finally, the upper clastic unit indicates an increasing predominance of oligohaline pelagic diatoms due to a higher fluvial influence. The most abundant limnic species is *Cyclotella meneghiniana* which occurs in the river Weser at present (Hustedt, 1957).

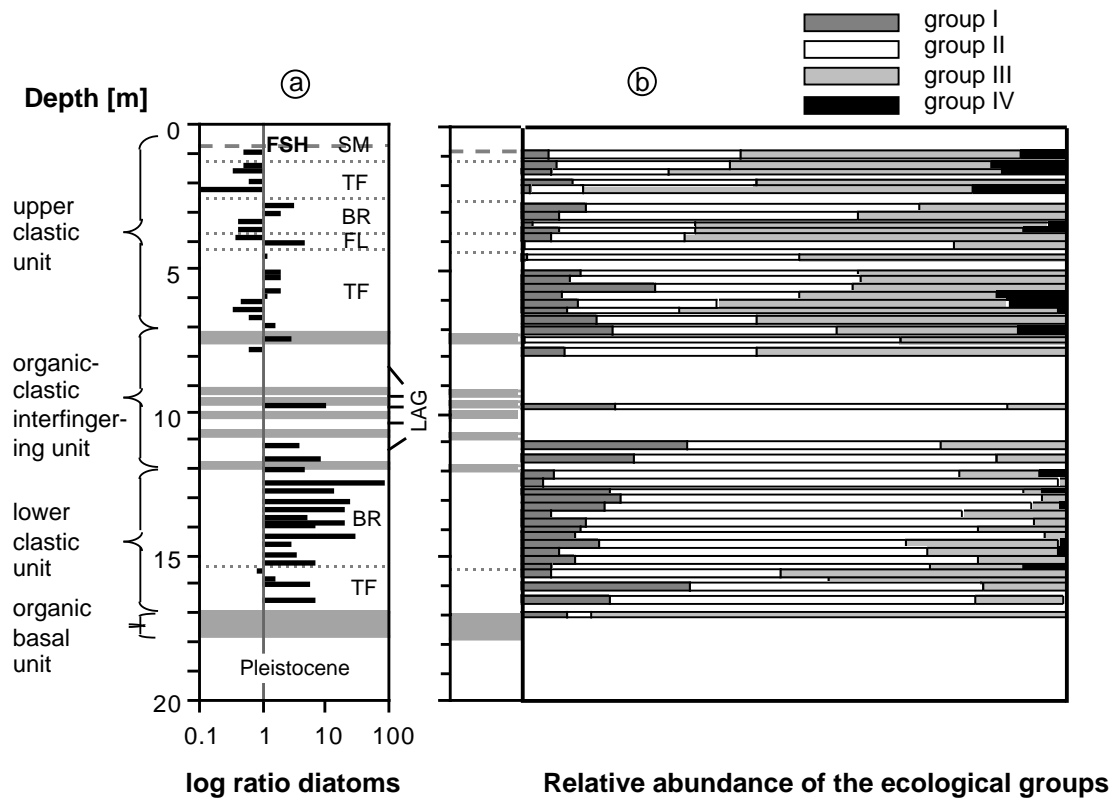


Figure 2.1.9: a) Ratio between polyhaline and oligohaline pelagic diatoms. At ratios <1, oligohaline species are dominant, while at ratios >1, polyhaline diatoms predominance. b) Relative abundance of the ecological groups listed in Table 2.1.1. (BR=brackish, FSH=fossil soil horizon, FL=fluvial levee, LAG=lagoonal, SM=salt marsh, TF=tidal flat).

The entire Holocene sequence is characterized by changing sedimentary environments, deposited under marine, brackish, and limnic-semiterrestrial conditions. The study reveals that pelagic diatoms from both open marine and fluvial conditions occur at different depths and facies. Pelagic diatoms may be transported over significant distances, thereby intermingling forms that did not originally live together. The pelagic diatoms in the coastal Holocene are useful markers for paleoenvironmental, e.g., paleosalinity gradients (Moore and McIntire, 1977) and sea level changes (Palmer and Clague, 1986). With respect to both paleosalinity signals and sea level contacts, the results presented in Figure 2.1.9a and b indicate that even the lagoonal and peat swamp

paleoenvironments have experienced several incursions of the seawater, probably on the occasion of storm events with exceptionally high water stands. The other explanation, however, could be that there was a continuous entrance through which the Holocene terrestrial deposits were provided with compounds from adjacent estuarine and open marine sources.

#### *Paleoenvironmental reconstruction*

The interdisciplinary approach used in this study including geochemical and microfacies analyses leads to a detailed picture of the environmental variations in the course of the Holocene.

*Basal unit* - The deposits of this unit reflect hydrological conditions typical of a fen bog: A limnic environment is represented in a nutrient-rich bog with a peat-forming vegetation dominated by Cyperaceae (e.g. *Carex* spp.), bushes and trees (e.g. birches). The presence of water led to a succession of sedimentary (mud) and sedentary (bog) conditions. A transgression-induced marine influence is not indicated.

*Lower clastic unit* - The sandy sediments overlying the basal unit clearly are marine influenced due to a rapid sea-level rise, immediately flooding the fluvial terrace sediments of the river Weser. The corresponding time interval is consistent with the phase of rapidly rising sea level in the sea level curve (Figure 2.1.2). The following phase of slowly rising sea level led to more brackish influenced depositional conditions. Here supplementary terrestrial-limnic effects due to fluvial run-off from the Weser or adjacent river systems became more evident.

*Organic-clastic interfingering unit* - Under the control of slowly rising sea level, stagnation or even temporary lowering of the sea level, the development of sheltered and fresh-water conditions is further pronounced. This results in an increased growth of *Phragmites* bogs and thus leads to an alternation of lagoonal sedimentation and sedentary bog growth. However, even within these deposits a marine influence is still visible that could derive from short-time events, e.g., at storm tides.

*Upper clastic unit* - The tidal flat deposits overlying the uppermost peat layer of the organic-clastic interfingering unit already document the estuarine influence due to the river Weser that gradually approached more and more its Recent course.

### Conclusions

Different disciplinary fields combined in this study have contributed to detailed information about the genesis of a Holocene sedimentary succession in NW Germany.

- Based on inorganic geochemical analyses, data are presented (e.g. on quartz [SiO<sub>2</sub>] and clay mineral contents [Al<sub>2</sub>O<sub>3</sub>, Rb]) that underline the suggested differentiation into sediments of marine, brackish and sedentary peat origin. The data also reflect changing hydrodynamic conditions involved in the buildup of the different sedimentary units (e.g., quartz-sandy sediments of the lower clastic unit reflect high-energy conditions and channel activities that probably were related to the rapid sea-level rise at this time). The data furthermore point to differences in the composition of the clastic units. This is, e.g., well documented by repeatedly increasing Ca/Sr-ratios even within those units. Higher Ca/Sr-ratios may be related to bioclastic material from marine organisms (e.g. molluscs).
- Results of diatom analyses underline the picture already drawn by the inorganic geochemical data. Considering the ratio between polyhaline (marine) and oligohaline (brackish-fluvial) diatom species, a ratio of >1 in sediments of the lower clastic unit supports the assumption of an initially rapid marine ingressions due to sea-level rise. Also prevailing marine species of low numbers point to high-energy and channel activities as already indicated by the geochemical data. Even within the fine-grained sediments intercalated between peat layers of the organic-clastic interfingering unit, the ratio between polyhaline (marine) and oligohaline (brackish-fluvial) species still is >1. On the other hand, the sediments of the upper clastic unit indicate an increasing influence of the river Weser as it is documented by a ratio of <1 between both ecological groups.

- Data on amino acids (THAA) contribute to the general picture already suggested by inorganic geochemical data and microfacies studies. The THAA values document a change in the organic matter origin in both the lower and the upper clastic units.
- The changing paleoenvironmental conditions are also documented by the results of the molecular organic geochemical investigations: The peat-forming vegetation of the basal unit is dominated by Cyperaceae, bushes and trees (e.g. birches) evident from high triterpenoid contents. Elevated amounts of *des-A*-triterpenoids document extensive bacterial reworking of the organic material. The high-energy paleoenvironment of the lower clastic unit is underlined by the presence of peat lumps and finely dispersed organic material. Their triterpenoid content implies a close relation to the organic matter in the organic basal unit. A more estuarine influenced sedimentation of the upper part of the lower clastic unit and the upper clastic unit is reflected by an enhanced level of C<sub>27</sub> and C<sub>28</sub> sterols. A frequent marine influence on the organic clastic interfingering unit is documented on the molecular level, e.g., by the occurrence of sterathiols. Their diagenetic formation depends on the presence of reduced sulfur species, hence marine sulfate has been present at least from time to time. Biomarker analysis could establish a close relationship between the so-called fossil soil horizon and the organic basal unit. This suggests its erosion-induced formation and is consistent with radiocarbon dating.

**Acknowledgements** - The authors acknowledge Prof. M. Geyh, NLfB Hannover, for radiocarbon measurements. Drs. A. Lückge, P. A. Meyers and H. Wilkes are thanked for their constructive comments on an earlier version of the manuscript. This project was financially supported by the Deutsche Forschungsgemeinschaft (DFG) as part of the priority program "Bio-geochemical changes over the last 15,000 years - continental sediments as an expression of changing environmental conditions" (DFG grants Scho 561/2-3, Ge 64/4-2, Li 352/6-3).

## 2.2. High-resolution reconstruction of a Holocene coastal sequence (NW Germany) using inorganic-geochemical data and diatom inventories

O. Dellwig, F. Watermann, H.-J. Brumsack and G. Gerdes

**Abstract** - Holocene deposits of the NW German coastal plain consist of many different lithological facies, e.g., tidal flats, brackish water sediments and peat beds. The effects of the Holocene sea-level rise on palaeoenvironmental conditions of this coastal sequence were studied by inorganic-geochemical methods in conjunction with diatom analyses. 300 samples from two parallel sediment cores which cover the entire NW German Holocene were taken at high resolution and were examined for major and minor elements and bulk parameters. Selected samples were analysed for redox-sensitive trace elements and REE distribution, reactive iron, and bulk sediment  $^{34}\text{S}/^{32}\text{S}$ -ratios. Chemical parameters, e.g., Si/Al-, Ca/Sr-ratios, and TOC contents correlate with depositional factors such as wave-energy and lithofacies changes, which allow a detailed reconstruction of the palaeoenvironment. Diatom analyses reveal information about changes between marine, brackish, and limnic conditions and serve to reconstruct palaeosalinity. Early diagenetic effects are evident in the TOC-rich intervals. Most peat layers are affected by sulphate reduction and resulting pyrite formation as well as by enrichments in redox-sensitive trace elements. The highest enrichments are seen for As, Mo, Re, and U, indicating a distinct seawater influence. S-isotope ratios of peat samples are compatible with pyrite formation under both open and closed system conditions, depending on exposition to seawater. The inorganic-geochemical and diatom data suggest limnic conditions at the base of the sequence, and repeated changes towards marine conditions within the overlying clastic units. On the other hand, data obtained from the clastic units yield evidence of a recurrent succession from open to restricted marine, brackish-lagoonal, and finally fen environments. Clastic sediments overlying peat layers, correlate with the increase of marine-derived geochemical signatures and pelagic diatoms attest transgressive overlaps. The analyses suggest that major controls on the palaeoenvironments were (i) climate-related oscillations of the coast line and (ii) the morphology of the coastal region allowing marine incursions even into distal semi-terrestrial lowlands.

## **Introduction**

The Holocene coastal sediments of NW-Germany result from the sea-level rise after the last glacial maximum, 18,000 years before present (BP). At that time the sea level was 110-130 m lower than today (Cameron *et al.*, 1987, Long *et al.*, 1988). The subsequent sea-level rise was 90-95% climatically controlled (Sindowski and Streif, 1974). From 10,000 to 8,100 years BP the deeper areas of the North Sea were characterized by brackish conditions (Eisma *et al.*, 1981). Reliable data about the late glacial and early Holocene sea-level rise in the study area are not available because of the shallow water depth (mostly less than 45 m) in the German Bight (Streif, 1990). Between 8,600-7,100 years BP the sea level was rising at a rate of about 2 m per 100 years and reached a depth of 15 m below the present level (Ludwig *et al.*, 1979). This steep rise probably lasted until 6,500 years BP (Menke, 1976) followed by a distinct slow down with phases of stagnation and even regression of the sea level. The time period since 1,000 years BP is strongly influenced by anthropogenic activities (dike building and draining), which hampered a natural sedimentation. However, some samples from the Eastfrisian Islands show that between 900 and 600 years BP the present mean sea level was achieved (Streif, 1986).

Sedimentological, palaeobotanical, and palynological studies have established the basis for the reconstruction of the sea level course as well as a lithological superstructure, which records the large number of the Holocene facies in the NW German coastal area (e.g. Streif, 1971; Barckhausen *et al.*, 1977; Linke, 1979, 1982; Preuss, 1979; Barckhausen and Müller, 1984). These facies can roughly be subdivided into three lithological units:

- (1) clastic sediments which were formed under marine influence (tidal flat)
- (2) semiterrestrial organic layers (predominantly peat)
- (3) interfingering units of clastic sediments and organic deposits.

Besides lithology, geochemical signatures constitute important tools for recognizing environmental changes preserved in Holocene coastal sequences. Until now, geochemical investigations are relative scarce when compared with palaeobotanical and

lithological studies (e.g. Behre *et al.*, 1985; Ludwig *et al.*, 1973). Diatom analysis also represents an important tool to reconstruct changes in palaeoenvironmental conditions, e.g., palaeo-salinity gradients (Moore and McIntire, 1977), palaeo-tide levels (Nelson and Kashima, 1993) or sea level change (Pientz *et al.*, 1991). In this contribution, a Holocene coastal sequence from NW Germany will be characterized using data from inorganic-geochemical and diatom analyses. The study will reveal detailed information about depositional dynamics and provenance of deposited materials. A second aim of this paper will be to find indications for early diagenetic processes, for instance, pyrite formation.

### Geographical and geological setting

Samples in this study originate from two adjacent drill holes (Archive No. 2517 Loxstedt, GE 430 GK B 32 and GE 431 GK C 32) of about 18 m total length covering the entire Holocene. The drill site is located in the marshland at the eastern bank of the river Weser about 20 km SW of Bremerhaven (Figure 2.2.1).

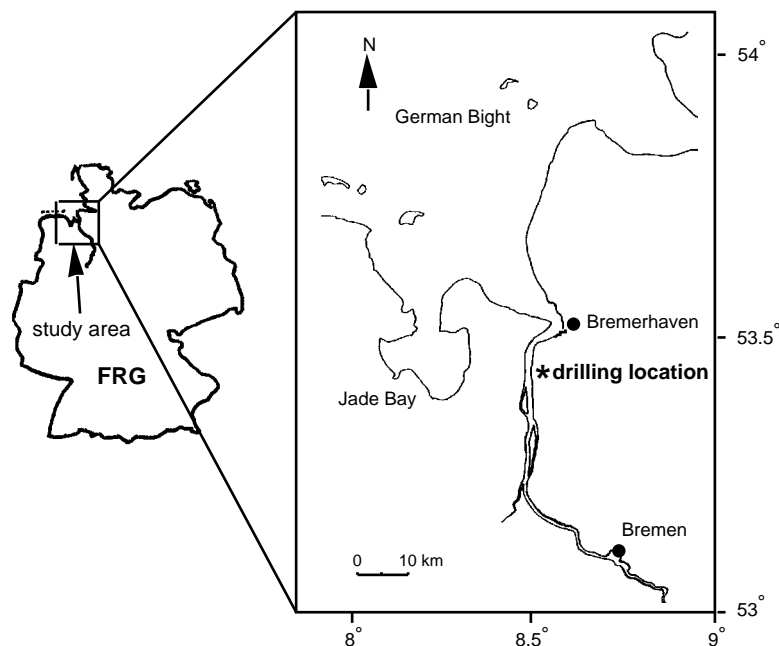


Figure 2.2.1: Study area and location of drill site.



The marshlands are situated funnel-like in the Pleistocene watercourse of the river Weser, which extended NW above glacial sands (often of eolian origin) and gravel (Müller, 1977). The cores were drilled with a drilling system provided by the Geological Survey of the Federal State of Lower Saxony, Germany (Merkt and Streif, 1970). On the basis of the lithological description and by using bulk parameters, major and minor element distributions, as well as microfacial analysis, the two cores were combined into one synthetic profile (Dellwig *et al.*, 1998). The resulting lithology of the composite core is given in Figure 2.2.2.

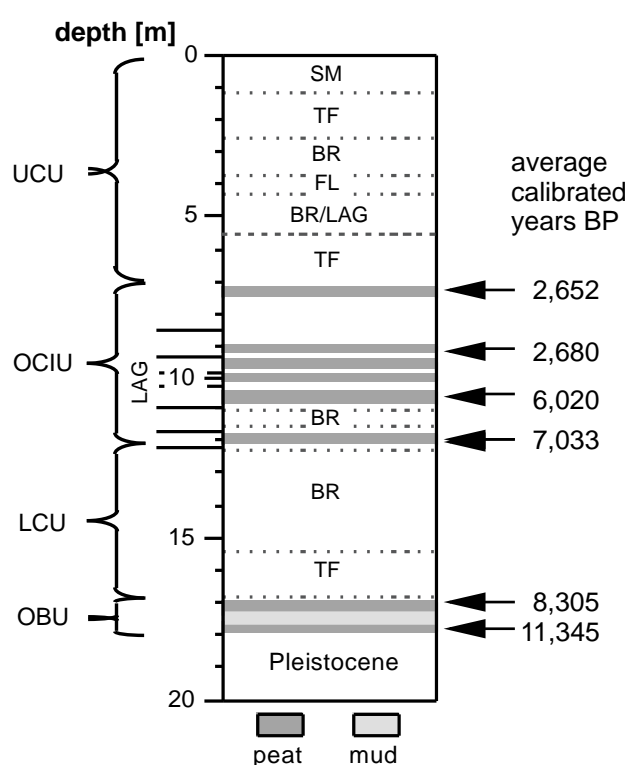


Figure 2.2.2: Profile of the composite core showing the lithology (SM=salt marsh, TF=tidal flat, BR=brackish, FL=fluvial levee, LAG=lagoon) and the four main sedimentary units (UCU=upper clastic unit, OCIU=organic clastic interfingering unit, LCU=lower clastic unit, OBU=organic basal unit) as well as  $^{14}\text{C}$ -age determinations of six peat samples [average calibrated years BP].

The core is composed of four main sedimentary units. The basis forms the organic basal unit (OBU) (17.86-17.00 m) consisting of different freshwater muds (organogenous,

silty, and sandy mud) between two peat layers. Microscopic examination of plant fragments from peat samples were kindly carried out by W. Bartels (LUFA, Soil-physical Laboratory) according to the methods given by Grosse-Brauckmann (1962).

The lower peat bed (17.86-17.57 m) represents a mixture of sedge peat (*Carex spp.*) and woodland peat (*Betula pubescens*) with a high contribution of freshwater muds while the upper peat bed (17.36-17.00 m) is a fen peat (*Phragmites australis*) with subordinate signals of bog vegetation (*Sphagnum spp.*). Six peat samples were chosen for  $^{14}\text{C}$ -age determinations, which were kindly performed by M.A. Geyh (Geological Survey of the Federal State of Lower Saxony, Germany). The resulting conventional ages (Dellwig *et al.*, 1998) and calibrated ages are presented in Table 2.2.1. The calibrated ages are calculated using the  $^{14}\text{C}$  age calibration program CALIB 3.0 (Stuiver and Reimer, 1993).

Table 2.2.1: Results of  $^{14}\text{C}$ -age determinations of peat samples from Holocene NW German coastal sediments.

depth interval [m]	conventional $^{14}\text{C}$ -age [years before 1950]	calibrated years BP	average calibrated years BP
7.30-7.40	2,630±200	2,935-2,370	2,652
9.18-9.30	2,640±170	2,875-2,485	2,680
10.60-10.82	5,250±155	6,265-5,775	6,020
11.89-12.03	6,160±100	7,175-6,890	7,033
17.00-17.22	7,540±205	8,490-8,120	8,305
17.57-17.82	9,920±410	12,205-10,485	11,345

The deepest sample (17.57-17.82 m) with an average age of 11,345 years BP originates from the transition zone between the Pleistocene and Holocene. The following sample at 17.32-17.28 m depth shows an average age of 8,300 years BP and represents the onset of the accumulation of the Holocene sedimentary wedge. Above the OBU tidal flat (17.00-15.40 m), brackish (15.40-12.15 m), and lagoonal sediments (12.15-12.03 m) are deposited, which according to our terminology form the lower clastic unit (LCU) (17.00-12.03 m). Between 12.03 and 7.30 m an organic-clastic interfingering unit (OCIU) occurs, consisting of brackish water sediments (brackish and lagoonal) and six intercalated reed peat beds (*Phragmites communis*). Four peat samples from this unit

were taken for  $^{14}\text{C}$ -age determination revealing an age of the OCIU from approximately 7,030 to 2,650 years BP. The OCIU is covered by an upper clastic unit (UCU) (7.30-0.52 m) consisting of tidal flat sediments (7.30-5.70 m and 2.60-1.12 m), brackish sediments (5.70-4.36 m and 3.67-2.60 m), and one layer formed by a fluvial levee (4.36-3.67 m). The top of the core is represented by salt marsh deposits (1.12-0.52 m). This variable sequence of lithological units in the UCU compared to the LCU reflects the unsteady sea level curve in this time interval as reported by Behre (1993). As mentioned above the sea-level rise was considerably steeper and more uniform during the formation of the LCU.

The described stratigraphic succession is typical for the investigated area. Age determinations of peats in the study area by Preuss (1979) show comparable ages. Thus, interfingering units occur between  $5,930 \pm 55$  and  $1,930 \pm 60$  years BP and datings of different basal peats vary from  $11,600 \pm 105$  to  $6,250 \pm 90$  years BP. The differences are the result of local variability, e.g., distance to the coastline as well as erosional effects during the deposition of the clastic sediments.

### **Material and methods**

*Geochemistry* - After splitting the cores into an archive and a working half, high resolution sampling was performed at 5 to 10 cm in clastic intervals and at 1 to 5 cm in organic-rich intervals, depending on the lithology. The samples were stored in polyethylen-bags, sealed, and immediately frozen. Porewater samples were obtained by centrifugation and were analysed for ammonia, reactive phosphate, chloride, and sulfate (Vetter and Liebezeit, 1996). The centrifuged samples were freeze-dried and homogenised in an agate mortar. The ground powder was used for all subsequent geochemical analyses.

A total number of 300 samples were analysed for major elements (Al, Ca, Fe, P, Si, Ti) and trace elements (As, Co, Cr, Ni, Pb, Sr, V, Y, Zn, and Zr) by XRF (Philips PW 2400, equipped with a Rh-tube) using fused borate glass beads. Samples with a total

organic carbon (TOC) content of more than 10% were heated to 500°C to remove TOC prior to adding lithiumtetraborate and fusing in Pt-Au-crucibles. Analytical precision and accuracy of XRF measurement was tested by replicate analysis of geostandards (GSD-7, GSD-10, and GSS-6) and several in-house standards (see appendix).

Total carbon (TC) and total sulphur (TS) were determined by combustion using an IR-analyser Leco SC-444. Inorganic carbon (IC) was determined with a Coulometrics Inc. CM 5012 CO<sub>2</sub> coulometer coupled to a CM 5130 acidification module (Huffman, 1977; Engleman *et al.*, 1985). The TOC content was calculated as the difference between TC and IC. The precision of bulk parameters was checked in series of double runs and accuracy was determined by using in-house standards (see appendix).

ICP-MS (Finigan MAT Element) was used to analyse for redox-sensitive trace metals (Co, Cr, Cu, Mo, Ni, Re, Tl, U, V, Y) and rare earth elements (REE) in 50 selected samples. Acid digestions were performed after Heinrichs and Herrmann (1990) in closed teflon vessels (PDS-6; Heinrichs *et al.*, 1986) heated for 6 h at 180°C by using two procedures (procedure A for redox-sensitive trace metals and procedure B for REE).

Procedure A: 100 mg sample + 2 ml HNO<sub>3</sub> (over night to oxidize TOC)  
+3 ml HF + 3 ml HClO<sub>4</sub>

Procedure B: 100 mg sample + 1 ml HNO<sub>3</sub> (over night to oxidize TOC)  
+3 ml HF + 3 ml H<sub>2</sub>SO<sub>4</sub>

After digestion the acids were evaporated using a heated metal block (A: 180°C, B: 240°C) and were re-dissolved and fumed off three times with 2 ml half-concentrated HCl, followed by re-dissolution with 1 ml conc. HNO<sub>3</sub> and dilution to 50 ml. The ICP-MS analyses were checked for precision and accuracy by parallel analysis of international reference materials SDO-1, GSD-3, and GSD-10, as well as in-house standards (see appendix). A more detailed description of the ICP-MS method is given by Schnetger (1997).

For 36 selected samples the reactive acid-soluble iron Fe<sub>x</sub> (as defined by treatment with 1N HCl at room temperature for 24 h) was measured by ICP-OES (Perkin Elmer Optima 3000XL) to determine the degree of pyritization (DOP) according to the method

of Leventhal and Taylor (1990). The  $\text{Fe}_x$  measurement was evaluated by using SDO-1 (see appendix).

For the investigation of the S-isotope composition, which was kindly performed by M. E. Böttcher (ICBM), 30 solid phase samples were first washed to remove chloride. Afterwards the samples were dried and directly analyzed by combustion isotope-ratio-monitoring mass spectrometry (C-irm MS) according to the method described by Böttcher *et al.* (1998). The reproducibility was better than  $\pm 0.3\%$ . Isotope ratios are given relative to the Vienna CTD.

*Diatoms* - Littoral and pelagic diatoms were isolated from selected samples according to Schrader (1973). To obtain information on relative abundance, counts were done in triplicate using counting chambers (Utermöhl, 1958). Counting was performed with an inverted microscope at 400-fold magnification. Quantification is based upon maximum counts of 400 frustules (Lund *et al.*, 1958). Frustules fragments  $> 1/2$  were counted as a whole frustule (Schrader and Gersonde, 1978). Taxonomy of the diatoms was facilitated by mounting the diatoms in Naphrax resin. The species were identified using a light microscope at 1000-fold magnification. In several cases an electron microscope was also used for taxonomic identification. Species identification is based on Drebes (1974), Hartley (1996), Hustedt (1957) and Pankow (1990). The diatom species are classified according to salinity groups after Simonsen (1962).

## **Results and discussion**

### *Major compounds*

As mentioned before the drill core is characterized by a large number of lithological units, which result from the mixture of different sedimentary and sedentary components owing to changes in depositional conditions. In the ternary plot  $\text{Al}_2\text{O}_3 \cdot 5\text{-SiO}_2\text{-TOC} \cdot 5$  (Figure 2.2.3) varying proportions of the main components, except carbonates, from the investigated sediments are visualized. No absolute concentrations are presented in this

plot but the relative proportions of the three components normalised to 100%. The three poles represent the end members clay (rich in  $\text{Al}_2\text{O}_3$ ), quartz ( $\text{SiO}_2$ ), and peat (TOC). Besides clay minerals, Al-containing feldspars may also be present in the silt-fraction of tidal flat sediments (van Straaten, 1954). Feldspars cannot be excluded from this diagram, but their presence will not affect the interpretation significantly in this case. Two discrete mixing trends are seen, which reflect the different conditions of deposition in low and higher wave-energy environments. On one hand the quartz-rich tidal flat sediments, which formed under higher wave-energy conditions, are indicated near the  $\text{SiO}_2$  pole. On the other hand, TOC-rich lagoonal sediments of the OCIU and the sedentary peats with partly higher clay proportions can clearly be distinguished. The two trends intersect in an area that is dominated by brackish and lagoonal sediments similar in composition to average shale (Wedepohl, 1971). In the following discussion the Holocene evolution of the depositional sequence will be documented using inorganic-geochemical and diatom data.

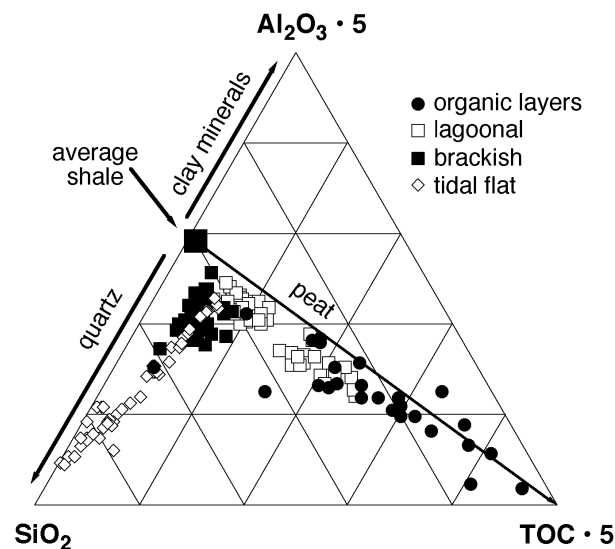


Figure 2.2.3: Ternary plot  $\text{Al}_2\text{O}_3 \cdot 5$ - $\text{SiO}_2$ - $\text{TOC} \cdot 5$  for sediment and peat samples from Holocene NW German coastal sediments.

#### *Palaeoenvironmental reconstruction*

*Organic basal unit (OBU)* - The base of the core is formed by the OBU, which comprises layers of different mud types (organogenous, silty, and sandy) intercalated

between a lower and an upper peat bed. The peat layers are easily recognized by their elevated TOC contents (Figure 2.2.4a). According to Berner and Raiswell (1984), TOC/TS-ratios may be a helpful indicator for palaeosalinity. Marine sediments are characterized by low (0.5 to 5) and freshwater sediments by higher values ( $>10$ ). The muds show an average TOC/TS-ratios of 35.8, which confirms that these muds are deposited under limnic conditions and were not influenced by the sea-level rise. This is also indicated by the occurrence of exclusively limnic diatoms, e.g., *Pinnularia* spp. (Figure 2.2.5a).

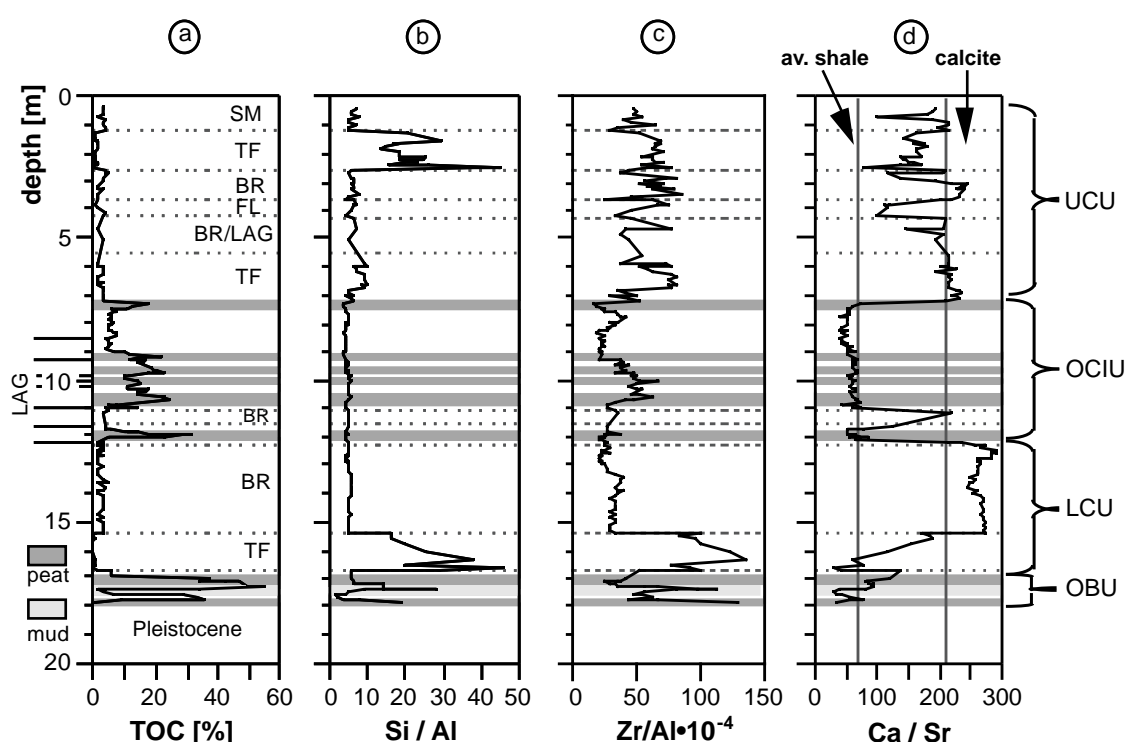


Figure 2.2.4: Depth profiles of TOC content, Si/Al-, Zr/Al-, and Ca/Sr-ratios of the drill core. Average shale after Wedepohl (1971). (SM=salt marsh, TF=tidal flat, BR=brackish, FL=fluvial levee, LAG=lagoonal).

A further indication of limnic conditions is given by the enrichment of  $P_2O_5$  in the lower part of the OBU (Figure 2.2.6d). This enrichment is due to the formation of vivianite, an indicator mineral for anoxic non-sulfidic conditions (Berner, 1981) which supports the assumption that the OBU is unaffected by the sea-level rise. The first signals of marine influence occur in the uppermost part of the upper peat layer of the OBU as indicated by a slight increase in marine pelagic diatoms (Figure 2.2.5b). This is not clearly visible in

the depth profile because of a very low number of frustules in comparison to the limnic diatoms. Nevertheless here the first marine influence seems apparent.

Furthermore an enrichment of TS in this peat layer due to pyrite formation (Figure 2.2.6a) reflects microbial reduction of seawater sulphate. The peat layer may have received sulphate from short-term flooding events as well as from the overlaying clastic sediments by diffusion and percolation, respectively.

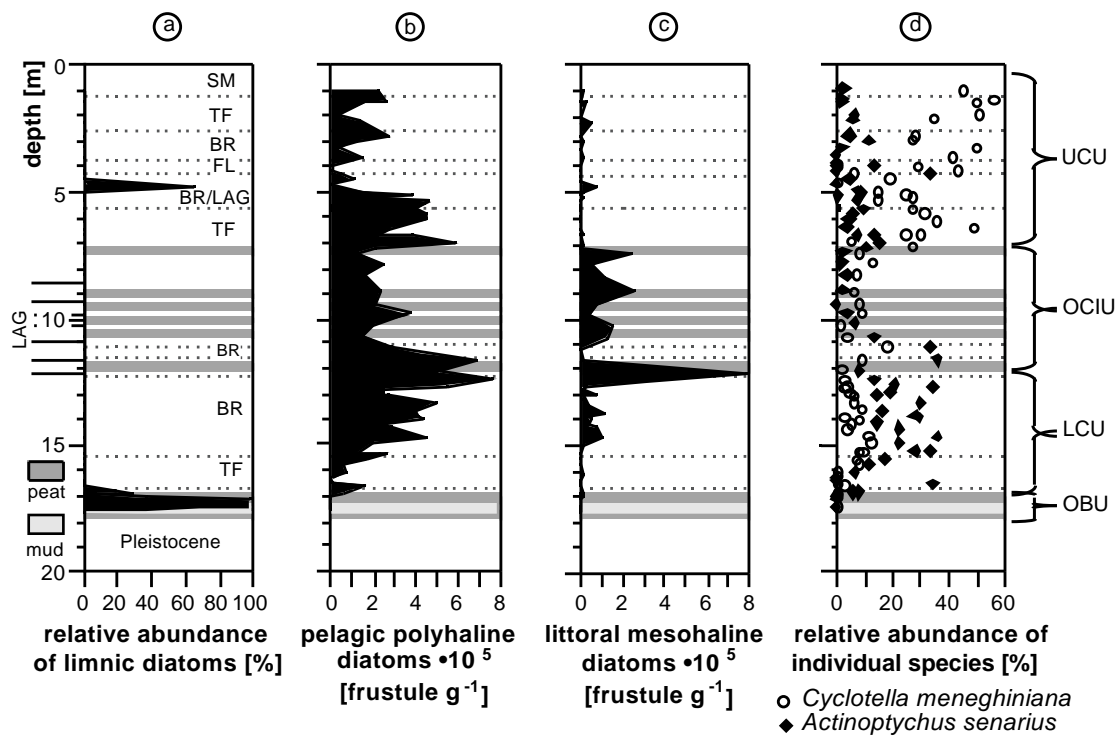


Figure 2.2.5: Depth profiles showing the diatom inventories of the drill core from limnic to marine species. (SM=salt marsh, TF=tidal flat, BR=brackish, FL=fluvial levee, LAG=lagoonal).

Except for this uppermost part the chemistry of the OBU seems influenced by eolian input. Correlations between  $\text{TiO}_2$ , Zr (Figure 2.2.7a), and Cr [not shown] are seen for the basal samples. Ti, Zr, and Cr form part of the refractory minerals (e.g. rutile, ilmenite, zircon, chromite), which are resistant to chemical and mechanical weathering. These minerals are preferentially enriched during the loess-forming process. Mean Jungwurm(JW)-loess from southern Lower Saxony and northern Hessia (FRG) (Schnetger, 1992), therefore, seems to contribute significantly to the terrigenous-detrital fraction of this interval. The younger reed peat samples of the OCIU show a much less



significant correlation with average shale as a possible endmember. Furthermore the similarity between the chemical composition of the OBU and the mean JW-loess becomes also evident in the pattern of the chondrite-normalized REE distribution (Boytton, 1984), elements that are also enriched in weathering resistant heavy minerals during loess forming processes (Figure 2.2.8). The basal samples plot close to the mean JW-loess and show the same enrichment in light relative to heavy REE when compared with the remaining clastic tidal flat sediments.

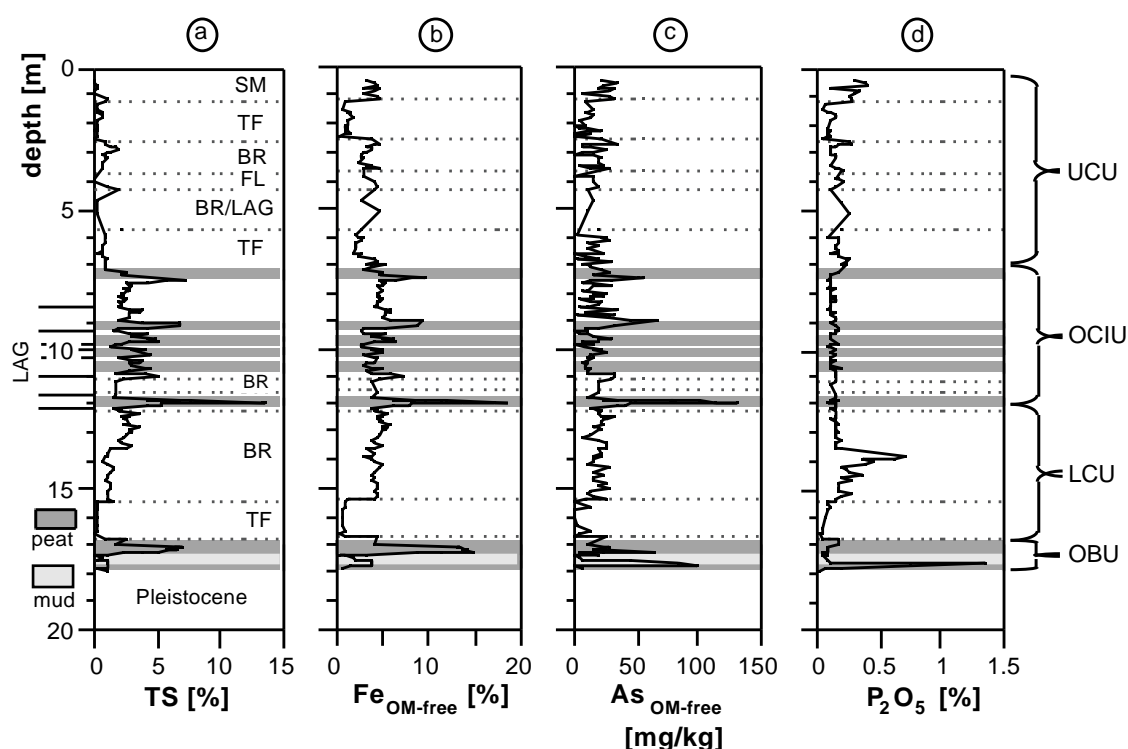


Figure 2.2.6: Depth profiles of TS, Fe, As, and P content of the drill core. The contents of Fe and As are calculated on an organic matter-free basis. (SM=salt marsh, TF=tidal flat, BR=brackish, FL=fluvial levee, LAG=lagoon).

*Lower clastic unit (LCU)* - In Figure 2.2.4b profiles of the Si/Al-ratios of the core are shown. The normalisation to Al eliminates dilution effects caused by quartz, carbonate, or organic matter and allows to compare the chemistry of sediments of different genesis. Al has been chosen for normalisation because its concentration is not influenced by biogenic cycles or anthropogenic activity.

The interval with the highest Si enrichment ( $\text{Si/Al} > 15$ ) in the LCU belongs to the sand flat facies where the  $\text{SiO}_2$  contents partly reach 95%. Furthermore Zr is strongly

enriched in this section (Figure 2.2.4c). The average Zr/Al-ratio of  $101 \cdot 10^{-4}$  is much higher than the average shale Zr/Al-ratio of  $22 \cdot 10^{-4}$  (Wedepohl, 1971). Zr as well as Ti are typical indicators for high-energy environments, because both elements are associated with the heavy mineral fraction, e.g., as ilmenite ( $\text{FeTiO}_3$ ), rutile ( $\text{TiO}_2$ ), and zircon ( $\text{ZrSiO}_4$ ). Figure 2.2.7b shows that these elements correlate in the sand flat sediments. Therefore, the diatom association is relatively poor in this section. However, in most cases marine pelagic species dominate the samples compared to the limnic diatoms (Figure 2.2.5a and b). Only strongly silicified, robust organisms occur. This result also emphasize a high energy regime throughout the sea-level rise. Taking into account the age of the upper peat of the OBU the described high energy environment for this section can be connected with the Calais I transgression which lasted from approximately 7,800-6,250 years BP (Brand *et al.*, 1965). Furthermore this section is in accordance with results of a mass-balance study of Holocene sediment accumulation on the southern North Sea coast of Germany by Hoselmann and Streif (1997), which shows that the highest sediment accumulation occurred in this time interval.

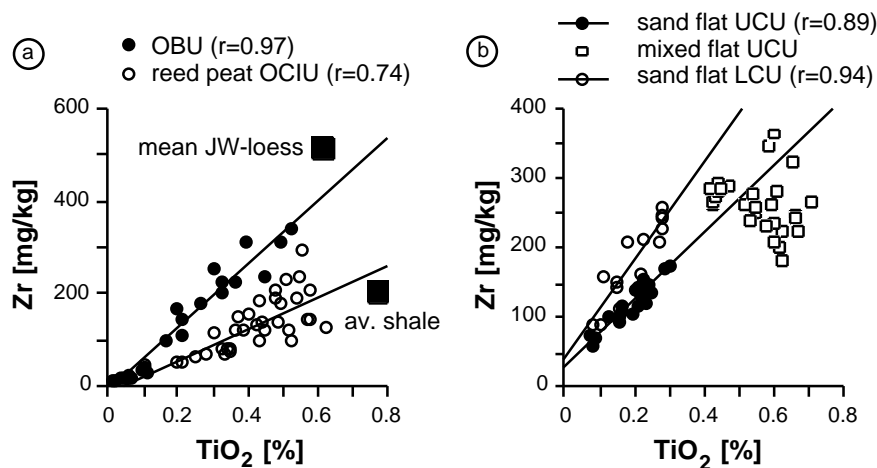


Figure 2.2.7: Scatter plots of  $\text{TiO}_2$  versus Zr of organic-rich layers and tidal flat sediments of the drill core. Mean Jungwurm-loess data from Schnetger (1992) and average shale data after Wedepohl (1971).

The overlying sediment layer is characterized by calmer conditions as reflected by lower Si/Al-ratios with an average value of about 4.0. This ratio is only slightly higher than the average shale value of 3.0 (Wedepohl, 1971) owing to the contribution of

quartz. A further difference to the underlying sand flat sediments is seen in the depth profile of the Ca/Sr-ratios (Figure 2.2.4d). For comparison, data from average shale (Ca/Sr=70, Wedepohl, 1971) and analyses of different mussel shells from the study area (Ca/Sr=210) are shown as well. The mussel shell ratio is in agreement with data for marine calcite as measured by Pingitore and Eastman (1985). This sediment layer is characterized by high Ca/Sr-ratios due to biogenic carbonate, while Ca/Sr-ratios similar to average shale are predominantly found in the sand flat section comprised mainly of detrital components. Diatom analyses reveal an increasing abundance of littoral species characteristic of brackish habitats (Figure 2.2.5c). The occurrence of marine pelagic diatoms also increases as a result of the still rising sea level (Figure 2.2.5b). Here it has to be mentioned that littoral diatoms characterize the environment because they are sedimented in their biotope, whereas pelagic diatoms reflect transport processes. This indicates a palaeoenvironment of relatively low energy and salinity in a coastal low land area.

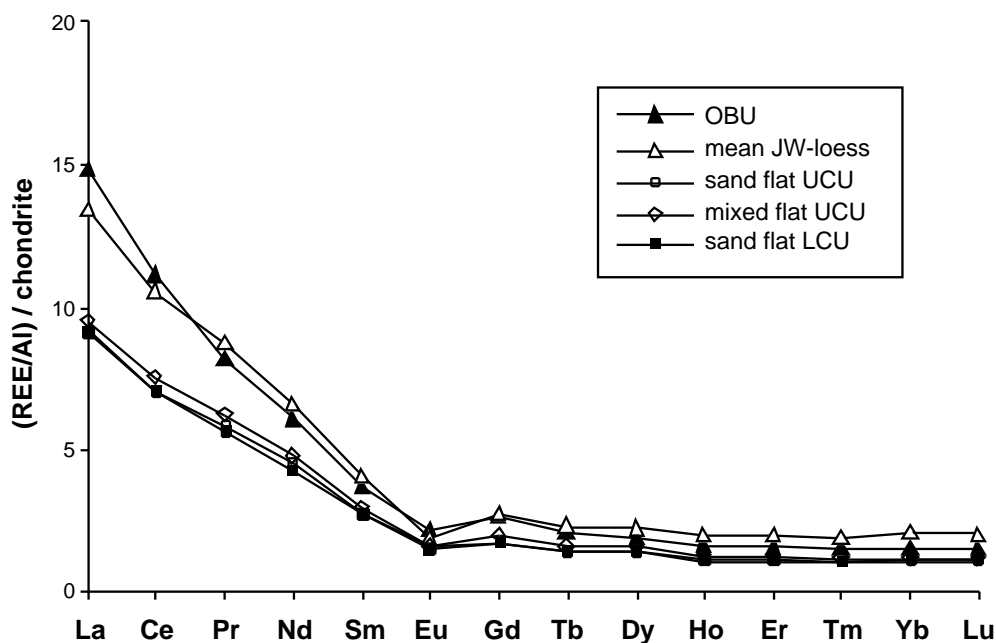


Figure 2.2.8: REE/Al-ratios normalised to chondrite for tidal flat sediments and samples of the organic basal unit. Chondrite data from Boynton (1984) and mean Jungwurm-loess data after Schnetger (1992).

In the upper part of the LCU a layer of about 10 cm thickness occurs, which is characterized by a decreasing Ca/Sr-ratio and an enrichment in littoral mesohaline

diatom species (Figure 2.2.5c). This interval forms the transition to the reed peat beds of the OCIU and can be classified as a lagoonal deposit.

*Organic clastic interfingering unit (OCIU)* - The OCIU consists of six reed peat beds intercalated between lagoonal sediments. The reed peat beds indicate a stagnation or perhaps decrease in sea-level rise (Streif, 1990) because reed is only able to grow under lower salinity conditions, which in this case requires a distinct freshening. It should also be considered that during a phase of less intense sea-level rise the rate of peat formation can balance this sea-level rise, leading to an apparent stand-still or even regression. The major element chemistry of these peats indicates flooding events, but possibly also riverine input, leading to a higher deposition of detrital matter. Hence the reed peats differ strongly from typical fen peats. For example, the average  $\text{Al}_2\text{O}_3$  content of the reed peats amounts to 8.8% (range 4.6-12.8%) and the average loss of ignition (LOI) to 36.4% (range 21.5-55.3%). The  $\text{Al}_2\text{O}_3$  value is significantly higher than the average  $\text{Al}_2\text{O}_3$  content of 1.9% (range 0.6-3.2%) as analysed by Naucke (1979) for 25 German fen peats. In accordance with the above data the LOI of the reed peat beds is considerably lower than for fen peats (average LOI 65%, range 44-78%). Furthermore the reed peat beds show TS and Fe enrichments (Figure 2.2.6a and b) as a result of pyrite formation due to the microbial reduction of seawater sulphate (see discussion on diagenetic effects below).

Gradual transitions between lagoonal sediments and peat beds exist especially in the centre of the OCIU. These lagoonal sediments are strongly influenced by the occurrence of reed rhizomes, as expressed by higher TOC contents (Figure 2.2.4a) in comparison to the adjacent clastic sediments. In general the lagoonal sediments are characterized by Ca/Sr-ratios close to average shale (Figure 2.2.4d). Only samples of the lowermost clastic section in the OCIU show higher Ca/Sr-ratios typical for biogenic carbonate. Here a stronger marine influence resulting from a brief transgressive pulse, possibly the Calais III transgression (Brand *et al.*, 1965), has to be assumed, which may have led to a chemical composition similar to brackish sediments. The diatom analyses confirm this assumption because the samples of the OCIU are clearly dominated by marine pelagic species, e.g. *Actinoptychus senarius* (Figure 2.2.5d) and indicate transport processes as

a result of the above mentioned transgressive pulse. The diatom assemblage in the upper part of the OCIU shows an increase in the brackish littoral diatom group (Figure 2.2.5c). At present, these species occur in inland waters of low salinity. Nevertheless the co-occurrence of marine planktonic diatoms indicates the close vicinity of the coastline (Figure 2.2.5b).

The described palaeoenvironment of the OCIU can be compared with a perimarine fluviatile coastal plain situation as suggested by van der Woude (1981) on the basis of investigations on Holocene deposits in the coastal area of the Netherlands. These fluviatile-lagoonal depositional areas are formed by ground water rise owing to a rising sea level. Under such conditions detrital material is delivered by small rivers and flooding events with brackish character increasing seawards.

*Upper clastic unit (UCU)* - As a result of a further transgressive event (presumably Dünkirchen I, 3,225-2,000 years BP; Brand *et al.*, 1965), which was less intense than transgression Calais I, tidal flat sediments were deposited on top of the upper peat layer of the OCIU. The abrupt transition from the uppermost peat layer to tidal flat sediments of the UCU indicates erosion effects. Therefore, the age determined for this peat provides no information about the precise onset of this transgression. The slightly higher Si/Al-ratios in comparison to the brackish sediments and the high Ca/Sr-ratios (Figure 2.2.4b and d), which indicate the presence of biogenic carbonate, allow a classification of this section as a mixed flat facies. TiO<sub>2</sub> and Zr are not correlated in these sediments (Figure 2.2.7b). In this case clay minerals, which were deposited under less energetic conditions in contrast to the sand flat sediments, seem to be the most important carrierphase for Ti. For this reason Ti and Al are highly correlated ( $r=0.99$ ) in this section.

The diatom assemblages change from littoral brackish to marine littoral and the proportion of marine pelagic diatoms increases in comparison to the OCIU (Figure 2.2.5d). Above the mixed flat section an interval of about 1.20 m thickness occurs, which represents the change from tidal flat to a fluvial levee deposit. These sediments show signals of biogenic calcite (Figure 2.2.4d) whereas the diatom analyses reveal a very high abundance of limnic species (Figure 2.2.5a). Therefore this part of the core

can be classified as a mixture of brackish and lagoonal sediments. The following fluvial levee is possibly an indication for the increasing influence of the river Weser and an increasing estuarine character in the UCU, respectively. After Hartung (1967) and Preuss (1979) the river Weser was flowing further to the west before  $3,275 \pm 50$  years BP. The fluvial levee represents the most elevated deposition area of brackish water sediments and is only exposed to seawater during extreme floods (Streif, 1990). Therefore, the fluvial levee sediments are characterized by low Ca/Sr-ratios (Figure 2.2.4d) comparable to average shale as well as low numbers of diatoms, contrasting with the enclosing sediments. The distinct increase in Ca/Sr-ratios in the following section is due to the presence of brackish sediments, which show a chemistry comparable to the brackish sediments of the LCU.

A final transgressive event is documented by the tidal flat sediments, which occur above the brackish section. The high Si/Al-ratios (Figure 2.2.4b) indicate that these sediments belong to the sand flat facies.  $\text{TiO}_2$  and Zr are correlated in this section (Figure 2.2.7 b), but in contrast to the sand flat sediments of the LCU a significant Zr enrichment does not occur (Figure 2.2.4c). The average Zr/Al-ratio of  $63 \cdot 10^{-4}$  is close to the mixed flat value with an average ratio of  $60 \cdot 10^{-4}$ . This difference between the sand flat sediments of the LCU and UCU is presumably a result of the influence of the river Weser. However, the REE distribution (Figure 2.2.8) shows a similar pattern for the tidal flat and brackish sediments of the whole core. Therefore, it can be stated that the river Weser has a stronger influence on the biocoenosis than on the composition of the deposited material. According to Hoselmann and Streif (1997) the riverine input is less important for the Holocene sediment accumulation in the study area. Therefore, a further reason for the lower Zr contents in the UCU may be an exhausted reservoir.

The most dominant species of the UCU is the limnic/brackish pelagic diatom *Cyclotella meneghiniana* (Figure 2.2.5d) which occurs in the river Weser at present (Hustedt, 1957). Thus, a distinct influence of the river Weser is indicated after 2,650 BP at the location of the drill site.

### Diagenetic effects

As mentioned above most of the peat beds are characterized by enrichments in TS and Fe as documented by element profiles of the drill core (Figure 2.2.6a and b). Owing to partly very low Al concentrations in the peat beds, Al does not appear as an appropriate element for normalisation in this context. Therefore, the contents of Fe and trace metals are calculated on an organic matter-free (OM-free) basis to eliminate dilution effects.

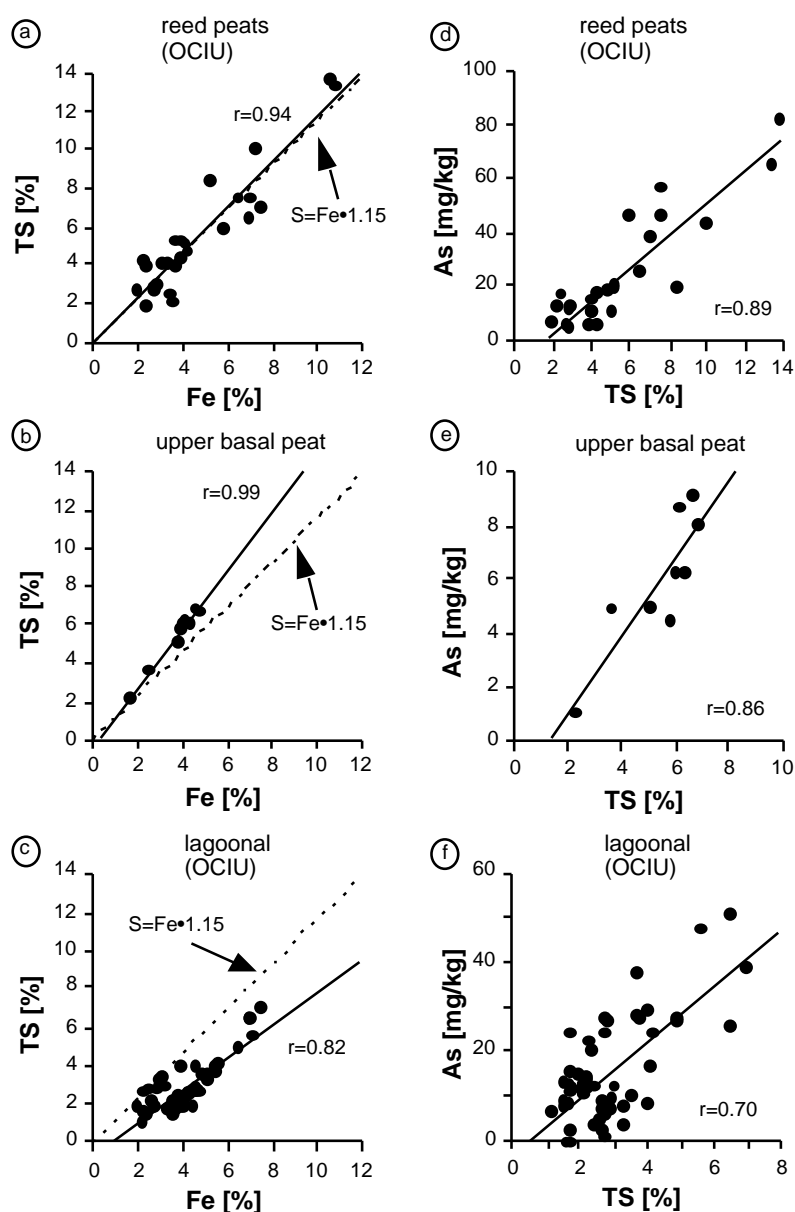


Figure 2.2.9: Scatter plots of Fe, TS, and As of reed peats, upper basal peat and lagoonal samples of the drill core.

TS is distinctly enriched in the peat beds of the OCIU and in the upper peat of the OBU. The high average TS-content of 5.46% (range 1.85-13.70%) show evidence for microbial reduction of seawater sulphate and resulting pyrite formation, respectively. Postma (1982) found similar TS values, ranging from 2 to 12% in brackish Skjernå delta swamp sediments (Denmark), while the investigation of freshwater peats in the Everglades (USA) by Price and Casagrande 1991 revealed lower TS amounts of 0.26 to 0.48%. This documents the important role of seawater sulfate for the amounts of pyrite in comparison to organic sulphur species occurring in peat.

Furthermore the lagoonal sediments and the upper section of the brackish sediments of the LCU show slight TS enrichments as well, presumably due to downward diffusion of  $\text{HS}^-$  from the overlaying peat beds where microbial sulphate reduction was quite intense. The Figures 2.3.9a-c show the correlation between Fe and TS for the reed peats and lagoonal sediments of the OCIU as well as for the upper basal peat layer. The regression line of the reed peat samples is almost identical to the theoretical pyrite ratio ( $\text{S}=\text{Fe}\cdot 1.15$ ) and intercepts the axis origin. This indicates that both elements are predominantly fixed as pyrite. The regression line of the upper basal peat is located above the pyrite line. This is possibly the result of a lower input of Fe because less detrital matter was delivered by flood and storm events and, therefore, higher amounts of organic sulphur compounds were formed. In contrast to this the regression line for the lagoonal sediments is located below the pyrite line due to a higher content of silicate-bound Fe, which is only in marginal amounts available for pyrite formation (Canfield and Raiswell, 1991). Only a few lagoonal samples from the centre of the OCIU in close vicinity to the peat beds show the theoretical pyrite ratio.

The refractory Fe fraction is taken into account in the ternary plot  $\text{Fe}_{\text{avail.}}\text{-TOC-S}\cdot 2$  as shown in Figure 2.2.10 (Brumsack, 1988). Additional information regarding limitation of pyrite formation for the different facies is obtained from this plot.

Factors limiting pyrite formation in normal marine sediments are (i) the amount of organic matter, which serves as an energy source for sulphate reducing bacteria, (ii) the sulphate concentration, (ii) the availability and reactivity of Fe, and (iv) the production



of elemental S (Berner, 1970; 1984). On the basis of the following empirical formula the available Fe ( $Fe_{avail.}$ ) for pyrite formation can be estimated:

$$Fe_{avail.} = Fe - 0.25 \cdot Al.$$

This calculation is based on the assumption that a certain Fe fraction is fixed in the silicate structures which empirically amounts to about 25% of the Al content. The line connecting TOC and pyrite may be regarded as a pyrite saturation line. Samples plotting on this line are considered to be completely pyritized.

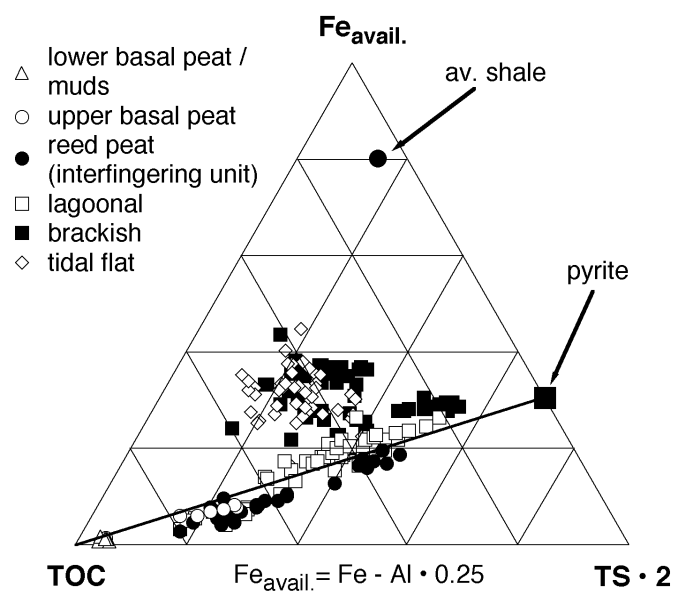


Figure 2.2.10: Ternary plot  $Fe_{avail.}$ -TOC- $S \cdot 2$  of different lithological units of the drill core. Average shale from Wedepohl (1971).

The peat samples of the OCIU and the upper peat of the OBU plot below the pyrite line, indicating an Fe-limited system and the presence of organic sulphur compounds, respectively. The lagoonal sediments of the OCIU almost all plot close to the pyrite-line indicating a high degree of pyritization. Especially the lagoonal samples next to the reed peat beds are strongly influenced by rhizomes as well as by diffusion of  $HS^-$  and are therefore completely pyritized. Contemporary peat deposits and lagoonal sediments unfortunately do not occur in the study area. However, recent salt marshes from the east coast of the USA can be regarded as comparable environments. Giblin (1988) found Fe limitation in peats of the saltmarshes of Great Sippewisset (USA) and in brackish water marsh sediments of the Rhode River Estuary (USA) on the basis of pyrite formation

experiments. Lord and Church (1983) reported similar results for TOC-rich marsh sediments of Delaware Bay (USA). Hence, the high production of hydrogen sulfide in these environments is due to high sulphate reduction rates (Howarth and Teal, 1979; Howarth and Giblin 1983; King *et al.*, 1985), which led to a fast consumption of the available iron. As a result only refractory silicate-bound Fe remains, which can not be easily converted into pyrite.

The freshwater mud samples and the lower peat of the OBU plot close to the TOC pole. These samples were formed under limnic S-limited conditions. Most of the brackish and tidal flat sediments are characterized by more oxidizing conditions. However, these samples plot distinctly closer to the pyrite-line in comparison with average shale.

Further information is given by the experimentally determined degree of pyritization (DOP). The DOP-value is based on the following formula (Raiswell *et al.*, 1988):

$$\text{DOP} = \text{Fe}_{\text{pyrite}} / (\text{Fe}_{\text{pyrite}} + \text{Fe}_x \text{ (analysed)}).$$

$\text{Fe}_x$  represents the acid-soluble reactive Fe-fraction (Fe-monosulfides, Fe-oxides, and Fe-oxyhydroxides) and  $\text{Fe}_{\text{pyrite}}$  is calculated from the TS content. Under oxic conditions DOP-values below 0.45 are obtained. More restricted suboxic sediments show values between 0.45 and 0.75. DOP values higher than 0.75 are indicative for anoxic conditions. The peat samples of the OCIU show DOP values between 0.82 and 0.97 (average 0.92) suggesting almost complete pyritization. The lagoonal sediments display slightly lower and more variable DOP values between 0.74 and 0.95 (average 0.81). Highest DOP values are found in samples close to peat beds, which supports the results seen in the triangular plot (Figure 2.2.10).

Evidence for microbial activity is given by bulk S-isotope values of selected peat samples of the OCIU and OBU. The reed peats of the OCIU show predominantly negative but also highly variable values between -25‰ and +5.6‰ indicating pyrite-formation as a result of microbial reduction of seawater sulphate. The most negative  $\text{d}^{34}\text{S}$ -values (range -25‰ to -4‰) and the highest isotopic fractionation relative to seawater (+20‰) occurs in the lowest reed peat bed. The remaining reed peats are characterized by less negative  $\text{d}^{34}\text{S}$ -values (range -12.1‰ to +5.6‰). This emphasizes

the distinct nature of the lowest reed peat bed, which is also characterized by pronounced trace metal enrichments (see discussion below). The S-isotopic composition of this peat layer is consistent with open system conditions and therefore this peat appears to be most strongly influenced by seawater. The remaining reed peats on the other hand show indications of a more closed, diffusion-controlled system.

In sediments under open system conditions typical isotopic fractionation values vary between -40 and -70‰ (Goldhaber and Kaplan, 1974). Therefore a dynamic system is suggested for the investigated reed peats where open and more closed system conditions alternate depending on exposition to seawater and concomitant distance to the coastline. However, it should also be considered that high sulphate reduction rates, which can be assumed for the reed peats, could cause a lower isotopic fractionation (Chambers and Trudinger, 1979). The upper peat of the OBU is characterized by positive  $\delta^{34}\text{S}$ -values close to the seawater value of +20‰, which tend towards more positive values with depth (range +10.2‰ to +17.1‰) indicating closed system conditions. The S source in this predominantly limnic environment, therefore, seems to be the sulphate, which reaches the peat via diffusion from overlying marine sediments.

Apart from high Fe and TS contents some of the peat samples are also characterized by enrichments in redox-sensitive trace elements, e.g., As, Co, Mo, Ni, V, and U in comparison to the enclosed clastic sediments. The  $A_{\text{SOM-free}}$  contents of the core are shown as an example in Figure 2.2.6b. Extreme enrichments are evident especially in the lowest reed peat of the OCIU and in the upper basal peat. The enrichment of As in the lower basal peat will be discussed below. As, Co, Mo, and Ni are fixed as sulphides and are more or less incorporated into pyrite (Huerta-Diaz and Morse, 1992), whereas U and V are preferentially bound to organic matter, according to experiments with humic acids isolated from peat performed by Szalay and Szilagyi (1967). In seawater U occurs as a carbonate complex ( $[\text{UO}_2(\text{CO}_3)_3]^{4-}$ ) (Langmuir, 1978) and V as an oxyanion (e.g.  $\text{HVO}_4^{2-}$ ) (Bruland, 1983). Under anoxic conditions, both elements are reduced to cations which then can be fixed by insoluble humic substances. Furthermore the reduction of U is influenced by sulfate reduction. On one hand the reduction of the U carbonate complex is initiated by  $\text{HS}^-$  produced by sulfate-reducing bacteria

(Klinkhammer and Palmer, 1991) and on the other hand U can be directly reduced by sulfate-reducing bacteria through enzymatical mechanisms (Lovley *et al.*, 1993). Both pathways lead to the precipitation of uraninite ( $\text{UO}_2$ ).

Figures 2.3.9d and e show correlation diagrams between As, an element which is easily incorporated into pyrite (Belzille and Lebel, 1986), and TS of reed peat beds ( $r=0.89$ ) and upper basal peat samples ( $r=0.86$ ). Further correlations with TS are found for Co ( $r=0.73/0.75$ ), Mo ( $r=0.81/0.53$ ), and Re ( $r=0.78/0.90$ ). An explanation for the less well expressed correlation between TS and Mo in the upper basal peat layer, which is characterized by TOC contents up to 55.5% (Figure 2.2.4a), could be the affinity of Mo to organic matter, as described by Brumsack and Gieskes (1983). The Re/Mo-ratios of the reed peat samples (average  $0.67 \cdot 10^{-4}$ ) and of the upper basal peat (average  $0.86 \cdot 10^{-4}$ ) are close to the seawater ratio ( $0.78 \cdot 10^{-4}$ ) reflecting anoxic-sulfidic conditions as suggested by Crusius *et al.* (1996). In the lagoonal sediments only As (Figure 2.2.9f) shows a correlation with the TS content ( $r=0.70$ ).

Enrichment factors relative to average shale for selected trace elements, Fe, and P on a OM-free basis ( $\text{EFS}_{\text{OMF}}$ ) are shown in Figure 2.2.11 for the peat beds. The calculation of EFS is based on the expression:

$$\text{EFS}_{\text{element}} = \text{element}_{(\text{OM-free}) \text{ sample}} / \text{element}_{\text{av. shale}}$$

It should be noticed that Mo and Re show highest enrichments in the reed peat beds (especially in the lowest reed peat) and in the upper basal peat. Furthermore As and U are enriched in these samples. As, Mo, Re, and U occur as oxyanions in relatively high concentrations in seawater (Bruland, 1983; Goldberg, 1987) while their geogenic background is comparatively low (Wedepohl, 1971; Colodner *et al.*, 1993). An exception is V which also occurs as an oxyanion in seawater, but which has a very high geogenic background value of about  $130 \text{ mg kg}^{-1}$  in average shale. Hence seawater has to be regarded as the main source for the trace metal enrichments. A reason for the lower enrichment of trace metals in the upper reed peats of the OCIU (Figure 2.2.11) may be related to the special topographic situation, possibly a fluvial levee with a decreasing marine and a distinct freshwater influence, respectively. Additional influence by the river Weser could have supported this freshening, too.

The remaining trace metals investigated show no significant enrichments or depletions relative to average shale (Figure 2.2.11). Hence it can be concluded, that in the reed peats and in the upper basal peat beds processes of element mobilization and fixation from surrounding clastic sediments are less important for the trace metal distribution. In this context it has to be considered that the lagoonal sediments are characterized by anoxic conditions as seen from the DOP-values. Therefore redox-sensitive elements are easily fixed and should not significantly be affected by mobilization processes.

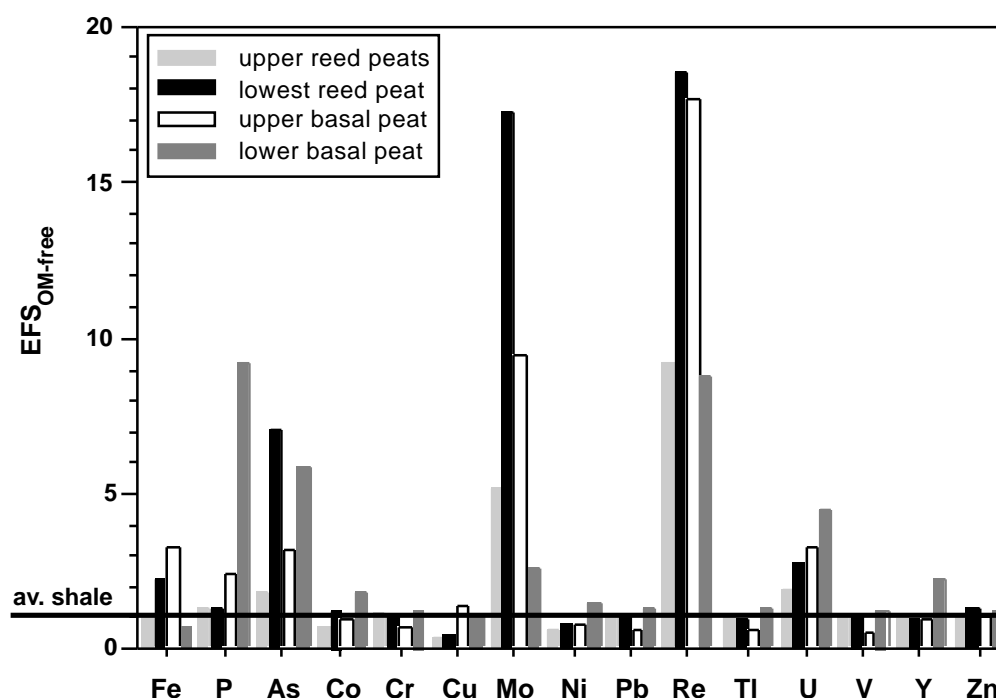


Figure 2.2.11: Enrichment factors for Fe, P, and selected trace elements versus average shale on an organic matter-free basis ( $EFS_{OMF}$ ) for different peat sections. Average shale from Wedepohl (1971).

In contrast to this scenario limnic conditions persisted in the lower part of the OBU. P is highly enriched in the lower basal peat (Figure 2.2.11). The P content partly reaches 1.35%  $P_2O_5$  (Figure 6d) presumably as a result of microbial degradation of organic matter and fixation of P as vivianite ( $Fe_3(PO_4)_2 \cdot 8H_2O$ ). P correlates in this section with Fe ( $r=0.87$ ), which supports the presence of vivianite, which is a typical indicator for anoxic, organic-rich, non-marine sediments, where not enough  $H_2S$  is produced to

convert the available reactive Fe into pyrite (Berner, 1980; 1981). This mineral is often found in moors and freshwater muds under S-limited conditions (Göttlich, 1990; Scheffer and Schachtschabel, 1992).

Furthermore the trace elements As, U, V, and Y which can be incorporated into phosphates (Nathan, 1984) are enriched in this section of the core (Figure 2.2.11). Further diagenetic mineral formation is evident in brackish sediments below the S-rich section in the depth interval 13.75-14.00 m with  $P_2O_5$  contents of about 0.7% (Figure 2.2.6d). Here a lower sulphate pore water concentration may be assumed. Enhanced organic matter decomposition would result in a more readily exhausted sulphate reservoir and lead to a higher probability of vivianite formation.

### **Summary and concluding remarks**

The inorganic-geochemical and diatom investigation carried out on a Holocene coastal sequence of NW Germany has led to a detailed description of the Holocene palaeoenvironment, which can be summarized as follows:

- The organic basal unit (OBU) formed under limnic conditions independent of the Holocene sea-level rise. This is indicated by high  $P_2O_5$  concentrations (probably related to the formation of vivianite), limnic diatoms and high TOC/TS-ratios. Mean Jungwurm-loess seems to contribute significantly to the terrigenous-detrital fraction of the OBU. Only the upper part of the OBU is characterized by a distinct pyrite enrichment resulting from microbial reduction of sulfate, which diffused downward from overlaying marine sediments. S-isotope values therefore reflect closed system conditions. Marine planktonic diatoms also record the first marine influence.
- The lower clastic unit (LCU) shows signals of high and lower wave-energy conditions, which correlate with the course of the Holocene sea level curve. The brackish sediments of the LCU are characterized by diagenetic overprints possibly resulting from changes in salinity. Therefore, pyrite is found enriched in the upper

part of this section while vivianite is present below. The diatom assemblages of the LCU change from marine pelagic to brackish littoral species.

- The organic-clastic interfingering unit (OCIU) is marked by an alternation of reed peat beds and clastic sediments. This unit is characterized by high contents of pyrite and enrichments in redox-sensitive trace elements. The distribution of trace metals suggests seawater as the main source for sulphate and trace metals. The amounts of pyrite and trace metals depend on exposition to seawater and thus distance to the coastline. S-isotope values are compatible with both, open and more closed system conditions. The dominance of littoral brackish diatoms in the OCIU reflects lower salinities and calm depositional conditions. Nevertheless the co-occurrence of marine pelagic diatoms shows the close distance to the former coastline.
- The upper clastic unit (UCI) with its variable succession of lithological facies reflects the fluctuating sea-level rise at this time interval. A distinct evidence for the increasing influence of the river Weser on the sediments under investigation could not be proven by our inorganic-geochemical data set, but the increase in abundance of *Cyclotella meneghiniana*, a characteristic species of the river Weser, indicates the fluvial influence on the UCI. Taking the  $^{14}\text{C}$ -age of the uppermost reed peat of the OCIU into account, the river Weser has reached its present position next to the drill site after 2,650 BP. The analyses suggest that major controls on the palaeoenvironments were (i) climate-related oscillations of the coast line and (ii) the morphology of the coastal region allowing marine incursions even into distal semi-terrestrial lowlands. The combination of inorganic-geochemical data with diatom analyses significantly improves the recognition of palaeoenvironmental changes and corroborates palaeoenvironmental reconstruction.

**Acknowledgements** - The authors wish to thank Prof. Dr. H. Streif and Dr. J. Barckhausen (Geological Survey of the Federal State of Lower Saxony, Germany) for the supply of sample material and for the lithological core descriptions. Furthermore we would like to thank Prof. M. A. Geyh for performing the  $^{14}\text{C}$ -age determinations

(Geological Survey of the Federal State of Lower Saxony, Germany), Dr. M. E. Böttcher (Max-Planck-Institute Bremen, Germany) for carrying out the S-isotope measurements, and W. Bartels (LUFA, Soil-physical Laboratory, Germany) for botanical macroresidual analyses. Thanks also to Prof. J. M. Gieskes for critically proofreading an earlier version of this manuscript and helpful comments.

This study is funded by the German Science Foundation (DFG) through grant No. Scho 561/2-3 and forms part of the interdisciplinary special research program "Biogeochemical changes over the last 15,000 years - continental sediments as an expression of changing environmental conditions".



### **2.3. Microfossils and geochemical data used as tools for palaeoenvironmental reconstruction of a Holocene depositional sequence from the coastlands of NW Germany**

F. Watermann, O. Dellwig, H.-J. Brumsack, G. Gerdes, W. E. Krumbein

**Abstract** - Holocene deposits of the coastal zone of NW Germany reflect former sea-level changes as a response to the climatic development. The sea level fluctuations led to lateral interfingerings of marine, brackish, and lagoonal sediments as well as peat layers. A drill core from the marshlands of NW Germany which covers the entire Holocene was analysed at high-resolution for diatoms, and foraminifera inventories as well as geochemical parameters. Ratios were calculated between diatom species which characterize different ecological groups with respect to salinity (polyhaline, mesohaline, and oligohaline) in order to obtain information about changing conditions in palaeosalinity. Ratios between marine pelagic and littoral diatom species were used for the interpretation of palaeotransport conditions and palaeohydrodynamics. Geochemical parameters, e.g., TOC content, Si/Al-, Zr/Al-, and Ca/Sr-ratios provide information about lithofacies changes, type and origin of deposited material, and depositional energy. The stratigraphic record of the core reveals four lithological units: (i) an organic basal unit (fen and bog peat), (ii) a lower clastic unit, (iii) an organic interfingering unit (fen peat), and (iv) an upper clastic unit. The top of the core forms a layer consisting of cultivated soil. Organic Basal unit: The abundance of diatoms differs fairly wide in the basal peat. In the lower part, which consists of fen woodland and bog peat, diatoms are almost absent, while the uppermost part (fen reed peat) is characterized by an increase of marine pelagic diatoms. All species are allochthonous. The presence of marine pelagic diatoms reflects a proximal coastline and periodical flooding. Increasing contents of lithogenic elements (Si, Rb, Zr), which coincide with a decrease in TOC, occur thin clastic layers (1-3 mm), brought in by tidal channel activities. Lower clastic unit: The frequent occurrence of marine pelagic diatoms (e.g. *Paralia sulcata*) documents increasing marine conditions which can be also evidenced by Ca/Sr-ratios in the range of biogenic calcite. Salinity changes are indicated by a varying dominance of littoral polyhaline, mesohaline, and oligohaline diatoms. As a result of the sea-level rise and, thus increasing marine influence, the lower part of the lower clastic unit is characterized by a change from lagoonal over brackish to tidal flat sediments. The upper part of this unit shows the reverse development as a result of a prograding coastline.

The development from lagoonal to tidal flat and again to lagoonal sediments resulted from changing depositional energy, which can be evidenced by the varying abundance of poorly silicified littoral species and Zr/Al-ratios. Organic interfingering unit: The prograding sequence finally merges in an intercalated reed peat layer whose diatom assemblage reflects brackish to freshwater conditions. Upper clastic unit: A further transgression led again to the deposition of lagoonal sediments. Furthermore this unit contains natural levee and salt marsh deposits. Littoral mesohaline and limnic diatoms in the upper clastic unit are typical for periodically drying-up brackish pools which are protected by a natural levee. Therefore, no fully marine conditions were ceased in the uppermost part of the core. Some horizons, however, show enrichments of marine pelagic diatoms and Zr indicating occasional storm events. Over all the microfossil distribution coincides well with geochemical parameters. Based on the synopsis of these data, the palaeogeographical position of the borehole may have been in a quite protected area, probably a shallow bay containing a rather broad silting-up zone. Seawater, supplied by tide currents, was mixed with freshwater from the hinterland, thus creating brackish water habitats even in close vicinity to the North sea.

### **Introduction**

The evolution of the NW German coastal area is decisively characterized by the Holocene sea level rise after the Weichselian glacial with its maximum 18,000 years BP. Since then the sea level rises with a generally decreasing rate from about -120 m to the actual niveau (Long *et al*, 1988). The time period between 9,000 - 6,000 years BP is characterized by a steep rise of about  $11 \text{ mm a}^{-1}$  (Behre, 1993) followed by a period of a distinct slow down with phases of stagnation and even regression (Behre, 1993; Streif, 1990). The Lower Saxonian coastlands with barrier islands, tidal flats, and marshes, were formed after 7,500 years BP (Streif, 1990). As a result of this development, various lithofacies, e.g., from tidal flats, brackish water environments, and peat developed.

In the scope of the special research programme "bio-geochemical changes over the last 15,000 years - continental sediments as an expression of changing environmental conditions" initiated by the German Science Foundation several cores were drilled with the support of the Geological Survey of the Federal State of Lower Saxony (Germany) at four locations in the NW German coastal area. These cores cover the entire Holocene deposits and were investigated at high-resolution for diatom inventories and geochemical parameters.

In the study presented here, a core from the Wangerland marshlands (Figure 2.3.1) was analysed at high-resolution for diatom and foraminifera inventories and geochemical parameters. The major aim was to document palaeoecological changes caused by the coastline shifting in relation to the fluctuating sea level. Palaeosalinity conditions, transport processes, depositional energy, and the provenance of the sediments were derived from the combined analysis of diatoms and foraminifera as well as geochemical parameters.

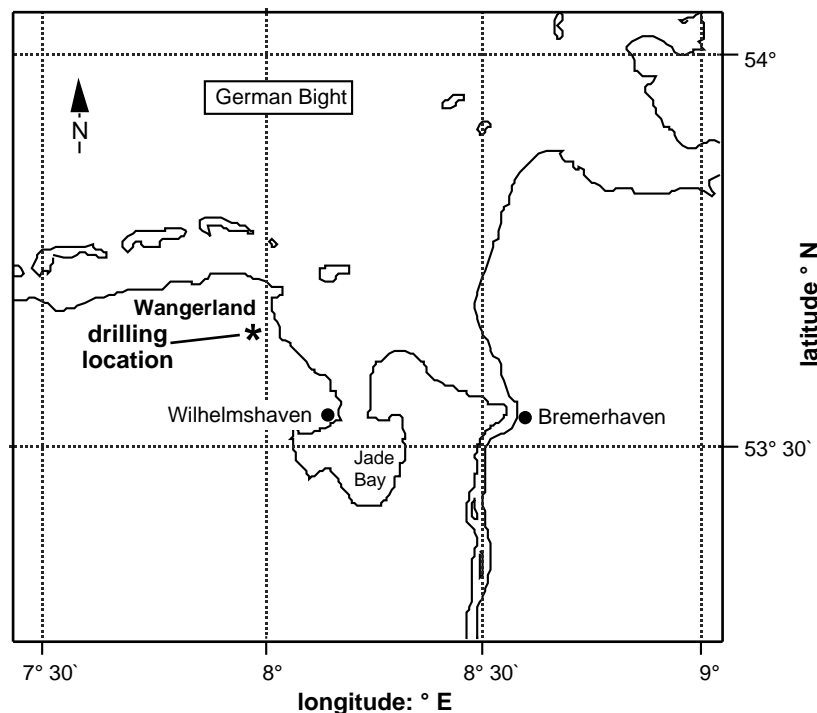


Figure 2.3.1: Study area and location of drill site in the marshlands of the Wangerland (NW Germany).

### **Regional setting and lithology**

This work bases on a drill core (W5; Archive No. KB 5950) from the Wangerland marshlands about 18 km NW of Wilhelmshaven close to the Jade Bay (Figure 2.3.1). The core was drilled in August 1996 with the support of the Geological Survey of the Federal State of Lower Saxony (Germany) using a drilling system after Merkt and Streif, (1970). The core has a total length of 6.80 m and covers the entire Holocene deposits.

The SE part of the Wangerland marshland area was formerly a sheltered so-called Crildumer Bay (Petzelberger, 1997), which was characterized by the occurrence of several deeps due to tidal channel activity.

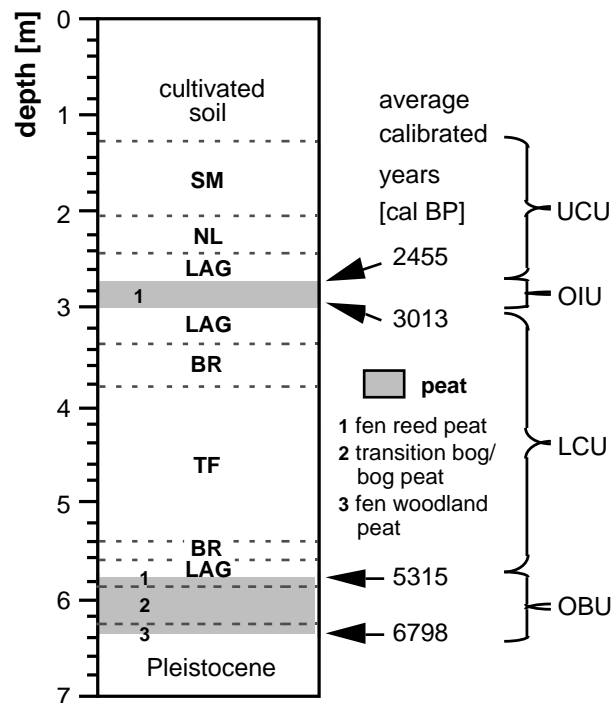


Figure 2.3.2: Profile of the drill core showing the lithology (BR=brackish, LAG=lagoonal, NL=natural levee, SM=salt marsh, TF=tidal flat) and the four main sedimentary units (OBU=organic basal unit, LCU=lower clastic unit, OIU=organic interfingering unit, UCU=upper clastic unit) as well as  $^{14}\text{C}$ -age determinations of four peat samples [average calibrated years BP]. Peat layers are indicated by grey areas.

According to the lithological classification after Barckhausen *et al.* (1977) the core W5 is composed of four different lithological units (Figure 2.3.2): (i) an organic basal unit (OBU) consisting of different fen and bog peats, (ii) a lower clastic unit (LCU) which contains lagoonal, brackish, and tidal flat sediments, (iii) an intercalated reed peat which represents the organic interfingering unit (OIU), and (iv) an upper clastic unit (UCU) consisting of lagoonal sediments, a natural levee, and salt marsh deposits.

Four peat samples were chosen for  $^{14}\text{C}$ -age determinations kindly carried out by M.A. Geyh (Geological Survey of the Federal State of Lower Saxony, Germany). The resulting average calibrated ages were calculated using the  $^{14}\text{C}$  age calibration program

CALIB 3.0 (Stuiver and Reimer, 1993) and are also presented in Figure 2.3.2. The deepest sample from the OBU with an average age of about 6,800 years BP reflects the onset of peat formation, while the age from the top of the OBU (5,315 years BP) coincides with the time when the first marine contact occurred. The formation of the intercalated reed peat layer of the OIU approximately occurred between 3,010 and 2,460 years BP.

### **Material and methods**

*Diatoms* - Littoral and pelagic diatoms were isolated from 53 selected samples according to Schrader (1973). To obtain evidence on relative abundance, counts were done with a microscope at 1000X magnification. Quantity analyses were based upon maximal counts of 200 frustules (Lund *et al.*, 1958). Diatom counts were made in triplicate of sample (0,1–1 ml depending of the suspension) using counting chambers (Utermöhl, 1958) under an inverted microscope (400X magnification). At some levels with very low valve concentration a smaller count was taken. Frustule fragments  $>1/2$  were counted as a whole (Schrader and Gersonde, 1978). If no diatoms were found by applying the method of Schrader (1973), the following application was used: The samples were homogenized and dried, treated with 15% hydrogenperoxide for one hour, suspended in water and passed through sieves of 500  $\mu\text{m}$  and 63  $\mu\text{m}$  mesh size. Afterwards the fractions were dried for 12 h at 60°C. The diatom contents were analysed in subsample triplicates of at least 500 mg. Diatoms of the  $>63 \mu\text{m}$  fraction were counted at 200X magnification using a Zeiss Stemi SV 11 binocular. The described method is used for peat samples which often contain poorly diatom inventories ( $<100 \text{ valves g}^{-1}$ ).

Taxonomy of the diatoms was facilitated by mounting diatoms in Naphrax resin. The species were identified using a light microscope (Zeiss Axiophot) at 1000X magnification. In several cases an electron microscope (Hitachi S-3200) was additionally used for taxonomic identification (Round *et al.*, 1990). Species identification was also based on Drebes (1974), Hartley (1996), Hustedt (1957) and Pankow (1990). The

diatom species were divided into different salinity tolerance groups according to Simonsen (1962): (i) polyhalobous-marine taxa (~30‰), (ii) mesohalobous-brackish taxa (0.2-30‰), and (iii) oligohalobous taxa (0-20‰). Halophilous taxa which can live in both brackish water and freshwater have their optimum in brackish water while the optimum of indifferent taxa is freshwater. An extensive classification is based on Vos and De Wolf (1993). These authors classified the diatoms not only in relation to their salinity optimum, but also according to their specific substrate demand.

*Foraminifera* - Sediment samples were collected from the borehole. Sampling was carried out in triplicate. The samples were dried, weighed and treated with H<sub>2</sub>O<sub>2</sub> to remove the organic material which makes the separation of foraminifera tests difficult. The samples were sieved on 500 and 63 µm meshes (Schröder *et al.* 1987), dried at 50°C and weighed.

Foraminifera were identified with the help of Bartenstein (1938), Boltovskoy and Wright (1976), Feyling-Hanssen (1972), Hansen and Lykke-Andersen (1976), Hofker (1977), Loeblich and Tappan (1988), Miller *et al.* (1982), Murray (1979), Richter (1964), and van Voorthuysen (1960). Foraminifera were counted on species level. Mean values were calculated from triplicates. Counts of individuals belonging to each species were characterized in terms of relative abundance.

*Geochemistry* - High resolution sampling was performed at 5 to 10 cm intervalls in clastic and 1 to 3 cm intervalls in peat samples. The samples were stored in polyethylen-bags, sealed, and immediately frozen. Afterwards the samples were freeze-dried and homogenized in an agate mortar. The ground powder was used for all subsequent geochemical analyses.

A total number of 163 samples were analysed for major elements (Al, Ca, Fe, K, Mg, Si, Ti) and trace elements (Mo, Rb, Sr, Y, Zr) by XRF (Philips PW 2400, equipped with a Rh-tube) using fused borate glass beads. Peat samples were heated to 500°C to remove TOC prior to adding lithiumtetraborate and fusing in Pt-Au-crucibles. Analytical precision and accuracy of XRF measurement was tested by replicate analysis of

geostandards (GSD-3, GSD-5, GSS-6, SDO-1, SGR-1) and several in-house standards (see appendix).

Bulk parameters were analysed in 124 samples. Total carbon (TC) and total sulphur (TS) were determined by combustion using an IR-analyser Leco SC-444. Inorganic carbon (TIC) was determined with a Coulometrics Inc. CM 5012 CO<sub>2</sub> coulometer coupled to a CM 5130 acidification module (Huffman, 1977; Engleman *et al.*, 1985). The TOC content was calculated as the difference between TC and TIC. The precision of bulk parameters was checked in series of double runs and accuracy was determined by using in-house standards (see appendix).

## **Results and discussion**

### *Identification of lithofacies*

With the help of the total organic carbon (TOC) profile (Figure 2.3.3a) a basal peat layer of about 65 cm thickness becomes discernible, which represents the organic basal unit (OBU; 5.79-6.44 m). The basal peat consists in the lowest part (6.45-6.36 m) of fen woodland peat which then change to raised bog peat and transition bog peat (6.36-5.84 m), followed by a fen reed peat layer in the uppermost part (5.84-5.78 m). For a more detailed description of the peat-forming vegetation see Dellwig and Brumsack (1999a). The highest TOC contents of maximum 52.6% are found in the raised bog peat of the OBU (average OBU 39.7%). The transition between the fen woodland peat and the raised bog peat of the OBU is characterized by a distinct decrease in TOC which coincides with elevated amounts of lithogenic elements as seen in increasing Si/Al-, Zr/Al-, and Rb/Al-ratios (Figures 2.3.3b-d). These enrichments of lithogenic elements occur in thin clastic layers within the peat as a result of tidal channel activities. The formation of these clastic layers and their effects on the palaeoenvironmental reconstruction is discussed in detail by Dellwig *et al.* (1999a).

The almost carbonate-free sediments (Figure 2.3.4a) of the lowest part (depth interval 5.79-5.60 m) of the lower clastic unit (LCU) reflect a shale-like composition

which is also documented by low Ca/Sr-ratios (Figure 2.3.4b) close to the average shale (Ca/Sr=70, Wedepohl, 1971). Therefore, this section can be classified as a lagoonal facies with a restricted marine influence. The following section (depth interval 5.60-5.40 m) shows an increasing marine influence which can be seen in high Ca/Sr-ratios (>210) indicative for biogenic carbonate (Figure 2.3.4b). The increasing Si/Al- and Zr/Al-ratios (Figures 2.3.3b and c) of the following deposits (5.40-3.80 m) with a maximum between 4.80-4.20 m reveal higher depositional energy conditions. Si/Al-ratios are indicative for elevated amounts of quartz while the Zr/Al-ratios reflect the occurrence of heavy minerals like zircon. Therefore, these signals of an increasing depositional energy allow to classify this section as tidal flat facies.

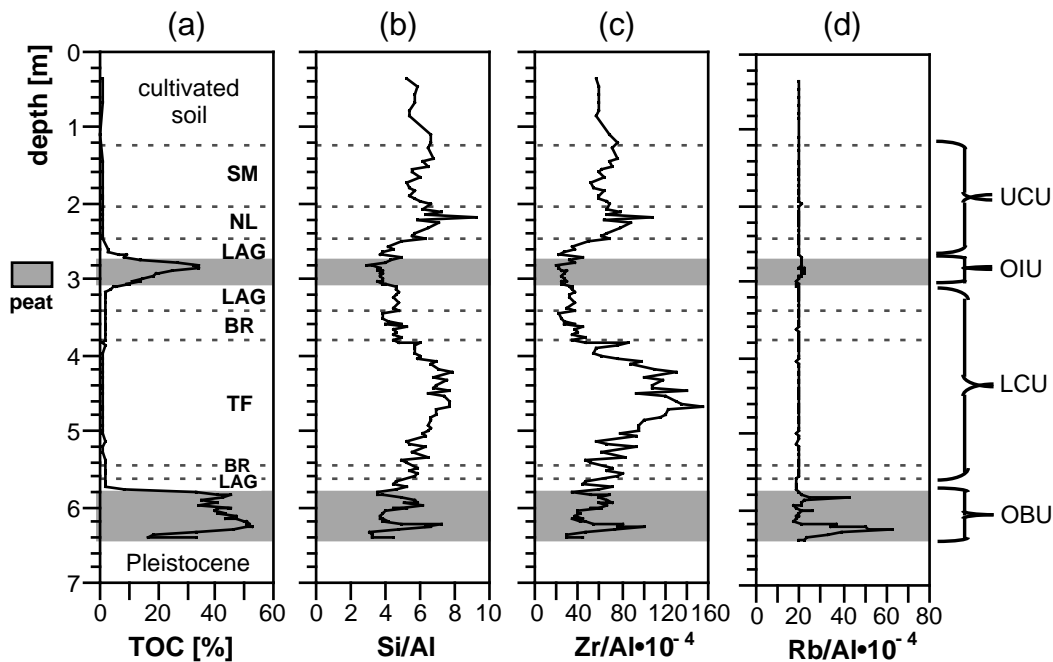


Figure 2.3.3: Depth profiles of TOC, Si/Al-, Zr/Al-, and Rb/Al-ratios of the drill core. (BR=brackish, LAG=lagoonal, NL=natural levee, SM=salt marsh, TF=tidal flat).

The profiles of TIC and Ca/Sr-ratios (Figures 2.3.4a and b) suggest a gradual transition from lagoonal over brackish to tidal flat conditions in this lower part of the LCU, i.e., a moderate transgressive development. Hence, erosion effects seem to be of minor importance, so that the average age of 5315 years BP of the upper reed peat of the OBU



dates the moment of the first direct marine contact. Above the tidal flat sediments a change to calmer depositional conditions is obvious as seen by decreasing Si/Al- and Zr/Al-ratios (Figures 2.3.3b and c). This section (3.80-3.38 m) can be again classified as a brackish facies. In the uppermost part of the LCU (3.38-3.03 m) the decreasing Ca/Sr-ratios evidence the occurrence of lagoonal sediments which form a transition to the following reed peat layer of the organic interfingering unit (OIU). This intercalated reed peat (2.73-3.03 m) is characterized by comparatively low TOC contents of average 25.8% due to higher proportions of clastic material via periodical flooding. The occurrence of the intercalated reed peat indicates a stagnation or even regression of the sea-level rise (Streif, 1990). However, it should be considered, that during a weak transgression the rate of peat formation can balance the sea level rise, leading to an apparent stagnation or regression. Therefore the intercalated reed peat was formed under moderate hydrodynamic conditions and a restricted marine influence.

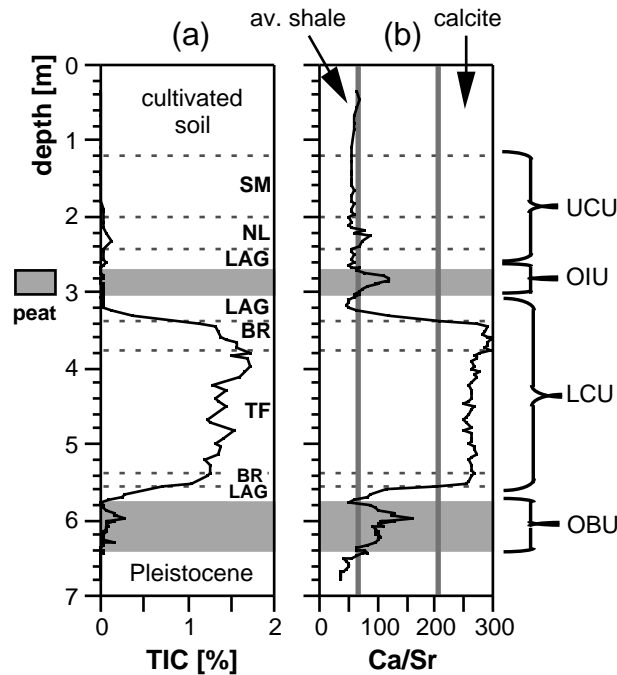


Figure 2.3.4: Depth profiles of TIC and Ca/Sr-ratios of the drill core. Average shale after Wedepohl (1971) and the range of Ca/Sr-ratios of calcite after Pingitore and Eastman (1985). (BR=brackish, LAG=lagoonal, NL=natural levee, SM=salt marsh, TF=tidal flat).

The intercalated reed peat is overlaid by clastic sediments of the upper clastic unit (UCU) as seen in a distinct decrease in TOC (Figure 2.3.3a). However, shale-like Ca/Sr ratios (Figure 2.3.4b) documented that no fully marine conditions were ceased within the UCU. The depth interval between 2.73-2.45 m can be classified again as a lagoonal facies while the section from 2.45-2.10 m consists of natural levee deposits. Such a levee forms the highest depositional facies of the Holocene coastal deposits (Streif, 1990). A marine influence on the natural levee occurred only during storm events as seen by peaks in Si/Al- and Zr/Al-ratios (Figures 2.3.3b and c). Above the natural levee salt marsh sediments are situated (2.10-1.27 m), which are identified by the visual core description kindly carried out by J. Barckhausen (Geological Survey of the Federal State of Lower Saxony, Germany).

#### *Abundance and diversity of diatoms*

**Organic basal unit: (OBU):** The concentration of diatoms in the OBU differs rather widely. A first increase of strongly silicified diatoms within the basal peat occurred at 6.11 m. The absence of diatoms below 6.11 m is possibly related to dissolution of diatom frustules (Vos and De Wolf, 1994). Thus, deposits isolated from a direct seawater influence, i.e., the basal peat, generally have a silica deficiency. Towards the uppermost part of the basal peat the number of diatoms increases from 60 to 3,340 frustules g<sup>-1</sup> accompanied with an increasing number of diatom taxa (Figure 2.3.5a and b). The occurrence of strongly silicified diatoms probably are results of the taphonomically enrichment due to dissolution of fragile species.

**Lower clastic unit (LCU):** The diatom abundance and diversity increases in the overlying clastic sediments in comparison to the underlying basal peat. The entire section of the LCU is characterized by the highest number of diatom taxa and diatoms in the core. The maximum of diatom number in the core is in the brackish section at 3.20m (Figure 2.3.5b).

**Organic interfingering unit (OIU):** In the OIU, which consists of an intercalated reed peat, the diatom abundance and diversity show a significant decrease. However, in

comparison to the basal reed peat (3,340 frustules  $\text{g}^{-1}$ ) the intercalated reed peat reveal a higher abundance of average 49,000 frustules  $\text{g}^{-1}$ .

*Upper clastic unit (UCU):* The UCU is again characterized by a decrease of diatom numbers. As mentioned above the intercalated peat is overlaid by a lagoonal section in which the abundance and diversity increases. Accompanied with the development of the natural levee the number of diatom taxa decreases again which is also true for the salt marsh sediments (Figure 2.3.5a).

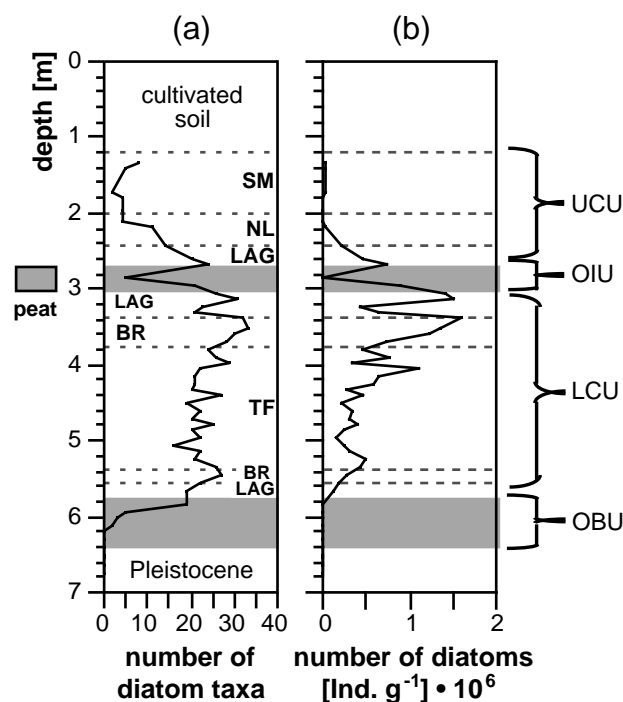


Figure 2.3.5: Depth profiles showing the number of diatom taxa and number of diatoms (individuals  $\text{g}^{-1} \cdot 10^6$ ). (BR=brackish, LAG=lagoonal, NL=natural levee, SM=salt marsh, TF=tidal flat).

#### *Comparison of the individual clastic facies*

The proportion of pelagic and littoral species for lagoonal, brackish and tidal flat sediments normalized to the total number of diatoms are shown in Figure 2.3.6a. Pelagic diatoms originate mainly from the open North Sea and indicate transport processes, whereas littoral species were deposited predominantly in or in neighbourhood to their

biotopes. Regarding the distribution of pelagic and littoral diatoms, the littoral species, which are particularly well preserved, generally show a higher abundance in clastic sediments. The littoral species occur particularly in the lagoonal and brackish facies. While the pelagic diatoms are more abundant in the tidal flat sediments.

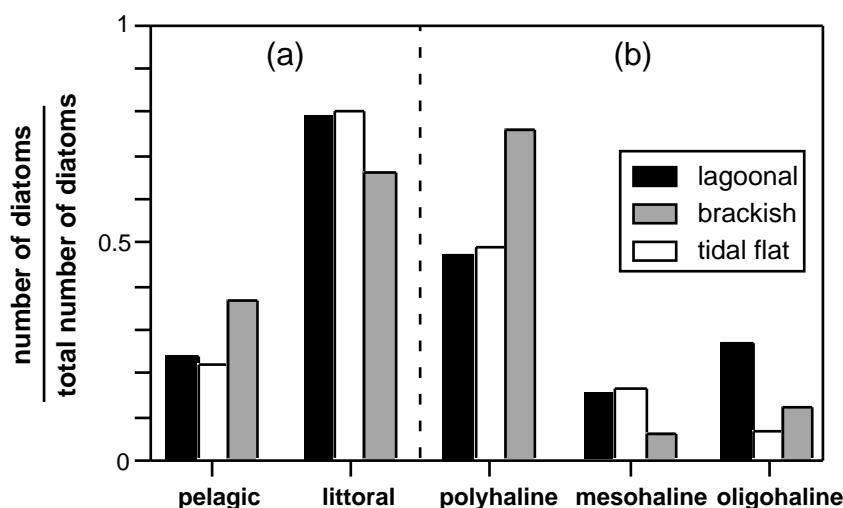


Figure 2.3.6: The proportion of (a) pelagic and littoral, as well as (b) poly-, meso-, and oligohaline species for lagoonal, brackish, and tidal flat sediments normalised to the total number of diatoms.

Figure 2.3.6b presents a differentiation of all diatoms between polyhaline, mesohaline, and oligohaline species. Generally, species tolerating polyhaline conditions are most abundant in tidal flat sediments due to the more pronounced marine conditions. The difference between lagoonal and brackish sediments is reflected by the dominance of oligohaline species in the lagoonal deposits. However, polyhaline species which occur in lagoonal and brackish sediments prove the marine influence ( storm events) as a result of the proximal shoreline. On the other hand, the co-occurrence of mesohaline and oligohaline diatoms in the tidal flat sediments document a varying salinity.

In Figure 2.3.7 the enrichment factors versus average shale (EFS) of selected major and trace elements for lagoonal, brackish, and tidal flat sediments are shown. The EFS values facilitate a comparison of the individual facies accompanied with a comparison to

an average sediment as represented by the average shale (Wedepohl, 1971, 1991). The EFS calculation bases on the following formula:

$$\text{EFS} = (\text{El}/\text{Al}_{\text{sample}})/(\text{El}/\text{Al}_{\text{av. shale}}).$$

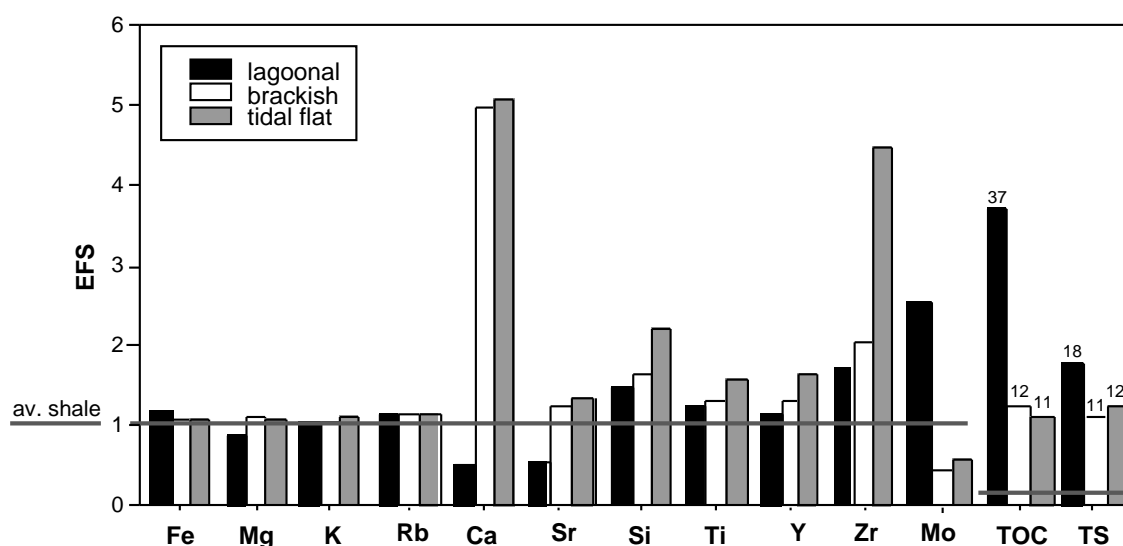


Figure 2.3.7: Enrichment factors for selected major and trace elements versus average shale (EFS) for lagoonal, brackish, and tidal flat sediments. TOC and TS values are divided by a factor of 10. Average shale from Wedepohl (1971, 1991).

The lithogenic elements Fe, Mg, K, and Rb plot close to the average shale-level, whereas Ca, Sr, Si, Ti, Y, Zr, Mo, TOC, and TS show significant enrichments in tidal flat and brackish facies. It should be noted that the TOC and TS values are divided by a factor of 10. The enrichment of Ca and Sr in the brackish and tidal flat sediments results from the above mentioned occurrence of biogenic carbonate under stronger marine conditions. The Si content and less pronounced the Ti content increases from the lagoonal sediments to the tidal flat sediments as a result of increasing wave-energy and increasing amounts of quartz and heavy minerals, respectively. Ti can be enriched in the heavy mineral fraction (e.g. ilmenite, rutile) just as Y and Zr. However, the highest enrichments show TOC and TS in all three facies. The elevated TOC content of the lagoonal sediments is to a large extent the result of the occurrence of reed rhizomes. Therefore, a higher availability of metabolizable organic matter can be assumed, which led to an enhanced formation of

pyrite as well as to an enrichment of redox-sensitive trace metals like Mo (Dellwig and Brumsack, 1999b).

Nevertheless, the amounts of TOC and TS in the brackish and especially in the tidal flat sediments are unusually high. Thus, a comparison of recent tidal flat sediments with the Holocene data set (Dellwig *et al.*, 1999b) has shown that Holocene sediments are characterized by higher amounts of fine material, i.e., clay and TOC, as a result of lower depositional energy because of lacking anthropogenic influences (e.g. dike-building).

### *Distribution of foraminifera*

Various foraminifera species, also known from modern coastal areas of NW Germany, occur in the sediment archives of the depositional sequence studied. According to their ecological requirements, the species are divided into four ecological groups. The relative abundance of each group is presented in Figure 2.3.8. Group 1 category (Figure 2.3.8a) includes agglutinated brackish water species, dominated by *Trochammina inflata* and *Jadammina polystoma*.

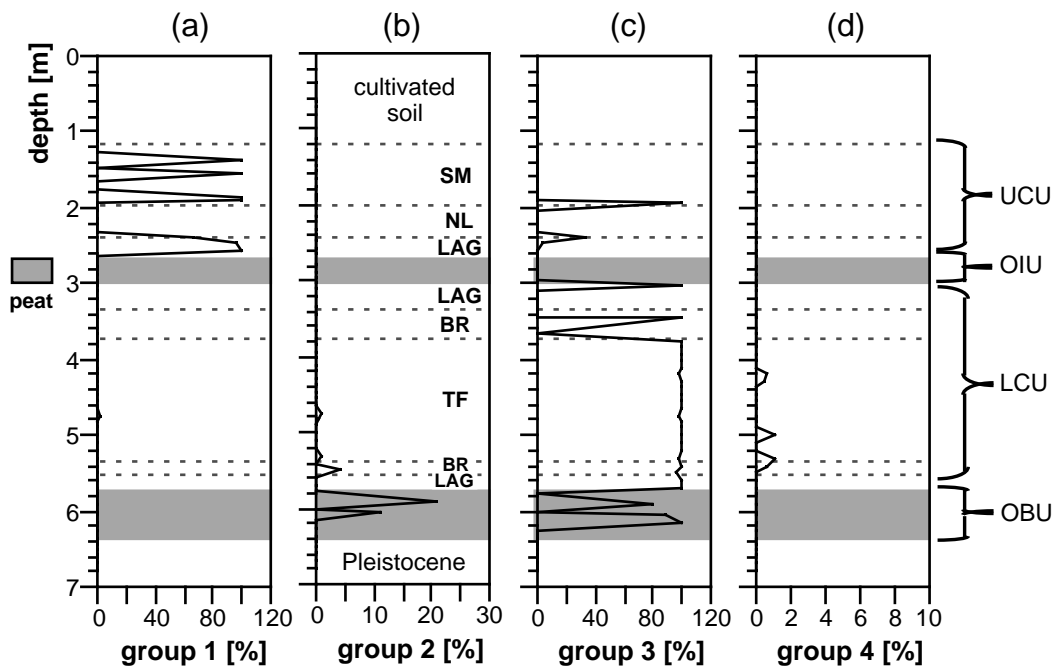


Figure 2.3.8: Relative abundance of foraminifera categorized in four ecological groups. (BR=brackish, LAG=lagoonal, NL=natural levee, SM=salt marsh, TF=tidal flat).

Figure 2.3.8b shows the Group 2 category which comprises calcifying brackish water species, e.g., *Elphidium guntheri*. Group 3 category (Fig 8c) includes calcareous species that occur widely in tidal flats (e.g., *Nonion depressulum*, *Elphidium selseyense*, *E. williamsoni*, *Ammonia beccarii*). Finally, Group 4 category (Figure 2.3.8d) comprises allochthonous marine species, introduced from the open marine realm into the coastal sediments. In the borehole strata, Group 3 and 4 categories are most abundant in the lower clastic unit, whereas Group 1 category is dominant in the upper clastic unit. Foraminifera of Group 3 and 2 categories occur already in the uppermost layers of the organic basal unit. The presence of Group 2 species points to brackish conditions. On the other hand, the occurrence of species of Group 3, coinciding well with the presence of polyhaline pelagic diatoms in these strata, supports the interpretation that the depositional environments of the basal peat experienced direct marine contact.

In the lower clastic unit, the transgressive sequence from initially lagoonal to brackish and finally tidal flat sediments (5.90 – 3.80 m) is characterized by species dominance of the Group 3 category. The other categories (Group 1, 2 and 4) are associated. The generally low concentration of Group 4 indicate a restricted access of sea water to the environment of deposition. Group 1 and 2 species underline repeated brackish intervals which may be supported by the local topography (shallow, protected, and influenced by freshwater). Similarly, the brackish intervals are also reflected by the presence of the diatom species (see below).

#### *Implications for the palaeoenvironment*

*Palaeosalinity* - Changes in salinity are best shown by the shift in the dominance of littoral diatoms. Littoral species (Figure 2.3.9a) are characteristic for palaeosalinity because these species are sedimented predominantly in their biotopes. Therefore, littoral or autochthonous species characterize the environment better than pelagic or allochthonous species.

As mentioned above the concentration of diatoms in the basal peat (OBU) differs widely and littoral species are absent. Hence, the reconstruction of the palaeosalinity during the formation of the basal peat is rather difficult. The abundance of marine pelagic

diatoms (e.g. *Aulacodiscus argus*, Figure 2.3.9b) in the transition between bog and reed peat layers (6.11-5.78 m) of the OBU indicates that this peat was formed during a first direct marine incursion. This incursion seems to be responsible for the change from bog peat to fen reed peat. In this context it has to be mentioned that the diatom profiles show the percentage of individual species in relation to the total inventory. Therefore the relatively high value of *Aulacodiscus argus* in the basal peat results from an extremely low total abundance.

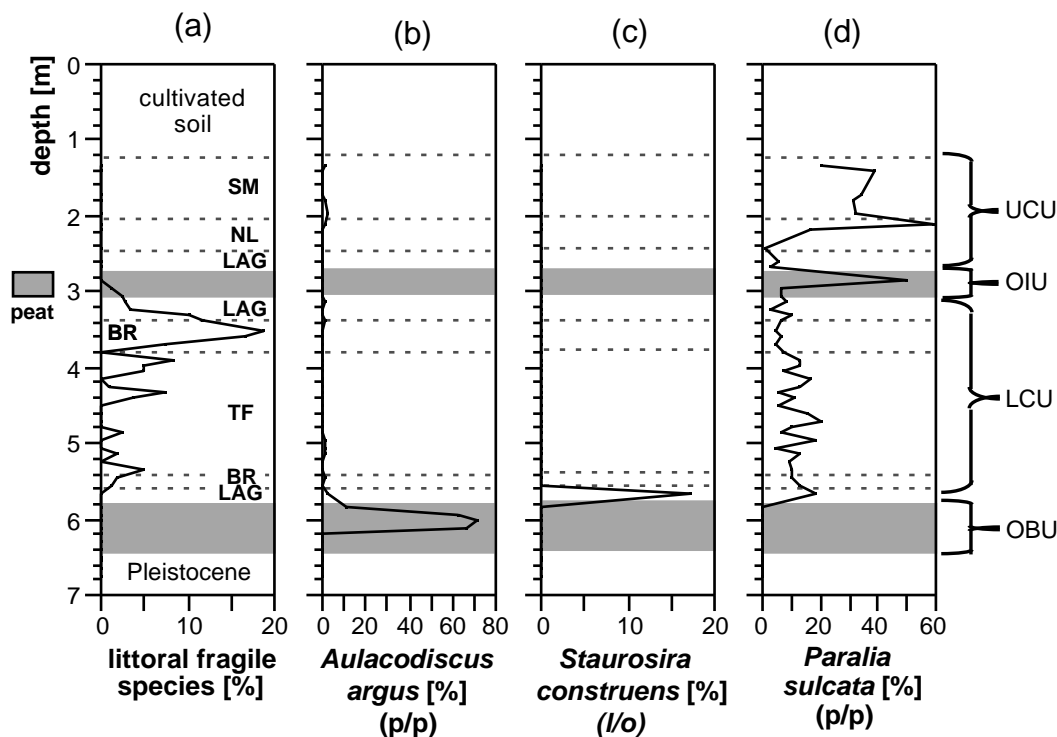


Figure 2.3.9: Depth profiles showing relative percentage of littoral fragile species as well as the relative abundance of *Aulacodiscus argus* (p/p=pelagic/polyhaline), *Staurosira construens* (l/o=littoral/oligohaline indifferent), and *Paralia sulcata* (p/p=pelagic/polyhaline). (BR=brackish, LAG=lagoonal, NL=natural levee, SM=salt marsh, TF=tidal flat).

The section between 5.78-5.60 m of the LCU is characterized by the oligohalobous-indifferent diatom *Staurosira construens* (Figure 2.3.9c) which is typical for shallow lakes and ponds (Vos and de Wolf, 1994). This species has been related to freshwater or brackish/freshwater groups (Vos and de Wolf, 1993). Additionally in this section the mesohalobous littoral species *Diploneis spp.* and *Navicula digitoradiatia* (not shown)



occur which points to a salinity of about 5‰. This finding supports the classification of this section as a lagoonal facies which is characterized by a restricted seawater influence. Therefore, an almost similar salinity has to be assumed for the reed peat layer of the OBU. Before a distinct marine incursion reached the LCU these deposits were influenced by single flooding events. Nevertheless, the coexistence of the polyhaline pelagic species *Paralia sulcata* (Figure 2.3.9d) documents the continuous seawater influence.

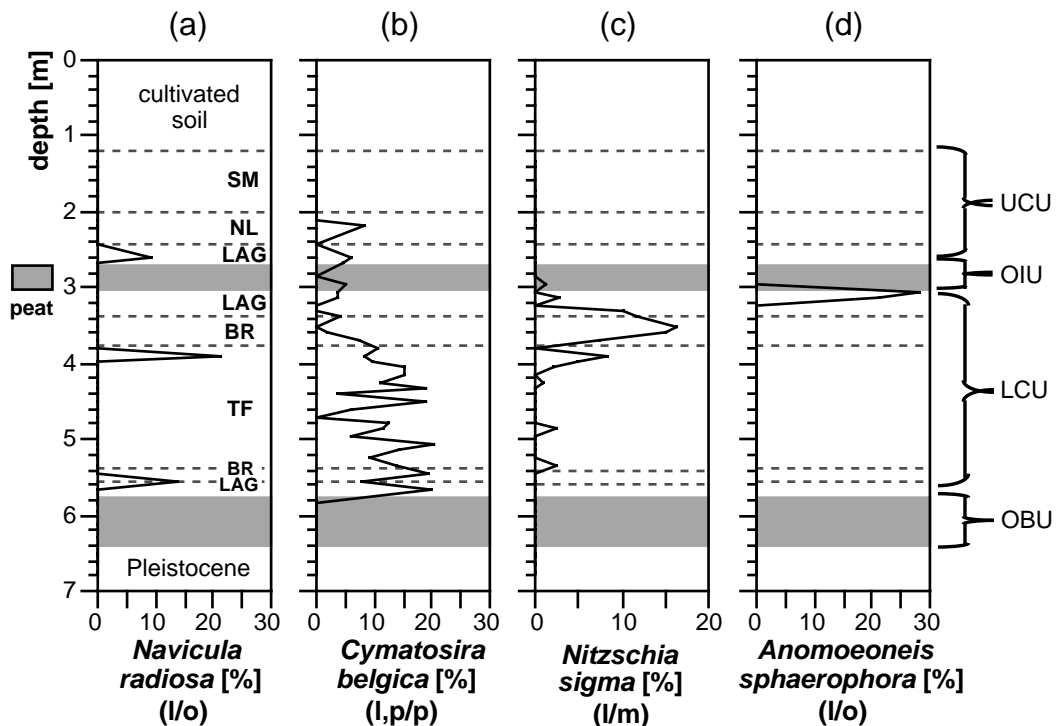


Figure 2.3.10: Depth profiles showing relative abundance of the diatom species *Navicula radiosa* (l/o=littoral/oligohaline), *Cymatosira belgica* (l/p=littoral/polyhaline), *Nitzschia sigma* (l/m=littoral/mesohaline), and *Anomoeoneis sphaerophora* (l/o=littoral/oligohaline). (BR=brackish, LAG=lagoonal, NL=natural levee, SM=salt marsh, TF=tidal flat).

Due to the persistent sea-level rise brackish mesohaline conditions appeared between 5.60-5.40 m as reflected by the decrease of oligohaline species and the increase of species with a wide salinity tolerance, e.g., *Navicula radiosa* (Figure 2.3.10a) which is indicative for a maximum salinity of 20‰ (Pankow, 1990). At the same time there is an increase in diversity and abundance of diatoms (Figures 2.3.5a and b). Polyhaline species

like *Paralia sulcata* and *Cymatosira belgica* (Figures 2.3.9d and 10b) show a higher abundance which reflects a slightly increasing tidal activity and a higher mean salinity.

In the tidal flat section (5.40-3.80 m) littoral polyhaline species reached a higher abundance (Figure 2.3.11a) and document therefore a distinct increase of mean salinity (20-30‰) and tidal activity. The dominance of littoral mesohaline species (Figure 2.3.11b) increases in the overlying brackish deposits (3.80-3.38 m) whereas the littoral polyhaline diatoms decreases. The frequent species *Nitzschia sigma* (Figure 2.3.10c) and *Scoliopleura tumida* (not shown) are mesohaline species and characterize mud-rich sediments above or close to the mean high-water level (Vos and De Wolf, 1988) indicating a highly variable salinity between 10 and 30‰.

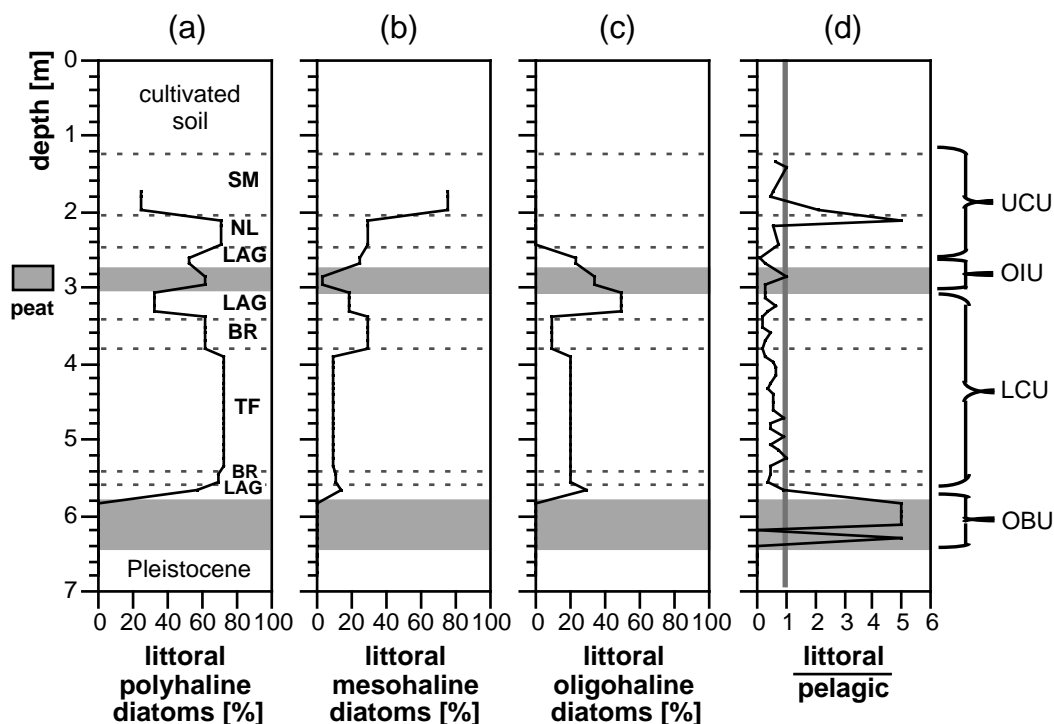


Figure 2.3.11: Depth profiles showing a-c) the relative abundance of littoral species in relation to the salinity tolerance (average values for individual lithological facies) and d) the ratio between littoral and pelagic diatoms. (BR=brackish, LAG=lagoonal, NL=natural levee, SM=salt marsh, TF=tidal flat).

The diatom assemblages in the lagoonal deposits of the uppermost part of the LCU (3.40-3.03 m) change from littoral mesohaline species (Figure 2.3.11b) to littoral oligohaline species (Figure 2.3.10c), e.g., *Anomoeoneis sphaerophora* (Figure 2.3.10d).

The diatom inventory describes this part of the LCU as a tidal lagoon with a small tidal range and a salinity of about 10-15‰. Therefore, the salinity was higher in comparison to the lagoonal sediments of the lower part of the LCU as seen for instance by the occurrence of the pelagic polyhaline species *Paralia sulcata* (Figure 2.3.9d). This development reflects the beginning of a distinct freshening and silting up process which culminate in the formation of the intercalated reed peat (OIU).

The diatom assemblage of the OIU reveals an oligohaline environment for the lower part of the OIU indicated by the littoral species *Pinnularia viridis* (Figure 2.3.12a). On the other hand, in the upper part of the OIU the diatom abundance is relatively poor but dominated by marine pelagic species (e.g. *Paralia sulcata*). Therefore, a higher mean salinity (10‰) can be assumed for the intercalated reed peat in comparison to the basal reed peat which partly reached 15‰.

As a result of a further transgression the intercalated reed peat is overlaid by lagoonal sediments which form part of the upper clastic unit (UCU). However, no fully marine conditions were ceased in the UCU as reflected by a significantly decrease in number of diatoms (Figure 2.3.5b). The lagoonal sediments (2.73-2.45 m) contain an elevated number of *Diploneis interrupta* (Figure 2.3.12b) and *Diploneis smithii* (not shown) as well as oligohaline diatoms, e.g., *Navicula radiosa* (Figure 2.3.10a). Foraminifera of the ecological Group 1 category is indicated also the brackish back-swamp character. The occurrence of *Diploneis interrupta* (Figure 2.3.12b) and *Diploneis smithii* indicate supratidal conditions (Vos & de Wolf, 1988).

*Hydrodynamic* - Features providing indications of changing depositional energy are (i) dominance shifts between littoral species of different fragility; (ii) ratios between littoral and pelagic diatoms (Figure 2.3.11d); and (iii) changing amounts of heavy minerals, as indicated by Zr/Al-ratios.

The few marine pelagic diatoms occurring in the upper basal reed peat are allochthonous and possess silica tests robust enough to withstand the transport from the open sea towards the inland settings. Such species are, e.g., *Aulacodiscus argus* (Figure 2.3.9b) and *Triceratium favus* (not shown). The dominance of species with robust silica tests in the peat thus may indicate rather a transport-selective than an

ecological phenomenon. In the succeeding lagoonal and brackish deposits, the number of littoral diatoms increases. This points to a gradual increase of calm, probably back-swamp conditions. Although the sediments are of marine origin, the calm intervals may have been long enough to support a rich microflora of littoral diatoms with relatively fragile silica tests. In the succeeding tidal flat deposits, a change towards higher depositional energy is evidenced by increasing Zr/Al and Si/Al-ratios (Figure 2.3.3b, c). This is also reflected by the decrease of littoral fragile diatoms (Figure 2.3.9a). Towards top of the tidal flat section, littoral fragile diatoms increase again, thus, indicating decreasing current or wave activities. A characteristic species of this high water zone is *Nitzschia sigma* (Figure 2.3.10c).

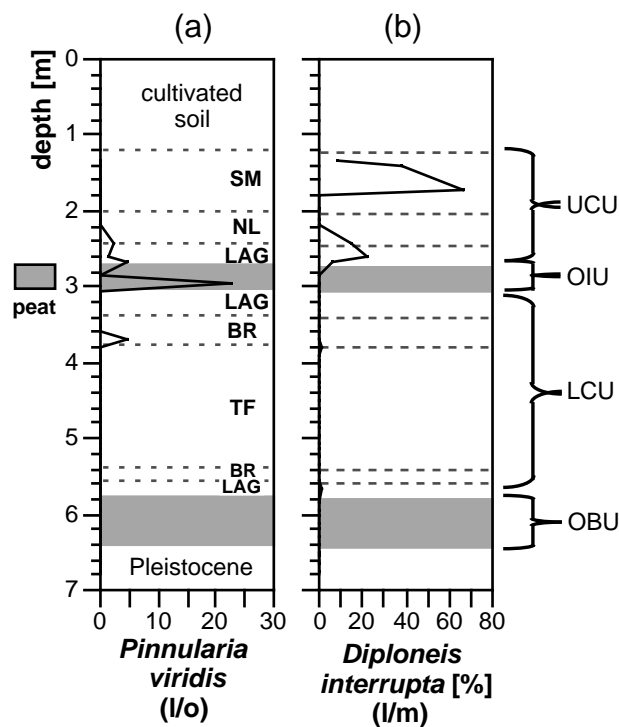


Figure 2.3.12: Depth profiles showing relative percentage of the diatom species *Diploneis interrupta* (l/m=littoral/mesohaline) and *Pinnularia viridis* (l/o=littoral/oligohaline). (BR=brackish, LAG=lagoonal, NL=natural levee, SM=salt marsh, TF=tidal flat).

In the UCU, a natural levee occurs which may have protected the depositional area against marine influence. The adjacent sediments are, thus, very fine-grained and of low quartz contents. The natural levee itself, however, may have been upheaval by

occasional storms which have brought material from nearby tidal flats. This is indicated by higher Zr/Al- and Si/Al-ratios, as well as by polyhaline pelagic diatoms, e.g., *Paralia sulcata* (Figure 2.3.9d), and finally by the foraminiferal contents (see next chapter).

Comparing the facies units representing lagoonal, brackish, tidal flat, and finally natural levee deposits, there is a correspondence between the number of diatom taxa and the quartz content. The number of taxa generally decreases with the coarsening-up sequence from lagoonal to brackish, and finally to tidal flat sediments (Figure 2.3.13). As the quartz content depends on the depositional energy, its correlation with diatom abundance and diversity provides clues on the hydrodynamical state of the palaeoenvironments as an ecological control. This was similarly stressed by de Jonge (1984).

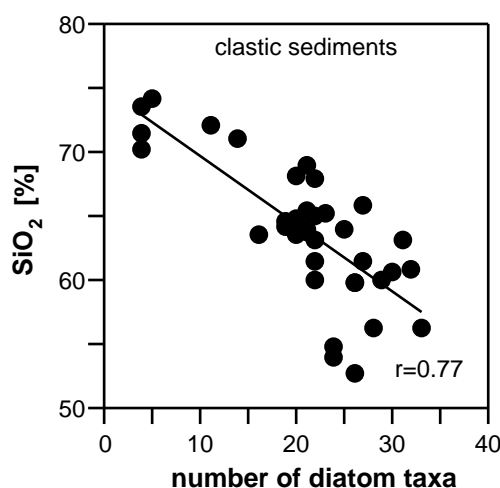


Figure 2.3.13: Scatter plot of SiO<sub>2</sub> versus the number of diatom taxa for the clastic sediments (lagoonal, brackish, tidal flat) of the drill core.

### Summary

A drill core from the marshlands close to the Jade Bay (NW Germany) was analysed at high-resolution for diatom and foraminifera inventories and geochemical parameters. The palaeoenvironmental development can be described as follows:

The investigated drill core documents two transgressive and one regressive phase as shown by the occurrence of a basal and an intercalated peat as well as clastic sediments

mainly of marine origin. The occurrence of marine pelagic diatoms and benthic foraminifera of the ecological Group 3 category only in the uppermost part of the basal peat indicate that most parts of this peat was formed without a direct seawater influence. Oligohaline littoral species and shale-like Ca/Sr-ratios indicate a salinity below 5‰ in the overlaying lagoonal sediments. The environment can be regarded as a shallow lagoon or pond with a restricted tidal influence. The following brackish deposits reflect the proceeded sea-level rise which led to a salinity up to 20‰. Diatoms and geochemical parameters (Ca/Sr-, Si/Al-, Zr/Al-ratios) reveal that tidal flat sediments of the centre part of the core are characterized by a salinity between 20 and 30‰ and increasing depositional energy. Foraminiferal assemblages, dominated by the Group 3 category, underline the tidal flat character. The overlaying brackish and lagoonal sediments are the result of a regressive phase and document therefore a silting up process. The salinity changed from polyhaline over mesohaline to oligohaline conditions accompanied with a change of the sedimentary environment from an intertidal to a supratidal zone. The silting up process culminates in the formation of an intercalated reed peat layer. The diatom inventory indicates a salinity of about 10‰. A further transgression led again to the formation of lagoonal sediments. The brackish back-swamp character also is indicated by the dominance of foraminifera of the ecological Group 1 category. The formation of a natural levee prevented the achievement a fully marine conditions.

**Acknowledgements** - The authors wish to thank J. Barckhausen (Geological Survey of the Federal State of Lower Saxony, Germany) for supporting the drill work and for the lithological core description. Furthermore we would like to thank M. A. Geyh for performing the <sup>14</sup>C-age determinations (Geological Survey of the Federal State of Lower Saxony, Germany). This study is funded by the German Science Foundation (DFG) through grant No GE 64/4-2 and No. Scho 561/3-2 and forms part of the special research program "Bio-geochemical changes over the last 15,000 years - continental sediments as an expression of changing environmental conditions".

## **2.4. Inorganic geochemistry of Holocene coastal deposits from NW Germany: An overview**

O. Dellwig and H.-J. Brumsack

**Abstract** - Coastal deposits of NW Germany were formed during the Holocene sea-level rise. These deposits consists mainly of tidal flat and brackish water sediments as well as peat layers (fen and bog peat). The peat layers can be distinguished into basal and intercalated peats. As the coastal zone reflect a very dynamic system nine drill cores from four locations were analysed at high-resolution for bulk parameter, major and trace elements by using geochemical methods (e.g. XRF, ICP-OES). Three locations are situated within (Arngast) or close to (Schweiburg, Wangerland) the present Jade Bay and one core originates from the right bank of the river Weser (Loxstedt).

In comparison to a reference peat core from the heathland the investigated peat layers show elevated contents of lithogenic elements (e.g. Al, Si, Ti) due to the influence of the rising North Sea. While the intercalated peats are characterized by periodical flooding, the basal peats are influenced by a process occurring after peat formation. As a result of tidal channel activities discrete clastic layers were formed within the basal peats which led to the inflow of seawater. Most of the peat layers are characterized by the occurrence of high amounts of pyrite due to microbial reduction of seawater sulphate as well as by enrichments of the trace metals As and Mo.

The clastic sediments can be differentiated by varying proportions of the main components quartz, clay, carbonate, and organic matter. Tidal flat sediments contain elevated amounts of quartz and heavy minerals as seen in enrichments of Si, Ti, Y, and Zr, whereas the brackish and lagoonal sediments were formed under comparatively calm depositional conditions. Especially the lagoonal sediments show an almost shale-like geochemical composition. The comparison of the four locations reveal differences between open, sheltered, and estuarine intertidal systems which are reflected by geochemical parameters (e.g. TOC, TS, As, Mn, Mo, Zr). These differences are caused by varying depositional energy and palaeosalinity and are most pronounced in the geochemistry of the peat layers and tidal flat sediments while the lagoonal and brackish show an almost similar composition for each location.

## Introduction

The coastal Holocene deposits of NW Germany were formed during the sea-level rise after the Weichselian Glacial. The rising North Sea pushed sedimentary material landwards („bulldozing effect“, Hagemann, 1969) which led to the formation of the so-called Holocene sedimentary wedge in the coastal area of Lower Laxony, NW Germany (Hoselmann and Streif, 1997). A detailed description of the Holocene evolution is given by, e.g., Long *et al.* (1988), Streif and Köster (1978), and Streif (1990). The coastal deposits contain a large number of different sediment facies which range from lagoonal to tidal flat sediments depending on exposition to the open sea. A further characteristic of the coastal area are peat layers, which can be differentiated into basal and intercalated peats. The formation of the basal peats, which overlay Pleistocene material, was often assisted by a rising groundwater level as a result of the approaching North Sea. By contrast, intercalated peat layers are situated between clastic sediments of predominantly marine origin owing to a stagnating or slowly rising sea level (Streif, 1990).

Such deposits are supposed to preserve information about the Holocene coastal development. However, geochemical studies are rare (e.g. Ludwig *et al.*, 1973; Behre *et al.*, 1985; Dellwig *et al.*, 1998) in comparison to sedimentological and palynological studies (e.g. Streif, 1971; Barckhausen *et al.*, 1977; Linke, 1979, 1982; Preuss, 1979; Barckhausen and Müller, 1984), although geochemical methods should enable a detailed reconstruction of the palaeoenvironment. Therefore, the major aim of this work is the inorganic-geochemical characterization of the different depositional facies and the use of these characteristics for a palaeoenvironmental reconstruction.

This work is based on nine drill cores from four locations (Figure 2.4.1) which presumably represent a sheltered bay (Wangerland), an open tidal flat area (Schweiburg, Arngast), and a riverine influenced tidal flat situation (Loxstedt). Except for the Arngast core the remaining cores cover the entire Holocene and contain the typical clastic facies (lagoonal, brackish, and tidal flat sediments) as well as several basal and intercalated peats.



The first part of this study provides an overview about the major component geochemistry of the investigated deposits while the second and third part focus on the geochemistry of the individual facies, i.e., peat layers and clastic sediments. The discussion of the peat layers is completed by an additional core from the heathland (Aurich Moor; Figure 2.4.1) which is used as a non-marine reference core. Furthermore, we will compare the drilling locations in the latter chapters in order to provide implications for the palaeoenvironment.

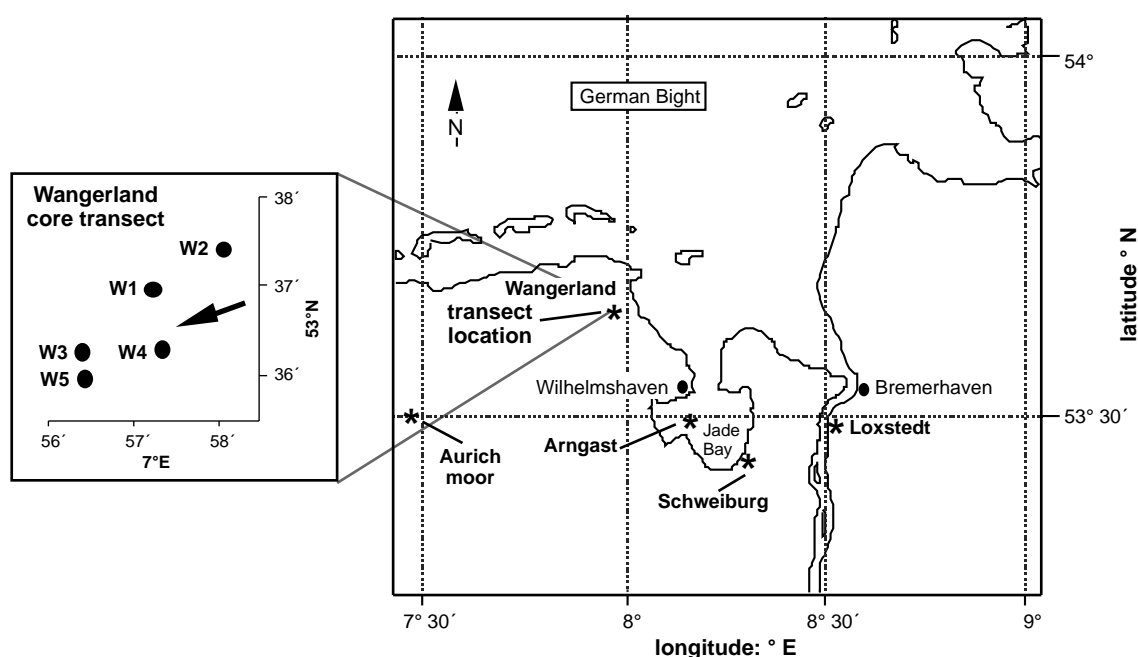


Figure 2.4.1: Map of the study area (drilling locations are indicated by asterisks) as well as the positions of the individual cores from the Wangerland transect. The arrow marks the assumed tidal channel direction.

### **Regional setting and lithology**

The cores were drilled with a drilling system (Merkt and Streif, 1970) of the Geological Survey of the Federal State of Lower Saxony, Hannover (Germany), while the reference core from the Aurich Moor was retrieved with the support of the Niedersächsisches Institut für Historische Küstenforschung, Wilhelmshaven (Germany).

The Loxstedt drill site is located about 20 km SW of Bremerhaven close to the river Weser (Figure 2.4.1) and consists of two parallel cores (Archive No. GE 430, 432) which were combined to one composite profile (Dellwig *et al.*, 1998). This site is located in the funnel-like Pleistocene watercourse of the river Weser (Müller, 1977) and therefore reflects a river influenced intertidal system.

The drill sites Schweiburg (Archive No. GE 707) and Arngast (Archive No. GE 117) from the Jade Bay (Figure 2.4.1) are supposed to reflect an open tidal flat area. The North Sea reached the present Jade Bay area about 7,000 years BP, as evidenced by age determinations of basal peats (Behre, 1978). At first an extended peat growing took place owing to the reduced drainage due to the rising sea level. The following 3,500 years are characterized by the development of an intertidal system (ancient Jade Bay) which was larger than the recent Jade Bay. Nevertheless, this phase was influenced by fluctuations of the sea level which led to the formation of several intercalated peats. It should be noted that the Arngast core (Figure 2.4.1) is only used for the discussion of peat geochemistry because recent processes of redeposition within the Jade Bay have influenced the clastic sediments.

The third location in the marshlands of the Wangerland about 18 km NW of Wilhelmshaven (Figure 2.4.1) is represented by a transect (about 3 km in length) of five drill cores (Archive No. W1=KB5552, W2=KB5156, W3=KB5750, W4=KB5752, W5=KB5950). This area was formerly a sheltered so-called Crildumer Bay which was presumably divided by a peninsula into a northern and a southern part (Petzelberger, 1997). The transect is located in the southern part of this bay. Due to tidal channel activities the Holocene basis shows a relatively uneven relief (Streif, 1990) which is reflected by the varying depth of the drill cores (Figure 2.4.2).

In Figure 2.4.2 the lithologies of the investigated cores are presented, as well. They are based on results from inorganic-geochemical and diatom analysis (Dellwig *et al.*, 1999c; Watermann *et al.*, 1999a; inorganic-geochemical data this study). The lithological classification (lagoonal, brackish, etc.) is based on the nomenclature given by Barckhausen *et al.* (1977).

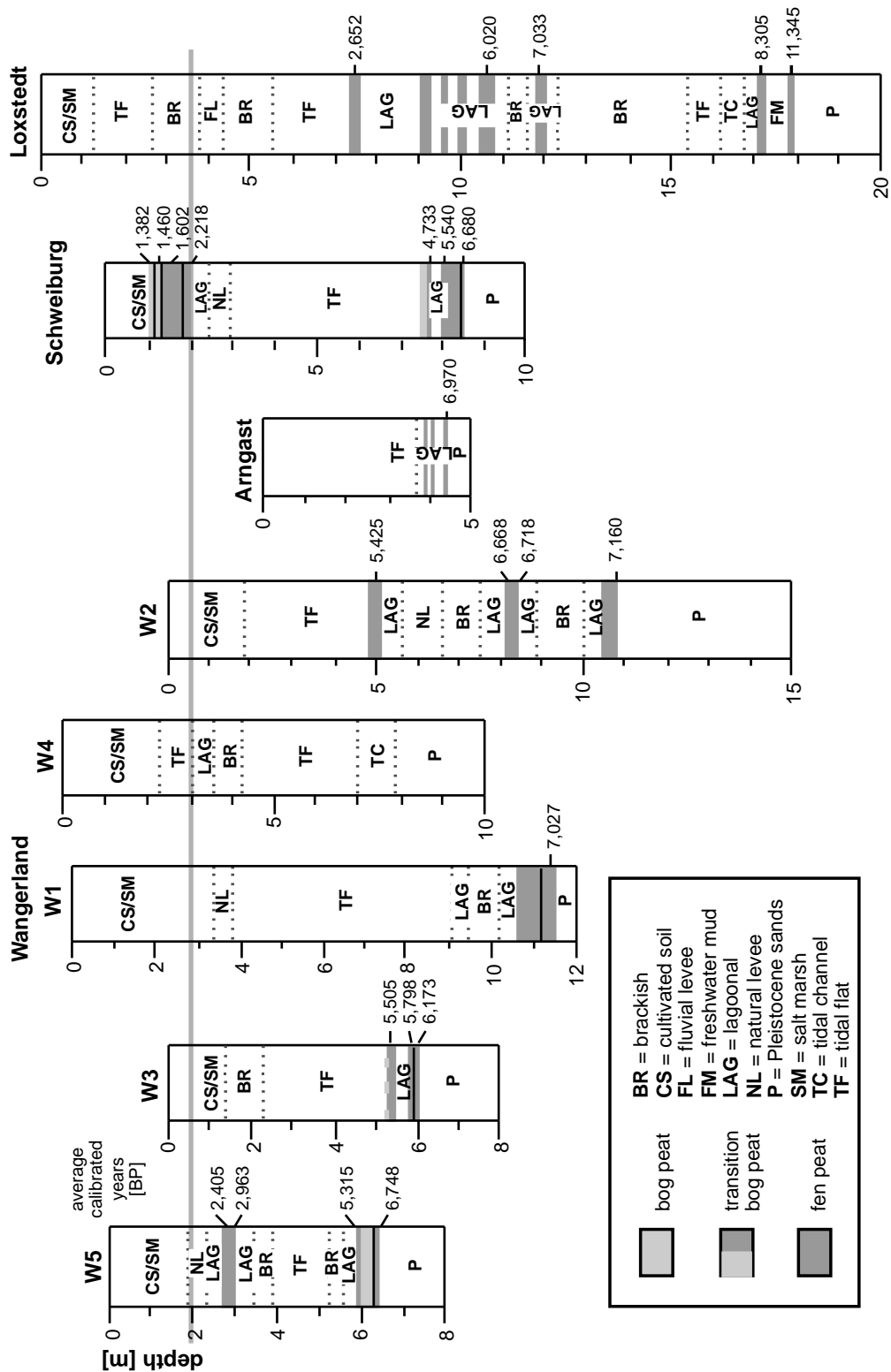


Figure 2.4.2: Lithologies and age determinations (average calibrated years BP) of the investigated drill cores. The peat layers are classified as fen and bog peat (TB = transitional bog). The black lines within the basal and intercalated peats of the cores W5, W3, W1, and Schweiburg indicate clastic layers and the grey line indicates the German zero datum [m NN].

Furthermore Figure 2.4.2 provides a simplified differentiation of the peat layers into fen and bog peat. A more detailed classification is given in Table 2.4.1, based on visual core descriptions kindly performed by J. Barckhausen and H. Streif (the Geological Survey of the Federal State of Lower Saxony, Germany) and microscopic examination of plant fragments which were carried out by W. Bartels (LUFA, Soil-physical Laboratory, Oldenburg) according to the methods given by Grosse-Brauckmann (1962).

Most intercalated peat layers consist of *Phragmites* fen peats because this plant tolerates a salinity of about 10‰ (Scheer, 1953). However, the occurrence of intercalated reed peats evidences a slowly rising or even regressive development of the sea level. An exception is the intercalated peat from the Schweiburg location which shows a development to bog vegetation. Most of the basal peats are characterized by a change from fen woodland peat to fen reed or sedge peat, which reflects an increasing marine influence. Only the Wangeland core W5 shows a development towards bog vegetation which again changed in a later stage to fen peat.

The deeper Pleistocene/Holocene boundary of the Loxstedt site led to an earlier peat formation in comparison to the remaining locations which can be seen from the age determinations presented in Figure 2.4.2. The age determinations of selected peat samples were kindly carried out by M. A. Geyh (Geological Survey of the Federal State of Lower Saxony, Germany) and were calculated using the  $^{14}\text{C}$  age calibration program CALIB 3.0 (Stuiver and Reimer, 1993). The scatter plot in Figure 2.4.3 shows the average calibrated ages of fen peat samples versus depth (relative to the German zero datum [m NN]). As most of the peat beds are directly linked to the sea level development this diagram can be used for a rough estimate of the sea-level rise rate. Therefore, the two Loxstedt basal peat samples (in brackets) are excluded because of a lacking direct relation to the rising North Sea. The reference value after Streif (1990) represents a first evidenced marine contact close to the study area. Two trends are visible: i) a rapid rise between 8,000 and 6,500 years BP and ii) a slower rise between 6,000 and 1,800 years BP. Although only a few data points are available from our cores the estimated rise rates are comparable to values reported for example by Streif (1990) and Behre (1993).

Table 2.4.1: Classification and characteristic vegetation of peat layers of the investigated drill cores.

core	depth interval [m]	peat classification	characteristic plants
Wangerland W1	10.75-11.20	fen reed peat	<i>Phragmites australis</i> <i>Cladium mariscus</i>
	11.20-11.40	fen woodland peat	<i>Alnus glutinosa</i>
W2	4.90-5.01	fen reed peat	<i>Phragmites australis</i>
	8.20-8.45	fen reed peat	<i>Phragmites australis</i>
	10.58-10.70	fen woodland peat	<i>Betula pubescens</i> <i>Sphagnum palustre</i> <i>Alnus glutinosa</i>
			<i>Sphagnum spp.</i>
W3	5.25-5.32	transition bog peat	<i>Phragmites australis</i>
	5.32-5.40	fen reed peat	<i>Phragmites australis</i>
	5.72-5.78	fen reed peat	<i>Phragmites australis</i>
	5.78-6.00	fen sedge peat	<i>Carex spp.</i>
	6.00-6.04	fen woodland peat	<i>Betula pubescens</i> <i>Carex spp.</i>
W5	2.72-3.03	fen reed peat	<i>Phragmites australis</i>
	5.78-5.83	fen reed peat	<i>Phragmites australis</i>
	5.83-6.36	bog peat	<i>Eriophorum vaginatum</i> <i>Calluna vulgaris</i> <i>Sphagnum spp.</i>
Arngast	6.36-6.45	fen woodland peat	<i>Betula pubescens</i>
	3.90-3.98	fen reed peat	<i>Phragmites australis</i>
	4.00-4.10	fen reed peat	<i>Phragmites australis</i>
	4.32-4.40	fen reed peat	<i>Phragmites australis</i>
Schweiburg	1.04-1.23	bog peat	<i>Sphagnum spp.</i>
	1.23-1.60	fen sedge peat	<i>Carex spp.</i>
	1.60-2.01	fen reed peat	<i>Phragmites australis</i>
	7.50-7.57	bog peat	<i>Sphagnum spp.</i>
	7.57-7.59	fen sedge peat	<i>Carex spp.</i>
Loxstedt	7.59-7.67	fen reed peat	<i>Phragmites australis</i>
	7.97-8.64	fen reed peat	<i>Phragmites australis</i>
	7.30-7.40	fen reed peat	<i>Phragmites australis</i>
	9.18-9.25	fen reed peat	<i>Phragmites australis</i>
	9.51-9.80	fen reed peat	<i>Phragmites australis</i>
	10.35-10.45	fen reed peat	<i>Phragmites australis</i>
	10.58-10.80	fen reed peat	<i>Phragmites australis</i>
	11.90-12.03	fen reed peat/freshwater mud	<i>Phragmites australis</i>
	17.00-17.28	fen reed peat	<i>Phragmites australis</i> <i>Sphagnum spp.</i>
	17.59-17.80	fen woodland/sedge peat	<i>Betula pubescens</i> <i>Carex spp.</i>
Aurich Moor	0-1.91	bog peat	<i>Eriophorum vaginatum</i>
	1.91-2.04	transition bog peat	<i>Erica tetralix</i> <i>Betula pubescens</i> <i>Eriophorum vaginatum</i>
			<i>Betula pubescens</i>
	2.04-2.45	fen woodland peat	<i>Betula pubescens</i>

The reference core from the Aurich Moor is 2.45 m in total length (Holocene basis) and the moor surface is +6.91 m above the German zero datum (NN). The core can be divided into three sections: i) fen woodland peat (*Betula pubescens*; 2.45-2.15 m), ii) transition bog peat (*Erica tetralix*, *Betula pubescens*; 2.15-1.91 m), and iii) bog peat (*Eriophorum vaginatum*; 1.91-0 m). An age determination of the peat basis revealed an age of 6,543 years BP (Petzelberger, pers. comm., Niedersächsisches Institut für historische Küstenforschung, Wilhelmshaven).

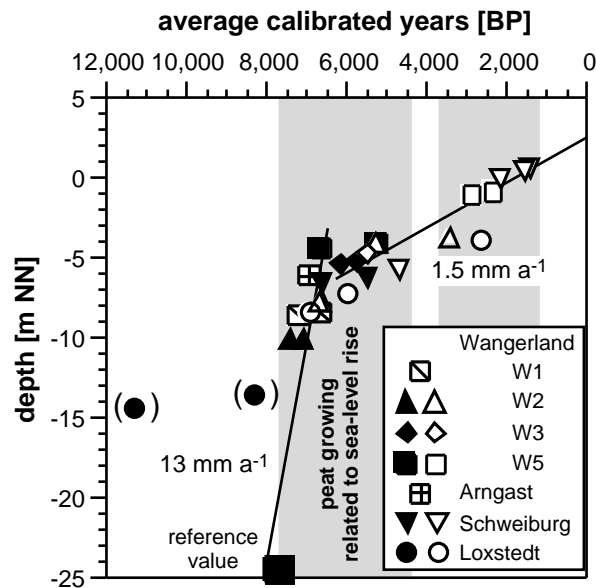


Figure 2.4.3: Scatter plot showing results of age determinations of peat samples from the investigated drill cores versus the depth related to the German zero datum (NN). Full symbols indicate basal peats and open symbols represent intercalated peats. Reference value after Streif (1990).

### Material and methods

High-resolution sampling was performed at 1 to 5 cm in peat intervals (248 samples) and at 5 to 10 cm in clastic intervals (1150 samples). The samples were stored in polyethylen bags, sealed, and immediately frozen. Afterwards the samples were freeze-

dried and homogenised in an agate mortar. The ground powder was used for all subsequent geochemical analyses.

All samples were analysed for major elements (Si, Ti, Al, Fe, Mg, Ca, Na, K, P) and trace elements (As, Ba, Co, Cr, Mn, Mo, Ni, Pb, Rb, Sr, V, Y, Zn, Zr) by XRF (Philips PW 2400, equipped with a Rh-tube) using fused borate glass beads. Due to detection limits of the XRF measurement As and Mo data were only used for peat and lagoonal samples. If samples contain total organic carbon (TOC) >10% they were heated to 500°C to remove TOC prior to adding lithiumtetraborate and fusing in Pt-Au-crucibles.

ICP-OES (Perkin Elmer Optima 3000XL) was used to analyse the reference core for major elements (Ti, Al, Fe, Mg, Ca, Na, K, P) and trace elements (As, Ba, Co, Cr, Mn, Ni, Pb, Sr, V, Y, Zn, Zr) in acid digestions performed after Heinrichs and Herrmann (1990) in closed teflon vessels (PDS-6; Heinrichs *et al.*, 1986). The samples (250-500 mg) were treated with 3 ml conc. HNO<sub>3</sub> for 24 hours to oxidize organic matter. Then 2 ml conc. HF and 2 ml conc. HClO<sub>4</sub> were added and the closed vessels were heated for 6 h at 180°C. After digestion the acids were evaporated on a heated metal block (180°C), re-dissolved and fumed off three times with 2 ml half-concentrated HCl, followed by re-dissolution with 0.5 ml conc. HNO<sub>3</sub> and dilution to 25 ml.

Total sulphur (TS) and total carbon (TC) were analysed in 1065 samples (248 peat samples, 817 clastic samples) after combustion using an IR-analyser Leco SC-444 while total inorganic carbon (TIC) was determined by a Coulometrics Inc. CM 5012 CO<sub>2</sub> coulometer coupled to a CM 5130 acidification module (Huffman, 1977, Engleman *et al.*, 1985). The content of total organic carbon (TOC) was calculated as the difference of TC and TIC.

Analytical precision and accuracy of XRF and ICP-OES measurements was tested by replicate analysis of geostandards (GSD-3, -5, -6, GSS-1, -6, LKSD-1, SDO-1, SGR-1) and several in-house standards. The precision of bulk parameter measurements was checked in series of double runs and accuracy was determined by using in-house standards (see appendix).

## Results and discussion

### Major components

Holocene deposits from the NW German coastal area consist of four main components (quartz, clay, carbonate, organic matter), whose relative distribution within the individual facies is presented in the ternary plots of Figures 2.4.4 and 2.4.5. In Figure 2.4.4 the relation between clay ( $\text{Al}_2\text{O}_3$ ), quartz ( $\text{SiO}_2$ ), and organic matter (TOC) is shown for the clastic sediments and peat samples.

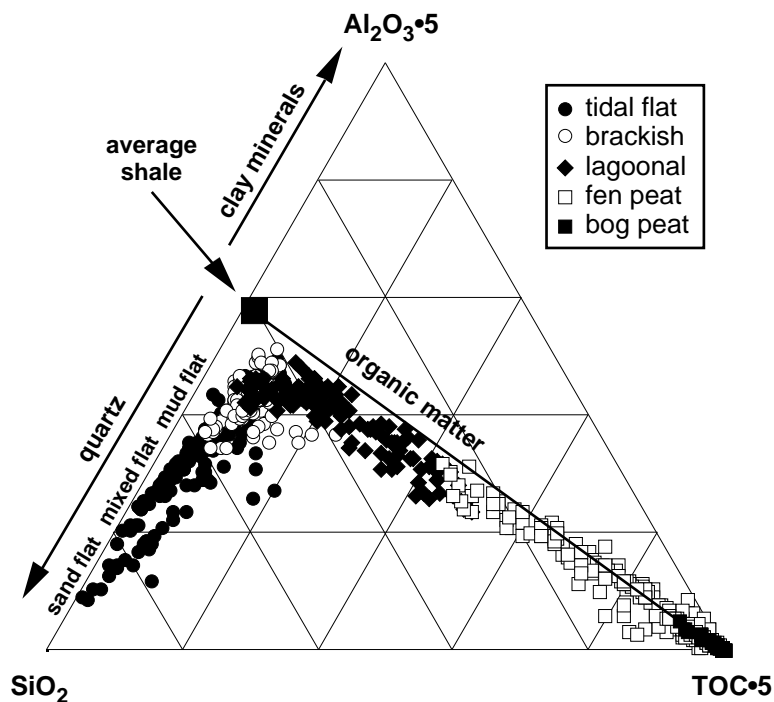


Figure 2.4.4: Ternary plot  $\text{Al}_2\text{O}_3 \cdot 5$ - $\text{SiO}_2$ - $\text{TOC} \cdot 5$  for sediment and peat samples from the investigated drill cores. Average shale data after Wedepohl (1971).

Sand flat sediments which were sedimentated under comparatively high wave-energy during transgressive phases plot close to the  $\text{SiO}_2$  pole. Under less energetic depositional conditions mixed and mud flat sediments were formed which contain higher amounts of clay. During regressive phases or at the first stage of a slight transgressive development brackish and lagoonal sediments occur which plot closer to the average shale data point (Wedepohl, 1971). However, the lagoonal sediments often contain enhanced amounts of



organic matter due to reed growing under comparatively low salinity. Thus, the lagoonal sediments plot on the mixing line between average shale and the TOC pole. A gradual transition between the lagoonal sediments and the fen peat samples, which consists predominantly of reed peat, is clearly visible. With decreasing marine influence the fen peats reach the TOC pole due to a lacking input of clastic material via flooding events. Close to the TOC pole the bog peats can be distinguished because no direct seawater influence occurred during peat formation.

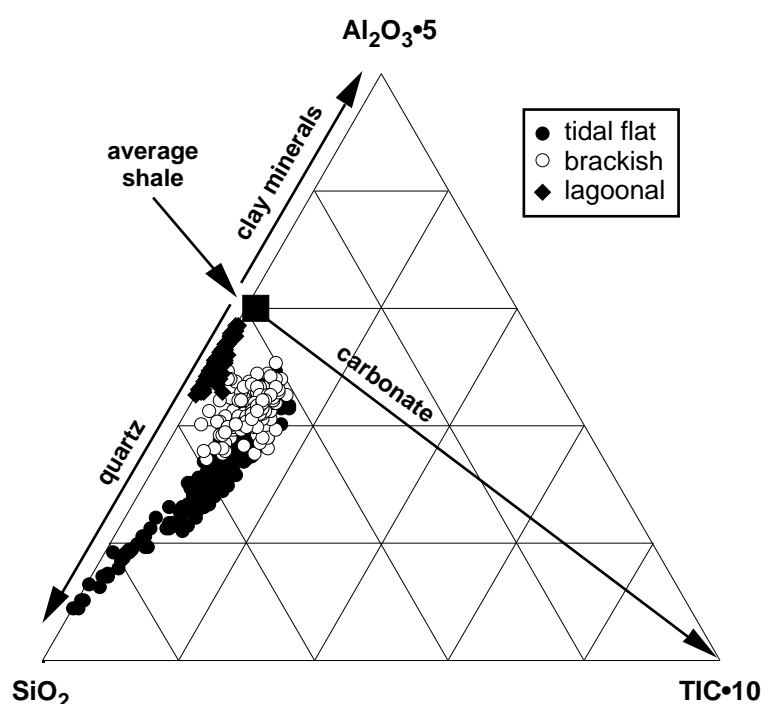


Figure 2.4.5: Ternary plot  $\text{Al}_2\text{O}_3 \cdot 5\text{-SiO}_2\text{-IC} \cdot 10$  for sediment samples from the investigated drill cores. Average shale after Wedepohl (1971).

The ternary plot presented in Figure 2.4.5 takes the carbonate content (TIC) into account. The majority of carbonate found in the sediments can be attributed to the occurrence of mussel shells while the amounts of authigenic carbonate are negligible (Irion, 1994). In the tidal flat sediments typical mussel species could be identified (e.g. *Cerastoderma edule*, *Scrobicularia plana*, *Macoma balthica*, *Mytilus edulis*) during visual core description.

Table 2.4.2: Average values of major [% dw] and selected trace elements [mg kg<sup>-1</sup> dw] for fen and bog peats of the drill cores. Reference peat is given by a core from the Aurich Moor.

element	reference bog peat	average bog peat	reference fen peat	average fen peat	intercalated reed peat	basal reed peat	fen wood-land peat
TOC	54.9	48.8	55.0	35.3	26.1	37.8	33.9
TS	0.4	2.8	0.3	5.2	4.3	5.4	7.1
TIC	<0.01	0.03	<0.01	0.02	<0.01	0.02	0.02
Si	n.d.	1.86	n.d.	15.00	25.33	12.00	7.54
Ti	0.01	0.02	0.07	0.19	0.33	0.14	0.11
Al	0.06	0.34	0.19	3.47	6.19	2.58	1.77
Fe	0.15	2.58	0.54	4.59	4.32	4.59	4.1
Mg	0.18	0.67	0.12	1.31	1.34	1.30	0.68
Ca	0.42	2.23	0.54	1.24	1.14	1.26	0.75
Na	0.04	0.16	0.07	1.07	0.94	1.41	0.87
K	0.02	0.12	0.02	0.71	1.08	0.51	0.55
P	0.03	0.05	0.02	0.09	0.11	0.09	0.03
As	<1	3	<2	10	11	9	20
Ba	14	29	65	89	140	78	87
Co	0.4	2	1	4	5	4	6
Cr	3	3	1	29	51	22	28
Mn	50	364	21	298	299	309	187
Mo	n.d.	1	n.d.	8	8	8	16
Ni	3	2	3	16	20	11	15
Pb	5	0.5	1	7	12	5	8
Rb	n.d.	6	n.d.	37	62	26	32
Sr	34	110	34	110	108	116	103
V	4	5	4	52	78	40	54
Y	0.5	2	4	11	15	9	13
Zn	5	9	2	28	37	25	32
Zr	3	9	3	55	97	42	75

n.d. = not determined

As the peat samples are almost carbonate-free (Table 2.4.2) only the clastic sediments are presented in the ternary plot of Figure 2.4.5. Similar to Figure 2.4.4 the carbonate-poor sand flat samples plot close to the SiO<sub>2</sub> pole, whereas the mixed and mud flat sediments contain elevated amounts of carbonate owing to decreasing wave-energy. The brackish sediments show again a major component chemistry similar to the mud flat deposits. Therefore a differentiation between brackish and mud flat sediments on the basis of the presented parameters is rather difficult. However, the mud flat sediments contain higher amounts of the trace metals Sr and Zr when compared with the brackish facies. The higher Sr contents of the mud flats are most likely due to a different organisms community under higher salinity conditions while the enhanced amounts of Zr result from slightly higher energy conditions (see below). On the other hand the

lagoonal sediments reveal a clearly different chemistry as seen for instance from the low TIC content due to a distinctly lower salinity. Diatom investigations on the Wangerland core W5 (Watermann *et al.*, 1999a) could show that the lagoonal sediments were most likely formed under a salinity below 10‰.

A further characteristic of the investigated Holocene deposits is the formation of authigenic minerals during early diagenesis, i.e., pyrite ( $\text{FeS}_2$ ) and to a lesser extent vivianite ( $\text{Fe}_3(\text{PO}_4)_2$ ). Vivianite is a typical mineral formed under suboxic/anoxic and sulphate-poor conditions and was proposed to be an indicator for palaeosalinity (Berner, 1980, 1981). The occurrence of vivianite is evidenced by P enrichments especially in some brackish sediments (0.3% P, average Holocene brackish sediments 0.06% P) as well as in the basal freshwater mud (0.7% P) of the Loxstedt core (Dellwig *et al.*, 1999c).

In case of the brackish sediments short-term freshening events must have occurred so that pyrite formation only took place in the very uppermost parts of the sediment. Therefore not all reactive Fe has been converted into sulphides and the concentration of dissolved Fe (possibly encouraged by microbial reduction of Fe oxides) must have increased until it reached the solubility product of vivianite. The freshening could be evidenced for the Loxstedt core by the investigation of diatom assemblages (Watermann *et al.*, 1999b). However, the most dominant authigenic mineral formed in the investigated sediments and peat layers is pyrite which amounts to a maximum value of 49.8%  $\text{FeS}_2$  in the basal peat of the Wangerland core W5. Especially the lagoonal sediments and most of the peat layers are characterized by a high abundance of pyrite. As mentioned above the lagoonal sediments were formed under a lower salinity in comparison to the brackish sediments. Therefore one would expect elevated contents of vivianite in the lagoonal facies. But in contrast to the brackish sediments, the lagoonal deposits provide better conditions for the formation of pyrite. Thus, the content of organic matter, which controls the sulphate reduction rate (Westrich and Berner, 1984), is distinctly higher in the lagoonal sediments due to plant growing (e.g. reed rhizomes). On the other hand, the sulphate concentration is sufficiently high even under lower mean salinity. For this

reason, the higher amounts of  $\text{H}_2\text{S}$  formed within the lagoonal sediments favour the formation of pyrite in comparison to vivianite.

The ternary plot  $\text{Fe}_{\text{avail.}}$ -TOC- $\text{TS}\cdot 2$  (Figure 2.4.6) provides information on pyrite formation and its limitations. In the ternary plot the main components which are necessary for the formation of pyrite are presented. It should be noted that not the total Fe content but the proportion of Fe which is available for pyrite formation ( $\text{Fe}_{\text{avail.}}$ ) is shown. The amount of  $\text{Fe}_{\text{avail.}}$  was calculated after the following formula suggested by Brumsack (1988):

$$\text{Fe}_{\text{avail.}} = \text{Fe}_{\text{total}} - \text{Al} \cdot 0.2.$$

This empirical formula is based on the assumption that the silicate-bound Fe fraction, which is not available for pyrite formation under normal sedimentary conditions (Canfield *et al.*, 1992), amounts to approximately 20% of the Al content. Data points which plot on the pyrite line are assumed to be completely pyritized while samples plotting above this line contain excess  $\text{Fe}_{\text{avail.}}$  but less organic matter and S. On the other hand the area below the pyrite line indicates Fe limitation and formation of organic sulphur compounds, respectively.

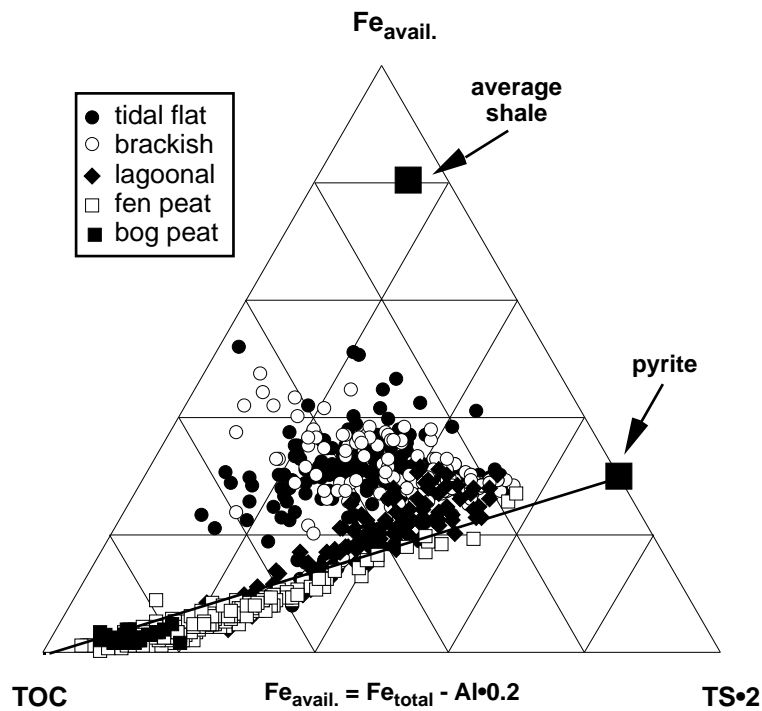


Figure 2.4.6: Ternary plot  $\text{Fe}_{\text{avail.}}$ -TOC- $\text{TS}\cdot 2$  for sediment and peat samples from the investigated drill cores. Average shale data after Wedepohl (1971).

Regarding the ternary plot in Figure 2.4.6 it seems obvious that most of the peat samples plot slightly below the pyrite line which indicates the above mentioned Fe limitation and formation of organic sulphur compounds. The lagoonal samples plot close to the pyrite line which points towards an almost complete transformation of  $\text{Fe}_{\text{avail.}}$  into pyrite. The brackish and tidal flat sediments show a large scatter but also a trend towards the pyrite line reflecting an enhanced degree of pyritization when compared with the average shale data point.

#### *Geochemistry of the peat layers*

In order to provide an overview about the geochemical composition of the investigated peats Table 2.4.2 presents the average contents of major and selected trace metals of bog and fen peat as well as a differentiation between fen reed peat (basal and intercalated) and fen woodland peat. As the geochemistry of peats strongly depends on, e.g., the composition of the underlying clastic sediments, the groundwater chemistry, and eolian input (Shotyk, 1988; and references therein) a comparison of peats from different locations is rather difficult. Therefore, the chemical composition of peats varies significantly as shown for example by Naucke (1979). He analysed several bog and fen peats from Lower Saxony (Germany) which evidences the dependence of peat composition on particular environmental conditions. For instance, the Al and Fe contents of the analysed peats show a wide range (Al: bog 0.02-0.36%, fen 0.3-1.7%; Fe: bog 0.03-0.47, fen 0.1-2.6%). For that reason, a reference core from the Aurich Moor (Figure 2.4.1), which contains fen and bog peat and originates from a comparable environment, was chosen for comparison. However, a distinct difference is given by the lacking direct seawater influence from the rising North Sea.

*Bog peat:* As seen from Table 2.4.1 the occurrence of bog peat is comparatively rare in the investigated cores. Bog sections are only found in the basal peat of the Wangerland core W5 and in the upper basal and intercalated peat of the Schweiburg core. Core W5 represents the most SW core of the Wangerland transect (Figure 2.4.1). At this location the Holocene basis is closer to the German zero datum in comparison to the remaining cores (Figure 2.4.2). Therefore, the rising North Sea reached this location later so that

bog vegetation could develop. The basal bog peat of the Schweiburg core represents only parts of its original extent because of erosion due to tidal channel activity. On the other hand, the bog peat of the intercalated peat section reflects a complete silting up process which was most likely caused by a natural levee within the ancient Jade Bay (see below).

Regarding Table 2.4.2 only TOC, P, Ba, Cr, and V reveal similar contents in the Wangerland and Schweiburg bog peats when compared with the reference core from the Aurich Moor whereas the remaining elements are enriched in the coastal peats. The only exception is the enrichment of Pb in the Aurich Moor due to anthropogenic activity. Especially the uppermost 50 cm of the Aurich bog peat are highly enriched in Pb (average  $36 \text{ mg kg}^{-1}$ , maximum  $118 \text{ mg kg}^{-1}$ ) while the underlying fen peat contains only  $1 \text{ mg kg}^{-1}$  Pb. The anthropogenic origin could be also evidenced by the investigation of  $^{206/207}\text{Pb}$  ratios by ICP-MS (O. Dellwig, unpubl. data). The first 50 cm show an average  $^{206/207}\text{Pb}$  ratio of 1.16 which reflects a distinct shift to the atmospheric Pb isotope signal of 1.11-1.14 (Döring *et al.*, 1997) when compared with the local geogenic background of 1.20 (Dellwig *et al.* 1999b).

The elevated contents of the lithogenic elements (e.g. Al, K, Ti, Y, Zr) in the coastal bog peats result from a process which occurred after peat formation. In Figure 2.4.2 the basal peats of the Wangerland cores W1, W3, and W5 as well as the peats of the Schweiburg core are marked by black lines which indicate the occurrence of clastic layers. These layers can be evidenced, e.g., by elevated  $\text{Al}_2\text{O}_3$  contents as shown in Figure 2.4.7 and are the result of tidal channel activities which led to an uplift of the peat at transition zones. Remnants of a tidal channel are seen in the Wangerland core W4 on the Pleistocene sands (Figure 2.4.2). This tidal channel developed most likely from NE to SW (Figure 2.4.1) and led to an uplift of parts of the basal peats of the cores W1, W3, W5 while the northern core W2 was untouched. From Figure 2.4.7 it can be seen that most of the clastic layers occur at fen/bog transitions or fen vegetation transitions. Due to the uplift of the peat the input of seawater and suspended particulate matter was possible. After that the peat settled down and a clastic layer remained whose interface to the peat acted as an aquifer and therefore allowed the inflow of seawater and

sulphate-rich groundwater, respectively. As a result of intense sulphate reduction  $\text{H}_2\text{S}$  was produced which reacted with Fe, derived from peatland waters, to pyrite. This phenomenon, which is discussed in more detail by Behre (1978) and Dellwig *et al.* (1999a), therefore explains the high TS contents within the originally limnic peat environments of the study area.

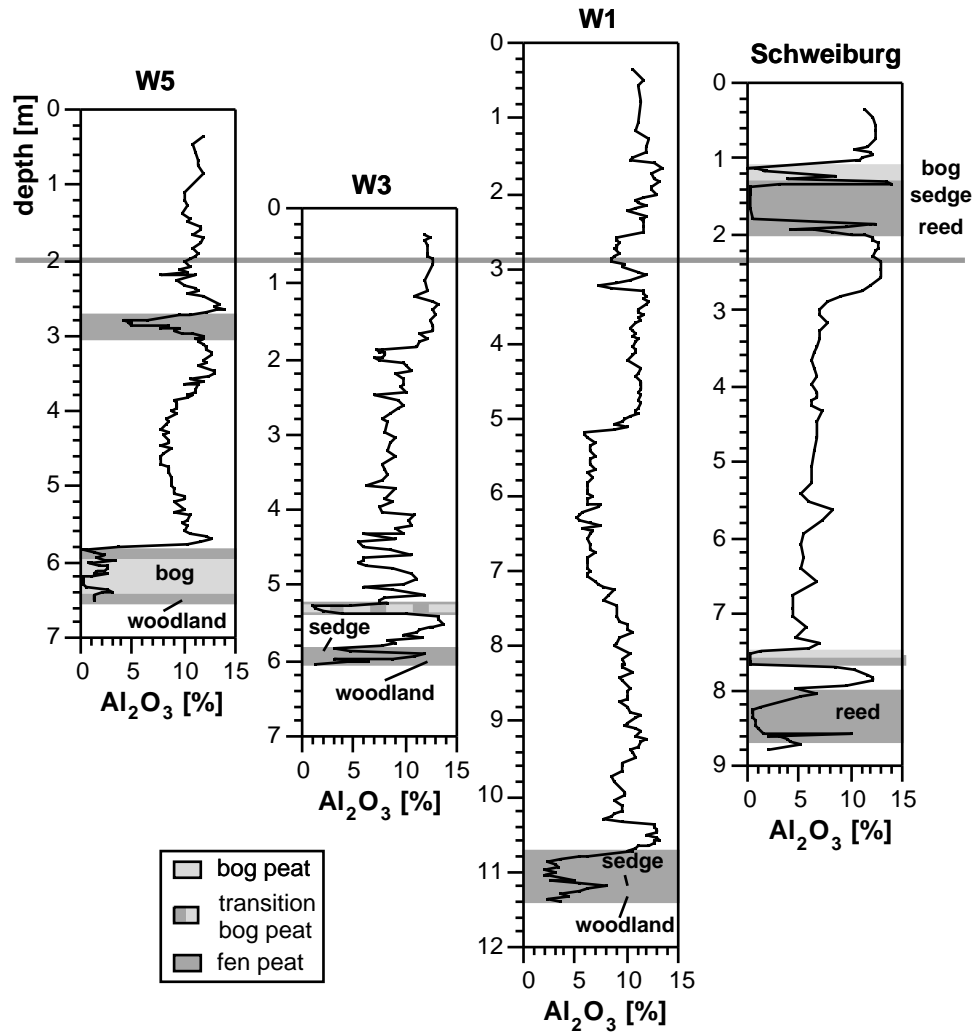


Figure 2.4.7: Depth profiles of the  $\text{Al}_2\text{O}_3$  content of the Wangerland cores (W1, W3, W5) and of the Schweiburg core. The grey line indicates the German zero datum [m NN].

The TS profiles of the four cores W5, W3, W1, and Schweiburg shown in Figure 2.4.8 reveal that the clastic layers coincide with enrichments in TS and pyrite, respectively. The investigated cores contain distinctly higher amounts of TS (core W5 maximum

28.2%) when compared with other coastal peat-forming environments. For instance, maximum TS contents in coastal swamps from the Florida Everglades vary between 6 and 10% TS (Given and Miller, 1985; Price and Casagrande, 1991).

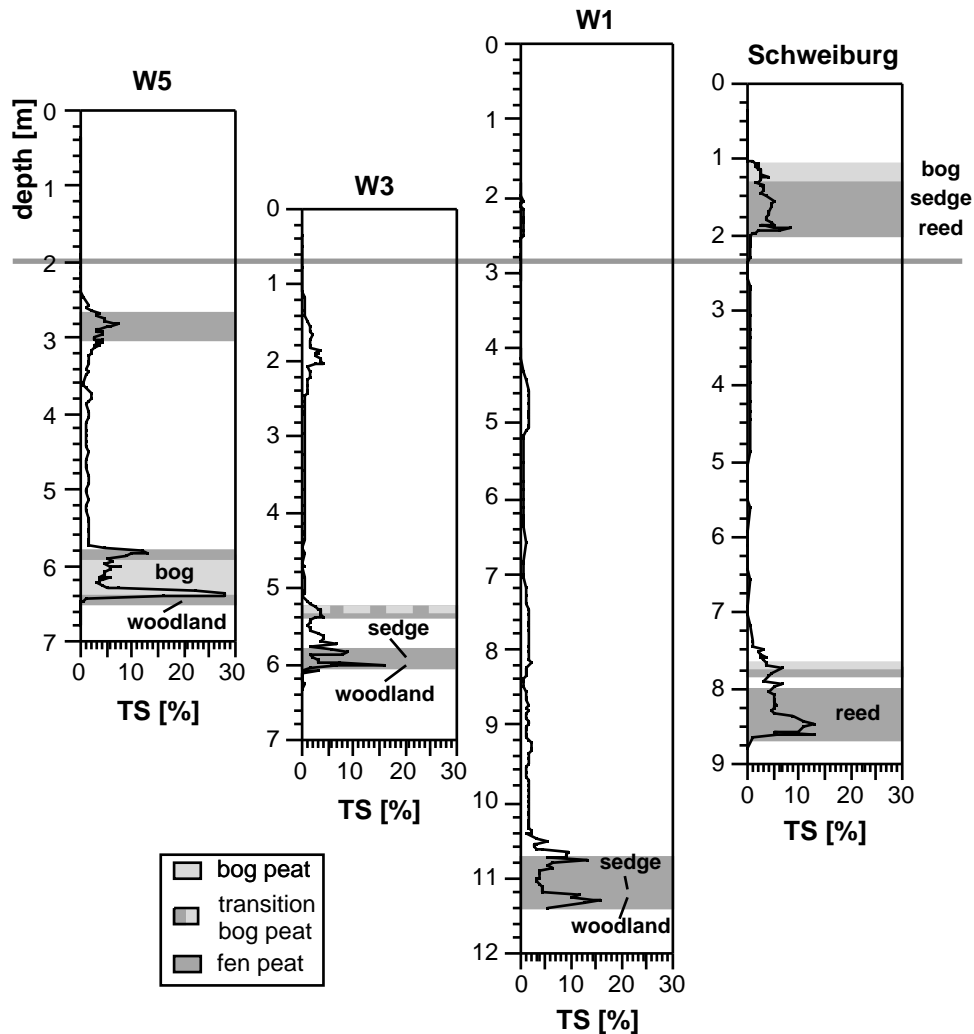


Figure 2.4.8: Depth profiles of the TS content of the Wangerland cores (W1, W3, W5) and of the Schweiburg core. The grey line indicates the German zero datum [m NN].

In order to compare the mineral matter of the peats with the geogenic background enrichment factors versus average shale were calculated on an organic matter free basis ( $EFS_{OMF}$ ). The  $EFS_{OMF}$  values for major and selected trace elements of the reference bog peat and the coastal bog peats (Figure 2.4.9a) reveal that most of the lithogenic elements (Al, Co, K, (Na), Ti, Y, Zr) are below or close to the shale-level and only Ca, Mg, and Sr are enriched in comparison to average shale. Furthermore, it can be seen that the



difference in the chemical composition of the reference and coastal bog peats is distinctly smaller than it was expected from the absolute concentrations presented in Table 2.4.2. As biomineralization leads to a vertical transport of nutrients and metals in bog peats, which receive mineral matter predominantly by eolian input, lithogenic elements are only enriched in the uppermost parts whereas the central part becomes poor in these elements (Naucke, 1990). Therefore, the  $EFS_{OMF}$  values of the above mentioned lithogenic elements are below the shale-level for the investigated bog peats.

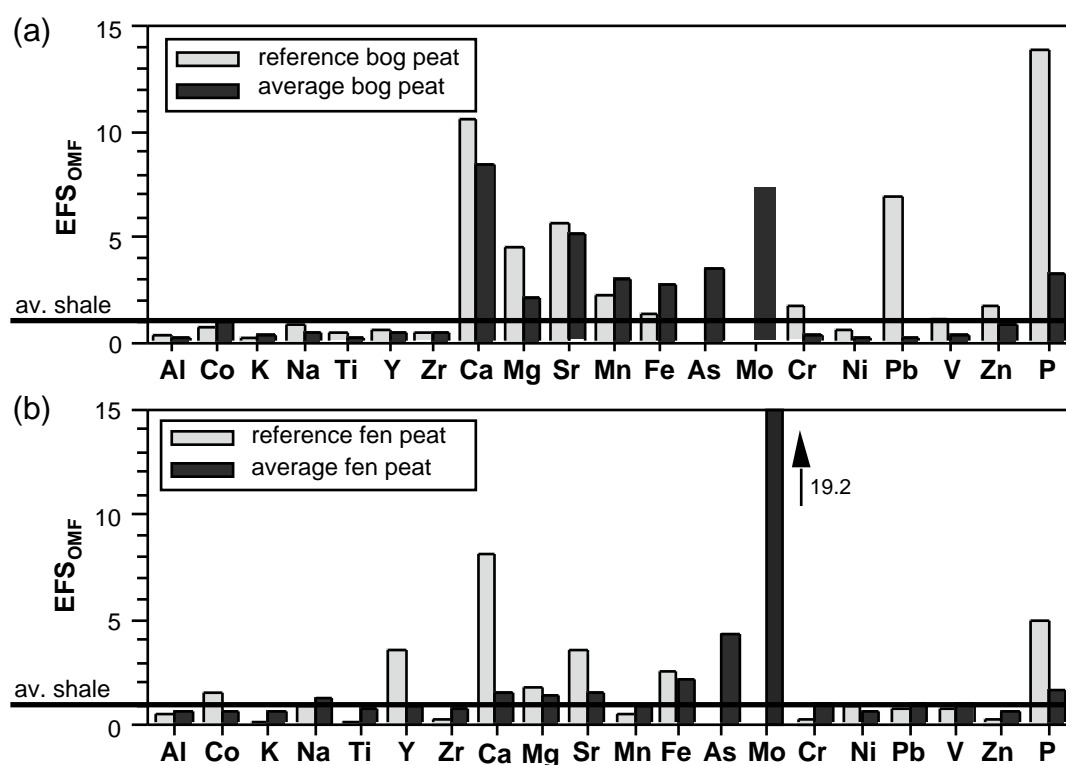


Figure 2.4.9: Enrichment factors for selected major and trace elements versus average shale on an organic matter-free basis ( $EFS_{OMF}$ ) for a) bog peats and b) fen peats. Average shale data from Wedepohl (1971, 1991).

According to Shotyk (1997) the amounts of Ca, Mg, Na, and Sr are influenced by sea spray. He showed that the concentrations of these elements in maritime peats exceed the contents of soil-derived aerosols by factors of 5 to 30. The investigated bog peats reveal an almost identical feature. The  $EFS_{OMF}$  values vary between 2 and 11 for Ca, Mg, and Sr. However, no enrichment is seen for Na which is possibly related to cation exchange processes and the high solubility of Na salts, respectively. Bog peats show a Ca-Mg

dominance with respect to monovalent cations (Zeitz, 1997) and especially Na is very rapidly removed from the peats (Damman, 1978).

A further element which is enriched in the reference bog peat and in the coastal peats is Mn. This enrichment can be explained by the Mn reservoir of the study area. The investigation of the geochemistry of rivers close to the Jade Bay carried out by Lipinski (1999) revealed that the freshwater environment of the study area is characterized by large amounts of Mn ( $Mn_{\text{particulate}} 3920 \text{ mg kg}^{-1}$ ,  $Mn_{\text{dissolved}} 370 \text{ } \mu\text{g l}^{-1}$ ) which exceed the average worldwide Mn concentration in rivers (Martin and Whitfield, 1983) by a factor of 4 and 45, respectively. Additionally, Mn is generally enriched in plants (Heinrichs, 1993), e.g., in the leaves of *Vaccinium spp.* (Wandtner, 1981) which could be indentified in some bog peat samples by microscopic examination.

The Fe enrichment in the coastal peats in comparison to the reference bog peat can be explained by the above mentioned formation of pyrite as a result of microbial reduction of seawater sulphate. Similar to Mn the freshwater environment contains also elevated amounts of Fe ( $Fe_{\text{particulate}} 9.7\%$ ,  $Fe_{\text{dissolved}} 1800 \text{ } \mu\text{g l}^{-1}$ ; Lipinski, 1999) when compared with concentrations of the average world-wide river composition ( $Fe_{\text{particulate}} 4.8\%$ ,  $Fe_{\text{dissolved}} 40 \text{ } \mu\text{g l}^{-1}$ ; Martin and Whitfield, 1983). As typical trace components of pyrite the redox-sensitive trace metals As and Mo are enriched in the coastal peats in comparison to average shale while the remaining trace metals (Co, Cr, Ni, Pb, V, Zn) reflect more or less the geogenic background. As and Mo form stable sulphides and can be incorporated into pyrite (e.g. Belzille and Lebel, 1986; Raiswell and Plant, 1980) and both elements are high in seawater whereas their geogenic background is relatively low (seawater: As  $1.5 \text{ } \mu\text{g l}^{-1}$ , Mo  $10 \text{ } \mu\text{g l}^{-1}$ , Martin and Whitfield, 1983; av. shale: As  $10 \text{ mg kg}^{-1}$ , Mo  $1.3 \text{ mg kg}^{-1}$ , Wedepohl, 1991). Therefore, the enrichment of As and Mo evidences a distinct influence of seawater on the coastal bog peats. However, as seawater does not contribute significant amounts of Fe, an interaction between freshwater and seawater has to be assumed.

As mentioned above the the heavy metal Pb is enriched in the reference bog peat in comparison to the coastal peats due to anthropogenic activity. Regarding the  $EFS_{\text{OMF}}$  it seems obvious that in contrast to the absolute concentrations the metals Cr, Ni, V, and

Zn are also enriched in the reference core. A further element which shows elevated contents in the reference core is P whose enrichment is related to the use of fertilizers (percolation, groundwater). As P serves as a nutrient for plants (Göttlich, 1990) the slight enrichment seen in the coastal peats is possibly the result of mobilization from underlying clastic sediments. Additionally, the increasing degree of peat decomposition releases P and therefore favours the formation of vivianite in microenvironments. However, the absolute P concentrations of the reference bog peat and coastal peats (Table 2.4.2) are at the lower P limit typically found in peats from Northern Germany (0.04-0.26% P; Naucke, 1990).

*Fen peat:* The comparison between the average composition of the coastal fen peats and the reference fen peat reveals again significant differences. The coastal fen peats are characterized by lower TOC contents but show distinctly higher amounts of lithogenic elements (Table 2.4.2) which result from periodical flooding and storm events. Regarding the EFS values shown in Figure 2.4.9b, however, the shale-like distribution of the lithogenic elements becomes evident. In contrast to the bog and reference fen peats the coastal fen peats show only a very slight enrichment in Ca, Mg, and Sr. Taking into account the elevated input of clastic material via flooding events it can be assumed that the sea spray signal is diluted by this material. Again high  $EFS_{OMF}$  values are seen for Fe, As, and Mo. The higher  $EFS_{OMF}$  values of Mo in comparison to the bog peats reflect a more pronounced seawater influence on the fen peats.

Anthropogenic influences are not seen within the fen peats. Therefore, the heavy metals (e.g. Pb, Zn) reflect the geogenic background. Only Y and to a lesser extent Co are enriched in the reference fen peat which coincides with enhanced contents of Fe and P and the formation of vivianite, respectively. Especially Y is incorporated into phosphates (Nathan, 1984) while Fe can be replaced by Co because of an almost similar ionic radius.

Regarding the average element contents of the intercalated and basal reed peats (Table 2.4.2) it is obvious that the basal reed peats are less influenced by flooding as is reflected by the higher TOC values and their lower amounts of lithogenic elements. In contrast to the intercalated reed peats, which were formed under a marine influence during a slowly

rising or stagnating sea level, the formation of the basal reed peats is often encouraged by a rising groundwater level due to the rising North Sea. Additionally, most of the basal reed peats were formed during a time period which was characterized by a steeper sea-level rise (Figure 2.4.3). Therefore, these peats were covered faster with clastic material, whereas the intercalated peats kept pace with the rising sea for a longer period. The comparable contents of TS, As and Mo evidence a distinct influence of seawater on the basal reed peats as well. However, it seems likely, that the formation of pyrite within the basal reed peats is diffusion controlled. For instance,  $^{34}\text{S}$  values of the basal reed peat of the Loxstedt core reflect closed system conditions with respect to seawater sulphate, while pyrite formation within the intercalated reed peats occurred under almost open system conditions (Dellwig *et al.*, 1999c).

The fen woodland peats, which in most cases form the basis of the basal peats, show similar contents of TOC and lithogenic elements like the basal reed peats. By contrast, the contents of TS, As, and Mo are slightly higher in the fen woodland peats due to the above mentioned occurrence of clastic layers within the peats.

*Comparison of the four locations:* Figure 2.4.10a shows the  $\text{EFS}_{\text{OMF}}$  values of selected major and trace elements of the bog peats from the Wangerland (core W5) and Schweiburg location. As the Holocene peats are not influenced by anthropogenic activity the heavy metals (e.g. Cr, Ni, Pb, Zn) plot close to the shale level just as the major elements (e.g. Al, K, Si). Only Ca, Sr, Fe, As, and Mo are enriched in the originally limnic bog peat environments which reflects the influence of seawater and sea spray. The enrichment in P results most likely from plant growing and vivianite formation in microenvironments. However, the two locations reveal no significant differences.

In contrast, the fen woodland peats of the Wangerland and Loxstedt location (Figure 2.4.10b) show a distinctly different chemistry. The fen woodlands peats from the Wangerland show the shale-like composition with respect to the lithogenic elements as well as enrichments in Fe, As, and Mo due to the formation of pyrite. On the other hand, the fen woodland peat from the Loxstedt location reflect no marine influence although especially As is highly enriched. This enrichment in As coincides with elevated

amounts of P which indicates the formation of vivianite. Furthermore, especially the trace metals As and Y can be incorporated into phosphates or, in the case of As, form stable Fe compounds (e.g.  $\text{Fe}_3(\text{AsO}_4)_2 \cdot 8\text{H}_2\text{O}$ ) under anoxic conditions (Ramdohr and Strunz, 1978; Nathan, 1984).

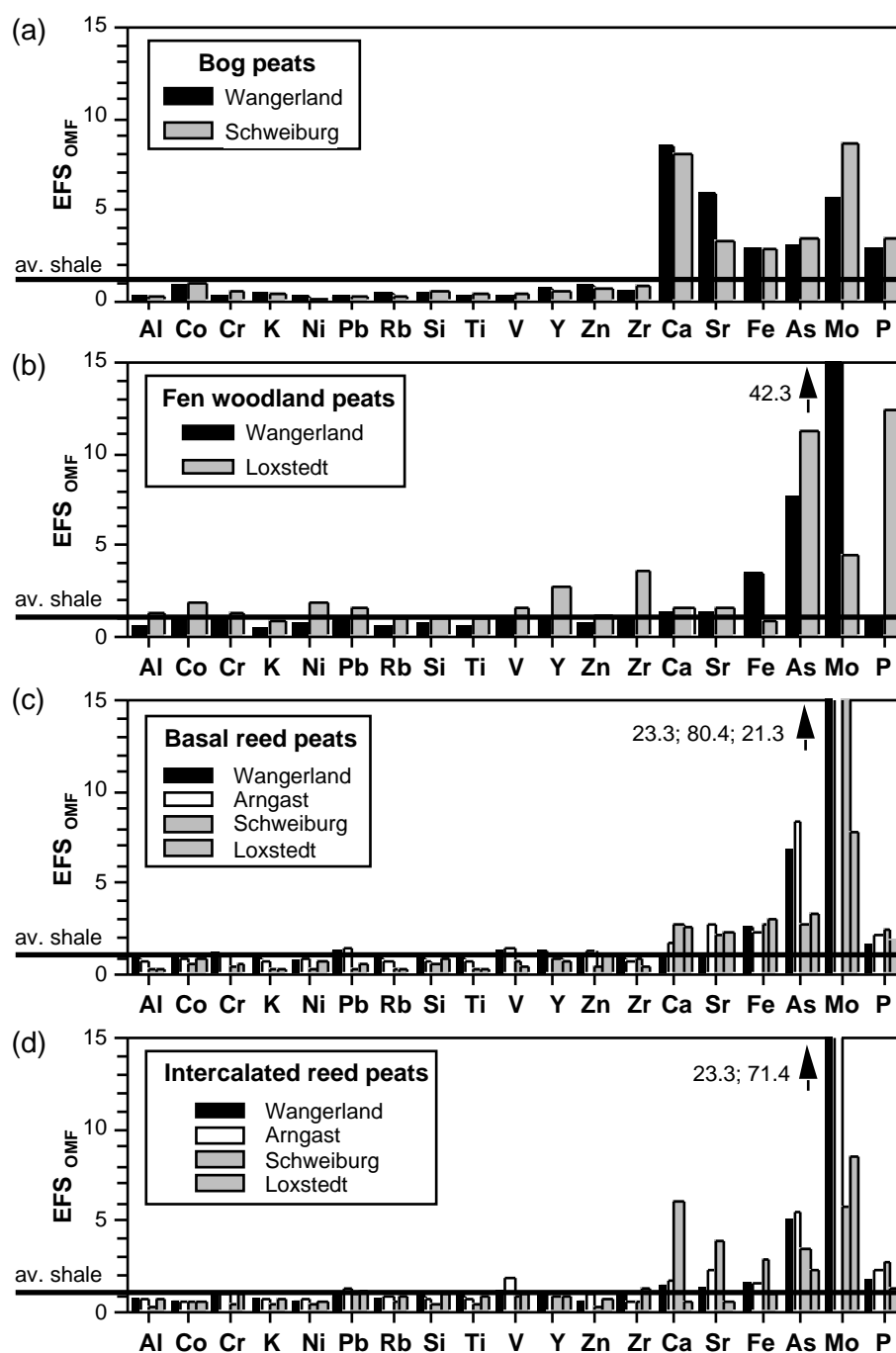


Figure 2.4.10: Enrichment factors for selected major and trace elements versus average shale on an organic matter-free basis (EFS<sub>OMF</sub>) for a) bog peats, b) fen woodland peats, c) basal reed peats, and d) intercalated reed peats of the individual drilling locations.

A further element which occurs in higher amounts in the Loxstedt fen woodland peat is the element Zr. According to Schnetger (1992) Zr serves as an indicator for eolian transported material like loess because refractory minerals, e.g., zircon, are enriched during the loess-forming process. Regarding the age of about 11,350 years BP of the woodland peat the input of eolian loess-like material seems to be likely. This finding is also evidenced by the investigation of rare earth elements (Dellwig *et al.*, 1999c) which show a pattern similar to an average Jungwurm-loess.

Regarding the the  $EFS_{OMF}$  values of the basal and intercalated reed peats (Figures 2.4.10c and d) an almost identical chemical composition is evident for the individual locations. The most significant difference reveals the enrichment of As and Mo which provides an idea of the palaeosalinity because the reed peats generally grew under seawater influence. The highest enrichments of As and especially Mo are seen in the basal and intercalated reed peats of the Arngast location which are therefore assumed to have formed under a comparatively high salinity due to the open access of the rising North Sea. On the other hand, the Loxstedt reed peats show lower  $EFS_{OMF}$  values due to a more estuarine situation because of the close proximity to the river Weser. The basal reed peat of the Schweiburg drill site show As and Mo enrichments comparable to those found in the Wangerland peats because both locations contain the above mentioned clastic layers which enable the inflow of seawater. By contrast, the two intercalated reed peat sections of the Schweiburg core reflect a very low salinity and a restricted marine influence. The formation of these intercalated reed peats forms part of a complete silting up process which culminated in the occurrence of bog vegetation (e.g. Table 2.4.1). The input of clastic material was considerably low in comparison to the intercalated peats of the remaining location, as seen for example in higher TOC contents (Schweiburg 48.7%; other cores 24%). The silting up process in the upper part of the core most likely results from the development of a natural levee within the ancient Jade Bay which prevented the direct inflow of seawater. Remnants of the levee are seen in the clastic sediments below the intercalated reed peat (Figure 2.4.2). On the other hand the lower intercalated reed peat seems to have formed before a distinct influence of the sea-level rise occurred.

*Geochemistry of the clastic sediments*

The clastic deposits of the Holocene sedimentary wedge consists mainly of the lagoonal, brackish and tidal flat facies. Salt marsh sediments as well as natural levee deposits were only found in the uppermost parts of the investigated drill cores. Therefore, this chapter focusses on the geochemistry of lagoonal, brackish, and tidal flat sediments because these deposits are supposed to preserve information about the palaeoenvironmental development, not at least owing to the lack of anthropogenic influences. Table 2.4.3 provides information about the average major and trace element geochemistry of the individual clastic facies.

Table 2.4.3: Average values of major [% dw] and selected trace elements [mg kg<sup>-1</sup> dw] for lagoonal, brackish, and tidal flat sediments of the drill cores (Loxstedt, Schweiburg, Wangerland). Average shale after Wedepohl (1971, 1991).

element	lagoonal	brackish	tidal flat	av. shale
TOC	6.3	2.2	1.3	0.2
TIC	0.02	1.1	1.2	0.15
TS	2.7	1.5	0.7	0.2
Si	26.0	27.9	32.1	27.1
Ti	0.41	0.38	0.32	0.47
Al	6.4	5.7	4.2	8.9
Fe	4.0	3.7	2.4	4.8
Mg	1.0	1.1	0.8	0.9
Ca	0.5	3.7	3.9	1.0
K	2.0	1.9	1.6	2.5
P	0.05	0.06	0.05	0.1
As	23	n.d.	n.d.	8
Ba	269	271	266	650
Co	11	10	8	19
Cr	91	81	67	95
Mn	348	449	387	850
Mo	8	n.d.	n.d.	1.3
Ni	31	27	15	68
Pb	22	20	14	22
Rb	120	108	78	150
Sr	92	143	165	230
V	117	103	69	130
Y	24	23	21	30
Zn	81	72	51	95
Zr	196	214	328	160

n.d. = not determined

In order to eliminate dilution effects, especially caused by quartz and organic matter, we calculated enrichment factors versus average shale (EFS) for selected major and trace elements of lagoonal, brackish, and mixed flat sediments which are presented in Figure

2.4.11. The mixed flat facies was chosen for comparison as it occurs in all cores. The EFS values are calculated using the following formula:

$$\text{EFS} = (\text{element}_{\text{sample}} / \text{Al}_{\text{sample}}) / (\text{element}_{\text{av. shale}} / \text{Al}_{\text{av. shale}}).$$

For normalisation we have chosen Al because its content is not influenced by biogenic cycles or anthropogenic activity and therefore allows comparing sediments of different genesis.

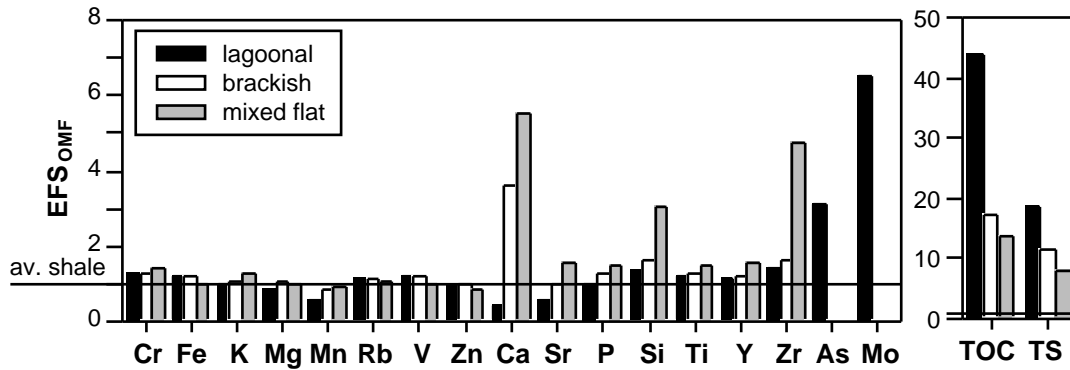


Figure 2.4.11: Enrichment factors for selected major and trace elements versus average shale (EFS) for lagoonal, brackish, and tidal flat sediments of the drill cores (Wangerland, Schweiburg, Loxstedt).

The EFS values reveal distinct differences between the individual facies, e.g., due to varying depositional energy and palaeosalinity. However, the lithogenic elements (Cr, Fe, K, Mg, Mn, Rb, V, Zn) show no significant differences in all three facies and plot more or less close to the shale level which reflects a similar provenance of the sedimented material (Figure 2.4.11). The elements Ca and Sr are enriched in the mixed flat sediments and in the brackish sediments owing to the occurrence of biogenic carbonate. This finding evidences that the brackish sediments were formed under more pronounced marine conditions and higher salinity in comparison to the lagoonal facies. On the other hand the low Ca and Sr content seen in the lagoonal facies is possibly the result of early diagenetic carbonate dissolution (Streif, 1990). In Figures 2.4.12a and b scatter plots of CaO and Sr are presented for the tidal flat, brackish and lagoonal sediments. A correlation between CaO and Sr is seen for the sand and mixed flat samples plotting close to the average ratio of mussel shells from the study area (Hild, 1997).



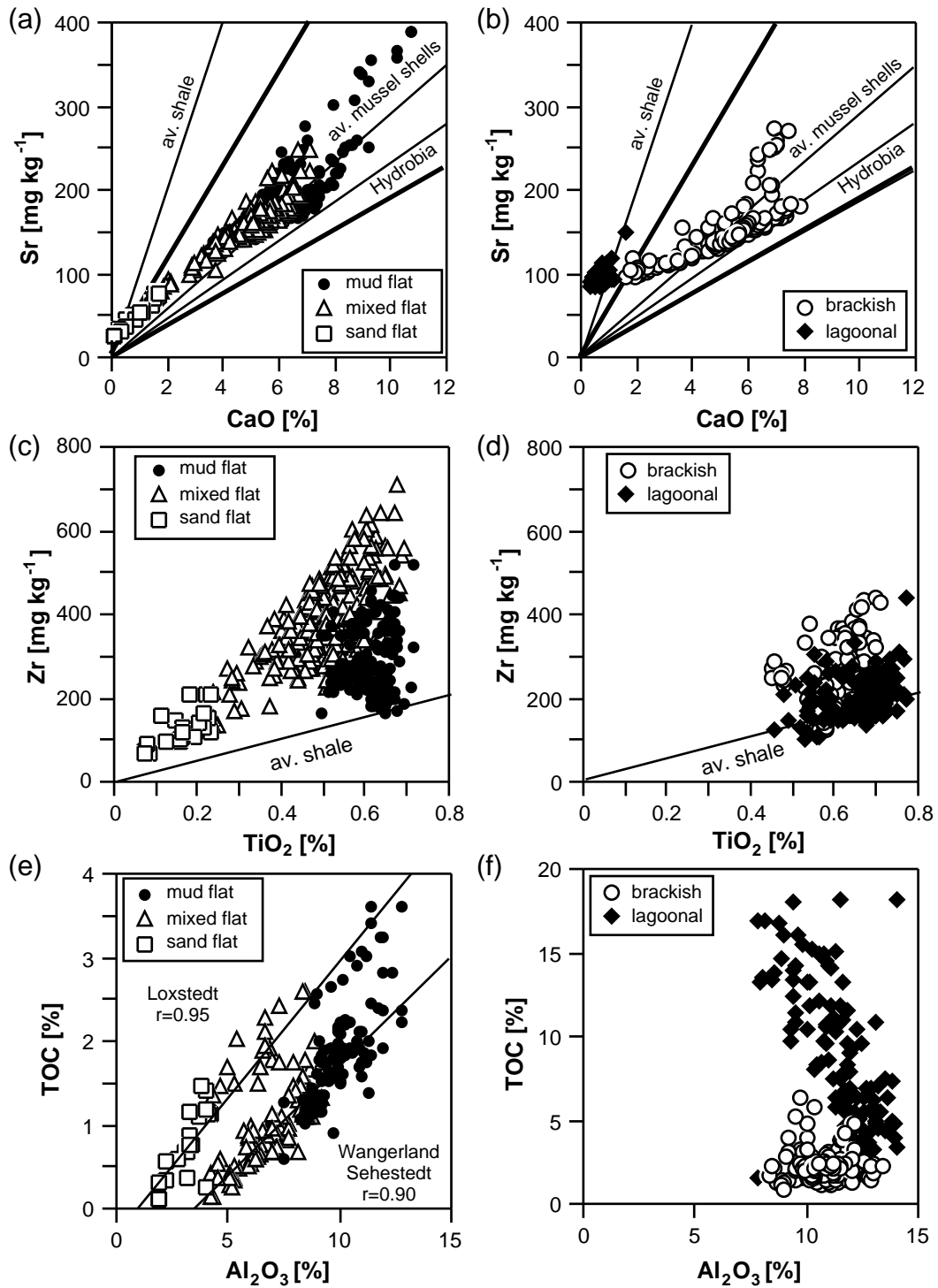


Figure 2.4.12: Scatter plots of Sr vs. CaO (a and b), Zr vs. TiO<sub>2</sub> (c and d), and TOC vs. Al<sub>2</sub>O<sub>3</sub> (e and f) for tidal flat, brackish, and lagoonal sediments. The bold lines indicate the range of mussel shells. Mussel shell and *Hydrobia* spp. data from Hild (1997).

In contrast, the mud flat sediments show a less pronounced correlation with some samples plotting slightly above the average mussel shell line. This bimodal pattern was also observed by Hild (1997) on the basis of grain size fractionations of tidal flat sediments from the Spiekeroog backbarrier area. He found differences in the carbonate composition of the  $<2\mu\text{m}$ ,  $2\text{--}63\mu\text{m}$ , and  $63\mu\text{m}\text{--}1\text{ mm}$  fraction with highest Sr contents in the  $<2\mu\text{m}$  fraction. Therefore, different carbonate sources have to be assumed for the grain size fractions and individual tidal flat facies.

Salomons (1975) and Irion (1994) pointed out that the fine fraction do not consists of biogenic shell fragments. Therefore, Salomons (1975) suggested Cretaceous carbonates from the the English Channel to be the major source for the fine fraction. On the other hand, enhanced proportions of clay which occur in the mud flat contribute high Sr and comparatively low Ca concentrations. By contrast, the coarser sediments are dominated by mussel shell fragments.

The lagoonal sediments show no Sr enrichment and plot close to the average shale line (Figure 2.4.12b) while the brackish sediments show also a development towards biogenic carbonate. Similar to the mud flat facies the clay-rich brackish sediments reveal two trends as well. The comparatively Sr-poor samples plot close to the ratio of *Hydrobia spp.* (Hild, 1997) which is, according to Streif (1990), a typical species in the brackish facies.

A further difference between the three facies is evident from the contents of quartz and heavy minerals due to varying wave-energy. The mixed flat sediments contain elevated amounts of quartz and heavy minerals, as seen in the enrichments of Si, Ti, V, Y, and Zr (Figure 2.4.11). Especially the elements Zr and Ti are useful indicators for high-energy environments, because both elements are often associated in the heavy mineral fraction (e.g. Sutherland, 1985), e.g., as zircon ( $\text{ZrSiO}_4$ ), ilmenite ( $\text{FeTiO}_3$ ), or rutile ( $\text{TiO}_2$ ). Transgressive reworking of older deposits therefore may lead to an enrichment of these minerals in coastal environments.

Regarding the scatter plots in Figures 2.4.12c and d it is obvious that the above mentioned relation between  $\text{TiO}_2$  and Zr is true for the sand flat sediments and to a lesser degree for the mixed flat sediments. The mud flat sediments show no correlation

and the data points reveal a trend towards average shale. A behaviour similar to the mud flats show the brackish and lagoonal sediments owing to comparatively calm depositional conditions. Especially the lagoonal sediments show a geochemical composition very similar to average shale reflecting elevated amounts of clay. A further element enriched in the mixed flat sediments is P which is most likely related to the occurrence of apatite ( $\text{Ca}_5(\text{PO}_4)_3(\text{OH}, \text{F}, \text{Cl})$ ) which also forms part of the heavy mineral fraction.

EFS values for TOC and TS (Figure 2.4.11) are very high in the lagoonal sediments which form the transition to the reed peats. The high amounts of organic matter (OM) in the lagoonal facies are predominantly due to the occurrence of reed rhizomes. Therefore, the formation of pyrite was favoured which explains the high TS content. This process led to the enrichment of the stable sulphide-forming trace metals As and Mo in the lagoonal sediments (Figure 2.4.11). Although the TOC and TS contents of the brackish and tidal flat sediments are distinctly lower, when compared with the lagoonal facies, these sediments show elevated EFS values as well. This finding is in agreement with the relatively high degree of pyritization as seen in the ternary plot in Figure 2.4.6.

The scatter plots in Figures 2.4.12e and f lead to the assumption that a different mechanism of OM deposition is characteristic for the individual facies. While the tidal flat sediments show a correlation between TOC and  $\text{Al}_2\text{O}_3$ , which indicates the adsorption of OM on clay particles, the brackish and lagoonal sediments show no such correlation. Therefore we assume that the sedimentary signal within the brackish and lagoonal sediments is obliterated by a sedentary process, i.e., plant growing. However, a difference between the tidal flat sediments of the Loxstedt and the two Jade Bay locations seems obvious. The TOC content of the Loxstedt tidal flat sediments is distinctly higher than the amounts seen for the remaining locations. An explanation could be the more pronounced riverine input at the Loxstedt site, which contributes higher amounts of OM to the system.

*Comparison of the locations:* Figures 2.4.13a-c present the EFS values for selected major and trace elements for lagoonal, brackish, and tidal flat sediments of the three locations Wangerland, Schweiburg, and Loxstedt.

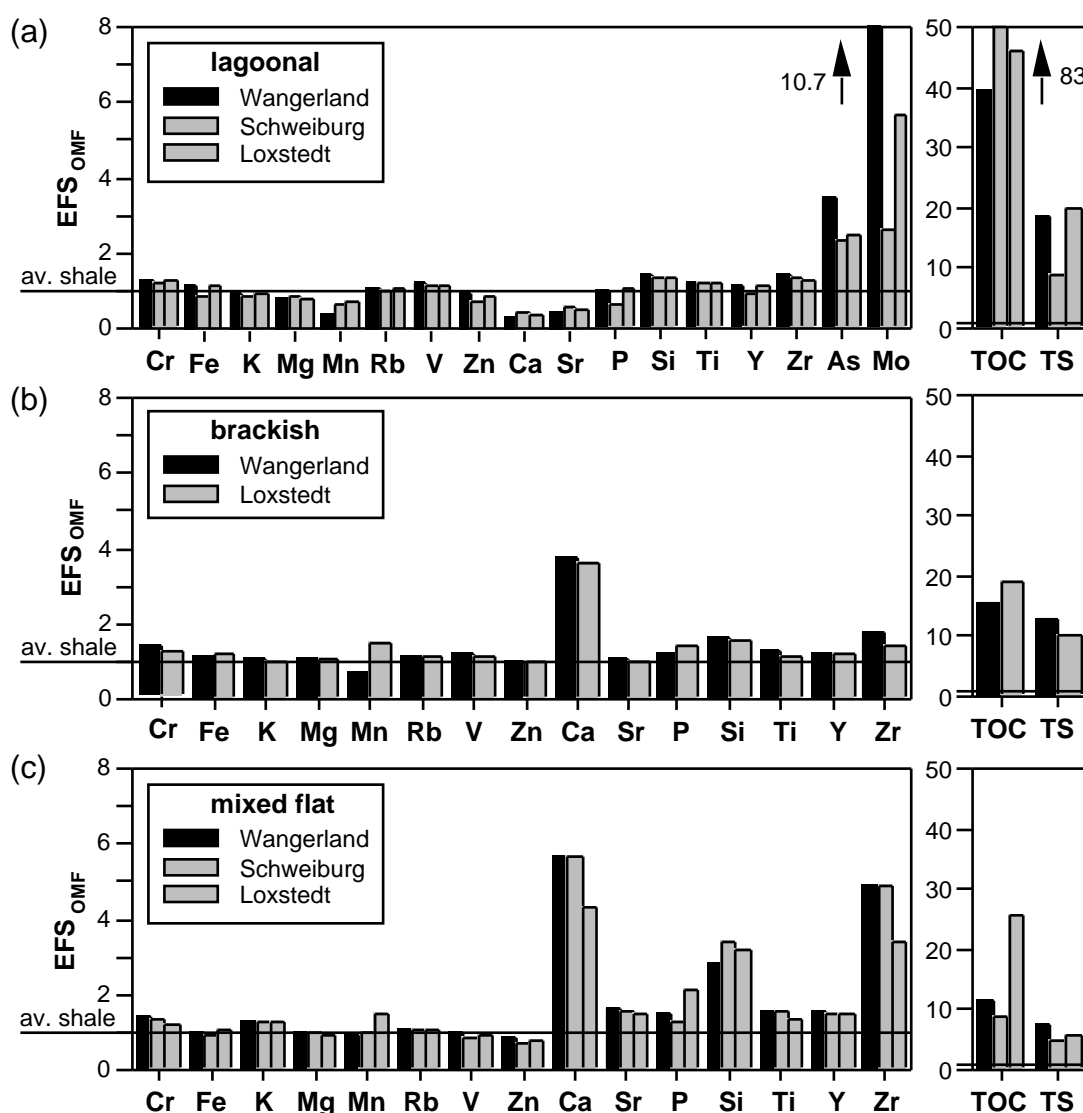


Figure 2.4.13: Enrichment factors for selected major and trace elements versus average shale (EFS) for lagoonal, brackish, and tidal flat sediments of the individual drilling locations (Wangerland, Schweiburg, Loxstedt).

Regarding the lagoonal sediments (Figure 2.4.13a) almost all elements show a similar distribution for the three locations. The only exception is the more pronounced enrichment of As and Mo in the Wangerland cores reflecting a higher salinity which possibly limited reed growing as seen from lower TOC contents. Thus, the lagoonal sediments from the Wangerland were often formed during transgressive phases as part of a development towards tidal flat conditions. Therefore an permanent influence of seawater has to be assumed for the Wangerland. On the other hand, the lagoonal

sediments of the Schweiburg site show the highest TOC enrichments while As, Mo, and TS are distinctly lower when compared with the remaining locations. The lagoonal sediments in the lower part of the Schweiburg core reflect only a very weak transgressive event, which explains the onset of peat growing above this section. Additionally the above mentioned formation of the natural levee in the upper part of the core protected the Schweiburg location against the rising North Sea and led to a significant freshening which promoted reed growth. As a result the input of seawater and redox-sensitive trace metals and sulphate was reduced. The Loxstedt core occupies an intermedium position with respect to the Wangerland and Schweiburg locations. The proximity to the river Weser led to the development of an estuarine tidal flat situation which is characterized by varying salinities as seen in the continuously changes between lagoonal sedimentation and peat-forming phases in the central part of the core (Figure 2.4.2). The similar TS values of the Loxstedt and Wangerland locations may lead to a misinterpretation concerning salinity. As the availability of metabolizable organic matter controls the rate of sulphate reduction the TS content is not an appropriate proxy for estimating palaeosalinity. The abundance of redox-sensitive trace metals like As and Mo, which are higher at the Wangerland site, instead should be used for comparison.

Figure 2.4.13b shows the EFS values for the brackish sediments only for the Loxstedt and Wangerland location because brackish sediments are presumably not preserved in the Schweiburg core. Regarding the abrupt change from bog peat to tidal flat sediments in the lower part of the Schweiburg core (Figure 2.4.2) one can imagine that formerly existing lagoonal and/or brackish sediments were eroded by a transgressive event. On the other hand the formation of the natural levee in the upper part of the core led to a lagoonal system and prevented brackish sedimentation. Nevertheless, the Loxstedt and Wangerland brackish sediments show a similar geochemical composition. Only a trend towards higher Mn and lower Zr contents is visible in the Loxstedt core. This trend continues in the mixed flat sediments (Figure 2.4.13c) and seems to be related to the estuarine character of the Loxstedt location. On one hand the riverine input contributes large amounts of Mn to the system (see above) and on the other hand Mn is removed from solution at low salinities (Knox *et al.* 1987). Hence, accompanied by flocculation

processes during estuarine mixing (Postma, 1967), these conditions may lead to Mn enrichments in the sediment as it is observed for the investigated samples.

However, the Mn concentrations vary in the Loxstedt profile. While the lower tidal flat sediments are characterized by Mn/Al ratios similar to the remaining cores (Mn/Al $\cdot 10^{-4}$ : Loxstedt 91, Wangerland/Schweiburg 97) the upper tidal flat sediments show a distinct enrichment (Mn/Al $\cdot 10^{-4}$  222) in the Loxstedt core. Therefore, we assume that the river Weser was characterized by a slightly oscillating watercourse during the Holocene. This assumption is supported by the investigation of diatoms (Dellwig *et al.*, 1999c). The abundance of *Cyclotella meneghiniana*, a typical species of the river Weser, increases only in the upper part of the Loxstedt core.

Regarding the lower EFS values for Zr it seems obvious that the Loxstedt core exhibits a significant lack in heavy minerals. This difference likely has to be attributed to the accumulation of heavy minerals in the coastal tidal flat sediments (Wangerland, Schweiburg) as a result of reworking of older sediments (Dill, 1998) while within the fluvially influenced estuarine situation (Loxstedt) heavy minerals are generally less abundant because of less pronounced reworking processes.

### Summary

This study provides an overview about the inorganic geochemistry of Holocene coastal deposits from NW Germany. The basis of this work form nine drill cores from four locations which were analysed at high-resolution for bulk parameters, major, and selected trace elements.

*Geochemical characteristics of the individual facies:* The investigated cores contain fen and bog peat deposits which can be subdivided into basal and intercalated peats. In comparison to a reference peat core from the heathland (Aurich Moor), the coastal peats contain elevated amounts of lithogenic elements (e.g. Al, Mg, Si, Ti). The intercalated peats received the lithogenic material predominantly from periodical flooding whereas the basal peats are influenced by a process occurring after peat growing. Tidal channel

activities led to a partial uplift of the basal peat and allowed the input of seawater and clastic material. As a result discrete clastic layers were formed within the basal peats which encouraged the further inflow of seawater. Most of the peat layers are characterized by intense pyrite formation as a result of microbial reduction of seawater sulphate. Accompanied with the formation of pyrite the seawater derived redox-sensitive trace metals As and Mo are enriched in pyrite-rich peat layers, while other trace metals like Co, Cr, Pb, or Zn reflect more or less the geogenic background. Like for the input of clastic material pyrite formation and trace metal enrichments occurred after two mechanisms: i) during peat growing (intercalated peats) and ii) subsequent to peat growing (basal peats).

The major clastic facies of the investigated Holocene deposits are tidal flat, brackish, and lagoonal sediments, which can be distinguished by varying proportions of the main components quartz, clay, carbonate, and organic matter due to varying depositional energy and palaeosalinity. The tidal flat sediments contain elevated amounts of quartz and heavy minerals as seen in enrichments of Si, Ti, Y, and Zr, while the brackish and lagoonal sediments were formed under comparatively calm depositional conditions. Especially the lagoonal sediments show an almost shale-like geochemical composition. The occurrence of biogenic carbonate in the brackish sediments, as seen in enrichments of Ca and Sr, reflect a distinctly higher salinity for this facies in comparison to the almost carbonate-free lagoonal facies. By contrast, the lagoonal facies contains higher amounts of TOC which is predominantly the result of reed growing under a considerably lower mean salinity (<10‰). Therefore, a higher availability of organic matter encouraged the formation of pyrite which explains enrichments of TS, As, and Mo in the lagoonal sediments.

*Implications for the palaeoenvironment:* The investigated drill cores originate from four locations which are supposed to represent different palaeoenvironmental developments. Three locations are situated within (Arngast) or close to (Schweiburg, Wangerland) the present Jade Bay and one site originates from the right bank of the river Weser (Loxstedt). On the basis of the geochemical characteristics of the individual facies estimates about their exposition to the coastline are possible. High enrichments of As

and Mo seen in the basal and intercalated peat of the Arngast core reflect an open intertidal system and a continuous seawater influence during peat formation. On the other hand low enrichments found in the intercalated peat of the Schweiburg core reflect a complete silting up process which culminated in the formation of bog peat. This silting up process is most likely encouraged by the development of a natural levee within the ancient Jade Bay. As a result the direct influence of seawater was reduced. The basal peats of the Wangerland cores show elevated As and Mo contents as well. However, these enrichments are favoured by clastic layers within the peat which enable the further input of seawater. For that reason an estimate of palaeosalinities on the basis of trace metal distributions would lead to a misinterpretation. The Loxstedt core reflects an estuarine intertidal situation as seen in enrichments of Mn and TOC in the clastic sediments. However, the influence of the river Weser changed during the Holocene as reflected by varying contents of Mn in the tidal flat sediments.

**Acknowledgements** - The authors wish to thank J. Barckhausen and H. Streif (Geological Survey of the Federal State of Lower Saxony, Germany) for supporting the drilling and for lithological core descriptions. Furthermore we would like to thank M. A. Geyh (Geological Survey of the Federal State of Lower Saxony, Germany) for performing the  $^{14}\text{C}$ -age determinations and W. Bartels (LUFA, Soil-Physical Laboratory, Germany) for botanical macroresidual analyses. Thanks also to B. E. M. Petzelberger (Niedersächsisches Institut für historische Küstenforschung, Wilhelmshaven, Germany) for the supply of the reference core from the Aurich Moor. This study was financially supported by the German Science Foundation (DFG) through grant No. Scho 561/3-2 and forms part of the special research program "Bio-geochemical changes over the last 15,000 years - continental sediments as an expression of changing environmental conditions".



## Chapter 3

### 3.1. Pyrite used as a tool for palaeoenvironmental reconstruction of a Holocene depositional sequence from the coastlands of NW Germany

O. Dellwig, F. Watermann, H.-J. Brumsack, G. Gerdes and W. E. Krumbein

**Abstract** - A drill core from the marshlands of NW Germany covering the entire Holocene deposits was analysed at high-resolution by geochemical (XRF, Cirm-MS) and microfacies methods (diatoms, thin sections, SEM) in order to provide information about the palaeoenvironmental development. The core contains an intercalated reed peat layer and a basal peat. The basal peat consists in the lowest part of fen woodland and raised bog peat while the upper part is formed by a reed peat bed. The peat layers are characterized by a distinct enrichment of pyrite which occurs only with framboidal texture. Fermentation experiments have shown that sulphate-reducing bacteria are strongly dependent on low molecular compounds produced by, e.g., cellulose fermenting fungi because peat provides only less metabolizable organic matter. The total sulphur content of the peat layers averages to 7.8% with a maximum value of 28.2% unusually found within the basal peat at the transition of fen woodland and raised bog peat. The pyrite enrichments can be explained by two different scenarios. On the one hand pyrite formation coincides with the peat growing, which is decisive for the reed peats. Here a brackish zone is assumed for the peat-forming environment which is influenced by iron-rich freshwater and sulphate-rich seawater. As the freshwater forms the major Fe source the amounts of pyrite increase to a certain degree with decreasing salinity in this environment. The palaeosalinity is estimated by the investigation of benthic and pelagic diatoms. On the other hand the unusual high contents of pyrite found within the basal peat at the transition of fen and bog peat points to a subsequent process after the peat was formed. Thin sections of this interval reveal clastic layers (1 to 3 mm) with completely pyritized interfaces. These clastic layers are most likely caused by tidal channel activities due to the sea-level rise, which led to an uplift of the peat at weak and crumbly transition zones. As a result of the uplift an input of suspended particulate matter is possible. When the peat settle down a clastic layer remains whose interface to the peat may have acted as an aquifer for waters of higher salinity. Therefore, an enhanced formation of pyrite was possible due to the combination of sulphate-rich ground water and iron-rich peatland waters. The marine origin of the clastic material is documented by the occurrence of marine pelagic diatoms.

## Introduction

Pyrite is a well known mineral, typically found in anoxic, sulfidic, marine sediments (e.g., Berner, 1970, 1984) while limnic systems are often characterized by the formation of siderite and vivianite (Berner, 1981; Postma, 1982). A transition between marine and limnic conditions exists, e.g., in recent salt marshes from the east coast of the U.S.A. and peat-forming coastal environments from the Florida Everglades which often contain enhanced amounts of pyrite (e.g. Giblin, 1988; Price & Casagrande, 1991). However, despite of its occurrence in various settings the mechanism of pyrite formation and its relation to texture (euhedral and framboidal) is not completely understood (e.g. Rickard, 1970; Sweeny & Kaplan, 1973; Raiswell, 1982; Schallreuter, 1984; Sawlowicz, 1993; Rickard, 1997).

During the Holocene the coastlands of NW Germany were characterized by the occurrence of extended areas of peat-forming vegetation. These peat-forming areas form part of silting up zones which have no recent example as a result of anthropogenic activity (e.g. dike-building). From a stratigraphic view basal and intercalated peat environments can be distinguished. The latter are encountered between clastic sediments of predominatly marine origin resulting from a shifting coastline, whereas the basal peats overlay Pleistocene deposits (Streif, 1990).

Holocene peats of the coastal area of NW Germany are often characterized by high amounts of pyrite (Dellwig *et al.*, 1999a). Such pyrite enrichments can only be explained by processes which have to be related to palaeoenvironmental changes during the Holocene sea-level rise. However, geochemical investigations in the study area regarding pyrite formation are very rare (Dellwig *et al.*, 1999a), although pyrite should preserve information about the palaeoenvironmental evolution. Therefore, the main objective of this work is to explain the processes which led to the formation of pyrite within the peat layers. For this reason, it seems necessary to characterize the element sources (Fe, S, organic matter) and their potential limitation during pyrite formation. Finally this investigation will complement the palaeoenvironmental reconstruction carried out by Watermann *et al.* (1999) based on the clastic sediments of the drill core.

### Regional setting and lithology

This work is based on the study of one drill core (W5; Archive No. KB 5950) which forms part of a transect of five cores in the NW German coastal area (Figure 3.1.1). The transect was drilled in summer 1996 with the support of the Geological Survey of the Federal State of Lower Saxony (Germany) in the marshlands of the Wangerland located about 18 km NW of Wilhelmshaven close to the Jade Bay. This area was formerly a sheltered so-called Crildumer Bay which was presumably divided by a peninsula into a northern and a southern part (Petzelberger, 1997). The transect is located in the southern part of this bay and is of about 3 km long. Core W5 was chosen for a detailed investigation based on its extreme amounts of pyrite especially within the basal part. The core is about 6.80 m long and covers the entire Holocene.

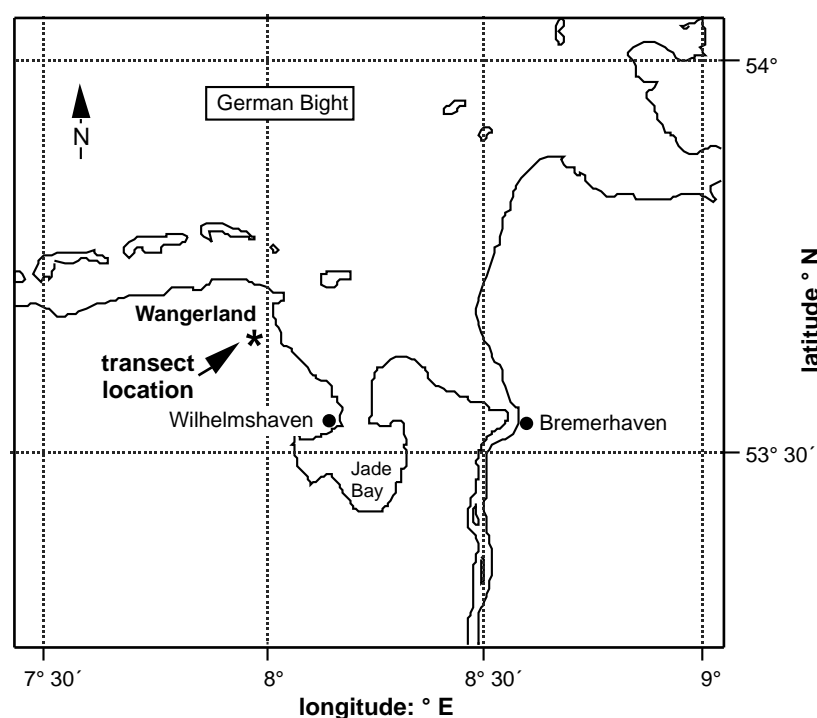


Figure 3.1.1: Map of the study area showing the transect location.

According to Barckhausen *et al.* (1977) core W5 is composed of four different lithological units. Figure 3.1.2 shows the lithology of the core as derived from geochemical and microfacies analysis (Watermann *et al.*, 1999) as well as from

microscopic examination of plant fragments from several peat samples. The microscopic analyses were kindly performed by W. Bartels (LUFA, Soil-Physical Laboratory) according to the methods given by Grosse-Brauckmann (1962). Furthermore four peat samples were chosen for  $^{14}\text{C}$ -age determination which kindly was carried out by M.A. Geyh (Geological Survey of the Federal State of Lower Saxony, Germany). The resulting average calibrated ages were calculated using the  $^{14}\text{C}$  age calibration program CALIB 3.0 (Stuiver & Reimer, 1993) and are presented in Figure 3.1.2 as well.

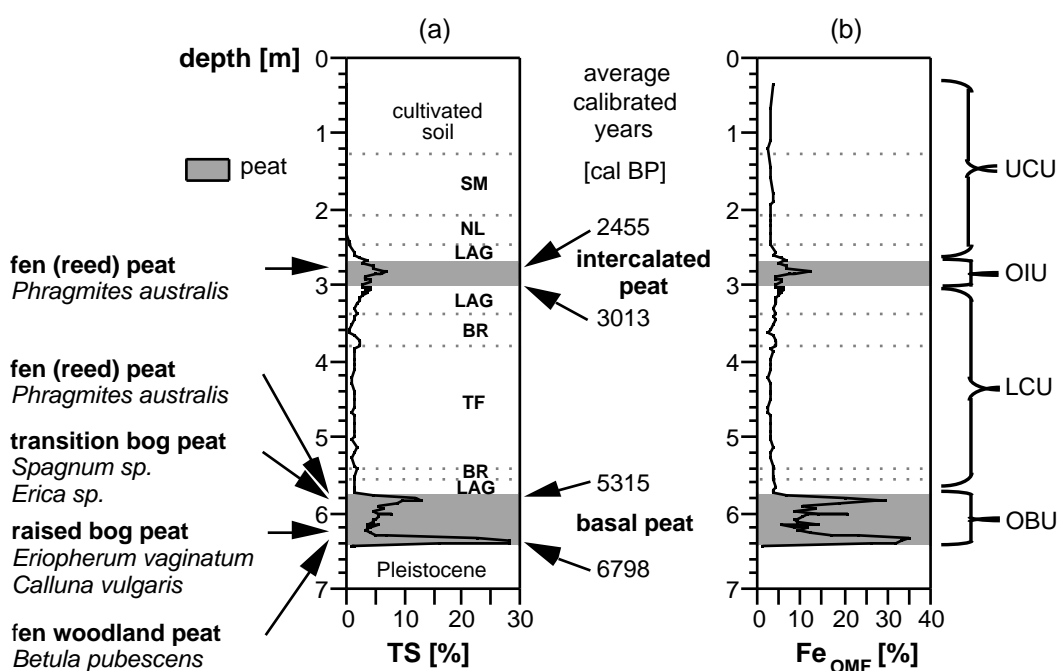


Figure 3.1.2: Depth profiles of TS and Fe on an organic matter-free basis as well as results from microscopic examination of plant fragments,  $^{14}\text{C}$ -age determinations of four peat samples [average calibrated years BP] and the lithology of the drill core W5 (BR=brackish, LAG=lagoonal, NL=natural levee, SM=salt marsh, TF=tidal flat) with the four main sedimentary units (UCU=upper clastic unit, OIU=organic interfingering unit, LCU=lower clastic unit, OBU=organic basal unit).

The organic basal unit (OBU), consisting of fen and bog peats, forms the basis of the core. This unit spans the time period from 6,800 to 5,315 years BP. The deepest sample reflects the onset of peat formation, while the age from the upper part of the basal peat likely represents the moment of the first marine contact. The overlying clastic sediments

form the lower clastic unit (LCU) which consists of material deposited under increasing marine conditions (lagoonal, brackish, and tidal flat sediments). The lower part of the LCU represents a transgressive flooding sequence whereas the upper part shows the reverse sequence due to increasing silting up. This process culminates in the formation of an intercalated reed peat layer representing the organic interfingering unit (OIU). The formation of this intercalated reed peat occurred between 3,000 and 2,450 years BP. After this time interval fully marine conditions ceased. The overlying upper clastic unit (UCU) consists of lagoonal sediments, a natural levee, and salt marsh deposits.

## **Material and methods**

### *Geochemistry*

High-resolution sampling (total of 163 samples) was performed at 5 to 10 cm in clastic and at 1 to 3 cm in organic-rich intervals, depending on lithology. After core recovery samples were stored in polyethylen bags, sealed, and immediately frozen. At the laboratory samples were freeze-dried and homogenised in an agate mortar. The ground powder was used for all subsequent geochemical analyses.

The samples were analysed for the major elements Al, Fe, Si as well as for the trace metals Rb and Zr by XRF (Philips PW 2400, equipped with a Rh-tube) using fused borate glass beads. Samples with a total organic carbon (TOC) content of more than 10% were heated to 500°C to remove TOC prior to adding lithiumtetraborate and fusing in Pt-Au-crucibles.

Total sulphur (TS) and Total carbon (TC) were analysed in 124 samples after combustion using an IR-analyser Leco SC-444. Total inorganic carbon (TIC) was determined with a UIC Coulometrics Inc. CM 5012 CO<sub>2</sub> coulometer coupled to a CM 5130 acidification module (Huffman, 1977; Engleman *et al.*, 1985). The total organic carbon (TOC) content was calculated as the difference between TC and TIC.

Analytical precision and accuracy of XRF measurements were tested by replicate analysis of geostandards (GSD-3, GSD-5, LKSD-1, SDO-1, SGR-1) and several in-

house standards (see appendix). The precision of TS, TC, and TIC measurements was checked in series of double runs and accuracy was determined by using in-house standards (see appendix).

For the investigation of the bulk sediment S-isotopic composition (kindly performed by M. E. Böttcher), 32 solid phase peat samples were first washed to remove chloride. Afterwards the samples were dried and directly analyzed by combustion isotope-ratio-monitoring mass spectrometry (C-irm MS) according to the method described by Böttcher *et al.* (1998). The precision was better than  $\pm 0.3\%$ . Isotope ratios are given relative to the Vienna-CDT.

### *Diatoms*

Benthic and pelagic diatoms were analyzed in 83 samples following the method of Schrader (1973). Specimen were counted and identified with a light microscope at 1000X magnification. Species identification is based on Round (1990), Pankow (1990) and Hartley (1994). The diatoms were classified into ecological groups which are related to specific sedimentary environments and salinity classes (Vos & de Wolf 1993). For a more detailed description of the methods used see Dellwig *et al.* (1998).

### *Thin sections*

Sediment samples were taken in small aluminum dishes (3.8 cm diameter and 2 cm height), treated with 5% formaldehyde in seawater for 5 days followed by a stepwise exchange of salt water from 25% to 100% freshwater. Dehydration was performed with acetone in steps of 5, 10, 25, 50, 75, 100% in water for 12 hours each. Spurr's Resin-Mixture (Spurr, 1969; Wachendörfer, 1991) in acetone was used for embedding (4 days each) in concentrations varying from 25, 50, 75, and 100% Spurr. The resin solidified during one day in 10°C steps from 30 to 70°C. Sawing and grinding of the resin block was performed with an Ecomet III and Thin Sectioning Petro System (Buehler). Samples were first sawed to a suitable size to fit the object holders followed by grinding on a rotation surface using P 320, 400, 600, 800, and 1200 grinding paper to a thickness of 20  $\mu\text{m}$ . Thin sections were investigated by using a binocular (Zeiss Stemi SV 11) as well as

an image processing system (Hitachi 3-CCD Color Camera Model HV-C20 and analySIS 3.0 software, Soft Imaging System).

#### *SEM investigations*

The sample material was dehydrated in ethanol and then dried by the critical point method. After that the samples were sputter-coated with gold and examined by a Hitachi S-3200 scanning electron microscope.

#### *Microbiology*

Two fermentations were performed under anoxic conditions at 20°C and almost neutral pH (6.5-7.2) using a Meredos fermenter and a BCC fermenter MINIBIOR I equipped with an amperometric H<sub>2</sub>S measuring sensor with a piko ammeter (AMT Rostock, H<sub>2</sub>S detection range 0.05-10 mg l<sup>-1</sup>). The fermentations were carried out with filtered and autoclaved seawater (salinity 30‰) and autoclaved raised bog peat. One fermentation was carried out only with sulphate-reducing bacteria while the second fermentation was done with a cellulose-fermenting fungi (*Acremonium* sp.) for 4 weeks prior to inoculate sulphate-reducing bacteria (*Desulfovibrio sapovorans*, *Desulfococcus multivorans*).

## **Results and discussion**

#### *Sulphur and iron in peat*

The depth profile of total sulphur (TS) of the drill core W5 shows three areas with distinct TS enrichment as a result of microbial sulphate reduction (Figure 3.1.2a): i) the intercalated reed peat in the organic interfingering unit (OIU), ii) the reed peat in the upper part of the organic basal unit (OBU), and iii) the lowest part of the OBU which covers the transition between fen woodland peat and raised bog peat. The TS values of the two reed peat layers (OIC: average 4.4%, range 2.6-7.1%; OBU: average 12.4%, range 11.8-13.1%) are in the order of magnitude typical for reed peats of the study area (Dellwig *et al.*, 1999a). Furthermore the TS values are comparable to results from other

peat-forming coastal environments. For instance, Casagrande *et al.* (1977) found TS contents between 1.3-10.1% (average 5.2%) in marine influenced peats from the Florida Everglades (U.S.A.). However, the maximum TS content of 28.2% in the lowest 10 cm thick part of the basal peat (OBU), consisting of fen woodland and raised bog peat which reflect limnic S-limited systems, is rather striking.

Regarding the Fe content on an organic matter-free basis ( $\text{Fe}_{\text{OMF}}$ ; Figure 3.1.2b) a profile similar to TS is evident. This indicates the presence of pyrite, which is confirmed by the scatter plots in Figures 3.1.3a and b. While in the depth profile  $\text{Fe}_{\text{OMF}}$  values are presented in order to eliminate dilution effects caused by organic matter, Figures 3.1.3a and b show the calculated Fe fraction which is available for pyrite formation ( $\text{Fe}_{\text{avail.}}$ ).

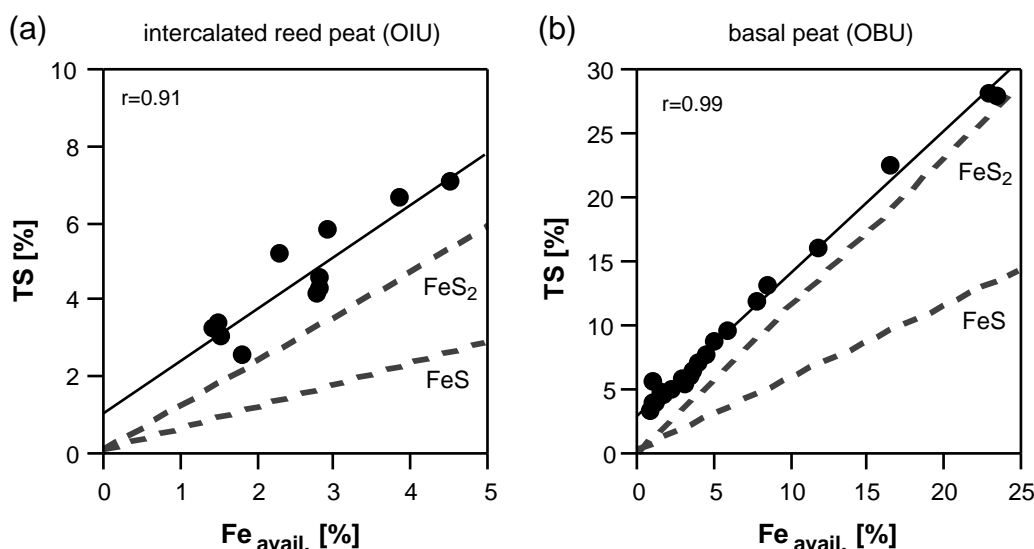


Figure 3.1.3: Scatter plots of TS versus Fe available for pyrite formation ( $\text{Fe}_{\text{avail.}}$ ) of the intercalated reed peat and the basal peat of the drill core.

This Fe fraction consists mainly of Fe-oxyhydroxides (e.g., ferrihydrite, haematite, goethite, lepidocroite) and is characterized by half-lives of hours to several days towards the reaction with dissolved sulphide (Canfield *et al.*, 1992). A further Fe fraction forms the silicate-bound Fe which is only marginally involved in the formation of pyrite (Canfield & Raiswell, 1991). The half-life of about 80,000 years for Fe from sheet silicates is extremely high when compared with reactive Fe minerals. The available Fe



(Fe<sub>avail.</sub>) shown in Figures 3.1.3a and b is calculated using the following empirical formula (Brumsack, 1988):

$$\text{Fe}_{\text{avail.}} = \text{Fe} - 0.2 \cdot \text{Al}.$$

This calculation bases on the assumption that the Fe fraction, which is fixed in silicate structures empirically amounts to about 20% of the Al content. Taking into account the high degree of pyritization (Raiswell *et al.*, 1988) of selected peat samples, which varies between 81-93% (average 90%), it can be assumed that almost all Fe<sub>avail.</sub> is fixed as pyrite. The scatter plots of Figures 3.1.3a and b reveal that Fe<sub>avail.</sub> is significantly correlated to the TS content of the intercalated reed peat (OIU) and basal peat (OBU) indicating its fixation in pyrite. However, the regression lines plot above the theoretical pyrite ratio. Therefore Fe-limitation and resulting formation of organic sulphur compounds have to be assumed while the significant presence of Fe-monosulphides (FeS<sub>x</sub>) can be excluded. This assumption is in accordance with studies on recent salt marshes (e.g. Howarth, 1979; Howarth & Teal, 1979).

Taking into account the high sulphate reduction rate occurring in organic-rich coastal environments (e.g. Howarth & Teal, 1979; Howarth & Giblin, 1983), one can imagine that excess H<sub>2</sub>S is produced which is not converted into pyrite due the lack of Fe<sub>avail.</sub>. As a result, H<sub>2</sub>S and its oxidation products may react with humic substances to form organic sulphur compounds (Francois, 1987). This non-pyritic sulphur fraction mainly consists of carbon-bound sulphur as documented by Casagrande *et al.* (1977). They report about 50% carbon-bound sulphur in a marine Everglades Swamp (U.S.A.) and up to 70% in freshwater peats from Okefenokee Swamp, Georgia (U.S.A.). Additionally, Ferdelman *et al.* (1991) investigated the sulphur enrichment in a *Spartina alterniflora* marsh sediment core from the Delaware salt marsh (U.S.A.) and reported a maximum value of 51% humic sulphur with respect to the amounts of total sulphur. This humic sulphur consists mainly of sulfoxides, sulfanes, and organic sulphides/polysulphides.

Considering the amounts of Fe<sub>avail.</sub> and TS the fraction of non-pyritic sulphur can be estimated. The calculated non-pyritic sulphur contents in the investigated peats are comparable to the above mentioned results. Although this sulphur fraction varies significantly in quantity (from 4 to 80%) the average value amounts to 38% and only

five samples are below 20%. Highest contents are found in the relatively pyrite-poor raised bog peat of the OBU (average 64%) while the pyrite-rich reed peat samples of the OIU and OBU are characterized by lower amounts of this fraction (average OIU 36%, average OBU 24%). The lowest proportions (averaging to 5.2%) are found in the lowest section of the OBU where highest TS contents of 28.2 % occur. Therefore it can be concluded that the availability of Fe plays an important role for the formation of pyrite within the peat-forming environments. For this reason high levels of non-pyritic sulphur occurring in the raised bog peat reflect the low input of detrital material into this environment. In contrast, the reed peat samples, which are stronger influenced by flooding, show lower contents of this sulphur fraction because enhanced amounts of  $\text{Fe}_{\text{avail.}}$  can react with  $\text{H}_2\text{S}$  derived from bacterial sulphate reduction.

#### *Pyrite texture*

Pyrite occurs in sediments predominantly in two textures: as euhedral and framboidal pyrite. The formation of framboidal pyrite most likely requires an intermediate step over greigite resulting from the reaction of initially formed Fe-monosulphides and elemental sulphur. On the other hand, euhedral pyrite is formed by the direct precipitation of Fe-oxyhydroxides or Fe-monosulphides in the presence of  $\text{H}_2\text{S}$  (Sweeney & Kaplan, 1973; Rickard, 1975). In marine sediments the pyrite texture seems to be controlled by the availability of Fe (Raiswell & Plant, 1980). Framboidal pyrite is formed locally within the sediment by the reaction of redistributed in situ Fe with sulphides, while euhedral Fe is formed when local sources are exhausted and the transport of Fe by diffusion from surrounding sediments is necessary. Therefore the porewater chemistry plays an important role. As reported by Raiswell (1982) in addition to the Fe availability the concentration of seawater sulphate is of crucial importance for the resulting texture. Framboids are formed under open system conditions at high sulphate reduction rates whereas inverse conditions are true for euhedral pyrite.

Investigations on recent TOC-rich salt marshes reveal an additional process. Luther *et al.* (1982) and Giblin (1988) found predominantly euhedral pyrite while framboidal

pyrite (size range 5 to 25  $\mu\text{m}$ ) was less abundant. They assume a very rapid pyrite formation within days or weeks, as mentioned by Howarth (1979), due to the porewater composition, which is supersaturated with respect to pyrite and undersaturated with respect to Fe-monosulphides. As a result of oxidation initiated by plant activity and tidal flushing polysulphides and elemental S were formed which react with reduced Fe to pyrite without Fe-monosulphide intermediates pointing towards euhedral pyrite.

Pyrite formation experiments with Fe and polysulphides at 25 and 100°C by Luther (1991) confirm the formation of euhedral pyrite at ambient temperature but with the occurrence of a FeS intermediate while framboids were only found at 100°C. On the other hand Lord (1980) reported the occurrence of FeS in the uppermost 10 cm of Great salt marsh sediments (U.S.A.) and Lord and Church (1983) found framboidal pyrite in the Delaware salt marsh (U.S.A.). According to Wang and Morse (1996) supersaturation of the porewater with respect to pyrite influences the resulting pyrite texture. Thus, the higher the supersaturation the more spherulitic pyrite is formed. The rapid formation of pyrite does not necessarily exclude the framboidal structure. Additionally their study stressed that the formation of framboidal pyrite can directly develop from a mackinawite cluster. This was also evidenced by Rickard (1997) who showed that the reaction between FeS and  $\text{H}_2\text{S}$  to pyrite without greigite intermediate is very rapid and has to be favoured in anoxic systems. Butler (1995) used this reaction and was able to produce framboidal pyrite.

SEM investigations on selected peat samples from the intercalated reed peat (OIU) and from the lowest pyrite-rich part of the basal peat reveal only framboidal pyrite (Figures 3.1.4a and b). The framboids vary in size from 10 to 30  $\mu\text{m}$  in diameter. A difference between the two peat sections is the random distribution of framboids within the peat matrix of the intercalated reed peat while in the basal peat often clusters of framboids are observed which can be called polyframboides after Postma (1982). As mentioned above oxidation processes occurring in salt marshes are thought to be of main importance for the formation of pyrite.

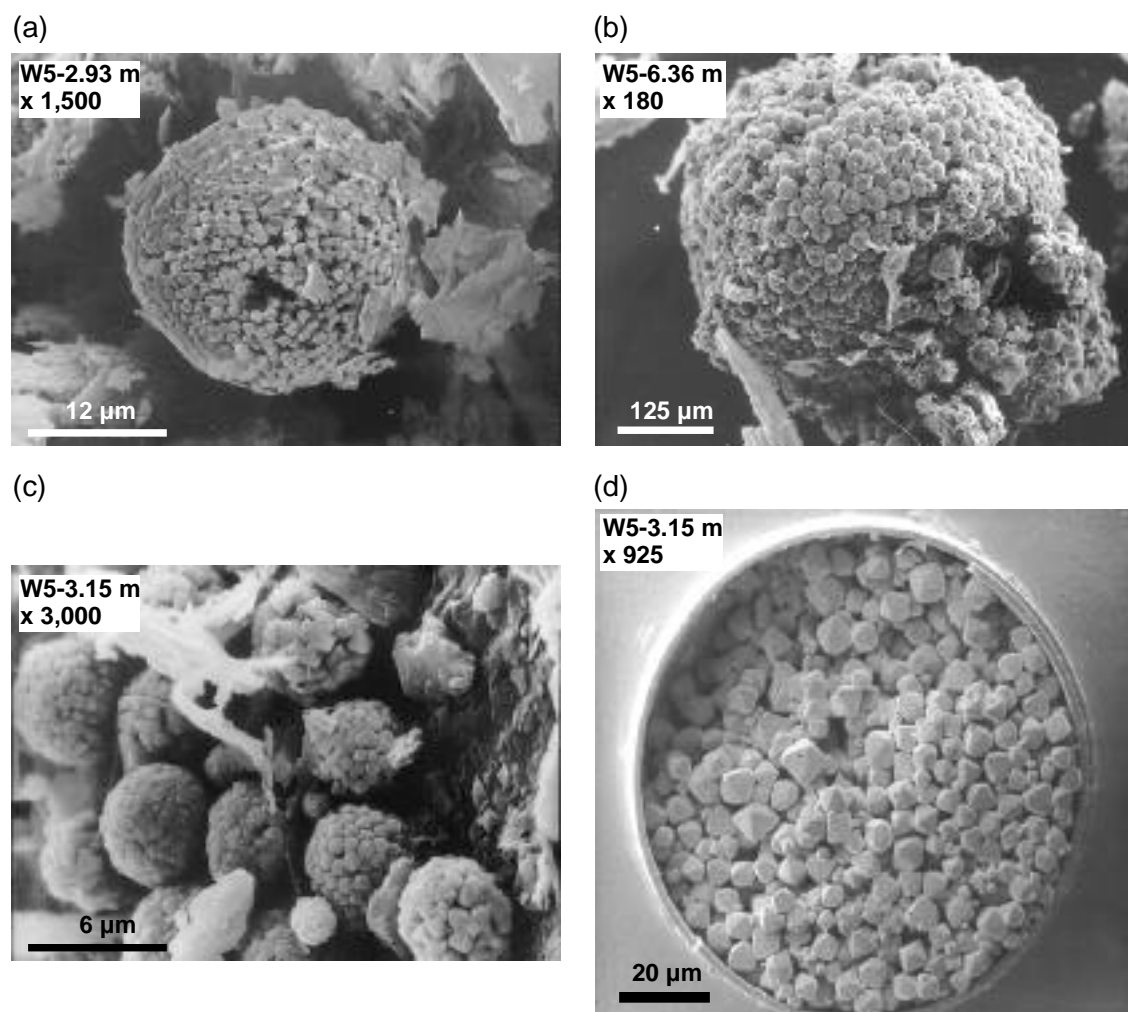


Figure 3.1.4: SEM photographs showing pyrite within peat and lagoonal sediments: a) framboid in the intercalated reed peat, b) polyframboid in the pyrite-rich part of the lower basal peat, c) framboidal pyrite in lagoonal sediments below the intercalated reed peat, and d) euhedral pyrite infillings of a diatom frustule found within the lagoonal sediments.

For example Howarth and Teal (1979) determined the sulphate reduction rate in salt marsh sediments and found that less pyrite (1.8-9%) was formed with respect to the high sulphate reduction rate. Therefore, the extremely high amounts of pyrite within the lowest part of the basal peat can be attributed to a lack of such oxidation processes because no tidal flushing and plant activity occurred. As this part of the basal peat is assumed to be characterized by strictly anoxic conditions the high rate of pyrite formation is in agreement with the results of Rickard (1997) mentioned above. For the partially oxygenated system of the intercalated reed peats the pathway via a greigite

intermediate state seems to be more significant, in accordance to results of Morse and Cornwell (1987). They presume greigite as an intermediate compound during the formation of framboidal pyrite in salt marsh sediments owing to the seasonal variation in redox states.

On the other hand, in the lagoonal sediments below the intercalated peat framboidal pyrite and euhedral pyrite as infillings of diatom frustules are found (Figures 3.1.4c and d) which indicate the formation of pyrite within microenvironments as proposed, e.g., by Schallreuter (1984). In comparison to the peat samples the framboids of the lagoonal sediments are distinctly smaller (about 5  $\mu\text{m}$  in diameter). The occurrence of euhedral pyrite within diatom frustules in the lagoonal sediments is possibly related to the availability and reactivity of Fe, as reported for instance by Passier *et al.* (1997) on Mediterranean sapropels and sediments. The pyrite infillings of the diatoms most likely reflect the fact that these species were alive where they are found. After their death and sedimentation the protoplasm is used for the production of  $\text{H}_2\text{S}$  by sulphate-reducing bacteria. Diatom tests form a microenvironment where  $\text{H}_2\text{S}$  can react with Fe, supplied by diffusion from the surrounding sediment, to euhedral pyrite.

#### *Element sources*

For the formation of pyrite three components have to be available (e.g. Berner, 1970, 1984): i) reactive Fe (mainly derived from Fe-oxyhydroxides), ii) sulphur species, i.e., sulphate (electron acceptor during bacterial sulphate respiration), sulphides (products of bacterial sulphate reduction), and elemental sulphur (resulting from oxidation processes), and iii) metabolizable organic matter (energy source for sulphate-reducing bacteria).

It can be assumed in a first approximation that sufficient organic compounds are available within the peat to satisfy the energy requirement of sulphate-reducing bacteria. However, the use of total organic carbon (TOC) which represents a bulk parameter bears uncertainties because no information is provided whether this organic matter is suitable for microorganisms. Westrich and Berner (1984) reported that the sulphate reduction rate depends directly on the concentration of metabolizable organic carbon. As terrestrial organic matter mainly derived from vascular plants (cellulose, lignin, resins,

waxes) is barely affected by microbial decomposition an organic carbon-limitation is likely during the beginning of sulphate reduction in peat. This assumption is also evidenced by the fact that sulphate-reducing bacteria prefer fatty acids of chain  $C_3$  and up (Belyaev *et al.*, 1981).

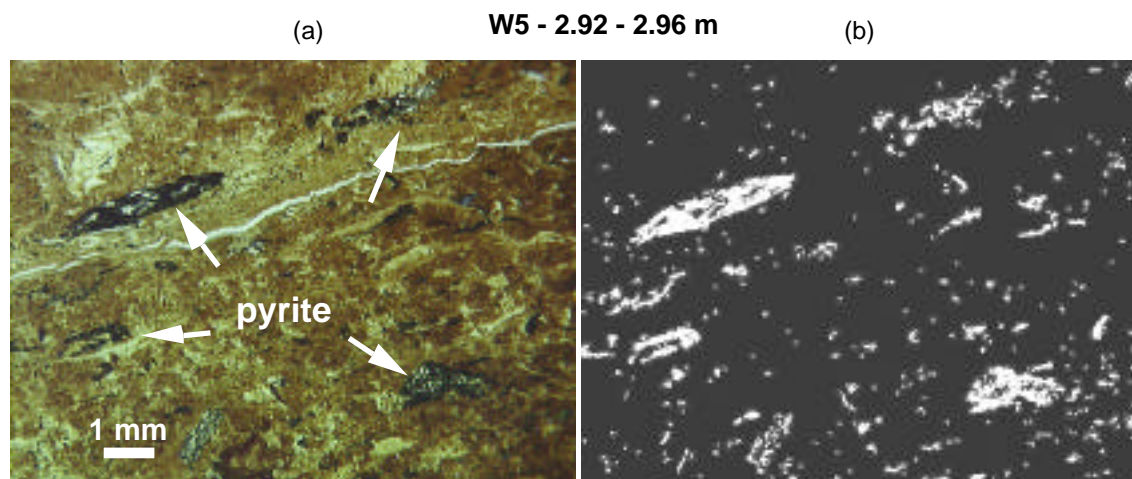


Figure 3.1.5: (a) Thin section and (b) its conversion by image processing (pyrite appears by white areas) of the intercalated reed peat of the drill core.

Figures 3.1.5a and b shows a photograph of a thin section of the intercalated reed peat (OIU) and its conversion by image processing where pyrite appears as a white area. The cluster-like distribution of pyrite within the peat matrix suggests microenvironments which provided better conditions for sulfate-reducing bacteria. It seems possible that in such environments formerly fungi or bacteria communities fermented cellulose, thereby producing low-molecular compounds which served as nutrition for the sulphate-reducing bacteria in a later stage. It is known that sulphate reducers grow in association with other bacteria which are able to ferment cellulose (e.g. *Clostridium spp.*) under anoxic conditions as mentioned by Belyaev *et al.* (1981).

In order to provide information about the availability of organic matter in peat for sulphate-reducing bacteria two fermentations were carried out with raised bog peat (*Eriophorum spp.* and *Sphagnum spp.*) as substrate and seawater under anoxic conditions. The first fermentation was directly inoculated with a mixture of sulphate-reducing bacteria (*Desulfovibro sapevorans* and *Desulfococcus multivorans*), while the

second fermentation was performed with the cellulose-fermenting fungi *Acremonium sp.* under anoxic conditions for four weeks prior to adding the sulphate-reducing bacteria. Figure 3.1.6 shows the total sulphide concentration of both fermentations after inoculating the sulphate-reducing bacteria for 10 days.

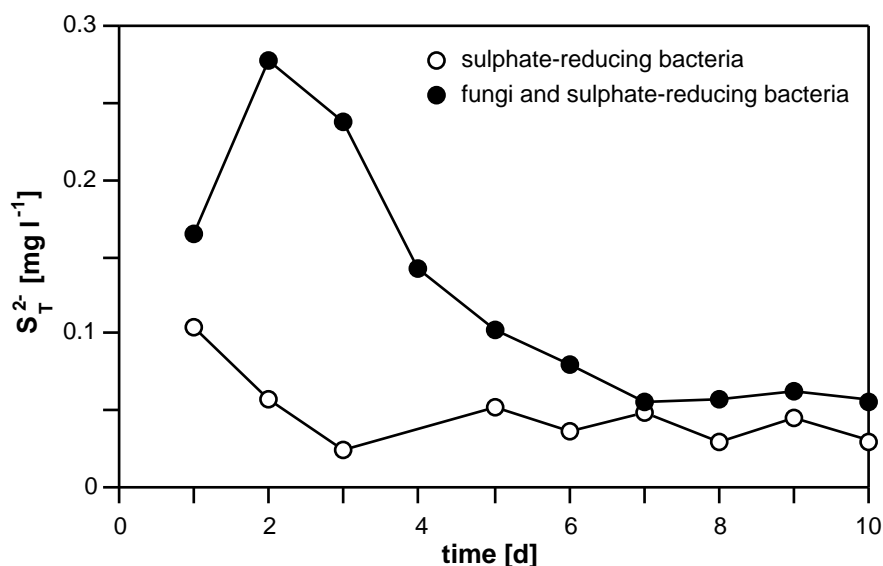


Figure 3.1.6: Total sulphide concentration of two fermentations of fungi and sulphate-reducing bacteria with seawater and raised bog peat.

The fermentation without fungi shows no significant adaptation to the peat substrate as can be seen from the total sulphide concentration which is very low and close to the detection limit. In contrast, the course of the total sulphide concentration of the second fermentation seems to be typical for a static (non-continuous) culture (Schlegel, 1992). The bacteria show an adaptation to the conditions in the fermenter. After an exponential growth phase a stationary phase is achieved and between the third and fourth day a change to the death phase is apparent. However, the enhanced production of sulphide during the second fermentation evidences the assumption that peat does not represent an appropriate substrate for sulphate-reducing bacteria. Therefore it can be concluded that the formation of pyrite in peat is at a first stage organic carbon-limited and sulphate-reducing bacteria have to rely on the preceding decomposition of peat by other organisms (fungi and/or bacteria). These organisms for their part also depend on

favourable conditions (e.g. almost neutral pH) most likely occurring in microenvironments.

The second component which is needed for pyrite formation are the above mentioned sulphur species. Regarding the constant marine influence especially on the reed peats, as documented by the occurrence of marine pelagic diatoms (Waterman *et al.*, 1999), seawater sulphate is considered to be the main sulphur source for the production of  $H_2S$  by sulphate-reducing bacteria. Furthermore sulphur is released during the microbial decomposition of organic sulphur compounds of the host flora. However, this fraction is small compared the sulphate derived from seawater owing to the low sulphur content of peat-forming plants (TS <0.01%; Behrens, 1996). As mentioned, e.g., by Berner (1970) the occurrence of elemental sulphur may be important for the transformation of initial Fe-monosulphides into pyrite. Elemental sulphur can be produced by oxidation of  $H_2S$  and  $FeS_x$  due to wave stirring and diffusion of oxygen. Additionally during the growth season plants oxidize the underlying deposits while during fall and winter more anoxic conditions prevail (Giblin & Howarth, 1984).

In order to provide information about the availability of seawater sulphate stable sulphur-isotope ratios serve as a useful tool. Bulk sediment  $^{34}S$  values of the peat sections reveal the easy availability of seawater sulphate and almost open system conditions. All samples show an enrichment in the light  $^{32}S$  isotope in comparison to the seawater value of +20‰ but also a large variation in sulphur-isotope ratios (average -11.5‰, range -2.6 to -26.7‰). The most negative values are found in the intercalated reed peat of the OIU (maximum -26.7‰) reflecting the almost permanent marine influence. The reed peat layer of the uppermost part of the OBU is also characterized by negative isotopic values (up to -12.0‰) but the fractionation is lower in comparison to the intercalated reed peat. Again, unexpected values are seen in the lowest part of the OBU. Samples with extremely high TS values show negative sulphur-isotope ratios (average -15.2‰; range -11.1 to -17.7‰) as well. The raised bog peat samples of the basal peat are characterized by less negative  $^{34}S$  values (-4.3 to -8.4‰; average -6.1‰) indicating a more diffusion controlled process. However, the average TS content of 5%



in this bog peat section is relatively high in comparison to values of marine unaffected raised bog peats from the study area (average 0.46%; Dellwig & Brumsack, 1999c).

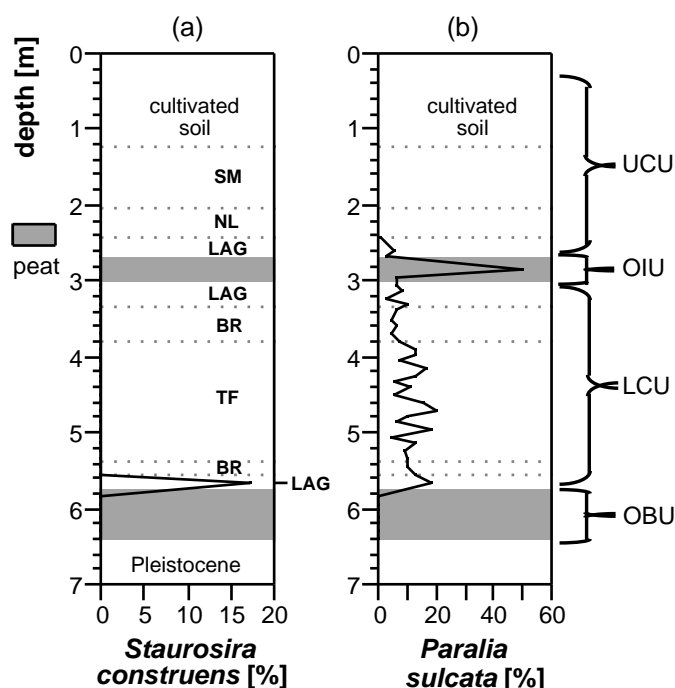


Figure 3.1.7: Relative abundance of two diatoms species (a) *Staurosira construens* (benthic oligohaline) and (b) *Paralia sulcata* (pelagic polyhaline) of the drill core (BR=brackish, LAG=lagoonal, NL=natural levee, SM=salt marsh, TF=tidal flat).

The final component necessary for pyrite formation is Fe. As mentioned above, one Fe source is the input of detrital material via periodical flooding and occasional storm events. This Fe source is considered to be of importance especially for the reed peat layers (OIU and OBU) which were formed under marine influence. However, a limnic input should be also considered due to the general occurrence of oligohaline benthic diatoms in the reed peats (Watermann *et al.*, 1999).

Figure 3.1.7 shows the relative percentage of *Staurosira construens* and *Paralia sulcata* versus depth in the drill core. The oligohaline benthic species *Staurosira construens* shows an enhanced abundance in the reed peat of the OBU and in the overlying lagoonal sediments. In contrast to this, the intercalated reed peat of the OIU is characterized by the occurrence of the pelagic polyhaline species *Paralia sulcata*. For

that reason, a higher salinity of 10 to 15‰ during the formation of the intercalated reed peat has to be assumed when compared to the reed peat of the OBU (salinity <5‰). An additional indicator for the palaeosalinity may be the occurrence of *Phragmites* reed itself because this plant tolerates a maximum salinity of about 10‰ while at higher levels its growth is significantly reduced depending on nutrient supply (Scheer, 1953). Therefore a brackish zone where seawater and freshwater are mixing has to be assumed for this environment. The resulting brackish water contains in a first approximation the dissolved and particulate Fe from terrestrial runoff and from the North Sea. Assuming an almost similar water composition in the past, the water volume necessary to explain the average Fe contents of the reed peat layers can be calculated from actual data. The data used to estimate the Fe concentration of this brackish water originate from i) small rivers close to the study area ( $\text{Fe}_{\text{diss.}} 1,680 \mu\text{g l}^{-1}$ ,  $\text{Fe}_{\text{part.}} 2,970 \mu\text{g l}^{-1}$ ; salinity <0.5‰; Lipinski, 1999), ii) average ocean water ( $\text{Fe}_{\text{diss.}} 2 \mu\text{g l}^{-1}$ ; Martin and Whitfield, 1983), and iii) the open North Sea ( $\text{Fe}_{\text{part.}} 87 \mu\text{g l}^{-1}$ ; salinity >30‰; Dellwig et al., 1999b).

To get an idea about the original peat composition the water content of on average 74% has to be considered. Furthermore it is necessary to get an estimate of compaction. According to Bennema *et al.* (1954) maximum compaction values of 85-90% were attained in Holocene bog peats being strongly dependend on the percentages of fine particles <2 $\mu$  and organic matter. Considering the relatively low TOC content (average 32.6%) of the intercalated reed peat compaction should be lower. The formation of intercalated reed peats depends on a moderate sea-level rise, which requires that the rate of peat formation and sea-level rise are comparable (Streif, 1990). Under this condition the time period in which the reed grew provides an idea of the original peat extent. As Behre (1993) pointed out the average rate of sea-level rise was about 3 mm a<sup>-1</sup> between 6,000 and 3,000 years BP while it dropped from 3,000 years BP to the present to an average value of 1 mm a<sup>-1</sup>. The lower rate seems to be appropriate for the intercalated reed peat because especially the time period between 3,600 and 2,800 years BP was characterized by a comparatively low sea-level rise (Streif, 1990). Furthermore this value is in accordance with results from <sup>14</sup>C age determinations on peats from the study area (Dellwig & Brumsack, 1999b).

Assuming a sea-level rise of  $1 \text{ mm a}^{-1}$ , a growing period of 560 a, and a thickness of 30 cm of the intercalated reed peat the resulting compaction is about 45%. This compaction falls in the range of observed values for Holocene fen peats of the study area (H. Streif, pers. comm., Geological Survey of the Federal State of Lower Saxony, Hannover). On the basis of these assumptions (water content of 74% and compaction of 45%), the average Fe content of 3.3% (d.w.) of the intercalated reed peat (OIU) was 0.48% in the original peat. Therefore the water volume which is necessary to explain the total Fe inventory of 1 kg of the intercalated reed peat layer (OIU) at a salinity of 5‰ amounts to  $1.2 \text{ m}^3$  (based on a total Fe-content of  $4,650 \mu\text{g l}^{-1}$  of the brackish water). At a salinity of 15‰ the volume increases to  $2.0 \text{ m}^3$  because the total Fe content of the brackish water decreases to a value of  $2,370 \mu\text{g l}^{-1}$ . This finding can be interpreted as follows: with increasing salinity the amounts of Fe added to the system decrease, leading to a more pronounced Fe limitation during pyrite formation. Especially the suspended particulate matter of the freshwater environment contributes large amounts of Fe to the peat-forming environment when compared with the North Sea water (see Fe concentrations above). Additionally it should be considered that the increase in salinity also leads to a decrease in dissolved Fe, as this element exhibits a non-conservative behavior during mixing of fresh and saline water masses. Particularly in the low-salinity region (0-10‰) large amounts of Fe are removed from solution (Holliday & Liss, 1976). As a result of such processes of flocculation and precipitation (Postma, 1967) the entire Fe content (dissolved and particulate) of higher salinity water decreases. These effects likely enhance the Fe limitation during pyrite formation at higher salinities.

As mentioned above the diatom inventory of the reed peat layers (OIU and OBU) confirms a higher salinity during the formation of the intercalated reed peat of the OIU while the reed peat of the OBU is characterized by more limnic conditions. Therefore the higher pyrite contents found in the reed peat of the OBU ( $\text{FeS}_2$  calculated from  $\text{Fe}_{\text{avail.}}$ : OBU 9.0%, OIU 2.6%) can be explained by the higher availability of Fe. The sulphate concentration does not seem to limit pyrite formation significantly because sufficient sulphate is available even at lower salinity. Additionally the S-isotopic data document the almost open system conditions presumably favoured by flooding events.

*Implications for the palaeoenvironment*

On the basis of the results presented a scenario of the near-coastal Holocene peat-forming environment arises which is comparable to a fluvatile coastal plain situation as suggested by van der Woude (1981) for Holocene deposits of the Netherlands.

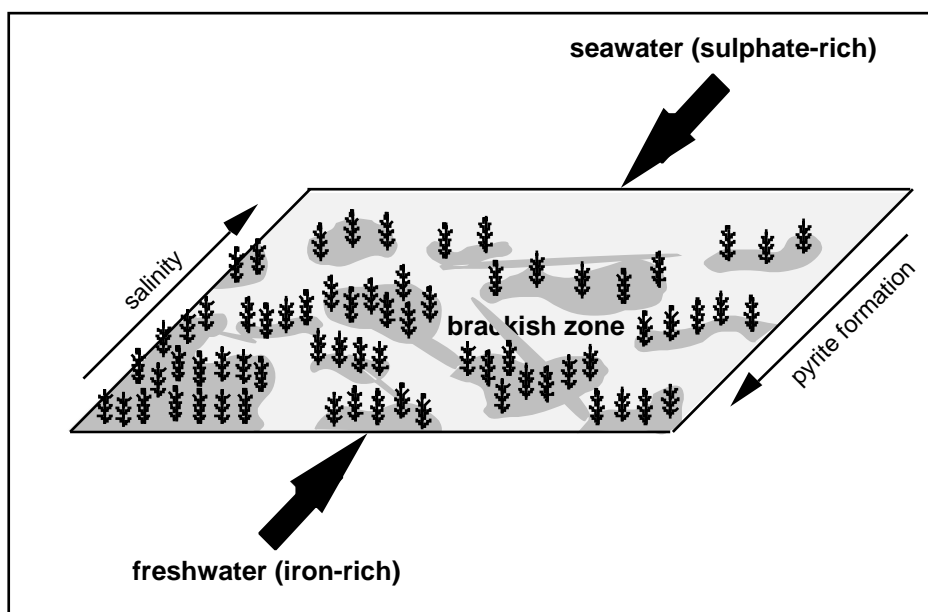


Figure 3.1.8: Picture of the coastlands of NW Germany during the Holocene showing a brackish water zone with moor islands and seawards decreasing stands of reed (modified after van der Woude, 1981).

In Figure 3.1.8 a simplified picture of the brackish zone is shown which is supposed to be characteristic for the Holocene coastlands of NW Germany. Fe-rich freshwater derived from terrestrial runoff and from rivers mix with sulphate-rich seawater. Therefore a brackish water zone with varying salinities exists where moor islands with seawards decreasing stands of reed are present. The brackish zone is characterized by relatively low wave-energy conditions due to the moderate sea-level rise. This environment was perhaps protected by a natural levee system as postulated by Barckhausen *et al.* (1979) which led to a lagoonal deposition area.

In contrast to the reed peat layers the pyrite enrichment in the lowest part of the OBU, covering the transition between fen woodland and raised bog peat, could not be explained by the occurrence of the above mentioned brackish zone. The peat-forming

vegetation of this part of the core reflects an exclusive limnic environment characterized by S-limitation (Göttlich, 1990). In contrast to S sufficient Fe seems to be available for the formation of pyrite in this environment because peatland waters are rich in humic substances and, due to complexation, rich in Fe ( $0.1\text{--}6\text{ mg l}^{-1}$ , Shotyk (1988) and references herein). However, the high amounts of pyrite found within this peat section (up to 50.3%) are in contrast to the assumed S-limitation. Therefore, a sulphur source is needed which is not related to a direct seawater inflow.

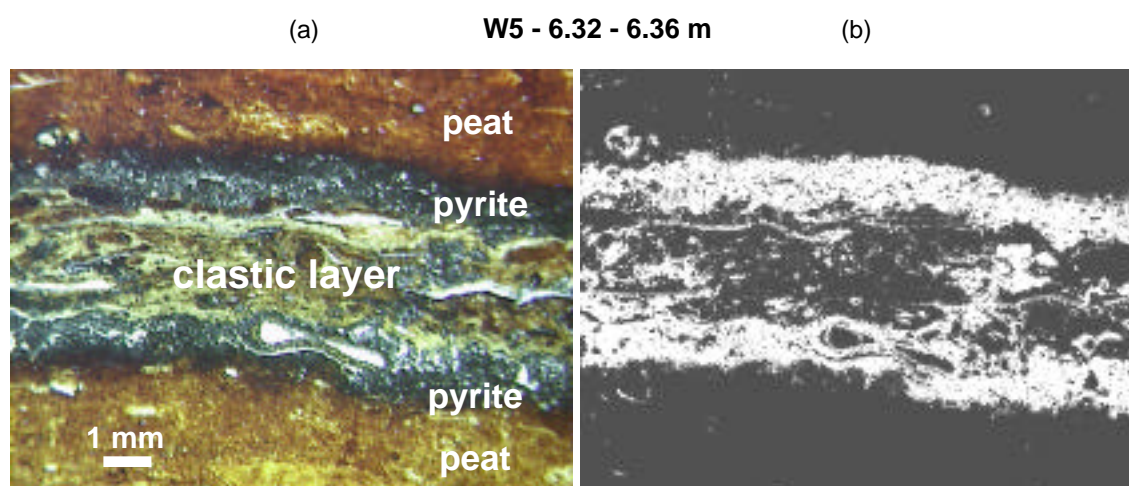


Figure 3.1.9: (a) Thin section and (b) its conversion by image processing (pyrite appears by white areas) of the lower part of the basal peat (pyrite-rich part containing clastic layers).

The thin section presented in Figure 3.1.9 shows this pyrite-rich peat section. Within the transition of fen and bog peat two clastic layers of 1 to 3 mm thickness occur (one layer is shown in Figure 3.1.9) whose boundaries to the surrounding peat are completely pyritized. The occurrence of these clastic layers is reflected in enhanced contents of lithogenic elements like Al, Si, Rb, and Zr in this peat interval. The examination of the entire core transect shown in Figure 3.1.10 reveals a possible explanation for the occurrence of these clastic layers. It is noticeable that core W4 contains no basal peat but tidal channel deposits. These deposits result from high energy tidal channel activities and often contain Pleistocene sands and gravel (Streif, 1990). During the transgressive evolution of the Crildumer Bay several tidal channels of different extent were formed in

SW direction which may have eroded parts of the basal peat. These erosion effects are presumably of major importance for the input of clastic material into the peat.

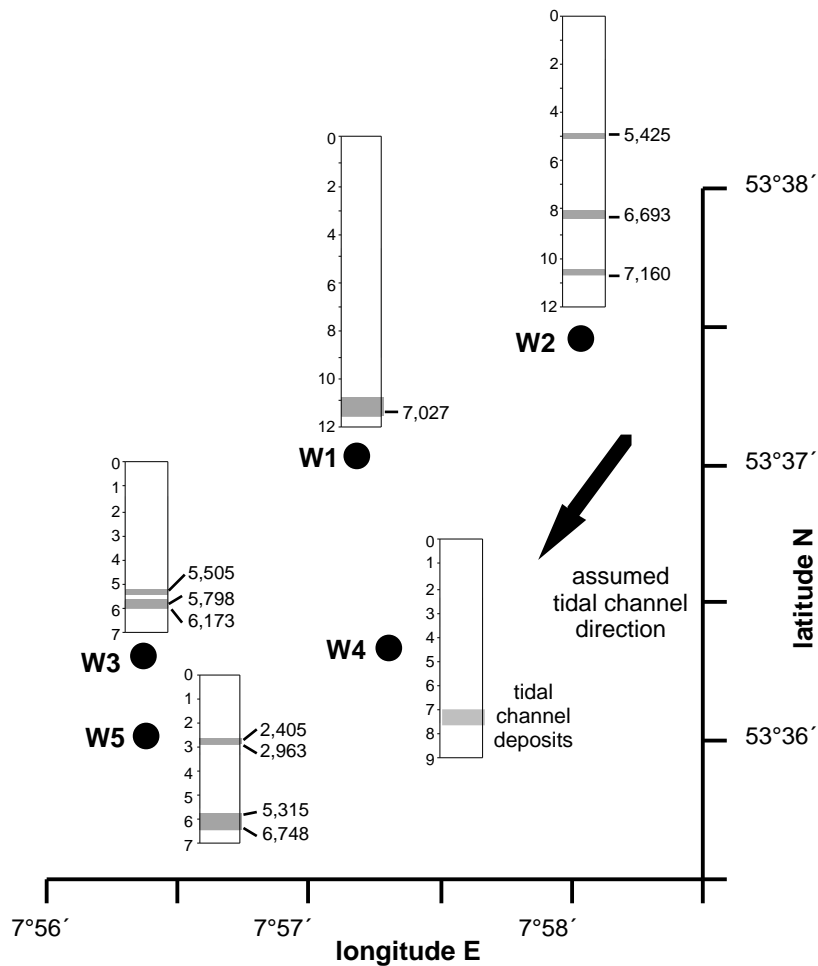


Figure 3.1.10: Location of the five drill cores from the Wangerland transect (peat layers are marked by grey bars).

The marine origin of the clastic material is documented by the occurrence of marine diatoms within the clay layer. Figure 3.1.11 shows a SEM photograph of *Paralia sulcata*, a marine pelagic species which indicates transport processes.

Figure 3.1.12 shows a model which relates tidal channel activities and the occurrence of the clastic layer in the basal peat. In Figure 3.1.12a the state of the evolution of the peat-forming environment before the first marine ingress is presented. At this stage pyrite formation only occurs in the upper part of the reed peat due to its contact with

the brackish zone. Owing to the rising sea-level a tidal channel seems to have eroded the basal peat in core W4 and led to an uplift of the peat. Uplifting typically occurs at weak and crumbly transition zones as, e.g., in the transition of fen woodland peat and raised bog peat (Figure 3.1.12 b). During the uplift phase of the raised bog peat the input of seawater and suspended particulate matter (SPM) is likely (Streif, 1990). After such an event a clastic layer remains and the boundary between peat and clastic material as well as the clastic layer itself may act as an aquifer for groundwater of higher salinity (Figure 3.1.12 c).

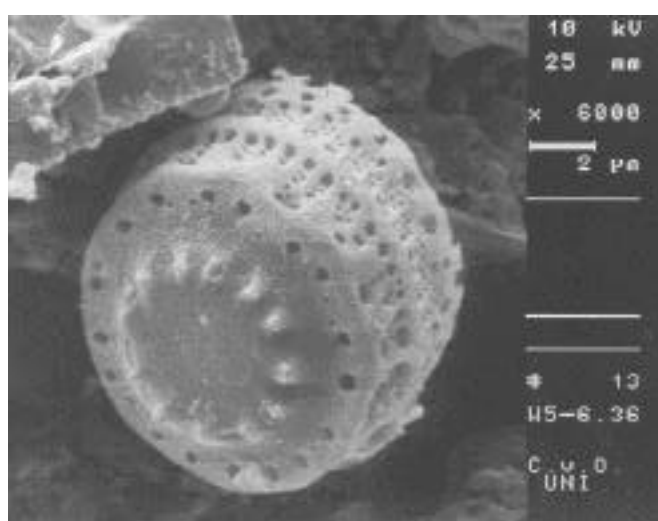


Figure 3.1.11: SEM photograph of the pelagic polyhaline diatom *Paralia sulcata* found within the clastic layer of the basal peat.

The association of Fe-rich peatland waters from below and saline porewaters from above therefore leads to the enhanced formation of pyrite. Unfortunately it is not possible to provide precise information about the chronology. However, it is most likely that the basal peat uplift occurred during the formation of the basal reed peat (about 5,315 years BP) parallel to the first marine contact. A modern example for the described scenario is found close to the study area at the eastern border of the Jade Bay. Here a peat bog seaward of the mainland dike is uplifted during storm events allowing input of SPM (Behre, 1982).

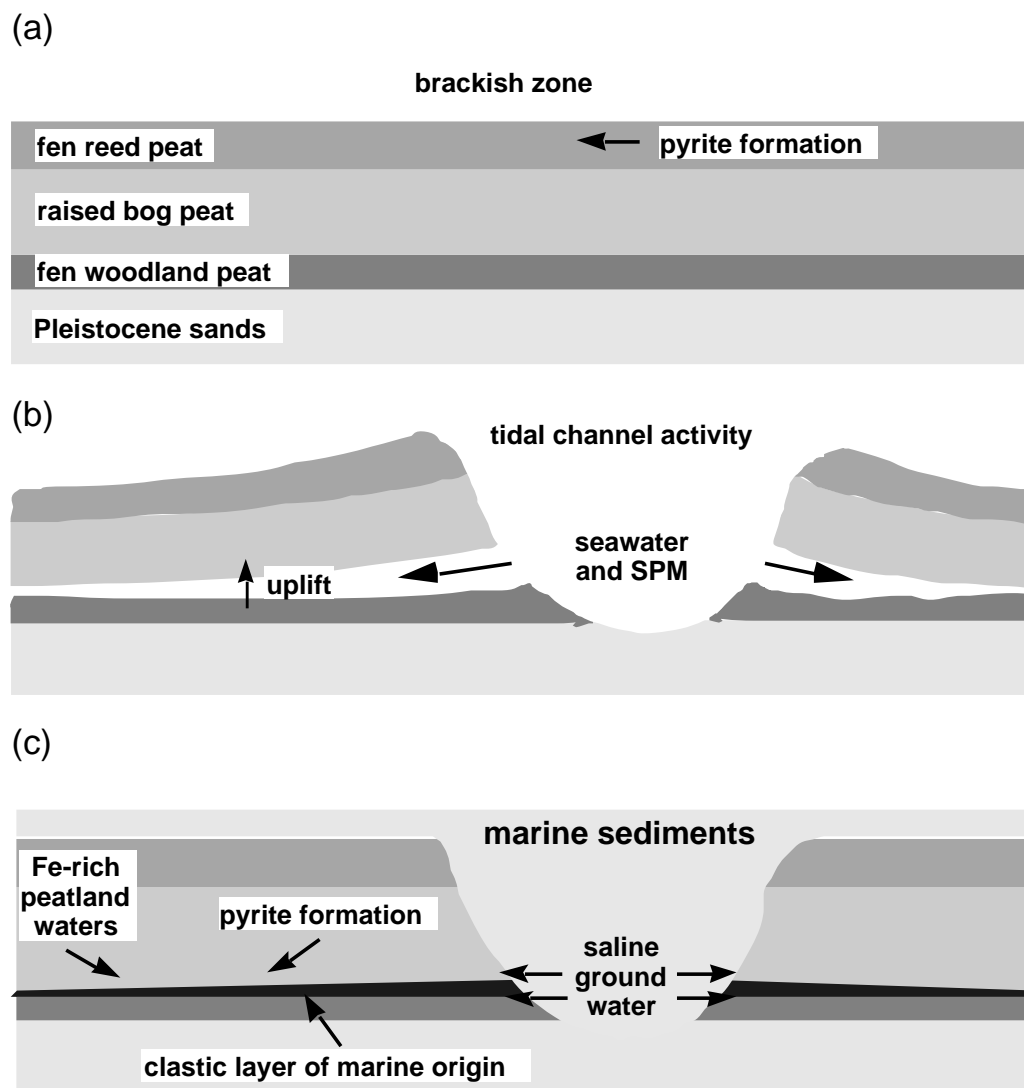


Figure 3.1.12: Model explaining the formation of clastic layers within the basal peat of the drill core.

### Summary

In this study a drill core from the marshlands of NW Germany covering the entire Holocene was analysed at high-resolution by inorganic-geochemical and microfacies methods. As the core contains two peat layers (an intercalated reed peat layer and a basal peat) characterized by distinct enrichments in pyrite the main objective was focussed on these peat layers in order to provide a palaeoenvironmental reconstruction



as carried out on the clastic sediments of this core by Watermann *et al.* (1999). The results obtained from this work can be summarized as follows:

- Microbial reduction of seawater sulphate under almost open system conditions within the peat layers led to the formation of high amounts of pyrite. The total sulphur content of the peat layers averages 7.8% with a maximum value of 28.2% found within the basal peat at a transition of fen woodland and raised bog peat.
- Fermentations carried out with sulphate-reducing bacteria and cellulose-fermenting fungi on peat reveal a dependence of sulphate-reducing bacteria on metabolites produced by fungi indicating a carbon limitation in the first stage of sulphate reduction.
- In contrast to sulphate the main Fe carrierphase is suggested to be freshwater. A brackish zone is assumed for the Holocene peat-forming environment. Diatom studies reveal a varying abundance of pelagic and benthic species which reflect a changing salinity during the formation of the basal reed peat when compared with the intercalated reed peat. Therefore, different pyrite contents within these peats can be explained by a varying Fe availability, which depends on freshwater supply.
- The pyrite enrichments within the investigated peats can be explained by two different scenarios. On one hand pyrite formation coincides with the peat growing due to the influence of the brackish zone which is specific for the reed peats. On the other hand the high amounts of pyrite found within the transition zone of fen and bog peat points to a process after peat formation. This process of pyrite formation is initiated by tidal channel activities which led to the uplift of the basal peat and allowed the deposition of suspended particulate matter. A thin clastic layers remained whose marine origin is evidenced by the occurrence of pelagic diatoms. The resulting clastic material/peat interface acted as an aquifer for waters of higher salinity, which led in combination with Fe-rich peatland waters, to the enhanced formation of pyrite.

**Acknowledgements** - The authors wish to thank J. Barckhausen (Geological Survey of the Federal State of Lower Saxony, Germany) for supporting the drill work and for lithological core descriptions. Furthermore we would like to thank M. E. Böttcher (Max-Planck-Institute Bremen, Germany) for carrying out the S-isotope measurements, M. A. Geyh for performing the  $^{14}\text{C}$ -age determinations (Geological Survey of the Federal State of Lower Saxony, Germany), and W. Bartels (LUFA, Soil-physical Laboratory, Germany) for botanical macroresidual analyses.

Thanks also to J. Overmann and H. Cypionka (ICBM Oldenburg) for the supply of bacteria as well as to T. Stratmann (Terramare Research Centre, Germany) and T. Kuiper (College of Biotechnology Emden, Germany) for controlling the fermentations. Our SEM investigations were kindly supported by R. Kort (ICBM Oldenburg). The authors are indebted to H.-J. Sach for conscientious sample preparation for geochemical analyses.

This study is funded by the German Science Foundation (DFG) through grant No. Scho 561/2-4 and GE 64/4-2 and forms part of the special research program "Bio-geochemical changes over the last 15,000 years - continental sediments as an expression of changing environmental conditions".

### **3.2. Trace metals in Holocene coastal peats (NW Germany) and their relation to pyrite formation**

O. Dellwig and H.-J. Brumsack

**Abstract** - Three drill cores from the marshlands of NW Germany, which cover the entire Holocene, were analysed at high-resolution for bulk parameters, Al, Fe, Si, and selected trace metals (using, e.g., ICP-MS). The drill cores contain two lithological types of peat: i) basal peats overlying Pleistocene sands and ii) intercalated peats situated between clastic sediments of predominantly marine origin. The peat layers are characterized by distinct enrichments in pyrite due to microbial reduction of seawater sulphate under almost open system conditions. Maximum pyrite accumulation (TS 28.2%) occurs in limnic basal peats which contain thin clastic layers as a result of tidal channel activities after peat formation. These layers may have acted as aquifers for the inflow of seawater and sulphate, respectively. The peat layers are also characterized by enrichments in redox-sensitive trace metals (As, Mo, Re, U) and Cd. On the other hand, Co, Cr, Cu, Mn, Ni, Pb, Tl, and Zn reflect the geogenic background. Seawater is the dominating source for As, Cd, Mo, Re, and U whereas the remaining elements seem to have a freshwater source. Therefore, a brackish water zone has to be assumed for the Holocene peat-forming environment. As, Co, Mo, Re, and Tl are predominantly fixed as sulphides and/or incorporated into pyrite while U is related to organic matter. The remaining trace metals show no distinct trend, only Cr reveals a strong relation to the lithogenic detritus. The seawater entering the basal peats is most likely depleted in redox-sensitive trace metals, e.g., owing to microbially induced reduction of trace metals and subsequent fixation by organic matter. Hence, the basal peats contain lower amounts of redox-sensitive trace metals in comparison to the intercalated peats which were formed under the direct influence of seawater and brackish water, respectively.

## Introduction

During the Holocene sea-level rise a so-called sedimentary wedge was formed in the coastal area of NW Germany which consists predominantly of sediments of marine origin (Hoselmann and Streif, 1997). A characteristic of these coastal deposits, however, are peat layers, which can be differentiated into basal and intercalated peats (e.g. Streif, 1990). The basal peats overlay Pleistocene sands, and their formation is often encouraged by decreasing drainage due to the approaching North Sea (Behre, 1982). On the other hand the intercalated peats, which occur between clastic sediments, were formed during phases of a weak, stagnating, or even regressive development of the sea level.

The geochemistry of Holocene peats from the study area so far is rather unknown. Only a few studies were recently carried out which mainly focussed on the palaeoenvironmental reconstruction of the Holocene development (e.g. Dellwig *et al.*, 1998, 1999c). As the coastal peats grew in close vicinity to the North sea they are supposed to reveal a geochemical composition different from peat-forming environments further inland (e.g. Naucke, 1990). On the other hand, similarities to TOC-rich marine sediments (e.g. sapropels, black shales, or sediments from upwelling areas), which often contain elevated amounts of pyrite and rather extreme enrichments in redox-sensitive and/or stable sulphide-forming trace metals (e.g. Brumsack, 1980, 1989; Calvert, 1990; Warning and Brumsack, 1998), seem to be evident.

Therefore, several peat layers, which originate from three cores drilled in the marshlands of NW Germany, were analysed at high-resolution for their trace metal inventory in order to provide information about trace metal sources and their fixation within the peat. As Holocene coastal peats are often characterized by a high abundance of pyrite (Dellwig and Brumsack, 1999a) we will also examine the relationship between pyrite formation and trace metal distribution. For that reason, the first part of this contribution focuses on pyrite formation while in the second part attention is given to the trace metal distribution.

### Regional setting and lithology

The investigated drill cores (Archive No. W2 KB5156, W3 KB5750, W5 KB 5950) originate from the marshlands of the Wangerland about 18 km NW of Wilhelmshaven close to the Jade Bay, Germany (Figure 3.2.1). The cores form part of a transect (five cores W1-W5), which was drilled with the support of the Geological Survey of the Federal State of Lower Saxony, Hannover. The cores W2, W3, and W5 were chosen for a detailed discussion because they contain basal and intercalated peat layers. The transect is of about 3 km in length and is located in a formerly sheltered so-called Crildumer Bay (Petzelberger, 1997).

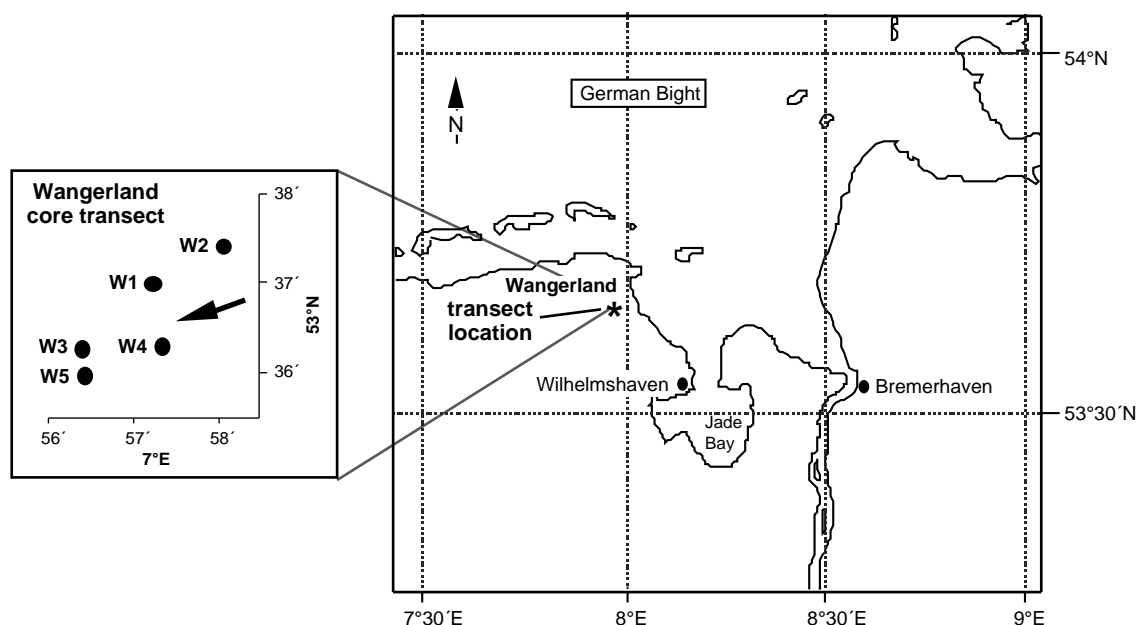


Figure 3.2.1: Map of the study area showing the transect location. The arrow marks an assumed tidal channel direction.

The lithologies of the cores W1-W5, which are based on results from inorganic-geochemical and microfacies analysis (Dellwig and Brumsack, 1999a; Watermann *et al.* 1999), are presented in Figure 3.2.2. The nomenclature used (e.g. lagoonal, brackish) is based on the lithological superstructure given by Barckhausen *et al.* (1977). Several peat samples have been chosen for  $^{14}\text{C}$ -age determinations (Figure 3.2.2), which were kindly carried out by M. A. Geyh (Geological Survey of the Federal State of Lower Saxony,

Germany). The resulting average calibrated ages were calculated using the  $^{14}\text{C}$  age calibration program CALIB 3.0 (Stuiver and Reimer, 1993).

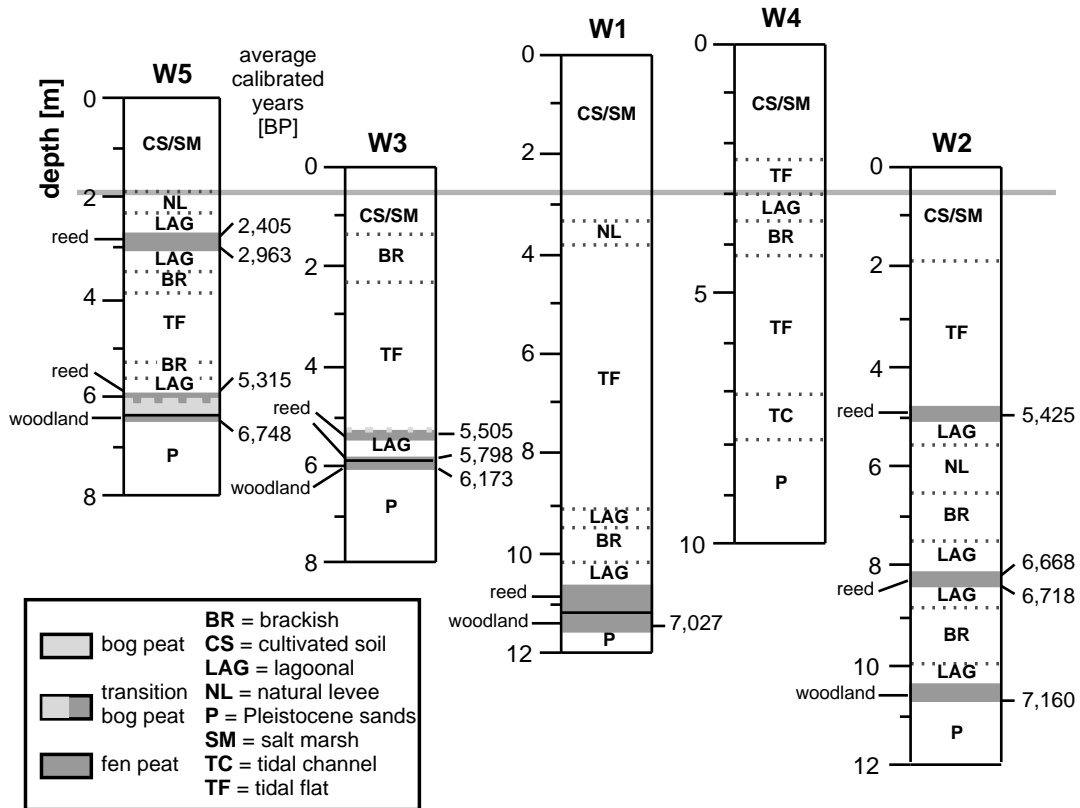


Figure 3.2.2: Profiles of the transect cores W1-W5 showing the lithology (BR = brackish, CS/SM = cultivated soil/salt marsh, LAG = lagoonal, TF = tidal flat) as well as  $^{14}\text{C}$ -age determinations of peat samples [average calibrated years BP]. The gray line indicates the German zero datum (NN) and the black lines within the basal peats of cores W3 and W5 mark clastic layers.

The age determinations reveal that the onset of peat formation occurred between app. 7,200-7,000 years BP in cores W1 and W2. The formation of the basal peats was induced by the approaching North Sea which prevented drainage and led to a rising groundwater level in the study area (e.g. Behre, 1982). After that the direct influence of seawater increased as reflected by the occurrence of lagoonal and brackish sediments (Figure 3.2.2). As a result of sea level fluctuations the first intercalated peat developed in core W2 about 6,700 years BP. It seems to be likely, that core W1 contained an intercalated peat above the second lagoonal section as well. However, this peat was

possibly eroded during the deposition of the tidal flat sediments which reflect increasing energy conditions. The development of the intercalated peat in core W2 coincides with the formation of basal peats in cores W3 and W5. While in the basal unit of core W5 continuous peat growing occurred, the peat formation in core W3 was interrupted 5,800 years BP for about 300 years, and an intercalated peat formed. A further transgression app. 5,300 years BP led again to the deposition of clastic sediments. The occurrence of tidal flat sediments in all cores reflects fully marine conditions in the study area for this time period. However, the abrupt transition from peat to tidal flat sediments in cores W2 and W3 indicates erosion effects. The intertidal system thereafter changed to supralittoral conditions as seen from the development of salt marsh sediments (Figure 3.2.2). This change coincided presumably with the formation of the intercalated peat in core W5 between 3,000-2,400 years BP. The formation of this intercalated peat correlates with a climatic cold event between 3,100-2,400 years BP reported by O'Brien (1995).

Core W4 contains no basal peat but tidal channel deposits which eroded most likely a formerly existing peat (Figure 3.2.2). This tidal channel, whose assumed direction is shown by a black arrow in Figure 3.2.1, had a decisive influence on the geochemical composition of the basal peats of cores W1, W3, and W5. Thus, especially during storm events, the intruding water masses may have led to a partial uplift of the basal peats at transition zones, e.g., the transition of fen woodland and bog peat in core W5. Therefore, the input of seawater and clastic material was possible which led to the formation of thin clastic layers within the basal peats of cores W1, W3, and W5 indicated by black lines in Figure 3.2.2. These clastic layers are 1-3 mm in thickness but can also reach a few cm at other locations of the study area (Behre, 1982). A more detailed description of this phenomenon is given by Dellwig *et al.* (1999a).

In order to provide information about the botanical peat composition visual core descriptions were kindly carried out by J. Barckhausen (Geological Survey of the Federal State of Lower Saxony, Hannover). Additionally microscopic examination of plant fragments from several peat samples were performed by W. Bartels (LUFA, Soil-physical Laboratory) according to the methods given by Grosse-Brauckmann (1962).

These analysis have shown that the intercalated peats consist mostly of reed peat (*Phragmites australis*) with partly low proportions of sedge peat (*Carex spp.*). The only exception is the intercalated peat of core W3 which contains in the upper part a transition bog section (*Phragmites australis*, *Sphagnum spp.*). On the other hand the basal peats are characterized by a more variable composition. The basis is formed in all cases by a fen woodland peat layer (*Betula pubescens*) which later develops into sedge and reed peat. The basal peat of core W5 even contains bog and transition bog peat (*Calluna vulgaris*, *Carex spp.*, *Eriophorum vaginatum*, *Sphagnum spp.*) within the central part (Figure 3.2.2).

### Material and methods

High-resolution sampling (847 samples) was performed at 5 to 10 cm in clastic intervals and at 0.5 to 3 cm in peat intervals, depending on lithology. The samples were stored in polyethylen bags, sealed, and immediately frozen. Afterwards the samples were freeze-dried and homogenised in an agate mortar. The ground powder was used for all subsequent geochemical analyses.

In order to provide an overview about the geochemical composition of the cores all samples were analysed for the major elements Al, Fe, Si and the trace metals As, Co, Cr, Mo, Mn, Ni, Pb, V, Zn, Zr by XRF (Philips PW 2400, equipped with a Rh-tube) using fused borate glass beads. Peat samples and sediment samples with a total organic carbon (TOC) content of more than 10% were heated to 500°C to remove TOC prior to adding lithiumtetraborate and fusing in Pt-Au-crucibles.

Total sulphur (TS) and total carbon (TC) were analysed in 601 samples after combustion using an IR-analyser Leco SC-444 while total inorganic carbon (TIC) was determined by a Coulometrics Inc. CM 5012 CO<sub>2</sub> coulometer coupled to a CM 5130 acidification module (Huffman, 1977, Engleman *et al.*, 1985). The content of total organic carbon (TOC) was calculated as the difference of TC and TIC.



ICP-MS (Finigan MAT Element) was used to analyse for trace metals (Cd, Co, Cr, Cu, Mo, Ni, Pb, Re, Tl, U) in acid digestions of 64 peat samples performed after Heinrichs and Herrmann (1990) in closed teflon vessels (PDS-6; Heinrichs *et al.*, 1986). The samples (50 mg) were treated with 2 ml HNO<sub>3</sub> over night to oxidize organic matter. After that 3 ml HF and 3 ml HClO<sub>4</sub> were added and the vessels were heated for 6 h at 180°C. After digestion the acids were evaporated on a heated metal block (180°C), re-dissolved and fumed off three times with 2 ml half-concentrated HCl, followed by re-dissolution with 1 ml conc. HNO<sub>3</sub> and dilution to 50 ml. The acid digestions were also analysed for Al, Fe, As, Mn, Zn, and V by ICP-OES (Perkin Elmer Optima 3000XL).

For 5 selected peat samples (250 mg) leaching experiments were performed according to the method described by Huerta-Diaz and Morse (1990). The resulting HCl, HF, and HNO<sub>3</sub> fractions were measured by ICP-OES for Fe, As, Mn, V, and Zn as well as for the aforementioned trace metals by ICP-MS. The recovery range between 78-112% (av. 94%).

Analytical precision and accuracy of XRF, ICP-OES, and ICP-MS measurements was tested by replicate analysis of geostandards (GSD-3, -5, -6, GSS-1, -6, LKSD-1, SDO-1, SGR-1) and several in-house standards. The precision of bulk parameter measurements was checked in series of double runs and accuracy was determined by using in-house standards (see appendix).

For the investigation of bulk sediment S-isotope composition, which was kindly performed by M. E. Böttcher (ICBM), 35 solid phase peat samples were first washed to remove chloride. Afterwards the samples were dried and directly analysed by combustion isotope-ratio-monitoring mass spectrometry (C-irm MS) according to the method described by Böttcher *et al.* (1998). The reproducibility was better than  $\pm 0.3\%$ . Isotope ratios are given relative to the Vienna-CDT.

## Results and discussion

### *Pyrite formation*

Figure 3.2.3 shows depth profiles of total sulphur of the drill cores W2, W3, and W5 on an organic matter-free basis ( $TS_{OMF}$ ). This normalisation eliminates dilution effects caused by organic matter of the sedentary peat layers. It can be clearly seen that the peat layers are highly enriched in sulphur. However, the peat layers reveal no uniform  $TS_{OMF}$  distribution. Except for core W2, the basal peats contain higher amounts of sulphur when compared with the intercalated peats.

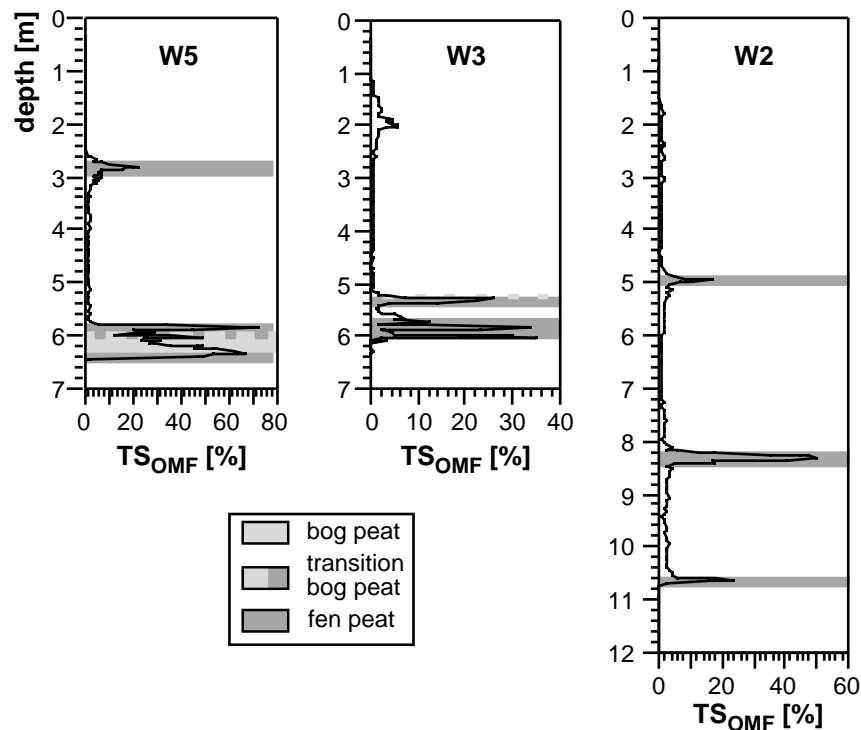


Figure 3.2.3: Depth profiles of TS on an organic matter-free basis ( $TS_{OMF}$ ) of the drill cores W2, W3, and W5.

The absolute TS contents of the intercalated peat layers average 5.0% (range 2.5-8.5%) and are comparable to TS values of marine influenced peat-forming environments within the Florida Everglades which range between 1.1-6.0% (Casagrande *et al.*, 1977; Given and Miller, 1985; Price and Casagrande, 1991). On the other hand the basal peats contain on average 8.5% TS (range 1.8-28.2%), though it should be noted that the lower values originate from the bog and transition bog peat samples of core W5. Although the

bog peat of core W5 is supposed to reflect a purely limnic and therefore sulphur-limited system, the average TS content of 5.9% is extremely high when compared with other freshwater influenced peat-forming environments. For instance TS values of the Everglades freshwater basin and of the Okefenokee Swamp, Georgia (USA) vary between 0.2-1.1% (Casagrande *et al.*, 1977; Altschuler *et al.*, 1983). The highest TS values of 16.0% in core W3 and 28.2% in core W5 occur at fen woodland peat/fen sedge peat and fen/bog transitions, respectively. These areas are characterized by decreasing TOC contents and increasing amounts in lithogenic elements like Al, Si, and Zr which indicate the occurrence of clastic layers within the basal peats of cores W3 and W5. As mentioned above these clastic layers resulted from tidal channel activities which led to a partial uplift of the basal peats at transition zones and therefore allowed the intrusion of seawater and clastic material (see regional setting and lithology). Thin sections evidence that in these peat samples peat discrete layers of pyrite occur between clastic material and peat (Dellwig *et al.*, 1999a).

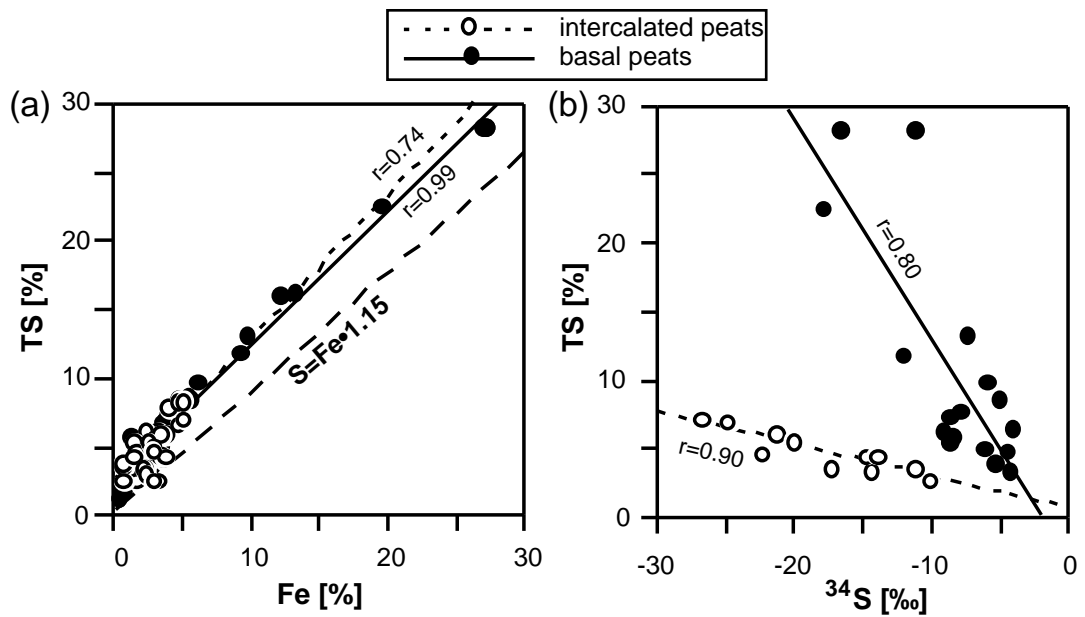


Figure 3.2.4: (a) Scatter plot of TS versus Fe of the intercalated and basal peats of the drill cores W2, W3, and W5 and (b) TS versus  $^{34}S$  values of the intercalated and basal peat of core W5.

Figure 3.2.4a shows the correlation of TS versus Fe for the intercalated and basal peats of the drill cores W2, W3, and W5. Although the distinct relation between TS and Fe evidences the formation of pyrite, the regression lines are situated above the theoretical pyrite ratio. Therefore, the formation of organic sulphur compounds, possibly induced by Fe limitation, has to be assumed. For instance Ferdelman *et al.* (1991) reported maximum contents of 60% organic sulphur of the total sulphur inventory in a *Spartina Alterniflora* salt marsh sediment core from the Delaware Bay (U.S.A.). They related this finding to a high sulphate reduction rate and a low Fe availability in comparison to produced  $H_2S$ . Furthermore, humic sulphur compounds show a high resistance towards reoxidation to sulphate. It can be also seen from Figure 3.2.4a that the highest amounts of pyrite occur within the basal peats. As seawater forms the only source which provides sufficient amounts of sulphate, the pyrite enrichments within the lower parts of the basal peats were unexpected because of the lacking direct seawater influence.

In contrast, the intercalated peats as well as the peat layers of the uppermost basal parts (max. 10 cm) consist predominantly of *Phragmites* reed which grew according to diatom analyses carried out by Watermann *et al.* (1999) under a mean salinity of 10‰ (range 5-15‰). Therefore, sufficient sulphate should be present for sulphate-reducing bacteria to produce  $H_2S$  for the formation of pyrite. As a direct seawater influence on the lower parts of the basal peats is hard to imagine Dellwig *et al.* (1999a) suggested that the clastic layers acted as aquifers and allowed a further inflow of seawater. Hence, pyrite formation occurred subsequent to peat growing in the lower parts of the basal sections. However, the question remains: Why do the lowest parts of the basal peats contain such high amounts of pyrite when compared with the reed peats?

For that reason, bulk sediment  $^{34}S$  values were determined for the intercalated and basal peat of core W5. Figure 3.2.5 shows that all peat samples are characterized by negative  $^{34}S$  values, i.e., an enrichment of the lighter  $^{32}S$  isotope, which indicates according to Jørgensen (1979) bacterial sulphate reduction under comparatively easy availability of seawater sulphate and rather open system conditions, respectively. On the other hand the  $^{34}S$  values also show large variations (range -2.6 to -26.7‰) which seem to be related to the TS content. Samples with high TS values show the most

negative  $^{34}\text{S}$  values. However, the correlation between TS and  $^{34}\text{S}$  values (Figure 3.2.4b) reveals two trends for the intercalated and basal peat. The intercalated peat shows only a little variation in TS when compared with the S-isotope ratios. By contrast, the basal peat is characterized by distinctly higher TS values although the S-isotope ratios are slightly less negative. This emphasizes that sulphate availability is not a limiting factor during pyrite formation in the investigated peat-forming environment. Therefore, it seems more likely that the sulphate reduction rate plays an important role for the amounts of produced sulphides and pyrite, respectively.

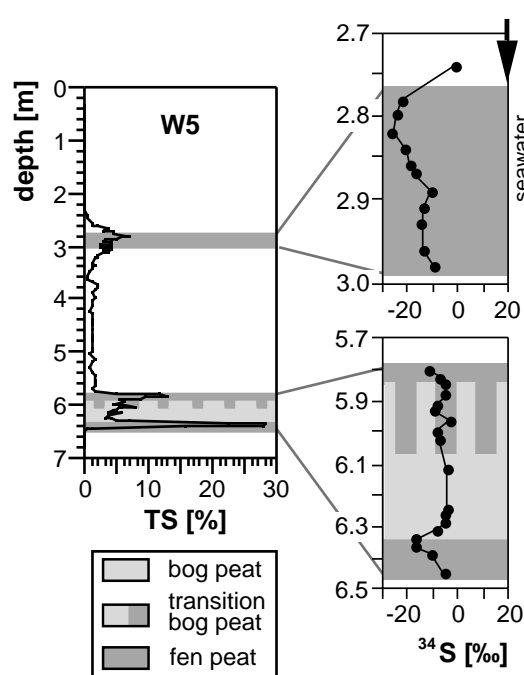


Figure 3.2.5: Depth profile of TS and  $^{34}\text{S}$  values for the intercalated and basal peat of core W5.

On the other hand organic-rich coastal environments are generally characterized by very high sulphate reduction rates (e.g. Howarth and Teal, 1979; Howarth and Giblin, 1983). In situ incubation experiments with peat in a salt marsh carried out by Giblin (1988) have shown that the amounts of accumulated pyrite are higher in peat containing living plants compared to peats with non-living plants. Therefore, plant activity presumably facilitates pyrite formation which points against the high amounts of pyrite found within the lowest parts of the basal peats (W3, W5), because here pyrite formation

occurred subsequent to peat growing (see above). However, the incubation experiments were carried out during fall when pyrite accumulation is highest. A study on pyrite formation in salt marshes over a two year period by Howarth and Teal (1979) showed that the net pyrite accumulation is too low considering the high sulphate reduction rate. They concluded that most of the pyrite is oxidized on an annual basis due to the metabolism of plant roots. Additionally, Fe limitation has to be considered. Thus, tidal flushing leads to a further input of oxygen and soluble Fe may be removed (Giblin and Howarth, 1984). Therefore, a better preservation of produced pyrite can be assumed for the basal peats owing to lacking tidal flushing as well as the longer time period in which pyrite formation occurred.

#### *Trace metal distribution*

Table 3.2.1 provides an overview about Fe and trace metal contents of the investigated peats (fen reed, fen woodland, and transition bog / bog peat) as well as of the pyrite-rich basal peat sections. The element contents reveal a large variability which is most likely caused by the changing palaeoenvironmental conditions during Holocene sea level fluctuations. The comparison of the data presented here with other peat-forming environments is rather difficult. In addition to the aforementioned climatic changes, the geochemistry of peat (especially fen peat) strongly depends on hydrogeological conditions (weathering), i.e., the source rock composition. Christanis *et al.* (1998) analysed Holocene fen peat samples from Greece for a large number of trace elements. They found for instance about 10-fold higher As and U contents which could be traced back in the case of U to the weathering of granitic rocks. On the other hand fen sedge peats from Finland analysed by Sillanpää (1972) show trace metal contents comparable to the fen reed peats presented in this study, only the Mo content is about 15-fold lower in the Finnish peats. Especially the Mo and Re concentrations of the fen reed peats are comparable to values reported for anoxic coastal sediments from the Saanich Inlet and Peru margin or for sapropels of the Black Sea (Goldberg, E. D., 1987; Crusius *et al.*, 1996). Additionally, when comparing peat data anthropogenic influences have to be taken into account, which can be neglected for the investigated Holocene peats.

<sup>206/207</sup>Pb ratios determined for several Holocene peat samples from the study area reflect the local geogenic background of 1.2 (O. Dellwig, unpublished data). The investigation of several trace metals on German fen and bog peats carried out by Naucke (1990) revealed distinctly higher amounts of Co, Cu, Ni, Pb, and Zn presumably indicating an anthropogenic origin. Lower contents in Co, Cu, and Pb are also found in the investigated Holocene bog peats in comparison to bog peat data from the Okefenokee Swamp (USA) reported by Casagrande and Erchull (1976).

Table 3.2.1: Average Fe and trace metal contents of fen reed peats (cores W2, 3, 5), fen woodland peats (cores W2, 3, 5), bog peat (Core W5), and pyrite-rich sections of the basal peats containing clastic layers (cores W3, 5). Ranges are presented in brackets.

element [mg kg <sup>-1</sup> ]	fen reed peat	fen wood- land peat	transition bog/ bog peat	basal peat (pyrite-rich)
Fe [%]	3.8 (0.9-9.8)	9.0 (0.6-27.3)	3.1 (1.0-6.1)	21.6 (12.3-27.3)
As	16 (5-28)	16 (7-22)	6 (2-13)	37 (14-98)
Cd	0.11 (0.02-0.3)	0.1 (0.05-0.3)	0.05 (0.02-0.1)	0.2 (0.1-0.3)
Co	5.7 (0.7-16)	5 (1-14)	1 (0.7-3)	9 (4-23)
Cr	42 (5-87)	29 (12-75)	12 (3-26)	26 (7-51)
Cu	9 (4-24)	8 (5-18)	6 (4-19)	6 (4-9)
Mn	230 (50-498)	182 (115-280)	142 (104-217)	379 (283-496)
Mo	13 (2-34)	11 (2-24)	2 (1-7)	18 (13-23)
Ni	18 (2-38)	11 (2-28)	5 (2-9)	16 (9-33)
Pb	9 (1-22)	6 (2-16)	2 (0.5-5)	6 (2-14)
Re [µg kg <sup>-1</sup> ]	6 (2-23)	4 (1-10)	2 (1-3)	4 (2-6)
Tl	0.3 (0.01-0.7)	0.2 (0.06-0.6)	0.06 (0.01-0.1)	0.2 (0.05-0.5)
U	3 (1-6)	4 (0.8-9)	1 (0.2-2)	3.2 (2.8-3.7)
V	61 (11-120)	25 (11-50)	15 (2-29)	32 (11-60)
Zn	34 (8-125)	28 (13-45)	13 (8-25)	54 (24-125)

As mentioned above the investigated peats show higher Mo contents in comparison to Finnish fen peats. Figure 3.2.6 shows the Mo<sub>OMF</sub> profiles of cores W2, W3, and W5. Similar to the TS<sub>OMF</sub> distribution (Figure 3.2.3) the Mo<sub>OMF</sub> profiles show enrichments in the peat layers. However, in contrast to TS<sub>OMF</sub>, almost all intercalated peats show higher Mo<sub>OMF</sub> values when compared with the lowest parts of the basal peats where the highest pyrite enrichments are seen.

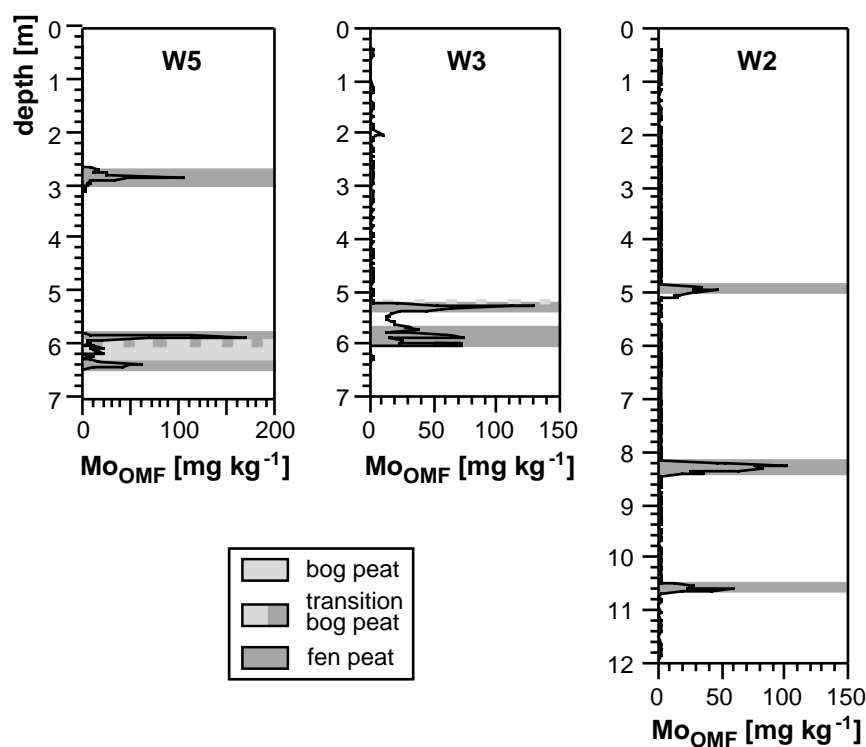


Figure 3.2.6: Depth profiles of Mo on an organic matter-free basis ( $\text{Mo}_{\text{OMF}}$ ) of the drill cores W2, W3, and W5.

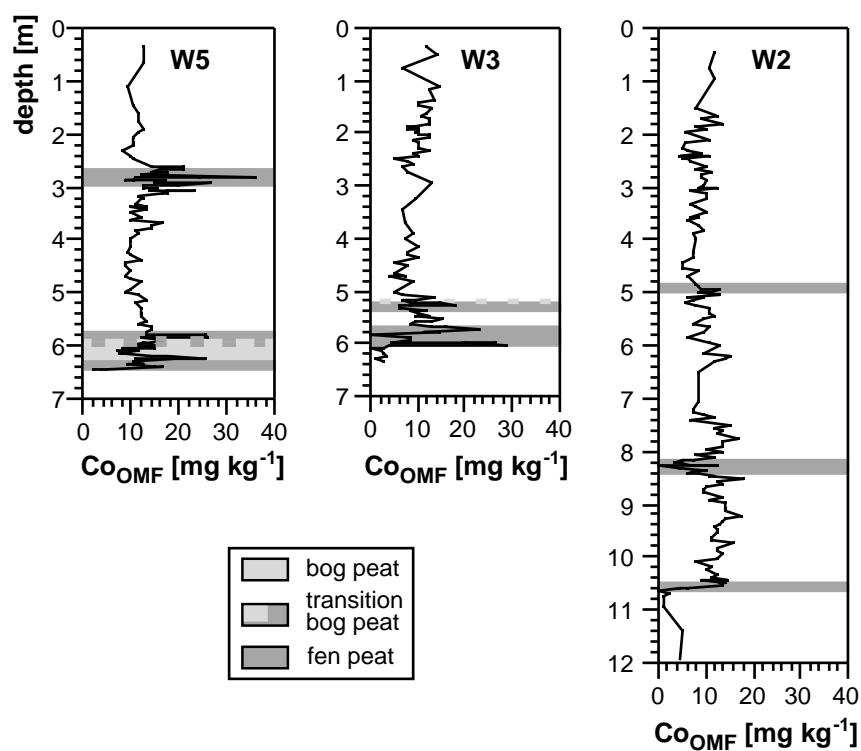


Figure 3.2.7: Depth profiles of Co on an organic matter-free basis ( $\text{Co}_{\text{OMF}}$ ) of the drill cores W2, W3, and W5.



Furthermore, the peat layers are highly enriched in the redox-sensitive trace elements As, Re, and U when compared with the clastic sediments of the drill cores. In Figures 3.2.7 and 3.2.8 the depth profiles of  $Co_{OMF}$  and  $Cr_{OMF}$  are presented for the cores W2, W3, and W5. The  $Co_{OMF}$  profiles reveal only slight enrichments in the peat layers of cores W3 and W5 in comparison to the clastic sediments while core W2 shows no significant variations. Cr is not enriched in the peats when compared with the clastic sediments, though it should be noted that some peat layers even contain distinctly lower amounts (e.g. basal peat W5).

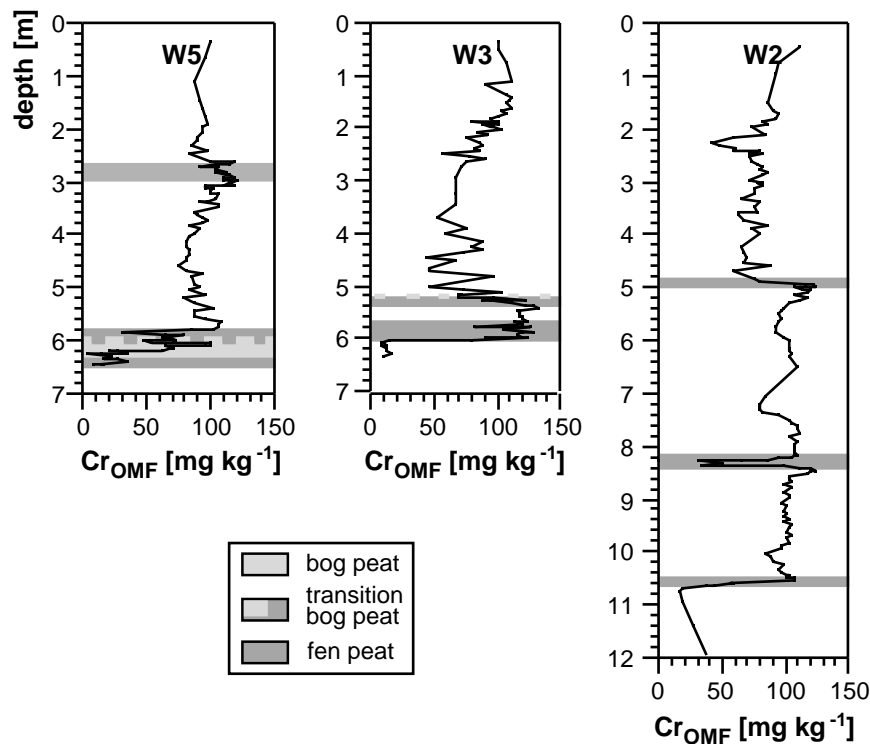


Figure 3.2.8: Depth profiles of Cr on an organic matter-free basis ( $TS_{OMF}$ ) of the drill cores W2, W3, and W5.

In order to provide a comparison of the Fe and trace metal inventory of the peat samples with the geogenic background we calculated enrichment factors versus average shale (Wedepohl, 1971, 1991; Re is represented by its crustal abundance after Colodner *et al.*, 1993) on an organic matter-free basis ( $EFS_{OMF}$ ). Figure 3.2.9 shows  $EFS_{OMF}$  values for the reed peats (intercalated and basal peats of cores W2, W3, W5) and for the pyrite-rich basal peat samples which contain clastic layers of cores W3 and W5.

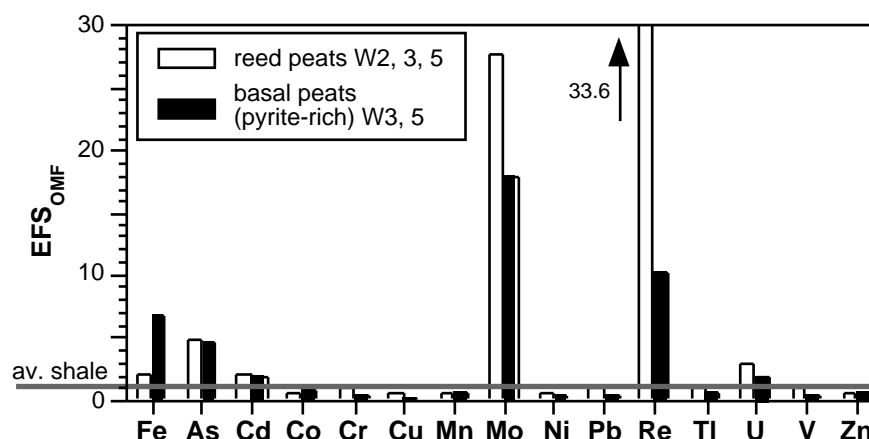


Figure 3.2.9: Enrichment factors for Fe and selected trace metals versus average shale on an organic matter-free basis ( $EFS_{OMF}$ ) for reed peats (W2, 3, 5), pyrite-rich basal peat samples containing clastic layers (cores W3, 5), and bog peat (core W5). Average shale data from Wedepohl (1971, 1991). Re value from crustal abundance after Colodner *et al.* (1993).

Highest enrichments are seen for Mo and Re accompanied with slight enrichments in As, Cd, and U. Except for Cd, the reed peats are characterized by higher  $EFS_{OMF}$  values for (As), Mo, Re, and U when compared with the pyrite-rich basal peats. On the other hand, Fe shows a higher abundance in the basal peats which reflects the pyrite distribution seen from the  $TS_{OMF}$  profiles (Figure 3.2.3). The remaining trace metals plot close to the shale level indicating no significant enrichment. This feature reveals a decisive difference to TOC-rich marine sediments which normally show a wide spectrum in trace metal enrichments (e.g. Warning and Brumsack, 1998).

In Table 3.2.2 seawater concentrations, average shale contents, and seawater/shale ratios of the investigated trace metals are presented. Regarding the seawater/shale ratios similarities between several trace metals become evident: i) Re and Mo show the highest seawater/shale ratios followed by U and As because these elements occur as oxoanions in relative high concentrations in oxygenated seawater while their geogenic background is comparatively low (Bruland, 1983; Martin and Whitfield, 1983; Colodner *et al.*, 1993; Goldberg, 1987; Wedepohl, 1991). The same holds for Cd even though it does not occur as an oxoanion in seawater ( $CdCl_2^0$ , Bruland 1983), ii) Cr and V occur as oxoanions in seawater as well, however, their geogenic background is high, and iii) Co, Cu, Mn, Ni,

Pb, Tl, and Zn form cations, carbonato, chloro, and/or hydroxy complexes and are characterized by low seawater concentrations in comparison to their geogenic background (Bruland, 1983; Wedepohl, 1971). The seawater content of both latter groups, therefore, should not contribute significant amounts of these elements to the peat.

Table 3.2.2: Seawater concentrations and average shale contents as well as seawater/shale ratios of the investigated trace metals.

element	seawater <sup>1</sup> [µg l <sup>-1</sup> ]	av. shale <sup>4</sup> [mg kg <sup>-1</sup> ]	seawater/ shale • 10 <sup>-3</sup>
As	1.7	10	0.17
Cd	0.08	0.13	0.62
Co	0.001	19	0.00005
Cr	0.21	95	0.002
Cu	0.25	39	0.006
Mn	0.27	850	0.0003
Mo	10.6	1.3	8.2
Ni	0.47	68	0.007
Pb	0.002	22	0.0001
Re	0.008 <sup>2</sup>	0.0005 <sup>5</sup>	16.6
Tl	0.01	0.68	0.02
U	3.2 <sup>3</sup>	3	1.1
V	1.8	130	0.014
Zn	0.39	115	0.003

<sup>1</sup> Bruland (1983)

<sup>2</sup> Goldberg (1987)

<sup>3</sup> Martin & Whitfield (1983)

<sup>4</sup> Wedepohl (1971, 1991)

<sup>5</sup> Crustal abundance Colodner *et al.* (1993)

It can be concluded that similar to sulphur the seawater represents the main source for As, Cd, Mo, Re, and U whereas the contents of the remaining trace metals can be explained by the geogenic background. Therefore, processes of element mobilisation from the surrounding clastic sediments and fixation within the peats seem to play only a minor role. However, regarding the Fe enrichment in Figure 3.2.9 a further element source is necessary to explain the geochemical composition of the investigated peats because the average seawater concentration of Fe is very low (range 0.006-0.14 µg l<sup>-1</sup>, Bruland, 1983).

Dellwig *et al.* (1999a) suggested a scenario of the Holocene peat-forming environment of the coastlands of NW Germany which is characterized by the occurrence of reed islands within a brackish water zone of comparatively low tidal activity. According to Watermann *et al.* (1999) the salinity of the brackish water ranged between 5 and 15‰ depending on the exposition to the open sea. Thus, the brackish water zone must result from a mixing of sulphate-rich seawater and freshwater. Table 3.2.3 presents a simple balance which provides an estimate of the brackish water volume needed for the Fe and trace metal inventory of 1 kg of the intercalated reed peat of core W5 at a salinity of 5 and 15‰, respectively. Additionally the element Al is chosen as it represents the detrital fraction. We focus the following discussion on core W5 as this core represents the largest database including age determinations which enable estimating compaction (see below).

Table 3.2.3: Dissolved and particulate concentrations of Al, Fe and selected trace metals in freshwater (small rivers close to the study area), average seawater, and North Sea water (Salinity >30‰) and element contents of the intercalated peat layer of core W5 (corrected for water content and compaction) as well as calculated volumes of brackish water (including dissolved and particulate phase) at a salinity of 5‰ and 15‰ necessary to explain the element inventory of 1 kg of the intercalated peat layer. The concentrations of the particulate phase are given per volume unit of water.

element	freshwater dissolved <sup>1</sup> [µg l <sup>-1</sup> ]	freshwater particulate <sup>1</sup> [µg l <sup>-1</sup> ]	seawater dissolved <sup>2</sup> [µg l <sup>-1</sup> ]	North Sea particulate <sup>4</sup> [µg l <sup>-1</sup> ]	intercalated peat <sub>corr.</sub> W5 <sup>6</sup> [mg kg <sup>-1</sup> ]	volume at 5‰ [m <sup>3</sup> ]	volume at 15‰ [m <sup>3</sup> ]
Al	300	729	0.54	125	5,500	6.3	9.6
Fe	1,678	2,973	0.06	87	4,844	1.2	2.0
Co	0.80	0.32	0.001	0.04 <sup>5</sup>	1	1.1	1.8
Cr	0.90	0.90	0.21	0.65	8	5.0	6.2
Mn	290	56	0.27	5.4	38	0.1	0.2
Mo	0.36	0.02	10.6	0.03 <sup>5</sup>	0.9	0.4	0.2
U	0.12	0.03	3.2 <sup>3</sup>	0.005 <sup>5</sup>	0.3	0.5	0.2
V	3.3	1.7	1.8	0.23	12	2.7	3.5

<sup>1</sup> Lipinski (1999)

<sup>2</sup> Bruland (1983)

<sup>3</sup> Martin & Whitfield (1983)

<sup>4</sup> Dellwig *et al.* (1999b)

<sup>5</sup> J. Hinrichs, ICBM, unpublished data

<sup>6</sup> this work

The balance is based on the assumption that the recent element concentrations of the freshwater environment and of the North Sea are comparable to the Holocene situation. Eolian input and processes during estuarine mixing (Chester, 1990) are disregarded. As the contents of many heavy metals in the recent environment are influenced by anthropogenic activity we restricted the balance to a few heavy metals (Co, Cr, Mn, Mo, U, V) which most likely reflect natural concentrations according to results reported by Lipinski (1999) whereas Cu, Ni, Pb, Tl, and Zn are excluded. We used dissolved and particulate element concentrations of rivers close to the study area (Lipinski, 1999) as well as dissolved element concentrations of average seawater (Bruland, 1983; Martin and Whitfield, 1983) and particulate matter of the North Sea (Dellwig *et al.*, 1999b; J. Hinrichs, ICBM, unpublished data). It should be noted, that the particulate element concentrations are given per volume unit water while the element contents of the intercalated reed peat layer of core W5 are corrected for water content and compaction (74%, 46%; Dellwig *et al.* 1999a).

Regarding the calculated water volumes, which are necessary to explain the composition of the intercalated reed peat layer of core W5, three element groups can be differentiated (Table 3.2.3). The highest volumes at a salinity of 5‰ are seen for Al, Cr, and V which are more abundant in freshwater in comparison to seawater. As Al represents the clay fraction its value reflects the volume needed for supplying the lithogenic component within the peat. However, it has to be considered that, in contrast to Cr or V, Al is not involved in redox-processes which may lead to element fixation and enrichment. Therefore, the dissolved phase should be disregarded, as a result of which the required volumes increase to values of 8.8 and 10.5 m<sup>3</sup>, respectively.

The second group is formed by Fe and Co, which are represented by an intermediate volume due to their elevated abundance in freshwater. The lowest volumes are seen for Mn, Mo, and U. Although the freshwater concentrations of Mo and U are comparatively low their high abundance in the dissolved seawater phase contributes sufficient amounts even at a salinity of 5‰. On the other hand the freshwater introduces high amounts of Mn to the system which explains its low volume. However, significant enrichments in comparison to average shale are not seen for Mn, which is possibly

related to its high solubility in the anoxic milieu of the peat layers. Furthermore, in contrast to Fe, its fixation is more difficult. Thus, the formation of MnS under normal conditions is quite uncommon but evidenced, e.g., by Suess (1979) and Böttcher and Huckriede (1997) in sediments of the Baltic Sea. A further possibility of Mn fixation is the formation of rhodochrosite ( $\text{MnCO}_3$ ) and reddingite ( $\text{Mn}_3(\text{PO}_4)_2$ ) due to the increasing  $\text{HCO}_3^-$  and  $\text{HPO}_4^{2-}$  concentration in porewaters during microbial decomposition of organic matter as reported for salt marsh sediments by Holdren (1977) and Lord and Church (1983).

Lipinski (1999) suggested that the high concentration of Fe and Mn in the freshwater environment of the study area result from the catchment area of the rivers, which is characterized by the occurrence of bogs and swamps. Thus, organic matter is presumably exported from bogs and swamps (Pettersen *et al.*, 1997) and forms complexes with metals which are mobilised from soil under reducing and acidic conditions (Viers *et al.*, 1997).

Regarding the water volumes at a salinity of 15‰ increasing volumes are seen for Al, Fe, Co, Cr, Mn, and V while Mo and U show a decrease by a factor of about 2, which reflects the importance of the interaction between freshwater and seawater within the investigated peat-forming environment.

As most of the trace metals determined in this study form stable sulphides leaching experiments according to the method described by Huerta-Diaz and Morse (1990) were performed on five pyrite-rich peat samples (core W5 reed peats and lower basal peat) in order to provide information about the fixation. From these leaching experiments three acid fractions were obtained which relative trace metal abundances are shown in Figure 3.2.10. While the HCl fraction contains the reactive compounds, HF and  $\text{HNO}_3$  react with clay minerals and pyrite, respectively.

Elements, which show highest abundance in the pyrite fraction (>60%) are As, Re, Tl, Mo, and Co. These metals may be incorporated into pyrite and/or form stable sulphides (Raiswell and Plant, 1980; Belzille and Lebel, 1986; Duchesne *et al.* 1986; Luther, 1991). However, the low Mo abundance of only 65% in the pyrite fraction is quite unexpected because Mo is one of the trace metals (besides As) typically enriched

in pyrite (Raiswell and Plant, 1980; Huerta-Diaz and Morse, 1992). The high concentration of on average  $6.6 \text{ mg kg}^{-1}$  Mo in the HF fraction excludes a detrital fixation, when considering the Mo content of  $1.3 \text{ mg kg}^{-1}$  in average shale (Wedepohl, 1991). For that reason, we assume that the affinity of Mo with organic matter, as suggested for instance by Brumsack and Gieskes (1983) and Christanis *et al.* (1998), caused this unexpected behaviour.

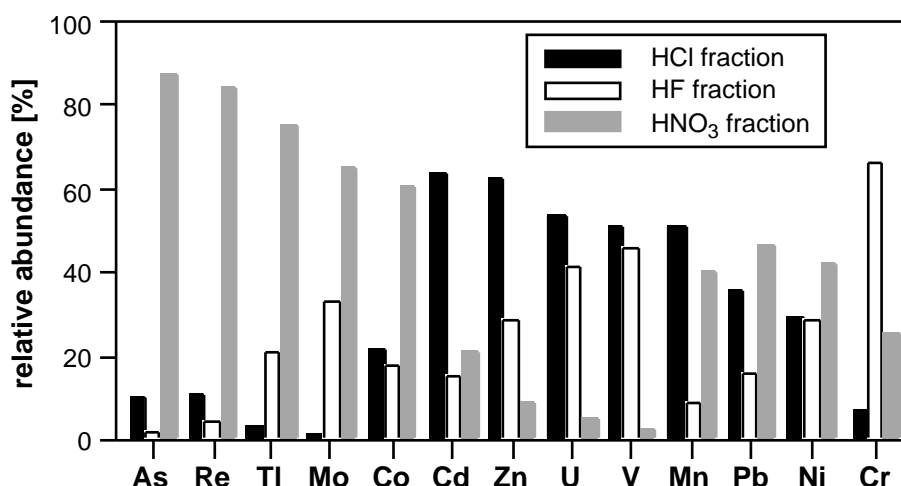


Figure 3.2.10: Relative abundance of selected trace metals in three acid fractions resulting from leaching experiments according to the method described by Huerta-Diaz and Morse (1990).

Less information is available about the fixation of Re. However, recent studies have shown that Re can be highly enriched in pyrite-rich anoxic marine sediments (e.g. Crusius *et al.*, 1996; Warning and Brumsack, 1998) which suggests its accumulation as sulphide. On the other hand Cd, Zn, U, and V are highest in the HCl fraction and enhanced in the HF fraction. According to Huerta-Diaz and Morse (1992) pyrite is generally an unimportant sink for Cd and Zn. Nevertheless, both elements are commonly present as sulphides (CdS, ZnS) in anoxic sulphidic sediments (Framson and Leckie, 1978; Elderfield *et al.*, 1979; Brumsack, 1980). As both sulphides are characterized by relatively high solubility products ( $1 \cdot 10^{-28}$ ,  $1 \cdot 10^{-24}$ ) when compared for example with CuS ( $8.5 \cdot 10^{-45}$ , Holleman, 1985), the leaching procedure may be responsible for their high abundance in the HCl fraction. The amounts of U and V in the

HCl and HF fraction can be explained by their relation to organic matter under anoxic conditions (Brumsack and Gieskes, 1983; Cheshire *et al.*, 1977, Szalay and Szilágyi, 1967). However, a correlation between both metals and TOC does not exist because the organic material resulted from the sedentary peat-forming process. Additionally, reduced U(IV) shows a high particle reactivity (Anderson *et al.*, 1989) which lead to an enrichment in the sediment.

Mn, Ni, and Pb are characterized by comparable amounts in the HCl and HNO<sub>3</sub> fraction which is possibly related to high solubility products of their sulphides, as well. For instance MnS and PbS are soluble in HCl (e.g. Murray *et al.*, 1978; Holleman, 1985). Different to all other trace metals, Cr shows the highest abundance in the HF fraction which is possibly caused by the instability of its sulphides in comparison to rapidly formed insoluble Cr-hydroxides (Smillie *et al.*, 1981; Eary and Rai, 1989). It should be kept in mind that the EFS<sub>OMF</sub> values reveal a shale-like distribution for most of the trace metals. Therefore, we assume that in the case of Co, Ni, Tl, Zn, and perhaps Cr and Mn the reactive, non-silicate bound phase reacted with H<sub>2</sub>S to sulphides or is partly incorporated into pyrite. This process would not lead to an element enrichment in the peats because the trace metals would only be transferred to a different mineral phase. The varying stability of the resulting sulphides, therefore, caused the different distribution of the trace metals in the acid fractions. Summarizing, it can be concluded that the leaching experiment provided information about the fixation of As, Co, Mo, Re, Tl, and perhaps U whereas the fixation of the other trace metals remains unclear.

Table 3.2.4 shows the interelement correlation coefficients of Al, Fe, and trace metals of the peat layers of core W5. The high coefficients between Al and the trace metals Cr, Ni, Pb, Tl, V, Zn indicate the relation of these trace metals to the clay fraction. This finding supports the aforementioned balance (Table 3.2.3) which has shown that similar brackish water volumes are necessary in order to explain the contents of Al, Cr and less pronounced V in the peats. Additionally the high abundance of Cr and perhaps V in the HF fraction can also be explained by these correlations which reveal an incorporation in silicate structures. On the other hand, Ni, Pb, Tl, and Zn seem to be adsorbed on clay particles in the brackish water so that the formation of sulphides in peat from this



reactive component is more likely. Co is also correlated to the above mentioned trace metals but its correlation to Al is less pronounced.

A further group which is characterized by high inter-element correlations form As, (Cd), Mn, Mo, Re, and U. Except for Mn, the relationship between these elements reflects their enhanced concentration in seawater. However, the elements likely originate from brackish water which contains elevated amounts of Mn. Additionally the effects of trace metal scavenging on Mn-rich phases, as reported for example for As by Peterson and Carpenter (1986), has to be considered. Therefore, both Mn and redox-sensitive trace metals may be introduced into the peat, so that a simultaneous fixation of Mn as MnS or perhaps MnCO<sub>3</sub> can not be ruled out. Moreover its abundance in the HNO<sub>3</sub> fraction is in accordance with results of Huerta-Diaz and Morse (1992). They reported that pyrite seems to be a moderately important sink for Mn. Fe shows no correlation to any of the presented elements owing to the different distribution of pyrite and trace metals in the intercalated and basal peats. If only the intercalated peats are considered the correlation coefficients between Fe and As, Mo, Re, and U increases (range 0.69-0.82).

Table 3.2.4: Correlation coefficients of Al, Fe, and trace metals for the peat samples of core W5.

	Al	Fe	As	Cd	Co	Cr	Cu	Mn	Mo	Ni	Pb	Re	Tl	U	V
Al	1														
Fe	-0.17	1													
As	0.30	0.43	1												
Cd	0.44	0.21	0.71	1											
Co	0.69	0.16	0.63	0.81	1										
Cr	1.00	-0.18	0.31	0.45	0.69	1									
Cu	0.48	-0.09	0.37	0.59	0.68	0.48	1								
Mn	0.33	0.47	0.81	0.61	0.46	0.32	0.13	1							
Mo	0.08	0.43	0.88	0.70	0.46	0.09	0.36	0.71	1						
Ni	0.87	-0.03	0.65	0.71	0.84	0.88	0.50	0.61	0.44	1					
Pb	0.94	-0.11	0.43	0.59	0.82	0.95	0.67	0.38	0.25	0.89	1				
Re	0.29	-0.07	0.77	0.60	0.44	0.29	0.25	0.72	0.70	0.64	0.35	1			
Tl	0.96	-0.11	0.39	0.57	0.80	0.95	0.62	0.37	0.19	0.87	0.96	0.35	1		
U	0.43	0.34	0.86	0.70	0.62	0.43	0.37	0.85	0.81	0.72	0.53	0.79	0.48	1	
V	0.96	-0.16	0.41	0.49	0.65	0.97	0.48	0.41	0.22	0.89	0.93	0.40	0.92	0.51	1
Zn	0.79	0.09	0.21	0.34	0.66	0.80	0.42	0.17	-0.05	0.68	0.75	-0.03	0.75	0.20	0.74

Hence, it has to be answered which process caused the different composition of redox-sensitive trace metals between the individual peat sections. As seawater is the ultimate source for S, As, Mo, Re, and U the higher trace metal enrichments in the reed peats (intercalated peats and uppermost parts of the basal peats) in comparison to the lower parts of the basal peats of cores W3 and W5 are rather unexpected, because in the latter peats the highest amounts of pyrite occur. The reed peats consist mainly of *Phragmites* reed peat which grew under a continuous seawater and brackish water influence, respectively. By contrast, the botanical composition of the lower parts of the basal peats (fen woodland and bog peat) reflects exclusively limnic conditions. Therefore, the difference in trace metal composition seems to be related to the different scenarios of pyrite formation, i.e., the direct or indirect seawater influence.

The scatter plot of Mo and U versus  $^{34}\text{S}$  values in core W5 (Figures 3.2.11a and b) reveals a general trend of increasing trace metal contents with increasing sulphate availability and open system conditions, respectively. This trend is clearly seen in the samples of the intercalated reed and basal peat. The samples with the highest Mo and U contents and the most negative  $^{34}\text{S}$  values originate from the upper part of the intercalated reed peat which was influenced by the onset of a transgressive development. Hence, an increasing salinity can be assumed as evidenced by the diatom inventory (Watermann *et al.*, 1999). The basal reed peat shows an indifferent behaviour especially with respect to Mo. The two uppermost samples contain enhanced amounts of Mo although the  $^{34}\text{S}$  values are less negative. As the mean salinity during the formation of the basal reed peat was lower in comparison to the intercalated peat (Watermann *et al.*, 1999), we assume that the inventory of redox-sensitive trace metals resulted to a certain degree from downward diffusing seawater from the brackish and tidal flat sediments, respectively.

As and Re show a behaviour similar to Mo, however, the Re contents are distinctly lower in basal reed peat samples in relation to Mo. The average Re/Mo-ratio ( $0.8 \cdot 10^3$ ) of the intercalated reed peat reflects the seawater ratio whereas the basal reed peat shows a lower ratio of  $0.2 \cdot 10^3$ . Crusius *et al.* (1996) reported that Re can be accumulated in suboxic sediments while Mo needs anoxic conditions. Therefore, it seems to be likely

that downward diffusing seawater is depleted in Re within the overlying suboxic clastic sediments before entering the basal reed peat.

Cd reveals a similar, but less pronounced, behaviour in comparison to the trace metals mentioned above. Except for Mn, the remaining trace metals show no relation to the  $^{34}\text{S}$  values. The correlation coefficients presented in Table 2.3.4 provided a first hint concerning a relation between Mn and the other redox-sensitive trace metals. Hence it is not unexpected that Mn correlates with  $^{34}\text{S}$  values ( $r=0.89$ ) in the peat samples owing to the same element source.

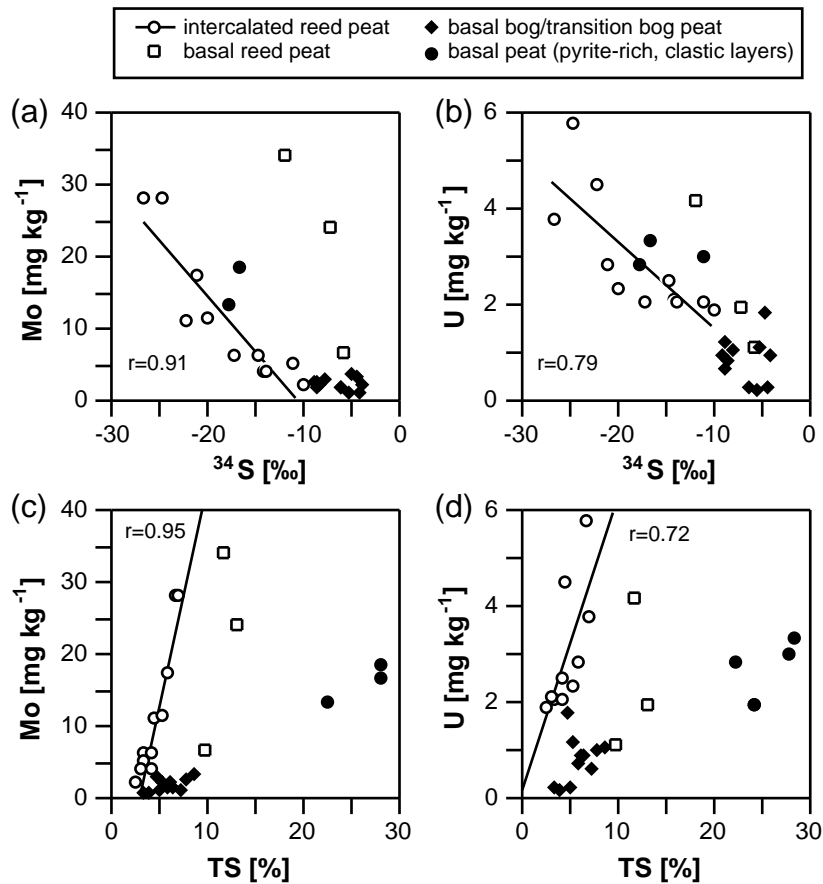


Figure 3.2.11: Scatter plots of Mo and U versus  $^{34}\text{S}$  values and TS of the intercalated reed peat and the basal peat of drill core W5. Samples in brackets originate from the upper reed peat of the OBU.

The scatter plots of Mo and U versus TS (Figures 3.2.11c and d) reflect the aforementioned difference between the intercalated reed peat and the lower basal peat, which can be also seen for As and Re. Two trends are obvious which are in accordance

with the scatter plot of TS versus  $^{34}\text{S}$  (Figure 3.2.4b). The basal reed peat samples show again a transitional behaviour. It should be noted that these relationships do not provide any information about the fixation of the trace metals. Even if As, Mo, and Re are fixed as sulphides it is not the case for U, as shown by the leaching experiments.

Taking into account, that S and redox-sensitive trace metals originate from the same source, the higher trace metal contents in relation to TS of the intercalated reed peat in comparison to the lower parts of the basal peats suggests a different water composition. The intercalated reed peat is directly influenced by brackish water, while the lowest pyrite-rich part of the basal peat, which contains the clastic layers, received saline water via groundwater transport. This water is most likely affected by diagenetic processes during transport which led to a partial removal of trace metals. Such diagenetic processes are for instance microbial reduction of trace metals through enzymatical mechanisms as shown by Lovley (1993) and fixation by organic matter which therefore lead to a decrease in trace metal content. Thus, the conservative  $\text{MoO}_4^{2-}$  anion shows a particle reactive behaviour after reaction with soft ligands like humic-bound thiols and the resulting compounds are more susceptible to reduction (Helz *et al.*, 1996). Furthermore, the reduction of U is initiated by dissolved sulphides produced by sulfate-reducing bacteria (Klinkhammer and Palmer, 1991) besides the direct reduction by sulfate-reducing bacteria as mentioned above. Similar to the basal reed peat the Re/Mo-ratio of this peat section ( $0.2 \cdot 10^3$ ) is distinctly lower than the seawater ratio of  $0.8 \cdot 10^3$  which indicates a stronger depletion of Re in comparison to Mo. This is also seen in the  $\text{EFS}_{\text{OMF}}$  values of the intercalated and basal peat in Figure 3.2.9.

On the other hand sulphate is supposed to be less affected by these processes because its concentration is orders of magnitude higher in comparison to the trace metals. For instance, considering the TS and Mo contents of the pyrite-rich basal part a 5-fold higher watervolume is necessary to explain the Mo content in comparison to TS. Additionally sulphate is not a limiting factor during pyrite formation in the investigated peat-forming environment as shown by stable sulphur isotope ratios.

## **Conclusions**

In this study three drill cores from the marshlands of NW Germany covering the entire Holocene were analysed at high-resolution for bulk parameters, stable sulphur isotopes, selected major elements, and trace metals especially in peat intervals. The results can be deliniated as follows:

- The peat layers can be differentiated in basal (mostly fen woodland and bog peat) and intercalated peats (mostly fen reed peat) which are characterized by elevated amounts of pyrite owing to microbial reduction of seawater sulphate under alsmost open system conditions. However, highest contents of pyrite are mostly seen in limnic basal peats. Thin clastic layers within the basal peats, as a result of tidal channel activities, may have acted as aquifers for a further intrusion of seawater after peat formation.
- The trace metals Mo and Re show highest enrichments in the peat layers followed by As, Cd, and U while Co, Cr, Cu, Mn, Ni, Pb, Tl, V, and Zn reflect the geogenic background. The trace metal composition of the peats can be explained by a brackish water zone (salinity 5-15‰) which consists of sulphate-rich seawater and Fe-rich freshwater. Seawater is the decisive source for As, Cd, Mo, Re, and U whereas the remaining elements originate from the freshwater environment.
- As, Co, Mo, Re, and Tl are predominantly fixed as sulphides and/or incorporated into pyrite while U is related to organic matter. The remaining trace metals show no distinct trend, only Cr reveals a strong relation to the lithogenic detritus.
- While pyrite shows its highest accumulation in the basal peats, the redox-sensitive trace metals As, Mo, Re, and U are highly enriched in the intercalated reed peats, although the metal source is the same. The intercalated reed peats were formed under the direct influence of seawater and brackish water, respectively. On the other hand, the seawater which enters the basal peats after their formation is most likely affected by diagenetic processes and is, therefore, partly depleted in redox-sensitive trace metals.

**Acknowledgements** - The authors wish to thank J. Barckhausen (Geological Survey of the Federal State of Lower Saxony, Germany) for supporting the drilling and for the lithological core descriptions. Furthermore we would like to thank M. E. Böttcher (Max-Planck-Institute Bremen, Germany) for carrying out the S-isotope measurements, M. A. Geyh for performing the  $^{14}\text{C}$ -age determinations (Geological Survey of the Federal State of Lower Saxony, Germany), and W. Bartels (LUFA, Soil-physical Laboratory, Germany) for botanical macroresidual analyses.

This study is funded by the German Science Foundation (DFG) through grant No. Scho 561/2-4 and forms part of the special research program "Bio-geochemical changes over the last 15,000 years - continental sediments as an expression of changing environmental conditions".

## Chapter 4

### **Suspended particulate matter geochemistry of the southern North Sea: the link between Holocene and recent tidal flat sediments**

O. Dellwig, J. Hinrichs, A. Hild, G. P. Klinkhammer, H.-J. Brumsack

**Abstract** - Six drill cores from the NW German coastal area covering the entire Holocene were sampled at high-resolution. Their geochemical composition was compared with recent surface samples from the Spiekeroog Island backbarrier area and Jade Bay. Additionally suspended particulate matter samples (SPM) from the Spiekeroog backbarrier area and from the German Bight as well as three short cores from the Helgoland mud hole were investigated. Samples were analysed for bulk parameters, major and trace elements (XRF and ICP-OES), Pb and  $^{206}\text{Pb}/^{207}\text{Pb}$  isotope ratios (ICP-MS). Holocene and recent tidal flat sediments are characterized in a first approximation by a comparable geochemical composition. They differ significantly in the amount of Zr, which is enriched in the recent sediments reflecting higher contents of heavy minerals. This seems to indicate a change to more energetic conditions from the Holocene to the recent situation. The Holocene tidal flat sediments contain elevated amounts of mud when compared to recent deposits that show a significant lack of this fine-fraction. This phenomenon is possibly related to modern dike-building because the mainland dike seems to act as an energy barrier for the deposition of the fine-fraction. The examination of SPM from this area demonstrates that the clay-fraction of the sediments is predominantly suspended in the water column and may be exported from the backbarrier area into the open North Sea. A nearby depocentre presumably is the Helgoland mud hole. The investigation of SPM from the Wadden Sea reveals a different behaviour among the redox-metals Fe and Mn. While Fe shows an abundance like average shale, Mn displays an enrichment with seasonal and regional variations. Lowest Mn enrichments occur in SPM from the backbarrier area during winter whereas summer samples show higher concentrations due to enhanced mobilisation processes presumably resulting from more pronounced anoxic conditions within the sediment. The anoxic tidal flat sediments therefore seem to act as a Mn source. A general decrease in  $\text{Mn}_{\text{diss}}/\text{Mn}_{\text{part}}$  ratios towards the open German Bight results from lower  $\text{Mn}_{\text{diss}}$  concentrations caused by oxidation and adsorption onto particles. The total Mn within the water column also decreases due to the sedimentation of particles. A vertical  $\text{Mn}_{\text{diss}}$  profile from the outer Jade Bay reveals a Mn enrichment below the photic zone similar to the one seen in the Columbia River estuary (USA). This phenomenon is most likely related to microbial activity.  $^{206}\text{Pb}/^{207}\text{Pb}$  ratios of SPM determined for two transects from the river Weser and Elbe estuaries (1.18) towards Helgoland Island (1.15) show a linear decrease with

increasing distance from the coast reflecting a change from the local geogenic background (1.20) to a more anthropogenic signal with lower  $^{206}\text{Pb}/^{207}\text{Pb}$  values. SPM from the Spiekeroog backbarrier area shows intermediate values of 1.17. The major factors controlling the observed Pb isotopic signature are the decreasing clay content and the increasing adsorption of atmospherically transported Pb. On the other hand  $^{206}\text{Pb}/^{207}\text{Pb}$  ratios of the backbarrier tidal flat sediments (1.20) and the Helgoland mud hole sediments (1.19) are similar to the geogenic background. The difference between SPM and sediment Pb isotopic ratios provides an additional indication for the small amount of SPM deposited in the recent tidal flat sediments.

## Introduction

The southern North Sea coastline has changed drastically from the Holocene to the present. The Holocene sedimentary wedge was deposited as a result of the bulldozing effect (Hagemann, 1969) caused by the sea level rise. Between 9,000 and 8,000 BP tidal flat sedimentation became more widespread and fully marine conditions prevailed most of the German Bight after 7,000 BP (Eisma *et al.*, 1981). Therefore the sediments of the NW German coastal area with its barrier islands, wadden seas, and marshes are comparatively young. The East Frisian barrier islands were formed since 7,500 BP (Streif, 1990).

Geochemical investigations on tidal flat sediments of the German Wadden Sea are comparatively rare (e.g. Gadow and Schäfer, 1973; Förstner and Reineck, 1974; Schwedhelm and Irion, 1985; Recke and Förstner, 1988; Irion and Müller 1990; Koopmann *et al.*, 1994) and often restricted to the investigation of nutrient elements and heavy metals.

This study focusses on the geochemical relation between tidal flat sediments and suspended particulate matter (SPM). In the first part we will compare the different chemical composition of Holocene and recent tidal flat sediments which we assume to be directly linked to the amounts of SPM deposited. The geochemical characteristics of SPM will be discussed in more detail in the second part of our contribution. In the third part we will use the Pb isotopic signal of sediments and SPM to provide information about the sources of the deposited material and possible anthropogenic influences.



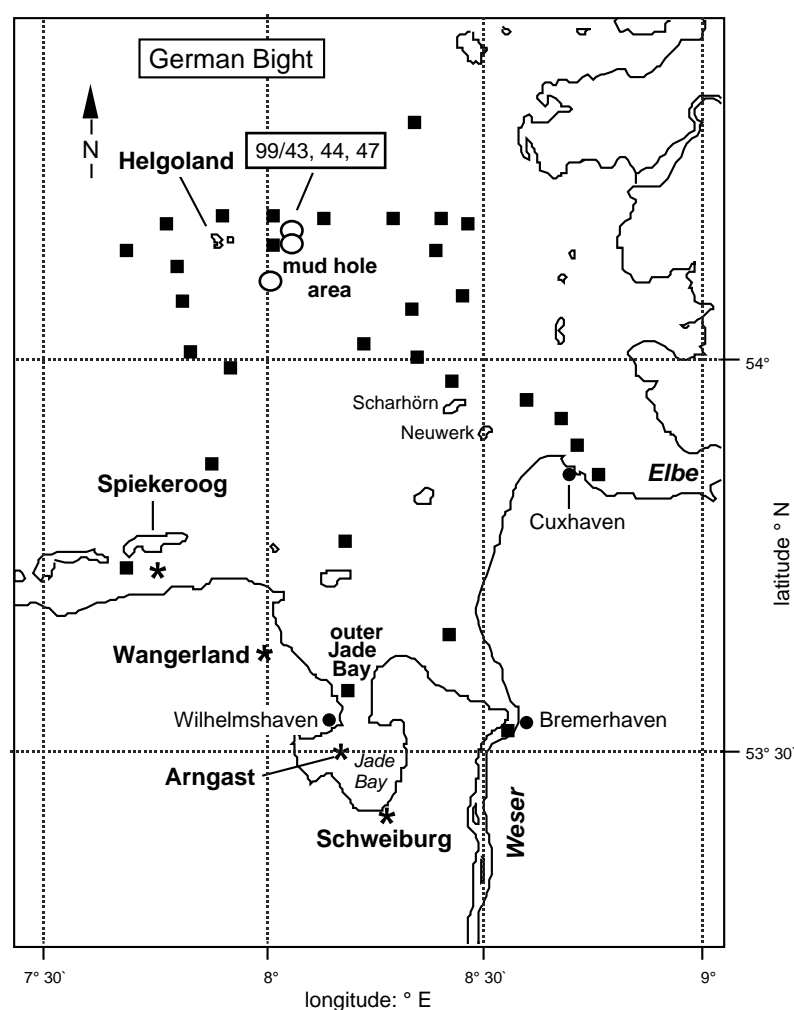


Figure 4.1: Map of the study area showing the sampling locations for sediments (asterisks, open circles) and SPM/seawater (squares).

### Geographical setting and sample material

The locations of the sediment and suspended particulate matter (SPM) samples, which will be described in detail below are shown in Figure 4.1. The Holocene tidal flat sediments were sampled from selected intervals of two drill sites: i) the Wangerland core transect (5 cores) representing sediments from a sheltered intertidal bay (Petzelberger, 1997), and ii) sediments from the ancient Jade Bay (core Schweiburg). The cores were drilled between 1996 and 1998 with the support of the Geological Survey of the Federal

State of Lower Saxony, Hannover, using a technique described by Merkt and Streif (1970). In Figure 4.2 the simplified lithology of the drill cores is presented.

The recent tidal flat sediments consist of surface samples collected from the Swinnplate which is located in the Spiekeroog Island backbarrier area. The samples were collected between winter 1994 and summer 1996 at 1-2 month intervals. Furthermore the recent sediments are supplemented by samples from one drill core (upper 2 m) from the Jade Bay (core Arngast). Additionally we investigated three short cores (length 22-26 cm, cores 99/43, 44 and 47) from the Helgoland mud hole which were collected during a FK Senckenberg cruise (03/99).

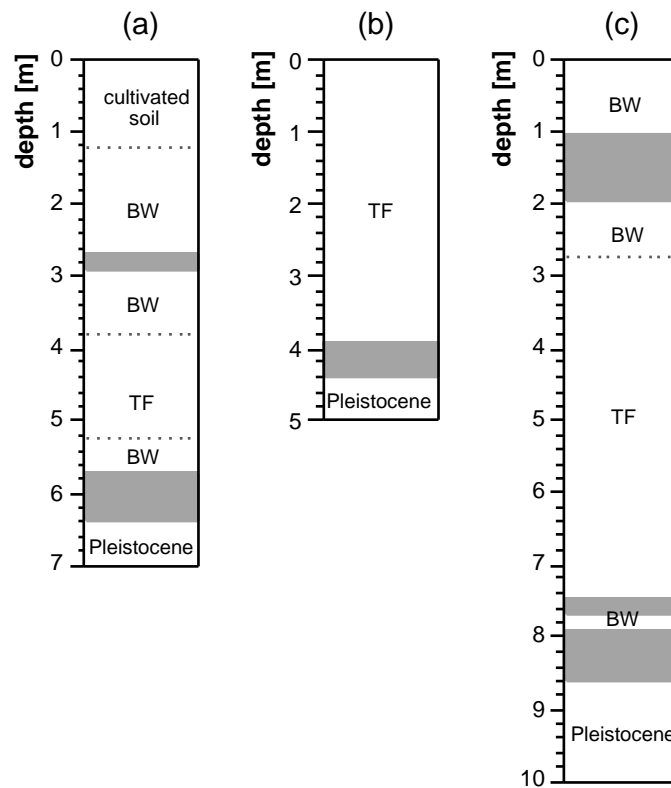


Figure 4.2: Depth profiles showing the lithology of the investigated drill cores: (a) Wangerland (one typical core of the transect), (b) Arngast, (c) Schweiburg. (BW = brackish water sediments, TF = tidal flat sediments, shaded areas indicate peat layers). The Holocene samples were taken from the TF intervals.

SPM samples originate from the backbarrier tidal area (several locations between Spiekeroog and the mainland coast) and from the German Bight (cruises Victor-Hensen, 8/97, WASCH 7/98 and monthly sampling in the backbarrier tidal flat, from 5/94 to

8/95). SPM samples from the German Bight include two transects from Bremerhaven and Cuxhaven to Helgoland Island. Around Helgoland, an algae bloom during Victor-Hensen cruise 8/97 was responsible for very high contents of biological materials in the SPM. Furthermore, a phytoplankton bloom occurred in June 95 in the backbarrier area of Spiekeroog Island (Hild, 1997).

Additionally water samples were taken from a depth profile in the outer Jade Bay (WASCH 7/98) as well as surface samples from the German Bight (Victor-Hensen 8/97).

### **Material and methods**

Sampling was performed on the Holocene drill cores at 5 to 10 cm depending on lithology and at 1 cm intervals on the three short cores from the Helgoland mud hole. The samples were stored in PE-bags, sealed, and immediately frozen. At our laboratory the samples were freeze-dried and homogenised in an agate mortar. The ground powder was used for all subsequent geochemical analyses. The recent surface samples from the Spiekeroog backbarrier area were treated in the same way as the drill core samples.

A total number of 615 sediment samples (Holocene 349, recent 194, Helgoland mud hole 72) were analysed for major elements (Al, Ca, Fe, Mg, K, P, Si, Ti) and trace metals (Ba, Cr, Mn, Pb, Rb, Sr, V, Zn, Zr) by XRF (Philips PW 2400, equipped with a Rh-tube) using fused lithiumtetraborate glass beads. Analytical precision and accuracy of XRF measurements were checked by replicate analysis of geological reference materials (GSD-3, GSD-5, GSS-6) and several in-house standards (see appendix). Five recent tidal flat samples were size-fractionated in order to separate the heavy mineral fraction (density  $>2.89 \text{ g cm}^{-3}$ ) and were analysed by XRF.

Total carbon (TC) and total sulphur (TS) were determined by combustion using an IR-analyser Leco SC-444. Inorganic carbon (TIC) was determined with a UIC Coulometrics Inc. CM 5012  $\text{CO}_2$  coulometer coupled to a CM 5130 acidification module (Huffman, 1977; Engleman *et al.*, 1985). The total organic carbon (TOC) content was calculated as the difference between TC and TIC. The precision of the bulk

parameter analysis was checked in series of double runs and accuracy was determined using in-house standards (see appendix).

SPM samples from the backbarrier tidal flat were taken between 5/94 and 8/95 (98 summer and 84 winter samples) and during the WASCH 98 cruise (7/98, 20 samples). From the German Bight, 33 samples were collected during the RV Victor-Hensen cruise 8/97. Onboard ship, 0.2-4 l of seawater were filtered through preweighed Millipore filters (0.45  $\mu\text{m}$ , for multi-element analyses) and Whatman quartz fiber filters (0.7  $\mu\text{m}$ , for TC and TIC analyses). The filters were rinsed with 18 M  $\Omega$  water, dried at 60°C and reweighed for the determination of total suspended material retained on the filters. For multi-element analysis, the Millipore filters were digested in closed PTFE autoclaves (Heinrichs *et al.*, 1986) at 180°C in a mixture of  $\text{HNO}_3$ ,  $\text{HClO}_4$  (purified by subboiling distillation) and HF (suprapure).

The major elements Al, Ca, Fe, P, and Ti as well as the minor elements Ba, Mn, Sr, Zn, and Zr were analysed by ICP-OES (Perkin Elmer Optima 3000XL). The trace metal Pb and the  $^{206}\text{Pb}/^{207}\text{Pb}$  isotope ratios were determined by ICP-MS (Finnigan MAT Element). Contamination effects can be excluded after measurements of filter and onboard procedural blanks. Precision and accuracy were checked by parallel analysis of international reference materials (GSD-3, GSD-5, GSD-6, GSS-1, GSS-6, LKSD-1), as well as in-house standards (see appendix), while the Pb isotope measurement was controlled by the NIST-Standard SRM 981.

Dissolved Mn was determined by GFAA on 53 filtered water samples (Victor-Hensen 8/97 28 and WASCH 7/98 25 samples). Precision and accuracy were checked by replicate measurement of the CASS-3 certified coastal seawater standard (see appendix). We compare these GFAA results to a dissolved Mn profile from the Columbia River estuary. The Columbia data were obtained using an *in situ* chemical analyser (Klinkhammer, 1994; Klinkhammer and McManus, 1999).

Inorganic carbon was determined coulometrically from the quartz fiber filters with the UIC instrument, total carbon was determined from a second quartz filter by high temperature combustion and coulometric detection of  $\text{CO}_2$  on a Ströhlein Coulomat 702. From stations where only one quartz filter was available, the filter was split into two

sections. One split was used for TIC, the other for TC. TOC was obtained by subtracting TIC from TC. For all methods, blank filters were digested and analysed. The blank values obtained were used for correcting the sample values, although blank concentrations were generally very low. Traces of Cr and Pb were detected in the Millipore filters, while shipboard contamination was insignificant. Accuracy and precision of the bulk parameter measurements are given in the appendix.

## Results and discussion

### *Comparison of recent and Holocene tidal flat sediments*

Figure 4.3 shows a ternary plot (Brumsack, 1989), which represents the three main inorganic components of the investigated sediment and SPM samples. The three poles represent the quartz ( $\text{SiO}_2$ ), clay ( $\text{Al}_2\text{O}_3$ ), and carbonate ( $\text{CaO}$ ) fraction.

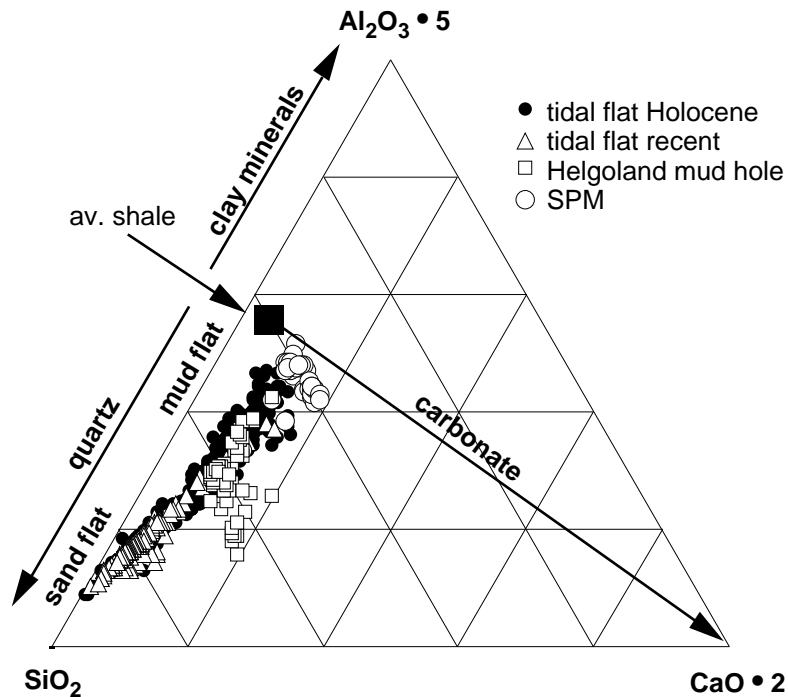


Figure 4.3: Ternary plot  $\text{Al}_2\text{O}_3 \cdot 5$ - $\text{SiO}_2$ - $\text{CaO} \cdot 2$  (Brumsack, 1989) representing the major inorganic components of the investigated sediments and SPM samples.

The quartz-rich sand flat sediments plot close to the  $\text{SiO}_2$  pole. The facies change with increasing clay and carbonate content to mixed and mud flat sediments. The Helgoland mud hole samples plot close to the Holocene mixed and mud flat sediments with some samples enriched in carbonate due to mussel shell fragments. Highest clay contents are found in SPM samples. Except for the higher carbonate content these samples are characterized by a chemical composition comparable to average shale (Wedepohl, 1971). In comparison to the Holocene samples the recent sediments show a less well developed mud flat character and lower clay contents. These differences are unlikely to be a result of sample selection as was shown by sedimentological investigations (Flemming and Davis, 1994), which confirmed that the largest part of the Spiekeroog backbarrier area consists of mixed and sand flat sediments while mud flats are relatively rare.

Enrichment factors versus average shale (EFS) were calculated for mud flat, mixed flat, and sand flat sediments to characterize the individual facies on a geochemical basis. In Figure 4.4, EFS of selected major and trace elements for different Holocene and recent tidal flat facies are presented. SPM samples from the Wadden Sea and German Bight (Figure 4.4a) and Helgoland mud hole samples (Figure 4.4b) were added for comparison. The EFS values are calculated as follows:

$$\text{EFS} = (\text{element}_{\text{sample}} / \text{Al}_{\text{sample}}) / (\text{element}_{\text{av. shale}} / \text{Al}_{\text{av. shale}})$$

The normalisation to Al eliminates dilution effects caused by quartz, carbonate, and organic matter, and allows to compare sediments of different genesis. The element Al was chosen because its abundance is directly linked to clay minerals and its content in sediments is not significantly affected by biogenic cycles or anthropogenic activity. The differentiation between sand, mixed, and mud flat is based on lithological core descriptions and on  $\text{SiO}_2$  contents ( $\text{SiO}_2 < 65\%$  = mud flat,  $\text{SiO}_2 65\text{--}80\%$  = mixed flat,  $\text{SiO}_2 > 80\%$  sand flat). EFS values of SPM and mud flat sediments as well as Helgoland mud hole samples and mixed flat sediments are plotted together because of their geochemical similarity as seen from the ternary plot (Figure 4.3). A compilation of the average values for sediments and SPM is presented in Tables 4.1a and b.

Figures 4.4a-c show that the recent and Holocene sediments are characterized as a first approximation by comparable EFS values. The detrital elements Ba, (Cr), Fe, K, Mg,

(Mn), Rb, and V plot close to the average shale composition. Regarding the EFS values of Mn it is obvious that the recent mud flat sediments and SPM contain higher amounts of this metal in comparison to the shale-like Holocene sediments (Figure 4.4a). We assume that the Holocene sediments lost their "excess" Mn by diagenetic mobilisation of the reduced  $\text{Mn}^{2+}$ -species. Further evidence for diagenetic effects can be seen from total sulphur (TS): While the Holocene mud flats contain 1.6 % TS, the recent mud flats show lower amounts of 0.4 %. This difference indicates a more pronounced formation of pyrite as a result of enhanced microbial sulphate reduction in the Holocene. Thus, the more reducing conditions during the Holocene led to an enhanced Mn mobilization. Because of the complex geochemistry of Mn this element will be discussed in more detail below.

Table 4.1: Average values of bulk parameters [%], major elements [%] and selected trace metals [ $\text{mg kg}^{-1}$ ] for (a) Holocene and recent tidal flat sediments, (b) Helgoland mud hole deposits, and SPM from the study area.

(a)

element	Holocene mud flat	Holocene mixed flat	Holocene sand flat	recent mud flat	recent mixed flat	recent sand flat
TOC	1.8	1.1	0.3	1.8	1.3	0.3
TIC	1.4	1.1	0.7	1.2	0.9	0.3
TS	1.2	0.7	0.2	0.4	0.3	0.1
$\text{SiO}_2$	61.4	71.3	81.7	57.8	75.8	87.9
$\text{TiO}_2$	0.60	0.53	0.33	0.46	0.38	0.29
$\text{Al}_2\text{O}_3$	9.5	7.4	5.0	7.4	5.5	3.5
$\text{Fe}_2\text{O}_3$	4.6	3.0	1.5	3.2	1.8	0.8
MgO	1.6	1.2	0.6	1.6	0.8	0.4
CaO	6.6	5.1	3.3	6.4	4.0	2.0
$\text{Na}_2\text{O}$	0.8	0.9	0.9	3.5	1.6	0.9
$\text{K}_2\text{O}$	2.1	1.9	1.5	1.8	1.6	1.2
$\text{P}_2\text{O}_5$	0.16	0.11	0.06	0.24	0.11	0.05
Ba	258	270	258	256	294	242
Cr	77	61	32	63	30	19
Mn	516	366	267	778	317	145
Pb	17	13	7	40	16	9
Rb	95	72	48	70	40	22
Sr	202	158	112	232	140	82
V	93	59	26	73	29	12
Zn	61	44	20	95	22	10
Zr	305	409	327	326	414	401

(b)

element	mud hole	SPM backbarrier	SPM offshore
TOC	1.2	5.2	n. d. *
TIC	1.5	1.6	n. d. *
TS	0.6	0.6	0.9
SiO <sub>2</sub>	68.3	51 **	21 **
TiO <sub>2</sub>	0.46	0.51	0.37
Al <sub>2</sub> O <sub>3</sub>	6.9	10.9	7.0
Fe <sub>2</sub> O <sub>3</sub>	2.6	4.4	3.7
MgO	1.2	1.7	1.5
CaO	6.6	7.9	5.6
Na <sub>2</sub> O	1.6	0.9	3.2
K <sub>2</sub> O	1.8	2.2	1.2
P <sub>2</sub> O <sub>5</sub>	0.09	0.36	0.61
Ba	268	277	274
Cr	50	144	176
Mn	312	1060	1785
Pb	24	66	260
Rb	68	94	67
Sr	193	296	253
V	52	97	74
Zn	64	200	777
Zr	395	161	98
SPM [mg kg <sup>-1</sup> ]		58	7

\* n.d. = not determined

\*\* data aquired with thin-film XRF after the method given by Wehausen (1995)

Elements which are enriched in comparison to average shale can be divided into three groups: i) Ca, Sr, ii) P, Pb, Zn, (Cr), and iii) Si, (Ti), Zr. The enrichment of Ca and Sr reflects the presence of carbonates while the enhanced amounts of the second group of elements is due to anthropogenic activity. P shows elevated concentrations especially in the recent mud and mixed flat sediments as well as in SPM reflecting an enhanced nutrient input (Radach *et al.*, 1990). Apparently organic matter is not a major source of P because there is no enrichment in Holocene samples. Pb is most enriched in SPM followed closely by recent sediments (tidal flat sediments and Helgoland mud hole), most probably indicating anthropogenic activity. Zn reveals a similar distribution but is not enriched in the sand flat sediments. This is possibly due to the different carrier phases of Pb and Zn. Pb is stronger influenced by atmospheric input (50 %) in



comparison to Zn (30 %) while the riverine contribution of Zn exceeds Pb by a factor of two (Schwedhelm and Irion, 1985). Owing to the comparatively low riverine input into the backbarrier area atmospheric input seems to be the most important factor. Additionally Pb is more particle reactive than Zn (Tappin *et al.*, 1995).

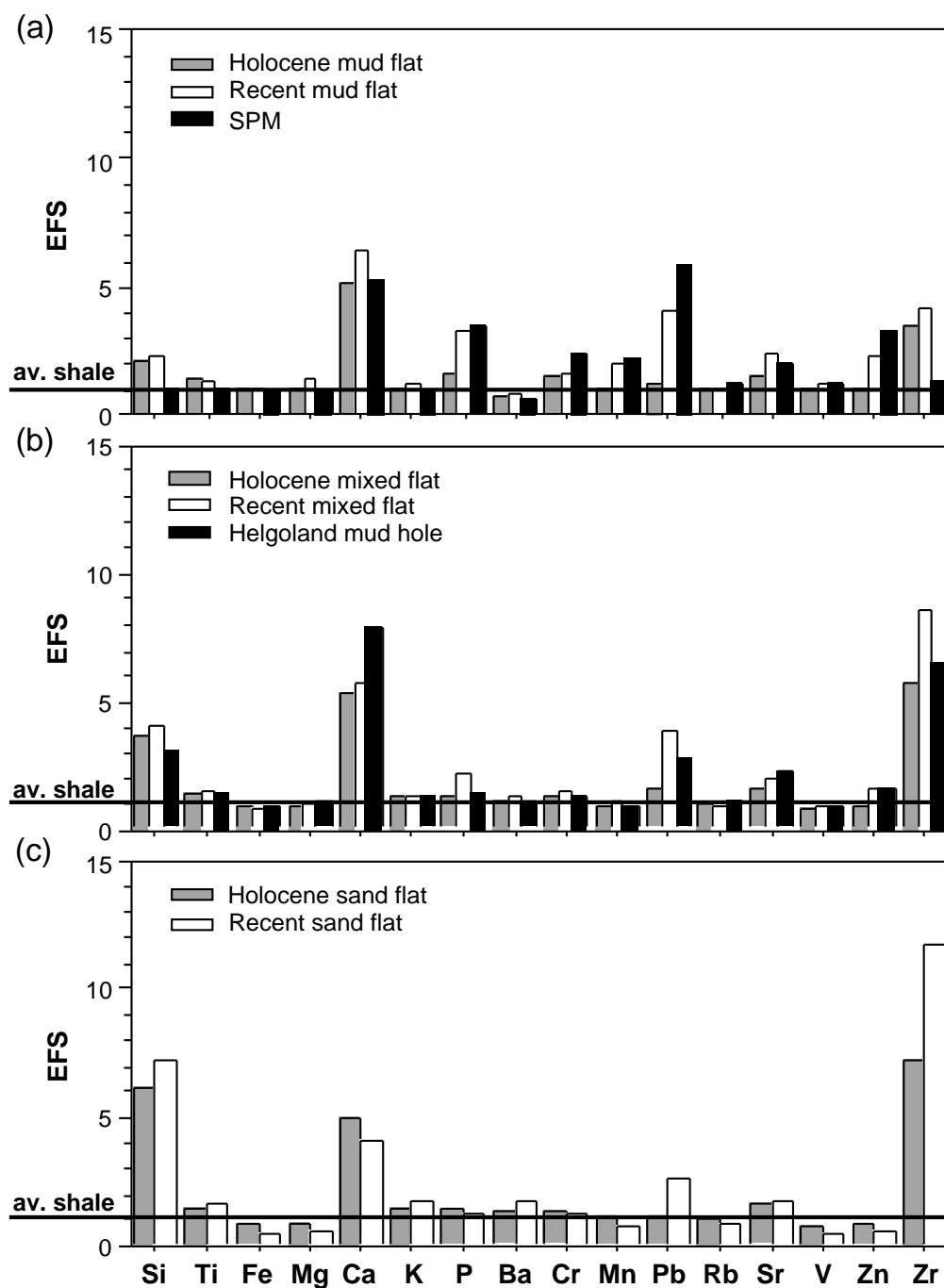


Figure 4.4: Enrichment factors versus average shale (EFS) for selected major and minor elements of different Holocene and recent tidal flat facies and SPM. Average shale data from Wedepohl (1971).

The third group consists of elements which can be used as indicators of depositional energy conditions. Enrichments in Si reflect higher amounts of quartz, whereas high Zr and Ti values point to an enhanced amount of heavy minerals (e.g., zircon, ilmenite, rutile). Only SPM is characterized by a shale-like composition while the sediments are enriched in these elements. Moreover, Zr reveals the most significant difference between the investigated recent and Holocene tidal flat sediments. Especially the recent sand flat sediments show a pronounced Zr enrichment in comparison to the Holocene sediments. Ti is only slightly enriched in recent sand flat sediments. This finding provides a first indication for a change in energetic conditions from the Holocene to the recent situation. The samples from the Helgoland mud hole can be compared with the Holocene sediments regarding their Si and Zr EFS values.

Figure 4.5a presents a scatter plot of Zr and  $\text{TiO}_2$  for sediments (tidal flat and Helgoland mud hole) and SPM. A broad correlation of  $\text{TiO}_2$  and Zr is evident for the recent sediments with data points tending towards the ratio determined for heavy mineral separates (from the Spiekeroog backbarrier area) whereas the SPM samples plot closer to the average shale ratio. No correlation is seen for the Holocene samples which plot between SPM and recent sediments. The Holocene tidal flat sediments therefore form a transition between two endmembers represented by the recent sediments and SPM. The samples from the Helgoland mud hole reflect the above mentioned similarity to the Holocene sediments.

Similar differences shows the scatter plot of  $\text{TiO}_2$  vs.  $\text{Al}_2\text{O}_3$  (Figure 4.5b). Again three groups can be distinguished. SPM samples plot close to average shale. The correlation of  $\text{Al}_2\text{O}_3$  and  $\text{TiO}_2$  for the Holocene sediments indicates the association of Ti with clay minerals. However, the fact that the regression line shows a significant positive intercept most probably reflects the presence of small amounts of heavy minerals. The Helgoland mud hole samples reveal once more a chemical composition which is comparable to the Holocene sediments. The recent tidal flat sediments show no correlation as a result of a higher contribution of heavy minerals. The higher  $\text{Al}_2\text{O}_3$  content of the Holocene tidal flat and Helgoland mud hole sediments is consistent with

the elevated mud-content while the recent deposits show a significant lack of this fine-fraction, but considerably higher and variable contents of heavy minerals.

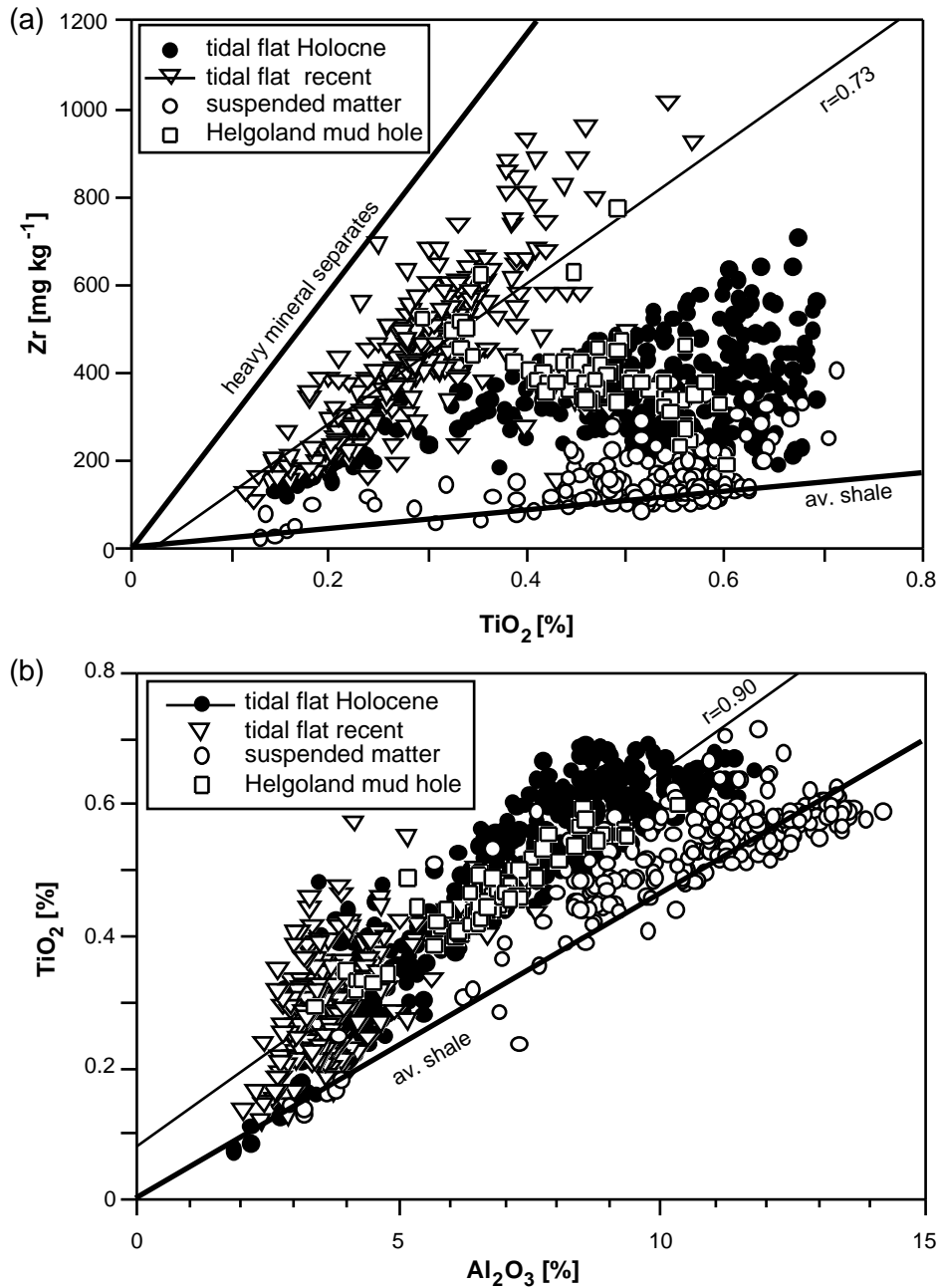


Figure 4.5: (a) Scatter plot of Zr vs. TiO<sub>2</sub> of sediment (Holocene and recent) and SPM samples. The bold lines indicate heavy mineral separates and average shale. (b) Scatter plot of TiO<sub>2</sub> vs. Al<sub>2</sub>O<sub>3</sub> of sediment (Holocene and recent) and SPM samples. The bold line indicates the average shale value.

A depletion of the mud-fraction was also observed by Flemming and Nyandwi (1994) on the basis of sedimentological investigations in the backbarrier area of Spiekeroog

Island. They related this phenomenon to modern dike-building because the mainland dike seems to act as an energy barrier for the deposition of the fine-fraction. The examination of SPM from this area demonstrates that the clay-fraction of the sediments is predominantly suspended in the water column and may be exported from the backbarrier area into the open North Sea by tidal flow.

The main area of deposition for the fine-fraction seems to be the western Skagerrak/Norwegian Channel, where presently about 50-70% of the total mass accumulation of the North Sea occurs (Eisma and Kalf, 1987). Furthermore the area of the Helgoland mud hole is considered as an additional depocentre. Most estimates of the recent sedimentation rate range from 5-18 mm yr<sup>-1</sup> (e.g. Förstner and Reineck, 1974; Dominik *et al.*, 1978; Eisma *et al.*, 1984; Baumann, 1991), while von Haugwitz *et al.* (1988) propose a significantly lower average sedimentation rate of 3.2 mm yr<sup>-1</sup> between 8,000 and 1,500 years BP. This difference can presumably be explained by the increasing SPM export from the Wadden Sea in addition to the dredged harbour mud mentioned by Dominik *et al.* (1978). Our finding is in accordance with the budget calculations presented by Puls *et al.* (1997). The authors point out that the main source of fine sediment in the Helgoland mud hole is the German Bight itself.

In order to estimate the total sediment accumulation in the study area, we compare recent SPM budgets and the Holocene clay accumulation in Table 4.2. For the calculation of the Holocene mass flux, we used a sediment volume of  $25 \times 10^9 \text{ m}^3$  for the sedimentary wedge of the Lower Saxonian coastlands (=study area) and a deposition time of 7500 a (Hoselmann and Streif, 1997). Assuming a mean density of  $1.25 \text{ t m}^{-3}$  for the Holocene sediments (mixed flat sediments, Puls *et al.*, 1997), the total deposited mass amounts to  $5.6 \text{ Mt yr}^{-1}$ . As a comparison to the recent SPM accumulation, we calculated the mean clay content of the Holocene sediments including tidal flat and brackish water sediments from the mean  $\text{Al}_2\text{O}_3$  concentration and the  $\text{Al}_2\text{O}_3$  content of average shale. This procedure assumes a dilution of clay material with quartz, which holds for the sediments used in this study (compare EFS values). From the mean  $\text{Al}_2\text{O}_3$  concentration of 9.2% we inferred a clay content of 55% of the Holocene sediments

which results in a clay deposition rate of  $2.3 \text{ Mt yr}^{-1}$ . This value is distinctly higher than the recent deposition rates presented in Table 4.2.

Table 4.2: Comparison of recent and Holocene estimates of deposition rates in the German Wadden Sea.

time period	author	input to the Wadden Sea [Mt yr <sup>-1</sup> ]
recent	Kirby (1987)	1.24
recent	Puls <i>et al.</i> (1997)	$1 \pm 1^*$
Holocene	this study	2.3

\* Value was calculated for the entire German Wadden Sea, i.e., the coastlands of Lower Saxony and Schleswig-Holstein

The comparison in Table 4.2 suggests that different energy conditions prevailed during these periods. It should be noted that the value given by Puls *et al.* (1997) integrates over the entire German coastal area; therefore this value has to be divided by a factor of 2 because the area of the Lower Saxonian coastlands amounts to about 43% of the total German Wadden Sea area (Lozán *et al.*, 1994).

It may be argued that quite different geographic locations are compared to each other, i.e., backbarrier tidal flats and intertidal bay sediments. However, the fossil sheltered bay of the Wangerland site reflects conditions comparable to the recent Spiekeroog backbarrier area. Furthermore the recent Jade Bay sediments are complemented by sediments of the ancient Jade Bay. In conclusion, while there are uncertainties, the geochemical balance indicates a large shift in depositional energy between the anthropogenically unaffected Holocene and recent times.

### *SPM geochemistry*

*Major compounds* - For a general characterization of the SPM, all samples are plotted in a ternary plot (Figure 4.6) with Al (clay minerals), Ca (from calcium carbonate), and TOC (organic matter) as endmembers. Element concentrations were used on a weight basis. Besides Si, which is of mainly detrital origin, these elements represent the main constituents of particles in the study area. For comparison, the values for average shale

and mean Wadden Sea sediment (recent surface and Holocene samples) as well as mean Helgoland mud hole sediments are also shown.

The SPM is characterized by an essentially constant Ca/Al-ratio without seasonal variations. Therefore fresh biogenic carbonate (e.g. foraminifera) seems not to be the major component as higher summer productivity should lead to a significant shift towards the Ca pole. According to Salomons (1975) the carbonate found in the fine fraction of tidal flat sediments (southern North Sea) consists of material from the English Channel (app. 80%) and from riverine input (app. 20%). The SPM data form a trend from the average tidal flat sediments to material with increasing TOC values, indicating a dilution of material with quite constant Ca/Al-ratios with varying amounts of TOC from biological activity. The mean value for recent sediment plots close to the SPM samples with the lowest TOC contents. The mean value for Holocene sediments shows a closer similarity to SPM, indicated by a higher TOC content, which possibly results from the change in depositional energy conditions mentioned before.

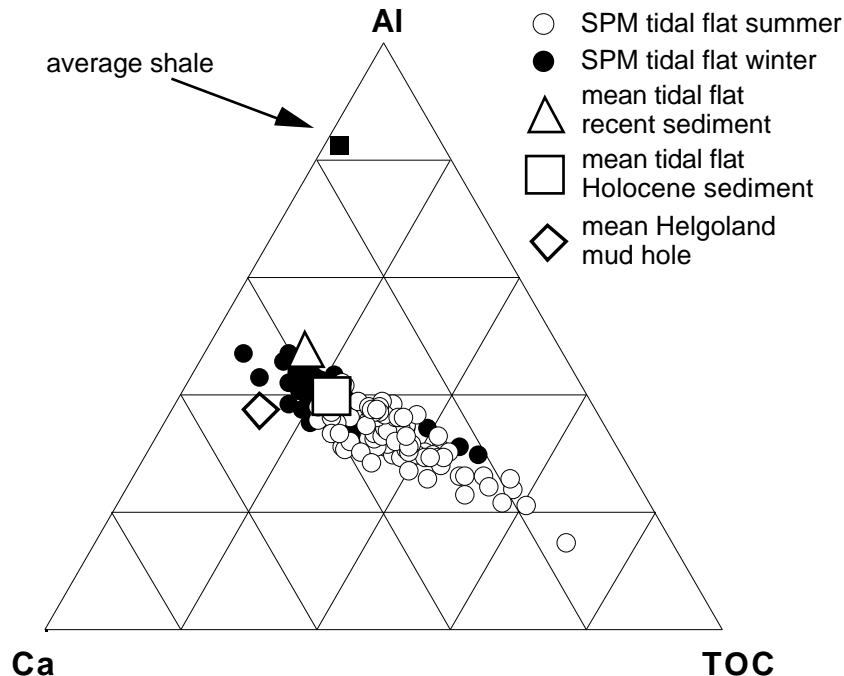


Figure 4.6: Ternary plot Al-Ca-TOC of SPM samples from the Spiekeroog island backbarrier area. Mean recent and Holocene tidal flat sediments are plotted for comparison.

Winter SPM samples from the backbarrier Wadden Sea are lower in TOC contents (range 1.4-6.3% w/w; mean  $4.4 \pm 1.3\%$  w/w) than those collected in summer (range 1.1-13.6% w/w; mean  $5.8 \pm 2.1\%$  w/w). Although both data sets partly overlap, they are consistent with higher bioproduction during summer conditions. The large variation in TOC is caused by algal blooms.

Concentrations of major and trace elements in particles are expected to vary widely in the North Sea and the Wadden Sea, depending on seasonal conditions and location (Postma, 1981). The importance of SPM for the distribution of trace metals like Pb, Zn, Cd is well known (e.g. Förstner and Müller, 1974), while major elements have rarely been analysed (Wirth and Seiffert, 1988; Hölemann and Wirth, 1988). We present data for selected elements of predominantly detrital origin and clay like element ratios and elements which are influenced to a larger extent by biological activity. In order to reveal deviations from average shale composition the concentrations of elements in particles are plotted versus Al which serves as a reference for detrital material. It should be noted that in Figure 4.7 concentrations per volume of sea water rather than on dry weight basis are presented as we intend to reveal variations in the composition of water masses and not in particle chemistry. EFS values that will be mentioned below are calculated from the difference of the slopes of the respective regression lines and the average shale ratio.

In the summer and winter samples from the Wadden Sea and the German Bight the elements Ti (Figure 4.7a), K, and Mg (not shown) are well correlated to Al and plot close to the average shale ratio, an indication for their detrital origin. Zr data of SPM (Figure 4.7b) show a larger scatter, possibly owing to wave action. Samples from the Wadden Sea are enriched in Zr while the SPM from the German Bight is characterised by a composition similar to average shale. High Zr concentrations in sediments are indicative of high energetic depositional conditions owing to the preferential accumulation of heavy minerals, as described above. Enhanced water velocities may even cause resuspension of heavy minerals. The fact that a Zr enrichment is not observed in the German Bight implies that the heavy minerals rapidly settle from the water column.

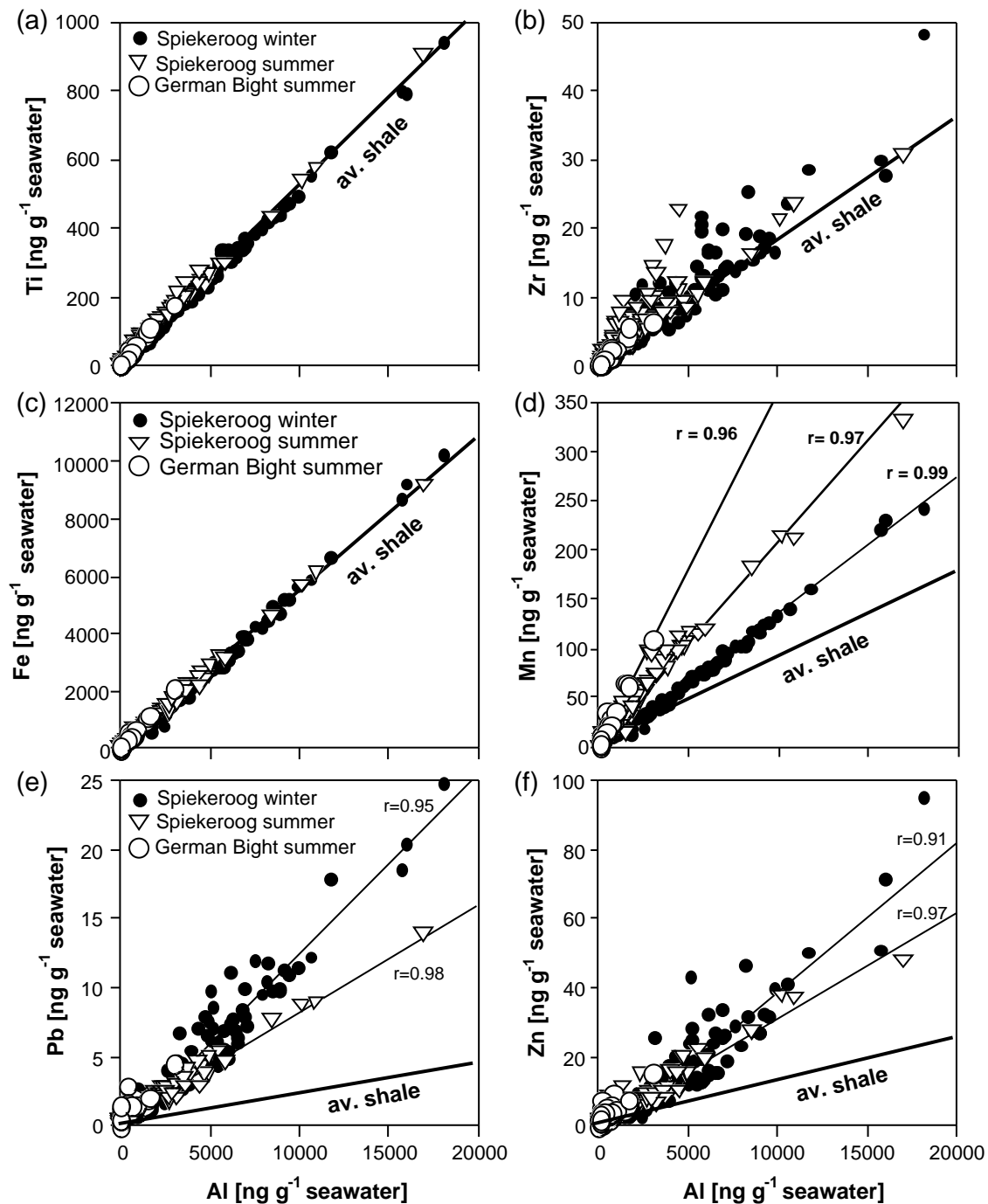


Figure 4.7: Scatter plots of Ti, Zr, Fe, Mn, Pb, and Zn vs. Al of SPM from the German Bight and Spiekeroog backbarrier area. The bold lines indicate average shale.

During summer the Wadden Sea sediments are characterised by enhanced microbial activity. Bacterial abundances (both sulphate reducing and heterotrophic bacteria) increase during summer and autumn (Gunkel and Klings, 1989), resulting in the release of remineralized nutrients and trace metals into interstitial waters (De Flaun and Mayer, 1983). By diffusion, activity of macrobenthos, tidal pumping and draining during low



tide the interstitial waters and the dissolved elements may enter the water column followed by adsorption on SPM (Morris *et al.*, 1982; McCaffrey *et al.*, 1980). The metals Fe and Mn are considerably involved in redox processes (e.g. Froelich *et al.*, 1979; Campbell *et al.*, 1988). Mn(IV) is transformed to the soluble Mn(II) under only mildly reducing sediment conditions. By contrast stronger reducing conditions are necessary to form Fe(II) from Fe(III) (Froelich *et al.*, 1979). Furthermore Fe(II) is rapidly fixed within the sediments as sulphides (Fe-monosulphides, pyrite) while Mn-sulphides are relatively unstable and Mn fixation will only occur as rhodochrosite under normal sedimentary conditions (Berner, 1981). However, Fe shows a shale-like abundance (Figure 4.7c) in SPM similar to Ti, K, Mg.

*Behaviour of Mn* - By contrast, Mn (Figure 4.7d) behaves differently. Besides the general enrichment in comparison to average shale, seasonal and regional variations are evident. The winter samples from the Wadden Sea show the lowest Mn enrichment (EFS=1.6) in comparison to all summer samples (EFS Spiekeroog summer=2.3 and EFS German Bight=4.3). During periods of enhanced oxygen depletion in summer Mn oxy/hydroxides are reduced to soluble Mn(II) in the tidal flat sediments which leads to a higher release of Mn(II) from the sediments. During low tide Hild (1997) determined high concentrations of dissolved Mn ( $30\text{--}110\ \mu\text{g l}^{-1}$ ) in the draining waters of the Spiekeroog backbarrier area (8/95). Tidal flat sediments therefore seem to act as a Mn source for the German Bight in summer.

On the other hand the Wadden Sea receives a large Mn supply by riverine input. Besides the large rivers Weser and Elbe, extremely high levels of dissolved (av.  $398$ , range  $50\text{--}1,180\ \mu\text{g l}^{-1}$ ) and particulate Mn (av.  $3,674$ , range  $470\text{--}9,800\ \text{mg kg}^{-1}$ ; Lipinski, 1999) in waters entering the Jade Bay and from the river Hunte (tributary of the river Weser) are introduced into the German Bight and the tidal flat areas. Presumably most Mn which is supplied by such small rivers is flocculated and redistributed within the intertidal system and thus elevated amounts of Mn are added to the tidal flat environment. Water samples originating from shallow depth close to the estuaries of the rivers Weser and Elbe are characterized by slightly enhanced Mn values of average  $3.1\ \mu\text{g l}^{-1}$  (range  $0.8\text{--}13\ \mu\text{g l}^{-1}$ , 21 samples, mean water depth 11 m). The surface seawater

value for the German Bight averages  $1.1 \mu\text{g l}^{-1}$  (range  $0.5\text{--}3 \mu\text{g l}^{-1}$ , 8 samples, mean water depth 26 m). The Mn concentration gradient from the backbarrier tidal flat to the deeper parts of the German Bight indicates the importance of the Wadden Sea for the Mn balance. For comparison, the average Mn level for the entire North Sea is in the range  $0.3\text{--}1.4 \mu\text{g l}^{-1}$  (Kremling, 1985; Shiller, 1997) while the open North Atlantic contains only  $0.05 \mu\text{g l}^{-1}$  (Kremling, 1985).

In order to give an overview about the Mn distribution in particulate ( $\text{Mn}_{\text{part}}$ ) and dissolved ( $\text{Mn}_{\text{diss}}$ ) form Figure 4.8 presents the ratio of  $\text{Mn}_{\text{diss}}/\text{Mn}_{\text{part}}$ . It should be noted that the preliminary results presented in this work are based on only a few data points from the SW part of the study area. The contours presented in this Figure were calculated with the statistic software JMP 3.1.6 (SAS Institute Inc.). Samples from the two southernmost Weser estuary show high values due to elevated concentrations of dissolved Mn in the low salinity water masses. The large data point from the backbarrier tidal flat represents the mean of 15 water samples, smoothing out tidal variations of the Mn concentrations. Although only few data points are available for the area close to the barrier islands, a general decrease of the  $\text{Mn}_{\text{diss}}/\text{Mn}_{\text{part}}$  ratios towards the open German Bight becomes obvious. This is likely the result of lower  $\text{Mn}_{\text{diss}}$  concentrations which are caused by oxidation and subsequent adsorption of Mn on particles. Additionally the total Mn amount within the water column decreases as well towards the German Bight due to sedimentation of particles. However, samples with the lowest total Mn content are characterized by the highest Mn concentrations per gram of dry SPM which is probably caused by enhanced coagulation (Eisma, 1993). This finding is confirmed by bulk particle concentrations, which average  $1,160 \text{ mg kg}^{-1}$  for SPM originating from the backbarrier area and  $1,860 \text{ mg kg}^{-1}$  for SPM sampled in the German Bight (salinity  $>30\text{‰}$ ). Another mechanism leading to enrichment of Mn in the German Bight SPM may be related to humic substances (DOC). Mn can be released during degradation of the organic matter and is then re-adsorbed on particles which are characterized by a higher specific surface area. Tappin *et al.* (1995) found elevated concentrations of dissolved Mn ( $0.6\text{--}3.0 \mu\text{g l}^{-1}$ ) throughout the Southern North Sea during summer while winter sampling revealed concentrations below  $0.6 \mu\text{g l}^{-1}$ .

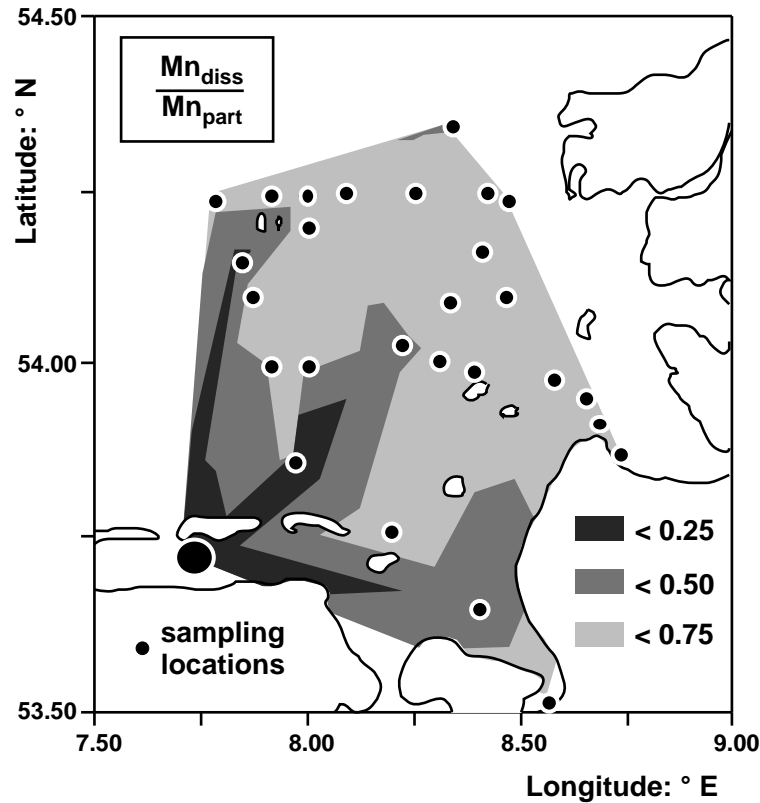


Figure 4.8: Map showing the distribution of the ratio of dissolved and particulate Mn ( $Mn_{diss}/Mn_{part}$ ) of the study area. The backbarrier tidal flat data point is a mean value of 15 samples.

The discussion presented above focussed on the lateral Mn distribution. However, vertical Mn concentration profiles reveal a more complex behaviour of Mn. Figure 4.9a shows a  $Mn_{diss}$  depth profile from the outer Jade Bay which was taken 1 h after high tide. The entire water column is well mixed at a salinity of  $28.41\text{‰} \pm 0.01$  (1). With the onset of the seaward tidal current the SPM concentrations are higher at the bottom in comparison to the top of the profile probably as a result of resuspension of bottom sediments. The  $Mn_{diss}$  data show a decrease from the deepest sample ( $3 \mu\text{g l}^{-1}$ , 16.2 m) by a factor of two within the lowermost 2 m of the water column. The source for the high concentrations is most likely Mn diffusing out of the tidal flat sediments. Between 12.8 and 10.7 m we observe a distinct Mn enrichment of at maximum  $3.5 \mu\text{g l}^{-1}$ . In the upper part of the profile the Mn concentrations decrease again to an average value of  $2.2 \mu\text{g l}^{-1}$ . Unfortunately the uppermost part of the profile could not be sampled due to

technical problems. If we assume an almost constant concentration within the remaining water column (0-6 m) a similarity to the profile of the Columbia River estuary (USA) seems evident (Figure 4.9b).

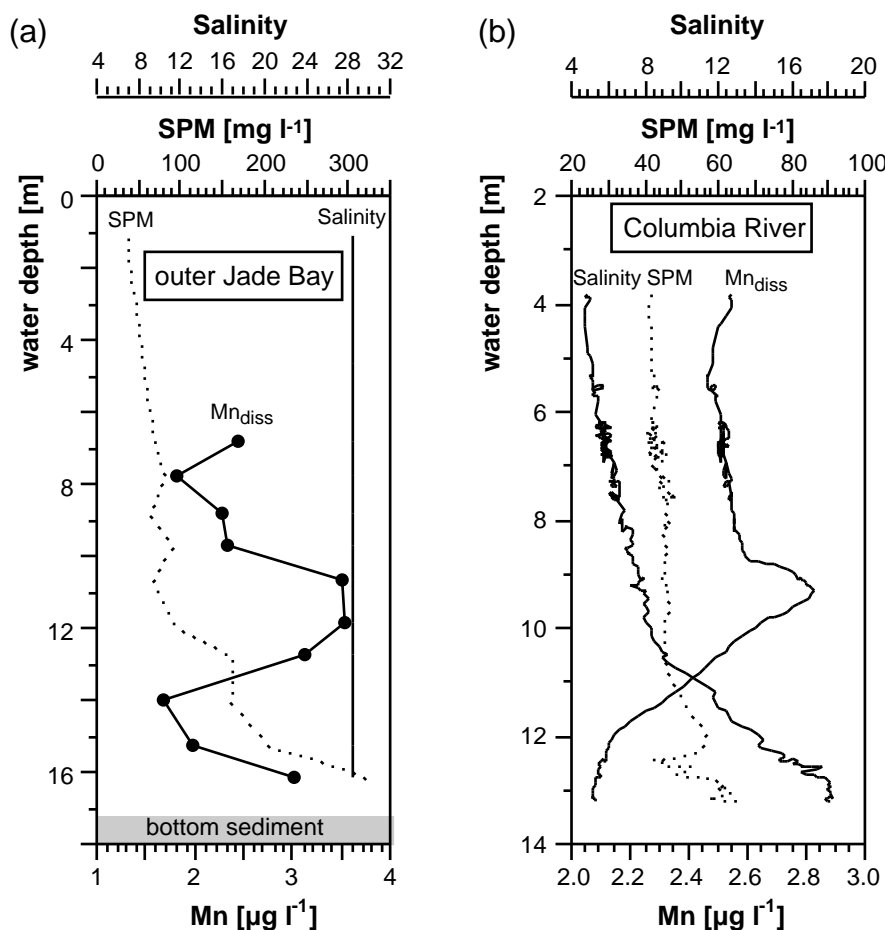


Figure 4.9: Water column profiles of dissolved Mn ( $Mn_{diss}$ ), suspended particulate matter (SPM), and salinity from (a) the outer Jade Bay and (b) Columbia River estuary (USA). The salinity of the Jade Bay profile is in the range of 28.40 - 28.42.

The most interesting thing about this feature is that it always occurs right at the base of the photic zone (as measured with a PAR sensor). Although we did not analyze this parameter in the outer Jade Bay, chlorophyll measurements during the Victor-Hensen cruise 8/97 in the outer Weser estuary indicate an extent of the photic zone to a depth of about 12 m.

We believe that the Mn maximum is produced by microbial oxidation of humic material using Mn oxides. How this Mn production cycle is related to photons remains

unclear but we may speculate that microbes use Mn oxides as energy storage devices. Sunlight produces oxides that serve two purposes: they protect the bacterial cells from UV radiation and store energy. When the microbes find themselves free of UV radiation, they use these coatings to produce energy by breaking down humics below the photic zone.

*Trace metals related to anthropogenic activity* - Further elements which are strongly enriched in particles are the heavy metals Pb and Zn (Figures 4.7e and f). Both metals are known to be affected by biogeochemical cycles (Kersten, *et al.*, 1992; Tappin *et al.*, 1995), and are concentrated on particle surfaces. The EFS values for Zn (summer 2.4, winter 3.0) are lower in comparison to Pb (summer 3.6, winter 5.4), which probably reflects the different sources of both metals (see above).

The bulk Pb content in the Wadden Sea SPM shows no significant seasonal differences (summer average 67 mg kg<sup>-1</sup>, range 25-202 mg kg<sup>-1</sup>; winter average 73 mg kg<sup>-1</sup>, range 12-197 mg kg<sup>-1</sup>). However, the EFS values of Pb per volume unit of seawater reveal higher enrichments in winter (summer 3.6, winter 5.4). This finding is possibly related to enhanced resuspension processes during winter owing to stronger winds and wave action.

SPM samples from the German Bight (salinity >30‰) exhibit an average Pb content of 235 µg g<sup>-1</sup> (range 62-959 µg g<sup>-1</sup>) and correspondingly a high EFS of 27.8. Tappin *et al.* (1995) determined Pb concentrations in SPM of >200 µg g<sup>-1</sup> during winter and approximately 50 µg g<sup>-1</sup> during the other seasons. They explain the winter enrichment by resuspension of Pb-rich material, a low plankton content of the SPM, and perhaps increased eolian input (Injuk *et al.*, 1992). During our sampling in the German Bight weather conditions were fair. For this reason we assume resuspension unlikely to be responsible for the elevated Pb contents. The samples were collected during an algae bloom, which probably indicates a biogeochemical mechanism of Pb incorporation into SPM. Additionally, Pb has a more pronounced scavenging reactivity, which may also contribute to the higher contents in the German Bight SPM when compared with the Wadden Sea SPM.

### *Lead isotopes*

The comparison of Holocene and recent tidal flat sediments revealed differences resulting from man-made influences on the morphology of the coastal area (dike-building). A further anthropogenic factor is manifested in heavy metal pollution (see above). According to Förstner and Wittmann (1979) especially Pb shows a high enrichment versus the geological background. Therefore, we examined the Pb isotopic ratios of SPM which provide more detailed information on the extent of pollution.

Continental sources from Europe contribute lead with a  $^{206}\text{Pb}/^{207}\text{Pb}$  ratio of approximately 1.18-1.20 (Elbaz-Poulichet *et al.*, 1986). This finding was confirmed by analysis of preindustrial Wadden Sea sediments ( $^{206}\text{Pb}/^{207}\text{Pb}$   $1.20 \pm 0.004$ ) which is considered to represent the local geogenic background. The anthropogenic signal of the study area is mainly influenced by the Pb ores used for Pb alkyl production which enter the atmosphere during combustion of leaded fuel and high temperature industrial processes (Erel *et al.*, 1997 and references therein). Most Pb ores are at present imported from Australian and Canadian Precambrian sources with low Pb isotopic ratios (Kersten *et al.*, 1992). The anthropogenic Pb is mainly distributed through the atmosphere and subsequently enters the terrestrial and marine environment by wet and dry deposition. Although recently the combustion of leaded fuel has decreased, the atmospheric Pb isotope signal is still significantly lower than the European geogenic signal (Döring *et al.*, 1997). Assuming an approximately homogenous mixing of Pb in the atmosphere, the entire water masses of the study area should receive roughly the same input of atmospheric Pb. Kersten *et al.*, (1992) found  $^{206}\text{Pb}/^{207}\text{Pb}$  ratios between 1.11 and 1.20 for aerosols from the North Sea, depending on the wind direction. Prevailing winds carried aerosols with low  $^{206}\text{Pb}/^{207}\text{Pb}$  ratios between 1.11 and 1.14 which were influenced by the highly industrialized UK and continental Europe while highest values of 1.20 indicated short term input of anthropogenically unaffected aerosols from the Atlantic. Pb on particles from North Atlantic surface water show  $^{206}\text{Pb}/^{207}\text{Pb}$  ratios of 1.18 (Véron *et al.*, 1994). This contribution is thus indistinguishable from the natural geogenic European isotopic signal. As Atlantic water is considered to be separated from the sampling area by the eastward flow of the Rhine into the North Sea (Eisma and

Irion, 1988; Tappin *et al.*, 1995), we expect to deal mainly with two sources: i) detrital riverine inflow with comparatively high  $^{206}\text{Pb}/^{207}\text{Pb}$  ratios and ii) atmospheric input with low  $^{206}\text{Pb}/^{207}\text{Pb}$  ratios.

Figure 4.10 provides an overview of the Pb-isotope distribution in the sampling area. The  $^{206}\text{Pb}/^{207}\text{Pb}$  ratio of SPM and sediments shows mixtures between the local geogenic background of 1.20 and the (atmospheric) anthropogenic endmember of app. 1.14. The offshore SPM data largely reflect the atmospheric signal, while in the underlying sediments of the Helgoland mud hole do not. A large part of the detrital Pb with a  $^{206}\text{Pb}/^{207}\text{Pb}$  ratio of app. 1.20 is considered to be deposited in the inner German Bight, while the remaining smallest size fraction becomes enriched in atmospheric Pb.

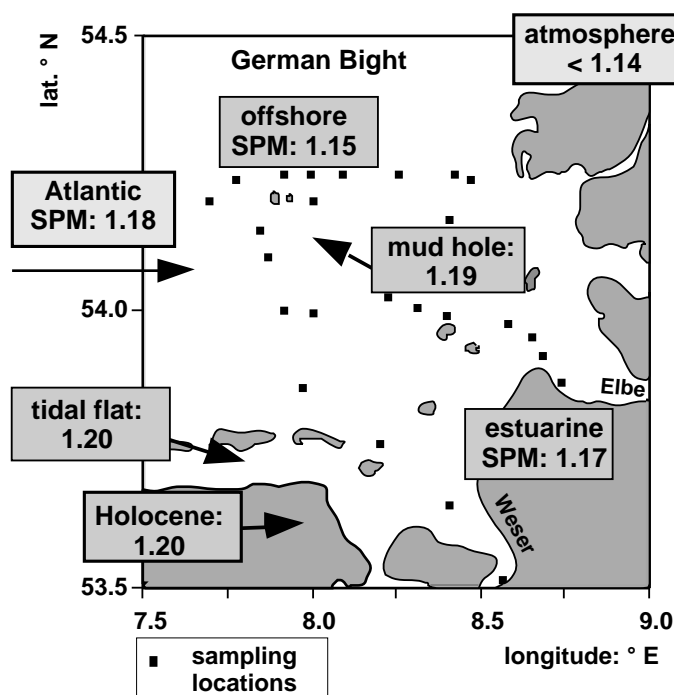


Figure 4.10: Map of the study area showing the distribution of mean  $^{206}/^{207}\text{Pb}$  ratios for sediments and suspended particulate matter.

A more detailed view is shown in Figures 4.11a and b where we plot the  $^{206}\text{Pb}/^{207}\text{Pb}$  ratios in surface water particles of two transects from the river Weser and Elbe estuary towards Helgoland Island. With increasing distance from the shore, the isotopic ratios show an almost linear decrease to values close to the anthropogenic signal. Lowest

values are found around Helgoland Island which is the most offshore location sampled in this study, and which is characterized by the smallest amounts of total and detrital SPM. The concentration of total SPM decreases from the Weser and Elbe estuaries towards Helgoland (Weser  $50 \text{ mg kg}^{-1}$ , Elbe  $11 \text{ mg kg}^{-1}$ , Helgoland  $1.4 \text{ mg kg}^{-1}$ ), as well as the amount of detrital SPM, which is reflected by the decreasing  $\text{Al}_2\text{O}_3$  contents (Weser 11.8%, Elbe 10.5%, Helgoland 3.6%).

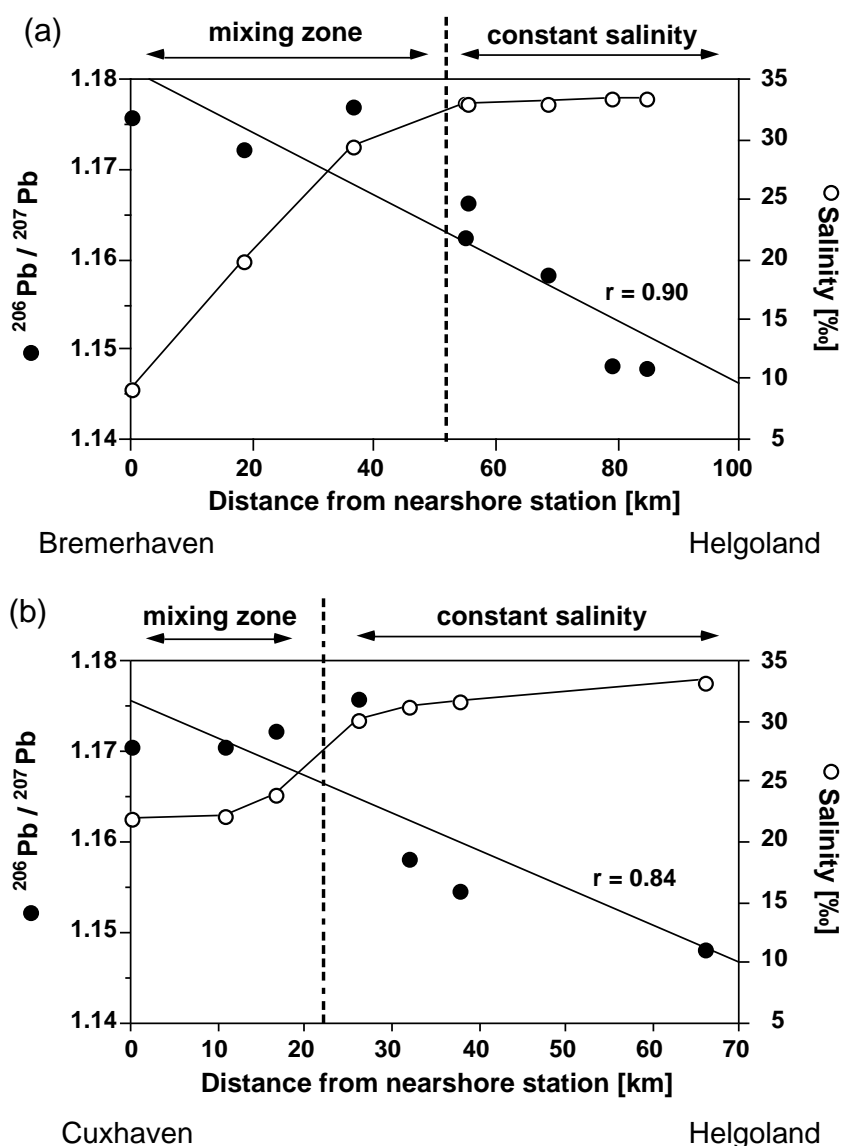


Figure 4.11:  $^{206}/^{207}\text{Pb}$  ratios and salinity data for two transects from (a) Bremerhaven (Weser estuary) and (b) Cuxhaven (Elbe estuary) to Helgoland island. Pb isotope ratios are indicated by filled circles and salinity by open circles.



Several contributions have to be considered in the interpretation of the observed  $^{206}\text{Pb}/^{207}\text{Pb}$  trends. Mixing of water masses can be traced by the salinity distribution which indicates the mixing zone of river and North Sea water. The smaller changes in salinity for the Elbe transect are due to a more seaward first sampling site of the transect. The mixing zone extends approximately half way from the coast to Helgoland Island, while the  $^{206}\text{Pb}/^{207}\text{Pb}$  ratios show a linear decrease from the shore towards Helgoland. Therefore, the Pb isotopic signal is not a simple mixing effect, as it does not parallel salinity. Additionally grain size effects have to be considered because fine grained material is expected to exhibit a largely anthropogenic Pb isotopic ratio due to the high particle reactivity of Pb together with the large surface/weight ratio and the pronounced ion exchange capacity of the fine size fraction of the SPM (Eisma, 1993). For the same reason, coarser grained material should show a largely local geogenic  $^{206}\text{Pb}/^{207}\text{Pb}$  signal. Grain size seems to be of minor importance because presumably most of the coarse grained material is deposited in the river bed itself.

Figure 4.12a shows the correlation between  $\text{Al}_2\text{O}_3$ , which represents the clay fraction, and the  $^{206}\text{Pb}/^{207}\text{Pb}$  ratio for the Weser estuary transect. The SPM of the Elbe transect is strongly influenced by material derived from the shallow area next to the islands Neuwerk and Scharhörn.

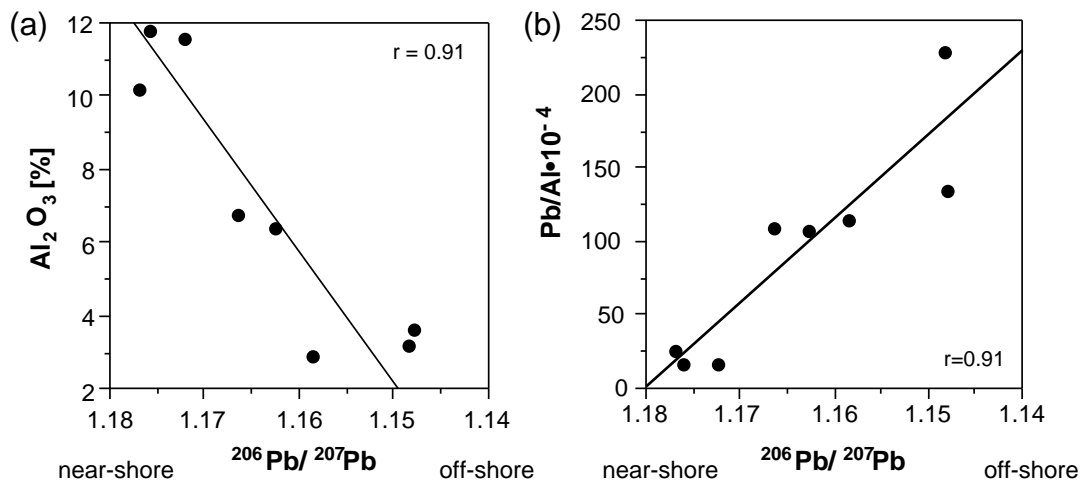


Figure 4.12: Correlations of  $\text{Al}_2\text{O}_3$  and Pb/Al ratios versus  $^{206}/^{207}\text{Pb}$  ratios for the Weser estuary.

With increasing distance from the coast a trend towards lower  $^{206}\text{Pb}/^{207}\text{Pb}$  values with decreasing amounts of clay minerals is evident. The decrease in  $\text{Al}_2\text{O}_3$  concentration is mainly caused by dilution with organic matter which dominates the SPM composition further offshore. The enhanced organic matter content in the open North Sea is related to the occurrence of an already mentioned algae bloom around Helgoland Island. As a result of this increase in biological activity predominantly dissolved Pb of atmospheric origin is incorporated into SPM. Figure 4.12b displays the Pb/Al ratio of the same transect versus the  $^{206}\text{Pb}/^{207}\text{Pb}$ -ratio, in order to eliminate dilution caused by organic matter. This scatter plot is suggestive of an uptake of Pb (increase in Pb/Al-ratio) owing to physically or biologically mediated absorption processes which were discussed for Mn in the open North Sea (see above).

The total Pb concentrations of SPM increase from the Weser estuary ( $91 \text{ mg kg}^{-1}$ ) to Helgoland ( $234 \text{ mg kg}^{-1}$ ). However, the Pb concentrations per volume unit of sea water display a reverse trend (Weser estuary  $4.5 \mu\text{g l}^{-1}$ , Helgoland  $0.3 \mu\text{g l}^{-1}$ ). Therefore it can be concluded that a large part of the heavy metal inventory remains in or close to the estuary. The  $^{206}\text{Pb}/^{207}\text{Pb}$  ratios from the Helgoland mud hole sediments are linearly related to total Pb content when normalized to Al (Figure 4.13). The sediment represents a mixture of geogenic and anthropogenically influenced material. The nearshore samples (salinity  $<30\text{‰}$ , dark grey bar) are enriched in Pb (Pb/Al range:  $8\text{--}20 \cdot 10^{-4}$ ), indicating one probable endmember for the Helgoland mud hole sediment. However, the mud hole sediments are characterised by a higher Pb isotopic ratio than the SPM. Taking into account the preferential deposition of detrital Pb with a  $^{206}\text{Pb}/^{207}\text{Pb}$  ratio of app. 1.20 in the inner German Bight, the transport of this material by bottom currents to the mud hole would explain a  $^{206}\text{Pb}/^{207}\text{Pb}$  ratio close to the geogenic signal in mud hole sediment. The offshore SPM ( $>30\text{‰}$ ) shows very high Pb/Al ratios of averaging  $95 \cdot 10^{-4}$ . For this reason only the range of the isotopic ratios is shown (light grey bar). Due to the high Pb/Al ratios the offshore SPM is unlikely to be an endmember for the mud hole sediment.

The backbarrier tidal flat sediments show  $^{206}\text{Pb}/^{207}\text{Pb}$  ratios similar to mud hole sediments. The larger scatter in the tidal flat is probably due to the feldspar and heavy

mineral content. This finding provides an additional indication for the small amount of SPM deposited in recent tidal flat sediments.

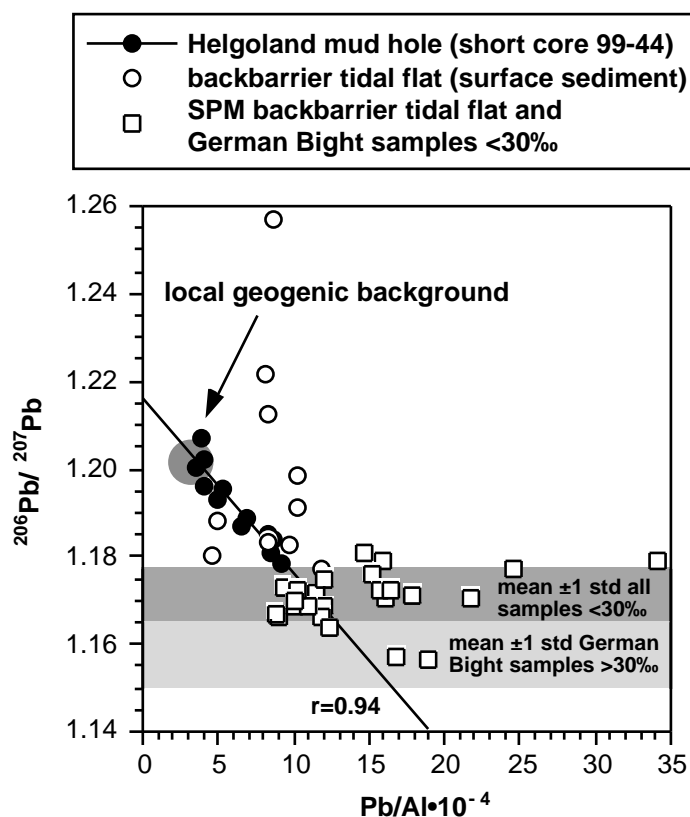


Figure 4.13: Scatter plot of  $^{206}/^{207}\text{Pb}$  vs.  $\text{Pb}/\text{Al}$  ratios for sediments (Helgoland mud hole, Spiekeroog backbarrier area) and suspended particulate matter (Spiekeroog backbarrier area, German Bight). Data points for offshore samples (salinity >30‰) are indicated by the light grey bar. Local geogenic background bases on Holocene tidal flat sediments.

### Summary and conclusions

In this study inorganic geochemical investigations of Holocene and recent tidal flat sediments as well as SPM from the NW German coastal area and the German Bight are presented. The results can be summarized as follows:

- The use of Zr and  $\text{TiO}_2$ , which occur in sediments as part of heavy minerals (e.g. zircon, ilmenite, rutile) and  $\text{Al}_2\text{O}_3$  representing clay minerals, reveals a rise in

depositional energy between Holocene and recent tidal flat sediments. On the basis of this change the recent tidal flat sediments are characterized by a significant lack of fine-grained material and higher amounts of heavy minerals, respectively. According to sedimentological investigations by Flemming and Nyandwi (1994) this phenomenon may possibly be traced back to the onset of human influence on the coastal morphology, e.g., by dike-building. The examination of SPM demonstrates that in the present situation the fine-grained material is predominantly suspended in the water column of the tidal flat area and therefore may be exported into the open North Sea.

- Regarding the contents of Ti, K, Mg, and Zr of SPM an almost shale-like composition is reflected indicating a detrital origin. However, Zr show enrichments versus average shale in the Wadden Sea reflecting an enhanced wave-energy which may cause even the suspension of heavy minerals. Although the metals Fe and Mn are considered to be involved in redox processes, only Mn is enriched in comparison to average shale accompanied by seasonal and regional variations. Winter samples from the Wadden Sea show lowest Mn enrichment in comparison to all summer samples due to more pronounced anoxic conditions during summer and enhanced mobilisation and release of Mn. A general decrease of the  $Mn_{diss}/Mn_{part}$  ratios towards the German Bight is the result of lower  $Mn_{diss}$  concentrations which are caused by oxidation and subsequent adsorption onto particles. The total Mn amount within the water column also decreases due to the settlement of particles. A vertical  $Mn_{diss}$  profile from the outer Jade Bay reveals a Mn enrichment below the photic zone similar to the Columbia River estuary (USA). This effect is most likely related to microbial activity. Thus microbially mediated redox reactions may also affect variations in SPM enrichment.
- The absolute Pb concentrations of SPM increase from the coast to the open North Sea. This finding is confirmed by the investigation of  $^{206}Pb/^{207}Pb$  ratios of SPM which show a decrease with increasing distance from the coast. This trend reflects a change from the local geogenic background to a more anthropogenic signal in the open

North Sea due to a decreasing clay content and an increasing adsorption of atmospherically transported Pb. However, the Pb concentrations per volume unit of sea water display lower Pb contents in the open North Sea. Therefore it can be concluded that a large part of the heavy metal inventory remains close to the coast. However, the uptake of Pb-rich particles by organisms should lead to an enhanced pollution of the open North Sea as well.

- In contrast the  $^{206}\text{Pb}/^{207}\text{Pb}$  ratios of the backbarrier tidal flat sediments and the Helgoland mud hole sediments are close to the geogenic background which provides an additional indication of the small amount of SPM deposited in the recent tidal flat sediments.

**Acknowledgements** - The authors wish to thank H. Streif and J. Barckhausen (Geological Survey of the Federal State of Lower Saxony, Germany) for the supply of sample material and for the lithological core descriptions. Further thanks to all personnel on board the cruises of FK Senckenberg and FS Victor Hensen as well as to R. Reuter and B. Warning. We appreciate the support of K. Bente (Institute of Crystallography/Mineralogy and Material Science Leipzig, Germany) and B. Hansen (IGDL Göttingen, Germany) who enabled the investigation of heavy mineral separates. This study was funded by: (i) the German Science Foundation (DFG) through grant No. Scho 561/2-3 and forms part of the interdisciplinary special research program "Bio-geochemical changes over the last 15,000 years - continental sediments as an expression of changing environmental conditions", (ii) the German Federal Environment Office (BMBF, grant no. 03F0112A/B) as part of the project "Ecosystem Research Lower Saxonian Wadden Sea (ÖSF)", and (iii) National Science Foundation (USA) grant OCE-9812376 to G. Klinkhammer.

## References

- Adam, P., Schmid, J.-C. and Albrecht, P. (1991) 2 $\alpha$  and 3 $\beta$  steroid thiols from reductive cleavage of macromolecular petroleum fraction. *Tetrahedron Letters* **32**, 2955-2958.
- Altschuler, Z. S., Schnepfe, M. M. Silber, C. C. and Simon, F. O. (1983) Sulphur diagenesis in Everglades peat and origin of pyrite in coal. *Science* **221**, 221-227.
- Anderson, R. F., Fleisher, M. Q. and LeHuray, A. P. (1989) Concentration, oxidation state, and particulate flux of uranium in the Black Sea. *Geochimica et Cosmochimica Acta* **53**, 2215-2224.
- Barckhausen, J., Preuss, H. and Streif, H. (1977) Ein lithologisches Ordnungsprinzip für das Küstenholozän und seine Darstellung in Form von Profiltypen. *Geologisches Jahrbuch* **A44**, 45-77.
- Barckhausen, J., Streif, H. and Vinken, R. (1979) Räumliche Erfassung von holozänen Küstenablagerungen in Niedersachsen. In DFG (Editor), *Sandbewegung im Küstenraum: Rückschau, Ergebnisse und Ausblick. Ein Abschlußbericht*, ed DFG, pp. 49-61, Boppard (Boldt).
- Barckhausen, J. and Müller, H. (1984) Ein Pollendiagramm aus der Leybucht. *Probleme der Küstenforschung im südlichen Nordseegebiet* **15**, 127-134.
- Bartenstein, H. (1938) Die Foraminiferen-Fauna des Jade-Gebietes 2 - Foraminiferen der meerischen und brackischen Bezirke des Jade-Gebietes. *Senckenbergiana maritima* **20**, 386-412.
- Baumann, M. (1991) Die Ablagerung von Tschernobyl-Radiocäsium in der Norwegischen See und in der Nordsee. *Berichte, Fachbereich Geowissenschaften, Universität Bremen* **14**, pp. 133.
- Behre, K.-E. (1978) Die Geschichte des Jadebusens und der Jade. In *Das Watt - Ablagerungs- und Lebensraum* ed H.-E. Rineck, pp. 39-49. Kramer Verlag, Frankfurt a.M.
- Behre, K.-E. (1982) Die Geschichte des Jadebusens und der Jade. In *Das Watt - Ablagerungs- und Lebensraum* ed H.-E. Rineck, pp. 39-49. Kramer Verlag, Frankfurt a.M.

- Behre, K.-E. (1993) Die nacheiszeitlichen Meeresspiegelbewegungen und ihre Auswirkungen auf die Küstenlandschaft und deren Besiedelung. In *Klimaänderung und Küste*, eds H.-J. Schellnhuber and H. Sterr, pp. 57-76. Springer, Berlin.
- Behre, K.-E. and Streif, H. (1980) Kriterien zu Meeresspiegel- und darauf bezogene Grundwasserabsenkungen. *Eiszeitalter und Gegenwart* **30**, 153-160.
- Behre, K.-E., Dörjes, J. and Irion, G. (1985) A dated Holocene sediment core from the bottom of the southern North Sea. *Eiszeitalter und Gegenwart* **35**, 9-13.
- Behrends, B. (1994) Aminosäuren und Proteine in Biodepositen einer Muschelbank. Diploma thesis, Universität Oldenburg, 88 pp.
- Behrens, I. (1996) Verteilungsmuster und molekulare Kohlenstoffisotopenzusammensetzung von Lipiden in rezenten torfbildenden Pflanzen. Diploma thesis, Fachhochschule Ostfriesland, Emden, 141 pp.
- Belyaev, S. S., Yy-Lein, A. and Ivanov, M. V. (1981) Role of methane-producing and sulphate-reducing bacteria in the destruction of organic matter. In *Biochemistry of ancient and modern environments*, eds P.A. Trudinger and M.R. Walter, pp. 235-242. Springer-Verlag, Berlin.
- Belzille, N. and Lebel, J. (1986) Capture of arsenic by pyrite in near-shore marine sediments. *Chemical Geology* **54**, 279-281.
- Bennema, J., Geue, E. C. W. A., Smits, H. and Wiggers, A. J. (1954) Soil compaction in relation to Quaternary movements of sea-level and subsidence of the land, especially in the Netherlands. *Geologie en Mijnbouw* **16**, 173-178.
- Berner, R. A. (1970) Sedimentary pyrite formation. *American Journal of Science* **268**, 1-23.
- Berner, R. A. (1980) *Early diagenesis: Atheoretical approach*. Princeton University press, Princeton, 241 pp.
- Berner, R. A. (1981) A new geochemical classification of sedimentary environments. *Journal of Sedimentary Petrology* **51**, 359-365.
- Berner, R. A. (1981) Authigenic mineral formation resulting from organic matter decomposition in modern sediments. *Fortschritte in der Mineralogie* **59(1)**, 117-135.

- Berner, R. A. (1984) Sedimentary pyrite formation: An update. *Geochimica et Cosmochimica Acta* **48**, 605-615.
- Berner, R. A. and Raiswell, R. (1984) C/S method for distinguishing freshwater from marine sedimentary rocks. *Geology* **12**, 365-368.
- Böttcher, M. E. and Huckriede, H. (1997) First occurrence and stable isotope composition of authigenic  $\text{-MnS}$  in the central Gotland Deep (Baltic Sea). *Marine Geology* **137**, 201-205.
- Böttcher, M. E., Brumsack, H.-J. and De Lange, G. J. (1998) Sulfate reduction and related stable isotope ( $^{34}\text{S}$ ,  $^{18}\text{O}$ ) variations in interstitial waters from the eastern Mediterranean (Leg 160). In *Proc. ODP Sci. Res.* ed K.-C. Emeis, A. H. F. Robertson, C. Richter and A. Camerlenghi, **160**, pp. 365-373. Ocean Drilling Program, College Station, TX.
- Boltovskoy, E. and Wright, R. (1976) *Recent Foraminifera*. Dr. W. Junk b.v. - Publishers - The Hague.
- Boynton, W.V. (1984) Geochemistry of rare earth elements: meteorite studies. In *Rare earth element geochemistry*, ed P. Henderson, pp. 63-114. Elsevier, Amsterdam,.
- Brand, G., Hageman, B. P., Jelgersma, S. and Sindowski, K. H. (1965) Die lithostratigraphische Unterteilung des marinen Holozäns an der Nordseeküste. *Geologisches Jahrbuch* **82**, 365-384.
- Bruland, K. W. (1983) Trace elements in sea-water. In *Chemical oceanography* **Vol. 8**. eds J. P. Riley and R. Chester, pp. 157-220. Academic Press, London.
- Brumsack, H.-J. (1980) Geochemistry of Cretaceous black shales from the Atlantic Ocean. *Chemical Geology* **31**, 1-25.
- Brumsack, H.-J. (1988) Rezente, Corg-reiche Sedimente als Schlüssel zum Verständnis fossiler Schwarzschiefer. Habilitation thesis, Universität Göttingen.
- Brumsack, H.-J. (1989) Geochemistry of recent TOC-rich sediments from the Gulf of California and the Black Sea. *Geologische Rundschau* **78**, 851-882.
- Brumsack, H.-J. and Gieskes, J. M. (1983) Interstitial water trace-metal chemistry of laminated sediments from the Gulf of California, Mexico. *Marine Chemistry* **14**, 89-106.



- Butler, I. B. (1995) Framboid formation. Ph.D. thesis, University of Wales. (cited after: Rickard, D. 1997 Kinetics of pyrite formation by the H<sub>2</sub>S oxidation of iron (II) monosulphide in aqueous solutions between 25 and 125°C: The rate equation. *Geochimica et Cosmochimica Acta* **61/1**, 115-134.)
- Calvert, S. E. (1990) Geochemistry and origin of the Holocene Sapropel in the Black Sea. In *Facets in modern Biogeochemistry* eds V. Ittekkot, S. Kempe, W. Michaelis, A. Spitzy, pp. 326-352. Springer, Berlin.
- Cameron, T. D. J., Stoker, M. S., and Long, D. (1987) The history of quaternary sedimentation in the UK sector of the North Sea Basin. *Journal Geological Society London* **144**, 43-58.
- Campbell, A. C., Gieskes, J. M., Lupton, J. E. and Lonsdale, P. F. (1988) Manganese Geochemistry in the Guaymas Basin, Gulf of California. *Geochimica et Cosmochimica Acta*, **52**, 345-357.
- Canfield, D. E. and Raiswell, R. (1991) Pyrite formation and fossil preservation. In *Topics in geobiology* **9**, eds P. A. Briggs and D. E. G. Allison, pp. 337-374. Plenum Press, New York.
- Canfield, D. E., Raiswell, R. and Bottrell, S. H. (1992) The reactivity of sedimentary iron minerals towards sulfide. *American Journal of Science* **292**, 659-683.
- Casagrande, D. J. and Erchull, L. D. (1976) Metals in Okefenokee peat-forming environments: relation to constituents found in coal. *Geochimica et Cosmochimica Acta* **40**, 387-393.
- Casagrande, D. J., Siefert, K., Berschinski, C. and Sutton, N. (1977) Sulfur in peat-forming systems of the Okefenokee Swamp and Florida Everglades: origin of sulfur in coal. *Geochimica et Cosmochimica Acta* **41**, 161-167.
- Chambers, L. A. and Trudinger, P. A. (1979) Microbiological fractionation of stable sulphur isotopes: A review and critique. *Geomicrobiology Journal* **1(3)**, 249-293.
- Chester, R. (1990) *Marine geochemistry*. Unwin Hyman Ltd, London, 698 pp.
- Cheshire, M. V., Berrow, M. L., Goodman, B. A. and Mundie, C. M. (1977) Metal distribution and nature of some Cu, Mn and V complexes in humic and fulvic acid fractions of soil organic matter. *Geochimica et Cosmochimica Acta* **41**, 1131-1138.

- Christanis, K., Georgakopoulos, A., Fernández-Turiel, J. L. and Bouzinos, A. (1998) Geological factors influencing the concentration of trace elements in the Philippi peatland, eastern Macedonia, Greece. *International Journal of Coal Geology* **36**, 295-313.
- Colodner, D., Sachs, J., Ravizza, G., Turekian, K., Edmond, J. and Boyle, E. (1993) The geochemical cycle of rhenium: a reconnaissance. *Earth and Planetary Science Letters* **117**, 205-221.
- Cowie, G. L. (1990) Marine organic diagenesis: A comparative study of amino acids, neutral sugars and lignin. PhD thesis, University of Washington. 193 pp.
- Cowie, G. L., Hedges, J. I. and Calvert, S. E. (1992) Sources and relative reactivities of amino acids, neutral sugars and lignin in an intermittently anoxic marine environment. *Geochimica et Cosmochimica Acta* **56**, 1963-1978.
- Crusius, J., Calvert, S., Pedersen, T. and Sage, D. (1996) Rhenium and molybdenum enrichments in sediments as indicators of oxic, suboxic, and sulfidic conditions of deposition. *Earth and Planetary Science Letters* **145**, 65-78.
- Damman, A. H. W. (1978) Distribution and movement of elements in ombrotrophic peat bogs. *Oikos*, **30**, 480-495.
- De Flaun, M. F. and Mayer, L. M. (1983) Relationships between bacteria and grain surfaces in intertidal sediments. *Limnological Oceanography* **28**, 873-881.
- Dehmer, J. (1988) Petrographische und organisch-geochemische Untersuchungen an rezenten Torfen und tertiären Braunkohlen - Ein Beitrag zur Fazies und Genese gebänderter Braunkohlen. PhD thesis, RWTH Aachen. 340 pp.
- Dellwig, O. and Brumsack, H.-J. (1999a) Inorganic geochemistry of Holocene coastal deposits from NW Germany: An overview. *Journal of Quaternary Science*. (submitted)
- Dellwig, O. and Brumsack, H.-J. (1999b) Trace metals in Holocene coastal peats (NW Germany) and their relation to pyrite formation. *Chemical Geology*. (submitted)
- Dellwig, O., Böttcher, M. E. and Brumsack, H.-J. (1996) Geochemical characterization of a Holocene sedimentary sequence from the NW German coastal area. In *Proceedings of the Fourth International Symposium on the Geochemistry of the*

- Earth's Surface*, eds S. H. Bottrell, A. C. Aplin, J. M. McArthur, R. J. Newton, M. Krom and R. Raiswell, pp. 43-46. University of Leeds.
- Dellwig, O., Gramberg, D., Vetter, D., Watermann, F., Barckhausen, J., Brumsack, H.-J., Gerdes, G., Rullkötter, J., Scholz-Böttcher, B. and Streif, H. (1998) Geochemical and microfacial characterisation of a Holocene depositional sequence of Northwest Germany. *Organic Geochemistry* **29**(5-7), 1687-1699.
- Dellwig, O., Watermann, F., Brumsack, H.-J., Gerdes, G. and Krumbein, W. E. (1999a) Pyrite used as a tool for palaeoenvironmental reconstruction of a Holocene depositional sequence from the coastlands of NW Germany. *Palaeogeography Palaeoclimatology Palaeoecology*. (submitted)
- Dellwig, O., Hinrichs, J., Hild, A., Klinkhammer, G. P., and Brumsack, H.-J. (1999b) Suspended particulate matter geochemistry of the southern North Sea: the link between Holocene and Recent tidal flat sediments. *Journal of Sea Research*. (submitted)
- Dellwig, O., Watermann, F., Brumsack, H.-J. and Gerdes, G. (1999c) High-resolution reconstruction of a Holocene coastal sequence (NW Germany) using inorganic-geochemical data and diatom inventories. *Estuarine, Coastal and Shelf Science* **48**, 617-633.
- Dill, H.G. (1998) A review of heavy minerals in clastic sediments with case studies from the alluvial-fan through the nearshore-marine environments. *Earth-Science Reviews* **45**, 103-132.
- Dominik, J., Förstner, U., Mangini, A. and Reineck, H.-E. (1978)  $^{210}\text{Pb}$  and  $^{137}\text{Cs}$  chronology of heavy metal pollution in a sediment core from the German Bight (North Sea). *Senckenbergiana maritima*, **10**, 213-227.
- Döring, T., Schwikowski, M. and Gäggeler, H. W. (1997) Determination of lead concentrations and isotope ratios in recent snow samples from high alpine sites with a double focusing ICP-MS. *Fresenius Journal of Analytical Chemistry* **359**, 382-384.
- Drebes, G. (1974) *Marines Phytoplankton*. Georg Thieme Verlag, Stuttgart. 186 pp.

- Duchesne, J. C., Rouhart, A., Schoumacher, C. and Dillen, H. (1983) Thallium, nickel, cobalt and other trace elements in iron sulfides from Belgian lead-zinc Vein deposits. *Mineralium Deposita* **18**, 303-313.
- Eary, L. E. and Rai, D. (1989) Kinetics of chromate reduction by ferrous ions. *American Journal of Science* **289**, 180-213.
- Eisma, D., 1993. *Suspended matter in the aquatic environment*. Springer-Verlag, Berlin.
- Eisma, D. and Irion, G. (1988) Suspended Matter and Sediment Transport. In *Pollution of the North Sea - An Assessment*, eds W. Salomons, B. L. Bayne, E. K. Duursma and U. Förstner, pp. 20-35. Springer-Verlag, Berlin, Heidelberg, New York.
- Eisma, D., Mook, W.G. and Laban, C. (1981) An early Holocene tidal flat in the Southern Bight. *Specific Publications of the international Association of Sedimentology* **5**, 229-237.
- Eisma, D., Jacobs, E., Berger, G. and Stolk, A. (1984) Mud-accumulation in the German Bight. In *Proceedings of a congress of the "Working group on marine sediments in relation to pollution"*. International Council for the Exploration of the Sea, Rostock Meeting.
- Elbaz-Poulichet, F., Holliger, P., Martin, J. M. and Petit, D. (1986) Stable lead isotopes ratios in major french rivers and estuaries. *The Science of the Total Environment* **54**, 61-76.
- Elderfield, H., Hepworth, A., Edwards, P. N. and Holliday, L. M. (1979) Zinc in the Conwy River and estuary. *Estuarine, Coastal Shelf Science* **9**, 403-422.
- Engleman, E. E., Jackson, L. L. and Norton, D. R. (1985) Determination of carbonate carbon in geological materials by coulometric titration. *Chemical Geology* **53**, 125-128.
- Erel, Y., Véron, A. and Halicz, L. (1997) Tracing the transport of anthropogenic lead in the atmosphere and in soils using isotopic ratios. *Geochimica et Cosmochimica Acta* **61**, 4495-4505.
- Ferdelman, T. G., Church, T. M. and Luther, G. W. III. (1991) Sulfur enrichment of humic substances in a Delaware salt marsh core. *Geochimica et Cosmochimica Acta* **55**, 979-988.

- Feyling-Hansen, R. W. (1972) The foraminifer *Elphidium excavatum* (Terquem) and its variant forms. *Micropaleontology* **18**, 337-354.
- Flemming, B. W. and Davis, R. A. (1994) Holocene evolution, morphodynamics and sedimentology of the Spiekeroog barrier island system (Southern North Sea). *Senckenbergiana maritima*, **24**, 117-155.
- Flemming, B.W. and Nyandwi, N. (1994) Land reclamation as a cause of fine grained sediment depletion in backbarrier tidal flats (Southern North Sea). *Netherlands Journal of Aquatic Ecology* **28**, 299-307.
- Förstner, U. and Reineck, H.-E. (1974) Die Anreicherung von Spurenelementen in den rezenten Sedimenten eines Profilkernes aus der Deutschen Bucht. *Senckenbergiana maritima* **6**, 175-184.
- Förstner, U. and Wittmann, G. T. U. (1979) *Metal pollution in the aquatic environment*. Springer, Berlin, 486 pp.
- Framson, P. E. and Leckie, J. D. (1978) Limits of coprecipitation of Cadmium and ferrous sulfides. *Environmental Science and Technology* **12**, 1075-1090.
- Francois, R. (1987) A study of sulphur enrichment in the humic fraction of marine sediments during early diagenesis. *Geochimica et Cosmochimica Acta* **51**, 17-27.
- Froelich, P. N., Klinkhammer, G. P., Bender, M. L., Luedtke, N. A., Heath, G. R., Cullin, D., Dauphin, P., Hammond, D., Hartman, B. and Maynard, V. (1979) Early oxidation of organic matter in pelagic sediments of the eastern equatorial Atlantic: suboxic diagenesis. *Geochimica et Cosmochimica Acta* **43**, 1075-1090.
- Gadow, S. and Schäfer, A. (1973) Die Sedimente der Deutschen Bucht: Korngrößen, Tonminerale und Schwermetalle. *Senckenbergiana maritima* **5**, 165-178.
- Geyh, M. A. (1971) *Die Anwendung der <sup>14</sup>C-Methode*. Clausthaler tektonische Hefte 11. Clausthal-Zellerfeld, 118 pp.
- Giblin, A. E. (1988) Pyrite formation in marshes during early diagenesis. *Geomicrobiology Journal* **6**, 77-97.
- Giblin, A. E., and Howarth, R. W. (1984) Porewater evidence for a dynamic sedimentary iron cycle in salt marshes. *Limnology and Oceanography* **29**, 47-63.

- Given, P. H. and Miller, R. N. (1985) Distribution of forms of sulfur in peats from saline environments in the Florida Everglades. *International Journal of Coal Geology* **5**, 397-409.
- Goldberg, E. D. (1987) Comparative chemistry of the platinum and other heavy metals in the marine environment. *Pure and Applied Chemistry* **59(4)**, 565-571.
- Goldhaber, M. B. and Kaplan, I. R. (1974) The sulphur cycle. In *The sea* **5**, ed E. D. Goldberg, pp. 895. Wiley, New York.
- Göttlich, K. (1990) *Moor-und Torfkunde*. E. Schweizerbart'sche Verlagsbuchhandlung, Stuttgart, 529 pp.
- Gramberg, D., Scholz-Böttcher, B. M. and Rullkötter, J. (1995) Column chromatographic separation and characterization of a complex mixture of heterocompounds in the extractable lipids of a phragmites peat. In *Organic Geochemistry: Developments and Applications to Energy, Climate, Environment and Human History*, eds. J. O. Grimalt and C. Dorronsoro, pp. 174-176. A.I.G.O.A., San Sebastian.
- Grosse-Brauckmann, G. (1962) Zur Moorgliederung und Ansprache. *Zeitschrift für Kulturtechnik* **3**, 6-29.
- Gunkel, W. and Klings, K. W. (1989) Mikrobiologische Langzeituntersuchungen bei Helgoland. *Jahresbericht 1988, Biologische Anstalt Helgoland*, 65-70.
- Hagemann, B. P. (1969) Development of the western part of the Netherlands during the Holocene. *Geologie en Mijnbouw* **48**, 373-388.
- Hansen, H. J. and Lykke-Anderson, A. L. (1976) Wall structure and classification of fossil and recent elphidiid and nonionid Foraminifera. *Fossils and Strata* **10**, 1-37.
- Hartley, B. B., Barber, H. G., Carter, J. R. (1996) *An atlas of British diatoms*. Biopress Limited, Bristol, pp. 601.
- Hartung, W. (1967) Das Gebiet zwischen Jade und Weser im Wandel der jüngsten Erdgeschichte. *Die Weser* **41**, 2-5.
- Heinrichs, H. (1993) Die Wirkung von Aerosolkomponenten auf Böden und Gewässer industrieferner Standorte: eine geochemische Bilanzierung. Habilitation thesis, Universität Göttingen, Germany.

- Heinrichs, H. and Herrmann, A. G. (1990) *Praktikum der Analytischen Geochemie*. Springer Verlag, Berlin, pp. 669.
- Heinrichs, H., Brumsack, H.-J., Loftfield, N. and König, N. (1986) Verbessertes Druckaufschlußsystem für biologische und anorganische Materialien. *Zeitschrift für Pflanzenernährung und Bodenkunde* **149**, 350-353.
- Helz, G. R., Miller, C. V., Charnock, J. M., Mosselmans, J. F. W., Patrick, R. A. D., Garner, C. D. and Vaughan, D. J. (1996) Mechanism of molybdenum removal from the sea and its concentration in black shales: EXAFS evidence. *Geochimica et Cosmochimica Acta* **60**, 3631-3642.
- Hild, A. (1997) Geochemie der Sedimente und Schwebstoffe im Rückseitenwatt von Spiekeroog und ihre Beeinflussung durch biologische Aktivität. *Forschungszentrum Terramare Berichte* **5**, 1-33.
- Hölemann, J. and Wirth, H. (1988) Concentration, Major Element Ratios and Scanning Electron Microscopy of Suspended Particulate Matter from the North Sea, Spring 1986. *Mitteilungen des Geologisch-Paläontologischen Instituts der Universität Hamburg* **65**, 183-206.
- Hofker, J. (1977) The Foraminifera of dutch tidal flats and salt marshes. *Netherlands Journal of Sea Research* **11**, 223-296.
- Holdren, G. R. (1977) Distribution and behavior of manganese in the interstitial waters of Chesapeake Bay sediments during early diagenesis. Ph.D. Thesis, University of Baltimore, 190 p. (cited after: Berner, R. A. (1980) *Early diagenesis. A theoretical approach*. Princeton University Press, Princeton, New Jersey, pp. 241.)
- Holleman, A. F. 1985. *Lehrbuch der anorganischen Chemie / Holleman-Wiberg*. Walter de Gruyter, Berlin, New York, 1451 pp.
- Holliday, L. M. and Liss, P. S. (1976) The behavior of dissolved iron, manganese and zinc in the Beaulieu Estuary. *Estuarine, Coastal and Shelf Science* **4**, 349-353.
- Hoselmann, C. and Streif, H. (1997) Bilanzierung der holozänen Sedimentakkumulation im niedersächsischen Küstenraum. *Zeitschrift der Deutschen Geologischen Gesellschaft* **148(3-4)**, 431-445.
- Howarth, R.W. (1979) Pyrite: Its rapid formation in a salt marsh and its importance in ecosystem metabolism. *Science* **203**, 49-51.

- Howarth, R. W. and Giblin, A. E. (1983) Sulphate reduction in the salt marshes at Sapelo. *Limnology and Oceanography* **28**, 70-82.
- Howarth, R. W. and Teal, J. M. (1979) Sulphate reduction in a New England salt marsh. *Limnology and Oceanography* **24**(6), 999-1013.
- Huang, W.-Y. and Meinschein, W. G. (1979) Sterols as ecological indicators. *Geochimica and Cosmochimica Acta* **41**, 739-745.
- Huerta-Diaz, M. A. and Morse, J. W. (1990) A quantitative method for determination of trace metal concentrations in sedimentary pyrite. *Marine Chemistry* **29**, 119-144.
- Huerta-Diaz, M. A. and Morse, J. W. (1992) Pyritization of trace metals in anoxic marine sediments. *Geochimica et Cosmochimica Acta* **56**, 2681-2702.
- Huffman, E. W. D. jun. (1977) Performance of a new automatic carbon dioxide coulometer. *Microchemical Journal* **22**, 567-573.
- Hustedt, F. (1930) *Die Kieselalgen*. Otto Koeltz Science Publishers. Vol. I, 920 pp., Vol. II, 845 pp., Vol. III, 816 pp.
- Hustedt, F. (1957) *Die Diatomeenflora des Flußsystems der Weser im Gebiet der Hansestadt Bremen*. Otto Koeltz Science Publishers, 441 pp.
- Injuk, J., Otten, P., Laane, R., Maenhaut, W. and van Grieken, R. (1992) Atmospheric concentrations and size distributions of aircraft-sampled Cd, Cu, Pb, and Zn over the Southern Bight of the North Sea. *Atmospheric Environment* **26A**, 2499-2508.
- Irion, G. (1994) Morphological, sedimentological and historical evolution of Jade bay, southern North sea. *Senckenbergiana maritima* **24**, 171-186.
- Irion, G. and Müller, G. (1990) Lateral distribution and sources of sediment-associated heavy metals in the North Sea. In *Facets of Modern Biogeochemistry*, eds V. Ittekkot, S. Kempe, W. Michaelis and A. Spitzy, pp. 175-201. Springer-Verlag, Berlin.
- De Jonge, V. N. (1984) The occurrence of epipsammic diatom populations: A result of interaction between physical sorting of sediment and certain properties of diatom species. *Estuarine, Coastal and Shelf Science* **21**, 607-622.
- Jöreskog, K. G., Klován, J. E. and Reymont, R. A. (1976) Geological Factor Analysis. *Methods in Geomathematics* **1**. Elsevier, Amsterdam, 178 pp.



- Jørgensen, B. B. (1979) A theoretical model of the stable sulfur isotope distribution in marine sediments. *Geochimica et Cosmochimica Acta* **43**, 363-374.
- Kersten, M., Förstner, U., Krause, P., Kriews, M., Dannecker, W., Garbe-Schönberg, C.-D., Höck, M., Terzenbach, U. and Graßl, H. (1992) Pollution source reconnaissance using stable lead isotope ratios ( $^{206}/^{207}\text{Pb}$ ). In *Impact of heavy metals on the environment*, ed J.-P. Vernet (Editor), pp. 311-325. Elsevier, Amsterdam.
- King, G. M., Howes, B. L. and Dacey, J. W. H. (1985) Short term endproducts of sulphate reduction in salt marsh sediments Significance of acid volatile sulfides, elemental sulphur, and pyrite. *Geochimica et Cosmochimica Acta* **49**, 1561-1566.
- Kirby, R. (1987) Sediment exchanges across the coastal margins of NW Europe. *Journal of the Geological Society of London* **144**, 121-126.
- Klinkhammer, G. (1994) Fiber optic spectrometers for *in situ* measurements in the oceans: The ZAPS probe. *Marine Chemistry* **47**, 13-20.
- Klinkhammer, G. P. and Palmer, M. R. (1991) Uranium in the oceans: Where it goes and why. *Geochimica et Cosmochimica Acta* **55**, 1799-1806.
- Klinkhammer, G. and McManus, J. (1999) Dissolved manganese and the turbidity maximum: High-resolution data from the Columbia River estuary. *Global Biogeochemical Cycles*. (submitted)
- Knox, S., Turner, D. E., Dickson, A. G., Liddicoat, M. I., Whitfield, M. and Butler, E.I. (1981) Statistical analysis of estuarine profiles: application to manganese and ammonium in the Tamar estuary. *Estuarine, Coastal Shelf Science* **13**, 357-371.
- Koopmann, C. F., J.; van Bernem, K.-H.; Prange, A. and Müller, A. (1993) *Schadstoffkartierung in Sedimenten des deutschen Wattenmeeres- Juni 1989-Juni 1992*. Abschlußbericht Jan. 1993, UBA-FuE-Vorhaben 10903377, 164 pp.
- Krammer K. (1986) *Kieselalgen: Biologie, Baupläne der Zellwand*. Kosmos Handbücher, Stuttgart. 139 pp.
- Kremling, K. (1985) The distribution of cadmium, copper, nickel, manganese, and aluminium in surface waters of the open Atlantic and European shelf area. *Deep-Sea Research* **32** (5), 531-555.

- Langmuir, D. (1978) Uranium solution-mineral equilibria at low temperatures with applications to sedimentary ore deposits. *Geochimica et Cosmochimica Acta* **42**, 547-569.
- Leventhal, J. and Taylor, C. (1990) Comparison of methods to determine degree of pyritization. *Geochimica et Cosmochimica Acta* **54**, 2621-2625.
- Linke, G. (1979) Ergebnisse geologischer Untersuchungen im Küstengebiet südlich Cuxhaven. *Probleme der Küstenforschung im südlichen Nordseegebiet* **11**, 119-143.
- Linke, G. (1982) Der Ablauf der holozänen Transgression der Nordsee aufgrund von Ergebnissen aus dem Gebiet Neuwerk/Scharhörn. *Probleme der Küstenforschung im südlichen Nordseegebiet* **14**, 123-157.
- Lipinski, M., 1999, Nährstoffelemente und Spurenmetalle in Wasserproben von Hunte und Jade. Diploma thesis, Universität Oldenburg, 77 pp.
- Loeblich, A.R. and Tappan, H. (1988) *Foraminiferal Genera and their Classification*. Van Nostrand Reinold, New York.
- Long, D., Laban, C., Streif, H., Cameron, T. D. J. and Schuettenhelm, R. T. E. (1988) The sedimentary record of climatic variation in the Southern North Sea. *Philosophical Transactions of the Royal Society of London* **B318**, 523-537.
- Lord, C. J. (1980) The chemistry and cycling of iron, manganese, and sulfur in salt marsh sediments. Ph.D. thesis, University of Delaware, USA. (cited after Lord, C. J. and Church, T. M. 1983 The geochemistry of salt marshes: sedimentary ion diffusion, sulfate reduction, and pyritization. *Geochimica et Cosmochimica Acta* **47**, 1381-1391.)
- Lord, C. J. and Church, T. M. (1983) The geochemistry of salt marshes: sedimentary ion diffusion, sulphate reduction, and pyritization. *Geochimica et Cosmochimica Acta* **47**, 1381-1391.
- Lovley, D. R. (1993) Dissimilatory metal reduction. *Annual Reviews in Microbiology* **47**, 263-290.

- Lovley, D. R., Roden, E. E., Phillips, E. J. P. and Woodward, J. C. (1993) Enzymatic iron and uranium reduction by sulfate-reducing bacteria. *Marine Geology* **113**, 41-53.
- Lozán, J. L., Rachor, E., Reise, K., v. Westernhagen, H., and Lenz, W. (1994) *Warnsignale aus dem Wattenmeer*. Blackwell Wissenschaftsverlag, Berlin.
- Ludwig, G., Müller, H. and Streif, H. (1979) Neuere Daten zum holozänen Meeresspiegelanstieg im Bereich der Deutschen Bucht. *Geologisches Jahrbuch* **D32**, 3-22.
- Ludwig, G., Barckhausen, J. and Streif, H. (1973) Geochemische Untersuchungen über Palaeosalinität und Ablagerungsraum holozäner Küstensedimente Ostfrieslands. *Geologisches Jahrbuch* **D3**, 35-54.
- Lund, J. W. G., Kipling, C. and Le Cren, E. D. (1958) The inverted microscope method of estimating algal numbers and the statistical basis of estimations by counting. *Hydrobiologica* **11**, 143-170.
- Luther, G. W. III. (1991) Pyrite synthesis via polysulfide compounds. *Geochimica et Cosmochimica Acta* **55**, 2839-2849.
- Luther, G. W. III., Giblin, A. E., Howarth, R. W. and Ryans, R. A. (1982) Pyrite oxidation in marsh sediments. *Geochimica et Cosmochimica Acta* **46**, 2665-2670.
- Martin, J. M. and Whitfield, M. (1983) The significance of the river input of chemical elements to the ocean. In *Trace metals in sea water*, eds C. S. Wong, E. Boyle, K. W. Bruland, J. D. Burton and E. D. Goldberg, pp. 265-296. Plenum, New York.
- McCaffrey, R. J., Myers, A. C., Davey, E., Morrison, G., Bender, M., Leudtke, N., Cullen, D., Froelich, P. and Klinkhammer, G. P. (1980) The relation between pore water chemistry and benthic fluxes of nutrients and manganese in Narragansett Bay, Rhode Island. *Limnological Oceanography* **25**, 31-44.
- Menke, B. (1976) Befunde und Überlegungen zum nacheiszeitlichen Meeresspiegelanstieg. *Probleme der Küstenforschung im südlichen Nordseegebiet* **11**, 145-161.
- Merkt, J. and Streif, H. (1970) Stechrohr-Bohrgeräte für limnische und marine Lockersedimente. *Geologisches Jahrbuch* **88**, 137-148.

- Meyers, P. A. and Ishiwatari, R. (1993) Lacustrine organic geochemistry - an overview of indicators of organic matter sources and diagenesis in lake sediments. *Organic Geochemistry* **20**, 867-900.
- Miller, A.A.L., Scott, D.B. and Medioli, F.S. (1982) *Elphidium excavatum* (Terquem): ecophenotypic versus subspecific variation. *Journal of Foraminiferal Research* **12**, 116-144.
- Moore, J. W. and McIntire, C. D. (1977) Spatial and seasonal distribution of littoral diatoms in Yaquina estuary, Oregon. *Botanica Marina* **20**, 99-109.
- Morris, A. W., Bale, A. J. and Howland, R. J. M. (1982) The dynamics of estuarine manganese cycling. *Estuarine, Coastal and Shelf Science* **14**, 175-192.
- Morse, J. W. and Cornwell, J. C. (1987) Analysis and distribution of iron sulfide minerals in recent anoxic marine sediments. *Marine Chemistry* **22**, 55-69.
- Müller, W. (1977) Geologie. Exkursion A (=E) Wesermarsch. *Mitteilungen der Deutschen Bodenkundlichen Gesellschaft Bremen* **24**, 15-29.
- Murray, J.W. (1979) *British Nearshore Foraminiferids*. Synopsis of the British Fauna No. 16, The Linnean Society of London.
- Murray, J. W., Grundmanis, V. and Smethie, W. M. (1978) Interstitial water chemistry in the sediments of Saanich Inlet. *Geochimica et Cosmochimica Acta* **42**, 1011-1026.
- Nathan, Y. (1984) The mineralogy and geochemistry of phosphorites. In *Phosphate minerals* eds J. O. Nriagu and P. B. Moore, pp. 275-291. Springer-Verlag, Berlin.
- Naucke, W. (1979) Untersuchung niedersächsischer Torfe zur Bewertung ihrer Eignung für die Moorthherapie, I. Zur stofflichen Zusammensetzung moorfrischer Badetorfe *Telma* **9**, 251-274.
- Naucke, W. (1990) Chemie von Moor und Torf. In *Moor- und Torfkunde*, ed K. Göttlich, pp. 237-259. Schweizerbart'sche Verlagsbuchhandlung, Stuttgart.
- Nelson, A. R. and Kashima, K. (1993) Diatom zonation in southern Oregon tidal marshes relative to vascular plants, foraminifera and sea-level. *Journal of Coastal Research* **9**, 673-697.

- Overbeck, F. (1975) *Botanisch-geologische Moorkunde unter besonderer Berücksichtigung der Moore Nordwestdeutschlands als Quellen zur Vegetations-, Klima- und Siedlungs-geschichte*. Wachholtz, Neumünster. 719 pp.
- O'Brien, S. R., Mayewski, P. A., Meeker, L. D., Meese, D. A., Twickler, M. S. and Whitlow, S. I. (1995) Complexity of Holocene climate as reconstructed from a Greenland ice core. *Science* **270**, 1962-1964.
- Palmer, A. J. M. and Clague, J. J. (1986) Diatom assemblage analysis and sea level change. In *Sea-Level Research - A Manual for the Collection and Evaluation of Data*, ed O. van de Plassche, pp. 457-487. Geo Books, Norwich.
- Pankow, H. (1990) *Ostsee-Algenflora*. Gustav Fischer Verlag, Jena. 648 pp.
- Pant, P. and Rastogi, R. P. (1979) The triterpenoids. *Phytochemistry* **18**, 1095-1108.
- Passier, H. F., Middelburg, J. J., de Lange, G. J. and Böttcher, M. E. (1997) Pyrite contents, microtextures, and sulphur isotopes in relation to formation of the youngest eastern Mediterranean sapropel. *Geology* **25**, 519-522.
- Peterson, M. L. and Carpenter, R. (1986) Arsenic distributions in porewaters and sediments in Puget Sound, Lake Washington, the Washington coast and Saanich Inlet, B.C. *Geochimica et Cosmochimica Acta* **50**, 353-369.
- Pettersson, C., Allard, B. and Boren (1997) River discharge of humic substances and humic-bound metals to the Gulf of Bothnia. *Estuarine, Coastal and Shelf Science* **44**, 533-541.
- Petzelberger, B. E. M. (1997) Geologische Untersuchungen zur Landschaftsgeschichte des jüngeren Holozäns in der ehemaligen Crildumer Bucht im Wangerland, Ldkr. Friesland. *Probleme der Küstenforschung im südlichen Nordseegebiet* **24**, 301-309.
- Pientz, R., Lortie, G. and Allard, M. 1991 Isolation of lacustrine basins and marine regression in the Kuujuaq area, Northern Quebec, as inferred from diatom analysis. *Geography and physics of the Quarternary* **45**, 155-174.
- Pingitore, N. E. and Eastman, M. E. (1985) Barium partitioning during the transformation of corals from aragonite to calcite. *Chemical Geology* **48**, 183-187.
- Postma, D. (1982) Pyrite and siderite formation in brackish and freshwater swamp sediments. *American Journal of Science* **282**, 1151-1183.

- Postma, H. (1967) Sediment transport and sedimentation in the estuarine environment. In *Estuaries*, ed G. H. Lauff, pp. 158-159. American Association of Advanced Science.
- Postma, H. (1981) Exchange of materials between the North Sea and the Wadden Sea. *Marine Geology* **40**, 199-213.
- Preuß, H. (1979) Die holozäne Entwicklung der Nordseeküste im Gebiet der östlichen Wesermarsch. *Geologisches Jahrbuch A* **53**, 3-84.
- Price, F. T. and Casagrande, D. J. (1991) Sulfur distribution and isotopic composition in peats from the Okefenokee Swamp, Georgia and the Everglades, Florida. *International Journal of Coal Geology* **17**, 1-20.
- Puls, W., Heinrichs, H. and Mayer, B. (1997) Suspended particulate matter budget for the German Bight. *Marine Pollution Bulletin* **34(6)**: 398-409.
- Radach, G., Schönfeld, W. and Lenhart, H. (1990) Nährstoffe in der Nordsee - Eutrophierung, Hypertrophierung und deren Auswirkungen. In *Warnsignale aus der Nordsee*, eds J. L. Lozán, W. Lenz, W. Rachor, B. Watermann, and H. von Westernhagen, H., pp. 48-65. Verlag Paul Parey, Berlin.
- Radke, M., Willsch, H. and Welte, D. H. (1980) Preparative hydrocarbon group type determination by automated medium pressure liquid chromatography. *Analytical Chemistry* **52**, 406-411.
- Raiswell, R. (1982) Pyrite texture, isotopic composition and the availability of iron. *American Journal of Science* **282**, 1244-1263.
- Raiswell, R. and Plant, J. (1980) The incorporation of trace elements into pyrite during diagenesis of Black Shales, Yorkshire, England. *Economic Geology* **75**, 684-699.
- Raiswell, R., Buckley, F., Berner, R. A. and Anderson, T. F. (1988) Degree of pyritization of iron as a paleoenvironmental indicator of bottom-water oxygenation. *Journal of Sedimentary Petrology* **58(5)**, 812-819.
- Ramdohr, P. and Strunz, H. (1978) *Klockmanns Lehrbuch der Mineralogie*. Enke Verlag, Stuttgart, 876 pp.
- Recke, M. and Förstner, U. (1988) Geochemical investigations on heavy metals in anoxic and oxic sediments from the North Sea and the East Frisian Wadden Sea.

- Mitteilungen des Geologisch-Paläontologischen Instituts der Universität Hamburg*, **65**, 313-344.
- Reed, D. J. (1995) The response of coastal marshes to sea-level rise: Survival or submergence?. *Earth Surface Processes and Landforms* **20**, 39-48.
- Richter, G. (1964) Zur Ökologie der Foraminiferen I. Die Foraminiferen-Gesellschaften des Jade-Gebietes. *Natur und Museum* **94**, 343-353.
- Rickard, D.T. (1975) Kinetics and mechanism of pyrite formation at low temperatures. *American Journal of Science* **275**, 636-652.
- Rickard, D. (1997) Kinetics of pyrite formation by the H<sub>2</sub>S oxidation of iron (II) monosulphide in aqueous solutions between 25 and 125°C: The rate equation. *Geochimica et Cosmochimica Acta* **61**, 115-134.
- Ries-Kautt, M. and Albrecht, P. (1989) Hopane-derived triterpenoids in soils. *Chemical Geology* **76**, 143-151.
- Round, F. E., Crawford, R. M., and Mann, D. G. (1990) *The Diatoms*. Cambridge University Press, Cambridge. 747 pp.
- Salomons, W. (1975) Chemical and isotopic composition of carbonates in recent sediments and soils from western Europe. *Journal of Sedimentary Petrology* **45**, 440-449.
- Sawlowicz, Z. (1993) Pyrite formation and their development: a new conceptual mechanism. *Geologische Rundschau* **82**, 148-156.
- Schallreuter, R. (1984) Framboidal pyrite in deep-sea sediments. *Initial Reports of the Deep Sea Drilling Project* **75**, 875-891.
- Scheer, K. (1953) Die Bedeutung von *Phragmites communis* Trin. für die Fragen der Küstenbildung. *Probleme der Küstenforschung im südlichen Nordseegebiet* **5**, 15-25.
- Scheffer, F. and Schachtschabel, P. (1992) *Lehrbuch der Bodenkunde*. Enke, Stuttgart, 491 pp.
- Schlegel, H.G. (1992) *Allgemeine Mikrobiologie*. Georg Thieme Verlag, Stuttgart, 634 pp.
- Schnetger, B. (1992) Chemical composition of loess from a local and worldwide view. *Neues Jahrbuch der Mineralogischen Abhandlungen, Monatshefte* **H1**, 29-47.

- Schnetger, B. (1997) Trace element analysis of sediments by HR-ICP-MS using low and medium resolution and different acid digestions. *Fresenius Journal of Analytical Chemistry* **359**, 468-472.
- Schrader, H. J. (1973) Proposal for a standardized method of cleaning diatom-bearing deep-sea and land-exposed marine sediments. *Nova Hedwigia Beihefte* **45**, 403-409.
- Schrader, H. J. and Gersonde, R. (1978) Diatoms and Silicoflagellates. In *Micropaleontological counting methods and techniques- an exercise on an eight metres section of the lower Pliocene of Capo Rossello, Sicily*, eds Zachariasee et al., pp. 129-176. *Micropaleontological Bulletin* **17**, Utrecht.
- Schröder, C.J., Scott, D.B. and Medioli, F.S. (1987) Can smaller benthic foraminifera be ignored in paleoenvironmental analyses?. *Journal of Foraminifera Research* **17**, 101-105
- Schwedhelm, E. and Irion, G. (1985) Schwermetalle und Nährelemente in den Sedimenten der deutschen Nordseewatten. *Courier des Forschungs-Instituts Senckenberg* **73**, 1-119.
- Shiller, A.M. (1997) Manganese in surface waters of the Atlantic Ocean. *Geophysical Research Letters* **24(12)**, 1495-1498.
- Shotyk, W. (1988) Review of the inorganic geochemistry of peats and peatland waters. *Earth-Science Reviews* **25**, 95-176.
- Shotyk, W. (1997) Atmospheric deposition and mass balance of major and trace elements in two oceanic peat bog profiles, northern Scotland and the Shetland Islands. *Chemical Geology* **138**, 55-72.
- Sillanpää, M. (1972) Distribution of trace elements in peat profiles. *Proceedings of the 4th International Peat Congress, Offsetpains, Helsinki*, **Vol. 5**, 185-191.
- Simonsen, R. (1962) *Untersuchungen zur Systematik und Ökologie der Bodendiatomeen der westlichen Ostsee*. Akademie-Verlag, Berlin. 147 pp.
- Sindowski, K.-H. and Streif, H. (1974) Die Geschichte der Nordsee am Ende der letzten Eiszeit und im Holozän. In *Norddeutschland und angrenzende Gebiete im Eiszeitalter*, eds P. Woldstedt and K. Duphorn, pp. 411-431. Köhler, Stuttgart,.



- Smillie, R.H., Hunter, K. and Loutit, M. (1981) Reduction of chromium(VI) by bacterially produced hydrogen sulphide in a marine environment. *Water Research* **15**, 1351-1354.
- Spurr, A. R. (1969) A Low-Viscosity Epoxy Resin Embedding Medium for Electron Microscopy. *Journal of Ultrastructure Research* **26**, 31-43.
- Streif, H. (1971) Stratigraphie und Faziesentwicklung im Küstengebiet von Woltzeten in Ostfriesland. *Beihefte zum Geologischen Jahrbuch* **119**, 1-61.
- Streif, H. (1986) Zur Altersstellung und Entwicklung der Ostfriesischen Inseln. *Offa* **43**, 29-44.
- Streif, H. (1990) Das ostfriesische Küstengebiet. Nordsee, Inseln, Watten und Marschen. *Sammlung Geologischer Führer* **57**, 2nd edition. Gebrüder Borntraeger, Stuttgart. 376 pp.
- Streif, H. (1993) Zum Ausmaß und Ablauf eustatischer Meeresspiegelschwankungen im südlichen Nordseegebiet seit Beginn des letzten Interglazials. In *Klimaänderung und Küste*, eds. H.- J. Schellnhuber and H. Sterr, pp. 231-249. Springer, Berlin.
- Streif, H. and Köster, R. (1978) Zur Geologie der deutschen Nordseeküste. *Die Küste* **32**, 30-49.
- Stuiver, M. and Reimer, P. J. (1993) Extended  $^{14}\text{C}$  database and revised CALIB 3.0  $^{14}\text{C}$  age calibration program. *Radiocarbon* **35**, 215-230.
- Suess, E., (1979) Mineral phases formed in anoxic sediments by microbial decomposition of organic matter. *Geochimica et Cosmochimica Acta* **43**, 339-352.
- Sutherland, D. G. (1985) Geomorphological controls on the distribution of placer deposits. *Journal of the Geological Society of London* **142**, 727-737.
- Sweeny, R. E. and Kaplan, I. R. (1973) Pyrite framboidal formation: Laboratory synthesis and marine sediments. *Economic Geology* **68**, 618-634.
- Szalay, A. and Szilágyi, M. (1967) The association of vanadium with humic acids. *Geochimica et Cosmochimica Acta* **31**, 1-6.
- Tappin, A. D., Millward, G. E., Statham, P. J., Burton, J. D. and Morris, A. W. (1995) Trace Metals in the Central and Southern North Sea. *Estuarine, Coastal and Shelf Science* **41**, 275-323.

- Trendel, J. M., Lohmann, F., Kintzinger, J. P. and Albrecht, P. (1989). Identification of des-A-triterpenoid hydrocarbons occurring in surface sediments. *Tetrahedron* **45**, 4457-4470.
- Utermöhl, H. (1958) Zur Vervollkommnung der quantitativen Phytoplanktonmethodik. *Mitteilungen der Internationalen Vereinigung der Limnologen* **9**, 1-38.
- van der Woude, J. D. (1981) Holocene palaeoenvironmental evolution of a perimarine fluvial area. Acad. Proefschr. Amsterdam, 112 pp. (Cited after: Reineck, H.-F. (1984) *Aktuo-Geologie klastischer Sedimente*. Senckenberg-Buch 61, Frankfurt a. M., 348 pp.)
- van Straaten, L. M. J. U. (1954) Composition and structure of recent marine sediments in the Netherlands. *Leidse Geologische Mededelingen* **19**, 1-110.
- van Voorthuysen, J.H. (1960) Die Foraminiferen des Dollart-Ems-Estuariums. In *Das Ems-Estuarium (Nordsee)*, Verh. Kon. Ned. Geol. Mijnb. k. Gen. Geol. Serie D1 19, 237-269.
- Véron, A. J., Church, T. M., Patterson, C. C. and Flegal, A. R. (1994) Use of stable lead isotopes to characterize the sources of anthropogenic lead in North Atlantic surface waters. *Geochimica et Cosmochimica Acta* **58**, 3199-3206.
- Vetter, D. and Liebezeit, G. (1996) Rekonstruktion des Kuestenholozäns mit geochemischen Methoden - Erste Ergebnisse der Porenwasseruntersuchungen. *Zentralblatt für Geologie und Paläontologie* **H1/2**, 375-386.
- Viers, J., Dupre, B., Polve, M., Schott, J. Dandurand, J.-L. and Braun, J.-J. (1997) Chemical weathering in the drainage basin of a tropical watershed (Nsimi-Zoetele site, Cameroon): comparison between organic-poor and organic-rich waters. *Chemical Geology* **140**, 181-206.
- von Haugwitz, W., Wong, H. K. and Salge, U. (1988) The mud area southeast of Helgoland: A reflection seismic study. *Mitteilungen des Geologisch-Paläontologischen Instituts der Universität Hamburg* **65**, 409-422.
- Vos P. C. and de Wolf, H. (1988) Methodological aspects of palaeo-ecological diatom research in coastal areas of the Netherlands. *Geologie en Mijnbouw* **67**, 31-40.

- Vos, P. C. and de Wolf, H. (1993) Reconstruction of sedimentary environments in Holocene coastal deposits of southwest Netherlands; the Poostvliet boring, a case study of palaeoenvironmental diatom research. *Hydrobiologica* **269/270**, 297-306.
- Vos P. C. and de Wolf, H. (1994) Palaeoenvironmental research on diatoms in early and middle Holocene deposits in central north Holland (The Netherlands). *Netherlands Journal of Aquatic Ecology* **28(1)**, 97-115.
- Wachendörfer, V. (1991) Parahistologische und Sediment-Mikrobiologische Untersuchungen an einem potentiellen silikoklastischen Stromatlithen. Ph. D. thesis. Universität Oldenburg.
- Wandtner, R., (1981) Indikatoreigenschaften der Vegetation von Hochmooren der Bundesrepublik Deutschland für Schwermetall-Immissionen. *Dissertationes Botanicae*, Cramer Verlag, Vaduz, **59**, 1-190.
- Wang, Q. and Morse, J. W. (1996) Pyrite formation under conditions approximating those in anoxic sediments I. Pathway and morphology. *Marine Chemistry* **52**, 99-121.
- Warning, B. and Brumsack, H.-J. (1998) Trace metal signatures of eastern Mediterranean sapropels. *Paleogeogr. Paleoclim. Paleoecol.* (accepted)
- Watermann, F., Dellwig, O., Brumsack, H.-J. and Gerdes, G., and Krumbein, W. E., 1999a. Diatoms and geochemical data used as tools for palaeoenvironmental reconstruction of a Holocene depositional sequence from the coastlands of NW Germany. *Palaeogeography Palaeoclimatology Palaeoecology*. (submitted)
- Watermann, F., Dellwig, O., Brumsack, H.-J. and Gerdes, G., 1999b. Microfacies and geochemical characteristics of an estuarine influenced Holocene intertidal system (NW Germany). (in preparation)
- Wedepohl, K. H. (1969) *Handbook of Geochemistry. Vol. II/4*. Springer, Berlin Heidelberg, New York. 37-K-1 - 37-K-2 pp.
- Wedepohl, K. H. (1971) Environmental influences on the chemical composition of shales and clays. In *Physics and Chemistry of the Earth* 8, eds. L. H. Ahrens, F. Press, S. K. Runcorn and H. C. Urey, 8, pp. 305-333. Pergamon, Oxford.

- Wedepohl, K. H., 1991. The composition of the upper earth's crust and the natural cycles of selected metals. Metals in natural raw materials. Natural resources. In *Metals and their compounds in the environment*, ed. E. Merian., pp. 3-17. VCH, Weinheim.
- Wehausen, R. (1995) Röntgenfluoreszenzanalytische Untersuchungen an Schwebstoffen aus dem Niedersächsischen Wattenmeer. Diploma thesis, Universität Oldenburg.
- Westrich, J. T. and Berner, R. A. (1984) The role of organic matter in bacterial sulfate reduction: The G-Model tested. *Limnology Oceanography* **29**, 236-249.
- Wirth, H. and Seifert, R. (1988) Mineralogy, Geochemistry and SEM-Observations of Suspended Particulate Matter from the North Sea, Spring 1984. *Mitteilungen des Geologisch-Paläontologischen Instituts der Universität Hamburg* **65**, 163-181.
- Zeitz, J. (1997) Zur Geochemie von Mooren. In *Geochemie und Umwelt*, eds J. Matschullat, H. J. Tobschall, H.-J. Voigt, pp.75-89. Springer, Berlin,.

## Appendix

A1: Drill core coordinates and age determinations	230
A2: Precision and accuracy of used methods	231
A3: Bulk parameters and XRF data	232
A4: Bulk parameters and ICP-OES data	285
A5: ICP-MS data	289
A6: $^{34}\text{S}$ -ratios	295

**A1: Drill core coordinates and age determinations**

Location	Archive No.	Coordinates				German zero datum [m NN]
		Longitude °E	Latitude °N	R	H	
Loxstedt	GE430/432	8.3012	53.2605	3466990	5922508	3.60
Arngast	GE117	8.1000	53.2900	3444687	5928124	-1.75
Wangerland						
W1	KB5552	7.5720	53.3701	3430895	5943186	2.90
W2	KB5156	7.5805	53.3745	3431745	5944516	0.65
W3	KB5750	7.5638	53.3629	3430100	5942200	0.65
W4	KB5752	7.5731	53.3632	3431082	5942270	3.00
W5	KB5950	7.5640	53.3601	3430132	5941315	2.00
Schweiburg	GE707	8.1541	53.2347	3450872	5918366	2.00
Aurich Moor		7.2554	53.3009	2594980	5930880	6.91

Location	Depth [m]	<sup>14</sup> C-age BP	av. calibrated age BP
Loxstedt	7.30-7.40	2,630±200	2,653
	9.18-9.30	2,640±170	2,680
	10.60-10.82	5,250±155	6,020
	11.89-12.03	6,160±100	7,033
	17.00-17.22	7,540±205	8,305
	17.57-17.82	9,920±410	11,345
Arngast	4.3	6,105±170	7,020
Wangerland			
W1	11.23-11.26	5,920±325	6,813
	11.37-11.40	6,465±305	7,340
W2	4.90-4.92	4,640±100	5,425
	8.24-8.25	5,850±125	6,668
	8.33-8.36	5,910±190	6,768
	10.67-10.71	6,285±300	7,160
W3	5.28-5.35	4,710±110	5,505
	5.75-5.80	4,985±125	5,798
	6.00-6.04	5,410±195	6,223
W5	2.74-2.76	2,380±75	2,405
	2.92-2.94	2,850±90	2,963
	6.10-6.12	4,595±65	5,315
	6.32-6.35	5,880±295	6,798
Schweiburg	1.09-1.13	1,420±105	1,382
	1.28-1.32	1,510±115	1,460
	1.41-1.46	1,660±95	1,602
	2.00-2.05	2,175±95	2,218
	2.10-2.13	1,540±100	1,472
	7.60-7.65	4,160±80	4,733
	8.05-8.10	4,800±120	5,540
	8.45-8.50	5,825±125	6,680
Aurich Moor	2.38-2.43	5,745±85	6,543

Age determinations were performed by M. A. Geyh (Geological Survey of the Federal State of Lower Saxony, Germany).

**A2: Precision and accuracy of used methods**

Element	Precision SD 2 [%]			Accuracy [%]		
	XRF	ICP-OES	ICP-MS	XRF	ICP-OES	ICP-MS
Si	0.8			0.8		
Ti	1.5	6.0		2.3	2.6	
Al	1.3	4.9		1.1	4.0	
Fe	1.1	4.9		0.9	2.6	
Mg	3.2	5.7		3.1	1.9	
Ca	0.9	5.4		4.8	2.1	
Na	7.8	11.8		7.2	19.2	
K	1.5	8.8		1.6	15.2	
P	3.5	8.1		6.7	4.3	
As	4.6	13.7		6.7	15.6	
Ba	2.8	6.1	9.0	3.9	3.5	7.1
Bi			12.6			5.8
Cd			11.7			10.7
Co	7.3	8.5	7.3	7.7	5.9	4.9
Cr	3.6	9.0	9.1	5.2	2.2	4.1
Cu	8.7	10.7	10.2	8.5	7.1	2.4
Mn	1.6	4.4		4.1	2.6	
Mo	15.3		9.9	15.2		5.3
Ni	3.9	10.2	7.8	8.7	3.2	3.6
Pb	5.6	21.2	12.4	2.7	14.9	5.1
<sup>206/207</sup> Pb			1.6			0.15
Re			18.6			-
Rb	3.3			2.4		
Sb			9.0			15.7
Sr	1.3	5.3	7.8	1.5	3.7	3.1
Tl			6.8			2.6
U			7.7			3.3
V	3.0	7.6	12.4	3.1	5.5	4.4
Y	3.3	5.0	8.2	6.7	4.1	5.3
Zn	3.4	4.7	13.5	4.9	7.7	14.0
Zr	2.3	5.6	13.7	1.5	11.8	18.7
La			6.7			6.0
Ce			8.9			3.6
Pr			8.3			10.9
Nd			12.6			6.7
Sm			10.0			5.4
Eu			8.2			4.2
Gd			8.2			3.5
Tb			9.6			14.5
Dy			10.2			4.1
Ho			12.6			5.1
Er			12.9			4.9
Tm			14.0			7.2
Yb			9.3			4.0
Lu			18.2			14.7
	IR-analyser	Coulometry		IR-analyser	Coulometry	
TS	2.3			6.2		
TC	4.0			1.3		
TIC		1.1			0.2	

Material and methods are described in the individual chapters.

**A3: Bulk parameters and XRF data**  
**Loxstedt core B (Archive No. GE 430)**

Depth [m]	TS	TC	TIC	SiO <sub>2</sub>	TiO <sub>2</sub>	Al <sub>2</sub> O <sub>3</sub>	Fe <sub>2</sub> O <sub>3</sub>	MgO	CaO	Na <sub>2</sub> O	K <sub>2</sub> O	P <sub>2</sub> O <sub>5</sub>
0.40	0.09	3.48	0.58	67.88	0.52	8.61	4.54	1.25	3.40	0.57	1.84	0.29
0.50	0.08	3.62	0.70	62.19	0.61	10.04	5.31	1.48	4.00	0.67	2.08	0.40
0.60	0.17	3.61	0.68	60.42	0.63	10.43	5.56	1.51	3.85	0.52	2.13	0.41
0.75	0.23	2.41	0.17	72.80	0.51	8.57	4.20	0.96	1.38	0.75	2.04	0.11
0.85	0.14	3.96	0.74	58.95	0.65	11.28	5.88	1.60	3.92	0.45	2.24	0.34
0.95	0.10	4.05	0.91	59.14	0.64	10.65	5.39	1.56	4.87	0.49	2.16	0.30
1.03	0.04	3.26	0.85	65.30	0.56	8.53	4.11	1.27	4.39	0.81	1.97	0.26
1.15	0.90	4.87	1.25	56.60	0.64	11.38	5.70	1.65	4.08	0.62	2.29	0.27
1.25	0.76	4.44	1.02	56.03	0.61	11.45	5.82	1.70	4.86	0.39	2.23	0.26
1.35	0.17	1.43	0.32	87.35	0.19	3.74	1.44	0.40	1.43	0.36	1.17	0.07
1.46	0.31	0.77	0.18	91.15	0.13	2.76	1.01	0.23	0.89	0.29	0.99	0.04
1.57	0.52	1.76	0.40	83.59	0.24	4.41	1.86	0.50	1.83	0.40	1.41	0.09
1.65	0.31	1.74	0.34	85.09	0.21	4.06	1.63	0.44	1.54	0.38	1.25	0.12
1.75	0.38	2.14	0.46	80.72	0.29	5.08	2.18	0.66	2.16	0.46	1.43	0.13
1.85	0.50	2.47	0.45	78.97	0.31	5.46	2.39	0.68	2.10	0.48	1.60	0.14
1.95	0.23	1.47	0.35	85.12	0.22	4.20	1.69	0.47	1.69	0.40	1.30	0.12
2.08	0.16	1.51	0.36	85.00	0.23	4.18	1.68	0.50	1.63	0.39	1.25	0.10
2.13	0.13	0.89	0.21	89.33	0.16	3.15	1.19	0.29	1.04	0.33	1.12	0.10
2.18	0.13	1.37	0.21	88.99	0.16	3.25	1.17	0.31	1.10	0.33	1.13	0.09
2.23	0.24	1.44	0.32	85.38	0.22	4.08	1.61	0.44	1.55	0.40	1.29	0.12
2.28	0.08	1.10	0.33	88.37	0.16	3.42	1.24	0.32	1.14	0.32	1.14	0.08
2.33	0.23	1.81	0.34	85.91	0.20	3.85	1.54	0.44	1.44	0.35	1.19	0.09
2.38	0.22	1.87	0.41	83.01	0.25	4.73	1.99	0.58	1.94	0.42	1.36	0.11
2.43	0.14	0.91	0.23	89.07	0.16	3.08	1.18	0.28	1.05	0.32	1.18	0.09
2.48	0.03	0.16	0.05	94.85	0.08	1.88	0.46	0.08	0.35	0.25	0.86	0.05
2.54	0.03	0.42	0.08	93.60	0.09	2.19	0.59	0.12	0.49	0.26	0.89	0.06
2.62	0.59	4.20	1.00	61.60	0.57	9.68	4.93	1.52	4.58	0.61	2.06	0.25
2.68	0.68	4.80	1.03	55.82	0.67	11.66	5.87	1.83	4.70	0.47	2.26	0.28
2.73	0.65	5.03	0.30	58.42	0.71	12.17	5.05	1.75	1.90	0.66	2.42	0.17
2.78	1.14	4.38	0.36	63.59	0.71	10.05	4.40	1.51	2.01	0.87	2.16	0.13
2.84	1.70	4.24	0.35	64.21	0.62	9.23	4.79	1.39	2.01	0.73	2.03	0.12
2.91	1.79	3.76	0.62	64.01	0.61	9.80	5.11	1.47	3.02	0.59	2.11	0.11
2.98	1.19	3.90	0.78	64.91	0.60	9.14	4.46	1.42	3.76	0.71	2.03	0.12
3.03	0.89	3.81	1.00	60.23	0.63	10.30	4.28	1.61	4.81	0.65	2.20	0.12
3.08	0.50	3.11	0.95	63.35	0.62	9.72	3.70	1.51	4.58	0.70	2.16	0.12
3.13	0.68	2.83	0.87	66.78	0.57	9.55	3.62	1.39	4.25	0.61	2.13	0.13
3.18	0.68	3.08	0.88	64.96	0.67	9.87	3.82	1.47	4.18	0.77	2.23	0.13
3.23	0.92	3.46	0.96	62.68	0.66	10.33	4.34	1.56	4.56	0.76	2.29	0.14
3.38	0.46	2.46	0.80	70.76	0.54	8.33	3.18	1.21	4.02	0.69	1.96	0.11
3.48	0.54	3.28	1.11	58.84	0.70	11.96	5.14	1.84	5.14	0.51	2.46	0.15
3.53	0.53	3.28	1.10	59.67	0.70	11.12	4.64	1.77	5.16	0.70	2.34	0.17
3.58	0.41	3.34	1.14	52.77	0.69	13.39	5.88	2.09	5.37	0.54	2.65	0.20
3.65	0.50	2.82	0.93	66.78	0.63	10.08	4.30	1.51	3.76	0.80	2.17	0.19
3.88	0.01	0.84	0.28	72.22	0.67	9.90	4.31	1.40	1.68	0.83	2.24	0.14
3.93	0.01	0.91	0.33	71.01	0.67	10.18	4.44	1.38	1.53	0.83	2.32	0.16
4.04	0.01	1.70	0.30	66.08	0.71	11.82	5.33	1.68	1.66	0.75	2.47	0.20
4.18	0.91	3.80	0.22	59.54	0.70	12.64	5.69	1.86	1.50	0.66	2.53	0.14
4.36	1.71	3.63	0.83	62.28	0.53	9.13	5.26	1.37	4.17	0.75	2.04	0.12
4.68	0.20	2.93	0.66	68.85	0.59	8.47	3.90	1.31	3.23	0.89	1.98	0.18
5.13	0.32	3.75	0.81	59.59	0.66	10.89	6.17	1.71	3.05	0.76	2.22	0.25

A detailed description of the used methods is given in the individual chapters.  
 Bulk parameters and major elements in %, trace metals in mg kg<sup>-1</sup>.



**Loxstedt core B (Archive No. GE 430)**

Depth [m]	As	Ba	Co	Cr	Mn	Mo	Ni	Pb	Rb	Sr	U	V	Y	Zn	Zr
0.40	19	407	8	79	1437	1	29	114	97	126	2	75	21	437	222
0.50	30	543	14	106	1569	0	38	143	107	152	3	88	24	584	267
0.60	20	577	18	107	2222	1	42	161	103	154	4	90	24	629	258
0.75	18	316	6	64	483	0	17	25	75	97	4	63	19	83	248
0.85	27	447	14	104	2715	1	42	157	112	152	4	107	25	486	227
0.95	24	375	14	94	1955	1	34	119	108	160	6	97	25	408	252
1.03	6	365	13	75	1353	1	24	75	86	147	1	72	21	255	291
1.15	23	352	13	87	1450	0	34	89	119	150	4	106	22	350	212
1.25	27	362	11	94	1934	2	34	122	116	162	4	106	23	447	181
1.35	10	226	9	17	257	1	7	30	37	63	1	24	9	132	106
1.46	15	198	4	17	319	1	6	20	33	45	1	16	10	73	99
1.57	11	240	7	23	623	3	7	36	43	77	2	30	13	117	150
1.65	8	222	4	25	540	0	5	33	37	70	3	28	8	105	145
1.75	14	273	5	30	658	1	11	40	54	87	3	37	13	150	172
1.85	13	274	7	36	695	3	10	41	50	90	3	43	14	136	176
1.95	4	238	5	24	623	3	6	33	36	73	1	28	9	119	155
2.08	10	229	5	24	553	2	6	33	42	70	1	29	9	132	119
2.13	0	220	4	12	420	2	2	24	27	54	1	16	7	79	102
2.18	4	203	4	20	430	3	2	26	25	55	2	17	8	83	106
2.23	10	246	6	22	574	0	5	33	35	77	1	30	11	114	132
2.28	19	243	7	25	411	1	9	26	37	55	0	20	10	97	116
2.33	10	227	7	21	498	2	6	32	41	65	1	24	10	124	142
2.38	5	276	7	27	664	2	9	38	42	82	0	33	11	139	136
2.43	13	209	5	16	352	2	8	25	28	55	1	20	7	78	94
2.48	3	166	5	2	188	2	0	13	13	32	1	6	3	34	76
2.54	1	179	5	4	226	2	0	16	16	38	1	9	7	43	69
2.62	18	347	10	74	1649	0	28	88	102	155	3	87	23	321	219
2.68	28	364	14	100	1699	1	37	113	120	165	3	110	26	392	223
2.73	6	372	12	95	563	2	33	113	131	119	4	110	24	375	248
2.78	6	340	14	88	248	1	26	94	105	107	4	87	25	246	430
2.84	12	344	11	74	262	1	23	74	98	104	2	78	23	176	353
2.91	21	296	10	77	336	1	26	69	105	114	4	82	23	167	292
2.98	15	293	8	70	338	0	22	58	95	120	3	74	25	127	345
3.03	6	326	9	79	384	2	22	66	110	140	2	86	23	128	291
3.08	0	310	9	74	372	1	21	56	102	136	3	79	22	108	346
3.13	15	281	9	66	397	0	26	54	102	129	3	79	18	104	298
3.18	18	313	10	74	400	1	22	55	102	132	4	79	26	104	419
3.23	16	305	11	74	440	2	24	58	104	136	3	83	25	105	334
3.38	16	291	8	59	356	0	21	44	87	125	5	64	22	70	379
3.48	21	307	12	91	897	0	32	68	123	159	4	103	25	110	281
3.53	4	318	10	80	919	1	26	62	116	160	2	91	25	97	323
3.58	11	319	15	93	1244	1	34	70	144	173	2	115	23	119	183
3.65	25	315	12	81	874	0	29	38	107	133	1	83	26	85	322
3.88	0	347	9	75	522	1	22	22	104	103	2	77	23	65	388
3.93	14	314	11	75	769	0	22	25	103	100	3	83	28	66	356
4.04	15	341	9	90	1504	2	28	28	125	104	4	107	26	85	285
4.18	16	340	15	96	278	2	38	27	136	107	2	116	24	98	216
4.36	10	314	8	68	624	1	23	21	98	144	2	78	19	60	224
4.68	14	285	6	68	815	0	19	19	86	112	2	70	21	48	345
5.13	10	295	10	81	1651	0	27	26	109	114	3	100	25	68	249

**Loxstedt core B (Archive No. GE 430)**

Depth [m]	TS	TC	TIC	SiO <sub>2</sub>	TiO <sub>2</sub>	Al <sub>2</sub> O <sub>3</sub>	Fe <sub>2</sub> O <sub>3</sub>	MgO	CaO	Na <sub>2</sub> O	K <sub>2</sub> O	P <sub>2</sub> O <sub>5</sub>
5.93	0.58	2.83	0.88	72.16	0.42	6.77	2.87	0.99	4.18	0.83	1.74	0.09
6.00	0.75	2.83	0.95	71.90	0.43	6.63	2.98	0.92	4.34	0.71	1.73	0.09
6.07	0.73	3.59	1.13	64.15	0.55	8.90	4.07	1.43	5.38	0.81	1.93	0.16
6.15	0.68	3.65	1.05	66.04	0.52	8.41	3.72	1.33	4.88	0.81	1.94	0.15
6.25	0.67	3.63	1.04	65.50	0.54	8.60	3.93	1.36	4.93	0.81	1.89	0.16
6.35	0.54	3.27	0.99	71.68	0.43	6.72	2.68	0.97	4.63	0.89	1.90	0.13
6.45	0.43	3.06	0.94	71.92	0.44	6.72	2.69	0.99	4.35	0.74	1.74	0.13
6.53	0.42	2.93	1.02	71.22	0.44	7.01	2.87	1.02	4.74	0.87	1.83	0.16
6.59	0.19	2.65	0.95	74.33	0.42	6.52	2.47	0.94	4.45	0.90	1.72	0.12
6.65	0.49	3.45	1.04	68.07	0.48	7.35	3.51	1.14	4.57	0.85	1.81	0.15
6.72	0.39	2.86	1.09	70.92	0.45	7.05	3.33	1.03	4.67	0.88	1.83	0.15
6.79	0.87	4.20	1.13	57.87	0.66	11.01	5.31	1.76	4.96	0.75	2.29	0.22
6.84	0.62	4.10	1.18	57.18	0.62	10.75	5.28	1.77	4.85	0.71	2.16	0.26
6.89	0.58	4.26	1.24	57.16	0.62	10.50	5.63	1.71	5.21	0.62	2.08	0.22
7.01	0.60	3.78	1.20	61.88	0.54	9.00	4.37	1.47	5.32	0.79	1.97	0.17
7.08	0.66	4.45	1.44	52.67	0.62	11.25	6.65	1.87	5.90	0.68	2.20	0.22
7.15	0.60	4.07	1.33	58.49	0.60	10.14	4.74	1.61	5.47	0.79	2.12	0.19
7.25	0.59	3.79	1.15	62.53	0.59	9.57	4.12	1.53	5.39	0.75	2.03	0.17
7.35	2.48	17.26	0.02	40.48	0.53	11.59	4.81	1.54	1.03	0.69	2.13	0.11
7.45	2.04	12.60	0.02	47.01	0.63	12.84	4.95	1.66	0.81	0.70	2.44	0.11
7.53	6.99	10.70	0.01	43.40	0.57	10.98	10.69	1.47	0.76	0.60	2.09	0.10
7.58	5.64	5.44	0.01	51.28	0.66	12.67	10.14	1.73	0.68	0.69	2.43	0.11
7.63	4.18	6.98	0.03	51.19	0.64	12.01	7.90	1.64	0.69	0.69	2.32	0.10
7.68	2.42	6.33	0.01	57.15	0.72	12.67	5.98	1.69	0.64	0.79	2.43	0.10
7.73	2.76	4.64	0.01	58.36	0.72	12.15	6.47	1.59	0.68	0.80	2.41	0.12
7.78	3.00	5.53	0.00	56.28	0.70	11.82	6.47	1.56	0.66	0.80	2.35	0.11
7.83	2.75	5.91	0.00	56.78	0.68	11.70	5.98	1.49	0.52	0.69	2.33	0.10
7.88	2.24	5.75	0.01	60.37	0.71	11.85	5.49	1.50	0.67	0.87	2.41	0.14
7.93	2.66	4.33	0.00	58.42	0.71	12.14	6.30	1.61	0.66	0.80	2.43	0.12
7.98	2.56	5.53	0.00	56.46	0.71	12.27	6.15	1.66	0.66	0.79	2.44	0.11
8.03	2.29	5.08	0.01	60.00	0.71	12.47	5.45	1.65	0.63	0.84	2.43	0.11
8.08	2.12	6.33	0.00	57.59	0.70	12.40	5.51	1.61	0.62	0.82	2.46	0.12
8.13	2.38	5.64	0.01	56.65	0.72	12.99	5.98	1.71	0.59	0.80	2.63	0.11
8.18	1.80	4.52	0.01	59.81	0.75	13.32	5.57	1.73	0.60	0.83	2.70	0.13
8.23	2.24	4.73	0.01	58.49	0.73	13.31	5.94	1.77	0.55	0.67	2.41	0.11
8.28	2.42	5.56	0.01	53.97	0.70	13.46	6.21	1.88	0.67	0.72	2.58	0.13
8.33	2.25	6.36	0.01	52.96	0.68	13.77	5.79	1.85	0.60	0.72	2.70	0.13
8.38	1.72	7.40	0.01	52.87	0.68	13.96	5.22	1.89	0.60	0.73	2.72	0.12
8.43	2.03	6.91	0.00	54.80	0.67	13.01	5.30	1.76	0.62	0.76	2.54	0.12
8.53	2.13	4.90	0.01	56.89	0.72	13.94	5.02	1.87	0.52	0.65	2.68	0.09
8.58	1.78	3.96	0.01	56.55	0.75	14.09	5.68	1.92	0.59	0.74	2.73	0.11
8.63	2.71	4.86	0.01	56.51	0.72	14.06	6.81	1.85	0.56	0.78	2.79	0.12
8.68	3.70	4.78	0.01	54.35	0.70	13.20	7.36	1.73	0.54	0.76	2.63	0.13
8.73	3.35	5.01	0.02	54.18	0.70	13.26	7.23	1.84	0.63	0.84	2.57	0.12
8.78	2.67	5.47	0.01	53.40	0.70	13.02	6.45	1.78	0.60	0.71	2.58	0.11
8.83	2.81	4.59	0.04	56.48	0.72	13.70	6.70	1.89	0.63	0.80	2.59	0.14
8.88	2.71	4.46	0.10	55.03	0.72	13.63	6.74	1.99	0.79	0.78	2.64	0.13
8.94	1.79	3.47	0.04	55.70	0.72	14.12	6.28	2.00	0.66	0.76	2.65	0.13
9.03	3.71	6.85	0.06	54.14	0.59	11.80	7.04	1.64	0.76	0.64	2.28	0.11
9.08	6.53	9.80	0.01	41.07	0.54	10.92	9.99	1.61	0.59	0.67	2.09	0.11
9.14	6.52	11.85	0.02	43.76	0.56	11.43	9.63	1.51	0.69	0.79	2.20	0.14
9.22	4.00	22.20	0.01	34.98	0.43	9.02	4.45	1.37	1.00	0.96	1.69	0.15
9.33	1.47	11.90	0.01	53.75	0.65	11.19	3.34	1.46	0.88	0.94	2.25	0.16
9.38	1.78	16.05	0.01	43.19	0.58	9.70	2.71	1.38	0.96	0.94	1.94	0.14

**Loxstedt core B (Archive No. GE 430)**

Depth [m]	As	Ba	Co	Cr	Mn	Mo	Ni	Pb	Rb	Sr	U	V	Y	Zn	Zr
5.93	2	308	6	49	386	2	11	16	59	138	1	51	17	38	263
6.00	22	284	8	56	388	0	14	17	57	142	4	48	18	35	269
6.07	21	289	8	69	583	1	23	19	96	194	2	75	22	66	250
6.15	18	290	8	61	545	0	19	18	86	153	4	69	20	47	263
6.25	23	298	10	70	605	1	22	20	93	185	1	70	24	58	278
6.35	10	278	5	52	429	2	12	18	60	149	3	50	19	30	275
6.45	17	278	9	57	506	0	16	17	58	143	3	47	20	31	294
6.53	10	279	5	52	585	0	14	16	70	153	3	52	17	38	280
6.59	20	287	8	51	487	2	16	12	72	148	1	42	20	40	285
6.65	0	307	6	55	862	2	14	16	63	150	3	60	19	42	288
6.72	9	282	10	48	931	1	12	14	66	152	3	51	20	36	286
6.79	16	284	10	84	947	2	30	25	111	156	3	106	27	73	241
6.84	2	313	9	81	952	2	25	23	110	149	1	101	21	68	199
6.89	25	271	11	86	1337	1	28	22	106	158	4	98	23	68	222
7.01	6	313	11	67	989	2	21	18	91	170	2	78	19	54	237
7.08	10	301	11	85	2117	2	28	22	120	185	2	108	22	72	182
7.15	12	272	9	75	1200	1	26	25	101	170	1	94	25	65	234
7.25	18	288	10	75	777	2	26	22	99	185	3	83	23	70	264
7.35	17	245	5	85	355	4	26	20	127	106	3	113	17	54	100
7.45	12	265	7	90	254	3	27	25	135	100	5	128	21	76	130
7.53	39	239	21	86	559	7	46	33	113	96	5	143	29	123	145
7.58	47	300	25	95	675	7	55	24	138	95	4	125	28	158	154
7.63	24	271	13	89	572	5	38	22	129	90	3	116	22	82	158
7.68	12	272	10	92	500	8	31	25	136	93	3	119	27	88	206
7.73	6	323	15	92	563	7	35	29	127	92	3	112	27	102	225
7.78	12	302	13	90	606	7	29	22	125	92	2	114	23	77	214
7.83	24	267	9	92	530	1	29	23	118	91	4	113	22	67	219
7.88	14	278	13	86	538	1	33	23	121	95	2	113	33	82	260
7.93	9	312	8	90	556	6	30	23	128	93	2	113	25	81	220
7.98	5	307	8	94	503	6	29	23	126	92	2	122	22	72	192
8.03	22	281	10	95	442	5	31	26	131	92	4	119	27	88	217
8.08	13	263	12	91	527	1	32	27	127	92	4	127	26	82	207
8.13	20	272	10	95	549	3	33	26	134	91	3	130	25	80	192
8.18	12	274	14	95	411	4	37	29	138	93	4	126	29	84	215
8.23	14	276	10	102	414	1	35	25	133	94	4	130	27	87	190
8.28	4	301	8	99	496	7	33	27	140	95	3	135	22	88	150
8.33	12	262	9	97	490	3	34	28	144	92	4	139	25	86	140
8.38	16	255	11	96	408	5	35	27	145	92	4	140	25	84	132
8.43	15	263	11	91	414	3	31	29	135	91	3	127	23	83	168
8.53	10	277	10	105	378	0	35	27	142	93	5	134	24	86	159
8.58	3	299	13	105	428	6	34	29	148	93	0	138	22	87	161
8.63	28	275	19	100	467	4	42	30	148	92	3	140	29	102	166
8.68	29	261	14	93	567	4	38	28	137	88	5	128	26	94	173
8.73	8	284	9	98	614	6	34	26	138	91	3	131	23	88	154
8.78	7	290	15	97	569	6	32	24	140	92	3	133	22	81	159
8.83	28	265	12	101	568	0	38	27	145	90	3	133	27	98	178
8.88	1	290	10	98	513	6	31	26	140	93	3	133	23	89	160
8.94	24	262	12	98	556	2	34	28	144	93	4	143	25	89	154
9.03	38	248	17	85	450	7	37	26	125	88	5	120	20	92	144
9.08	51	228	13	81	432	10	34	20	123	82	5	122	23	73	113
9.14	15	233	8	78	736	5	27	18	124	90	5	118	22	80	146
9.22	10	169	5	61	427	10	19	18	97	104	4	91	16	55	100
9.33	8	246	7	79	249	2	24	22	115	107	5	98	24	52	228
9.38	0	226	6	71	190	5	20	17	109	106	3	89	19	39	183

**Loxstedt core B (Archive No. GE 430)**

Depth [m]	TS	TC	TIC	SiO <sub>2</sub>	TiO <sub>2</sub>	Al <sub>2</sub> O <sub>3</sub>	Fe <sub>2</sub> O <sub>3</sub>	MgO	CaO	Na <sub>2</sub> O	K <sub>2</sub> O	P <sub>2</sub> O <sub>5</sub>
9.43	2.68	15.21	0.01	43.69	0.57	10.37	3.23	1.50	0.88	0.96	2.05	0.13
9.49	3.99	14.00	0.02	45.85	0.58	9.52	5.54	1.40	0.74	0.91	1.93	0.11
9.55	2.89	18.00	0.01	44.34	0.54	9.51	3.74	1.47	0.78	0.99	1.88	0.11
9.63	4.74	19.50	0.01	40.18	0.49	8.54	5.81	1.30	0.72	0.93	1.73	0.11
9.68	4.06	20.30	0.01	36.52	0.41	7.39	4.30	1.24	0.76	0.93	1.50	0.10
9.73	5.08	22.48	0.01	36.43	0.44	8.34	5.71	1.42	0.83	1.00	1.57	0.15
9.78	2.80	16.95	0.02	42.51	0.48	7.94	3.80	1.29	0.87	0.97	1.66	0.12
9.83	2.08	11.79	0.01	53.95	0.62	10.21	3.72	1.36	0.67	0.87	2.09	0.10
9.88	1.56	10.43	0.01	54.61	0.59	9.45	3.16	1.28	0.76	0.98	2.00	0.11
9.93	1.09	9.66	0.01	57.74	0.64	10.87	2.93	1.37	0.74	1.03	2.27	0.14
10.03	3.96	13.58	0.01	48.47	0.51	8.18	5.15	1.16	0.84	0.97	1.82	0.11
10.08	3.02	13.33	0.01	52.62	0.56	8.67	4.06	1.21	0.81	1.05	1.83	0.12
10.15	4.24	14.65	0.01	47.23	0.54	8.87	5.33	1.32	0.77	0.97	1.80	0.12
10.23	1.78	10.58	0.01	55.47	0.67	10.95	3.75	1.47	0.74	1.01	2.25	0.12
10.33	2.97	10.90	0.01	51.95	0.62	9.57	4.68	1.36	0.74	1.00	2.00	0.11
10.38	3.53	16.95	0.01	46.09	0.53	8.27	4.35	1.30	0.89	1.08	1.74	0.13
10.43	3.37	16.73	0.01	45.58	0.54	8.87	4.09	1.34	0.81	1.08	1.83	0.12
10.48	2.83	13.33	0.01	51.07	0.60	9.49	3.90	1.26	0.72	1.02	2.00	0.11
10.54	2.90	13.85	0.01	50.34	0.57	8.69	3.55	1.16	0.71	0.97	1.83	0.09
10.61	3.84	22.53	0.01	36.93	0.43	7.27	3.25	1.30	1.12	1.12	1.41	0.17
10.69	4.22	22.03	0.01	29.45	0.35	6.24	3.59	1.13	0.86	0.90	1.22	0.13
10.76	2.71	24.98	0.01	34.35	0.42	7.58	2.66	1.49	1.14	1.09	1.50	0.13
10.83	1.65	6.95	0.01	56.73	0.71	12.75	4.74	1.74	0.59	0.93	2.57	0.13
10.88	3.78	5.03	0.09	56.82	0.69	12.33	7.76	1.85	0.74	0.88	2.41	0.13
10.93	4.91	13.44	0.15	53.25	0.66	11.75	9.19	1.87	0.90	0.83	2.36	0.13
10.98	4.89	4.01	0.09	54.39	0.68	12.13	9.23	1.80	0.70	0.84	2.43	0.13
11.02	2.37	4.59	0.42	59.53	0.68	11.75	5.93	1.95	1.92	0.95	2.36	0.14
11.14	1.63	3.67	0.83	59.55	0.64	10.99	4.76	1.91	3.54	0.78	2.25	0.12
11.63	1.55	3.58	0.39	61.42	0.68	12.16	5.65	2.05	1.60	0.76	2.44	0.13
11.71	1.46	3.50	0.20	61.68	0.73	13.15	5.10	2.06	0.97	0.91	2.65	0.15
11.78	1.49	5.47	0.03	59.00	0.70	13.28	5.04	1.81	0.63	0.93	2.74	0.14
11.83	6.52	9.80	0.02	48.12	0.54	9.41	9.77	1.39	0.65	0.79	1.89	0.11
11.88	4.07	13.23	0.03	45.96	0.53	10.18	6.49	1.54	0.89	1.00	2.04	0.14
11.93	9.27	26.90	0.02	17.86	0.24	4.51	8.80	1.12	0.83	0.94	0.92	0.09
11.99	8.88	19.85	0.02	31.52	0.35	6.92	10.50	1.28	0.73	0.87	1.34	0.12
12.07	4.03	4.78	0.11	55.84	0.62	11.87	7.85	1.83	0.73	0.80	2.36	0.13
12.13	1.60	2.82	0.79	59.89	0.65	12.02	5.15	1.99	3.51	0.92	2.56	0.14
12.18	1.39	3.57	0.90	58.45	0.64	12.06	5.04	2.04	4.00	0.76	2.42	0.12
12.23	2.05	3.41	1.02	56.92	0.62	11.72	5.80	1.92	4.59	0.87	2.47	0.14
12.28	1.89	3.42	1.16	57.00	0.61	11.48	5.46	1.90	5.24	0.87	2.34	0.14
12.33	3.45	3.54	1.09	56.00	0.56	10.50	7.16	1.74	4.86	0.85	2.19	0.14
12.43	1.97	3.21	1.43	54.99	0.59	11.16	5.68	1.86	6.23	0.85	2.35	0.14
12.48	2.74	3.69	1.41	53.52	0.58	11.27	6.59	1.89	6.44	0.68	2.21	0.12
12.53	2.28	3.09	1.35	56.59	0.55	10.23	5.64	1.71	6.30	0.87	2.16	0.13
12.58	2.55	3.68	1.42	54.58	0.57	11.13	6.25	1.91	6.47	0.83	2.26	0.14
12.63	2.68	3.72	1.38	52.43	0.58	11.46	6.48	1.89	6.32	0.80	2.29	0.15
12.68	2.32	3.50	1.43	54.10	0.57	11.24	6.01	1.84	6.42	0.83	2.36	0.14
12.73	3.48	3.55	1.46	51.73	0.56	11.21	7.36	1.84	6.64	0.81	2.31	0.14
12.78	3.39	3.50	1.36	50.99	0.57	11.20	7.48	1.86	6.19	0.76	2.24	0.13
12.83	2.65	3.57	1.34	53.98	0.58	11.30	6.49	1.89	5.99	0.68	2.25	0.13
12.87	3.01	3.42	1.33	52.27	0.58	11.47	7.04	1.94	6.03	0.78	2.28	0.14
12.93	3.00	3.41	1.28	53.77	0.58	11.15	6.95	1.85	5.83	0.82	2.25	0.15
12.98	2.70	3.56	1.30	53.65	0.58	11.06	6.50	1.88	5.88	0.84	2.25	0.13
13.08	2.43	3.52	1.24	55.08	0.57	10.90	6.10	1.78	5.73	0.83	2.33	0.14

**Loxstedt core B (Archive No. GE 430)**

Depth [m]	As	Ba	Co	Cr	Mn	Mo	Ni	Pb	Rb	Sr	U	V	Y	Zn	Zr
9.43	3	224	6	75	238	3	23	21	108	102	7	97	24	44	179
9.49	9	238	10	73	457	9	29	19	98	89	4	82	20	73	215
9.55	11	219	6	68	273	12	21	20	103	92	5	86	18	64	188
9.63	19	199	6	63	314	7	20	19	88	83	5	82	17	53	179
9.68	10	184	6	57	248	7	19	13	79	82	4	77	16	43	156
9.73	20	175	7	65	286	2	28	18	85	88	2	82	18	69	141
9.78	5	204	5	64	220	5	20	16	86	92	4	73	19	44	205
9.83	12	238	7	86	220	3	21	22	102	93	4	89	20	46	244
9.88	0	246	5	73	188	6	20	19	95	91	3	83	20	55	254
9.93	6	282	6	78	226	0	21	21	112	96	4	98	21	49	253
10.03	15	207	6	66	288	6	23	19	83	92	5	83	22	59	228
10.08	18	229	6	75	283	2	23	15	90	93	5	83	23	52	280
10.15	18	202	9	73	420	8	25	19	92	92	4	88	21	73	228
10.23	10	264	7	79	287	2	23	21	111	94	6	106	22	59	234
10.33	9	236	8	75	275	7	23	20	101	90	4	89	22	62	256
10.38	10	203	8	65	324	4	23	19	84	96	5	82	24	52	242
10.43	4	207	6	65	364	5	20	21	90	93	6	88	19	45	209
10.48	8	240	7	72	331	6	19	19	96	92	5	93	21	45	257
10.54	8	221	7	71	324	8	18	17	87	91	5	79	21	48	263
10.61	11	177	6	58	320	9	23	15	72	129	4	72	24	52	166
10.69	3	157	7	49	366	5	24	13	59	93	4	59	15	54	124
10.76	11	173	5	63	281	4	23	12	79	127	4	80	20	47	128
10.83	8	281	10	90	297	0	29	26	129	91	4	119	27	74	189
10.88	28	254	14	91	440	10	32	26	133	86	3	118	28	100	181
10.93	28	293	10	88	929	5	32	27	125	86	3	117	24	77	169
10.98	27	290	8	90	865	6	29	26	129	87	2	120	25	79	171
11.02	26	273	15	94	582	1	39	24	120	97	2	114	26	83	204
11.14	16	258	10	88	421	2	30	24	108	113	3	100	24	70	200
11.63	16	267	10	96	434	2	33	30	120	95	5	114	22	82	183
11.71	9	286	12	94	383	0	33	27	133	90	4	121	27	86	192
11.78	13	282	9	97	355	2	35	26	135	92	4	127	28	82	190
11.83	26	225	18	74	410	6	34	18	86	89	5	99	27	75	179
11.88	17	234	5	70	415	4	24	16	106	97	6	107	19	52	151
11.93	44	113	11	39	534	25	27	15	45	74	10	96	20	49	72
11.99	62	168	25	52	689	28	52	18	69	76	6	98	26	189	93
12.07	29	264	12	87	727	7	36	25	123	83	4	114	22	95	149
12.13	13	293	12	86	629	3	35	26	121	116	4	108	24	78	177
12.18	14	250	12	94	567	1	35	29	119	120	5	110	22	78	159
12.23	17	268	11	81	613	4	31	24	122	127	4	112	24	75	156
12.28	19	257	13	82	647	1	31	25	116	135	3	111	27	76	157
12.33	15	267	6	73	889	1	24	21	109	129	3	100	20	71	159
12.43	18	256	12	77	1682	3	31	27	114	153	3	109	25	75	151
12.48	28	252	13	84	969	4	31	24	114	164	4	106	23	74	142
12.53	21	263	9	71	728	1	27	22	106	154	4	95	21	66	162
12.58	20	253	10	80	838	2	31	24	117	164	5	105	22	75	139
12.63	18	271	12	77	894	1	30	26	117	159	3	112	21	80	124
12.68	18	255	10	77	810	4	30	25	118	162	2	111	23	74	134
12.73	18	247	13	78	826	2	31	26	116	167	4	110	23	74	128
12.78	19	261	8	82	805	2	30	26	122	167	2	112	21	78	125
12.83	15	260	10	83	845	0	32	24	114	158	5	108	21	77	138
12.87	16	243	11	81	811	0	29	22	120	162	4	112	22	78	128
12.93	18	243	11	80	892	0	29	24	118	155	3	110	19	77	141
12.98	16	274	12	81	834	2	32	23	117	158	3	105	20	77	142
13.08	12	256	10	79	884	1	27	23	112	154	4	103	24	71	152

**Loxstedt core B (Archive No. GE 430)**

Depth [m]	TS	TC	TIC	SiO <sub>2</sub>	TiO <sub>2</sub>	Al <sub>2</sub> O <sub>3</sub>	Fe <sub>2</sub> O <sub>3</sub>	MgO	CaO	Na <sub>2</sub> O	K <sub>2</sub> O	P <sub>2</sub> O <sub>5</sub>
13.15	2.21	3.18	1.17	57.16	0.55	10.45	5.82	1.76	5.28	0.82	2.19	0.13
13.25	1.79	3.14	1.15	58.34	0.56	10.37	5.09	1.71	5.43	0.89	2.24	0.18
13.35	1.94	3.24	1.09	61.44	0.54	9.55	5.22	1.59	4.74	0.88	2.07	0.13
13.45	3.02	3.45	1.09	58.96	0.55	9.70	6.74	1.59	4.80	0.88	2.20	0.13
13.53	2.50	5.91	1.12	60.48	0.56	10.03	5.38	1.64	4.85	0.86	2.24	0.13
13.58	1.11	3.24	1.08	61.65	0.54	9.83	4.65	1.65	4.78	0.75	2.12	0.18
13.75	0.81	4.37	1.09	58.83	0.54	10.01	5.19	1.73	4.71	0.75	2.12	0.70
13.83	0.85	3.46	1.14	60.56	0.55	9.92	5.00	1.69	4.97	0.86	2.14	0.60
13.90	0.59	3.22	1.20	61.81	0.59	9.91	4.32	1.70	5.24	0.97	2.25	0.36
13.98	0.55	3.45	1.19	59.51	0.59	10.53	4.77	1.82	5.11	0.78	2.19	0.44
14.05	0.80	3.47	1.19	59.00	0.56	10.36	5.28	1.72	5.15	0.89	2.19	0.39
14.15	1.45	3.74	1.31	55.24	0.56	10.28	6.29	1.78	5.51	0.85	2.15	0.19
14.25	1.27	3.77	1.39	57.22	0.57	10.56	6.02	1.81	5.74	0.87	2.14	0.22
14.35	1.04	3.76	1.33	58.03	0.57	10.53	5.27	1.77	5.77	0.91	2.22	0.24
14.45	0.87	3.73	1.29	58.30	0.57	10.53	5.03	1.84	5.85	0.88	2.21	0.37
14.55	0.88	3.79	1.30	57.81	0.58	10.79	5.24	1.83	5.62	0.75	2.21	0.18
14.65	0.74	3.39	1.24	60.50	0.56	10.31	5.02	1.70	5.38	0.87	2.28	0.27
14.75	1.14	3.73	1.34	57.22	0.59	10.84	5.68	1.84	5.80	0.86	2.20	0.15
14.85	1.17	3.44	1.34	57.36	0.59	10.85	5.72	1.81	5.64	0.87	2.33	0.15
14.95	1.06	3.67	1.29	57.78	0.60	10.93	5.78	1.88	5.65	0.88	2.19	0.15
15.05	0.92	3.52	1.18	58.01	0.58	10.85	5.39	1.81	5.30	0.88	2.26	0.28
15.15	0.92	3.59	1.29	57.51	0.59	11.07	5.56	1.84	5.48	0.87	2.29	0.17
15.25	0.98	3.70	1.29	57.42	0.60	11.22	5.62	1.89	5.45	0.71	2.27	0.14
15.33	1.25	3.64	1.28	58.31	0.56	10.56	5.41	1.80	5.68	0.84	2.19	0.14
15.41	0.26	0.99	0.45	84.34	0.28	4.68	1.55	0.57	2.01	0.55	1.51	0.10
15.51	0.19	0.82	0.46	84.47	0.28	4.68	1.35	0.55	2.18	0.74	1.60	0.09
15.61	0.18	1.06	0.47	84.26	0.28	4.78	1.43	0.58	2.18	0.78	1.51	0.11
15.72	0.12	0.56	0.30	87.91	0.22	3.99	1.05	0.38	1.48	0.64	1.56	0.09
15.94	0.18	0.54	0.16	90.12	0.18	3.17	0.96	0.24	0.78	0.46	1.26	0.08
16.25	0.20	0.59	0.04	93.62	0.11	2.20	0.65	0.12	0.28	0.31	0.96	0.04
16.47	0.32	1.28	0.09	87.44	0.22	3.99	1.25	0.39	0.51	0.52	1.26	0.04
16.62	0.09	0.31	0.00	95.10	0.08	1.86	0.41	0.09	0.11	0.24	0.78	0.02
16.75	0.61	2.18	0.01	90.22	0.15	2.75	1.22	0.22	0.22	0.31	0.93	0.05
17.05	3.49	41.70	0.03	10.99	0.08	1.67	3.52	1.05	1.34	0.67	0.34	0.06
17.16	0.75	33.53	0.02	28.49	0.16	1.85	1.22	0.81	1.33	0.65	0.51	0.09
17.27	0.09	3.44	0.00	88.88	0.21	3.13	0.44	0.21	0.27	0.38	1.01	0.05
17.36	0.04	1.94	0.00	79.49	0.53	7.83	1.40	0.65	0.45	0.79	1.97	0.05
17.45	0.35	2.74	0.00	69.26	0.77	13.04	2.61	1.30	0.49	0.95	2.68	0.08
17.56	0.14	6.37	0.00	62.47	0.74	13.76	2.76	1.47	0.51	0.74	2.67	0.09
17.63	0.89	28.63	0.04	20.48	0.38	10.65	2.29	1.58	2.00	0.78	1.33	1.34
17.70	0.95	33.24	0.02	19.56	0.31	8.11	2.03	1.47	1.71	0.67	1.05	0.74
17.77	0.93	35.95	0.02	16.66	0.23	5.37	1.63	1.14	1.34	0.54	0.81	0.19
17.83	0.24	9.34	0.01	64.15	0.42	7.31	1.68	0.96	0.66	0.63	1.61	0.07
17.91	0.03	0.90	0.00	89.43	0.26	4.09	0.78	0.35	0.24	0.45	1.32	0.03

**Loxstedt core B (Archive No. GE 430)**

Depth [m]	As	Ba	Co	Cr	Mn	Mo	Ni	Pb	Rb	Sr	U	V	Y	Zn	Zr
13.15	6	301	12	75	723	2	26	19	109	143	1	97	19	70	154
13.25	16	273	9	73	862	2	26	23	107	147	4	95	23	67	176
13.35	22	266	10	68	1765	0	21	20	98	135	3	90	22	58	196
13.45	22	266	9	67	1048	2	24	22	98	132	3	85	22	61	188
13.53	22	270	12	70	1173	4	24	23	102	135	3	93	23	63	188
13.58	16	259	8	74	1327	1	26	26	97	136	2	88	21	62	193
13.75	19	273	10	78	2838	1	29	25	98	137	3	96	21	67	174
13.83	15	265	10	69	1887	1	23	22	101	137	3	90	23	65	179
13.90	17	280	10	71	1044	3	24	20	101	143	3	88	26	60	208
13.98	15	278	12	82	1273	0	28	21	103	142	4	94	24	68	186
14.05	13	264	13	71	1352	0	23	25	101	137	4	97	22	67	175
14.15	9	295	9	75	1353	2	26	23	104	145	2	95	20	64	157
14.25	24	284	8	84	1325	0	31	20	111	151	1	97	22	75	174
14.35	15	275	9	75	994	1	27	23	108	154	3	96	28	69	175
14.45	20	279	10	74	1057	1	25	24	108	154	4	93	23	65	174
14.55	13	276	12	81	897	2	30	25	106	148	4	97	21	72	167
14.65	13	271	12	71	890	3	25	24	105	144	3	93	24	67	173
14.75	21	294	11	86	845	1	33	20	111	152	3	100	24	77	172
14.85	16	288	12	76	840	2	29	23	114	149	3	101	26	69	178
14.95	23	297	11	87	844	0	35	20	116	147	0	100	25	76	185
15.05	11	276	8	77	893	2	28	23	110	138	4	101	21	71	173
15.15	10	274	13	76	841	0	29	24	110	142	3	103	23	74	175
15.25	14	283	10	85	786	2	33	25	114	143	4	98	24	74	174
15.33	21	267	14	73	689	1	27	22	108	146	4	94	23	64	172
15.41	9	248	4	31	229	0	6	15	42	85	2	25	13	17	248
15.51	0	326	4	24	203	1	2	11	36	86	1	21	8	13	209
15.61	13	277	8	30	267	0	9	10	47	84	1	24	15	23	243
15.72	1	246	5	15	184	2	2	13	37	69	1	16	11	8	211
15.94	1	224	4	12	397	0	0	12	23	50	1	15	7	8	207
16.25	3	168	4	11	276	1	0	11	17	33	1	10	5	5	158
16.47	13	232	6	25	192	2	10	11	40	46	0	22	13	22	165
16.62	5	156	3	4	27	1	0	7	20	26	0	6	3	19	90
16.75	0	159	5	11	120	0	0	8	18	34	3	16	8	10	145
17.05	0	73	1	13	390	5	6	4	17	116	2	20	7	22	31
17.16	4	166	2	14	249	2	6	5	16	129	1	12	8	10	138
17.27	5	208	3	10	44	2	0	8	31	46	0	12	6	18	170
17.36	0	332	5	45	93	2	6	17	66	80	1	40	13	17	340
17.45	12	362	4	79	179	0	26	23	112	102	3	80	24	51	384
17.56	13	365	6	83	171	1	26	27	111	111	5	93	25	52	323
17.63	20	904	12	58	341	1	57	24	65	306	8	92	45	58	287
17.70	28	496	15	43	270	2	52	12	52	214	7	74	29	50	244
17.77	29	175	19	34	198	1	43	11	40	133	6	53	19	35	109
17.83	0	252	10	41	138	1	23	15	71	87	3	49	15	30	253
17.91	6	225	8	22	63	1	8	11	42	47	2	20	10	29	282

## Loxstedt core C (Archive No. GE 432)

Depth [m]	TS	SiO <sub>2</sub>	TiO <sub>2</sub>	Al <sub>2</sub> O <sub>3</sub>	Fe <sub>2</sub> O <sub>3</sub>	MgO	CaO	Na <sub>2</sub> O	K <sub>2</sub> O	P <sub>2</sub> O <sub>5</sub>
0.57	0.24	60.32	0.65	10.69	5.68	1.55	4.06	0.68	2.19	0.46
0.73	0.23	74.19	0.46	7.58	3.56	0.86	1.5	0.95	1.93	0.13
0.80	0.17	56.18	0.67	11.65	6.11	1.7	3.97	0.58	2.27	0.37
0.99	0.14	58.05	0.60	10.03	5.93	1.5	4.59	0.61	2.04	0.38
1.55	0.2	74.58	0.20	4.06	1.54	0.45	1.71	0.42	1.29	0.11
2.03	0.08	80.2	0.08	1.89	0.53	0.11	0.4	0.24	0.74	0.04
2.49	0.18	67.32	0.66	10.51	3.76	1.54	1.85	0.72	2.23	0.14
2.98	1.14	61.55	0.65	10.65	4.76	1.62	4.49	0.6	2.25	0.13
3.44	0.48	69.97	0.56	8.38	3.19	1.21	3.6	0.7	1.95	0.11
3.94	0.07	74.44	0.60	8.63	3.29	1.2	2.77	0.89	2.06	0.11
4.73	0.87	64.81	0.71	12.18	5.97	1.8	2.28	0.72	2.48	0.27
4.92	0.87	57.12	0.60	10.59	5.03	1.57	4.05	0.66	2.16	0.19
5.58	0.17	63.36	0.61	9.59	5.72	1.51	3.61	0.8	2.04	0.24
5.88	0.51	58.58	0.67	11.31	5.47	1.81	4.15	0.73	2.22	0.25
6.00	0.16	69.03	0.55	8.99	3.26	1.35	4.11	0.83	2.03	0.13
6.95	0.65	59.07	0.58	9.58	4.52	1.53	5.11	0.78	2	0.18
7.28	0.71	62.09	0.66	9.79	4.23	1.6	5.36	0.86	2.05	0.19
7.48	2.3	44.57	0.60	12.13	4.77	1.63	0.87	0.74	2.28	0.10
7.53	2.37	53.81	0.71	13.45	5.96	1.73	0.67	0.73	2.59	0.09
7.97	3.58	57.13	0.70	12.39	7.51	1.64	0.67	0.8	2.42	0.12
8.46	2.28	54.48	0.69	13.28	6.1	1.81	0.64	0.77	2.54	0.11
8.97	2.81	51.09	0.66	13.43	6.71	1.85	0.66	0.75	2.54	0.13
9.05	5.72	44.26	0.56	11.4	9.91	1.62	0.61	0.72	2.16	0.12
9.29	3.92	32.29	0.35	7.01	4.18	1.01	0.82	0.76	1.37	0.13
9.37	1.95	36.63	0.44	8.4	3.07	1.12	0.67	0.76	1.63	0.12
9.45	2.25	43.48	0.57	9.85	3.41	1.3	0.88	0.94	1.95	0.14
9.51	2.69	21.63	0.29	5.4	2.25	0.93	0.71	0.68	1.04	0.09
9.56	3.68	41.11	0.54	9.25	4.95	1.36	0.78	0.92	1.83	0.12
9.89	3.23	41.24	0.48	7.9	4.18	1.22	0.81	1.03	1.64	0.11
9.96	3.13	50.56	0.57	8.84	4.65	1.2	0.74	1.04	1.87	0.10
10.02	2.69	54.88	0.59	9.83	4.82	1.32	0.75	1.02	2.03	0.13
10.08	1.58	56.4	0.59	10.08	3.39	1.31	0.75	1.03	2.11	0.12
10.47	5.61	42.02	0.49	7.81	6.8	1.25	0.87	1.05	1.61	0.12
10.65	2.1	53.49	0.39	6.77	5.12	0.97	1.19	0.74	1.49	0.12
10.73	2.18	32.94	0.39	6.75	1.96	1.14	0.9	0.98	1.36	0.13
10.87	3.25	33.78	0.38	6.24	3.23	1.06	0.8	0.9	1.28	0.10
10.93	2.86	32.37	0.37	6.45	2.57	1.26	1.05	1.06	1.31	0.12
11.04	1.13	55.33	0.70	12.69	4.05	1.79	0.7	0.98	2.51	0.12
11.10	1.51	59.62	0.73	12.79	4.92	1.72	0.6	0.96	2.56	0.12
11.41	3.43	57.05	0.68	12.04	7.7	1.81	0.83	0.92	2.42	0.13
11.48	2.48	59.5	0.66	11.29	6.2	1.91	1.64	0.97	2.32	0.13
11.55	2.13	60.91	0.65	10.79	5.66	1.87	2.21	0.98	2.25	0.13
11.83	5.61	40.88	0.48	8.85	7.98	1.39	0.72	0.89	1.76	0.13
11.95	5.79	19.93	0.21	4.19	4.64	0.9	0.63	0.77	0.83	0.10
12.09	2.06	55.74	0.62	12.19	6.06	1.98	3.79	0.83	2.42	0.14
12.17	2.42	54.28	0.60	11.79	6.35	1.94	5.29	0.82	2.34	0.14
12.45	2.61	55.34	0.57	10.9	6.32	1.83	5.96	0.85	2.21	0.14
12.75	3.17	54.07	0.57	11.08	7.23	1.84	5.85	0.82	2.23	0.14
12.96	1.69	61.18	0.54	10.1	5.03	1.64	4.91	0.89	2.17	0.12
13.97	0.67	61.02	0.55	10.11	4.7	1.7	5.09	0.9	2.17	0.52
14.19	0.57	56.04	0.57	10.58	6.74	1.86	5.14	0.82	2.16	0.98
14.59	0.53	55.87	0.58	10.8	5.75	1.83	6.12	0.86	2.2	0.37
14.91	0.5	57.56	0.57	10.39	5.67	1.79	5.95	0.91	2.15	0.34



## Loxstedt core C (Archive No. GE 432)

Depth [m]	As	Ba	Co	Cr	Mn	Mo	Ni	Pb	Rb	Sr	U	V	Y	Zn	Zr
0.57	18	599	13	106	2203	1	36	162	110	159	3	94	23	649	269
0.73	1	340	10	48	968	1	15	28	61	92	2	49	16	104	245
0.80	10	452	18	102	2614	1	41	168	117	147	2	114	22	518	194
0.99	13	401	14	82	2785	1	28	104	102	156	2	95	21	383	231
1.55	1	247	7	22	535	1	4	33	29	72	3	25	7	106	115
2.03	1	127	3	2	129	1	0	15	1	29	1	6	1	30	59
2.49	1	350	12	83	246	1	25	84	100	100	2	87	19	228	301
2.98	6	298	11	79	366	1	26	65	110	130	2	93	21	125	311
3.44	1	284	7	64	313	1	15	49	82	114	3	63	19	76	423
3.94	1	311	6	70	433	1	17	20	78	111	2	64	20	52	364
4.73	11	320	11	88	484	1	28	28	132	112	3	107	23	90	268
4.92	7	288	13	77	964	1	26	26	111	140	2	96	19	68	206
5.58	4	288	10	75	1608	1	21	22	91	118	4	83	21	54	281
5.88	8	299	13	84	834	1	27	23	111	136	1	107	21	69	223
6.00	1	307	7	67	298	1	19	18	84	127	4	74	18	50	258
6.95	2	273	8	74	817	1	19	22	88	157	3	84	19	83	229
7.28	8	274	13	81	753	1	21	22	95	163	2	85	22	83	323
7.48	5	247	9	86	170	1	26	32	128	93	4	127	15	97	109
7.53	5	277	10	96	241	2	30	30	142	91	3	128	19	94	152
7.97	28	271	13	91	618	1	34	27	134	90	4	124	23	93	199
8.46	16	264	11	94	477	1	35	30	142	88	3	131	21	97	146
8.97	16	255	13	95	459	1	37	32	139	87	3	139	19	89	126
9.05	49	220	13	80	455	2	36	33	128	82	5	126	25	83	121
9.29	1	148	6	48	293	2	16	20	68	79	3	77	11	160	83
9.37	1	175	5	57	156	1	17	17	82	76	4	77	13	82	122
9.45	3	219	5	70	204	3	19	20	108	97	4	94	18	78	179
9.51	1	115	3	39	129	1	13	17	54	65	2	59	8	61	73
9.56	13	210	9	66	317	2	26	21	101	89	5	85	17	99	178
9.89	8	190	5	61	209	1	17	19	85	84	4	80	16	94	192
9.96	13	227	6	68	181	1	20	20	94	86	4	82	17	88	255
10.02	9	243	5	73	199	1	22	24	102	89	4	85	19	99	245
10.08	1	249	6	75	182	1	18	24	105	90	3	94	18	78	240
10.47	20	196	13	60	526	4	26	24	69	89	5	77	21	72	199
10.65	1	204	5	53	439	1	17	27	57	79	2	63	13	76	139
10.73	1	157	4	51	247	1	13	12	60	81	3	67	12	26	123
10.87	1	155	6	46	212	1	16	13	55	76	2	56	11	32	150
10.93	6	155	6	50	264	1	17	14	65	96	4	64	14	37	122
11.04	1	278	9	92	258	1	26	26	131	91	3	118	20	69	167
11.11	1	290	15	93	255	1	30	30	125	85	2	122	22	70	187
11.41	38	274	17	90	394	1	35	27	130	86	3	122	22	77	183
11.48	17	270	8	82	344	1	29	25	115	92	2	107	22	70	205
11.55	12	274	11	81	325	1	26	25	106	96	4	100	22	64	214
11.83	29	200	12	67	336	1	33	20	89	80	4	111	22	85	137
11.95	1	94	5	32	364	8	13	11	33	55	4	59	7	32	50
12.09	13	269	16	87	850	1	32	28	125	114	3	113	20	82	134
12.17	18	258	14	83	869	1	32	25	120	132	2	112	19	79	132
12.45	16	257	13	79	969	1	29	25	107	151	4	105	19	71	137
12.75	21	256	8	79	906	1	29	27	111	154	3	107	20	74	136
12.96	15	278	12	69	999	1	24	24	100	134	1	88	17	63	168
13.97	1	279	11	72	1351	1	24	24	89	136	4	90	17	58	173
14.19	7	273	13	77	4224	1	26	25	98	137	4	103	19	65	153
14.59	2	281	12	76	1918	1	26	26	95	155	2	100	19	63	151
14.91	10	282	12	74	2103	1	24	23	96	153	3	97	20	63	158

**Loxstedt core C (Archive No. GE 432)**

Depth [m]	TS	SiO <sub>2</sub>	TiO <sub>2</sub>	Al <sub>2</sub> O <sub>3</sub>	Fe <sub>2</sub> O <sub>3</sub>	MgO	CaO	Na <sub>2</sub> O	K <sub>2</sub> O	P <sub>2</sub> O <sub>5</sub>
14.99	0.39	73.95	0.37	6.51	2.85	0.98	3.41	0.72	1.64	0.17
15.07	0.49	58.01	0.57	10.32	5.45	1.77	5.85	0.91	2.15	0.34
15.27	3.89	42.97	0.10	2.33	4.13	0.72	1.01	0.62	0.61	0.07
15.44		86.17	0.28	4.73	1.68	0.57	2.18	0.72	1.51	0.09
15.55	0.26	83.91	0.29	4.94	1.63	0.6	2.41	0.82	1.58	0.10
16.05	0.34	81.34	0.15	2.86	1.03	0.23	0.65	0.38	1.06	0.03
16.56	0.14	73.42	0.16	2.79	1.16	0.23	0.46	0.32	0.97	0.04
16.92	0.44	86.52	0.21	4.05	1.41	0.37	0.33	0.46	1.27	0.04
17.02	0.15	76.8	0.10	2.32	0.54	0.13	0.19	0.3	0.91	0.02
17.12	0.33	75.37	0.36	6.65	2.97	0.98	3.34	0.68	1.67	0.16
17.18	5.45	9.69	0.06	1.4	5.68	1.15	1.63	0.87	0.26	0.09
17.26	2.02	2.79	0.02	0.54	1.98	1.24	1.91	0.81	0.11	0.06
17.34	0.76	45.75	0.22	3.08	1.18	0.74	1.08	0.66	0.79	0.07
17.54	0.4	53.26	0.33	8.44	1.67	0.8	1.03	0.61	1.42	0.76
17.57	0.93	28.14	0.32	8.13	2.02	1.32	1.39	0.66	1.2	0.62
17.61	1	21.98	0.26	6.45	1.92	1.25	1.51	0.63	0.94	0.51
17.64	0.44	52.69	0.45	8.85	2.16	1.24	0.92	0.65	1.64	0.12
17.69	0.12	75.65	0.36	6.37	1.49	0.73	0.45	0.54	1.49	0.05
17.75	0.04	81.95	0.10	2.04	0.33	0.08	0.19	0.26	0.84	0.01
17.82		92.98	0.17	2.9	0.44	0.14	0.23	0.39	1.17	0.02

Depth [m]	As	Ba	Co	Cr	Mn	Mo	Ni	Pb	Rb	Sr	U	V	Y	Zn	Zr
14.99	1	252	8	39	722	1	11	18	44	98	3	49	12	32	191
15.07	1	284	9	73	1859	1	23	25	76	139	1	95	17	61	147
15.27	4	117	3	13	636	1	8	10	18	74	3	23	7	23	71
15.44	1	265	2	30	229	1	5	13	35	84	1	26	9	16	261
15.55	1	283	5	27	233	1	5	14	34	90	3	23	10	17	228
16.05	1	206	6	11	340	1	1	10	10	42	1	13	4	2	154
16.56	1	171	2	15	278	1	1	12	7	36	1	15	2	7	113
16.92	1	224	4	34	81	1	4	15	21	46	1	23	4	15	143
17.02	1	168	3	6	11	1	1	11	5	31	1	7	1	1	88
17.12	1	256	7	44	523	1	15	16	49	96	2	50	11	34	198
17.18	17	80	1	11	638	2	10	5	12	136	3	17	10	28	26
17.26	4	59	1	4	275	1	2	2	0	139	1	8	2	1	13
17.34	1	178	2	17	183	1	5	9	19	95	2	19	7	6	144
17.54	1	455	8	33	191	1	20	20	38	151	4	46	14	24	204
17.57	13	502	8	42	226	1	29	15	60	187	6	76	22	41	226
17.61	18	422	12	38	234	1	37	13	44	182	7	71	27	32	180
17.64	6	255	14	51	163	1	32	21	81	107	4	71	22	37	242
17.69	1	236	11	34	91	1	17	16	43	64	2	38	12	23	228
17.75	1	168	3	1	11	1	1	11	3	29	1	5	2	1	135
17.82	1	222	4	8	41	1	1	10	18	38	2	8	5	3	250

## Arngast core (Archive No. GE 117)

Depth [m]	TS	TC	TIC	SiO <sub>2</sub>	TiO <sub>2</sub>	Al <sub>2</sub> O <sub>3</sub>	Fe <sub>2</sub> O <sub>3</sub>	MgO	CaO	Na <sub>2</sub> O	K <sub>2</sub> O	P <sub>2</sub> O <sub>5</sub>
0.03	0.04	0.34	0.33	88.88	0.31	3.50	0.76	0.32	1.77	0.94	1.26	0.04
0.08				89.93	0.28	3.24	0.66	0.29	1.67	0.89	1.19	0.03
0.12				86.24	0.18	3.98	0.73	0.39	2.65	1.08	1.47	0.03
0.16	0.05	0.46	0.44	87.61	0.26	3.79	0.74	0.37	2.24	1.04	1.37	0.04
0.20				88.13	0.25	3.75	0.72	0.35	2.05	1.04	1.36	0.03
0.24				87.93	0.23	3.93	0.74	0.37	2.21	1.09	1.44	0.04
0.29	0.04	0.34	0.33	89.56	0.21	3.53	0.62	0.31	1.71	1.13	1.33	0.03
0.33				80.05	0.27	5.19	1.70	0.71	3.41	1.31	1.61	0.06
0.37				88.27	0.20	3.77	0.77	0.36	1.98	1.03	1.38	0.04
0.41	0.05	0.38	0.33	89.38	0.22	3.57	0.67	0.32	1.76	0.97	1.31	0.03
0.46				82.54	0.26	4.69	1.34	0.59	2.98	1.19	1.52	0.05
0.50				87.65	0.26	3.73	0.81	0.37	1.96	1.01	1.33	0.04
0.54	0.04	0.35	0.34	88.72	0.32	3.54	0.73	0.33	1.85	0.93	1.27	0.04
0.59				89.27	0.35	3.42	0.76	0.31	1.68	0.93	1.21	0.04
0.67				89.65	0.21	3.42	0.59	0.30	1.66	0.93	1.27	0.03
0.73	0.04	0.36	0.35	89.13	0.20	3.60	0.65	0.32	1.84	0.98	1.34	0.04
0.77				86.07	0.28	3.94	0.94	0.42	2.54	1.06	1.39	0.05
0.81	0.05	0.35	0.33	89.26	0.39	3.54	0.80	0.32	1.78	0.93	1.26	0.04
0.82				85.99	0.23	4.13	0.96	0.44	2.63	1.05	1.45	0.04
0.85				86.62	0.35	3.74	0.90	0.39	2.19	1.01	1.32	0.04
0.86				88.17	0.20	3.78	0.66	0.34	2.08	1.02	1.41	0.04
0.88	0.03	0.27	0.27	90.26	0.45	3.35	0.78	0.30	1.57	0.91	1.18	0.04
0.93	0.03	0.31	0.31	89.84	0.23	3.52	0.63	0.30	1.69	0.96	1.30	0.03
0.99				90.12	0.22	3.38	0.59	0.30	1.63	0.92	1.24	0.03
1.07				89.31	0.21	3.57	0.63	0.32	1.82	0.95	1.32	0.03
1.13	0.07	0.70	0.56	85.33	0.29	4.01	0.93	0.43	2.84	1.05	1.41	0.05
1.18				90.80	0.24	3.11	0.59	0.27	1.46	0.84	1.12	0.03
1.23				89.58	0.36	3.32	0.73	0.30	1.62	0.90	1.17	0.04
1.28	0.04	0.70	0.26	89.77	0.36	3.24	0.77	0.29	1.49	0.88	1.15	0.04
1.33				90.43	0.27	3.31	0.66	0.28	1.49	0.90	1.23	0.03
1.38				88.33	0.23	3.82	0.72	0.35	2.07	1.02	1.39	0.04
1.44	0.05	0.46	0.45	87.46	0.29	3.98	0.82	0.38	2.28	1.03	1.42	0.04
1.50				88.06	0.39	3.72	0.81	0.36	2.05	0.96	1.32	0.04
1.56				88.58	0.36	3.50	0.79	0.34	1.97	0.86	1.25	0.05
1.62	0.04	0.60	0.36	88.77	0.19	3.65	0.63	0.32	1.84	0.96	1.36	0.04
1.68				88.87	0.19	3.64	0.64	0.32	1.89	0.99	1.38	0.04
1.74				89.58	0.21	3.52	0.63	0.30	1.73	0.94	1.33	0.03
1.78	0.05	0.43	0.39	88.51	0.22	3.77	0.77	0.35	1.98	0.98	1.37	0.04
1.82				89.11	0.21	3.63	0.67	0.31	1.86	0.99	1.36	0.04
1.87				89.06	0.18	3.65	0.66	0.32	1.86	0.95	1.35	0.03
1.90	0.06	0.46	0.40	87.90	0.21	3.94	0.84	0.37	2.05	1.00	1.41	0.04
1.94				88.67	0.20	3.66	0.68	0.32	1.87	0.97	1.36	0.03
1.99				87.75	0.20	3.80	0.75	0.35	2.09	1.00	1.39	0.04
2.05				88.31	0.21	3.75	0.72	0.34	2.00	1.01	1.39	0.03
2.10				88.30	0.17	3.81	0.70	0.34	2.08	1.06	1.43	0.04
2.17	0.07	0.61	0.41	87.84	0.19	3.90	0.76	0.36	2.08	1.05	1.42	0.04
2.22				88.64	0.21	3.70	0.69	0.33	1.98	0.98	1.36	0.04
2.26				87.62	0.24	3.88	0.78	0.37	2.23	1.03	1.42	0.04
2.32	0.06	0.51	0.44	87.71	0.21	3.88	0.77	0.36	2.21	1.01	1.41	0.04
2.39				88.02	0.18	3.85	0.68	0.35	2.11	1.05	1.44	0.03
2.43				88.31	0.16	3.81	0.67	0.34	2.04	1.05	1.43	0.03
3.04	0.12	0.83	0.48	86.35	0.27	3.74	1.02	0.40	2.42	1.03	1.31	0.04
3.11				87.04	0.28	3.74	1.03	0.38	2.27	0.98	1.32	0.04

## Arngast core (Archive No. GE 117)

Depth [m]	As	Ba	Co	Cr	Mn	Mo	Ni	Pb	Rb	Sr	U	V	Y	Zn	Zr
0.03		256	4	28	129		1	10	24	79	2	11	10	12	455
0.08		260	5	23	115		1	11	19	76	1	10	8	9	397
0.12		277	6	16	96		2	12	32	103	1	15	8	10	166
0.16		281	5	24	123		1	10	25	91	2	13	9	7	342
0.20		260	3	23	115		1	11	29	89	1	13	10	9	357
0.24		278	6	19	110		1	12	25	89	2	13	7	10	236
0.29		270	4	16	93		1	10	26	78	1	9	7	7	252
0.33		291	5	32	192		8	18	42	119	1	31	10	24	187
0.37		265	3	17	122		1	10	23	83	1	15	6	9	193
0.41		281	5	18	116		1	10	21	80	1	9	8	7	277
0.46		273	6	27	179		4	14	38	111	0	26	10	20	233
0.50		271	4	24	136		1	11	28	86	1	14	9	11	350
0.54		248	2	29	143		1	8	22	81	2	15	11	8	538
0.59		274	5	30	155		1	11	22	78	1	11	11	8	664
0.67		257	1	16	101		1	10	24	77	2	7	7	5	244
0.73		264	4	16	100		1	8	23	81	2	9	7	8	210
0.77		262	6	25	148		3	17	26	100	1	17	9	14	305
0.81		259	4	32	173		1	10	19	80	2	15	12	10	732
0.82		261	4	19	145		1	12	28	102	1	17	9	14	235
0.85		283	5	30	160		1	13	28	92	2	16	13	10	572
0.86		288	3	16	98		1	7	30	88	1	11	7	9	199
0.88		257	5	37	184		1	9	14	75	2	13	13	8	882
0.93		273	5	15	111		1	10	21	76	2	10	6	6	271
0.99		259	5	19	102		1	8	24	76	1	9	8	7	270
1.07		263	6	14	101		1	8	25	80	1	10	8	5	239
1.13		267	6	26	151		1	10	29	107	2	18	10	12	384
1.18		249	3	18	105		1	8	21	70	2	9	8	6	330
1.23		237	4	33	154		1	9	21	75	2	9	12	11	605
1.28		238	7	33	154		1	7	18	73	2	13	12	6	626
1.33		244	4	25	116		1	11	16	71	1	10	7	6	425
1.38		270	4	16	107		1	9	22	86	2	13	7	16	217
1.44		276	5	28	131		1	7	22	90	1	14	9	8	338
1.50		260	3	38	152		1	11	25	86	2	16	14	8	643
1.56		255	2	31	154		1	12	21	83	1	13	11	6	554
1.62		265	3	14	94		1	8	28	82	1	9	7	7	196
1.68		268	4	11	91		1	8	25	82	1	10	6	5	170
1.74		274	3	15	101		1	8	23	77	0	8	6	5	262
1.78		262	1	16	112		1	9	24	84	3	13	8	9	297
1.82		263	5	12	98		1	11	23	82	0	10	7	7	226
1.87		263	5	14	90		1	8	29	82	0	11	7	7	180
1.90		267	5	18	110		1	9	27	87	3	14	7	12	215
1.94		273	3	16	94		1	10	28	83	1	12	7	9	215
1.99		267	4	18	104		1	10	29	87	0	12	7	7	195
2.05		264	4	15	105		1	8	30	87	1	12	8	12	244
2.10		276	5	14	93		1	9	24	87	1	8	5	6	166
2.17		274	3	14	102		1	9	24	86	2	11	6	7	179
2.22		276	5	16	103		1	8	23	85	2	11	8	7	231
2.26		267	4	20	114		1	6	24	92	2	13	8	8	265
2.32		274	5	19	107		1	11	25	91	2	12	7	7	211
2.39		288	4	16	93		1	10	29	90	2	11	7	8	176
2.43		289	3	12	87		1	9	30	87	0	10	6	9	150
3.04		247	6	23	145		2	14	28	98	0	16	9	21	373
3.11		264	5	25	149		1	13	28	95	1	14	10	19	422

## Arngast core (Archive No. GE 117)

Depth [m]	TS	TC	TIC	SiO <sub>2</sub>	TiO <sub>2</sub>	Al <sub>2</sub> O <sub>3</sub>	Fe <sub>2</sub> O <sub>3</sub>	MgO	CaO	Na <sub>2</sub> O	K <sub>2</sub> O	P <sub>2</sub> O <sub>5</sub>
3.16				86.59	0.28	3.76	0.96	0.40	2.54	1.00	1.31	0.04
3.23	0.06	0.55	0.47	86.89	0.27	3.87	0.88	0.39	2.39	1.07	1.39	0.04
3.32				88.02	0.32	3.82	0.76	0.37	2.07	1.04	1.36	0.04
3.40				84.54	0.26	4.25	1.02	0.47	2.85	1.13	1.50	0.04
3.46	0.07	0.49	0.42	87.25	0.28	3.88	0.82	0.38	2.17	1.03	1.39	0.04
3.50				88.88	0.22	3.69	0.70	0.32	1.83	0.97	1.37	0.03
3.54				89.03	0.25	3.64	0.72	0.33	1.83	0.98	1.34	0.03
3.61	0.43	1.19	0.74	47.41	0.35	3.46	1.29	0.48	2.21	0.69	0.96	0.04
3.68				70.59	0.48	7.24	2.96	1.17	4.63	1.42	1.87	0.09
3.74				60.13	0.65	10.89	6.48	1.82	1.61	1.71	2.34	0.11
3.77	3.85	4.49	0.11	54.20	0.71	13.15	8.20	2.15	0.75	2.01	2.72	0.12
3.79				53.83	0.71	13.01	8.53	2.13	0.76	2.00	2.71	0.12
3.81				52.09	0.69	13.06	8.18	2.09	0.67	2.03	2.67	0.12
3.83	4.58	7.19	0.03	48.74	0.64	12.60	8.58	2.04	0.58	2.17	2.57	0.12
3.85	4.50	9.28	0.02	45.71	0.59	11.97	7.99	2.00	0.60	2.31	2.44	0.11
3.87	5.27	10.50	0.01	42.64	0.54	11.05	8.82	1.89	0.60	2.44	2.26	0.11
3.89	6.82	16.20	0.02	35.01	0.43	8.91	9.18	1.74	0.69	2.79	1.84	0.10
3.91	6.89	26.50	0.02	21.56	0.27	5.66	7.49	1.59	0.91	3.46	1.21	0.10
3.93	4.95	36.75	0.02	13.03	0.18	3.83	3.08	1.61	1.14	4.09	0.86	0.10
3.95	4.07	34.85	0.02	14.19	0.19	3.98	2.26	1.67	1.26	4.10	0.90	0.11
3.97	5.11	37.65	0.02	6.48	0.09	1.99	1.89	0.94	0.70	2.41	0.45	0.07
3.99	4.24	11.05	0.02	45.93	0.62	11.73	7.33	1.99	0.73	2.22	2.42	0.12
4.00	4.52	13.10	0.05	44.27	0.57	10.72	7.08	1.88	0.76	2.25	2.23	0.12
4.01	5.19	41.40	0.03	8.88	0.13	2.58	2.79	1.56	1.28	4.02	0.61	0.11
4.04	8.78	33.80	0.02	13.80	0.18	4.37	8.47	1.55	1.09	3.54	0.94	0.13
4.06	4.24	9.69	0.01	45.64	0.54	12.06	7.55	1.89	0.64	2.19	2.45	0.15
4.09	7.99	26.10	0.03	21.35	0.26	5.38	8.56	1.52	1.11	3.10	1.14	0.14
4.12	7.13	26.35	0.01	28.76	0.23	4.03	6.75	1.29	1.37	2.94	0.97	0.11
4.13	7.06	33.10	0.02	16.74	0.23	4.43	5.97	1.55	1.22	3.41	0.96	0.13
4.15	7.55	23.55	0.02	28.55	0.36	6.85	7.96	1.57	0.99	2.74	1.42	0.13
4.17	6.91	28.85	0.03	21.34	0.28	5.64	6.60	1.59	1.15	3.13	1.19	0.12
4.18	6.80	31.05	0.02	18.48	0.25	5.50	6.64	1.62	1.19	3.22	1.14	0.12
4.20	7.05	35.15	0.02	14.33	0.20	4.48	6.08	1.58	1.29	3.41	0.95	0.11
4.22	5.83	32.45	0.04	16.53	0.23	4.78	5.00	1.62	1.42	3.33	1.03	0.10
4.23	5.75	26.95	0.02	24.87	0.27	5.59	5.71	1.54	1.14	3.07	1.17	0.12
4.25	5.70	28.25	0.01	25.08	0.25	5.03	5.04	1.46	1.12	2.98	1.06	0.12
4.27	5.30	25.40	0.01	27.64	0.27	5.52	4.94	1.44	1.03	2.85	1.16	0.11
4.29	5.01	21.05	0.03	33.52	0.40	7.65	5.78	1.59	1.07	2.54	1.59	0.15
4.31	5.13	19.15	0.02	34.06	0.44	7.86	6.12	1.55	0.99	2.42	1.65	0.11
4.33	6.48	39.55	0.02	9.30	0.14	2.75	3.90	1.31	1.26	3.40	0.63	0.08
4.35				16.98	0.19	3.54	2.29	1.25	1.20	3.23	0.81	0.09
4.37				22.88	0.20	3.42	1.61	1.28	1.41	3.01	0.81	0.09
4.39	3.21	26.15	0.01	37.44	0.17	2.49	1.61	0.96	1.19	2.42	0.69	0.06
4.41	0.30	1.07	0.01	92.87	0.21	1.96	0.62	0.10	0.28	0.52	0.81	0.01
4.44	0.16	0.81	0.02	93.16	0.23	2.18	0.58	0.11	0.32	0.50	0.86	0.02
4.46	0.17	0.77	0.01	92.67	0.23	2.33	0.61	0.12	0.31	0.46	0.89	0.02
4.49	0.21	0.82	0.01	92.90	0.23	2.46	0.66	0.13	0.31	0.48	0.91	0.02
4.52	0.33	1.09	0.00	91.97	0.24	2.51	0.76	0.14	0.30	0.51	0.90	0.02
4.55	0.23	0.69	0.00	92.80	0.24	2.64	0.69	0.14	0.29	0.47	0.92	0.02

## Arngast core (Archive No. GE 117)

Depth [m]	As	Ba	Co	Cr	Mn	Mo	Ni	Pb	Rb	Sr	U	V	Y	Zn	Zr
3.16		262	2	27	144		1	12	27	101	2	15	9	16	399
3.23		280	4	23	133		1	15	29	99	2	15	9	22	371
3.32		282	3	31	133		1	12	26	88	1	14	10	7	431
3.40		290	3	25	144		1	14	33	110	2	20	9	10	314
3.46		268	5	23	130		1	11	27	91	0	14	10	8	360
3.50		273	5	18	111		1	8	29	82	1	12	9	9	291
3.54		273	2	23	114		1	11	25	82	0	11	7	6	285
3.61		191	2	39	147		1	11	12	75	0	24	10	0	537
3.68		299	7	59	346		13	22	68	155	3	57	18	42	413
3.74	27	294	9	85	489	12	28	25	116	104	5	115	24	78	334
3.77	23	272	9	101	580	12	38	30	131	96	4	140	24	93	166
3.79	30	275	12	105	583	13	36	28	133	97	5	142	24	93	173
3.81	28	277	13	99	472	14	36	28	138	99	6	141	23	93	156
3.83	32	269	14	93	390	18	39	26	137	101	9	141	22	88	134
3.85	28	257	18	88	307	16	37	25	127	103	10	140	21	86	115
3.87	35	292	13	83	273	21	40	24	122	103	12	132	19	79	107
3.89	28	192	10	66	281	36	33	19	100	107	14	120	18	70	90
3.91	21	131	3	44	298	38	22	17	57	122	14	98	18	51	61
3.93	14	87	4	31	348	38	17	10	44	160	14	77	9	37	40
3.95	11	90	4	32	398	29	16	7	45	176	11	59	9	30	42
3.97	3	49	4	20	298	28	10	4	18	95	7	49	5	21	21
3.99	23	254	12	88	655	22	36	24	119	109	10	116	19	92	128
4.00	21	225	9	85	661	28	34	22	109	109	9	107	18	83	133
4.01	15	65	5	23	428	40	15	8	24	175	16	62	8	49	32
4.04	28	96	18	38	483	65	33	20	43	164	32	97	18	116	43
4.06	8	269	16	84	395	46	43	24	128	119	25	121	16	130	93
4.09	31	141	8	48	631	59	26	36	54	170	24	83	20	110	73
4.12	21	138	5	33	573	30	17	12	40	169	10	49	12	67	123
4.13	22	101	7	38	822	30	19	11	42	185	10	54	14	72	52
4.15	28	157	8	52	1148	21	22	17	69	168	6	69	16	79	86
4.17	24	133	6	45	679	23	22	14	58	189	8	68	14	77	71
4.18	24	119	8	43	571	20	21	15	58	198	8	70	14	78	55
4.20	22	112	5	36	606	16	19	16	45	207	6	62	17	61	49
4.22	18	112	5	38	511	14	18	12	51	212	6	59	12	59	55
4.23	20	135	8	45	800	19	25	12	57	190	7	61	12	78	60
4.25	19	130	9	38	769	20	21	12	53	187	8	60	11	77	56
4.27	16	130	7	42	773	22	22	13	61	176	6	67	11	80	63
4.29	18	179	9	58	878	20	28	17	83	182	7	83	15	87	98
4.31	22	183	7	62	1094	15	26	19	86	182	4	76	16	75	127
4.33	13	67	2	24	317	20	10	10	27	198	5	46	8	40	36
4.35	11	92	3	28	225	19	11	9	39	186	5	46	7	37	63
4.37	7	109	3	28	259	10	11	11	37	230	4	39	7	28	97
4.39	2	114	2	22	204	7	5	10	24	198	4	26	7	21	180
4.41		186	3	12	67			13	13	41	0	6	5	7	383
4.44		196	4	25	73			8	17	44	1	9	6	15	392
4.46		196	3	10	82			8	16	47	2	8	7	13	488
4.49		213	3	10	89			10	15	50	2	11	6	8	409
4.52		216	4	16	86			8	17	52	1	10	7	7	425
4.55		213	1	14	84			9	16	50	2	9	6	7	432

## Arngast core (Archive No. GE 117)

Depth [m]	TS	TC	TIC	SiO <sub>2</sub>	TiO <sub>2</sub>	Al <sub>2</sub> O <sub>3</sub>	Fe <sub>2</sub> O <sub>3</sub>	MgO	CaO	Na <sub>2</sub> O	K <sub>2</sub> O	P <sub>2</sub> O <sub>5</sub>
4.58				92.51	0.24	2.69	0.68	0.14	0.31	0.48	0.91	0.03
4.60	0.25	0.86	0.00	92.04	0.25	2.79	0.75	0.15	0.32	0.48	0.93	0.04
4.63	0.23	0.77	0.00	92.33	0.25	2.73	0.76	0.14	0.30	0.46	0.90	0.03
4.66	0.27	0.56	0.00	92.85	0.23	2.70	0.76	0.13	0.28	0.44	0.90	0.03
4.68				92.74	0.22	2.60	0.72	0.12	0.27	0.46	0.87	0.03
4.71	0.19	0.35	0.00	93.61	0.21	2.49	0.65	0.11	0.25	0.40	0.85	0.02
4.72				92.31	0.19	2.39	0.62	0.11	0.24	0.38	0.83	0.02
4.75				94.28	0.19	2.41	0.64	0.10	0.24	0.39	0.85	0.02
4.79	0.19	0.21	0.00	94.50	0.17	2.26	0.62	0.09	0.23	0.36	0.81	0.02
4.82				94.71	0.17	2.20	0.63	0.08	0.22	0.37	0.78	0.03
4.84				94.23	0.19	2.20	0.69	0.09	0.24	0.36	0.78	0.03
4.87	0.27	0.28	0.00	94.05	0.22	2.27	0.76	0.09	0.25	0.37	0.81	0.03
4.90				93.95	0.20	2.30	0.69	0.09	0.23	0.39	0.85	0.03
4.93				94.37	0.16	2.18	0.69	0.08	0.23	0.34	0.80	0.02
4.96	0.22	0.17	0.00	93.78	0.17	2.30	0.67	0.09	0.23	0.41	0.85	0.02
5.00				93.62	0.17	2.26	0.58	0.08	0.22	0.36	0.84	0.02
5.07	0.17	0.08	0.00	94.23	0.15	2.37	0.56	0.08	0.23	0.37	0.89	0.02
5.10	0.15	0.04	0.00	95.20	0.14	2.29	0.49	0.08	0.21	0.37	0.88	0.02

Depth [m]	As	Ba	Co	Cr	Mn	Mo	Ni	Pb	Rb	Sr	U	V	Y	Zn	Zr
4.58		198	1	12	92			9	13	52	1	12	6	6	429
4.60		212	4	16	97			8	16	57	3	12	7	8	434
4.63		207	3	11	101			8	15	53	3	10	7	7	433
4.66		204	3	14	97			8	14	50	0	9	6	6	428
4.68		197	2	13	93			7	15	49	2	7	6	6	439
4.71		207	4	12	90			6	12	44	1	9	5	5	400
4.72		215	3	9	85			4	13	42	0	5	5	7	414
4.75		202	3	17	83			9	14	43	0	7	6	9	393
4.79		195	3	9	82			8	14	40	1	4	5	9	361
4.82		191	2	7	76			7	11	40	3	6	5	8	408
4.84		201	4	8	81			7	11	43	1	5	5	10	410
4.87		196	1	12	100			7	12	43	2	5	5	10	549
4.90		264	2	11	94			7	12	41	0	5	5	6	389
4.93		200	4	3	89			8	7	40	1	5	3	10	289
4.96		196	3	8	75			7	12	41	1	4	4	5	393
5.00		194	3	7	73			6	6	40	1	5	3	1	278
5.07		200	2	2	66			8	6	41	1	6	3	2	245
5.10		204	2	3	64			6	9	38	1	4	3	2	276

## Wangerland core W1 (Archive No. KB 5552)

Depth [m]	TS	TC	TIC	SiO <sub>2</sub>	TiO <sub>2</sub>	Al <sub>2</sub> O <sub>3</sub>	Fe <sub>2</sub> O <sub>3</sub>	MgO	CaO	Na <sub>2</sub> O	K <sub>2</sub> O	P <sub>2</sub> O <sub>5</sub>
0.34	0.03	1.41	0.03	71.17	0.65	10.68	4.69	1.34	1.10	0.74	2.55	0.39
0.48				69.60	0.69	11.51	5.15	1.56	1.38	0.70	2.70	0.37
0.58				69.88	0.69	11.04	4.85	1.50	1.47	0.72	2.64	0.45
0.79				69.99	0.72	11.33	5.04	1.61	1.19	0.74	2.70	0.35
1.06				68.80	0.71	11.13	4.96	1.66	1.85	0.73	2.65	0.44
1.17	0.03	1.17	0.07	71.40	0.71	10.96	4.56	1.43	1.10	0.77	2.67	0.41
1.27				69.38	0.76	12.15	5.36	1.61	0.93	0.73	2.87	0.35
1.37	0.05	0.64	0.03	69.94	0.75	11.80	5.71	1.53	0.79	0.74	2.81	0.24
1.45	0.02	0.60	0.06	70.10	0.75	11.92	5.17	1.48	0.86	0.74	2.82	0.19
1.51				67.84	0.68	10.72	4.29	1.59	2.86	0.73	2.53	0.19
1.56	0.03	1.19	0.45	70.29	0.69	10.40	4.31	1.53	2.30	0.76	2.50	0.20
1.61				64.82	0.74	12.67	6.34	1.81	1.18	0.63	3.04	0.40
1.66				64.18	0.75	13.43	5.72	1.76	0.81	0.63	3.30	0.21
1.73				69.17	0.75	12.53	5.01	1.54	0.74	0.70	3.14	0.18
1.79				69.62	0.76	12.59	5.11	1.48	0.61	0.72	3.17	0.20
1.84	0.07	0.93	0.01	67.19	0.77	13.29	5.63	1.55	0.56	0.65	3.34	0.28
1.90				70.14	0.76	12.50	4.92	1.43	0.54	0.73	3.15	0.23
1.95				69.56	0.77	12.38	5.24	1.37	0.51	0.73	3.20	0.21
2.01	0.14	0.71	0.04	68.72	0.77	13.01	5.04	1.50	0.65	0.69	3.24	0.13
2.06	0.34	1.32	0.19	68.64	0.72	11.64	5.17	1.57	1.20	0.71	2.96	0.21
2.10	0.11	1.48	0.41	68.55	0.71	10.81	4.63	1.63	1.98	0.71	2.81	0.29
2.13				67.02	0.68	11.09	4.76	1.62	2.11	0.69	2.88	0.27
2.16	0.19	2.17	0.73	62.56	0.67	11.95	5.35	1.87	3.44	0.61	3.01	0.20
2.20	0.28	1.92	0.84	64.25	0.65	10.91	4.98	1.72	3.87	0.67	2.80	0.19
2.24				66.65	0.65	10.01	4.75	1.58	3.94	0.74	2.60	0.20
2.29	0.54	5.49	0.29	59.60	0.64	11.86	5.84	1.66	1.06	0.54	3.05	0.47
2.33	0.51	5.46	0.08	59.83	0.63	11.74	5.67	1.66	1.06	0.54	3.03	0.42
2.35	0.44	5.41	0.15	59.54	0.63	11.41	5.54	1.65	1.27	0.57	2.96	0.45
2.37	0.43	5.82	0.07	60.08	0.63	11.63	5.62	1.67	0.97	0.55	3.00	0.49
2.46	0.28	5.09	0.16	61.14	0.63	11.58	5.53	1.69	1.31	0.54	2.98	0.43
2.53	0.29	4.50	0.25	62.22	0.64	11.55	5.32	1.76	1.57	0.73	2.99	0.35
2.58	0.21	2.93	0.36	69.25	0.63	9.15	4.04	1.40	1.94	0.77	2.49	0.37
2.61	0.16	2.82	0.30	70.91	0.62	8.96	3.79	1.36	1.66	0.79	2.47	0.33
2.65	0.14	2.67	0.31	70.50	0.63	9.19	3.89	1.42	1.89	0.78	2.51	0.46
2.68	0.09	1.56	0.57	71.02	0.63	9.17	3.88	1.43	2.71	0.77	2.48	0.31
2.71				71.49	0.65	9.18	3.75	1.46	3.15	0.79	2.45	0.22
2.74				73.36	0.64	8.90	3.59	1.39	2.40	0.81	2.40	0.19
2.78	0.11	0.79	0.39	73.91	0.64	9.30	3.71	1.43	1.80	0.82	2.47	0.14
2.82				75.38	0.62	8.90	3.48	1.37	1.60	0.83	2.40	0.15
2.86	0.04	0.56	0.27	77.43	0.62	8.46	3.17	1.28	1.22	0.88	2.32	0.14
2.90				77.72	0.65	8.52	3.19	1.28	1.09	0.85	2.33	0.16
2.95				73.70	0.68	9.94	4.09	1.49	1.07	0.81	2.59	0.23
2.99	0.03	0.54	0.18	75.21	0.67	9.59	3.52	1.37	0.97	0.83	2.52	0.17
3.04	0.05	0.80	0.19	69.60	0.68	11.07	5.32	1.68	1.00	0.74	2.85	0.41
3.09				70.12	0.74	11.88	4.50	1.70	1.00	0.74	2.94	0.15
3.14	0.03	0.75	0.24	73.95	0.71	10.22	3.60	1.54	1.13	0.82	2.61	0.14
3.18	0.03	0.85	0.38	75.68	0.72	9.00	3.02	1.40	1.72	0.88	2.36	0.12
3.22				78.88	0.75	7.35	2.24	1.13	2.01	0.91	2.04	0.12
3.25	0.02	0.59	0.23	77.71	0.73	8.42	2.80	1.22	1.16	0.86	2.27	0.12
3.29				69.90	0.74	11.61	5.18	1.80	1.05	0.73	2.98	0.14
3.32				69.10	0.71	11.65	5.50	1.86	1.14	0.71	2.98	0.18
3.36	0.04	0.74	0.23	68.23	0.70	11.80	5.72	1.90	1.07	0.70	3.01	0.24



## Wangerland core W1 (Archive No. KB 5552)

Depth [m]	As	Ba	Co	Cr	Mn	Mo	Ni	Pb	Rb	Sr	U	V	Y	Zn	Zr
0.34	12	299	8	84	589	2	25	20	109	100	3	98	27	82	339
0.48	14	303	13	91	666	2	28	21	116	101	3	105	29	81	313
0.58	14	299	9	88	627	2	23	20	114	105	2	103	27	76	339
0.79	14	307	10	89	713	2	26	22	115	97	2	105	29	75	349
1.06	21	300	10	91	782	2	25	19	109	106	3	108	29	71	358
1.17	19	298	9	87	287	2	23	19	110	100	4	95	28	74	372
1.27	21	306	10	99	658	4	27	21	122	95	2	115	31	71	356
1.37	19	304	12	94	689	3	26	20	117	88	3	117	30	70	355
1.45	16	309	13	95	596	3	25	21	118	88	3	119	31	65	352
1.51	18	281	10	87	248	1	25	19	105	107	3	105	28	64	348
1.56	24	283	8	87	279	2	21	18	101	101	3	95	29	62	378
1.61	39	290	12	96	294	4	30	22	130	94	2	128	29	84	256
1.66	29	292	12	99	263	8	32	22	140	83	4	132	29	91	223
1.73	16	314	13	94	256	3	28	21	127	84	4	119	30	76	304
1.79	13	312	12	96	256	4	26	21	128	84	4	122	31	74	318
1.84	14	312	12	99	294	1	26	24	138	81	3	130	30	82	253
1.90	12	313	10	98	263	1	24	20	128	82	4	118	28	74	301
1.95	16	306	10	98	263	2	26	20	128	81	3	112	28	75	284
2.01	13	316	10	100	240	2	26	23	131	85	4	125	30	78	285
2.06	21	298	12	90	333	2	26	20	119	89	2	112	28	71	344
2.10	14	293	10	88	449	2	24	20	108	95	4	105	29	68	382
2.13	17	291	11	87	511	2	27	20	116	101	2	107	26	76	331
2.16	16	271	14	91	604	2	29	20	123	121	3	115	27	82	235
2.20	17	285	12	83	658	4	25	19	110	129	2	104	26	76	289
2.24	25	276	10	81	658	0	22	17	101	128	2	90	25	61	340
2.29	36	266	12	89	589	3	27	20	123	87	3	121	24	103	203
2.33	36	259	8	88	573	2	28	19	122	89	4	114	24	104	207
2.35	35	256	10	86	589	4	27	20	118	91	3	115	23	98	213
2.37	36	264	11	89	589	2	26	19	119	87	3	114	24	101	205
2.46	31	269	10	88	550	2	27	20	119	89	2	114	25	99	214
2.53	29	263	13	89	496	2	27	18	119	95	1	114	27	92	232
2.58	22	277	9	75	542	2	18	17	91	99	4	78	24	70	359
2.61	21	280	9	73	480	1	17	17	89	94	2	72	26	67	365
2.65	20	277	10	73	472	1	18	16	93	96	2	79	23	74	364
2.68	14	289	9	78	596	2	18	16	91	108	2	73	25	60	395
2.71	11	294	9	78	488	2	18	16	89	111	2	78	25	54	396
2.74	12	294	10	80	410	2	18	16	85	101	4	76	27	49	463
2.78	16	298	11	77	387	6	21	15	89	92	3	81	25	50	415
2.82	14	293	9	74	364	3	18	14	85	89	2	74	25	48	405
2.86	11	296	9	73	395	2	17	15	82	85	3	68	25	43	447
2.90	10	303	8	75	387	1	15	14	80	81	3	70	26	42	518
2.95	12	301	8	84	550	1	21	17	94	84	2	93	29	54	423
2.99	10	303	8	79	294	1	17	16	90	83	3	77	28	51	413
3.04	15	284	9	86	658	1	22	23	111	84	2	116	29	68	352
3.09	10	303	9	95	263	1	24	21	119	87	2	106	29	70	356
3.14	9	310	8	86	248	1	20	18	96	86	2	87	30	61	424
3.18	9	303	7	85	240	1	18	15	88	93	3	73	31	49	563
3.22	8	306	7	86	232	2	12	14	69	96	4	55	32	34	826
3.25	9	310	5	81	217	1	11	15	81	87	3	66	31	43	684
3.29	11	293	8	93	240	2	23	19	117	89	3	110	28	74	382
3.32	11	305	13	93	287	2	25	20	113	88	3	108	29	73	333
3.36	12	293	11	90	325	1	26	21	118	88	2	124	29	76	305

## Wangerland core W1 (Archive No. KB 5552)

Depth [m]	TS	TC	TIC	SiO <sub>2</sub>	TiO <sub>2</sub>	Al <sub>2</sub> O <sub>3</sub>	Fe <sub>2</sub> O <sub>3</sub>	MgO	CaO	Na <sub>2</sub> O	K <sub>2</sub> O	P <sub>2</sub> O <sub>5</sub>
3.39				69.56	0.73	11.63	4.73	1.57	0.78	0.72	2.98	0.17
3.43	0.10	1.84	0.08	67.85	0.73	12.20	4.83	1.58	0.72	0.67	3.08	0.17
3.48	0.10	1.62	0.08	68.51	0.72	11.98	4.91	1.60	0.72	0.68	3.02	0.20
3.53				70.31	0.70	11.07	4.59	1.49	0.83	0.76	2.85	0.23
3.57				69.33	0.69	11.17	4.82	1.53	1.08	0.74	2.85	0.25
3.61	0.12	1.79	0.21	68.09	0.70	11.58	4.97	1.64	1.18	0.73	2.94	0.17
3.65				67.76	0.69	11.19	4.98	1.78	2.62	0.70	2.83	0.13
3.69				64.11	0.67	11.26	5.24	1.91	4.23	0.67	2.79	0.14
3.73	0.04	1.52	1.03	64.01	0.66	10.94	5.45	1.88	4.61	0.68	2.74	0.15
3.77				66.02	0.64	10.28	4.58	1.76	4.61	0.71	2.59	0.13
3.81				64.79	0.67	10.66	4.46	1.82	5.23	0.71	2.63	0.13
3.85	0.04	1.74	1.25	62.49	0.64	10.85	4.88	1.86	5.66	0.64	2.67	0.13
3.89				64.07	0.63	10.53	4.57	1.79	5.51	0.65	2.59	0.12
3.94	0.05	1.88	1.38	62.19	0.66	11.09	4.59	1.87	6.19	0.66	2.67	0.13
3.98				60.65	0.64	10.99	4.51	1.87	6.67	0.61	2.61	0.13
4.03	0.14	1.92	1.39	62.80	0.64	10.60	4.21	1.78	6.30	0.65	2.55	0.13
4.08				60.93	0.65	10.97	4.31	1.83	6.57	0.62	2.59	0.13
4.12				62.78	0.64	10.83	4.32	1.83	6.08	0.68	2.57	0.13
4.15	0.16	2.05	1.37	62.89	0.63	10.51	4.28	1.76	6.21	0.65	2.51	0.13
4.20				63.63	0.60	10.09	4.09	1.69	6.34	0.67	2.43	0.13
4.32	0.67	2.99	1.60	57.42	0.65	11.35	4.97	1.94	7.27	0.60	2.60	0.14
4.38				58.14	0.65	11.15	4.86	1.87	6.82	0.58	2.54	0.14
4.44	0.93	3.03	1.44	59.19	0.64	10.98	4.59	1.83	6.64	0.59	2.50	0.14
4.48				58.22	0.65	11.37	4.92	1.90	6.46	0.57	2.55	0.14
4.53				57.73	0.65	11.38	5.04	1.92	6.74	0.56	2.54	0.15
4.59	1.73	3.34	1.51	56.08	0.65	11.46	5.63	1.90	6.96	0.54	2.54	0.15
4.63	1.55	3.38	1.60	56.38	0.64	11.21	5.27	1.88	7.33	0.56	2.50	0.15
4.68				56.27	0.65	11.39	5.34	1.94	7.38	0.55	2.51	0.15
4.74	1.34	3.22	1.49	58.27	0.65	11.02	4.78	1.84	6.86	0.57	2.46	0.15
4.79				54.42	0.65	11.36	5.25	1.94	8.01	0.53	2.49	0.16
4.84	1.61	3.51	1.77	55.25	0.64	11.23	5.17	1.94	8.20	0.55	2.45	0.16
4.89				53.90	0.63	10.88	6.08	1.89	8.30	0.54	2.38	0.17
4.91	1.72	3.78	1.87	53.72	0.63	10.93	5.20	1.93	8.78	0.54	2.37	0.17
4.93	1.82	3.73	1.86	53.66	0.63	11.10	5.35	1.91	8.65	0.52	2.41	0.17
4.96				55.57	0.60	10.39	5.01	1.79	8.36	0.57	2.30	0.17
4.99				58.51	0.60	9.95	4.87	1.71	7.94	0.61	2.26	0.16
5.02	1.50	3.25	1.72	59.10	0.59	9.49	4.50	1.62	7.90	0.61	2.19	0.16
5.05				62.71	0.56	8.85	3.85	1.51	7.43	0.66	2.09	0.15
5.08	1.60	3.45	1.85	56.40	0.60	10.12	4.78	1.74	8.55	0.55	2.27	0.17
5.12	1.28	2.99	1.61	62.46	0.57	8.76	3.92	1.48	7.40	0.69	2.08	0.15
5.16	0.57	1.70	1.15	74.55	0.52	6.07	2.14	0.95	5.33	0.80	1.71	0.14
5.20	0.57	1.62	1.09	75.11	0.52	6.07	2.09	0.94	5.02	0.80	1.72	0.13
5.25				74.16	0.53	6.19	2.23	0.97	5.20	0.81	1.74	0.12
5.30				71.52	0.54	6.90	2.70	1.12	5.59	0.81	1.85	0.12
5.35				73.53	0.50	6.35	2.31	0.99	5.42	0.82	1.74	0.11
5.40				72.82	0.50	6.50	2.40	1.04	5.61	0.83	1.77	0.10
5.47				70.88	0.50	6.88	2.60	1.15	6.14	0.83	1.82	0.11
5.53	0.64	1.84	1.23	73.29	0.47	6.35	2.26	1.02	5.60	0.82	1.74	0.10
5.59				73.56	0.48	6.40	2.24	1.02	5.78	0.85	1.75	0.10
5.65				70.69	0.49	6.87	2.58	1.14	6.37	0.85	1.79	0.11
5.71				74.53	0.49	6.16	2.20	0.95	5.10	0.80	1.71	0.09
5.77	0.79	1.93	1.22	72.13	0.50	6.72	2.62	1.07	5.60	0.78	1.78	0.10

## Wangerland core W1 (Archive No. KB 5552)

Depth [m]	As	Ba	Co	Cr	Mn	Mo	Ni	Pb	Rb	Sr	U	V	Y	Zn	Zr
3.39	13	305	9	93	256	2	24	22	119	88	3	114	29	77	327
3.43	19	309	12	92	240	1	29	23	129	88	3	130	28	86	294
3.48	18	299	10	92	256	1	26	20	124	87	3	117	28	83	281
3.53	17	296	10	87	256	1	23	21	115	87	2	104	28	74	326
3.57	21	304	10	85	263	2	22	20	115	93	4	103	27	72	313
3.61	21	293	12	88	240	2	24	21	119	92	2	112	27	71	297
3.65	12	293	9	85	256	1	23	19	112	109	3	103	28	65	315
3.69	11	283	11	85	271	1	26	18	112	126	2	106	29	68	265
3.73	11	279	10	85	279	2	21	19	109	131	3	104	27	64	264
3.77	9	285	8	79	256	2	21	17	102	131	2	96	27	61	322
3.81	9	283	9	86	263	1	21	18	107	142	2	100	27	64	331
3.85	10	280	11	84	271	2	22	18	108	150	1	105	26	64	260
3.89	9	278	10	81	256	2	21	17	102	146	3	100	26	64	286
3.94	12	283	13	85	271	1	30	19	108	159	4	110	27	68	255
3.98	19	276	14	83	271	2	31	19	108	170	3	110	26	72	239
4.03	19	273	12	82	271	2	30	17	103	162	3	107	25	65	265
4.08	19	274	11	86	263	2	26	19	107	165	3	115	26	69	256
4.12	18	280	9	86	256	2	26	18	106	158	3	106	27	65	289
4.15	17	268	9	84	256	3	25	17	103	159	3	105	25	64	263
4.20	25	273	9	84	256	2	26	18	98	159	2	102	24	60	247
4.32	30	264	13	87	294	3	30	19	112	178	4	117	26	74	216
4.38	33	265	12	92	356	4	30	20	108	169	3	114	26	71	220
4.44	24	260	11	86	318	3	30	19	107	166	2	107	25	71	230
4.48	15	266	13	87	318	3	29	19	110	165	3	115	26	73	225
4.53	13	262	11	89	325	2	29	20	111	171	3	114	27	74	236
4.59	25	253	12	89	356	3	30	19	110	175	3	116	26	75	203
4.63	13	259	11	85	395	2	29	19	110	183	3	114	26	73	210
4.68	15	247	13	89	434	3	28	19	111	190	3	116	26	73	222
4.74	17	262	11	85	434	3	26	19	107	180	2	113	26	71	253
4.79	19	253	13	89	480	3	29	20	111	219	3	113	26	76	207
4.84	17	258	13	85	534	4	29	19	112	225	3	115	25	73	213
4.89	30	263	11	86	643	4	30	19	107	244	4	110	25	73	223
4.91	16	248	12	83	651	3	26	19	108	259	2	114	25	72	217
4.93	17	243	12	88	666	5	30	19	108	254	3	117	25	78	200
4.96	17	253	11	81	573	2	26	18	101	250	2	104	25	68	234
4.99	19	254	8	76	565	3	26	17	96	234	1	99	26	67	262
5.02	17	252	9	76	643	3	22	17	93	238	2	93	25	61	296
5.05	12	264	9	72	558	3	20	16	85	223	2	84	23	56	327
5.08	15	249	10	80	573	2	26	17	98	255	3	100	24	69	237
5.12	13	263	9	70	496	3	21	14	85	220	3	82	23	52	350
5.16	9	274	6	59	333	2	8	12	58	162	3	42	23	27	515
5.20	10	270	7	58	302	2	8	10	58	155	2	42	23	30	517
5.25	10	269	8	61	318	2	8	11	60	160	4	47	23	28	536
5.30	12	268	7	61	356	2	13	12	66	170	3	55	24	35	470
5.35	10	256	5	56	325	2	9	12	60	166	3	48	21	31	468
5.40	10	266	7	56	318	3	9	12	64	167	2	49	21	32	438
5.47	11	273	7	56	341	2	13	11	66	179	2	54	22	37	391
5.53	9	276	7	52	279	1	10	12	61	169	2	47	20	31	385
5.59	9	273	4	56	271	1	10	13	60	172	3	46	21	34	406
5.65	10	264	6	58	302	2	12	12	66	188	2	54	21	37	383
5.71	10	267	7	53	279	2	9	12	61	159	2	47	21	29	484
5.77	13	268	7	58	310	4	11	12	66	170	3	48	21	34	459

## Wangerland core W1 (Archive No. KB 5552)

Depth [m]	TS	TC	TIC	SiO <sub>2</sub>	TiO <sub>2</sub>	Al <sub>2</sub> O <sub>3</sub>	Fe <sub>2</sub> O <sub>3</sub>	MgO	CaO	Na <sub>2</sub> O	K <sub>2</sub> O	P <sub>2</sub> O <sub>5</sub>
5.83				74.47	0.46	6.08	2.18	0.94	5.44	0.84	1.70	0.09
5.88	0.66	1.73	1.05	74.38	0.47	6.29	2.29	0.96	4.89	0.79	1.72	0.09
5.93				74.82	0.47	6.09	2.21	0.92	5.17	0.80	1.69	0.09
5.98				73.27	0.47	6.20	2.34	0.96	5.71	0.80	1.69	0.09
6.03	0.78	2.04	1.29	71.74	0.51	6.65	2.60	1.08	5.90	0.80	1.75	0.10
6.07				73.11	0.45	6.27	2.31	0.98	5.49	0.78	1.71	0.09
6.11	0.67	1.81	1.22	73.48	0.44	6.31	2.28	1.00	5.59	0.83	1.71	0.09
6.14				68.95	0.51	7.39	2.89	1.22	6.46	0.77	1.85	0.11
6.17				68.70	0.48	7.37	2.88	1.20	6.47	0.77	1.85	0.11
6.22	0.49	1.65	1.18	75.64	0.39	5.65	1.91	0.87	5.45	0.86	1.63	0.08
6.26	0.47	1.45	1.10	77.31	0.34	5.36	1.72	0.78	5.04	0.85	1.59	0.07
6.29	0.41	1.33	1.06	78.15	0.33	5.15	1.57	0.75	4.83	0.86	1.55	0.07
6.33	0.49	1.39	1.06	77.46	0.35	5.35	1.74	0.78	4.84	0.83	1.58	0.07
6.37	0.62	1.89	1.27	72.97	0.46	6.43	2.32	1.03	5.79	0.81	1.72	0.09
6.41				66.33	0.48	7.61	3.28	1.27	6.60	0.72	1.86	0.11
6.45				76.44	0.40	5.68	2.03	0.84	4.81	0.83	1.63	0.08
6.49				72.45	0.47	6.68	2.72	1.07	5.38	0.81	1.74	0.10
6.53				72.06	0.45	6.38	2.59	1.02	5.87	0.81	1.69	0.10
6.58	0.81	2.00	1.21	72.89	0.46	6.26	2.48	1.01	5.58	0.85	1.68	0.09
6.64				70.25	0.47	6.36	2.64	1.02	6.88	0.82	1.66	0.10
6.71				73.05	0.48	6.53	2.57	1.03	5.13	0.82	1.71	0.10
6.77				71.48	0.49	6.88	2.84	1.11	5.74	0.83	1.75	0.10
6.83	0.71	1.93	1.30	72.95	0.47	6.23	2.41	0.98	5.91	0.86	1.66	0.09
6.87	0.66	1.91	1.20	73.75	0.46	6.19	2.29	0.98	5.50	0.86	1.67	0.09
6.92				73.37	0.45	6.08	2.20	0.97	5.78	0.85	1.63	0.09
6.97				75.01	0.47	6.26	2.16	0.97	5.16	0.85	1.67	0.09
7.01	0.63	1.86	1.18	73.46	0.48	6.38	2.32	1.02	5.43	0.85	1.69	0.09
7.05	0.64	1.77	1.22	73.32	0.53	6.15	2.29	1.01	5.55	0.88	1.65	0.10
7.09				71.44	0.47	6.22	2.44	0.97	6.59	0.83	1.64	0.09
7.14				68.02	0.50	6.95	2.99	1.12	7.19	0.81	1.71	0.10
7.18	1.17	2.23	1.26	69.71	0.55	7.25	3.24	1.18	5.75	0.77	1.75	0.11
7.22				69.11	0.60	7.84	3.44	1.27	5.16	0.80	1.88	0.11
7.27	1.17	2.34	1.16	66.45	0.65	8.92	3.81	1.49	5.31	0.84	2.05	0.12
7.33				69.83	0.65	8.28	3.38	1.33	4.38	0.85	1.96	0.11
7.39	0.95	1.94	0.98	71.10	0.62	7.81	3.15	1.23	4.50	0.85	1.89	0.11
7.46	1.34	2.69	1.36	63.97	0.61	9.04	4.05	1.49	6.11	0.84	2.03	0.12
7.62	1.62	2.67	1.32	63.74	0.60	9.12	4.38	1.49	6.10	0.86	2.02	0.12
7.68	1.57	2.67	1.31	63.76	0.60	9.27	4.42	1.54	6.02	0.87	2.04	0.12
7.73	1.62	2.85	1.34	61.58	0.62	10.04	4.71	1.69	6.13	0.82	2.16	0.13
7.78				61.04	0.63	10.05	4.73	1.68	5.98	0.81	2.17	0.13
7.83				61.42	0.66	10.69	4.88	1.79	5.55	0.83	2.27	0.14
7.90				64.62	0.66	9.41	4.22	1.59	5.39	0.86	2.11	0.13
7.96	1.57	2.87	1.36	63.03	0.63	9.15	4.44	1.52	6.24	0.86	2.05	0.12
8.01	1.53	2.63	1.19	65.56	0.59	8.75	4.28	1.48	5.45	0.90	2.00	0.12
8.12	1.75	3.23	1.39	59.49	0.62	10.28	5.18	1.75	6.25	0.83	2.19	0.14
8.17	1.95	3.22	1.41	60.19	0.61	9.67	5.20	1.68	6.38	0.87	2.11	0.14
8.25	1.19	2.98	1.30	64.26	0.67	9.89	4.62	1.60	4.32	0.87	2.18	0.15
8.26	0.92	2.70	1.14	64.52	0.63	9.57	4.07	1.63	5.12	0.90	2.14	0.15
8.30	1.04	2.81	1.19	63.94	0.60	9.56	4.18	1.59	5.30	0.90	2.12	0.13
8.34	0.96	3.05	1.19	61.07	0.65	10.55	4.58	1.76	5.30	0.89	2.26	0.17
8.37	0.76	3.06	1.17	61.21	0.65	10.65	4.43	1.78	5.21	0.87	2.29	0.21

## Wangerland core W1 (Archive No. KB 5552)

Depth [m]	As	Ba	Co	Cr	Mn	Mo	Ni	Pb	Rb	Sr	U	V	Y	Zn	Zr
5.83	10	270	7	50	287	3	8	11	58	169	2	47	20	28	416
5.88	11	277	5	52	271	2	8	11	61	152	3	49	20	35	458
5.93	10	271	6	52	279	2	10	11	61	163	4	46	20	29	471
5.98	13	252	8	55	302	2	10	12	61	178	2	48	22	31	470
6.03	11	270	8	57	341	3	10	11	63	176	2	50	23	33	482
6.07	10	271	5	53	318	2	9	12	60	171	2	49	18	32	401
6.11	10	274	7	49	302	2	9	11	60	175	2	46	19	34	374
6.14	13	267	8	60	349	3	14	12	70	193	3	60	23	39	362
6.17	12	263	7	59	364	1	15	13	71	200	2	63	19	41	331
6.22	8	275	5	42	294	1	8	10	55	174	2	37	18	29	304
6.26	8	267	5	36	279	2	6	8	54	165	1	29	14	24	287
6.29	6	273	5	35	287	2	6	9	52	157	0	29	15	20	274
6.33	7	266	4	37	310	1	6	10	52	158	2	32	16	25	301
6.37	9	268	5	50	426	2	10	10	62	183	3	48	20	31	372
6.41	12	259	7	61	488	2	16	15	74	207	2	69	21	44	311
6.45	10	266	5	45	302	2	7	11	54	154	2	38	18	26	362
6.49	12	273	8	55	333	3	12	13	64	168	4	50	22	32	393
6.53	12	265	8	52	310	2	11	12	62	183	3	52	21	33	390
6.58	11	261	7	49	294	2	10	12	62	173	2	48	20	32	435
6.64	13	256	6	58	294	2	13	13	63	221	2	52	20	31	456
6.71	11	264	6	55	294	2	12	13	62	158	2	49	20	32	434
6.77	13	271	6	58	318	3	13	14	67	177	3	56	21	38	417
6.83	11	270	6	58	279	2	9	12	61	183	3	47	21	30	450
6.87	11	259	7	54	271	2	11	11	60	172	2	43	20	30	394
6.92	9	263	5	49	279	3	9	12	58	179	2	43	20	28	381
6.97	9	269	5	51	263	2	8	10	59	159	2	44	21	30	427
7.01	10	266	6	58	279	1	11	11	63	166	4	46	21	31	451
7.05	10	264	4	57	310	2	9	10	58	167	3	42	22	31	522
7.09	13	251	8	52	325	2	10	11	59	201	2	44	20	32	456
7.14	16	263	8	58	364	2	13	13	67	221	3	59	22	38	446
7.18	17	257	8	64	387	3	15	14	70	178	3	63	22	41	523
7.22	17	269	8	70	403	3	16	15	73	161	4	68	26	48	525
7.27	14	279	9	73	441	4	18	17	85	163	3	82	26	52	492
7.33	12	269	9	73	372	2	15	15	78	141	4	73	28	48	558
7.39	11	280	8	73	341	3	15	16	77	144	3	70	26	42	565
7.46	16	264	9	77	410	3	20	14	88	190	3	86	24	54	398
7.62	19	255	11	75	395	4	20	18	90	185	2	88	26	54	395
7.68	19	268	11	78	434	3	23	19	88	184	3	91	26	60	384
7.73	18	260	11	77	472	4	25	18	95	183	4	102	26	63	327
7.78	18	266	10	78	480	3	23	17	96	181	3	97	26	65	319
7.83	17	268	13	84	472	2	25	17	102	171	4	111	26	67	318
7.90	16	270	9	83	410	2	19	16	90	161	3	89	29	56	443
7.96	21	271	10	76	519	4	22	16	88	195	4	86	26	58	410
8.01	17	268	9	72	542	3	19	16	86	175	4	77	23	54	364
8.12	20	273	11	80	627	4	25	19	101	196	3	102	26	64	278
8.17	19	260	8	77	550	3	22	19	93	196	4	98	24	65	264
8.25	20	272	11	84	527	4	22	16	95	146	3	94	27	62	404
8.26	19	278	7	76	441	1	20	16	92	161	2	92	26	61	354
8.30	20	279	11	75	496	2	21	17	93	169	2	90	25	61	307
8.34	20	268	11	82	565	2	26	20	100	165	3	107	25	69	264
8.37	18	281	11	81	565	1	25	19	103	166	4	105	26	72	248

## Wangerland core W1 (Archive No. KB 5552)

Depth [m]	TS	TC	TIC	SiO <sub>2</sub>	TiO <sub>2</sub>	Al <sub>2</sub> O <sub>3</sub>	Fe <sub>2</sub> O <sub>3</sub>	MgO	CaO	Na <sub>2</sub> O	K <sub>2</sub> O	P <sub>2</sub> O <sub>5</sub>
8.41	0.68	2.85	1.14	64.56	0.60	9.40	3.89	1.63	5.05	0.96	2.11	0.27
8.47	0.70	2.85	1.00	65.21	0.62	9.54	4.11	1.63	4.46	0.92	2.12	0.35
8.55	0.82	3.15	0.94	63.39	0.65	10.25	4.49	1.73	4.22	0.93	2.23	0.34
8.61	1.14	2.88	1.03	63.19	0.65	10.19	4.64	1.69	4.66	0.91	2.21	0.15
8.67	1.33	2.99	1.17	62.45	0.66	10.16	4.80	1.68	5.30	0.91	2.18	0.15
8.72	1.34	2.97	1.05	62.36	0.63	10.15	4.77	1.66	4.75	0.88	2.20	0.15
8.76	1.01	2.71	0.98	66.23	0.60	9.27	4.01	1.49	4.45	0.93	2.10	0.13
8.80	1.41	2.84	0.96	63.86	0.66	9.97	4.75	1.60	4.37	0.93	2.18	0.14
8.89	1.25	2.69	0.81	64.34	0.68	10.32	4.72	1.66	3.67	0.93	2.26	0.15
8.92	1.52	3.20	0.76	61.47	0.71	11.36	5.39	1.85	3.51	0.92	2.38	0.15
8.96	1.47	2.99	0.88	62.43	0.68	10.94	5.16	1.75	4.00	0.92	2.32	0.14
9.01	1.29	2.71	0.91	64.82	0.66	10.02	4.61	1.61	4.12	0.94	2.20	0.13
9.05	1.03	2.52	0.82	66.61	0.64	9.73	4.17	1.53	3.71	0.92	2.17	0.13
9.10	1.04	2.93	0.94	63.40	0.68	10.79	4.58	1.74	4.27	0.92	2.28	0.16
9.15	1.33	2.87	0.87	61.99	0.68	11.31	5.07	1.79	3.95	0.89	2.37	0.14
9.19	1.86	2.92	0.82	62.54	0.66	10.86	5.51	1.72	3.73	0.91	2.30	0.13
9.23	2.28	3.04	0.20	63.87	0.71	11.88	6.24	1.69	1.11	0.97	2.47	0.14
9.29	2.04	2.89	0.56	62.44	0.69	11.40	6.06	1.87	2.43	0.95	2.40	0.14
9.33	2.16	3.09	0.78	61.29	0.67	11.21	6.10	1.85	3.44	0.93	2.34	0.14
9.37	1.59	2.69	0.80	64.52	0.65	10.46	4.89	1.69	3.57	0.93	2.28	0.13
9.43	1.37	2.92	0.83	63.69	0.67	10.59	4.84	1.74	3.64	0.95	2.27	0.13
9.49	1.67	3.18	0.01	61.64	0.68	10.96	5.43	1.82	4.41	0.93	2.29	0.13
9.55	1.19	2.59	0.91	66.55	0.65	9.53	4.26	1.59	4.05	0.99	2.14	0.12
9.61	1.17	2.63	1.01	66.16	0.63	9.63	4.16	1.58	4.40	0.98	2.14	0.12
9.67	1.30	2.56	1.06	65.70	0.64	9.50	4.25	1.61	4.69	1.00	2.11	0.12
9.73	1.48	2.31	1.05	68.02	0.61	8.62	4.12	1.45	4.66	1.02	2.01	0.12
9.80	1.49	2.36	1.04	67.24	0.62	8.88	4.18	1.48	4.63	0.99	2.04	0.12
9.93	1.72	2.61	1.03	64.13	0.68	9.85	4.76	1.67	4.57	0.97	2.14	0.13
9.99	1.85	2.66	1.01	64.33	0.69	9.76	4.84	1.71	4.48	1.01	2.13	0.13
10.05	1.68	2.41	0.98	66.84	0.65	8.89	4.36	1.49	4.37	1.00	2.03	0.12
10.12	1.71	2.32	0.87	66.58	0.66	9.50	4.58	1.53	3.91	0.99	2.13	0.12
10.18	1.57	1.58	0.18	72.48	0.68	9.54	4.21	1.28	1.03	1.06	2.18	0.13
10.23	1.51	1.32	0.01	75.17	0.69	8.84	3.88	0.98	0.55	1.08	2.10	0.12
10.27	1.56	1.17	0.99	76.62	0.70	8.45	3.84	0.89	0.55	1.07	2.04	0.11
10.31	1.40	1.00	0.01	78.07	0.69	7.88	3.41	0.80	0.55	1.06	1.97	0.11
10.35	1.85	1.74	0.01	72.63	0.73	9.59	4.53	1.11	0.54	1.01	2.19	0.12
10.38	1.88	3.07	0.02	64.33	0.75	12.67	5.60	1.65	0.49	0.99	2.61	0.13
10.41	1.95	3.88	0.01	62.52	0.73	12.72	5.67	1.70	0.49	1.02	2.61	0.14
10.43	1.29	3.08	0.01	64.31	0.75	12.88	4.93	1.70	0.48	1.01	2.65	0.13
10.48	3.01	4.40	0.01	58.74	0.71	12.96	7.25	1.77	0.53	1.02	2.58	0.16
10.52	5.18	4.71	0.01	56.24	0.68	11.95	9.42	1.63	0.50	1.05	2.40	0.16
10.55	3.02	3.64	0.01	60.59	0.73	12.93	7.01	1.70	0.45	1.01	2.63	0.12
10.57	2.78	4.94	0.01	58.41	0.72	13.26	6.62	1.76	0.45	0.97	2.65	0.11
10.59	2.74	4.03	0.01	60.76	0.72	12.73	6.48	1.66	0.44	1.00	2.60	0.11
10.62	3.44	4.45	0.01	58.78	0.71	12.69	7.52	1.68	0.44	0.98	2.59	0.11
10.64	4.09	5.58	0.01	57.48	0.69	12.07	8.12	1.59	0.45	0.99	2.47	0.11
10.67	9.63	8.66	0.01	45.61	0.62	11.10	13.99	1.45	0.41	0.92	2.27	0.09
10.69	8.94	8.44	0.01	46.69	0.60	10.78	13.44	1.44	0.43	0.92	2.14	0.10
10.72	9.07	10.45	0.02	45.78	0.55	10.10	12.42	1.43	0.49	1.00	1.96	0.11
10.74	5.39	12.07	0.02	48.16	0.60	10.62	7.85	1.50	0.55	1.05	2.12	0.11
10.78	13.15	18.90	0.04	28.64	0.33	6.12	15.98	1.12	0.70	0.95	1.20	0.11
10.81	6.60	28.95	0.02	25.14	0.32	5.36	6.92	1.31	0.94	1.30	1.07	0.12

## Wangerland core W1 (Archive No. KB 5552)

Depth [m]	As	Ba	Co	Cr	Mn	Mo	Ni	Pb	Rb	Sr	U	V	Y	Zn	Zr
8.41	18	280	9	73	550	2	19	15	89	160	2	86	25	58	287
8.47	18	278	10	75	612	3	21	17	92	148	3	90	25	59	333
8.55	20	278	9	81	558	3	24	16	97	142	3	102	26	62	320
8.61	21	283	12	80	488	5	24	17	97	152	3	98	26	62	309
8.67	19	271	11	85	480	2	22	18	96	175	3	97	28	62	374
8.72	20	284	12	81	519	4	24	17	100	156	4	100	25	65	316
8.76	16	286	7	74	403	2	21	18	88	147	3	83	24	53	338
8.80	21	278	11	82	496	2	24	18	95	145	3	97	26	62	393
8.89	19	282	10	83	465	3	24	18	98	129	4	101	28	67	363
8.92	22	260	11	91	511	4	28	19	109	128	3	113	29	71	319
8.96	22	286	10	84	426	3	26	19	107	140	3	110	26	69	319
9.01	21	280	11	81	395	3	20	16	95	143	3	98	27	59	363
9.05	17	288	9	78	325	2	20	18	92	134	3	93	25	61	347
9.10	20	281	11	91	380	3	26	17	103	148	5	101	26	68	339
9.15	22	277	11	88	341	2	28	20	107	138	3	115	29	73	289
9.19	28	284	11	85	387	3	27	19	103	137	2	106	28	69	273
9.23	29	302	13	94	263	4	30	21	113	95	1	124	28	76	250
9.29	22	287	13	91	349	3	28	21	108	106	2	119	27	76	246
9.33	24	272	13	86	372	3	30	19	105	119	1	117	28	73	242
9.37	17	292	11	83	364	3	27	21	97	122	1	103	26	63	287
9.43	18	282	12	83	325	2	25	18	99	124	3	108	26	63	285
9.49	30	284	12	88	380	4	28	19	104	138	3	114	28	69	255
9.55	20	277	12	80	325	3	21	18	89	131	2	87	27	57	335
9.61	22	280	10	79	356	3	21	17	88	138	3	90	27	56	318
9.67	21	282	8	74	341	2	20	18	89	145	3	89	26	57	319
9.73	17	292	8	72	341	2	18	16	80	145	3	79	25	49	365
9.80	14	293	9	72	356	4	22	15	83	145	4	74	26	50	364
9.93	17	293	11	82	457	3	22	18	94	143	3	96	28	62	343
9.99	19	284	12	83	449	2	22	17	92	137	2	93	28	60	338
10.05	17	281	8	76	434	3	20	16	84	138	2	83	27	53	382
10.12	16	293	10	78	403	3	22	17	91	131	2	86	27	57	365
10.18	16	311	9	80	372	4	22	17	89	91	4	84	28	53	418
10.23	16	308	9	80	333	2	17	17	81	85	2	78	28	49	497
10.27	18	303	8	80	349	2	19	17	77	83	2	67	31	47	577
10.31	15	304	8	77	410	2	16	15	72	83	3	58	30	39	612
10.35	24	309	10	87	496	3	23	18	89	86	3	83	30	58	533
10.38	26	302	14	97	380	3	31	23	120	91	4	125	30	82	241
10.41	26	303	16	119	325	6	45	24	121	89	3	133	29	90	214
10.43	20	303	13	98	294	2	31	23	121	89	2	128	28	88	206
10.48	32	275	14	98	380	5	36	24	120	93	4	136	29	92	173
10.52	43	277	18	92	380	9	34	23	111	91	4	124	29	89	189
10.55	19	302	11	96	302	5	32	22	123	88	4	128	28	83	200
10.57	17	286	16	99	294	5	34	23	128	88	4	138	27	93	182
10.59	21	305	18	95	279	5	36	22	122	87	4	122	26	82	207
10.62	29	287	16	97	271	7	39	25	124	87	4	126	27	80	207
10.64	33	274	16	94	263	9	38	23	117	87	5	131	27	89	205
10.67	89	244	30	84	356	19	52	24	113	81	5	138	23	86	144
10.69	88	238	27	80	372	17	51	23	105	81	4	117	23	93	150
10.72	82	223	35	73	339	19	62	20	97	84	4	107	21	112	148
10.74	16	243	9	80	273	7	24	14	102	89	4	113	22	53	169
10.78	41	138	10	50	504	21	27	14	58	79	5	83	16	63	104
10.81	14	131	5	44	309	9	19	10	51	104	5	76	18	56	112

## Wangerland core W1 (Archive No. KB 5552)

Depth [m]	TS	TC	TIC	SiO <sub>2</sub>	TiO <sub>2</sub>	Al <sub>2</sub> O <sub>3</sub>	Fe <sub>2</sub> O <sub>3</sub>	MgO	CaO	Na <sub>2</sub> O	K <sub>2</sub> O	P <sub>2</sub> O <sub>5</sub>
10.84	5.49	39.60	0.02	13.20	0.20	3.51	3.86	1.30	1.09	1.44	0.71	0.11
10.87	6.13	44.20	0.04	7.49	0.12	2.25	3.77	1.55	1.55	1.59	0.44	0.12
10.90	3.62	46.40	0.02	7.20	0.17	3.04	3.35	1.12	0.95	1.25	0.61	0.10
10.93	3.90	51.23	0.02	3.98	0.19	3.47	9.06	0.63	0.40	0.54	0.68	0.06
10.96	3.48	53.90	0.03	1.01	0.13	2.14	2.02	0.95	0.85	1.22	0.41	0.08
11.00	3.51	53.90	0.02	1.64	0.19	3.19	1.79	0.68	0.47	0.80	0.63	0.06
11.03	3.18	55.90	0.02	1.10	0.12	2.19	3.66	1.50	1.50	1.55	0.43	0.11
11.06	3.07	50.90	0.02	5.01	0.13	2.44	3.00	0.35	0.12	0.24	0.47	0.03
11.10	3.84	50.25	0.01	2.69	0.27	4.90	3.62	0.69	0.25	0.48	0.98	0.05
11.13	4.02	45.55	0.02	10.10	0.16	2.65	2.50	1.18	1.05	1.52	0.51	0.10
11.16	4.01	35.30	0.02	20.65	0.31	5.37	3.01	1.14	0.78	1.34	1.06	0.10
11.19	4.06	26.75	0.02	31.35	0.46	8.06	4.26	1.27	0.68	1.27	1.60	0.10
11.22	11.35	26.65	0.02	24.34	0.36	6.28	13.06	1.10	0.64	1.12	1.25	0.09
11.25	9.95	29.20	0.04	19.96	0.30	5.32	11.01	1.08	0.73	1.19	1.04	0.07
11.28	14.00	31.30	0.02	11.99	0.19	3.73	16.45	1.01	0.84	1.15	0.71	0.07
11.31	15.65	26.20	0.02	16.00	0.24	4.36	18.71	1.04	0.73	1.11	0.85	0.07
11.35	12.55	37.85	0.04	7.54	0.11	2.26	13.62	1.03	1.02	1.28	0.41	0.08
11.39	5.17	46.85	0.10	8.03	0.21	3.49	4.51	0.85	0.61	0.85	0.70	0.08

Depth [m]	As	Ba	Co	Cr	Mn	Mo	Ni	Pb	Rb	Sr	U	V	Y	Zn	Zr
10.84	11	80	3	29	229	7	12	7	34	110	4	54	11	21	53
10.87	12	56	3	22	350	8	11	5	19	145	5	48	11	20	34
10.90	10	69	3	25	199	6	11	6	29	95	4	47	10	18	46
10.93	23	78	5	28	286	12	16	8	33	45	3	47	9	36	59
10.96	7	49	4	19	108	2	8	4	21	80	2	30	7	10	32
11.00	7	72	4	25	74	3	10	6	34	53	3	35	7	12	41
11.03	11	55	3	21	340	8	10	5	18	141	5	47	11	19	33
11.06	20	54	8	18	82	5	15	5	23	20	1	26	5	27	36
11.10	8	112	4	37	126	3	11	7	47	41	2	52	10	24	78
11.13	9	61	5	24	134	3	10	5	26	99	3	37	8	12	39
11.16	11	121	7	43	124	5	17	10	57	90	4	59	12	21	68
11.19	13	184	9	60	140	5	24	12	84	92	6	77	15	37	107
11.22	29	149	36	50	248	16	45	16	65	84	7	63	14	62	96
11.25	37	122	32	42	231	19	40	8	52	90	8	66	13	41	77
11.28	94	89	53	32	362	57	57	9	36	96	15	64	13	86	47
11.31	96	104	72	38	417	48	68	10	43	91	10	64	20	81	68
11.35	119	56	287	22	189	27	183	4	20	102	6	62	41	222	36
11.39	9	85	3	28	201	6	12	7	33	68	3	50	12	37	73



## Wangerland core W2 (Archive No. KB 5156)

Depth [m]	TS	TC	TIC	SiO <sub>2</sub>	TiO <sub>2</sub>	Al <sub>2</sub> O <sub>3</sub>	Fe <sub>2</sub> O <sub>3</sub>	MgO	CaO	Na <sub>2</sub> O	K <sub>2</sub> O	P <sub>2</sub> O <sub>5</sub>
0.38	0.04	0.94	0.01	71.58	0.71	11.62	5.09	1.28	0.89	0.75	2.44	0.12
0.44				68.25	0.71	12.94	6.17	1.67	0.98	0.71	2.58	0.11
0.52				66.94	0.70	12.52	5.90	1.90	2.27	0.70	2.49	0.12
0.61				65.00	0.68	12.06	5.74	1.94	3.89	0.69	2.41	0.13
0.76	0.03	1.56	0.49	67.82	0.67	11.12	5.67	1.55	2.83	0.74	2.32	0.13
0.81				63.53	0.68	12.19	6.11	1.98	4.28	0.64	2.43	0.16
0.88				64.81	0.65	10.94	5.24	1.78	4.83	0.70	2.27	0.23
1.07				63.24	0.69	11.89	5.41	1.91	5.12	0.66	2.40	0.17
1.12				62.96	0.70	12.44	4.81	1.95	4.92	0.62	2.48	0.14
1.18				63.74	0.68	11.62	4.05	1.82	5.57	0.66	2.37	0.12
1.29				61.80	0.67	11.88	4.68	1.89	5.91	0.63	2.38	0.14
1.38				64.09	0.64	10.82	5.16	1.76	5.44	0.66	2.26	0.17
1.42				65.46	0.62	10.16	4.49	1.63	5.30	0.72	2.18	0.16
1.52	0.10	2.49	1.03	66.18	0.61	9.94	4.27	1.57	5.14	0.73	2.17	0.15
1.64	0.60	2.92	1.08	62.43	0.62	10.16	4.43	1.60	5.42	0.68	2.18	0.13
1.72	1.10	3.25	1.28	61.27	0.64	10.77	4.81	1.72	6.20	0.67	2.28	0.12
1.81	1.22	3.36	1.32	60.00	0.63	10.83	4.91	1.76	6.36	0.63	2.29	0.12
1.88	0.89	2.92	1.26	64.26	0.60	9.71	4.07	1.54	6.14	0.69	2.15	0.11
1.92	0.81	2.88	1.27	64.37	0.60	9.74	3.96	1.56	6.07	0.70	2.16	0.11
1.98	0.87	2.62	1.33	68.26	0.56	8.28	3.40	1.34	6.27	0.81	1.98	0.10
2.1	0.92	2.86	1.26	65.37	0.58	9.60	3.99	1.55	6.00	0.74	2.16	0.11
2.19	0.80	2.30	1.11	71.85	0.48	7.45	3.01	1.14	5.30	0.80	1.89	0.09
2.27	0.49	1.80	1.04	77.05	0.37	6.15	2.05	0.87	4.95	0.88	1.77	0.07
2.33	0.61	2.55	1.07	74.77	0.39	6.47	2.33	0.95	5.14	0.83	1.79	0.08
2.355	1.23	5.25	0.95	69.43	0.42	6.39	2.95	0.97	4.79	0.76	1.71	0.08
2.44	0.70	2.87	1.13	71.35	0.44	7.40	2.80	1.13	5.41	0.88	1.92	0.09
2.445	1.60	5.87	1.02	65.64	0.53	6.77	3.48	1.11	5.11	0.78	1.71	0.10
2.45	0.52	1.72	1.02	75.73	0.60	6.33	2.36	0.94	4.93	0.81	1.70	0.09
2.48	0.58	1.56	0.98	76.55	0.69	6.37	2.41	0.98	4.64	0.85	1.71	0.10
2.54	0.86	2.41	1.45	69.56	0.57	7.27	3.06	1.16	6.76	0.81	1.80	0.10
2.61	1.41	2.81	1.57	61.48	0.52	7.98	4.32	1.31	7.04	0.74	1.89	0.10
2.68	1.54	3.21	1.48	62.21	0.54	9.44	4.74	1.61	6.81	0.80	2.10	0.12
2.73	1.15	3.10	1.45	62.44	0.56	9.86	4.53	1.68	6.77	0.80	2.18	0.12
2.78	0.97	2.96	1.41	63.14	0.57	9.81	4.37	1.67	6.54	0.78	2.17	0.15
2.83	0.95	3.18	1.39	60.80	0.58	10.27	4.68	1.78	6.46	0.78	2.23	0.19
2.88	0.87	3.15	1.39	59.61	0.56	9.74	4.56	1.70	6.38	0.76	2.14	0.18
2.95	0.51	2.24	1.19	67.01	0.52	8.44	4.51	1.41	5.63	0.81	2.06	0.23
3	1.50	5.00	1.88	54.17	0.52	8.82	6.03	1.62	8.68	0.80	1.99	0.15
3.01	1.32	3.69	1.22	61.74	0.54	8.64	5.75	1.54	5.89	0.86	2.04	0.15
3.06	1.19	2.74	1.54	58.63	0.57	9.32	7.51	1.72	6.93	0.80	2.17	0.38
3.14	0.74	2.93	1.73	60.50	0.55	9.01	5.37	1.58	7.98	0.82	2.09	0.22
3.23	1.08	3.69	2.23	56.95	0.53	8.86	4.95	1.53	10.26	0.84	2.01	0.12
3.31	0.56	3.24	2.34	59.77	0.50	7.55	4.70	1.31	10.71	0.83	1.82	0.26
3.4	0.40	3.08	2.14	54.56	0.53	8.87	8.15	1.69	9.28	0.84	2.07	0.57
3.48	0.76	3.04	2.06	58.97	0.54	8.08	6.76	1.47	8.88	0.85	1.93	0.41
3.53				54.91	0.57	9.56	7.32	1.79	8.96	0.84	2.18	0.57
3.57	0.46	2.20	0.88	67.70	0.58	9.25	5.12	1.31	4.38	0.80	2.12	0.20
3.59	0.74	2.03	1.01	70.98	0.51	7.46	4.08	1.23	4.74	0.90	1.90	0.24
3.63	0.67	1.96	0.88	74.84	0.48	7.15	2.98	1.09	4.15	0.92	1.86	0.08
3.68				75.17	0.53	6.95	2.88	1.06	3.99	0.92	1.83	0.08
3.74	0.55	1.96	0.87	73.37	0.54	7.55	3.20	1.17	4.14	0.89	1.91	0.11
3.78	0.53	2.22	1.00	81.19	0.50	5.68	1.89	0.77	3.28	0.86	1.66	0.08
3.8				67.94	0.56	8.60	3.90	1.44	4.69	0.95	2.06	0.19
3.815				69.14	0.63	8.68	3.82	1.41	4.71	0.89	2.07	0.12

## Wangerland core W2 (Archive No. KB 5156)

Depth [m]	As	Ba	Co	Cr	Mn	Mo	Ni	Pb	Rb	Sr	U	V	Y	Zn	Zr
0.38	1	313	9	92	364	1	20	27	93	88	5	104	25	79	301
0.44	22	295	11	105	793	1	35	22	135	91	2	121	24	82	278
0.52	15	315	20	98	3343	1	44	21	124	109	3	127	23	80	265
0.61	15	295	14	93	1678	1	34	20	121	124	4	119	24	77	263
0.76	14	321	10	89	716	1	25	32	115	111	4	99	22	83	300
0.81	20	283	9	94	572	1	28	20	130	130	4	117	23	81	245
0.88	20	280	11	86	793	1	24	20	114	140	4	107	23	70	279
1.07	8	275	9	92	338	1	25	20	120	140	3	108	22	76	238
1.12	4	278	9	94	284	1	26	21	130	138	4	108	22	82	232
1.18	4	273	6	88	251	1	24	17	123	148	3	96	22	78	258
1.29	8	272	8	89	324	1	25	17	99	155	4	108	24	80	234
1.38	12	276	11	85	557	1	24	17	110	149	5	100	21	73	264
1.42	6	274	10	80	413	1	22	17	102	146	1	89	19	77	272
1.52	8	274	7	79	341	1	20	13	98	145	3	86	19	61	286
1.64	14	273	11	80	376	1	22	16	82	153	4	94	22	67	286
1.72	21	262	8	86	384	1	24	18	115	176	4	101	21	73	262
1.81	17	259	12	83	421	1	24	18	114	185	2	102	20	75	252
1.88	11	267	7	75	442	1	19	16	96	180	2	88	20	64	304
1.92	14	256	9	78	498	1	22	17	101	195	3	85	21	64	309
1.98	3	261	5	68	379	1	14	12	70	197	3	68	19	52	328
2.1	8	274	10	77	438	1	24	15	96	177	4	84	19	63	287
2.19	13	280	5	55	533	1	10	10	51	171	5	57	18	46	306
2.27	3	280	5	41	375	1	6	11	47	160	3	38	14	31	247
2.33	9	268	6	45	463	1	7	10	51	166	3	45	15	35	253
2.355	17	253	8	55	653	1	12	14	52	156	3	70	16	42	317
2.44	9	273	4	55	506	1	10	14	61	170	4	59	16	45	244
2.445	16	252	9	69	546	1	12	16	54	162	3	79	20	54	510
2.45	3	264	5	67	317	1	8	10	49	150	6	42	23	38	798
2.48	1	261	6	78	332	2	8	12	44	145	6	44	28	35	914
2.54	5	244	6	67	351	2	11	12	55	245	5	58	22	45	605
2.61	2	219	9	65	370	1	12	15	63	260	4	75	19	33	372
2.68	29	243	7	70	435	1	20	17	96	243	3	89	19	62	260
2.73	31	253	10	74	432	1	22	18	80	232	2	92	21	67	248
2.78	26	250	8	73	445	1	21	17	101	224	2	90	19	63	269
2.83	26	257	8	78	531	1	24	21	105	228	3	96	19	67	244
2.88	30	247	9	72	538	1	22	20	77	225	3	92	22	65	241
2.95	15	255	9	65	484	1	15	22	88	211	4	79	17	53	279
3	50	228	7	70	691	1	19	16	86	306	3	107	20	63	237
3.01	37	255	11	69	531	1	19	18	85	206	4	95	21	53	281
3.06	30	249	6	73	717	1	22	29	94	277	3	101	23	63	265
3.14	27	244	9	69	520	1	18	22	96	301	1	88	20	56	280
3.23	35	240	9	67	442	1	18	15	57	365	4	84	22	57	259
3.31	23	228	6	59	593	1	13	15	47	390	4	74	22	48	349
3.4	26	231	7	72	961	1	19	29	82	355	3	107	24	58	235
3.48	23	238	9	69	785	1	17	20	69	340	2	85	23	49	351
3.53	31	234	8	75	547	1	22	26	94	337	3	104	23	66	249
3.57	13	278	6	73	439	1	18	22	97	163	3	86	20	62	313
3.59	23	261	8	59	323	1	14	15	67	159	3	63	19	46	361
3.63	18	262	6	59	310	1	11	12	55	138	3	54	16	43	354
3.68	16	267	8	61	302	1	8	12	58	134	4	50	19	41	538
3.74	16	256	8	63	356	1	13	13	71	138	3	61	18	48	471
3.78	5	269	3	52	261	1	3	8	45	118	4	34	17	29	636
3.8	23	260	9	69	422	1	16	15	85	150	2	76	18	53	338
3.815	19	273	9	80	414	1	18	13	83	153	4	74	22	54	488

## Wangerland core W2 (Archive No. KB 5156)

Depth [m]	TS	TC	TIC	SiO <sub>2</sub>	TiO <sub>2</sub>	Al <sub>2</sub> O <sub>3</sub>	Fe <sub>2</sub> O <sub>3</sub>	MgO	CaO	Na <sub>2</sub> O	K <sub>2</sub> O	P <sub>2</sub> O <sub>5</sub>
3.84				73.06	0.62	7.53	3.16	1.19	4.30	0.90	1.90	0.12
3.86				70.76	0.52	8.20	3.65	1.33	4.31	0.94	2.02	0.13
3.89				70.54	0.58	8.22	3.65	1.34	4.55	0.93	2.02	0.15
3.92				68.86	0.59	8.68	4.18	1.42	4.82	0.93	2.08	0.20
4	0.43	2.54	1.38	64.80	0.59	9.17	4.74	1.52	6.05	0.94	2.15	0.23
4.1				69.01	0.60	9.29	4.30	1.49	3.90	0.95	2.21	0.25
4.17				70.62	0.63	8.11	3.40	1.34	5.02	1.00	1.99	0.13
4.2				69.88	0.60	8.24	3.68	1.35	4.82	1.03	2.03	0.11
4.25	0.55	1.81	0.97	73.06	0.56	7.81	3.13	1.26	4.46	1.03	1.97	0.10
4.28				72.91	0.64	7.61	3.08	1.22	4.34	1.01	1.93	0.11
4.35	0.44	1.69	0.97	75.35	0.60	7.24	2.75	1.13	4.24	1.02	1.88	0.10
4.4				74.12	0.60	7.37	2.86	1.15	4.39	1.02	1.90	0.10
4.42	0.39	1.48	0.81	76.22	0.58	7.06	2.64	1.07	3.83	1.00	1.86	0.09
4.42				71.31	0.61	8.24	3.41	1.35	4.46	1.06	2.03	0.12
4.45				77.37	0.69	6.84	2.53	1.02	3.63	0.98	1.82	0.10
4.49				77.08	0.56	6.99	2.75	1.05	3.49	1.00	1.85	0.09
4.55	0.56	1.45	0.71	75.97	0.56	7.27	2.95	1.08	3.37	0.99	1.89	0.09
4.6	0.67	2.12	1.00	69.42	0.68	8.46	3.59	1.38	4.64	1.03	2.04	0.11
4.64				74.86	0.60	7.16	2.74	1.10	4.12	0.99	1.88	0.09
4.71	0.90	2.28	1.29	71.05	0.47	7.36	3.01	1.21	5.94	1.03	1.88	0.09
4.78				69.80	0.44	7.40	3.05	1.23	6.14	1.05	1.89	0.10
4.85	1.98	4.75	0.96	66.54	0.57	7.67	3.97	1.26	4.56	1.06	1.85	0.10
4.89	3.39	13.20	1.14	49.32	0.46	7.33	4.66	1.40	5.58	1.29	1.66	0.10
4.93	4.11	26.30	0.22	31.81	0.42	7.28	3.68	1.63	1.81	1.80	1.54	0.10
4.96	6.03	35.40	0.05	19.39	0.28	4.98	4.74	1.58	1.02	2.06	1.07	0.11
4.99	4.95	26.10	0.04	31.47	0.41	7.45	5.29	1.69	0.83	1.79	1.57	0.11
5.01	4.14	21.00	0.09	39.56	0.45	7.60	5.05	1.56	0.88	1.72	1.66	0.11
5.03	2.71	13.25	0.04	49.34	0.58	10.29	5.10	1.69	0.67	1.50	2.16	0.10
5.06	2.59	11.20	0.04	50.99	0.62	11.27	5.27	1.84	0.63	1.47	2.34	0.11
5.08	1.96	9.28	0.02	53.46	0.66	11.98	6.99	1.87	0.57	1.37	2.47	0.11
5.11	2.18	7.13	0.02	54.77	0.69	12.18	4.69	1.80	0.53	1.40	2.51	0.10
5.14	3.42	8.38	0.03	58.87	0.70	11.67	5.46	1.67	0.58	1.26	2.49	0.10
5.19	2.13	3.24	0.02	59.63	0.75	13.12	6.31	1.88	0.52	1.20	2.75	0.12
5.25	2.86	2.41	0.03	63.17	0.77	12.97	7.16	1.83	0.53	1.20	2.75	0.12
5.3	2.46	1.67	0.08	65.85	0.75	12.45	6.61	1.79	0.63	1.20	2.71	0.12
5.37	1.82	1.21	0.17	68.74	0.74	11.65	5.65	1.78	0.90	1.22	2.60	0.12
5.44	1.55	1.24	0.21	68.95	0.74	11.58	5.29	1.83	1.00	1.22	2.59	0.12
5.51	1.92	1.03	0.21	70.09	0.72	10.85	5.55	1.72	1.01	1.20	2.49	0.11
5.58	1.57	1.07	0.25	71.04	0.72	10.74	5.27	1.75	1.09	1.25	2.49	0.12
5.65	1.31	1.04	0.24	70.68	0.73	11.09	5.08	1.79	1.06	1.25	2.54	0.12
5.73	1.29	1.09	0.25	70.93	0.71	10.79	4.99	1.79	1.13	1.28	2.49	0.12
5.8				71.34	0.70	10.28	4.86	1.75	1.20	1.27	2.42	0.11
5.86	1.72	1.24	0.30	70.01	0.72	10.73	5.46	1.83	1.21	1.30	2.48	0.12
5.93	1.81	1.45	0.26	66.94	0.73	11.63	6.27	1.97	1.11	1.30	2.61	0.13
6.01	0.83	1.46	0.26	67.16	0.75	12.03	5.63	2.06	1.10	1.32	2.68	0.26
6.07				65.24	0.75	12.46	6.06	2.09	0.95	1.37	2.74	0.50
6.14	0.49	1.65	0.19	67.02	0.75	12.16	5.47	1.98	0.91	1.37	2.71	0.30
6.19	0.72	1.66	0.16	68.66	0.74	11.83	5.19	1.83	0.86	1.38	2.65	0.15
6.24	0.86	1.65	0.15	67.01	0.74	11.90	5.74	1.88	0.83	1.40	2.65	0.24
6.29				66.26	0.74	12.04	5.55	1.91	0.85	1.41	2.68	0.22
6.32	0.91	1.78	0.19	66.75	0.74	11.88	5.58	1.92	0.93	1.40	2.64	0.16
6.36				67.83	0.74	11.97	4.84	1.95	0.99	1.43	2.67	0.13
6.41				67.29	0.73	12.03	4.94	1.99	1.03	1.40	2.67	0.13

## Wangerland core W2 (Archive No. KB 5156)

Depth [m]	As	Ba	Co	Cr	Mn	Mo	Ni	Pb	Rb	Sr	U	V	Y	Zn	Zr
3.84	12	264	8	71	401	1	12	16	64	142	3	60	22	45	612
3.86	17	262	10	63	397	1	14	13	78	139	3	71	17	50	305
3.89	19	273	7	68	501	1	15	9	79	147	3	69	20	52	420
3.92	17	265	7	70	518	1	16	19	83	164	2	76	20	55	408
4	21	266	7	74	609	1	18	14	93	244	3	84	21	57	388
4.1	14	276	12	72	502	1	19	16	98	143	4	88	19	60	340
4.17	16	266	5	76	357	1	15	14	75	159	4	64	23	49	557
4.2	18	273	8	69	391	1	14	14	70	151	4	68	21	51	460
4.25	12	280	7	62	300	1	12	17	64	140	4	60	20	46	401
4.28	12	274	3	76	323	1	14	14	64	139	3	56	24	46	642
4.35	9	274	7	65	288	1	11	9	55	138	4	54	21	42	579
4.4	8	268	6	67	283	1	11	9	39	139	2	55	23	43	603
4.42	8	280	5	67	262	1	9	11	61	127	5	51	20	51	578
4.42	14	281	7	72	329	1	13	13	76	141	3	64	20	53	438
4.45	3	269	6	77	285	1	10	12	49	121	4	50	24	38	884
4.49	14	268	6	65	264	1	9	15	54	121	5	53	21	41	535
4.55	16	271	5	64	250	1	9	13	61	122	4	52	21	42	562
4.6	20	266	8	81	324	1	15	14	81	146	5	69	25	53	708
4.64	14	275	6	71	281	1	12	14	59	134	4	53	22	44	636
4.71	27	268	6	56	412	1	12	11	60	178	2	56	17	45	289
4.78	27	263	7	53	432	1	14	10	65	214	1	56	16	44	248
4.85	25	239	7	67	523	2	14	14	63	147	4	66	20	48	492
4.89	22	198	6	58	460	2	19	14	49	228	6	76	20	49	275
4.93	13	167	4	58	204	14	18	13	58	156	6	82	15	35	125
4.96	24	110	5	43	155	17	19	10	39	115	5	76	14	54	71
4.99	25	160	6	63	213	15	23	16	65	96	5	105	18	69	109
5.01	20	187	5	63	251	17	20	17	61	87	4	100	19	65	158
5.03	17	230	9	82	223	12	30	20	86	88	5	110	22	101	177
5.06	9	238	10	90	224	10	29	21	91	91	6	130	22	84	163
5.08	36	251	5	95	260	1	32	22	102	88	3	140	25	98	164
5.11	11	263	7	93	211	1	27	21	98	87	4	116	22	81	184
5.14	10	276	6	90	249	1	24	19	118	89	4	110	21	78	221
5.19	30	281	5	103	348	1	28	25	105	86	4	129	27	87	201
5.25	34	287	7	101	372	1	29	23	129	86	4	131	24	88	241
5.3	24	284	10	96	320	1	26	25	124	87	5	121	25	83	270
5.37	19	306	10	162	307	1	56	19	94	88	3	110	28	76	302
5.44	18	310	11	90	294	1	29	20	92	89	5	113	28	75	296
5.51	18	304	9	89	258	1	23	19	111	89	4	99	24	74	336
5.58	11	301	7	92	354	1	24	22	83	88	3	97	26	68	336
5.65	3	300	10	89	340	1	25	20	82	87	5	105	27	72	310
5.73	14	300	9	87	287	1	22	18	85	89	5	99	28	71	340
5.8	11	296	8	86	263	1	16	19	104	89	3	90	25	63	347
5.86	13	298	6	88	279	1	21	19	107	88	3	98	25	68	340
5.93	18	290	10	92	248	1	28	22	118	90	4	116	26	76	295
6.01	13	297	12	97	245	1	26	24	120	90	4	116	27	78	292
6.07	11	286	7	97	282	1	26	23	122	88	5	127	25	79	265
6.14	13	303	9	97	223	1	26	22	120	89	4	123	26	74	278
6.19	13	298	14	96	181	1	34	20	91	89	4	121	27	81	287
6.24	20	305	13	97	200	1	30	23	118	89	4	120	25	78	282
6.29	11	291	11	95	190	1	27	22	119	89	4	124	24	77	268
6.32	22	292	11	95	179	1	29	20	117	89	3	123	25	81	273
6.36	12	289	6	95	189	1	23	23	116	89	3	119	25	72	281
6.41	24	290	11	96	189	1	26	23	118	90	2	119	25	78	273

## Wangerland core W2 (Archive No. KB 5156)

Depth [m]	TS	TC	TIC	SiO <sub>2</sub>	TiO <sub>2</sub>	Al <sub>2</sub> O <sub>3</sub>	Fe <sub>2</sub> O <sub>3</sub>	MgO	CaO	Na <sub>2</sub> O	K <sub>2</sub> O	P <sub>2</sub> O <sub>5</sub>
6.49	0.62	1.95	0.28	66.36	0.74	12.17	4.96	2.08	1.13	1.37	2.67	0.13
6.54				64.02	0.74	12.42	5.62	2.14	1.12	1.39	2.69	0.13
7.05	1.08	2.35	0.98	67.43	0.66	9.22	4.24	1.66	4.39	1.28	2.17	0.12
7.13				66.09	0.65	9.37	4.33	1.70	4.74	1.29	2.18	0.12
7.19	1.13	2.45	1.06	67.98	0.63	8.84	4.05	1.58	4.76	1.22	2.10	0.11
7.25	1.23	2.31	1.02	67.72	0.63	8.93	4.22	1.59	4.54	1.24	2.13	0.11
7.32	0.72	2.09	0.02	70.17	0.65	8.57	3.67	1.53	4.24	1.25	2.09	0.11
7.38	0.92	1.98	0.86	69.72	0.67	8.88	3.81	1.56	3.80	1.24	2.14	0.12
7.43	1.27	2.23	0.59	66.63	0.70	10.87	4.92	1.87	2.60	1.27	2.44	0.13
7.49	1.33	2.20	0.29	65.72	0.73	12.18	5.33	2.04	1.25	1.33	2.67	0.13
7.55	1.37	2.31	0.27	65.54	0.72	12.19	5.39	2.06	1.15	1.36	2.65	0.13
7.62	2.05	2.45	0.13	63.20	0.74	12.79	6.42	1.95	0.78	1.37	2.71	0.13
7.68	1.67	2.15	0.13	62.19	0.72	12.41	5.83	1.91	0.75	1.35	2.66	0.13
7.74	1.76	2.56	0.16	60.88	0.73	12.68	5.96	1.98	0.77	1.39	2.70	0.13
7.82	1.62	2.99	0.03	65.38	0.71	12.09	5.45	1.69	0.54	1.44	2.63	0.12
7.91	1.33	2.48	0.02	64.85	0.74	12.76	5.27	1.78	0.53	1.41	2.75	0.13
7.97	1.14	2.96	0.01	65.52	0.74	12.58	4.92	1.75	0.54	1.45	2.71	0.13
8.02	1.41	3.89	0.01	65.37	0.74	11.63	4.80	1.61	0.59	1.48	2.56	0.12
8.07	1.99	3.59	0.04	63.99	0.74	12.16	5.76	1.68	0.55	1.46	2.63	0.12
8.12	3.57	6.36	0.03	57.82	0.68	11.41	7.07	1.62	0.62	1.50	2.43	0.11
8.16	2.32	7.51	0.03	57.51	0.69	11.60	5.01	1.59	0.64	1.60	2.50	0.11
8.18	3.74	16.05	0.14	46.68	0.55	9.07	5.06	1.42	0.83	1.88	1.98	0.10
8.21	5.75	28.25	0.14	27.11	0.32	5.72	5.68	1.59	1.60	2.17	1.25	0.13
8.23	7.24	30.15	0.06	22.80	0.27	4.76	7.12	1.59	1.64	2.23	1.06	0.13
8.26	7.88	41.05	0.06	6.68	0.09	1.91	6.79	1.72	1.65	2.67	0.44	0.14
8.27	7.89	43.10	0.02	3.93	0.05	1.11	6.15	1.66	1.59	2.70	0.29	0.11
8.29	8.47	44.17	0.05	5.07	0.02	0.59	6.57	1.46	1.27	2.64	0.19	0.09
8.32	6.21	48.60	0.03	1.84	0.03	0.60	3.49	1.64	1.49	2.94	0.22	0.09
8.35	5.38	47.23	0.06	4.25	0.02	0.43	2.38	1.60	1.41	2.80	0.18	0.09
8.38	5.44	36.65	0.03	17.67	0.23	3.95	4.22	1.43	1.04	2.40	0.89	0.11
8.42	4.61	39.20	0.04	14.01	0.19	3.47	2.62	1.40	0.97	2.48	0.78	0.11
8.44	2.68	22.00	0.04	36.96	0.51	9.29	3.69	1.72	0.80	1.90	1.94	0.11
8.46	2.10	14.50	0.03	47.40	0.61	10.97	3.94	1.81	0.69	1.75	2.28	0.11
8.49	2.19	11.60	0.03	50.16	0.65	11.84	4.77	1.88	0.64	1.64	2.46	0.11
8.52	3.46	10.75	0.31	50.75	0.65	11.51	6.62	1.83	0.61	1.62	2.40	0.11
8.56	2.77	4.48	0.01	62.07	0.72	12.06	6.35	1.67	0.56	1.40	2.61	0.12
8.61	2.86	3.03	0.01	63.56	0.73	12.31	6.76	1.68	0.54	1.35	2.66	0.12
8.66	2.90	2.31	0.02	64.19	0.75	12.73	6.90	1.73	0.54	1.32	2.75	0.13
8.71	2.17	1.58	0.06	67.31	0.73	12.34	5.98	1.71	0.66	1.30	2.72	0.13
8.77	2.47	1.83	0.25	63.72	0.74	12.86	6.81	2.14	1.09	1.25	2.78	0.13
8.85	2.39	1.75	0.32	63.45	0.71	12.11	6.63	2.12	1.28	1.26	2.63	0.13
8.91	2.39	2.38	0.41	63.25	0.72	12.40	6.81	2.18	1.23	1.26	2.68	0.12
8.99	2.18	1.84	0.31	64.52	0.73	12.21	6.33	2.13	1.25	1.27	2.67	0.13
9.09	3.44	1.90	0.41	63.20	0.68	11.32	8.36	1.94	1.76	1.25	2.50	0.12
9.14	2.23	1.99	0.48	63.93	0.73	12.24	6.84	2.16	1.45	1.30	2.67	0.13
9.19				63.39	0.73	12.43	6.42	2.21	1.43	1.32	2.69	0.15
9.25	2.06	2.19	0.50	64.65	0.71	11.60	5.85	2.06	1.94	1.32	2.57	0.12
9.29	1.87	2.29	0.55	64.28	0.70	11.82	5.81	2.07	2.11	1.31	2.58	0.12
9.33	1.96	2.75	0.56	63.06	0.69	11.69	5.98	2.06	2.44	1.28	2.55	0.12
9.39	1.55	2.55	0.54	63.66	0.70	11.96	5.56	2.09	2.34	1.30	2.60	0.12
9.44	1.00	2.50	0.55	64.80	0.71	11.80	4.64	2.06	2.44	1.33	2.60	0.13
9.48	1.20	2.59	0.49	63.54	0.72	12.23	5.00	2.15	2.35	1.32	2.64	0.13
9.54	1.60	2.68	0.49	63.26	0.71	12.20	5.59	2.12	2.15	1.32	2.62	0.13
9.62	2.17	3.26	0.56	61.91	0.69	11.81	6.03	2.07	2.47	1.30	2.53	0.13

## Wangerland core W2 (Archive No. KB 5156)

Depth [m]	As	Ba	Co	Cr	Mn	Mo	Ni	Pb	Rb	Sr	U	V	Y	Zn	Zr
6.49	35	294	8	100	189	1	26	21	124	91	4	123	25	81	272
6.54	47	298	14	101	191	1	35	22	125	90	6	128	24	120	243
7.05	11	270	8	77	324	1	18	18	87	130	5	83	24	59	373
7.13	14	278	10	77	335	1	20	17	89	137	5	84	24	61	348
7.19	5	268	7	74	327	1	17	17	75	135	4	77	22	56	344
7.25	17	280	7	73	320	1	16	15	88	138	4	80	23	60	349
7.32	6	280	9	75	300	1	16	16	80	130	4	70	23	54	409
7.38	7	291	11	76	293	1	16	14	84	124	4	76	24	62	432
7.43	11	289	6	88	289	1	24	19	106	108	5	104	23	76	329
7.49	18	283	14	94	259	1	28	23	125	91	4	118	25	79	263
7.55	11	285	11	96	402	1	26	24	95	90	3	126	26	82	255
7.62	24	293	12	99	463	1	32	20	107	89	4	133	27	87	217
7.68	11	274	11	96	472	1	29	22	127	87	4	121	24	86	218
7.74	9	276	15	98	746	1	31	23	130	88	4	131	24	86	206
7.82	28	297	12	94	360	1	31	21	119	88	6	128	23	77	244
7.91	13	295	12	99	436	1	29	21	131	89	3	129	24	83	242
7.97	5	303	9	98	296	1	30	24	96	88	5	125	26	75	249
8.02	12	297	12	95	210	5	25	23	112	88	6	116	23	66	290
8.07	28	292	7	96	211	16	26	24	122	89	6	124	26	70	265
8.12	35	269	10	90	184	21	29	24	95	89	8	123	27	58	226
8.16	5	266	6	90	175	17	22	18	96	93	8	108	24	59	205
8.18	12	218	4	73	157	20	17	14	78	102	9	99	23	42	183
8.21	17	133	2	48	189	21	21	10	38	137	8	80	18	33	104
8.23	22	119	2	40	222	22	20	7	31	131	7	61	22	33	95
8.26	28	44	2	19	227	22	15	5	12	158	7	37	15	23	34
8.27	27	29	2	12	206	17	11	3	7	149	6	25	11	18	21
8.29	26	16	0	6	169	14	5	0	2	123	4	14	9	13	8
8.32	19	20	1	6	189	10	3	0	5	138	3	15	7	11	12
8.35	10	12	1	4	171	8	2	0	0	130	2	15	3	8	11
8.38	19	89	3	32	181	8	12	5	37	105	3	49	10	30	69
8.42	12	73	2	29	176	9	11	5	29	102	4	57	11	28	51
8.44	4	202	5	69	212	5	21	14	75	91	4	96	18	52	113
8.46	4	244	8	87	206	1	30	20	90	90	4	108	22	80	143
8.49	8	262	8	89	228	1	29	20	96	89	5	117	24	87	147
8.52	29	252	14	91	314	1	35	20	96	87	4	125	24	103	154
8.56	28	299	11	91	349	1	32	25	121	89	4	114	24	88	212
8.61	33	295	12	93	403	1	32	22	126	87	3	114	23	86	217
8.66	21	308	9	97	453	1	31	24	132	90	4	117	24	92	211
8.71	19	307	9	92	364	1	31	21	127	89	4	108	24	85	221
8.77	31	298	9	96	411	1	33	22	133	90	3	122	25	91	202
8.85	29	295	12	90	485	1	31	20	126	89	3	116	24	84	206
8.91	25	283	10	95	566	1	31	21	125	90	4	121	24	83	202
8.99	23	300	13	94	490	1	29	21	126	91	5	114	25	83	226
9.09	36	290	13	88	447	1	30	22	92	100	5	104	26	81	223
9.14	15	290	13	93	1176	1	31	22	98	94	4	115	27	86	215
9.19	11	290	10	95	1340	1	29	24	124	94	3	119	26	85	216
9.25	28	293	16	90	503	1	33	21	120	100	4	111	24	82	234
9.29	31	294	13	92	371	1	32	21	117	100	5	113	24	79	237
9.33	34	290	12	90	351	1	32	19	122	104	5	113	24	83	224
9.39	22	291	12	94	310	1	30	20	98	104	4	113	26	86	220
9.44	7	287	11	91	279	1	28	21	113	103	4	110	23	79	231
9.48	16	283	11	95	277	1	28	21	124	102	3	116	24	81	221
9.54	19	288	11	93	265	1	30	23	124	101	5	116	24	83	218
9.62	22	268	10	91	281	1	30	24	119	103	6	115	24	85	226

## Wangerland core W2 (Archive No. KB 5156)

Depth [m]	TS	TC	TIC	SiO <sub>2</sub>	TiO <sub>2</sub>	Al <sub>2</sub> O <sub>3</sub>	Fe <sub>2</sub> O <sub>3</sub>	MgO	CaO	Na <sub>2</sub> O	K <sub>2</sub> O	P <sub>2</sub> O <sub>5</sub>
9.69	2.06	3.24	0.97	61.67	0.72	12.30	6.01	2.14	2.13	1.35	2.62	0.13
9.75	1.89	3.31	0.61	61.84	0.70	11.91	5.71	2.09	2.70	1.34	2.56	0.13
9.81	2.20	3.38	0.80	60.36	0.68	11.43	6.01	2.02	3.56	1.27	2.45	0.12
9.87	2.41	3.48	0.17	59.14	0.67	11.37	6.26	2.01	4.30	1.26	2.44	0.12
9.93	2.88	3.15	0.86	59.76	0.67	11.23	6.79	1.98	3.88	1.31	2.41	0.12
10.01	2.35	2.84	0.93	63.62	0.60	9.94	5.71	1.75	4.21	1.15	2.20	0.11
10.09	2.43	3.00	0.83	62.50	0.63	10.55	5.96	1.84	3.75	1.19	2.31	0.11
10.16	2.27	2.93	0.71	64.30	0.63	10.26	5.69	1.75	3.16	1.20	2.27	0.11
10.24	2.64	3.17	0.79	60.14	0.69	11.54	6.55	2.04	3.51	1.28	2.47	0.12
10.32	2.60	2.96	0.78	60.73	0.70	11.56	6.42	2.05	3.48	1.28	2.48	0.12
10.39	2.66	2.95	0.64	62.42	0.71	11.35	6.31	1.99	2.82	1.28	2.46	0.12
10.44	3.26	3.26	0.52	60.83	0.70	11.62	6.99	2.01	2.36	1.30	2.48	0.13
10.46	3.28	3.80	0.55	58.87	0.69	11.84	7.06	2.03	2.49	1.33	2.50	0.13
10.49	3.37	4.68	0.78	55.63	0.66	11.62	6.95	2.00	3.63	1.35	2.43	0.14
10.51	3.53	5.37	0.36	56.85	0.67	11.72	7.21	2.01	1.76	1.41	2.46	0.13
10.54	3.65	7.62	0.23	54.07	0.64	11.31	6.91	1.92	0.99	1.46	2.37	0.14
10.57	4.03	14.75	0.06	54.28	0.33	4.99	5.11	1.12	1.58	1.30	1.25	0.07
10.59	6.62	33.10	0.07	23.98	0.16	2.35	5.00	1.32	1.38	1.94	0.62	0.05
10.62	8.24	34.55	0.04	20.07	0.11	1.49	6.83	1.38	1.41	2.38	0.47	0.05
10.65	5.48	35.75	0.02	23.91	0.10	1.12	3.61	1.09	1.08	2.11	0.41	0.04
10.69	1.76	14.43	0.00	68.24	0.24	2.04	1.23	0.53	0.66	1.04	0.79	0.03
10.73	0.34	2.30	0.00	90.98	0.32	2.61	0.59	0.17	0.31	0.57	1.05	0.02
10.78				94.00	0.34	2.78	0.45	0.13	0.27	0.52	1.09	0.02
10.83				93.79	0.32	2.95	0.50	0.14	0.27	0.50	1.13	0.02
10.89				93.29	0.32	3.20	0.57	0.18	0.29	0.51	1.14	0.03
10.96	0.14	0.72	0.00	86.62	0.30	3.33	0.64	0.21	0.29	0.50	1.09	0.04
11.02				92.52	0.33	3.57	0.65	0.21	0.30	0.53	1.19	0.04
11.1				92.72	0.38	3.70	0.62	0.20	0.30	0.56	1.30	0.03
11.2				93.50	0.40	3.53	0.57	0.18	0.28	0.55	1.29	0.02
11.31				93.57	0.33	3.47	0.54	0.18	0.26	0.52	1.26	0.03
11.38	0.04	0.10	0.00	92.30	0.48	4.09	0.71	0.23	0.31	0.61	1.40	0.03
11.48				92.81	0.44	4.03	0.68	0.22	0.31	0.59	1.43	0.03
11.63				90.19	0.46	5.22	0.93	0.34	0.34	0.70	1.65	0.03
11.75				88.36	0.55	6.21	1.25	0.45	0.35	0.70	1.71	0.04
11.84				89.17	0.47	5.65	1.09	0.38	0.34	0.71	1.69	0.04
11.94				88.28	0.51	5.98	1.19	0.43	0.34	0.71	1.72	0.04
12.05	0.07	0.09	0.00	88.41	0.53	6.09	1.21	0.43	0.35	0.77	1.77	0.04
12.15				89.10	0.52	5.57	1.10	0.37	0.34	0.73	1.67	0.03
12.25				90.30	0.47	5.02	0.97	0.33	0.31	0.64	1.53	0.03
12.38				87.29	0.56	6.66	1.36	0.50	0.35	0.79	1.81	0.04
12.48				87.70	0.53	6.38	1.29	0.48	0.33	0.75	1.74	0.04
12.57				90.53	0.42	4.94	0.96	0.34	0.29	0.62	1.50	0.03
12.67	0.04	0.05	0.00	93.38	0.34	3.70	0.67	0.21	0.24	0.48	1.30	0.02
12.74				85.50	0.63	7.48	1.54	0.56	0.39	0.89	1.98	0.05
12.8				90.66	0.52	4.81	0.99	0.31	0.30	0.62	1.48	0.03
12.87				86.23	0.62	6.90	1.47	0.52	0.36	0.78	1.83	0.05
12.94	0.08	0.10	0.00	89.00	0.54	5.53	1.12	0.37	0.34	0.73	1.66	0.04
13.02				83.59	0.72	8.21	1.75	0.65	0.39	0.91	2.05	0.05
13.09	0.07	0.34	0.00	85.34	0.67	7.37	1.51	0.54	0.37	0.83	1.90	0.05
13.17				85.51	0.65	7.24	1.48	0.52	0.37	0.85	1.89	0.05
13.26	0.09	0.36	0.00	88.65	0.57	5.60	1.11	0.36	0.31	0.70	1.61	0.04
13.35	0.14	1.55	0.01	78.84	0.75	9.32	1.98	0.77	0.43	0.99	2.09	0.07

## Wangerland core W2 (Archive No. KB 5156)

Depth [m]	As	Ba	Co	Cr	Mn	Mo	Ni	Pb	Rb	Sr	U	V	Y	Zn	Zr
9.69	8	276	10	96	274	1	32	26	98	101	5	118	27	89	209
9.75	22	279	14	91	291	1	30	20	124	108	3	115	24	85	221
9.81	20	272	11	91	339	1	30	20	119	118	6	113	23	84	215
9.87	19	260	11	86	370	1	27	21	116	127	4	107	24	83	214
9.93	31	268	12	86	364	1	33	19	117	123	4	105	23	85	211
10.01	22	264	11	76	353	1	26	17	103	132	3	92	21	71	217
10.09	19	268	7	79	430	1	25	19	109	122	4	98	21	78	210
10.16	4	274	10	81	463	1	24	22	70	110	4	93	23	73	215
10.24	15	275	9	89	468	1	29	20	92	118	4	106	26	81	202
10.32	25	267	11	85	446	1	28	22	117	121	5	106	26	84	213
10.39	20	287	10	88	457	1	27	19	91	111	3	102	27	83	233
10.44	18	275	13	90	550	1	29	25	90	108	6	107	26	87	207
10.46	19	278	8	90	666	2	31	23	95	116	5	110	27	88	189
10.49	16	264	12	87	635	2	30	24	117	156	6	114	23	88	175
10.51	11	261	11	91	673	2	30	20	92	104	7	112	24	87	187
10.54	24	257	11	87	731	5	33	23	95	92	8	108	25	89	185
10.57	16	169	4	40	280	16	11	9	31	92	6	55	13	42	207
10.59	21	83	2	22	211	22	7	2	17	130	8	40	8	25	103
10.62	22	67	0	16	189	15	5	3	10	129	5	18	12	21	102
10.65	13	65	0	12	136	7	2	2	6	105	2	13	4	13	119
10.69	0	149	2	14	119	1	0	5	3	64	2	10	7	8	309
10.73	0	210	1	16	85	1	0	6	2	46	2	8	8	7	398
10.78	0	214	5	13	90	1	0	7	16	42	1	8	8	10	425
10.83	0	221	1	13	90	1	0	4	25	43	2	9	7	11	384
10.89	0	212	1	15	89	1	0	8	25	45	0	9	5	11	378
10.96	0	201	1	18	84	1	0	7	15	45	1	12	5	11	347
11.02	0	225	5	16	97	1	0	7	25	46	4	13	7	14	396
11.1	0	249	1	18	100	1	0	4	24	49	3	13	7	13	388
11.2	0	251	4	17	98	1	0	6	22	46	4	11	9	15	440
11.31	0	240	4	16	87	1	0	6	25	46	1	10	6	15	327
11.38	0	274	5	28	122	1	0	7	11	51	1	15	12	17	528
11.48	0	281	4	21	107	1	0	10	22	52	2	13	8	13	439
11.63	0	300	2	32	109	1	0	10	39	58	3	22	10	22	400
11.75	0	297	6	41	129	1	3	13	45	61	4	32	12	27	460
11.84	0	298	4	31	109	1	0	10	38	60	2	24	11	22	392
11.94	0	300	3	42	113	1	1	11	50	61	3	28	14	25	435
12.05	0	315	4	39	115	1	2	8	42	63	4	30	13	22	396
12.15	0	307	3	41	119	1	2	12	42	61	2	26	14	23	467
12.25	0	291	4	32	109	1	0	9	34	55	2	22	10	19	425
12.38	0	320	4	40	125	1	3	7	42	65	1	37	16	29	434
12.48	0	303	8	42	116	1	2	12	45	63	4	32	14	27	362
12.57	0	272	3	31	104	1	0	11	34	53	3	24	13	18	324
12.67	0	248	4	22	87	1	0	10	21	44	3	16	9	15	285
12.74	0	345	4	53	136	1	4	12	66	69	1	44	19	32	490
12.8	0	276	4	34	121	1	1	7	33	53	3	25	13	25	540
12.87	0	327	6	49	141	1	3	12	58	66	5	39	20	34	577
12.94	0	310	6	36	119	1	1	11	39	61	3	27	15	24	550
13.02	0	347	3	63	150	1	6	13	70	72	2	48	23	43	655
13.09	0	326	8	56	145	1	6	14	66	69	3	43	22	42	585
13.17	0	327	6	55	143	1	4	11	64	68	3	46	23	39	585
13.26	0	285	4	42	133	1	3	9	37	57	4	32	20	29	666
13.35	0	345	8	71	153	1	15	14	83	75	3	74	30	87	665



## Wangerland core W3 (Archive No. KB 5750)

Depth [m]	TS	TC	TIC	SiO <sub>2</sub>	TiO <sub>2</sub>	Al <sub>2</sub> O <sub>3</sub>	Fe <sub>2</sub> O <sub>3</sub>	MgO	CaO	Na <sub>2</sub> O	K <sub>2</sub> O	P <sub>2</sub> O <sub>5</sub>
0.34	0.02	1.73	0.02	69.45	0.73	11.97	5.45	1.35	0.84	0.74	2.40	0.12
0.38				69.75	0.74	12.45	5.78	1.60	0.82	0.74	2.50	0.10
0.43				71.10	0.72	11.95	5.59	1.60	0.89	0.76	2.47	0.10
0.51	0.01	0.72	0.32	67.00	0.70	12.06	6.64	1.94	1.89	0.66	2.46	0.11
0.59				65.90	0.71	12.11	5.37	1.96	3.40	0.68	2.46	0.10
0.64				63.17	0.70	12.29	5.79	2.02	4.42	0.63	2.47	0.11
0.69				59.42	0.70	12.71	5.96	2.07	5.82	0.57	2.48	0.13
0.76	0.03	1.98	1.25	59.52	0.71	12.66	5.46	2.03	6.11	0.57	2.49	0.11
0.96				62.59	0.69	11.98	4.90	1.83	5.03	0.63	2.41	0.11
1.10	0.05	2.55	0.91	60.32	0.70	12.16	6.15	1.93	4.62	0.60	2.43	0.22
1.17	0.71	3.85	1.42	59.09	0.60	10.88	4.42	1.87	6.36	1.04	2.29	0.15
1.23				55.73	0.67	12.61	5.60	1.96	4.41	0.53	2.44	0.13
1.29				57.71	0.71	13.08	6.32	2.02	4.29	0.55	2.54	0.15
1.35	0.34	3.32	0.93	57.16	0.68	12.57	6.29	1.93	4.80	0.54	2.45	0.16
1.40	0.66	3.54	1.11	55.69	0.69	12.96	6.33	2.01	5.61	0.53	2.51	0.16
1.47	1.30	3.98	1.40	54.52	0.67	12.50	5.93	1.97	6.87	0.56	2.44	0.14
1.54	1.35	3.97	1.41	53.97	0.68	12.62	5.86	2.02	6.87	0.56	2.47	0.14
1.61	1.60	3.97	1.40	53.50	0.68	12.59	5.96	2.03	6.77	0.59	2.49	0.14
1.67	2.02	5.07	1.29	54.56	0.63	11.51	5.92	1.88	6.33	0.63	2.33	0.14
1.73	1.77	4.11	1.22	55.96	0.66	12.05	5.83	1.97	5.90	0.65	2.44	0.14
1.78	1.74	3.95	1.20	58.31	0.65	11.48	5.53	1.87	5.81	0.69	2.37	0.13
1.83	1.72	3.97	1.31	58.50	0.62	11.04	5.16	1.83	6.20	0.71	2.30	0.13
1.86	3.62	11.00	1.22	49.66	0.49	7.80	5.91	1.44	6.33	0.72	1.72	0.12
1.88	3.23	11.30	1.48	48.43	0.45	7.24	5.23	1.38	7.48	0.71	1.63	0.12
1.90	2.54	8.15	1.41	54.50	0.45	7.53	4.66	1.32	6.96	0.74	1.72	0.11
1.91	3.20	10.60	1.38	48.64	0.48	8.12	5.51	1.49	6.96	0.71	1.76	0.13
1.94	2.74	8.65	1.44	53.62	0.48	8.10	5.06	1.45	7.04	0.74	1.80	0.12
1.97	3.43	12.23	1.39	47.61	0.48	7.67	5.61	1.44	7.01	0.74	1.68	0.12
1.99	3.88	14.35	1.21	44.86	0.46	6.99	5.82	1.39	6.37	0.76	1.56	0.12
2.03	4.05	14.00	1.37	43.64	0.48	7.56	6.19	1.51	6.97	0.77	1.63	0.18
2.05	2.73	7.69	1.37	51.63	0.57	9.75	5.78	1.76	6.73	0.76	2.04	0.14
2.08	1.29	3.71	1.48	60.02	0.59	10.03	4.41	1.73	6.87	0.81	2.17	0.13
2.14	1.67	3.58	1.36	59.50	0.61	10.49	4.98	1.78	6.32	0.79	2.23	0.13
2.20	1.45	3.03	1.27	64.54	0.56	9.15	4.32	1.54	5.83	0.86	2.10	0.11
2.27	0.92	3.39	1.28	62.83	0.60	9.95	4.14	1.67	5.88	0.84	2.19	0.13
2.33	0.98	3.18	1.19	63.34	0.61	9.95	4.36	1.68	5.53	0.88	2.19	0.18
2.38	0.84	3.21	1.30	63.76	0.58	9.61	4.11	1.64	5.96	0.88	2.15	0.16
2.43	0.84	3.42	1.35	61.69	0.59	10.03	4.30	1.74	6.22	0.93	2.20	0.18
2.47	0.55	2.17	1.09	73.53	0.46	7.05	2.62	1.12	5.04	0.96	1.85	0.13
2.53	0.67	3.24	1.36	63.69	0.54	9.31	3.93	1.61	6.18	0.92	2.11	0.16
2.60	0.75	3.54	1.40	58.44	0.59	9.95	4.53	1.76	6.19	0.87	2.15	0.20
2.66	0.67	3.20	1.38	63.99	0.56	9.20	4.11	1.61	5.97	0.94	2.09	0.17
2.72	0.65	2.89	1.32	66.96	0.52	8.42	3.49	1.44	5.85	0.96	2.00	0.13
2.80				69.95	0.52	7.84	3.43	1.30	5.29	0.97	1.93	0.12
2.83				67.40	0.54	8.39	3.61	1.43	5.44	0.99	2.00	0.14
2.96	0.56	2.96	1.22	68.68	0.50	8.07	3.42	1.34	5.30	0.97	1.97	0.13
3.05				67.02	0.56	8.99	3.85	1.50	5.10	0.97	2.09	0.15
3.12				68.64	0.52	8.48	3.51	1.41	5.05	0.98	2.02	0.13
3.23	0.51	2.62	1.15	68.67	0.51	8.39	3.48	1.39	5.02	0.98	2.02	0.13
3.30				66.66	0.56	8.95	3.78	1.50	5.23	0.99	2.09	0.15
3.38				69.78	0.47	7.84	3.24	1.28	4.96	1.00	1.95	0.13
3.46	0.50	2.52	1.11	69.99	0.53	8.12	3.43	1.33	4.73	0.98	1.98	0.13
3.54				68.87	0.52	8.32	3.45	1.38	4.86	1.01	2.00	0.13
3.62				71.00	0.49	7.79	3.16	1.26	4.70	1.00	1.94	0.13

## Wangerland core W3 (Archive No. KB 5750)

Depth [m]	As	Ba	Co	Cr	Mn	Mo	Ni	Pb	Rb	Sr	U	V	Y	Zn	Zr
0.34	17	305	11	94	506	1	24	31	128	88	3	112	23	76	270
0.38	19	320	11	98	1590	1	36	24	131	92	3	118	25	75	270
0.43	30	311	13	97	1122	1	35	21	124	92	4	118	25	71	298
0.51	39	300	13	96	1427	1	37	24	125	100	2	130	23	75	252
0.59	9	290	9	95	667	1	27	21	126	116	2	110	23	75	255
0.64	15	277	10	96	628	1	28	26	131	129	4	118	24	79	224
0.69	17	252	12	98	474	1	30	24	133	153	3	131	23	82	192
0.76	13	271	6	98	281	1	27	19	132	164	2	126	23	84	214
0.96	6	271	9	93	296	1	27	20	124	146	3	112	22	79	233
1.10	27	263	13	101	315	1	32	23	127	141	3	125	23	82	221
1.17	14	257	11	81	549	1	25	20	115	231	3	107	19	71	201
1.23	17	247	8	95	248	1	31	23	131	132	5	136	22	82	176
1.29	21	270	12	100	291	1	33	22	134	131	4	130	23	88	183
1.35	17	258	12	95	310	1	30	23	131	140	4	126	22	83	199
1.40	20	266	9	98	344	1	32	21	136	157	5	134	22	90	171
1.47	24	253	9	95	420	1	30	21	136	195	5	127	23	86	181
1.54	24	245	11	94	446	1	30	19	135	207	3	128	22	91	175
1.61	24	253	10	97	531	1	31	23	133	205	5	129	23	90	174
1.67	27	254	9	89	596	1	30	24	122	223	5	122	20	84	196
1.73	22	258	11	94	565	1	30	23	129	183	4	123	21	85	195
1.78	22	262	11	90	598	1	27	19	125	181	3	116	22	80	227
1.83	17	247	11	84	644	1	26	22	118	209	5	104	21	89	215
1.86	35	208	7	74	1158	1	23	20	70	236	2	104	19	66	263
1.88	35	200	6	75	1176	1	22	17	65	270	3	95	19	64	269
1.90	30	213	8	64	839	1	17	12	66	252	3	85	19	59	248
1.91	29	205	6	76	1047	1	23	20	72	252	5	100	18	66	230
1.94	30	228	8	71	973	1	21	18	74	258	3	91	19	64	241
1.97	32	203	7	70	781	1	20	14	68	255	2	98	17	63	259
1.99	32	189	7	68	848	1	21	20	60	241	3	102	19	61	288
2.03	39	194	7	73	1028	1	21	15	67	272	2	105	19	68	247
2.05	34	235	10	84	832	1	26	20	105	248	4	116	20	76	229
2.08	15	254	11	75	605	1	21	16	105	248	3	94	19	70	240
2.14	21	246	8	82	665	1	24	18	112	233	4	101	20	70	249
2.20	15	262	9	68	540	1	18	16	95	211	4	84	18	62	271
2.27	12	267	9	77	542	1	21	17	101	219	4	93	20	65	280
2.33	11	259	11	80	518	1	22	17	104	175	3	92	20	65	290
2.38	13	263	8	75	490	1	21	16	101	213	3	90	19	63	287
2.43	13	264	9	78	532	1	21	18	105	225	2	94	19	67	246
2.47	10	267	5	53	356	1	8	8	65	174	2	53	16	40	302
2.53	12	253	7	70	571	1	19	15	99	230	4	86	17	58	232
2.60	13	245	8	79	909	1	20	16	101	229	2	95	19	64	233
2.66	14	261	6	69	973	1	16	15	94	213	2	83	19	60	259
2.72	12	267	7	66	596	1	15	14	80	220	3	71	18	53	273
2.80	9	266	5	63	596	1	13	14	65	170	3	62	18	49	312
2.83	9	273	8	69	722	1	15	15	86	182	4	72	17	52	324
2.96	6	270	12	62	644	1	16	11	77	172	4	70	16	51	275
3.05	8	261	8	70	550	1	17	15	91	166	3	77	19	59	303
3.12	6	271	10	62	552	1	14	13	84	165	4	71	16	51	261
3.23	5	271	9	62	610	1	15	13	74	161	3	70	16	50	243
3.30	9	271	5	67	531	1	17	15	93	182	3	77	17	55	289
3.38	11	277	6	58	481	1	14	13	76	167	3	64	16	49	268
3.46	9	267	6	62	568	1	13	16	80	158	4	67	17	49	328
3.54	8	268	8	66	464	1	15	13	85	161	3	73	17	52	287
3.62	6	268	8	61	463	1	12	12	79	156	2	62	16	45	319

## Wangerland core W3 (Archive No. KB 5750)

Depth [m]	TS	TC	TIC	SiO <sub>2</sub>	TiO <sub>2</sub>	Al <sub>2</sub> O <sub>3</sub>	Fe <sub>2</sub> O <sub>3</sub>	MgO	CaO	Na <sub>2</sub> O	K <sub>2</sub> O	P <sub>2</sub> O <sub>5</sub>
3.68	0.29	1.87	0.93	77.48	0.42	6.19	2.13	0.92	4.20	0.95	1.74	0.10
3.73				66.26	0.59	9.16	3.87	1.53	5.26	1.01	2.10	0.16
3.84				70.61	0.52	8.08	3.32	1.30	4.52	0.98	1.97	0.14
3.90	0.48	2.89	1.22	66.76	0.53	8.76	3.81	1.47	5.25	1.06	2.06	0.15
3.97				71.83	0.49	7.61	2.99	1.22	4.60	1.00	1.92	0.14
4.02	0.48	2.35	1.01	71.56	0.46	7.77	3.00	1.23	4.62	0.99	1.94	0.12
4.07				59.26	0.63	10.77	4.97	1.90	5.82	1.08	2.31	0.18
4.14	0.68	3.60	1.34	61.00	0.58	10.23	4.70	1.79	5.79	1.03	2.24	0.20
4.21				58.47	0.63	10.73	5.28	1.91	6.12	1.03	2.27	0.20
4.26	0.59	3.28	1.29	63.92	0.56	9.14	4.16	1.57	5.43	1.03	2.08	0.16
4.30	0.60	3.52	1.35	61.52	0.58	9.91	4.62	1.72	5.67	1.03	2.16	0.18
4.33				77.99	0.44	6.06	2.05	0.88	4.09	0.99	1.72	0.09
4.37	0.56	3.04	1.26	64.88	0.53	9.07	3.96	1.53	5.40	1.03	2.08	0.15
4.42				80.18	0.36	5.51	1.67	0.74	3.83	0.97	1.67	0.08
4.48	0.23	1.67	0.93	78.48	0.42	5.89	1.93	0.85	4.14	0.98	1.70	0.09
4.53	0.51	3.02	1.25	67.01	0.51	8.59	3.55	1.46	5.46	1.07	2.03	0.14
4.59				60.40	0.60	10.56	4.96	1.82	5.65	1.04	2.26	0.18
4.63				79.77	0.42	5.83	1.90	0.81	3.66	0.93	1.67	0.08
4.67	0.26	1.82	0.94	77.36	0.41	6.00	2.03	0.88	4.30	0.98	1.72	0.09
4.70	0.31	2.29	0.80	79.17	0.41	5.37	1.73	0.77	3.79	1.00	1.63	0.09
4.73	0.25	1.72	0.95	77.73	0.38	6.14	2.03	0.89	4.31	1.00	1.75	0.09
4.78				68.03	0.52	8.73	3.68	1.44	5.08	1.00	2.06	0.15
4.84	0.69	3.33	1.42	59.53	0.64	10.50	4.89	1.84	5.94	1.05	2.25	0.19
4.91				58.31	0.63	11.11	5.14	1.93	6.02	1.05	2.34	0.20
4.97				63.09	0.58	9.84	4.22	1.66	5.68	1.05	2.19	0.17
5.03	0.29	1.77	0.90	78.02	0.40	6.03	1.88	0.87	4.20	0.99	1.74	0.10
5.07	0.65	3.16	1.15	66.30	0.53	8.93	3.49	1.47	5.22	1.03	2.07	0.12
5.11	0.06	2.97	1.04	60.47	0.71	11.92	5.46	1.92	5.17	0.64	2.39	0.13
5.16	0.86	2.59	1.11	69.84	0.50	8.00	3.28	1.27	5.10	1.01	1.95	0.10
5.19	1.42	3.50	2.23	60.92	0.52	7.46	3.75	1.22	10.23	0.95	1.75	0.10
5.22	1.54	5.11	1.99	59.50	0.51	7.61	3.83	1.31	9.22	0.97	1.77	0.10
5.25	2.47	12.60	1.35	44.74	0.49	8.38	4.57	1.71	6.47	1.20	1.74	0.13
5.26	3.17	26.40	0.60	26.42	0.28	4.78	3.77	1.66	3.40	1.68	1.03	0.10
5.27	3.45	47.50	0.11	4.73	0.05	1.10	1.60	1.64	1.41	2.22	0.25	0.09
5.30	3.63	49.80	0.05	6.04	0.07	1.37	1.31	1.51	1.18	2.22	0.30	0.10
5.34	3.84	46.60	0.04	8.88	0.05	1.98	1.26	1.33	0.90	1.94	0.35	0.10
5.37	4.10	37.80	0.04	17.09	0.19	4.01	2.50	1.35	0.81	1.82	0.77	0.12
5.39	2.50	21.50	0.26	40.60	0.55	10.09	2.73	1.52	0.61	1.44	1.99	0.09
5.42	1.33	10.85	0.02	52.97	0.72	13.23	3.65	1.79	0.49	1.26	2.60	0.09
5.46	1.42	7.09	0.02	59.42	0.77	13.26	4.08	1.70	0.48	1.22	2.68	0.08
5.50	1.04	7.55	0.01	58.22	0.77	13.65	3.91	1.81	0.48	1.21	2.76	0.09
5.54	1.41	9.54	0.02	55.73	0.72	12.55	3.77	1.73	0.55	1.27	2.56	0.09
5.56	1.82	10.40	0.01	54.04	0.72	12.39	4.07	1.69	0.61	1.29	2.55	0.09
5.59	3.37	15.10	0.02	45.86	0.62	11.40	5.04	1.73	0.63	1.38	2.32	0.10
5.62	4.27	14.05	0.02	46.45	0.62	11.23	6.16	1.65	0.60	1.31	2.30	0.09
5.66	4.38	19.35	0.02	38.81	0.53	9.96	5.29	1.53	0.62	1.41	2.02	0.10
5.70	3.80	10.95	0.01	51.25	0.67	11.69	6.09	1.54	0.56	1.27	2.41	0.10
5.74	6.64	23.85	0.03	31.72	0.42	8.27	7.26	1.56	0.76	1.45	1.61	0.12
5.77	1.40	8.40	0.40	61.23	0.53	9.15	3.27	1.38	2.23	1.14	2.05	0.11
5.80	5.59	25.35	0.03	29.18	0.41	7.73	5.90	1.58	0.87	1.53	1.54	0.12
5.84	8.79	37.20	0.02	10.59	0.15	3.05	7.44	1.36	1.10	1.63	0.58	0.11
5.87	7.67	33.30	0.00	17.57	0.25	4.62	6.29	1.31	0.92	1.49	0.88	0.09
5.89	1.67	12.45	0.03	52.16	0.68	11.81	3.38	1.65	0.70	1.31	2.19	0.17

## Wangerland core W3 (Archive No. KB 5750)

Depth [m]	As	Ba	Co	Cr	Mn	Mo	Ni	Pb	Rb	Sr	U	V	Y	Zn	Zr
3.68	0	273	7	50	339	1	7	9	49	141	3	43	13	32	318
3.73	8	264	9	73	546	1	17	15	92	173	3	80	19	58	319
3.84	8	258	5	63	573	1	13	13	78	150	2	67	17	51	309
3.90	7	254	8	69	642	1	16	17	82	168	3	74	17	57	278
3.97	6	265	8	58	455	1	10	11	68	153	3	61	17	48	319
4.02	8	271	7	55	362	1	12	15	77	155	2	61	15	51	263
4.07	16	265	9	93	575	1	25	18	112	191	2	105	20	76	236
4.14	19	261	9	78	610	1	24	18	108	182	2	97	19	75	210
4.21	17	249	11	83	956	1	24	17	112	212	3	105	21	76	244
4.26	11	257	7	71	819	1	17	13	92	173	2	83	17	62	256
4.30	13	253	7	78	854	1	20	17	103	199	3	95	18	70	227
4.33	4	276	7	48	350	1	7	11	50	141	2	40	16	33	392
4.37	12	268	9	66	671	1	19	11	95	182	2	83	17	67	230
4.42	-2	270	5	36	279	1	2	7	44	134	3	30	13	26	310
4.48	0	275	5	43	321	1	6	9	46	142	3	35	14	34	362
4.53	10	255	7	61	547	1	16	13	90	183	5	74	16	55	225
4.59	13	253	10	79	926	1	21	18	109	186	3	101	19	74	220
4.63	0	261	5	44	275	1	5	8	46	129	3	39	14	30	384
4.67	4	275	5	44	314	1	6	8	51	147	3	40	14	31	342
4.70	3	261	7	44	263	1	5	8	43	133	3	37	14	31	391
4.73	0	277	4	44	333	1	6	9	48	144	3	41	11	66	268
4.78	11	269	8	67	665	1	17	14	91	166	1	74	17	56	255
4.84	15	256	8	85	902	1	22	20	109	197	4	101	22	68	274
4.91	17	262	9	85	1049	1	26	19	115	212	5	113	21	76	230
4.97	12	261	9	75	800	1	20	15	101	186	2	91	18	65	250
5.03	4	275	5	44	274	1	5	7	50	144	2	39	15	33	328
5.07	9	255	6	67	374	1	17	16	93	171	2	80	17	56	266
5.11	16	262	12	94	263	1	29	23	125	142	3	120	23	79	225
5.16	12	273	9	66	338	12	13	14	75	165	3	68	17	50	324
5.19	22	229	6	63	334	15	14	14	65	357	7	65	20	49	404
5.22	23	229	7	61	346	14	17	14	67	330	6	72	19	52	348
5.25	26	204	10	68	354	14	27	17	80	239	10	101	22	62	210
5.26	20	129	8	97	247	23	51	10	45	163	11	90	14	38	132
5.27	8	25	1	12	90	17	4	1	5	130	7	30	5	11	20
5.30	1	32	1	13	95	16	2	2	4	110	4	31	5	9	17
5.34	5	25	1	19	50	11	5	2	13	94	2	39	6	10	12
5.37	7	74	3	35	60	12	12	9	38	94	4	64	10	19	42
5.39	0	209	5	77	97	14	19	16	87	84	4	107	11	40	111
5.42	0	270	8	102	161	13	30	25	131	91	4	118	17	73	157
5.46	0	298	10	97	181	10	26	25	127	91	5	112	17	82	201
5.50	0	291	8	98	166	12	26	26	136	93	4	115	18	80	190
5.54	1	279	12	94	161	11	30	24	126	94	6	108	19	103	196
5.56	0	268	10	91	112	13	14	17	99	96	3	112	10	35	150
5.59	9	244	7	83	171	13	27	13	116	98	7	110	18	66	142
5.62	16	244	6	84	184	14	24	14	116	95	7	107	18	66	158
5.66	12	208	8	75	132	19	26	22	100	91	6	107	17	73	127
5.70	6	257	12	87	151	21	25	17	119	93	6	109	19	70	197
5.74	19	164	12	63	179	20	40	24	81	94	8	98	26	125	98
5.77	4	260	9	68	232	11	23	14	95	116	4	74	16	72	223
5.80	21	162	7	62	166	14	24	14	83	103	6	87	17	61	103
5.84	33	66	0	28	159	17	13	11	32	120	7	53	18	24	43
5.87	11	96	3	43	95	24	19	14	45	89	6	70	16	26	59
5.89	4	261	6	89	157	12	24	25	106	104	5	104	19	46	172

**Wangerland core W3 (Archive No. KB 5750)**

Depth [m]	TS	TC	TIC	SiO <sub>2</sub>	TiO <sub>2</sub>	Al <sub>2</sub> O <sub>3</sub>	Fe <sub>2</sub> O <sub>3</sub>	MgO	CaO	Na <sub>2</sub> O	K <sub>2</sub> O	P <sub>2</sub> O <sub>5</sub>
5.91	1.89	12.65	0.01	50.39	0.68	11.99	3.27	1.46	0.55	1.26	2.23	0.13
5.94	2.87	16.05	0.01	46.63	0.65	10.82	3.64	1.40	0.64	1.35	2.22	0.08
5.97	3.13	21.90	0.02	39.77	0.54	8.80	3.50	1.51	0.88	1.49	1.73	0.13
5.99	7.06	40.30	0.02	10.94	0.17	3.19	5.61	1.18	0.90	1.54	0.58	0.09
6.00	15.95	16.00	0.01	25.27	0.36	6.46	17.62	1.11	0.51	0.89	1.29	0.08
6.01	5.65	37.65	0.02	16.28	0.24	4.50	4.58	1.38	1.01	1.59	0.85	0.10
6.03	6.85	44.45	0.02	8.42	0.11	1.36	5.49	1.15	1.22	1.52	0.27	0.12
6.06	1.59	11.50	0.01	73.65	0.24	1.76	1.58	0.34	0.48	0.58	0.65	0.05
6.08	0.26	3.95	0.01	90.59	0.24	1.89	0.32	0.15	0.26	0.37	0.76	0.03
6.10	3.32	2.15	0.01	88.28	0.27	1.95	3.81	0.12	0.23	0.33	0.79	0.02
6.13	0.13	1.81	0.01	93.29	0.26	2.13	0.30	0.12	0.23	0.34	0.85	0.02
6.15	0.13	1.43	0.01	93.33	0.28	2.27	0.37	0.12	0.25	0.34	0.89	0.02
6.18	0.12	1.97	0.01	90.73	0.26	2.49	0.37	0.16	0.29	0.35	0.93	0.04
6.22	0.15	1.89	0.01	89.56	0.26	2.72	0.46	0.19	0.31	0.40	0.95	0.06
6.27	0.33	0.85	0.01	92.62	0.27	3.16	0.85	0.18	0.27	0.41	1.04	0.04
6.33	0.12	1.22	0.01	92.44	0.27	3.13	0.56	0.19	0.30	0.43	1.03	0.05

Depth [m]	As	Ba	Co	Cr	Mn	Mo	Ni	Pb	Rb	Sr	U	V	Y	Zn	Zr
5.91	7	254	6	85	124	10	21	17	110	95	6	112	19	34	155
5.94	1	249	6	79	106	17	16	16	119	95	6	104	16	30	172
5.97	5	205	2	71	149	13	19	15	93	106	5	87	15	37	134
5.99	0	66	6	27	71	17	9	5	27	77	3	55	7	17	32
6.00	98	136	14	48	283	27	33	13	65	69	6	64	26	125	96
6.01	19	95	6	38	115	18	17	9	52	112	6	63	14	45	64
6.03	13	57	6	16	116	14	9	4	5	124	4	33	10	12	113
6.06	0	135	3	12	88	9	0	5	6	56	2	9	5	8	314
6.08	0	163	3	8	67	9	0	8	5	38	1	5	3	4	309
6.10	0	164	0	10	170	10	0	5	12	35	3	8	5	6	347
6.13	0	168	2	13	64	1	0	5	12	36	2	5	3	4	310
6.15	0	186	2	9	68	1	0	7	14	37	2	9	3	4	336
6.18	0	184	3	12	66	1	0	5	13	43	0	11	3	9	284
6.22	0	194	3	12	74	1	0	4	18	47	2	9	5	6	299
6.27	0	205	1	16	86	1	0	3	21	43	2	9	5	11	327
6.33	0	197	3	11	84	1	0	9	20	45	3	11	5	10	307

## Wangerland core W4 (Archive No. KB 5752)

Depth [m]	TS	TC	TIC	SiO <sub>2</sub>	TiO <sub>2</sub>	Al <sub>2</sub> O <sub>3</sub>	Fe <sub>2</sub> O <sub>3</sub>	MgO	CaO	Na <sub>2</sub> O	K <sub>2</sub> O	P <sub>2</sub> O <sub>5</sub>
0.39	0.05	1.25	0.02	67.86	0.65	11.40	4.93	1.48	1.65	0.70	2.40	1.25
0.51				70.24	0.71	11.29	4.83	1.52	1.24	0.76	2.43	0.61
0.73	0.10	1.10	0.17	67.02	0.73	11.90	5.90	1.76	1.47	0.71	2.53	0.73
0.90	0.04	1.04	0.17	67.77	0.74	12.30	5.38	1.80	1.26	0.70	2.62	0.35
1.05				68.16	0.71	11.48	5.15	1.71	1.79	0.73	2.48	0.58
1.15				70.38	0.70	11.46	4.42	1.44	1.16	0.75	2.45	0.31
1.22	0.12	3.11	0.17	63.20	0.69	11.96	4.98	1.57	1.62	0.62	2.48	0.64
1.26				66.13	0.69	12.01	4.99	1.64	2.30	0.64	2.48	0.36
1.35				66.21	0.69	11.01	4.27	1.63	1.73	0.71	2.42	0.43
1.45	1.32	23.20	0.20	38.03	0.35	5.37	3.28	0.94	2.47	0.39	1.27	0.69
1.55	1.08	19.43	0.37	44.78	0.42	6.65	3.25	1.18	3.31	0.47	1.61	0.71
1.67	0.87	14.20	0.35	51.01	0.49	7.69	3.59	1.36	2.72	0.55	1.87	0.62
1.78	0.44	7.57	0.34	62.43	0.56	8.44	3.68	1.39	2.22	0.67	2.11	0.72
1.87				71.94	0.64	9.25	3.76	1.48	1.53	0.81	2.31	0.64
1.96	0.38	5.83	0.49	60.67	0.54	8.29	5.26	1.32	2.90	0.68	1.98	0.56
2.07	0.68	7.48	0.50	56.42	0.61	10.50	4.80	1.74	2.87	0.57	2.48	0.45
2.17				57.92	0.64	11.52	5.10	1.95	3.59	0.58	2.62	0.61
2.28	0.32	4.62	0.71	58.14	0.66	12.10	5.00	1.98	3.55	0.56	2.73	0.49
2.41	0.64	4.49	0.76	58.74	0.66	11.74	5.10	1.89	3.71	0.58	2.69	0.34
2.51				56.92	0.65	11.57	5.45	1.88	4.43	0.56	2.66	0.22
2.60	1.15	4.23	0.99	55.85	0.64	11.79	5.67	1.91	4.80	0.54	2.69	0.19
2.68	0.90	3.57	0.74	59.80	0.67	11.94	5.31	1.92	3.63	0.62	2.75	0.18
2.75	1.19	4.01	1.19	54.92	0.65	12.39	5.80	2.00	5.58	0.52	2.80	0.20
2.80	1.12	4.27	1.03	56.23	0.65	11.97	5.57	1.95	4.88	0.55	2.73	0.19
2.86	1.11	3.36	1.00	58.32	0.67	11.98	5.52	1.96	4.68	0.59	2.73	0.18
2.94	1.23	2.93	1.63	61.86	0.59	8.69	3.94	1.50	7.40	0.69	2.09	0.14
3.02	1.29	3.28	1.04	56.83	0.69	12.83	5.88	2.04	4.84	0.53	2.85	0.17
3.09	1.90	3.60	1.23	53.44	0.68	12.82	6.31	2.01	5.77	0.46	2.79	0.17
3.16	0.96	3.07	0.48	66.60	0.70	11.80	3.98	1.34	0.85	0.70	2.73	0.08
3.23	1.76	2.61	0.04	67.63	0.70	11.37	5.13	1.41	0.68	0.74	2.62	0.12
3.29	1.76	2.16	0.10	66.63	0.69	11.37	5.35	1.52	0.84	0.71	2.67	0.14
3.33	1.89	1.62	0.30	68.16	0.66	10.55	5.22	1.69	1.35	0.77	2.51	0.13
3.37	2.05	1.89	0.45	63.36	0.68	11.67	6.05	1.94	1.95	0.66	2.69	0.14
3.41	1.00	2.14	0.90	62.00	0.66	11.43	4.81	1.89	3.99	0.64	2.63	0.13
3.45	1.07	3.20	1.26	61.69	0.63	10.98	4.59	1.85	5.68	0.64	2.54	0.13
3.49	0.68	2.57	1.46	59.85	0.63	11.12	4.35	1.86	6.61	0.62	2.57	0.13
3.52	0.62	2.82	1.62	59.10	0.60	10.68	4.14	1.80	7.39	0.62	2.47	0.13
3.56	0.68	2.90	1.59	58.21	0.63	10.97	4.34	1.86	7.22	0.60	2.52	0.14
3.60	0.78	2.79	1.47	59.94	0.60	10.44	4.29	1.76	6.75	0.61	2.43	0.13
3.62	0.73	2.30	1.40	63.87	0.62	9.00	3.80	1.56	6.28	0.75	2.20	0.12
3.65				66.28	0.58	9.02	3.41	1.52	5.80	0.74	2.22	0.12
3.69				68.31	0.53	8.03	2.89	1.33	5.58	0.77	2.05	0.11
3.73	0.61	2.97	1.54	58.09	0.62	10.86	4.31	1.85	7.00	0.59	2.51	0.13
3.79	0.65	3.22	1.74	54.25	0.65	11.85	4.75	2.03	7.86	0.51	2.65	0.15
3.85				54.84	0.65	11.95	4.83	2.05	7.89	0.50	2.69	0.15
3.89				56.65	0.61	11.00	4.18	1.83	7.32	0.53	2.50	0.14
3.96				60.91	0.63	10.26	3.76	1.73	6.92	0.63	2.40	0.14
4.03	1.09	2.97	1.40	61.46	0.64	10.03	4.38	1.71	6.38	0.65	2.34	0.16
4.09	1.37	2.35	1.40	66.58	0.60	7.85	3.89	1.33	6.37	0.77	1.99	0.13
4.17				67.87	0.61	7.47	3.36	1.30	6.40	0.78	1.93	0.12
4.25	1.26	2.59	1.52	64.58	0.59	8.27	3.79	1.43	6.96	0.73	2.04	0.13
4.32				72.71	0.55	6.62	2.58	1.08	5.52	0.80	1.81	0.11
4.35				71.61	0.56	6.57	2.52	1.12	5.67	0.83	1.79	0.11

**Wangerland core W4 (Archive No. KB 5752)**

Depth [m]	As	Ba	Co	Cr	Mn	Mo	Ni	Pb	Rb	Sr	U	V	Y	Zn	Zr
0.39	17	277	12	84	573	1	26	42	120	151	3	102	24	122	254
0.51	16	305	11	91	472	1	26	21	118	107	2	105	27	85	315
0.73	40	294	12	90	589	1	29	20	126	108	2	139	28	84	283
0.90	17	308	10	93	418	1	29	22	127	92	3	116	28	82	257
1.05	27	298	10	96	573	1	27	20	121	109	3	112	25	83	285
1.15	20	305	10	86	279	1	24	19	116	93	3	108	22	63	302
1.22	21	286	10	89	318	1	28	22	122	109	2	120	26	74	240
1.26	16	289	15	91	534	1	25	19	122	105	1	124	25	73	245
1.35	14	290	9	84	325	1	24	19	113	94	3	105	25	77	273
1.45	23	150	6	44	648	5	16	9	55	101	1	54	14	118	146
1.55	12	187	7	55	849	5	18	12	72	151	1	65	15	109	180
1.67	13	213	7	60	628	2	17	14	80	125	3	71	18	81	207
1.78	18	253	11	69	1208	1	20	16	85	108	1	80	22	71	313
1.87	10	300	10	71	860	1	19	16	95	96	2	80	25	58	421
1.96	17	241	8	72	558	1	20	14	84	128	3	74	20	116	249
2.07	16	248	11	80	457	1	24	18	112	130	2	108	22	92	205
2.17	16	269	11	85	558	1	27	19	122	140	4	107	22	88	202
2.28	16	270	11	95	488	1	28	20	126	135	4	122	24	88	196
2.41	18	271	13	87	441	1	29	19	124	141	2	120	25	85	206
2.51	20	263	11	92	418	1	28	19	119	156	2	122	23	83	187
2.60	17	256	12	90	418	1	29	19	122	168	2	123	23	85	176
2.68	13	272	11	88	372	1	29	21	126	139	3	127	24	85	216
2.75	17	251	14	89	527	1	32	20	133	188	3	134	23	85	164
2.80	14	260	12	87	488	1	31	20	127	168	3	129	24	85	181
2.86	16	267	12	86	534	1	30	19	126	161	4	125	25	81	200
2.94	17	257	9	74	496	1	19	16	90	207	4	87	23	76	376
3.02	29	273	15	97	403	1	34	22	131	154	2	138	24	401	188
3.09	22	260	13	89	441	1	34	23	133	186	3	134	24	84	170
3.16	29	296	12	92	194	1	26	21	120	100	4	115	21	132	259
3.23	45	299	17	87	225	1	41	19	116	98	3	110	30	100	284
3.29	24	290	12	86	263	1	26	19	115	89	3	112	28	86	253
3.33	15	298	7	78	248	1	24	18	110	91	2	98	25	91	264
3.37	20	279	12	91	256	1	29	19	116	96	2	116	25	74	215
3.41	16	275	12	88	271	1	29	21	117	118	3	114	25	567	212
3.45	15	256	11	80	294	1	25	17	114	143	3	109	24	71	208
3.49	12	269	9	82	318	1	24	19	114	155	3	113	23	70	191
3.52	12	256	9	81	318	1	22	19	112	169	3	110	23	68	196
3.56	14	252	10	79	333	1	26	18	113	167	2	113	23	69	194
3.60	15	262	10	77	333	1	24	20	110	163	3	102	23	66	218
3.62	16	259	8	74	302	1	20	15	94	155	3	83	25	101	352
3.65	13	269	8	70	279	1	21	16	92	146	2	83	22	54	291
3.69	16	274	8	64	263	1	20	14	83	141	1	70	21	45	331
3.73	15	259	10	81	341	1	24	19	112	165	3	112	22	76	199
3.79	14	239	10	88	387	1	30	20	125	180	1	125	23	89	167
3.85	15	257	11	93	418	1	29	20	123	181	1	128	23	80	173
3.89	21	249	11	84	349	1	25	20	114	174	1	113	22	103	180
3.96	17	262	10	78	302	1	23	19	107	166	2	101	24	64	278
4.03	25	259	12	78	349	1	23	16	103	161	4	103	25	64	298
4.09	15	265	8	79	364	1	16	13	84	171	3	71	26	45	469
4.17	14	271	8	72	418	1	15	14	78	175	2	65	26	44	526
4.25	17	256	10	75	441	1	19	14	88	187	4	77	23	50	406
4.32	10	273	7	63	341	1	12	12	71	160	2	52	23	36	520
4.35	10	271	6	58	341	1	9	10	68	158	3	52	23	56	485

## Wangerland core W4 (Archive No. KB 5752)

Depth [m]	TS	TC	TIC	SiO <sub>2</sub>	TiO <sub>2</sub>	Al <sub>2</sub> O <sub>3</sub>	Fe <sub>2</sub> O <sub>3</sub>	MgO	CaO	Na <sub>2</sub> O	K <sub>2</sub> O	P <sub>2</sub> O <sub>5</sub>
4.40	0.80	2.09	1.32	70.37	0.56	6.82	2.72	1.14	6.03	0.81	1.83	0.11
4.45				68.49	0.58	7.60	3.29	1.28	6.18	0.77	1.95	0.12
4.49	1.36	2.83	1.53	63.03	0.60	8.78	4.07	1.51	6.97	0.70	2.11	0.14
4.52				69.32	0.50	7.40	2.92	1.18	5.60	0.74	1.93	0.11
4.57	1.01	2.48	1.49	67.27	0.54	7.72	3.28	1.34	6.75	0.78	1.96	0.12
4.62	0.78	2.13	1.41	70.16	0.51	6.96	2.72	1.17	6.32	0.83	1.86	0.11
4.69				72.10	0.52	6.66	2.48	1.11	5.71	0.81	1.82	0.11
4.75				72.63	0.52	6.67	2.45	1.10	5.58	0.86	1.82	0.10
4.81				71.62	0.54	6.80	2.48	1.14	5.93	0.85	1.85	0.11
4.87	0.87	2.43	1.49	66.90	0.53	7.57	3.08	1.29	6.75	0.79	1.94	0.12
4.93				67.25	0.56	7.79	3.08	1.31	6.82	0.78	1.99	0.12
4.98				64.66	0.63	8.69	3.46	1.53	6.88	0.75	2.12	0.13
5.03	0.98	2.65	1.51	64.16	0.58	8.76	3.62	1.49	6.86	0.71	2.15	0.13
5.09				68.93	0.55	7.73	2.98	1.26	6.20	0.76	1.99	0.12
5.15				62.11	0.60	9.36	3.97	1.61	7.10	0.67	2.22	0.13
5.21	1.00	2.59	1.57	64.62	0.57	8.43	3.53	1.44	7.17	0.74	2.08	0.13
5.27				69.21	0.56	7.51	2.89	1.23	5.92	0.78	1.93	0.11
5.32				72.87	0.54	6.97	2.63	1.09	4.95	0.78	1.86	0.10
5.37	0.95	2.29	1.43	68.75	0.51	7.35	3.11	1.18	6.56	0.76	1.91	0.11
5.42				72.29	0.50	6.92	2.63	1.11	5.49	0.78	1.87	0.10
5.46				69.63	0.48	7.29	2.89	1.17	5.84	0.75	1.92	0.10
5.50				74.12	0.47	6.56	2.45	1.01	4.93	0.77	1.81	0.09
5.53	1.11	3.45	1.06	56.05	0.65	11.76	5.46	1.93	4.98	0.54	2.66	0.17
5.57	0.60	1.93	1.17	72.67	0.49	6.81	2.48	1.07	5.33	0.80	1.85	0.10
5.61				76.34	0.42	6.06	2.04	0.90	4.68	0.82	1.74	0.09
5.66	0.64	1.92	1.15	72.77	0.52	6.82	2.56	1.08	5.28	0.80	1.86	0.10
5.71				72.50	0.51	6.74	2.42	1.09	5.22	0.83	1.86	0.10
5.76				68.88	0.53	7.65	3.00	1.28	6.16	0.78	1.98	0.11
5.80				65.72	0.55	8.41	3.43	1.45	6.52	0.77	2.10	0.12
5.85	0.89	2.57	1.44	67.94	0.50	7.65	3.03	1.30	6.26	0.79	1.97	0.11
5.89				66.14	0.54	8.13	3.25	1.37	6.26	0.75	2.05	0.11
5.93	1.04	2.78	1.48	64.22	0.52	8.39	3.60	1.42	6.74	0.72	2.09	0.12
5.97				69.97	0.48	7.34	2.85	1.20	5.87	0.81	1.96	0.10
6.03				69.15	0.50	7.58	2.98	1.25	5.88	0.79	1.98	0.11
6.08	0.57	1.86	1.10	73.58	0.44	6.53	2.32	1.02	5.06	0.82	1.83	0.09
6.14				70.70	0.51	7.36	2.84	1.19	5.53	0.80	1.95	0.10
6.19				64.67	0.56	8.53	3.55	1.44	6.59	0.72	2.11	0.12
6.23	0.79	2.09	1.22	69.99	0.49	7.32	2.87	1.18	5.54	0.85	1.96	0.10
6.28				66.43	0.54	8.36	3.51	1.39	6.24	0.71	2.09	0.11
6.33				71.82	0.43	6.69	2.59	1.05	5.42	0.78	1.83	0.09
6.39	0.82	2.36	1.35	68.99	0.48	7.33	2.96	1.22	6.18	0.79	1.93	0.10
6.44				66.32	0.54	8.24	3.32	1.39	6.39	0.73	2.07	0.11
6.48				61.25	0.58	9.57	3.92	1.62	6.92	0.67	2.29	0.13
6.53	0.66	2.33	1.33	67.91	0.54	7.78	3.00	1.30	6.02	0.79	2.00	0.11
6.59				69.03	0.53	7.76	2.99	1.29	5.71	0.79	2.00	0.11
6.66				59.48	0.59	9.90	4.31	1.68	7.25	0.62	2.33	0.13
6.71				59.27	0.60	10.26	4.46	1.71	7.10	0.58	2.37	0.13
6.76	0.88	2.36	1.47	60.85	0.56	9.68	4.21	1.62	6.69	0.61	2.30	0.13
6.82	1.44	3.06	1.43	61.32	0.60	9.78	4.56	1.63	6.45	0.65	2.31	0.13
6.88	1.22	2.94	1.50	62.69	0.51	8.79	3.91	1.45	6.86	0.66	2.13	0.12
6.93	1.22	3.02	1.42	62.37	0.53	8.94	3.95	1.48	6.48	0.60	2.13	0.12
6.98	0.81	1.83	0.84	75.86	0.37	6.10	2.71	0.97	3.82	0.36	1.48	0.08
7.05	0.14	0.26	0.10	88.01	0.22	1.70	0.65	0.17	0.52	0.16	0.60	0.03
7.12	0.22	0.54	0.21	84.11	0.24	2.52	0.99	0.33	1.06	0.20	0.74	0.06



## Wangerland core W4 (Archive No. KB 5752)

Depth [m]	As	Ba	Co	Cr	Mn	Mo	Ni	Pb	Rb	Sr	U	V	Y	Zn	Zr
4.40	11	257	6	62	356	1	12	13	72	174	4	54	23	39	493
4.45	15	264	10	68	395	1	15	16	80	176	4	69	24	43	478
4.49	18	252	10	75	465	1	19	16	90	191	3	84	24	53	357
4.52	14	261	10	60	325	1	15	12	77	164	2	67	19	77	384
4.57	14	272	9	65	403	1	16	14	83	193	3	67	21	44	374
4.62	11	266	8	51	302	1	12	12	73	179	2	56	21	39	387
4.69	10	267	7	57	271	1	12	11	70	165	1	52	22	35	450
4.75	10	272	7	63	271	1	9	12	70	159	3	51	22	115	430
4.81	11	268	6	64	279	1	12	12	72	170	2	58	21	36	468
4.87	14	278	7	65	325	1	16	13	81	193	3	69	21	44	362
4.93	12	259	9	67	333	1	16	13	82	191	3	73	23	43	398
4.98	14	265	9	72	341	1	20	15	92	182	3	77	25	51	422
5.03	14	269	10	73	341	1	20	14	92	189	2	82	24	51	354
5.09	13	273	10	69	294	1	14	12	79	173	3	64	21	45	401
5.15	16	260	9	76	364	1	21	17	94	189	2	87	23	59	302
5.21	15	267	8	69	333	1	16	15	88	200	4	76	24	49	376
5.27	11	262	6	64	287	1	15	14	77	168	3	61	21	43	447
5.32	13	267	9	60	271	1	12	12	73	145	3	57	22	35	496
5.37	19	260	9	61	310	1	14	12	77	199	2	60	21	48	406
5.42	11	288	5	57	287	1	12	13	72	154	2	53	20	38	399
5.46	13	261	7	58	310	1	14	12	76	165	3	61	19	42	336
5.50	12	277	7	56	287	1	12	10	71	150	2	48	19	34	412
5.53	21	254	13	85	519	1	28	21	123	168	4	121	24	92	192
5.57	11	264	5	54	302	1	10	10	73	158	4	52	20	36	420
5.61	8	277	7	49	256	1	7	10	64	142	2	45	16	28	364
5.66	11	269	7	62	325	1	12	11	72	157	2	51	19	37	489
5.71	10	269	6	62	302	1	12	12	70	147	1	53	22	36	417
5.76	13	263	9	67	349	1	14	12	81	175	3	65	21	132	380
5.80	13	271	10	59	387	1	18	15	85	179	2	73	23	50	308
5.85	12	267	6	56	349	1	16	12	81	179	3	63	20	44	298
5.89	12	266	7	72	372	1	18	13	84	174	3	69	21	170	325
5.93	17	273	9	66	418	1	18	15	88	192	1	80	20	51	257
5.97	12	274	7	58	349	1	15	12	79	173	1	57	18	40	294
6.03	12	268	9	55	364	1	13	13	79	171	2	65	20	42	339
6.08	10	283	6	54	294	1	11	11	70	154	1	47	18	98	332
6.14	12	270	7	61	356	1	14	13	77	160	2	61	20	40	346
6.19	15	266	9	63	426	1	17	13	90	187	3	77	21	51	356
6.23	12	273	7	60	333	1	13	13	77	164	1	59	18	48	357
6.28	15	265	9	67	395	1	15	15	89	182	4	72	21	49	340
6.33	11	256	8	50	294	1	12	12	71	164	2	49	17	92	308
6.39	14	263	9	58	325	1	14	13	78	179	2	60	19	42	268
6.44	15	260	9	65	364	1	19	15	88	186	0	71	21	50	356
6.48	16	255	9	73	434	1	21	18	101	195	4	91	23	62	255
6.53	13	267	9	62	341	1	15	14	82	175	2	65	21	45	363
6.59	14	268	9	62	318	1	14	13	81	165	3	68	21	44	353
6.66	19	247	11	79	434	1	23	18	103	201	4	97	22	65	244
6.71	19	242	12	80	496	1	24	18	107	200	3	102	23	66	260
6.76	21	259	11	76	511	1	23	15	99	192	4	100	20	62	222
6.82	17	259	9	80	472	1	22	17	102	186	3	94	22	60	261
6.88	16	261	11	66	418	1	19	15	91	195	3	82	19	54	213
6.93	16	247	10	68	349	1	21	15	95	176	2	86	20	68	216
6.98	10	178	8	47	225	1	14	11	67	101	1	56	13	40	183
7.05	3	134	3	8	77	1	1	4	26	29	2	7	7	26	259
7.12	5	140	2	15	108	1	0	3	33	41	0	19	8	14	183

**Wangerland core W4 (Archive No. KB 5752)**

Depth [m]	TS	TC	TIC	SiO <sub>2</sub>	TiO <sub>2</sub>	Al <sub>2</sub> O <sub>3</sub>	Fe <sub>2</sub> O <sub>3</sub>	MgO	CaO	Na <sub>2</sub> O	K <sub>2</sub> O	P <sub>2</sub> O <sub>5</sub>
7.21	0.11	0.20	0.08	85.97	0.14	1.29	0.47	0.13	0.42	0.11	0.45	0.02
7.32	0.09	0.15	0.06	93.89	0.11	1.25	0.43	0.10	0.33	0.13	0.46	0.02
7.42	0.31	0.53	0.19	88.95	0.29	3.16	1.21	0.38	0.96	0.27	0.96	0.04
7.53	0.31	0.28	0.02	91.71	0.45	2.91	1.17	0.27	0.30	0.25	0.90	0.03
7.60	0.11	0.14	0.01	89.93	0.44	4.16	0.94	0.22	0.22	0.34	1.54	0.03
7.65				89.90	0.45	4.40	0.86	0.22	0.22	0.37	1.67	0.03
7.75				89.40	0.44	4.61	0.85	0.22	0.22	0.39	1.78	0.03
7.86	0.04	0.06	0.01	89.28	0.45	5.02	0.91	0.24	0.23	0.43	1.89	0.03
7.96				90.32	0.41	4.39	0.80	0.21	0.21	0.38	1.74	0.02
8.07				90.66	0.39	4.16	0.75	0.19	0.21	0.38	1.68	0.02
8.18	0.03	0.04	0.01	91.22	0.37	3.93	0.71	0.17	0.21	0.37	1.63	0.02
8.26				90.75	0.46	4.11	0.78	0.18	0.23	0.38	1.64	0.02
8.35				89.77	0.43	4.68	0.86	0.23	0.22	0.41	1.82	0.03
8.45	0.04	0.04	0.01	90.08	0.41	4.44	0.83	0.20	0.22	0.40	1.75	0.02

Depth [m]	As	Ba	Co	Cr	Mn	Mo	Ni	Pb	Rb	Sr	U	V	Y	Zn	Zr
7.21	3	101	4	3	54	1	1	2	22	22	0	6	6	7	132
7.32	3	118	3	8	70	1	1	2	22	21	1	7	5	8	116
7.42	5	165	6	29	124	1	4	7	44	45	1	27	8	17	302
7.53	6	167	4	33	132	1	4	8	39	36	2	21	10	17	461
7.60	4	274	4	29	85	1	1	8	48	43	1	21	12	26	421
7.65	3	299	2	35	77	1	1	9	51	45	3	17	12	16	459
7.75	2	314	3	41	70	1	1	8	53	47	1	19	11	15	414
7.86	2	333	4	31	70	1	2	9	57	50	2	23	11	16	397
7.96	2	313	3	24	62	1	1	7	52	46	1	19	13	13	379
8.07	2	316	1	39	62	1	5	8	51	46	2	17	12	14	382
8.18	2	309	2	24	62	1	0	7	50	47	0	16	9	15	335
8.26	2	305	3	30	77	1	1	9	50	46	3	20	12	13	477
8.35	3	330	4	29	70	1	2	8	57	50	1	21	11	16	386
8.45	2	319	3	27	62	1	1	10	51	46	0	17	10	15	364

## Wangerland core W5 (Archive No. KB 5950)

Depth [m]	TS	TC	TIC	SiO <sub>2</sub>	TiO <sub>2</sub>	Al <sub>2</sub> O <sub>3</sub>	Fe <sub>2</sub> O <sub>3</sub>	MgO	CaO	Na <sub>2</sub> O	K <sub>2</sub> O	P <sub>2</sub> O <sub>5</sub>
0.35	0.03	0.71	0.01	70.79	0.75	11.89	4.96	1.30	0.87	0.72	2.43	0.29
0.45				71.45	0.66	10.89	4.57	1.24	1.18	0.75	2.37	0.73
0.55				71.67	0.69	11.03	4.62	1.27	1.03	0.75	2.40	0.57
0.66	0.02	0.66	0.01	72.27	0.72	11.33	4.56	1.29	0.79	0.77	2.42	0.27
0.76				71.02	0.73	11.50	4.99	1.35	0.77	0.75	2.44	0.24
0.85				71.83	0.74	11.85	4.71	1.40	0.72	0.76	2.50	0.15
1.09	0.03	0.42	0.01	75.95	0.69	10.08	3.80	1.11	0.64	0.82	2.31	0.13
1.21	0.02	0.60	0.01	75.72	0.67	10.06	3.72	1.12	0.71	0.83	2.32	0.22
1.26				75.30	0.70	10.33	3.80	1.16	0.68	0.82	2.34	0.18
1.40				75.34	0.67	9.92	4.25	1.14	0.69	0.81	2.27	0.22
1.44	0.02	0.64	0.01	74.16	0.69	10.54	4.05	1.22	0.68	0.79	2.37	0.18
1.50				74.55	0.67	10.25	4.25	1.19	0.68	0.81	2.32	0.19
1.56				72.52	0.73	11.58	4.09	1.35	0.69	0.77	2.50	0.15
1.60	0.03	0.73	0.01	71.94	0.73	11.56	4.11	1.36	0.66	0.79	2.49	0.14
1.65				72.93	0.69	10.81	4.21	1.23	0.70	0.79	2.41	0.21
1.71				70.15	0.75	11.94	5.08	1.43	0.69	0.75	2.58	0.18
1.78	0.02	1.02	0.01	70.23	0.73	11.67	5.13	1.38	0.69	0.75	2.53	0.19
1.84				70.42	0.71	10.92	5.51	1.30	0.72	0.77	2.43	0.28
1.90	0.06	1.25	0.02	69.84	0.72	11.37	5.09	1.36	0.73	0.75	2.55	0.28
1.95	0.18	1.22	0.05	71.40	0.72	11.15	4.48	1.29	0.67	0.78	2.54	0.17
1.97				70.82	0.69	10.50	4.42	1.24	0.72	0.76	2.43	0.27
2.02				74.37	0.70	9.97	3.63	1.07	0.59	0.83	2.37	0.16
2.07	0.12	0.97	0.02	73.53	0.68	10.58	3.95	1.19	0.61	0.82	2.47	0.13
2.11				77.08	0.68	9.46	3.13	0.96	0.55	0.90	2.31	0.10
2.15	0.14	1.08	0.03	73.59	0.70	10.32	3.75	1.16	0.63	0.79	2.43	0.12
2.18				80.25	0.55	7.67	2.77	1.01	0.87	0.87	2.02	0.14
2.21	0.11	1.13	0.06	72.13	0.71	11.00	4.19	1.36	0.72	0.80	2.53	0.13
2.26				75.14	0.65	9.40	3.95	1.40	1.03	0.87	2.26	0.20
2.33	0.13	0.80	0.11	73.98	0.67	10.17	3.91	1.37	0.86	0.83	2.39	0.17
2.38				71.82	0.73	11.12	4.05	1.51	0.87	0.81	2.52	0.14
2.41	0.26	1.06	0.04	71.05	0.72	11.31	4.35	1.40	0.69	0.79	2.59	0.16
2.45	0.32	1.22	0.03	73.72	0.68	10.25	3.78	1.18	0.64	0.84	2.43	0.12
2.49				67.55	0.72	12.02	4.93	1.57	0.76	0.74	2.63	0.13
2.57	1.34	2.54	0.02	63.93	0.75	13.35	5.45	1.74	0.70	0.67	2.83	0.13
2.61	1.16	2.99	0.05	64.88	0.75	13.01	5.10	1.70	0.76	0.71	2.77	0.13
2.64	2.18	2.90	0.02	60.81	0.75	14.06	6.79	1.84	0.62	0.61	2.91	0.13
2.67	3.75	6.26	0.01	54.02	0.70	13.15	8.39	1.77	0.71	0.52	2.72	0.11
2.69	3.19	9.09	0.01	51.46	0.64	12.04	7.04	1.65	0.90	0.52	2.51	0.11
2.72	2.95	8.34	0.01	58.23	0.63	10.61	5.60	1.27	0.85	0.65	2.31	0.10
2.74	4.60	14.30	0.01	46.18	0.54	9.64	6.84	1.26	1.13	0.55	2.02	0.12
2.78	4.57	27.15	0.02	29.69	0.37	6.53	5.03	1.21	2.12	0.48	1.33	0.14
2.80	6.64	34.15	0.02	13.83	0.18	4.23	6.59	1.33	2.80	0.36	0.82	0.17
2.82	7.08	32.20	0.01	17.53	0.23	4.83	7.46	1.24	2.47	0.38	0.95	0.15
2.84	5.84	33.90	0.01	19.75	0.25	4.76	5.04	1.18	2.11	0.40	0.97	0.13
2.86	5.21	33.80	0.01	19.57	0.26	4.99	3.97	1.18	2.00	0.40	1.00	0.12
2.87	3.38	25.05	0.01	33.22	0.45	8.46	3.42	1.30	1.53	0.50	1.70	0.11
2.89	3.30	25.15	0.02	34.37	0.43	7.80	3.29	1.28	1.53	0.50	1.60	0.14
2.91	3.04	20.40	0.02	39.34	0.52	9.48	3.52	1.31	1.19	0.56	1.93	0.10
2.93	4.30	19.55	0.03	39.56	0.51	9.14	5.32	1.31	1.12	0.57	1.85	0.10
2.96	4.18	18.05	0.02	41.23	0.52	9.79	5.52	1.39	1.03	0.57	1.94	0.11
2.98	2.58	14.95	0.02	47.70	0.59	10.89	4.22	1.51	0.94	0.61	2.18	0.10
3.01	2.58	11.55	0.02	51.92	0.66	11.98	4.72	1.60	0.82	0.67	2.43	0.09
3.03	4.35	14.20	0.02	45.43	0.60	11.11	6.55	1.61	0.93	0.61	2.21	0.10
3.05	3.06	9.64	0.02	52.73	0.66	11.89	5.75	1.63	0.77	0.64	2.42	0.11

## Wangerland core W5 (Archive No. KB 5950)

Depth [m]	As	Ba	Co	Cr	Mn	Mo	Ni	Pb	Rb	Sr	U	V	Y	Zn	Zr
0.35	16	315	12	96	503	1	26	23	123	94	2	112	28	80	360
0.45	18	291	9	83	658	1	28	20	116	119	3	98	25	100	339
0.55	20	292	10	83	550	1	26	18	115	110	3	103	27	86	341
0.66	20	313	12	92	364	1	23	20	121	93	3	107	27	70	361
0.76	21	305	13	94	449	1	25	22	119	91	3	115	27	72	366
0.85	17	309	11	92	380	1	27	20	123	89	3	118	26	71	357
1.09	16	308	9	84	364	1	17	16	105	83	3	87	25	55	374
1.21	13	300	9	85	217	0	18	19	105	89	4	84	24	63	404
1.26	12	313	9	84	217	1	19	18	109	87	4	85	26	62	395
1.40	21	302	9	80	325	1	19	18	102	86	4	91	25	58	403
1.44	15	310	10	87	217	1	22	18	111	86	4	94	25	63	385
1.50	18	306	11	83	349	1	23	17	106	85	1	99	26	60	388
1.56	12	310	9	87	256	1	25	21	119	87	3	111	27	72	376
1.60	12	305	11	90	434	1	23	22	121	86	4	111	27	67	357
1.65	19	303	11	90	573	0	23	19	112	86	3	101	28	64	370
1.71	20	308	15	92	1177	2	28	21	126	88	3	118	26	69	327
1.78	19	303	11	91	751	1	25	22	124	88	3	110	27	71	335
1.84	23	302	13	83	426	1	22	18	115	89	3	102	27	65	365
1.90	17	306	12	93	418	0	25	20	119	91	3	107	27	67	354
1.95	17	313	11	89	527	1	25	22	116	84	4	106	27	65	349
1.97	21	299	10	85	457	1	21	18	113	86	3	99	27	66	363
2.02	14	301	8	80	325	1	16	17	105	81	3	87	24	54	369
2.07	11	305	10	90	271	1	21	18	112	82	1	92	25	60	369
2.11	8	319	7	77	209	1	14	17	101	81	3	78	25	48	400
2.15	12	303	10	85	271	1	21	19	107	82	3	91	26	57	363
2.18	9	297	6	66	294	1	13	13	81	80	2	59	21	37	441
2.21	13	305	10	85	310	0	25	19	116	85	4	102	25	63	368
2.26	12	300	9	79	333	1	17	17	96	84	2	82	27	53	445
2.33	13	303	8	82	372	1	18	18	108	85	3	90	24	57	424
2.38	13	310	10	94	248	1	26	19	115	89	2	109	28	65	392
2.41	15	307	10	92	283	1	25	20	120	88	3	107	27	68	371
2.45	14	310	10	79	248	1	21	17	110	86	4	91	26	60	379
2.49	40	305	10	94	318	1	27	21	123	88	4	119	27	72	317
2.57	37	300	11	107	341	1	32	23	138	91	5	140	27	80	243
2.61	29	300	13	92	294	1	30	22	133	93	4	138	28	77	259
2.64	38	294	19	108	310	7	40	26	149	91	6	147	27	90	196
2.67	32	273	18	97	287	13	51	20	146	90	9	143	24	89	159
2.69	18	245	13	84	290	12	47	22	131	95	13	126	24	75	155
2.72	11	263	12	75	232	8	31	21	116	93	9	96	23	53	242
2.74	14	216	13	75	271	16	36	22	106	101	10	101	20	46	162
2.78	13	142	6	51	415	12	21	14	71	136	6	86	17	18	125
2.80	26	67	12	37	498	32	33	9	45	165	7	79	15	14	46
2.82	24	89	10	40	429	33	28	9	57	149	5	74	15	15	54
2.84	14	97	4	38	362	17	19	6	54	124	2	73	11	27	57
2.86	12	98	4	40	342	11	18	8	59	123	2	70	11	13	58
2.87	8	174	4	59	274	6	18	13	98	113	3	91	13	23	107
2.89	13	167	9	59	273	4	21	13	88	108	3	88	13	27	118
2.91	9	203	9	71	225	3	18	13	102	100	4	93	16	32	141
2.93	11	195	16	68	223	5	26	17	95	96	2	91	16	45	135
2.96	11	200	13	71	226	4	28	18	100	97	3	98	18	68	131
2.98	9	234	9	85	217	0	26	16	107	94	2	104	21	63	162
3.01	10	256	10	90	223	2	29	18	123	96	3	115	22	70	192
3.03	20	228	11	82	262	2	36	21	112	96	4	119	22	81	147
3.05	16	253	11	87	271	1	33	21	120	92	1	114	19	79	172

## Wangerland core W5 (Archive No. KB 5950)

Depth [m]	TS	TC	TIC	SiO <sub>2</sub>	TiO <sub>2</sub>	Al <sub>2</sub> O <sub>3</sub>	Fe <sub>2</sub> O <sub>3</sub>	MgO	CaO	Na <sub>2</sub> O	K <sub>2</sub> O	P <sub>2</sub> O <sub>5</sub>
3.07	4.24	10.25	0.02	50.91	0.63	11.40	7.03	1.60	0.74	0.59	2.32	0.10
3.09	2.86	5.86	0.02	59.60	0.67	11.41	6.16	1.51	0.60	0.69	2.36	0.10
3.11	3.61	4.23	0.02	61.16	0.69	11.86	7.05	1.55	0.57	0.71	2.45	0.10
3.14	2.83	3.67	0.02	63.18	0.71	12.04	6.21	1.55	0.60	0.74	2.52	0.10
3.17	2.26	2.14	0.02	65.84	0.71	12.07	5.88	1.56	0.59	0.78	2.56	0.12
3.21	2.09	1.96	0.03	65.26	0.70	12.63	5.81	1.65	0.62	0.75	2.65	0.14
3.24	1.79	2.01	0.11	64.67	0.72	12.77	5.58	1.81	0.82	0.73	2.66	0.14
3.32	1.32	2.19	0.38	65.37	0.69	11.98	4.77	1.99	1.64	0.75	2.54	0.13
3.36	1.68	2.60		60.96	0.70	12.27	5.45	2.09	3.26	0.69	2.53	0.13
3.40	1.31	2.62	1.15	60.83	0.66	11.30	4.78	1.96	5.18	0.70	2.38	0.13
3.45	1.39	2.87	1.33	56.05	0.68	12.81	5.51	2.17	6.00	0.59	2.60	0.13
3.50	1.00	2.84	1.36	56.33	0.69	12.92	4.99	2.18	6.17	0.60	2.60	0.13
3.54				58.50	0.67	12.31	4.37	2.08	5.95	0.65	2.51	0.13
3.58	0.63	3.02	1.37	60.60	0.61	10.72	3.74	1.80	6.26	0.69	2.29	0.12
3.61				54.98	0.66	12.03	4.56	2.05	7.33	0.61	2.44	0.13
3.63	0.59	2.92	1.45	60.91	0.60	10.15	3.49	1.71	6.60	0.68	2.17	0.12
3.66	1.22	3.32	1.56	57.10	0.67	11.37	4.64	1.98	7.04	0.67	2.32	0.14
3.70				56.99	0.68	11.00	5.38	1.93	7.02	0.68	2.26	0.14
3.74	2.25	3.29	1.58	55.54	0.67	11.17	5.83	1.96	7.20	0.64	2.26	0.14
3.77				56.71	0.65	10.30	5.32	1.84	7.55	0.69	2.14	0.14
3.80	2.24	3.43	1.74	54.81	0.64	10.93	5.84	1.89	7.92	0.65	2.24	0.14
3.82				56.51	0.64	10.36	5.58	1.77	7.48	0.66	2.15	0.15
3.84	1.57	2.78	1.51	61.89	0.65	9.02	4.32	1.59	6.95	0.77	1.99	0.12
3.88	1.21	3.23	1.69	59.71	0.65	9.31	4.34	1.67	7.68	0.77	2.02	0.13
3.92				59.67	0.60	9.28	4.29	1.63	8.11	0.78	2.03	0.12
3.96	1.51	3.09	1.73	59.98	0.60	9.31	4.30	1.64	7.85	0.75	2.03	0.12
4.00				59.49	0.57	8.74	3.94	1.51	9.22	0.75	1.93	0.12
4.04	1.37	2.89	1.66	61.50	0.64	9.23	4.09	1.65	7.47	0.77	2.03	0.12
4.09				64.84	0.61	8.35	3.45	1.48	6.82	0.83	1.92	0.12
4.13	1.24	2.68	1.61	63.79	0.63	8.60	3.70	1.54	7.26	0.81	1.96	0.12
4.18				66.36	0.62	8.21	3.37	1.42	6.47	0.82	1.91	0.11
4.23	0.94	2.09	1.28	68.91	0.61	7.70	3.08	1.28	5.86	0.80	1.85	0.11
4.28	1.15	2.61	1.44	64.51	0.62	8.50	3.75	1.45	6.53	0.81	1.95	0.12
4.33				67.31	0.61	7.92	3.46	1.32	5.99	0.83	1.87	0.11
4.38	1.25	2.45	1.32	65.83	0.64	8.44	3.67	1.44	6.07	0.81	1.95	0.11
4.42	1.31	2.50	1.36	65.47	0.65	8.63	3.86	1.46	6.24	0.79	1.97	0.12
4.46				68.42	0.63	7.84	3.40	1.30	5.68	0.82	1.87	0.11
4.50	1.33	2.59	1.45	64.22	0.61	8.74	3.86	1.47	6.60	0.79	1.99	0.12
4.55				67.55	0.61	8.03	3.35	1.31	5.79	0.78	1.89	0.11
4.60	1.18	2.20	1.33	67.98	0.62	7.87	3.42	1.30	5.85	0.83	1.89	0.11
4.65				67.92	0.65	7.86	3.40	1.32	5.87	0.84	1.87	0.11
4.69	1.13	2.17	1.23	68.18	0.67	7.77	3.37	1.31	5.64	0.86	1.86	0.11
4.73	1.26	2.38	1.27	66.28	0.69	8.53	3.74	1.45	5.76	0.83	1.96	0.12
4.77				65.68	0.69	8.44	3.82	1.46	5.97	0.84	1.94	0.12
4.81	1.36	2.69	1.54	63.94	0.67	8.56	3.89	1.47	6.99	0.81	1.94	0.11
4.87				65.35	0.68	8.69	3.94	1.54	6.19	0.84	1.97	0.11
4.92	1.38	2.60	1.43	63.63	0.68	8.79	4.03	1.58	6.44	0.84	1.98	0.12
4.95				64.83	0.67	8.68	3.93	1.54	6.09	0.85	1.97	0.12
4.99	1.27	2.43	1.33	65.03	0.68	8.83	3.88	1.54	5.98	0.84	2.00	0.12
5.03	1.02	2.64	1.39	63.66	0.67	9.03	3.88	1.60	6.25	0.85	2.02	0.12
5.08				64.00	0.68	8.98	4.07	1.57	6.20	0.84	2.00	0.12
5.12	1.77	2.87	1.37	60.11	0.67	10.05	4.90	1.72	6.20	0.77	2.15	0.12
5.17				61.21	0.67	10.07	4.87	1.72	5.92	0.78	2.16	0.12
5.21	1.21	2.52	1.21	65.33	0.66	9.08	3.91	1.53	5.51	0.82	2.05	0.12

## Wangerland core W5 (Archive No. KB 5950)

Depth [m]	As	Ba	Co	Cr	Mn	Mo	Ni	Pb	Rb	Sr	U	V	Y	Zn	Zr
3.07	20	247	18	92	287	2	38	20	116	87	4	121	21	112	155
3.09	18	255	15	82	356	1	31	20	117	83	3	107	23	103	202
3.11	25	274	16	86	449	0	34	19	121	83	4	114	23	90	206
3.14	17	280	15	92	341	1	33	21	122	87	3	114	25	88	224
3.17	14	291	11	93	329	1	30	21	124	88	4	112	27	81	238
3.21	15	285	12	92	302	1	30	22	129	90	2	128	26	81	211
3.24	17	289	11	98	271	1	34	22	131	91	3	125	26	81	215
3.32	17	287	10	95	240	1	27	20	123	97	2	120	26	76	236
3.36	19	282	12	89	271	1	30	21	126	113	4	127	27	80	198
3.40	14	268	9	83	287	1	28	20	118	136	2	114	25	72	219
3.45	17	269	12	96	364	1	31	20	130	147	2	136	24	85	154
3.50	15	270	9	95	380	1	30	22	132	153	2	136	23	83	160
3.54	15	267	12	93	333	1	29	19	129	152	2	127	25	78	179
3.58	15	262	11	79	302	1	25	19	110	153	2	107	23	69	212
3.61	16	265	10	88	387	1	28	21	126	178	2	132	26	79	174
3.63	13	254	9	79	302	1	24	17	102	159	3	99	23	63	234
3.66	30	263	15	83	341	1	34	20	117	174	3	118	24	76	221
3.70	34	256	12	88	372	1	28	17	112	172	4	109	27	75	229
3.74	19	248	13	88	380	0	29	20	117	180	3	113	26	76	209
3.77	17	245	10	80	395	0	27	17	106	184	2	109	25	66	257
3.80	20	237	13	84	480	0	28	21	113	205	2	116	25	74	203
3.82	17	249	11	87	519	1	27	19	107	198	2	109	25	70	254
3.84	20	255	10	76	403	0	20	16	93	181	4	87	26	57	409
3.88	18	253	11	82	418	1	23	17	97	203	3	91	27	60	381
3.92	18	244	10	74	426	1	24	16	98	219	3	90	23	62	278
3.96	16	252	9	78	472	1	21	16	96	208	3	89	23	59	261
4.00	15	244	9	72	472	1	20	15	91	251	2	79	23	56	279
4.04	16	254	9	76	503	1	20	16	93	192	3	89	25	58	372
4.09	15	263	9	69	380	1	18	13	88	181	1	76	26	49	434
4.13	16	258	9	74	364	0	19	14	91	190	4	80	24	53	405
4.18	14	258	9	69	349	1	17	14	87	177	3	75	26	49	484
4.23	15	266	9	76	325	1	16	13	80	162	3	68	25	45	536
4.28	19	260	9	76	352	1	20	15	89	176	3	81	26	52	456
4.33	18	261	8	74	372	0	16	14	82	164	3	73	25	47	499
4.38	18	274	11	76	387	1	18	15	88	166	3	80	26	51	484
4.42	18	260	8	75	395	1	17	15	92	174	3	83	26	52	496
4.46	15	255	9	74	380	1	16	15	82	163	3	68	27	47	585
4.50	17	259	8	75	372	1	20	15	90	176	4	81	23	55	430
4.55	16	267	9	76	356	1	17	14	82	156	3	71	25	48	510
4.60	19	277	9	69	349	1	17	15	83	162	3	70	25	46	539
4.65	17	266	9	76	372	0	17	14	81	166	3	69	27	47	563
4.69	16	266	8	76	356	1	17	15	81	161	3	69	28	45	640
4.73	18	271	9	86	387	1	18	15	88	163	4	79	28	53	559
4.77	18	267	8	80	387	1	18	14	86	163	4	78	29	51	542
4.81	18	258	11	78	395	0	19	17	89	199	2	79	26	51	520
4.87	15	259	10	77	380	0	19	17	90	168	4	79	29	52	466
4.92	15	261	9	79	395	0	19	14	90	174	2	84	28	57	442
4.95	15	269	11	82	387	1	20	14	89	165	3	81	28	53	445
4.99	14	260	8	84	395	1	19	16	89	164	3	82	27	52	449
5.03	14	269	11	76	434	1	20	16	93	167	3	82	27	55	380
5.08	14	264	10	81	465	1	20	17	91	165	3	83	30	53	440
5.12	18	261	12	87	449	1	27	17	101	162	2	101	24	65	304
5.17	17	270	11	93	410	1	26	17	105	162	4	97	25	64	354
5.21	14	269	10	73	341	1	20	17	92	152	3	89	26	55	444

## Wangerland core W5 (Archive No. KB 5950)

Depth [m]	TS	TC	TIC	SiO <sub>2</sub>	TiO <sub>2</sub>	Al <sub>2</sub> O <sub>3</sub>	Fe <sub>2</sub> O <sub>3</sub>	MgO	CaO	Na <sub>2</sub> O	K <sub>2</sub> O	P <sub>2</sub> O <sub>5</sub>
5.29	0.84	1.87	1.27	62.54	0.65	10.09	4.21	1.70	5.80	0.80	2.19	0.12
5.33				66.19	0.64	9.08	3.60	1.52	5.35	0.85	2.06	0.11
5.38	1.45	2.93	1.26	59.77	0.64	10.74	4.62	1.78	5.72	0.75	2.27	0.12
5.43	1.64	2.80	1.23	61.51	0.64	10.37	4.45	1.73	5.64	0.76	2.22	0.12
5.48				64.62	0.65	9.80	4.08	1.61	5.06	0.79	2.16	0.12
5.53	1.51	2.70	1.04	63.07	0.66	10.35	4.58	1.68	4.74	0.76	2.21	0.12
5.57	1.62	2.20	0.70	66.71	0.70	10.21	4.71	1.68	3.20	0.82	2.23	0.12
5.61				68.02	0.72	10.63	4.52	1.72	1.54	0.86	2.30	0.12
5.66	1.49	2.36	0.27	64.66	0.76	12.20	5.26	1.97	1.13	0.82	2.53	0.13
5.70	1.47	2.28	0.25	64.39	0.77	12.65	5.17	2.02	1.08	0.80	2.59	0.13
5.74	1.56	2.33	0.09	67.43	0.77	11.53	4.81	1.58	0.72	0.86	2.45	0.13
5.78	4.85	7.99	0.01	54.66	0.65	10.45	8.21	1.50	0.63	0.77	2.17	0.12
5.80	11.80	33.15	0.03	14.35	0.20	3.66	13.67	1.19	1.13	0.66	0.74	0.08
5.83	13.07	40.20	0.02	2.27	0.04	0.58	14.03	1.01	1.22	0.65	0.13	0.06
5.85	9.64	45.60	0.02	1.19	0.01	0.27	8.79	1.02	1.17	0.68	0.07	0.05
5.88	8.75	42.35	0.05	6.76	0.07	1.23	7.83	1.27	1.52	0.71	0.28	0.06
5.91	5.42	35.60	0.17	15.24	0.15	2.36	4.70	1.13	1.80	0.66	0.53	0.06
5.93	6.12	40.80	0.17	10.12	0.10	1.52	5.24	1.15	1.79	0.69	0.36	0.06
5.96	6.43	40.20	0.17	13.80	0.16	2.37	6.95	1.55	2.39	0.89	0.56	0.08
5.98	4.49	34.07	0.29	22.83	0.22	3.28	5.29	1.47	2.77	0.87	0.77	0.09
6.00	5.76	45.05	0.09	6.32	0.07	1.12	4.51	1.30	1.78	0.71	0.26	0.06
6.02	7.76	44.73	0.06	4.15	0.05	0.82	6.98	1.26	1.60	0.71	0.20	0.05
6.03	5.73	40.50	0.17	10.97	0.12	1.84	4.70	1.19	1.80	0.69	0.41	0.07
6.05	5.61	39.35	0.07	11.55	0.18	2.60	4.30	1.18	1.42	0.72	0.55	0.07
6.08	4.86	43.30	0.10	10.94	0.16	2.55	3.35	1.27	1.57	0.75	0.55	0.07
6.10	4.64	40.60	0.05	10.52	0.16	2.43	2.97	1.29	1.53	0.73	0.51	0.06
6.12	4.74	46.70	0.06	6.88	0.11	1.67	2.66	1.32	1.62	0.76	0.33	0.07
6.14	3.82	43.87	0.04	4.94	0.07	1.17	3.69	1.37	1.73	0.75	0.26	0.06
6.15	5.65	47.10	0.06	10.84	0.18	2.50	1.92	1.19	1.40	0.74	0.48	0.07
6.18	3.93	50.20	0.04	4.33	0.06	0.94	1.91	1.28	1.61	0.66	0.21	0.05
6.20	3.84	50.65	0.04	1.50	0.02	0.34	1.96	1.35	1.74	0.67	0.11	0.04
6.22	3.74	52.00	0.04	1.85	0.02	0.33	1.68	1.40	1.72	0.71	0.13	0.04
6.24	3.32	50.40	0.03	1.65	0.01	0.20	1.45	1.44	1.72	0.70	0.11	0.04
6.26	3.98	52.63	0.04	1.02	0.01	0.14	1.98	1.56	1.88	0.74	0.11	0.04
6.29	5.00	50.75	0.15	1.12	0.01	0.15	3.55	1.54	1.78	0.74	0.10	0.04
6.31	7.10	46.60	0.02	1.37	0.01	0.25	6.10	1.31	1.50	0.67	0.10	0.04
6.34	22.50	33.00	0.02	2.01	0.04	0.57	28.19	1.01	1.18	0.56	0.16	0.04
6.37	28.20	18.93	0.01	9.08	0.14	2.47	38.45	0.84	0.74	0.45	0.52	0.05
6.39	28.00	16.67	0.01	11.71	0.17	3.18	39.07	0.84	0.67	0.44	0.62	0.06
6.41	16.00	33.05	0.03	10.36	0.11	2.04	18.91	0.95	1.08	0.57	0.42	0.06
6.44	1.15	21.43	0.02	57.16	0.17	1.30	0.93	0.63	0.97	0.41	0.43	0.05
6.45	1.19	14.40	0.01	69.61	0.16	1.21	1.05	0.36	0.55	0.34	0.43	0.04
6.46	0.33	7.06	0.00	83.95	0.19	1.30	0.32	0.22	0.38	0.26	0.51	0.03
6.49	0.14	3.30	0.00	90.77	0.18	1.34	0.19	0.12	0.25	0.22	0.56	0.03
6.52	0.11	1.97	0.00	92.49	0.18	1.52	0.20	0.09	0.19	0.22	0.63	0.02
6.54	0.11	1.78	0.00	92.29	0.19	1.71	0.23	0.10	0.21	0.24	0.69	0.03
6.57	0.11	2.33	0.00	90.16	0.19	1.99	0.22	0.15	0.28	0.28	0.74	0.04
6.59	0.12	2.41	0.00	89.84	0.19	2.25	0.25	0.19	0.32	0.29	0.79	0.06
6.61	0.10	2.26	0.00	90.06	0.18	2.30	0.25	0.17	0.31	0.30	0.78	0.07
6.64	0.11	1.26	0.00	91.33	0.20	2.42	0.37	0.13	0.25	0.29	0.83	0.07
6.67	0.09	0.83	0.00	92.81	0.18	2.44	0.38	0.12	0.22	0.30	0.83	0.07
6.73	0.05	0.34	0.00	93.55	0.18	2.37	0.37	0.09	0.17	0.29	0.82	0.05
6.77	0.05	0.23	0.00	94.10	0.20	2.34	0.38	0.09	0.17	0.29	0.81	0.04
6.79	0.04	0.18	0.00	94.40	0.22	2.28	0.39	0.08	0.17	0.29	0.80	0.04

## Wangerland core W5 (Archive No. KB 5950)

Depth [m]	As	Ba	Co	Cr	Mn	Mo	Ni	Pb	Rb	Sr	U	V	Y	Zn	Zr
5.29	16	271	11	80	364	1	24	16	103	157	4	101	26	65	335
5.33	14	286	10	73	333	1	20	16	92	146	2	83	24	57	406
5.38	17	268	11	91	380	1	26	20	110	152	3	109	25	69	266
5.43	17	270	11	78	372	1	25	18	106	152	3	102	24	69	280
5.48	15	274	9	91	325	1	22	17	100	139	2	89	25	62	369
5.53	19	276	12	80	325	1	23	18	105	133	4	105	26	65	368
5.57	18	300	11	88	302	0	24	17	104	113	1	105	28	64	439
5.61	18	290	12	88	287	1	23	19	107	95	4	107	28	68	433
5.66	22	303	13	99	290	1	31	21	122	90	4	126	29	79	307
5.70	20	301	13	97	287	0	31	22	125	92	4	129	30	82	290
5.74	21	302	13	98	248	1	28	21	116	89	4	110	30	73	434
5.78	37	269	11	83	343	6	30	20	106	90	5	120	26	70	327
5.80	21	96	11	36	271	41	19	12	40	92	4	79	11	32	65
5.83	15	32	7	8	194	34	11	3	7	92	2	33	3	16	16
5.85	8	22	2	6	134	9	5	1	6	85	2	25	3	8	10
5.88	8	48	4	15	162	4	6	3	14	108	1	28	4	14	38
5.91	13	79	5	23	171	1	9	4	26	99	1	34	8	23	81
5.93	10	63	3	15	160	1	7	2	17	101	1	25	5	19	57
5.96	9	86	4	22	217	2	10	5	22	132	1	34	7	25	73
5.98	10	110	4	29	236	0	13	6	32	123	1	39	8	37	117
6.00	6	56	3	9	145	2	5	2	13	111	1	17	5	12	35
6.02	6	40	2	10	147	3	4	2	11	108	1	14	3	13	22
6.03	6	63	4	17	151	2	6	4	20	99	2	23	5	22	61
6.05	4	78	2	25	121	2	5	4	27	99	1	30	5	14	54
6.08	4	75	3	23	122	3	7	4	26	103	2	29	5	16	53
6.10	4	76	2	21	116	4	6	4	25	116	2	26	5	11	54
6.12	4	60	2	11	115	3	4	2	16	119	2	19	5	9	33
6.14	4	47	1	11	125	3	5	2	11	123	1	14	3	12	28
6.15	3	78	2	14	104	0	3	3	23	102	1	19	6	8	46
6.18	3	50	2	7	136	1	2	1	11	116	1	10	3	9	21
6.20	3	34	1	2	141	1	1	0	7	124	0	3	2	8	9
6.22	2	35	2	2	125	0	2	1	6	118	1	3	2	8	10
6.24	2	33	2	3	120	0	1	0	5	121	0	2	1	8	9
6.26	2	28	1	1	132	1	2	0	4	133	0	2	1	8	6
6.29	2	29	2	0	142	1	2	0	5	128	0	2	2	12	8
6.31	3	24	2	3	132	2	3	0	5	111	1	4	2	12	10
6.34	14	55	6	8	435	21	14	2	10	99	3	12	3	24	14
6.37	16	134	7	19	496	27	17	5	31	82	5	26	4	33	37
6.39	18	118	11	27	304	24	20	5	37	72	5	29	5	36	48
6.41	7	66	7	16	159	4	13	4	21	98	2	16	4	23	47
6.44	1	110	3	10	120	1	0	3	14	84	1	4	6	5	192
6.45	2	113	3	12	65	1	1	3	16	53	1	0	5	2	185
6.46	2	126	2	8	62	1	1	2	19	43	1	1	5	2	225
6.49	2	142	3	10	46	1	1	2	22	33	0	1	6	2	223
6.52	1	152	2	12	46	1	1	3	24	31	1	1	6	2	223
6.54	1	161	2	7	46	1	1	4	27	33	0	4	5	5	224
6.57	1	165	1	13	54	1	1	4	29	40	0	2	6	4	214
6.59	1	175	3	7	54	1	1	5	30	44	2	5	6	5	198
6.61	1	168	2	8	54	1	1	6	29	42	2	6	6	4	208
6.64	1	183	2	10	54	1	1	6	31	40	0	3	7	7	220
6.67	2	186	4	9	46	1	1	4	32	37	0	6	6	7	219
6.73	2	175	2	9	54	1	1	4	30	33	1	7	5	5	224
6.77	2	174	2	8	62	1	1	4	32	32	1	4	6	5	335
6.79	1	176	2	11	77	1	1	5	31	32	0	4	6	5	361



## Schweiburg (Archive No. GE 707)

Depth [m]	TS	TC	TIC	SiO <sub>2</sub>	TiO <sub>2</sub>	Al <sub>2</sub> O <sub>3</sub>	Fe <sub>2</sub> O <sub>3</sub>	MgO	CaO	Na <sub>2</sub> O	K <sub>2</sub> O	P <sub>2</sub> O <sub>5</sub>
0.350	0.09	2.76	0.93	59.76	0.67	11.43	5.73	1.71	4.72	0.57	2.40	0.25
0.450				58.99	0.70	12.22	5.44	1.84	5.61	0.59	2.52	0.20
0.550				58.17	0.70	12.54	5.71	1.88	6.00	0.56	2.54	0.17
0.750	0.06	2.08	1.17	59.14	0.72	12.30	5.28	1.85	5.71	0.59	2.49	0.17
0.835				62.76	0.70	11.60	4.87	1.75	5.07	0.66	2.39	0.14
0.925				60.84	0.68	12.01	4.72	1.74	5.40	0.61	2.39	0.12
0.965	0.09	2.13	0.98	60.22	0.68	12.18	5.88	1.76	5.00	0.58	2.40	0.14
0.990				64.95	0.70	11.17	5.66	1.31	1.34	0.70	2.35	0.14
1.015	0.16	4.42	0.02	63.91	0.69	10.96	5.67	1.19	1.24	0.69	2.31	0.13
1.035	0.95	20.20	0.01	48.84	0.54	10.51	4.67	1.31	3.49	0.54	2.10	0.13
1.110	1.80	48.50	0.01	0.55	0.00	0.11	2.74	0.41	3.51	0.05	0.01	0.05
1.130	2.09	52.70	0.01	0.69	0.00	0.06	1.74	0.42	3.30	0.07	0.02	0.06
1.140	2.60	45.00	0.01	6.32	0.04	0.82	2.58	0.41	2.51	0.06	0.14	0.08
1.145	2.80	44.70	0.01	9.86	0.10	1.77	3.24	0.55	2.61	0.16	0.37	0.12
1.165	2.70	44.80	0.01	10.03	0.09	1.51	3.28	0.50	2.27	0.14	0.31	0.10
1.240	2.74	23.00	0.01	35.11	0.46	8.53	4.59	1.27	1.77	0.35	1.63	0.10
1.270	2.78	39.00	0.01	16.15	0.21	3.87	3.28	0.89	2.35	0.22	0.76	0.08
1.298	1.95	8.00	0.13	51.80	0.69	13.46	5.72	1.90	1.44	0.41	2.54	0.13
1.323	1.78	6.22	0.16	54.51	0.72	13.94	5.78	1.96	1.41	0.45	2.64	0.13
1.340	3.30	36.10	0.01	12.52	0.16	3.21	3.06	0.65	1.64	0.06	0.56	0.04
1.355	2.69	50.50	0.01	2.15	0.02	0.39	1.68	0.49	1.93	0.08	0.06	0.05
1.380	3.08	55.70	0.01	1.19	0.01	0.23	1.74	0.47	1.84	0.10	0.05	0.05
1.410	2.96	56.00	0.01	1.53	0.01	0.27	1.64	0.48	1.88	0.10	0.05	0.05
1.445	2.79	50.70	0.01	1.18	0.01	0.26	1.78	0.50	1.92	0.13	0.07	0.06
1.490	3.55	52.40	0.01	0.76	0.01	0.14	2.12	0.46	1.73	0.13	0.04	0.04
1.640	4.78	51.20	0.01	0.88	0.01	0.21	3.23	0.72	2.74	0.14	0.05	0.04
1.780	3.45	49.20	0.01	2.17	0.03	0.57	2.29	0.94	2.89	0.14	0.09	0.05
1.870	2.71	9.27	0.02	51.38	0.66	12.43	6.47	1.76	1.02	0.49	2.38	0.12
1.880	3.26	9.24	0.02	50.71	0.66	11.84	6.80	1.66	0.91	0.50	2.31	0.11
1.890	5.16	16.00	0.02	38.04	0.50	9.49	8.43	1.52	1.23	0.39	1.81	0.10
1.925	6.15	34.90	0.01	16.56	0.23	4.05	7.20	1.21	1.98	0.28	0.75	0.07
1.940				22.47	0.28	4.64	2.40	1.01	1.77	0.25	0.74	0.05
1.950	2.05	27.80	0.01	30.64	0.39	6.36	3.09	1.39	2.31	0.42	1.08	0.08
1.975	1.79	21.10	0.01	39.54	0.50	8.26	3.23	1.56	2.05	0.49	1.39	0.07
1.995	1.07	15.50	0.02	47.93	0.59	9.97	3.42	1.67	1.67	0.56	1.76	0.07
2.015	0.54	10.50	0.02	54.87	0.66	11.32	3.64	1.63	1.15	0.59	2.09	0.06
2.040	0.55	7.97	0.02	57.76	0.69	12.08	4.10	1.70	1.00	0.59	2.22	0.06
2.075	0.51	5.28	0.01	62.66	0.70	12.13	4.25	1.67	0.81	0.66	2.33	0.07
2.120	0.53	3.05	0.01	64.79	0.72	12.75	4.57	1.75	0.72	0.67	2.51	0.07
2.165	0.63	2.82	0.09	64.91	0.71	12.64	4.75	1.84	0.87	0.65	2.52	0.09
2.215				63.39	0.71	12.48	4.89	2.08	2.04	0.64	2.53	0.10
2.280	0.45	2.11	0.82	62.51	0.68	12.07	4.85	1.98	3.83	0.64	2.47	0.10
2.365	0.16	2.77	0.94	58.64	0.71	13.02	5.30	2.19	4.40	0.59	2.60	0.11
2.465				55.81	0.68	12.89	5.54	2.14	5.35	0.55	2.54	0.29
2.560	0.20	3.50	1.22	55.89	0.67	12.89	5.23	2.10	5.46	0.57	2.56	0.16
2.675	0.30	3.26	1.12	58.94	0.65	11.82	5.12	1.96	4.98	0.64	2.41	0.26
2.735	0.40	3.10	1.13	60.47	0.64	11.21	4.79	1.84	5.18	0.66	2.32	0.18
2.815				65.03	0.55	9.05	4.05	1.51	5.63	0.77	2.04	0.12
2.975				71.49	0.52	7.10	2.83	1.16	5.21	0.84	1.78	0.08
3.065	0.46	2.06	1.22	71.09	0.53	7.05	2.75	1.19	5.58	0.96	1.77	0.11
3.265	0.44	2.01	1.19	71.99	0.55	6.95	2.63	1.14	5.31	0.90	1.76	0.08
3.365	0.40	1.86	1.17	71.84	0.54	6.97	2.60	1.16	5.30	0.90	1.77	0.08
3.465				72.91	0.55	6.77	2.45	1.12	5.29	0.92	1.75	0.08
3.665	0.39	1.63	1.01	75.33	0.48	6.25	2.23	0.95	4.57	0.89	1.70	0.07

**Schweiburg (Archive No. GE 707)**

Depth [m]	As	Ba	Co	Cr	Mn	Mo	Ni	Pb	Rb	Sr	U	V	Y	Zn	Zr
0.350	21	277	14	82	658	2	27	30	115	128	4	109	22	94	209
0.450	24	282	13	85	720	1	30	28	121	144	3	118	24	85	200
0.550	25	276	12	87	496	1	30	27	124	151	2	117	23	82	194
0.750	23	281	11	87	434	1	26	22	119	151	4	111	24	78	221
0.835	19	298	12	84	426	3	28	21	114	140	2	106	24	72	254
0.925	17	282	13	82	697	0	29	20	117	148	2	107	22	75	209
0.965	32	288	17	84	829	2	28	26	121	149	3	117	24	79	209
0.990	28	288	11	81	349	1	27	23	113	106	3	103	24	72	273
1.015	21	287	9	80	310	1	22	22	108	105	3	98	24	65	271
1.035	23	218	7	79	452	8	32	23	106	170	11	108	23	56	209
1.110	4	7	3	0	369	0	0	0	3	118	0	1	0	10	4
1.130	3	9	3	0	387	1	1	0	3	110	0	0	0	19	5
1.140	5	31	7	2	364	1	1	1	15	78	1	6	0	28	25
1.145	5	50	6	13	386	1	5	4	20	87	0	18	3	25	40
1.165	5	49	4	12	381	2	1	2	17	75	1	12	3	18	42
1.240	11	173	10	61	557	4	23	17	84	103	1	87	15	63	116
1.270	9	87	4	31	604	3	12	8	38	103	1	52	13	31	62
1.298	21	266	12	93	604	1	31	23	132	103	3	133	22	96	143
1.323	20	283	15	94	542	2	33	24	138	103	4	131	24	98	160
1.340	9	64	4	19	465	0	0	3	32	62	3	46	6	21	35
1.355	4	11	1	1	508	0	0	0	6	63	1	7	2	3	10
1.380	2	8	1	1	495	1	0	0	4	63	0	4	0	3	7
1.410	2	8	1	2	516	0	0	0	6	65	0	3	0	2	9
1.445	2	8	1	2	539	2	0	1	4	70	0	4	1	3	7
1.490	2	7	2	0	524	0	0	1	4	63	1	3	0	2	5
1.640	3	10	1	1	901	1	0	7	3	109	1	5	1	3	6
1.780	5	16	3	4	948	1	2	2	7	135	0	14	3	7	13
1.870	20	256	14	83	465	2	30	22	122	108	2	112	20	92	157
1.880	17	241	12	83	417	5	29	22	117	103	2	111	20	87	173
1.890	14	187	10	68	484	2	25	19	95	110	1	91	16	80	125
1.925	12	83	6	31	703	3	13	10	38	133	1	52	10	33	67
1.940	9	93	2	31	736	0	0	8	34	105	3	51	10	13	78
1.950	10	131	4	49	978	3	14	13	50	163	2	71	18	21	132
1.975	8	171	4	60	883	1	16	14	67	158	2	88	19	34	161
1.995	10	207	7	72	699	1	24	17	84	146	3	102	20	49	192
2.015	13	250	10	79	488	0	21	16	96	116	3	107	20	62	200
2.040	12	263	11	84	457	0	25	21	104	109	3	114	20	66	203
2.075	11	281	11	85	410	0	23	21	107	102	4	111	21	62	226
2.120	9	292	11	91	449	2	25	22	120	100	3	116	23	70	235
2.165	8	290	12	91	480	2	27	22	122	98	3	122	25	69	238
2.215	8	285	10	89	945	2	26	20	119	104	4	116	26	72	222
2.280	8	283	12	90	387	0	25	19	116	121	3	112	24	68	211
2.365	9	271	14	91	372	0	32	21	121	128	3	121	24	82	178
2.465	13	266	13	91	736	0	39	22	121	140	4	131	26	85	167
2.560	14	269	15	89	914	1	37	20	121	143	3	128	24	87	162
2.675	15	267	14	83	821	0	31	19	114	138	1	112	24	74	199
2.735	15	263	10	80	465	3	24	18	107	142	2	105	23	70	238
2.815	27	271	9	65	472	2	21	14	87	150	3	73	20	53	231
2.975	16	270	5	59	364	1	15	9	68	144	3	48	19	36	368
3.065	12	288	7	54	380	0	12	10	69	159	3	49	20	37	346
3.265	9	266	7	54	341	1	11	12	67	146	3	47	21	33	397
3.365	9	279	7	56	318	0	10	10	64	146	3	47	20	35	389
3.465	8	285	8	57	318	2	10	10	64	150	4	46	20	33	419
3.665	8	282	6	49	271	2	7	10	61	139	3	38	19	29	411

## Schweiburg (Archive No. GE 707)

Depth [m]	TS	TC	TIC	SiO <sub>2</sub>	TiO <sub>2</sub>	Al <sub>2</sub> O <sub>3</sub>	Fe <sub>2</sub> O <sub>3</sub>	MgO	CaO	Na <sub>2</sub> O	K <sub>2</sub> O	P <sub>2</sub> O <sub>5</sub>
3.765				75.90	0.50	6.44	2.39	0.99	4.78	0.94	1.73	0.08
3.965	0.45	1.76	1.09	74.73	0.46	6.31	2.25	0.96	4.88	0.93	1.70	0.07
4.065				73.43	0.50	6.71	2.46	1.04	4.92	0.96	1.74	0.08
4.200	0.41	1.81	1.02	74.87	0.43	6.28	2.26	0.94	4.65	0.90	1.70	0.07
4.265				74.27	0.46	6.30	2.35	0.97	4.86	0.91	1.70	0.09
4.340	0.42	2.13	1.23	71.34	0.54	7.16	2.81	1.19	5.46	0.89	1.78	0.09
4.465	0.42	1.95	1.08	72.89	0.51	6.85	2.58	1.08	4.92	0.95	1.76	0.09
4.665				73.43	0.51	6.82	2.61	1.06	4.91	0.95	1.77	0.08
4.865	0.41	1.65	1.00	74.66	0.56	6.58	2.42	1.00	4.52	0.95	1.72	0.08
5.065	0.26	1.53	0.90	76.39	0.49	6.22	2.14	0.91	4.11	0.90	1.65	0.08
5.265				75.62	0.47	6.15	2.35	0.92	4.59	0.95	1.64	0.10
5.415	0.15	1.12	0.86	79.08	0.35	5.28	1.47	0.72	4.28	0.96	1.60	0.07
5.515	0.24	1.45	0.95	76.46	0.39	5.98	1.96	0.85	4.37	1.00	1.69	0.10
5.630	0.45	2.36	1.17	68.46	0.57	8.32	3.58	1.36	5.23	1.06	1.94	0.16
5.780				72.07	0.48	7.12	2.97	1.09	4.66	1.00	1.78	0.13
5.940	0.22	1.26	0.75	79.20	0.41	5.43	1.75	0.71	3.72	0.96	1.56	0.07
6.090	0.19	1.24	0.82	80.23	0.30	5.19	1.49	0.66	3.77	1.00	1.58	0.06
6.265				79.98	0.38	5.34	1.81	0.71	3.42	0.98	1.52	0.10
6.415	0.23	1.12	0.76	81.23	0.37	5.22	1.68	0.67	3.49	0.90	1.54	0.07
6.565	0.35	1.82	0.90	74.52	0.45	6.64	2.75	1.00	3.89	0.98	1.65	0.13
6.765				82.42	0.29	4.53	1.46	0.58	2.85	0.83	1.33	0.08
6.915	0.18	0.99	0.58	83.26	0.27	4.38	1.25	0.51	2.97	0.89	1.37	0.05
7.015	0.09	0.77	0.63	84.25	0.24	4.39	0.94	0.48	3.06	1.02	1.47	0.04
7.165	0.34	1.78	0.85	76.55	0.38	5.82	2.10	0.86	3.90	1.02	1.51	0.11
7.315				80.96	0.32	4.71	1.76	0.66	3.08	0.79	1.27	0.04
7.395	0.96	1.79	0.77	73.13	0.73	7.05	3.13	1.05	3.70	1.00	1.69	0.09
7.455	1.24	1.44	0.60	76.83	0.69	5.99	3.19	0.85	2.94	0.92	1.51	0.08
7.500	3.37	33.30	0.01	24.85	0.37	1.19	3.22	0.95	1.41	2.63	0.39	0.07
7.525	2.07	46.80	0.01	1.86	0.02	0.24	0.46	1.27	1.60	3.07	0.12	0.04
7.620	3.18	50.90	0.01	1.04	0.01	0.17	0.94	1.37	1.85	2.70	0.09	0.05
7.650	3.80	49.00	0.01	1.52	0.02	0.36	1.71	1.07	1.34	2.58	0.10	0.05
7.690	3.71	28.40	0.01	26.27	0.40	8.42	3.87	1.35	0.82	2.12	1.56	0.09
7.740	6.97	20.00	0.01	32.02	0.47	10.31	9.44	1.50	0.73	1.82	1.86	0.12
7.790	4.53	18.20	0.02	36.78	0.53	11.61	6.67	1.68	0.74	1.72	2.10	0.12
7.840	4.35	16.10	0.01	38.64	0.57	12.12	6.98	1.73	0.66	1.68	2.21	0.11
7.890	3.14	17.10	0.01	38.31	0.56	12.25	5.53	1.76	0.70	1.68	2.19	0.11
7.940	6.61	21.50	0.01	29.14	0.43	9.59	8.57	1.56	0.79	1.74	1.72	0.11
7.990	5.25	37.70	0.01	12.05	0.19	4.65	4.59	1.40	1.42	2.35	0.79	0.23
8.040	4.19	34.60	0.01	19.19	0.29	6.64	3.46	1.42	1.04	2.10	1.21	0.13
8.090	5.44	36.70	0.01	14.68	0.23	5.16	4.14	1.42	1.29	2.09	0.94	0.14
8.215	5.65	38.20	0.01	15.18	0.07	1.39	3.75	1.35	1.93	2.25	0.34	0.09
8.260	5.43	49.50	0.01	1.54	0.01	0.46	2.52	1.50	2.03	2.23	0.11	0.07
8.290	4.53	47.20	0.01	2.93	0.02	0.44	1.90	1.28	1.68	1.92	0.12	0.06
8.370	8.57	46.30	0.01	4.39	0.03	0.51	7.49	1.20	1.54	1.75	0.12	0.07
8.420	11.05	43.90	0.01	4.95	0.03	0.66	10.58	1.24	1.58	1.62	0.14	0.06
8.470	13.10	38.80	0.01	7.06	0.04	0.70	12.15	0.98	1.24	1.26	0.14	0.05
8.520	10.95	37.85	0.01	9.81	0.06	0.98	11.89	1.11	1.42	1.42	0.20	0.07
8.565	9.96	35.85	0.01	16.29	0.12	1.57	10.15	1.04	1.40	1.24	0.31	0.08
8.595	5.44	15.20	0.01	41.35	0.50	10.19	7.68	1.50	0.79	1.06	1.92	0.10
8.610	13.10	27.15	0.01	25.31	0.16	2.09	14.82	0.84	1.08	1.09	0.45	0.07
8.625	5.64	14.80	0.01	54.56	0.29	3.21	6.56	0.51	0.73	0.89	0.81	0.05
8.640	1.27	3.30	0.00	82.94	0.39	3.91	1.84	0.21	0.39	0.66	1.09	0.02
8.790	0.18	0.13	0.00	94.15	0.17	2.05	0.52	0.05	0.16	0.31	0.80	0.00

## Schweiburg (Archive No. GE 707)

Depth [m]	As	Ba	Co	Cr	Mn	Mo	Ni	Pb	Rb	Sr	U	V	Y	Zn	Zr
3.765	9	283	6	52	294	0	9	9	60	139	2	40	17	29	396
3.965	9	277	6	48	279	1	8	9	65	148	2	39	17	33	358
4.065	9	282	7	51	294	0	11	10	65	145	2	46	19	33	360
4.200	10	287	6	44	302	1	6	10	63	144	3	42	16	28	317
4.265	10	285	6	48	325	0	7	9	61	144	2	42	18	28	355
4.340	10	280	6	56	356	2	12	12	68	150	2	52	21	41	390
4.465	10	288	6	53	333	1	9	9	65	146	2	47	19	33	379
4.665	9	282	7	53	380	2	9	12	67	148	2	45	19	31	391
4.865	9	274	6	59	294	0	11	10	64	137	2	48	20	32	548
5.065	8	281	6	54	287	0	10	9	61	127	2	39	19	29	473
5.265	8	282	4	48	325	2	10	9	61	141	2	39	17	28	379
5.415	6	291	4	34	271	0	4	8	51	134	2	22	12	19	304
5.515	8	287	6	36	395	0	8	9	57	137	2	33	14	25	287
5.630	13	273	8	68	751	4	18	13	83	157	2	65	20	44	352
5.780	12	277	7	55	697	1	13	10	66	139	3	56	16	35	317
5.940	8	284	5	41	302	2	5	8	56	125	4	30	15	23	421
6.090	7	272	3	29	294	0	5	7	54	123	1	22	10	18	234
6.265	8	275	5	42	395	1	5	8	53	116	2	29	12	21	390
6.415	7	282	5	35	325	0	4	8	51	113	2	28	13	19	373
6.565	10	256	7	50	565	0	10	11	68	121	2	50	15	34	345
6.765	6	234	6	27	263	0	4	7	47	95	2	25	10	18	261
6.915	6	249	4	22	225	1	3	7	47	105	2	20	9	16	269
7.015	5	278	4	21	186	0	0	5	47	110	2	13	8	12	213
7.165	10	236	6	41	434	0	9	8	59	121	3	39	13	29	317
7.315	8	206	5	36	302	0	5	8	49	101	2	34	11	24	320
7.395	12	266	8	83	418	3	13	11	71	124	2	55	31	39	996
7.455	9	240	6	74	356	4	10	11	63	106	2	40	27	30	1093
7.500	11	76	3	46	321	4	2	3	14	85	1	50	16	8	116
7.525	4	21	1	3	252	1	0	0	4	99	1	4	1	2	20
7.620	4	21	1	1	302	1	0	0	4	116	1	5	1	2	10
7.650	5	23	1	2	231	0	0	0	5	85	1	6	1	3	10
7.690	13	163	9	57	249	5	22	14	84	91	2	82	9	33	70
7.740	29	194	16	71	397	11	32	18	101	93	3	113	16	63	86
7.790	17	216	11	79	427	8	31	21	112	97	4	134	18	74	95
7.840	17	226	14	82	364	5	35	21	120	96	3	129	18	79	101
7.890	13	227	11	82	283	7	34	20	117	98	6	128	20	76	102
7.940	22	183	16	65	295	17	37	18	92	97	8	120	20	59	87
7.990	9	124	7	34	364	13	19	7	40	136	7	121	18	44	43
8.040	8	131	6	44	239	10	19	12	63	102	4	99	14	36	53
8.090	7	112	8	35	324	10	17	9	46	119	7	76	12	35	49
8.215	5	75	2	10	447	8	5	2	14	147	4	19	4	12	67
8.260	3	32	2	3	430	4	0	0	5	158	3	10	2	8	11
8.290	4	28	1	3	333	2	1	0	5	126	2	7	3	7	18
8.370	6	33	3	5	388	5	5	0	5	122	1	13	5	9	36
8.420	7	37	6	5	388	5	5	1	6	127	1	16	6	9	40
8.470	5	38	3	6	360	4	3	1	7	94	1	17	7	7	41
8.520	6	49	3	10	375	7	5	2	8	114	2	31	11	8	64
8.565	15	75	4	14	413	15	7	3	12	113	4	36	17	10	124
8.595	19	230	11	70	392	12	30	16	97	102	8	92	18	75	148
8.610	10	99	7	17	392	10	6	3	20	94	5	35	16	12	181
8.625	7	167	4	20	219	1	1	5	28	77	2	28	15	5	345
8.640	4	232	2	25	131	0	1	6	34	56	1	18	11	4	508
8.790	2	184	1	10	70	0	0	4	26	30	1	3	3	1	413

**A5: Bulk parameters and ICP-OES data:****Loxstedt core C (Archive No. GE 432)**

Depth [m]	TS	TC	TIC	TiO <sub>2</sub>	Al <sub>2</sub> O <sub>3</sub>	Fe <sub>2</sub> O <sub>3</sub>	MgO	CaO	Na <sub>2</sub> O	K <sub>2</sub> O	P <sub>2</sub> O <sub>5</sub>
11.87	6.0	11.4	0.01	0.517	9.62	8.33	1.56	0.75	0.85	1.67	0.15
11.88	7.6	12.5	0.01	0.489	9.47	9.93	1.57	0.70	0.80	1.63	0.12
11.91	7.6	13.3	0.01	0.455	8.04	9.27	1.33	0.80	1.01	1.43	0.14
11.93	13.4	17.3	0.01	0.249	4.97	15.33	1.05	0.78	0.76	0.78	0.13
11.95	13.7	20.0	0.01	0.343	6.83	15.14	1.26	0.67	0.82	1.08	0.09
11.97	10.0	23.1	0.01	0.327	6.01	10.29	1.29	0.78	0.97	1.04	0.11
11.99	8.5	31.2	0.01	0.201	4.00	7.47	1.10	0.88	0.89	0.68	0.13
12.01	5.1	28.2	0.01	0.337	6.62	5.14	1.44	0.83	0.95	1.12	0.14
12.04	5.2	22.4	0.01	0.350	7.19	5.47	1.40	0.77	0.92	1.21	0.13
17.08	6.9	36.9	0.01	0.102	2.38	6.57	1.07	1.36	0.65	0.39	0.09
17.10	6.1	37.2	0.01	0.100	2.30	6.14	1.05	1.34	0.67	0.38	0.08
17.12	6.7	36.6	0.01	0.112	2.66	6.76	1.19	1.50	0.68	0.41	0.09
17.14	5.8	34.5	0.01	0.056	1.44	5.55	0.97	1.31	0.69	0.22	0.09
17.16	6.3	43.1	0.01	0.046	1.15	5.84	1.12	1.58	0.70	0.19	0.10
17.18	6.0	47.0	0.01	0.063	1.44	5.72	1.31	1.88	0.79	0.24	0.09
17.25	5.0	49.3	0.01	0.035	0.93	5.39	1.19	1.89	0.61	0.16	0.08
17.28	3.6	53.9	0.01	0.013	0.36	3.65	1.39	2.09	0.73	0.08	0.05
17.31	2.3	55.5	0.01	0.013	0.33	2.38	1.36	2.02	0.65	0.07	0.05
17.36	0.9	34.8	0.01	0.161	1.90	1.20	0.93	1.54	0.63	0.40	0.10

Depth [m]	As	Ba	Co	Cr	Cu	Mn	Ni	Pb	Sr	V	Y	Zn	Zr
11.87	47	224	24	77	14	414	40	18	92	107	23	113	116
11.88	47	216	17	80	16	417	41	17	89	125	23	94	131
11.91	57	201	23	66	13	463	32	15	91	86	20	67	114
11.93	65	119	16	37	14	1503	30	10	74	71	13	89	64
11.95	82	157	28	49	17	808	36	14	86	84	15	62	81
11.97	43	153	12	51	12	794	29	13	82	87	14	70	85
11.99	20	92	11	35	9	614	27	7	75	71	10	78	50
12.01	20	157	7	57	14	463	24	10	87	88	14	46	76
12.04	20	163	12	60	14	552	29	12	82	84	15	95	78
17.08	8	90	6	21	12	1071	15	4	108	30	9	37	43
17.10	9	90	5	20	12	1003	15	3	105	23	8	36	39
17.12	9	94	6	22	13	1104	17	3	117	28	8	43	37
17.14	4	61	4	13	11	824	12	1	99	15	5	32	23
17.16	6	67	3	13	11	649	11	2	119	14	5	31	22
17.18	6	81	3	13	10	609	10	2	142	15	5	29	25
17.25	17	79	4	8	15	367	10	0	144	11	4	15	18
17.28	5	56	3	3	14	301	6	0	147	6	2	4	12
17.31	1	53	2	4	13	299	5	0	140	5	2	3	13
17.36	4	191	2	18	24	240	9	3	127	13	7	9	98

A detailed description of the used methods is given in the individual chapters.  
Bulk parameters and major elements in %, trace metals in mg kg<sup>-1</sup>.

**Schweiburg core (Archive No. GE 707)**

Depth [m]	TS	TC	TIC	TiO <sub>2</sub>	Al <sub>2</sub> O <sub>3</sub>	Fe <sub>2</sub> O <sub>3</sub>	MgO	CaO	Na <sub>2</sub> O	K <sub>2</sub> O	P <sub>2</sub> O <sub>5</sub>
1.045	1.71	35.8	0.01	0.120	3.67	3.09	0.74	4.12	0.19	0.60	0.10
1.060	2.06	45.4	0.01	0.039	1.38	2.48	0.56	4.63	0.10	0.21	0.07
1.085	2.04	49.8	0.01	0.025	0.70	2.70	0.54	4.66	0.10	0.12	0.07
1.190	2.47	48.9	0.01	0.058	0.97	2.43	0.49	2.23	0.15	0.20	0.11
1.215	2.81	48.1	0.01	0.075	1.28	2.87	0.62	2.54	0.17	0.24	0.09
1.220	4.32	48.8	0.01	0.027	0.55	3.25	0.67	3.15	0.10	0.11	0.04
1.340	3.3	36.1	0.01	0.232	4.48	4.31	0.96	2.13	0.24	0.71	0.08
1.540	5.39	52	0.01	0.015	0.29	4.59	0.60	2.19	0.13	0.07	0.05
1.590	4.52	52.8	0.01	0.015	0.31	3.07	0.74	2.92	0.15	0.08	0.05
1.690	4.15	50.2	0.01	0.011	0.25	2.67	0.88	3.10	0.16	0.07	0.04
1.740	3.99	48.5	0.01	0.013	0.28	2.77	0.98	3.18	0.17	0.07	0.05
1.810	3.64	52.5	0.01	0.028	0.52	2.67	1.00	3.13	0.19	0.10	0.06
1.835	4.92	46.5	0.01	0.087	1.58	4.87	1.08	2.60	0.20	0.26	0.07
1.855	4.97	46.1	0.01	0.126	2.34	5.07	1.28	2.78	0.23	0.40	0.07
1.905	8.37	34.4	0.01	0.171	3.24	9.34	1.27	2.01	0.26	0.58	0.08
7.550	3.37	33.3	0.01	0.006	0.12	1.08	1.42	1.71	0.05	0.12	0.04
7.575	3.42	48.5	0.01	0.016	0.27	2.03	1.40	1.73	1.53	0.15	0.06
7.595	2.66	52.3	0.01	0.016	0.26	0.63	1.40	1.70	1.26	0.13	0.06
7.620	3.18	50.9	0.01	0.019	0.44	0.98	1.49	1.86	2.58	0.15	0.06
7.990	5.25	37.7	0.01	0.173	4.42	4.34	1.35	1.28	1.96	0.67	0.23
8.140	5.05	46	0.01	0.069	1.92	1.95	1.42	1.61	1.07	0.36	0.14
8.190	5.02	49.8	0.01	0.025	0.77	1.43	1.43	1.60	0.95	0.16	0.11
8.235	4.98	47.8	0.01	0.029	0.82	2.14	1.77	2.35	1.05	0.18	0.10
8.325	4.96	50.9	0.01	0.021	0.45	2.38	1.44	1.77	0.90	0.14	0.07
8.470	13.1	38.8	0.01	0.044	1.00	13.40	1.12	1.32	1.19	0.19	0.06

Depth [m]	As	Ba	Co	Cr	Cu	Mn	Ni	Pb	Sr	V	Y	Zn	Zr
1.045	38.6	56	7.5	32	8	390	19.7	6.6	146	39	7	21	38
1.060	14.5	20	2.7	10	3	454	8.4	2.3	161	12	2	10	13
1.085	3.5	10	2.3	4	2	455	5.9	0.1	161	6	1	9	6
1.190	1.7	24	2.4	9	6	380	4.3	3.5	78	7	2	9	20
1.215	0.8	33	2.4	11	6	466	4.4	2.6	86	10	3	10	26
1.220	0.7	13	1.1	5	3	697	1.8	1.3	105	8	2	4	9
1.340	11.4	95	2.9	38	11	641	15.2	9.6	95	65	12	36	46
1.540	1.1	4	0.7	1	3	751	0.4	12.0	84	7	1	4	4
1.590	0.6	5	0.6	2	3	916	0.3	5.1	112	10	1	2	5
1.690	0.8	3	0.5	1	4	995	0.7	4.5	136	10	2	3	4
1.740	1.7	4	0.9	2	6	983	2.3	1.4	142	13	2	3	5
1.810	0.4	6	1.0	3	6	1011	3.5	2.2	153	14	4	4	10
1.835	4.0	33	2.9	14	9	858	7.3	4.3	130	25	7	13	26
1.855	14.2	47	4.2	22	9	910	10.0	6.0	144	42	11	22	35
1.905	6.5	75	4.5	27	10	637	8.6	11.5	126	38	9	56	45
7.550	0.7	13	0.3	10	2	275	3.8	0.1	110	2	1	0	2
7.575	0.6	17	0.3	2	1	339	0.3	0.2	113	3	1	2	7
7.595	2.5	14	0.3	3	2	292	0.2	1.5	105	3	1	1	8
7.620	0.4	22	0.2	6	11	318	3.3	4.8	126	9	1	5	13
7.990	0.2	122	4.6	35	12	344	19.7	6.7	123	110	17	45	47
8.140	4.6	53	2.0	13	4	288	6.8	2.3	130	39	6	12	15
8.190	0.2	29	0.3	4	3	292	2.4	0.2	123	16	3	5	7
8.235	1.8	43	1.0	7	4	446	3.7	1.0	177	14	4	10	14
8.325	1.3	24	0.5	4	3	344	0.8	0.3	127	8	4	4	16
8.470	2.8	43	0.3	8	9	403	3.7	5.8	104	24	8	9	36

**Aurich Moor core**

Depth [m]	TS	TC	TIC	TiO <sub>2</sub>	Al <sub>2</sub> O <sub>3</sub>	Fe <sub>2</sub> O <sub>3</sub>	MgO	CaO	Na <sub>2</sub> O	K <sub>2</sub> O	P <sub>2</sub> O <sub>5</sub>
0.025	0.56	46.4	0.01	0.109	1.27	1.57	0.25	3.22	0.09	0.17	0.83
0.075	0.49	48.8	0.01	0.064	0.80	0.90	0.17	2.76	0.05	0.10	0.45
0.12	0.43	49.8	0.01	0.020	0.34	0.20	0.13	2.07	0.02	0.03	0.12
0.16				0.015	0.25	0.14	0.11	1.60	0.02	0.02	0.08
0.21				0.012	0.20	0.08	0.12	1.33	0.02	0.02	0.06
0.33	0.44	54.2	0.01	0.011	0.20	0.07	0.19	1.06	0.02	0.02	0.06
0.38	0.45	54.5	0.01	0.014	0.19	0.08	0.19	0.75	0.03	0.02	0.08
0.49	0.49	47.0	0.01	0.076	0.89	1.08	0.23	2.37	0.07	0.12	0.57
0.58	0.44	51.0	0.01	0.028	0.34	0.38	0.23	0.85	0.04	0.05	0.22
0.63	0.44	52.7	0.01	0.018	0.24	0.21	0.26	0.74	0.03	0.03	0.13
0.68				0.015	0.20	0.15	0.34	0.61	0.03	0.02	0.08
0.73				0.007	0.11	0.07	0.36	0.45	0.03	0.01	0.05
0.78				0.009	0.12	0.11	0.44	0.49	0.03	0.02	0.06
0.88				0.005	0.09	0.12	0.63	0.47	0.04	0.01	0.04
0.93				0.009	0.10	0.13	0.55	0.44	0.05	0.02	0.04
1.05				0.038	0.48	0.57	0.34	1.19	0.07	0.07	0.24
1.15	0.47	56.1	0.01	0.006	0.09	0.18	0.47	0.44	0.06	0.02	0.04
1.35				0.003	0.08	0.21	0.48	0.51	0.08	0.02	0.03
1.45				0.003	0.06	0.22	0.38	0.51	0.09	0.02	0.04
1.55				0.005	0.08	0.21	0.24	0.45	0.09	0.02	0.06
1.63				0.005	0.09	0.31	0.30	0.57	0.10	0.02	0.05
1.7	0.35	55.2	0.01	0.004	0.11	0.37	0.32	0.63	0.10	0.02	0.04
1.8				0.004	0.15	0.47	0.30	0.75	0.09	0.02	0.05
1.89				0.003	0.17	0.42	0.24	0.62	0.09	0.01	0.05
1.96				0.004	0.26	0.54	0.27	0.73	0.10	0.02	0.05
2.03				0.004	0.27	0.49	0.21	0.63	0.08	0.02	0.06
2.07				0.005	0.34	0.65	0.22	0.79	0.09	0.01	0.05
2.13				0.004	0.37	0.75	0.24	0.76	0.09	0.01	0.05
2.18				0.005	0.38	0.72	0.21	0.77	0.08	0.01	0.05
2.24				0.005	0.37	1.00	0.23	1.11	0.10	0.02	0.03
2.33				0.056	0.65	0.92	0.16	0.83	0.12	0.16	0.02
2.38				0.077	0.98	0.77	0.12	0.64	0.16	0.25	0.02

**Aurich Moor core**

Depth [m]	As	Ba	Co	Cr	Cu	Mn	Ni	Pb	Sr	V	Y	Zn	Zr
0.025	3	85	3.4	150	21	1721	7.0	117.8	104	265	6.4	189	32
0.075		48	2.3	98	13	937	4.4	61.0	79	189	3.2	137	16
0.12		20	0.8	19	4	316	2.1	13.8	54	45	0.9	51	5
0.16		14	0.5	13	3	196	1.7	7.5	45	25	0.7	24	5
0.21		12	0.4	6	3	128	1.0	3.5	38	10	0.5	13	3
0.33		14	0.3	3	3	57	0.7	1.6	42	4	0.5	5	3
0.38		12	0.2	6	4	78	0.7	4.0	34	10	0.7	8	4
0.49	2	62	2.4	80	15	1289	4.0	74.3	73	186	4.7	131	19
0.58	1	25	0.9	26	6	418	1.7	29.4	38	70	1.6	42	3
0.63		15	0.5	15	7	191	1.2	14.1	33	35	0.9	25	6
0.68		15	0.3	8	3	139	0.8	10.9	35	19	0.6	11	3
0.73	1	8	0.2	4	2	34	0.7	6.3	31	6	0.3	4	2
0.78		12	0.2	5	3	75	0.9	5.6	36	10	0.4	6	3
0.88		11	0.1	1	4	21	0.4	8.3	40	2	0.2	1	1
0.93		9	0.1	2	4	19	0.9	2.7	35	3	0.3	2	2
1.05		34	1.5	36	9	710	2.8	33.4	47	101	2.0	59	7
1.15		13	0.7	1	2	34	0.5	1.0	30	5	0.3	3	1
1.35		14	0.3	1	3	8	0.5	0.8	32	1	0.1	1	1
1.45		16	0.2	1	2	11	0.3	0.4	30	2	0.1	1	1
1.55		15	0.4	3	3	50	0.9	2.2	22	8	0.2	5	1
1.63		26	0.5	2	5	23	0.9	1.9	29	4	0.3	3	1
1.7		33	0.6	1	2	17	1.2	1.4	31	2	0.4	2	1
1.8	4	48	0.8	2	3	17	2.0	2.1	33	2	0.8	2	1
1.89	5	40	0.9	1	3	14	1.5	1.9	26	2	1.2	2	1
1.96	8	50	1.2	1	4	20	2.1	1.6	33	3	2.7	2	2
2.03	6	41	1.5	1	8	17	1.9	0.5	25	4	3.0	3	2
2.07	3	63	1.5	1	8	17	2.3	0.6	31	5	4.3	2	2
2.13	3	65	1.6	1	8	19	2.2	0.4	34	5	5.3	2	2
2.18	3	59	1.4	1	7	17	2.4	0.5	30	5	5.4	1	3
2.24		79	1.4	1	8	24	2.9	0.6	40	3	4.6	5	4
2.33	1	97	1.0	4	8	31	4.6	1.3	39	2	2.5	2	49
2.38	1	108	0.6	8	11	35	5.2	2.4	35	3	2.6	2	61



## A5: ICP-MS data

## Loxstedt core B (Archive No. GE 430)

Depth [m]	Bi	Cd	Co	Cr	Cu	Mo	Ni	Pb	Re	Sb	Tl	U	Y	Zn
7.35	0.16	0.08	6	60	8	1.6	25	15	1.5	0.14	0.48	3.1	17	50
7.45	0.33	0.12	9	96	10	3.1	30	21	1.9	0.43	0.63	3.0	19	81
9.22	0.17	0.10	6	61	8	4.2	22	16	3.3	0.43	0.42	4.4	16	48
9.28	0.22	0.11	7	79	15	4.0	26	17	2.1	0.37	0.49	4.0	18	73
9.63	0.23	0.15	7	62	9	7.8	23	16	4.0	0.55	0.44	3.3	14	57
9.73	0.20	0.14	9	59	8	2.1	27	14	3.5	0.37	0.38	2.3	18	67
10.03	0.19	0.14	7	69	9	4.9	24	15	2.5	0.51	0.44	3.0	18	63
10.03	0.22	0.17	9	70	8	4.8	26	15	2.7	0.48	0.46	3.5	19	72
10.69	0.19	0.23	11	52	9	6.0	25	14	2.6	0.30	0.40	4.2	17	63
10.76	0.12	0.09	5	60	7	4.0	21	10	3.2	0.26	0.35	4.2	18	47
11.99	0.31	0.48	26	57	28	21.7	59	20	4.5	0.81	0.42	5.2	17	182
13.75	0.23	0.14	9	65	8	0.6	27	17	1.0	0.42	0.44	1.7	21	66
17.27	0.05	0.06	1	27	5	0.2	5	8	0.3	0.16	0.28	1.3	11	11
17.63	0.22	0.85	10	55	21	1.8	52	18	2.3	0.85	0.48	6.0	38	63
17.7	0.15	0.51	12	45	20	4.6	45	11	1.9	0.63	0.40	5.4	26	52
17.77	0.14	0.40	20	37	18	1.0	40	10	1.5	0.42	0.28	6.3	23	43
17.83	0.17	0.19	11	55	14	0.5	29	15	0.7	0.50	0.47	3.3	17	39
17.91	0.06	0.08	5	29	5	0.1	12	8	0.3	0.17	0.25	1.1	8	20

Depth [m]	La	Ce	Pr	Nd	Sm	Eu	Gd	Tb	Dy	Ho	Er	Tm	Yb	Lu
1.46	9.9	20.0	2.2	8.4	1.6	0.35	1.31	0.20	1.31	0.24	0.68	0.10	0.64	0.11
1.95	12.0	24.4	2.8	10.6	2.0	0.44	1.89	0.29	1.91	0.34	1.00	0.15	0.94	0.15
2.28	10.2	19.8	2.4	9.1	1.8	0.38	1.48	0.21	1.41	0.24	0.67	0.10	0.68	0.11
3.18	33.6	67.3	7.9	29.0	5.9	1.10	5.18	0.76	5.11	0.95	2.82	0.40	2.64	0.41
4.04	34.3	70.5	8.1	30.3	6.3	1.25	5.36	0.81	5.11	0.98	2.94	0.40	2.63	0.39
5.04	32.5	67.0	7.7	29.2	5.7	1.15	5.16	0.76	5.23	0.93	2.74	0.39	2.49	0.39
7.01	28.7	58.6	6.7	25.4	5.1	1.01	4.38	0.65	4.12	0.76	2.12	0.31	2.08	0.32
7.45	24.5	55.9	7.3	25.0	5.4	1.04	4.86	0.64	4.39	0.73	2.10	0.31	2.04	0.29
9.22	18.8	41.8	5.7	19.4	4.3	0.83	3.95	0.52	3.52	0.59	1.66	0.24	1.57	0.23
9.28	20.9	52.3	6.6	22.4	5.0	0.91	4.50	0.60	4.10	0.68	1.99	0.29	1.99	0.28
9.63	19.6	38.2	6.1	20.4	4.5	0.84	4.01	0.53	3.51	0.57	1.66	0.24	1.63	0.23
9.73	19.2	44.4	6.0	19.9	4.6	0.87	4.29	0.57	3.90	0.64	1.83	0.26	1.70	0.25
10.03	21.8	49.3	6.7	23.0	5.0	0.93	4.53	0.61	4.13	0.69	1.98	0.29	1.95	0.28
10.16	24.5	52.7	7.1	24.2	5.3	0.98	4.93	0.67	4.62	0.77	2.24	0.32	2.12	0.31
10.69	19.3	40.1	5.7	19.3	4.2	0.78	4.00	0.54	3.67	0.63	1.76	0.26	1.69	0.24
10.76	18.4	41.4	5.7	19.4	4.4	0.85	4.07	0.56	3.75	0.63	1.78	0.25	1.66	0.24
12.68	33.2	66.7	7.7	28.4	5.6	1.19	4.89	0.73	4.63	0.87	2.34	0.35	2.29	0.33
13.75	30.8	62.8	7.2	27.8	5.3	1.14	4.87	0.72	4.71	0.88	2.52	0.36	2.34	0.36
15.41	15.7	31.6	3.6	13.3	2.7	0.51	2.23	0.34	2.27	0.41	1.22	0.18	1.23	0.19
16.25	5.5	10.7	1.2	4.3	0.9	0.21	0.82	0.13	0.83	0.15	0.42	0.06	0.42	0.08
16.75	8.4	16.8	1.9	7.2	1.4	0.29	1.18	0.18	1.18	0.21	0.64	0.09	0.60	0.10
17.27	10.9	21.4	2.3	8.5	1.6	0.31	1.43	0.23	1.59	0.32	1.01	0.15	1.03	0.16
17.63	76.2	147.0	14.0	48.6	10.3	2.23	10.3	1.33	8.57	1.50	4.20	0.59	3.89	0.57
17.70	44.6	98.4	8.8	27.0	5.6	1.13	5.79	0.70	4.80	0.85	2.60	0.39	2.72	0.42
17.77	28.7	68.5	7.1	23.3	5.2	1.03	5.06	0.65	4.41	0.77	2.26	0.33	2.33	0.36
17.83	23.1	51.2	6.1	20.9	4.3	0.85	3.90	0.56	3.70	0.67	1.95	0.29	1.93	0.30

A detailed description of the used methods is given in the individual chapters.  
 Except for Re [ $\mu\text{g kg}^{-1}$ ] trace metals are given in  $\text{mg kg}^{-1}$ .

**Loxstedt core C (Archive No. GE 432)**

Depth [m]	Bi	Cd	Co	Cr	Cu	Mo	Ni	Pb	Re	Sb	Tl	U	Y	Zn
11.95	0.19	0.20	11	48	10	19.5	25	12	7.6	0.74	0.33	5.6	14	68
11.97	0.13	0.12	10	36	8	20.2	26	10	4.9	0.46	0.22	5.2	11	82
11.99	0.20	0.09	6	56	12	12.4	22	12	6.3	0.38	0.35	4.5	15	49
12.01	0.22	0.25	11	58	13	12.0	28	14	5.4	0.48	0.40	4.8	16	99
12.04	0.05	0.13	4	13	9	2.8	11	3	2.7	0.15	0.08	3.0	6	33
11.87	0.33	0.18	16	85	15	3.4	41	20	3.6	0.66	0.51	3.6	26	100
11.88	0.33	0.20	25	85	13	4.8	41	21	2.9	0.76	0.56	5.0	26	129
11.91	0.19	0.21	17	43	10	17.3	31	13	7.2	0.83	0.32	4.8	15	93
11.93	0.32	0.20	29	61	14	24.0	36	19	6.5	1.06	0.48	6.8	17	70
17.08	0.09	0.17	6	24	11	3.4	16	6	3.3	0.32	0.16	3.3	10	42
17.1	0.08	0.16	5	21	11	2.8	15	5	3.0	0.26	0.16	2.9	9	40
17.12	0.09	0.18	6	22	12	3.2	16	5	2.7	0.26	0.16	3.1	8	45
17.14	0.06	0.12	4	13	9	4.2	11	3	2.8	0.17	0.10	2.7	5	34
17.16	0.01	0.09	4	4	12	2.4	6	1	0.9	0.09	0.01	0.9	3	6
17.18	0.05	0.10	3	13	9	2.8	10	3	1.8	0.15	0.09	3.1	5	30
17.25	0.03	0.14	4	8	14	5.0	10	2	2.0	0.18	0.05	2.8	4	17
17.28	0.29	0.16	20	65	12	7.1	30	18	3.9	0.60	0.40	4.4	21	71
17.31	0.01	0.09	2	4	12	0.7	5	1	0.5	0.07	0.02	0.3	2	5
17.36	0.03	0.15	1	17	23	0.5	8	4	0.7	0.19	0.14	0.8	8	12

Depth [m]	La	Ce	Pr	Nd	Sm	Eu	Gd	Tb	Dy	Ho	Er	Tm	Yb	Lu
11.91	15.7	28.3	4.2	14.6	3.3	0.65	3.08	0.42	2.84	0.47	1.31	0.19	1.23	0.17
11.93	22.4	46.0	6.5	21.4	4.8	0.94	4.40	0.59	4.02	0.66	1.90	0.27	1.77	0.26
11.87	34.1	58.8	7.5	30.1	5.7	1.23	5.76	0.80	4.51	0.88	2.68	0.37	2.45	0.34
11.88	36.9	73.2	8.2	30.0	6.6	1.35	6.40	0.88	5.13	0.99	2.87	0.40	2.61	0.37
11.91	15.8	36.4	4.2	16.1	3.3	0.75	3.37	0.47	2.67	0.52	1.49	0.21	1.40	0.19
11.93	18.6	38.2	4.7	18.1	3.7	0.75	3.32	0.47	2.79	0.54	1.48	0.22	1.46	0.20
11.95	16.9	36.3	4.3	16.1	3.2	0.64	2.89	0.43	2.41	0.47	1.28	0.19	1.27	0.18
11.97	12.0	23.4	2.8	11.4	2.4	0.53	2.29	0.35	2.00	0.40	1.10	0.16	1.05	0.14
11.99	17.8	31.9	3.8	15.1	3.0	0.66	2.97	0.43	2.43	0.48	1.41	0.20	1.24	0.19
12.01	20.6	37.3	4.8	17.0	3.8	0.81	3.55	0.52	3.07	0.57	1.64	0.23	1.55	0.21
12.04	4.8	11.7	1.2	4.9	1.1	0.26	1.14	0.17	0.91	0.19	0.56	0.08	0.51	0.07
17.08	8.0	15.6	2.1	8.2	1.8	0.40	1.79	0.26	1.60	0.32	0.93	0.13	0.90	0.15
17.10	8.1	15.1	1.9	7.5	1.7	0.37	1.69	0.25	1.46	0.31	0.85	0.12	0.82	0.11
17.12	8.9	18.2	2.2	8.2	1.7	0.38	1.69	0.24	1.41	0.28	0.79	0.11	0.76	0.11
17.14	5.3	10.6	1.2	4.6	1.0	0.22	1.04	0.14	0.87	0.16	0.48	0.07	0.44	0.07
17.16	2.7	5.5	0.7	2.5	0.6	0.14	0.58	0.08	0.46	0.09	0.25	0.03	0.23	0.03
17.18	5.7	11.1	1.4	5.7	1.1	0.25	1.10	0.16	0.94	0.18	0.53	0.07	0.51	0.07
17.25	4.6	9.8	1.2	4.2	0.9	0.22	0.95	0.14	0.80	0.15	0.41	0.05	0.37	0.05
17.28	23.3	49.4	5.9	23.4	4.4	0.93	4.43	0.60	3.46	0.71	1.89	0.28	1.94	0.26
17.31	2.2	4.5	0.5	2.1	0.4	0.11	0.46	0.06	0.39	0.07	0.20	0.03	0.18	0.04
17.36	10.0	20.2	2.2	8.2	1.6	0.32	1.67	0.23	1.34	0.27	0.80	0.11	0.77	0.14

**Arngast core (Archive No. GE 117)**

Depth [m]	Bi	Cd	Co	Cr	Cu	Mo	Ni	Pb	Re	Sb	Tl	U	Y	Zn
3.87	0.25	0.19	15	82	15	16.6	40	20	12.9	0.66	0.60	11.4	18	90
3.91	0.12	0.14	5	44	11	32.0	21	15	13.4	0.58	0.33	13.2	11	55
3.95	0.07	0.07	4	30	11	23.6	15	9	7.8	0.32	0.21	11.3	9	33
3.99	0.31	0.21	12	86	13	18.8	33	23	7.4	0.78	0.61	7.6	19	104
4.04	0.22	0.33	17	38	18	53.4	30	20	22.1	1.19	0.43	27.9	8	124
4.09	0.22	0.36	12	46	22	48.6	24	30	13.9	1.62	0.37	21.5	10	124
4.15	0.18	0.19	7	49	10	14.5	20	14	4.5	0.56	0.36	4.8	12	84
4.18	0.17	0.19	7	41	11	14.8	20	14	3.8	0.41	0.28	7.0	10	87
4.23	0.15	0.27	7	44	13	14.3	25	12	8.4	0.45	0.34	5.9	10	96
4.31	0.21	0.22	9	62	11	11.0	25	18	3.6	0.63	0.44	4.2	14	83
4.37	0.08	0.09	2	27	8	6.4	11	10	4.7	0.33	0.18	4.1	7	29

**Wangerland core W1 (Archive No. KB 5552)**

Depth [m]	Bi	Cd	Co	Cr	Cu	Mo	Ni	Pb	Re	Sb	Tl	U	Y	Zn
2.01	0.27	0.05	10	105	13	0.1	31	23	0.8	0.06	0.59	2.8	27	113
3.04	0.27	0.11	8	98	11	0.2	27	24	0.6	0.22	0.53	2.3	26	95
4.03	0.23	0.23	11	92	10	0.5	33	19	1.0	0.22	0.56	2.7	23	90
5.08	0.23	0.11	9	83	9	0.8	28	17	1.4	0.29	0.51	2.1	22	85
7.05	0.09	0.09	5	57	4	0.6	12	10	0.9	0.42	0.32	2.2	19	38
8.47	0.19	0.09	9	88	7	0.7	24	18	1.5	0.45	0.49	2.3	25	72
8.55	0.23	0.11	10	83	8	0.9	26	19	1.7	0.50	0.54	2.5	25	80
9.15	0.24	0.07	10	91	8	1.1	28	19	1.5	0.59	0.51	2.5	25	84
9.19	0.23	0.10	10	85	9	1.1	28	19	1.5	0.28	0.58	2.5	24	81
9.23	0.28	0.12	12	95	9	1.3	32	22	1.6	0.48	0.62	2.5	25	87
10.38	0.31	0.14	13	100	11	2.7	33	24	1.7	0.67	0.66	3.1	27	97
10.52	0.31	0.16	17	94	13	6.6	38	24	4.3	0.71	0.60	3.9	27	101
10.64	0.30	0.16	15	84	11	6.6	37	23	3.0	0.71	0.59	4.1	23	86
10.67	0.46	0.36	31	85	13	17.0	53	22	5.0	0.95	0.74	4.4	20	72
10.69	0.31	0.29	27	76	12	14.5	46	23	6.0	0.78	0.61	3.6	18	76
10.72	0.19	0.33	31	71	9	15.9	58	19	5.0	0.73	0.56	3.5	18	96
10.74	0.15	0.08	6	71	9	4.8	24	13	3.4	0.51	0.52	4.1	19	55
10.78	0.18	0.20	10	49	10	16.4	27	14	5.5	0.74	0.37	5.0	15	58
10.81	0.15	0.12	6	49	7	6.8	20	11	2.9	0.38	0.28	4.4	16	54
10.84	0.09	0.08	3	33	5	5.3	13	6	3.8	0.19	0.18	4.1	11	19
10.87	0.07	0.07	2	21	5	6.4	9	4	3.7	0.23	0.11	4.1	10	19
10.96	0.01	0.11	1	7	2	1.0	4	1	0.5	0.05	0.04	0.6	2	10
11.00	0.01	0.06	1	5	1	1.0	2	1	0.8	0.04	0.02	0.6	2	1
11.03	0.01	0.11	1	7	2	1.0	3	1	0.9	0.05	0.02	0.6	2	10
11.06	0.04	0.06	2	15	3	1.9	5	3	1.2	0.10	0.10	1.4	5	7
11.13	0.07	0.06	4	24	5	2.1	10	4	3.2	0.15	0.13	2.2	7	13
11.16	0.11	0.08	6	42	6	3.5	18	9	3.8	0.23	0.29	3.7	10	21
11.22	0.21	0.28	38	51	11	12.1	43	16	6.3	0.52	0.42	6.3	13	61
11.25	0.13	0.11	33	42	9	15.8	38	10	4.3	0.41	0.30	7.8	11	37
11.28	0.16	0.32	53	30	9	44.6	50	9	5.4	0.77	0.30	13.4	11	77
11.31	0.15	0.20	74	35	9	37.2	60	10	3.3	0.64	0.43	8.3	16	68
11.35	0.07	0.23	277	21	16	19.4	167	5	6.1	0.44	1.45	4.9	35	199
11.39	0.03	0.09	83	13	8	3.8	63	3	4.6	0.23	2.40	1.6	41	36

**Wangerland core W2 (Archive No. KB 5156)**

Depth [m]	Bi	Cd	Co	Cr	Cu	Mo	Ni	Pb	Re	Sb	Tl	U	Y	Zn
4.89	0.18	0.17	7	53	7	15.6	19	13	9.0	0.48	0.37	4.6	16	38
4.93	0.15	0.11	4	52	10	9.2	19	13	4.2	0.35	0.36	4.7	13	39
4.96	0.15	0.13	6	55	8	13.1	27	10	6.4	0.37	0.26	3.2	11	44
4.99	0.20	0.09	6	54	10	10.6	21	14	3.7	0.42	0.35	3.1	15	57
8.16	0.17	0.09	6	80	9	8.5	22	16	3.4	0.38	0.53	6.7	22	54
8.21	0.12	0.09	3	43	6	16.8	21	10	5.3	0.28	0.28	6.4	15	28
8.23	0.09	0.09	4	35	5	17.0	18	7	5.9	0.33	0.22	5.2	11	26
8.26	0.13	0.11	3	15	5	17.1	13	4	6.6	0.26	0.16	4.8	7	17
8.27	0.07	0.09	5	11	6	14.1	10	3	4.1	0.31	0.09	3.7	5	16
8.29	0.03	0.04	3	6	4	9.3	5	1	2.6	0.27	0.04	2.3	3	11
8.32	0.02	0.03	2	6	4	7.1	3	1	2.8	0.12	0.04	2.3	3	9
8.35	0.02	0.02	1	5	4	4.5	2	1	2.4	0.05	0.01	1.3	2	6
8.38	0.07	0.05	3	29	5	4.7	11	5	3.4	0.18	0.18	2.0	8	26
8.42	0.05	0.04	2	26	4	5.7	11	4	3.4	0.15	0.15	2.3	9	20
10.57	0.11	0.10	5	39	7	10.4	13	10	3.0	0.32	0.28	4.8	11	33
10.59	0.03	0.06	3	21	5	15.9	7	3	3.0	0.29	0.13	6.3	6	21
10.62	0.03	0.06	2	15	5	9.6	5	3	3.3	0.26	0.08	3.0	4	16
10.65	0.02	0.05	1	12	5	2.4	2	2	2.3	0.11	0.06	0.8	3	10
10.69	0.02	0.02	0	19	4	0.9	2	4	0.7	0.12	0.12	0.9	6	9

**Wangerland core W3 (Archive No. KB 5750)**

Depth [m]	Bi	Cd	Co	Cr	Cu	Mo	Ni	Pb	Re	Sb	Tl	U	Y	Zn
1.99	0.30	0.54	10	71	16	2.6	26	18	7.6	0.92	0.42	2.1	19	177
2.03	0.25	0.24	8	58	16	1.8	21	16	5.7	0.54	0.37	1.8	17	56
2.05	0.29	0.17	10	79	10	1.2	26	20	4.0	0.62	0.49	1.9	21	65
5.25	0.25	0.22	10	63	14	12.2	27	17	19.2	0.84	0.45	10.0	20	70
5.26	0.13	0.18	7	48	13	15.7	20	9	28.6	0.55	0.29	8.8	12	35
5.30	0.02	0.03	1	11	6	13.9	3	2	4.8	0.18	0.04	3.6	6	8
5.34	0.05	0.05	1	21	8	8.9	6	3	3.9	0.17	0.11	2.4	6	12
5.37	0.15	0.04	3	33	8	11.3	10	8	2.7	0.22	0.22	2.7	9	17
5.39	0.27	0.11	4	71	11	10.8	18	15	2.5	0.42	0.46	3.5	12	38
5.66	0.36	0.21	11	84	14	15.5	28	22	6.9	0.64	0.58	5.4	15	67
5.74	0.21	0.29	15	67	11	16.5	38	22	8.4	0.72	0.45	6.2	17	100
5.87	0.22	0.12	6	42	11	26.1	16	13	4.3	0.50	0.34	5.4	12	24
5.94	0.26	0.10	4	82	10	12.2	17	16	2.9	0.47	0.53	3.8	13	36
5.97	0.18	0.11	5	67	14	6.8	20	16	2.7	0.48	0.43	4.3	16	36
5.99	0.11	0.10	8	38	8	17.1	21	5	3.5	0.32	0.22	4.2	10	23
6.00	0.21	0.28	23	51	9	22.6	33	14	6.0	1.04	0.53	3.7	12	130
6.01	0.31	0.25	13	75	18	23.6	28	16	9.7	0.57	0.56	8.6	19	70

**Wangerland core W5 (Archive No. KB 5950)**

Depth [m]	Bi	Cd	Co	Cr	Cu	Mo	Ni	Pb	Re	Sb	Tl	U	Y	Zn
2.74	0.21	0.30	10	69	12	14.2	34	18	11.1	0.48	0.53	6.7	14	48
2.78	0.14	0.10	4	50	8	11.0	20	12	10.8	0.40	0.31	4.5	16	20
2.8	0.12	0.21	11	38	10	28.1	31	8	23.1	0.64	0.29	5.8	14	20
2.82	0.10	0.14	8	35	10	28.0	23	8	17.6	0.58	0.30	3.8	13	10
2.84	0.09	0.11	4	35	10	17.6	17	7	11.1	0.35	0.28	2.9	12	25
2.87	0.14	0.10	3	65	9	6.3	18	11	5.9	0.34	0.37	2.1	13	26
2.89	0.15	0.13	8	59	12	5.0	21	12	5.2	0.42	0.44	2.1	13	28
2.93	0.28	0.19	16	70	21	6.4	27	19	3.9	0.49	0.60	2.5	18	46
2.96	0.25	0.10	11	75	10	4.1	28	15	2.6	0.43	0.47	2.1	14	71
2.98	0.20	0.10	6	87	10	2.1	27	14	2.1	0.37	0.49	1.9	14	65
3.01	0.27	0.11	7	90	11	2.9	28	15	1.7	0.45	0.56	2.0	15	74
3.05	0.31	0.11	10	93	12	3.8	34	21	2.1	0.54	0.61	3.0	21	74
3.07	0.31	0.20	16	84	15	4.7	40	20	2.5	0.56	0.60	2.7	20	99
3.11	0.27	0.15	14	87	12	2.3	34	21	1.3	0.67	0.61	2.7	22	75
3.17	0.27	0.13	10	90	10	0.7	30	21	0.8	0.63	0.62	2.5	24	69
3.24	0.30	0.08	11	93	11	0.6	33	22	0.9	0.46	0.58	2.5	26	71
3.36	0.31	0.11	10	89	11	0.8	32	21	1.0	0.55	0.61	2.4	26	67
5.8	0.20	0.18	9	33	24	34.0	15	13	6.8	0.50	0.32	4.2	12	23
5.85	0.04	0.02	1	7	4	6.8	5	1	3.3	0.25	0.01	1.1	2	7
5.91	0.06	0.06	3	23	9	2.1	9	5	3.2	0.26	0.12	1.2	7	23
5.93	0.05	0.05	2	15	6	2.3	7	3	2.9	0.26	0.07	0.9	5	23
6	0.04	0.04	2	13	4	1.8	6	3	1.9	0.16	0.05	0.8	3	15
6.1	0.04	0.04	1	26	5	3.0	8	3	1.3	0.13	0.10	1.8	4	11
6.12	0.03	0.05	1	16	5	2.8	7	2	1.5	0.10	0.06	1.8	4	10
6.16	0.04	0.04	1	20	4	2.1	5	3	2.4	0.13	0.11	1.5	6	8
6.18	0.04	0.04	1	9	5	1.6	3	2	1.3	0.08	0.05	0.9	3	9
6.24	0.01	0.05	1	3	4	0.9	2	1	0.7	0.06	0.01	0.2	1	6
6.26	0.01	0.07	1	3	8	0.8	2	0	0.7	0.08	0.01	0.2	1	10
6.34	0.03	0.10	4	8	4	13.3	9	2	2.4	0.32	0.04	2.7	3	18
6.37	0.06	0.10	4	20	5	18.7	10	4	1.9	0.38	0.15	3.4	4	25
6.39	0.07	0.10	6	26	5	16.7	13	5	3.3	0.40	0.17	3.0	5	30
6.41	0.05	0.11	6	14	10	1.9	9	4	1.2	0.17	0.20	1.5	4	27
6.44	0.02	0.07	1	13	5	0.3	4	3	0.4	0.13	0.06	0.7	5	11
6.45	0.02	0.06	1	12	4	0.3	4	3	0.3	0.13	0.07	0.6	4	8

**$^{206}\text{Pb}/^{207}\text{Pb}$  isotope ratios**

Core	Depth [m]	$^{206}/^{207}\text{Pb}$	Core	Depth [m]	$^{206}/^{207}\text{Pb}$
<b>Loxstedt GE430</b>	0.40	1.170	<b>Wangerland W1</b>	3.61	1.222
	0.50	1.168		5.08	1.202
	0.60	1.168		6.03	1.217
	0.75	1.194		7.05	1.215
	0.85	1.168		8.47	1.220
	0.95	1.169	<b>Wangerland W2</b>	8.55	1.209
	1.07	1.175		3.06	1.198
	1.25	1.165		3.40	1.205
	1.25	1.167		3.53	1.199
	1.35	1.169		6.07	1.192
	2.68	1.167		6.14	1.208
	3.18	1.189	<b>Wangerland W3</b>	2.00	1.202
	4.04	1.207		2.05	1.203
	7.01	1.206	<b>Aurich Moor</b>	0.03	1.157
	7.25	1.205		0.08	1.156
	7.35	1.207		0.16	1.155
	7.45	1.203		0.33	1.181
	9.63	1.209		0.38	1.157
	10.16	1.211		0.49	1.161
	11.83	1.215		0.58	1.159
	13.75	1.214		0.63	1.172
	15.41	1.200		0.73	1.165
	16.75	1.197		0.78	1.168
	17.27	1.214		0.93	1.167
<b>Arngast</b>	17.91	1.211		1.05	1.158
	0.03	1.193		1.15	1.168
	0.88	1.233		1.55	1.158
	1.62	1.190		1.70	1.163
	2.32	1.173		2.33	1.212
				2.37	1.205

A6:  $^{34}\text{S}$  ratios

Core	Depth [m]	$^{34}\text{S}$	Core	Depth [m]	$^{34}\text{S}$
<b>Loxstedt GE430</b>	7.35	5.6	<b>Wangerland W5</b>	2.74	-1.2
	7.58	-1.4		2.78	-22.25
	7.63	-0.4		2.8	-24.7
	7.78	5.4		2.82	-26.7
	7.93	9.9		2.84	-21.2
	8.13	5.6		2.86	-19.9
	8.38	6.3		2.87	-17.3
	8.73	5.1		2.89	-11.1
	8.88	-0.1		2.91	-14.05
	9.14	-6		2.93	-14.8
	9.38	0.2		2.96	-13.9
	9.49	-9		2.98	-10.1
	9.63	-12.1		3.03	-24.2
	9.78	3.6		5.8	-11.95
	10.03	-9		5.825	-7.2
	10.23	-7.2		5.85	-5.9
	10.38	-10.5		5.88	-5
	10.43	-10.3		5.91	-8.5
	10.69	-11.8		5.93	-8.95
	10.93	11.8		5.95	-3.9
	10.98	12.9		6	-8.4
<b>Loxstedt GE432</b>	11.85	-10.4		6.02	-7.9
	11.88	-9.1		6.03	-8.9
	11.93	-13.8		6.08	-5.8
	11.95	-7.2		6.12	-4.45
	11.99	-25		6.14	-6.9
	12.01	-4		6.2	-11.3
	17.08	10.2		6.24	-4.3
	17.10	10.8		6.26	-5.3
	17.16	13.9		6.29	-6
	17.31	15.8		6.31	-8.75
	17.36	17.1		6.34	-17.65
<b>Wangerland W3</b>	1.86	0.5		6.365	-16.7
	1.91	5.2		6.39	-11.1
	2.03	4.3		6.435	-2.6
	2.05	3.4		6.45	-5.6
	2.27	0.3			
	4.14	-4			
	5.16	-9.7			
	5.27	3.2			
	5.37	4.6			
	5.46	-10.1			
	5.54	-11.8			
	5.59	-12.7			
	5.66	-18.2			
	5.74	-21.5			
	5.84	-14			
	5.94	2.7			
	6	-11.05			
	6.06	7.4			

Measurements of stable sulphur isotopes were performed by M. E. Böttcher using Cirm-MS.  
 $^{34}\text{S}$  ratios are given in ‰ (rel. V-CDT). A detailed description is provided by Böttcher *et al.* (1998).

## **Danksagung**

Besonderer Dank gilt meinem Doktorvater Prof. Dr. Hans-Jürgen Brumsack für sein Vertrauen in meine Arbeit. Er gab mir die Freiheit meinen eigenen Weg in der Geochemie zu finden, stand mir jedoch immer mit Rat und Tat zur Seite.

Bei Prof. Dr. Jürgen Rullkötter bedanke ich mich für die Begutachtung dieser Arbeit.

Ebenso bin ich Dr. Bernhard Schnetger zu Dank verpflichtet, da er mir neben meßtechnischen Ratschlägen die Denkweise eines Analytikers näherbrachte.

Mein spezieller Dank gilt Frank Watermann für die fantastische Zusammenarbeit.

Dr. J. Barckhausen und Prof. Dr. H. Streif (Niedersächsisches Landesamt für Bodenforschung, Hannover) danke ich für die bohrtechnische Unterstützung sowie für ihre rege Anteilnahme an unserem Projekt.

Hans-Jochim Sach schulde ich Dank für seine gewissenhafte Unterstützung bei Probenpräparation und Pauschalparameterbestimmungen.

Dr. Michael E. Böttcher gilt mein Dank für die Durchführung der S-Isotopenmessungen.

Weiterhin möchte ich meinen Dank Dr. Gisela Gerdes, Dörte Gramberg, Eleonore Gründken, Joachim Hinrichs und Dr. Barbara Scholz-Böttcher aussprechen, da sie auf die eine oder andere Art zum Gelingen dieser Arbeit beigetragen haben.

Nicht zuletzt möchte ich mich noch bei allen nicht namentlich genannten Mitgliedern der AG Mikrobiogeochemie für die anregenden „Jever-Events“ bedanken.

Diese Arbeit wurde finanziell durch die Deutsche Forschungsgemeinschaft im Rahmen des Schwerpunktprogramms „Wandel der Geo-Biosphäre während der letzten 15,000 Jahre - Kontinentale Sedimente als Ausdruck sich verändernder Umweltbedingungen“ gefördert.



## **Curriculum Vitae**

Olaf Dellwig wurde am 18. April 1967 in Unna (Nordrhein-Westfalen) geboren. Er besuchte zwischen 1973 und 1987 Grundschule, Orientierungsstufe, Realschule und Gymnasium in Buxtehude und beendete seine schulische Laufbahn mit dem Abitur. Von 1988 bis 1989 leistete er seinen Wehrdienst in Stade ab. Im Wintersemester 1989/1990 begann er ein Chemie-Studium an der Carl von Ossietzky Universität Oldenburg, das er im Januar 1996 mit dem Diplom abschloß (Titel der Diplomarbeit: „Anorganisch-geochemische Untersuchungen an holozänen Ablagerungen im norddeutschen Küstenraum (Bohrung Loxstedt 32B)“). Von 1996 bis 1999 arbeitete er als wissenschaftlicher Angestellter in der Arbeitsgruppe Mikrobiogeochemie von Prof. Dr. H.-J. Brumsack im Institut für Chemie und Biologie des Meeres der Carl von Ossietzky Universität Oldenburg. Seit seiner Diplomarbeit beschäftigt er sich mit den Themen, die in dieser Arbeit vorgestellt werden.

Hiermit versichere ich, daß ich diese Arbeit selbständig verfaßt und keine anderen als die angegebenen Quellen und Hilfsmittel benutzt habe.

Oldenburg, den 01.11.1999

A handwritten signature in black ink, reading 'Olaf Dellwig'. The signature is written in a cursive style with a large, stylized 'D'.

Olaf Dellwig